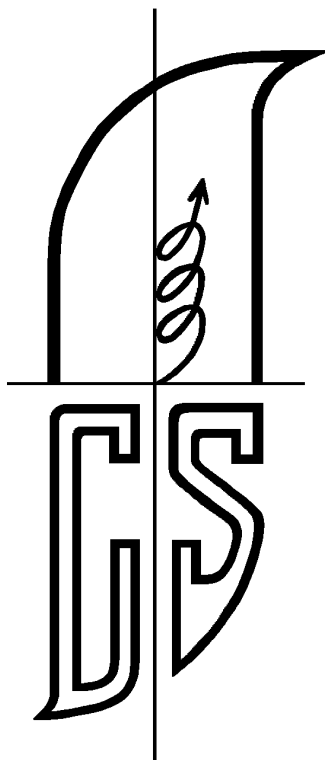


**15<sup>th</sup> Czech and Slovak  
Conference on Magnetism  
CSMAG'13**



**June 17. - 21., 2013  
KOŠICE**

**PROGRAMME  
ABSTRACTS**



***Sponsored by:***

***Quantum Design***  
***LOT-Oriel Group Europe***

***CRYOGENIC Limited***

***CRYOSOFT s.r.o., Košice***

***ChromSpec Slovakia s.r.o., Šaľa***

***ŠEVT a.s., Košice***

## **Book of Abstracts and Programme**

### **15<sup>th</sup> Czech and Slovak Conference on Magnetism**

Faculty of Sciences, P.J. Šafárik University in Košice  
Institute of Experimental Physics, SAS in Kosice

Editors: Pavol Sovák, Ivan Škorvánek, Peter Kollár, Martin Orendáč,  
Jozef Marcin, Gabriel Pavlík and Rastislav Varga.

©2013 Pavol Jozef Šafárik Univerzity in Košice

All rights reserved. Non of the parts of this book or its entirety may be reproduced, stored in information systems, or disseminated in any other way without the prior consent granted by the copyright owner

The authors of individual abstracts to this volume are accountable for the professional level and language correctness. The language and arrangement of the manuscript have not been revised.

ISBN 978-80-8152-015-0

## INTERNATIONAL ADVISORY COMMITTEE

<b>Tadeusz Balcerzak</b>	<b>Łódź</b>
<b>Andrej Bobák</b>	<b>Košice</b>
<b>Horia Chiriac</b>	<b>Iași</b>
<b>Alexander Feher</b>	<b>Košice</b>
<b>Karol Flachbart</b>	<b>Košice</b>
<b>Bogdan Idzikowski</b>	<b>Poznań</b>
<b>Pavel Javorský</b>	<b>Prague</b>
<b>Jiří Kamarád</b>	<b>Prague</b>
<b>Mark W. Meisel</b>	<b>Gainesville</b>
<b>Marcel Miglierini</b>	<b>Bratislava</b>
<b>Marek Pekała</b>	<b>Warsaw</b>
<b>Jaromír Pištora</b>	<b>Ostrava</b>
<b>Oldřich Schneeweiss</b>	<b>Brno</b>
<b>Vladimír Sechovský</b>	<b>Prague</b>
<b>Józef Spalek</b>	<b>Kraków</b>
<b>Henryk Szymczak</b>	<b>Warsaw</b>
<b>Peter Švec</b>	<b>Bratislava</b>
<b>Ilja Turek</b>	<b>Brno</b>
<b>Lajos K. Varga</b>	<b>Budapest</b>

## Organizing Committee

Conference Chairmen:	<b>Pavol Sovák</b>	<b>FS UPJŠ Košice</b>
	<b>Ivan Škorvánek</b>	<b>IEP SAS Košice</b>
Programme:	<b>Peter Kollár</b>	<b>FS UPJŠ Košice</b>
	<b>Martin Orendáč</b>	<b>FS UPJŠ Košice</b>
	<b>Jozef Marcin</b>	<b>IEP SAS Košice</b>
Publication:	<b>Rastislav Varga</b>	<b>FS UPJŠ Košice</b>
	<b>Jozef Kováč</b>	<b>IEP SAS Košice</b>
Local Committee:	<b>Ján Füzer</b>	<b>FS UPJŠ Košice</b>
Treasurer:	<b>Marián Reiffers</b>	<b>IEP SAS Košice</b>
Members:	<b>Adriana Zelenáková</b>	<b>FS UPJŠ Košice</b>
	<b>Milan Timko</b>	<b>IEP SAS Košice</b>
	<b>Martina Koneracká</b>	<b>IEP SAS Košice</b>
	<b>Adriana Orfanusová</b>	<b>FS UPJŠ Košice</b>

**The Conference is organized by**

Faculty of Sciences P. J. Šafárik University (FS UPJŠ) and Institute of Experimental Physics, Slovak Academy of Sciences (IEP SAS), Košice in cooperation with Technical University in Košice, Slovak Physical Society, Czech Physical Society and Slovak Magnetic Society.

**CSMAG `13 Conference Secretariat**

Institute of Physics, P. J. Šafárik University  
Park Angelinum 9  
041 54 Košice,  
Slovakia

www: <http://csmag.saske.sk>  
e-mail: [csmag-secr@saske.sk](mailto:csmag-secr@saske.sk)

**Conference Date and Location**

The conference holds on June 17-21, 2013. Conference sessions will take place in the Lecture hall Aula Maxima, Technical University, Letná 9, Košice. Poster sessions will take place in the Library foyer, Technical University, Boženy Němcovej 7, Košice.

**Scientific programme**

The programme of the conference covers the following areas:

1. Theoretical problems of magnetically ordered materials, magnetization processes.
2. Amorphous, nanocrystalline and other soft magnetic materials.
3. Magnetic materials for energy applications (permanent magnets, magnetocaloric materials, motors, transformers,...).
4. Magnetic thin films and surfaces, spintronics, particles and nanostructures.
5. Low-dimensional magnetic materials, molecular magnets and ferrofluids.
6. Rare-earth and 5f-systems.
7. Strongly correlated electron systems, superconducting materials.
8. Multifunctional magnetic materials (multiferroic, magnetoelastic, shape memory,...).
9. Other magnetic materials and applications not included in 1-8.

The scientific programme consists of invited and contributed talks and poster sessions.

**Conference Language**

The working language of the conference is English.

**Proceedings**

The Proceedings of the Conference will be published in Acta Physica Polonica, the Journal recognised by the Current Contents database.

# **P R O G R A M M E**

# MONDAY, JUNE 17

<b>09:30</b>		<b>Registration</b>
<b>12:30</b>	<b>14:00</b>	<b>Lunch</b>
<b>14:00</b>	<b>14:15</b>	<b>Opening</b>
<b>14:15</b>	<b>14:55</b>	<b>I3-01, M.E. McHenry (invited)</b> NANOCOMPOSITE MAGNETS FOR POWER ELECTRONIC APPLICATIONS
<b>14:55</b>	<b>15:35</b>	<b>I3-02, V. Franco (invited)</b> THE MAGNETOCALORIC EFFECT OF MULTIPHASE MATERIALS AND NANOSTRUCTURES
<b>15:35</b>	<b>15:50</b>	<b>O3-01, S. Rivoirard</b> MAGNETIC FIELD ENHANCED SOFT MAGNETIC PROPERTIES OF Fe-Co ALLOYS
<b>15:50</b>	<b>16:05</b>	<b>O3-02, L.K. Varga</b> MINOR LOOP SCALING RULES FOR SOFT MAGNETIC CORES
<b>16:05</b>	<b>16:30</b>	<b>Coffee break</b>
<b>16:30</b>	<b>17:10</b>	<b>I2-01, G. Herzer (invited)</b> STATUS AND TRENDS OF AMORPHOUS AND NANOCRYSTALLINE ALLOYS FOR SOFT MAGNETIC APPLICATIONS
<b>17:10</b>	<b>17:25</b>	<b>O2-01, R. Szewczyk</b> INFLUENCE OF THERMOMAGNETIC TREATMENT ON MAGNETOELASTIC PROPERTIES OF FeNiMoB AMORPHOUS ALLOY
<b>17:25</b>	<b>17:40</b>	<b>O2-02, M. Pavlovič</b> INFLUENCE OF HIGH-ENERGY HEAVY IONS ON MAGNETIC SUSCEPTIBILITY OF SOFT MAGNETIC METALLIC GLASSES
<b>17:40</b>	<b>17:55</b>	<b>O2-03, Š. Michalik</b> IDENTIFICATION OF THE CURIE POINT IN FINEMET BASED ALLOYS USING IN-SITU X-RAY DIFFRACTION
<b>18:00</b>	<b>21:00</b>	<b>Welcome Reception</b>



## TUESDAY, JUNE 18

<b>08:20</b>	<b>09:00</b>	<b>I2-02, F. Mazaleyrat (invited)</b> TRENDS AND CHALLENGES IN SOFT MAGNETS FOR HIGHER FREQUENCY APPLICATIONS
<b>09:00</b>	<b>09:15</b>	<b>O2-04, M. Miglierini</b> DEPTH-SELECTIVE STUDY OF SURFACE CRYSTALLIZATION IN NANOPERM-TYPE ALLOYS
<b>09:15</b>	<b>09:30</b>	<b>O2-05, A. Lančok</b> MÖSSBAUER AND MAGNETIC STUDY OF THE MAGNETITE NANOPARTICLES
<b>09:30</b>	<b>09:45</b>	<b>O2-06, A. Hendrych</b> THE SURFACE STRUCTURE AND MAGNETIC PROPERTIES OF Fe-Al ALLOYS
<b>09:45</b>	<b>10:00</b>	<b>O2-07, M. Čilliková</b> MAGNETIC EVALUATION OF RESIDUAL STRESSES AND STRUCTURE TRANSFORMATIONS INDUCED IN SOFT STEEL AFTER TURNING
<b>10:00</b>	<b>10:15</b>	<b>O2-08, Z. Śniadecki</b> GLASS FORMING ABILITY AND MAGNETISM OF Co-BASED TERNARY METALLIC GLASSES
<b>10:15</b>	<b>10:35</b>	<b>Coffee break</b>
<b>10:35</b>	<b>11:15</b>	<b>I1-01, A. Zhukov (invited)</b> FAST MAGNETIZATION SWITCHING IN AMORPHOUS MICROWIRES
<b>11:15</b>	<b>11:30</b>	<b>O1-01, J. Richter</b> THERMODYNAMICS OF FRUSTRATED QUANTUM J1-J2 HEISENBERG MAGNETS
<b>11:30</b>	<b>11:45</b>	<b>O1-02, M. L. Lyra</b> KINETICALLY-DRIVEN FRUSTRATION IN HYBRID LADDERS WITH LOCALIZED AND DELOCALIZED SPINS
<b>11:45</b>	<b>12:00</b>	<b>O1-03, K. Carva</b> ULTRAFast DEMAGNETIZATION AND ELECTRON-PHONON SPIN-FLIP PROCESSES FROM FIRST PRINCIPLES
<b>12:00</b>	<b>12:15</b>	<b>O1-04, D. Legut</b> VIBRATIONAL PROPERTIES AND THE ENERGETIC STABILITY OF THE MAGNETIC KCuF3 PHASES – A QUASI-ONE-DIMENSIONAL MAGNET

<b>12:15</b>	<b>12:30</b>	<b>O1-05, M. Borovský</b> THERMAL PROPERTIES OF A DILUTED TRIANGULAR ISING ANTIFERROMAGNET IN A FIELD
<b>12:30</b>	<b>14:00</b>	<b>Lunch</b>
<b>14:00</b>	<b>14:40</b>	<b>I5-01, F. Mila (invited)</b> NEW DEVELOPMENTS IN QUANTUM MAGNETISM WITH $S > 1/2$
<b>14:40</b>	<b>14:55</b>	<b>O5-01, M. W. Meisel</b> MAGNETIC RESPONSE OF Mn(III)F(salen) AT LOW TEMPERATURES
<b>14:55</b>	<b>15:10</b>	<b>O5-02, H. Szymczak</b> SPIN-GLASS TRANSITION IN THE RCoGaO <sub>4</sub> (R=Lu, Yb, Tm) LAYERED COBALTITES
<b>15:10</b>	<b>15:25</b>	<b>O5-03, R. Pelka</b> CRITICAL BEHAVIOR OF Mn <sub>2</sub> [Nb(CN) <sub>8</sub> ] MOLECULAR MAGNET THROUGH COMPLEMENTARY EXPERIMENTAL METHODS
<b>15:25</b>	<b>15:40</b>	<b>O5-04, R. Tarasenko</b> NEUTRON AND EPR STUDY OF Cu(tn)Cl <sub>2</sub> – A TWO - DIMENSIONAL SPATIALLY ANISOTROPIC TRIANGULAR LATTICE ANTIFERROMAGNET
<b>15:40</b>	<b>15:55</b>	<b>O5-05, B. Brzostowski</b> ASSESSMENT OF SPIN HAMILTONIAN PARAMETERS FOR MOLECULAR NANOMAGNETS BY THE SINGLE-CRYSTAL MAGNETIZATION PROFILES AND DFT CALCULATIONS
<b>15:55</b>	<b>16:10</b>	<b>O5-06, K. Szalowski</b> INDIRECT COUPLING BETWEEN LOCALIZED MAGNETIC MOMENTS IN GRAPHENE NANOSTRUCTURES
<b>16:10</b>	<b>16:30</b>	<b>Coffee break</b>
<b>16:30</b>	<b>18:00</b>	<b>Poster sessions P2, P3</b>
<b>19:00</b>		<b>Concert</b>

08:20	09:00	<b>I4-01, S. Lipiński (invited)</b> CORRELATION EFFECTS AND SPIN DEPENDENT TRANSPORT IN CARBON NANOSTRUCTURES
09:00	09:15	<b>O4-01, M. Gmitra</b> SPIN-ORBIT COUPLING ENHANCEMENT AND EXCHANGE INTERACTIONS IN HYDROGENATED GRAPHENE
09:15	09:30	<b>O4-02, S. Krompiewski</b> ELECTRONIC TRANSPORT IN MULTI-TERMINAL GRAPHENE DEVICES WITH VARIOUS ARRANGEMENTS OF ELECTRODES
09:30	09:45	<b>O4-03, J. Hamrle</b> QUADRATIC MAGNETO-OPTICAL KERR EFFECT SPECTRA IN 3d METALS Fe, Co AND Ni
09:45	10:00	<b>O4-04, D. Kubániová</b> PHASE COMPOSITION OF FERRIC OXIDE IN $\text{Fe}_2\text{O}_3/\text{SiO}_2$ SYSTEM
10:00	10:15	<b>O4-05, I. Turek</b> MAGNETIC ANISOTROPIES IN TETRAGONAL Fe-Co ALLOYS
10:15	10:30	<b>O4-06, K. Výborný</b> MAGNETIC LINEAR DICHROISM AND BIREFRINGENCE IN DILUTE MAGNETIC SEMICONDUCTOR (Ga,Mn)As
10:30	10:50	<b>Coffee break</b>
10:50	11:30	<b>I8-01, N. Lupu (invited)</b> Fe-Ga MAGNETOSTRICTIVE POLYCRYSTALLINE MATERIALS: FROM BULK SHAPED SAMPLES TO NANOWIRES
11:30	11:45	<b>O8-01, O. Heczko</b> MAGNETIC DOMAINS IN 10M MARTENSITE OF Ni-Mn- Ga EXHIBITING MAGNETIC SHAPE MEMORY EFFECT
11:45	12:00	<b>O8-02, Z. Jagličić</b> MAGNETIC MEMORY EFFECT IN $\text{K}_3\text{M}_3^{\text{II}}\text{M}_2^{\text{III}}\text{F}_{15}$ FAMILY OF MULTIFERROICS
12:00	12:15	<b>O8-03, J. Kaštil</b> OUTSTANDING MAGNETIC PROPERTIES OF Co- SUBSTITUTED AND Er-DOPED $\text{Ni}_2\text{MnGa}$ COMPOUND

<b>12:15</b>	<b>12:30</b>	<b>O8-04, N. Randrianantoandro</b> STRUCTURAL AND MAGNETIC PROPERTIES OF GLASS-COVERED FePtNbB-BASED MICROWIRES
<b>12:30</b>	<b>14:00</b>	<b>Lunch</b>
<b>14:00</b>	<b>14:40</b>	<b>I6-01, C. Lacroix (invited)</b> THE KONDO LATTICE: SOME NEW ASPECTS
<b>14:40</b>	<b>14:55</b>	<b>O6-01, P. Javorský</b> PRESSURE INFLUENCE ON STRUCTURAL AND MAGNETIC PROPERTIES OF TbNiAl
<b>14:55</b>	<b>15:10</b>	<b>O6-02, S. Mašková</b> LARGE MAGNETOCALORIC EFFECT IN Nd <sub>2</sub> Ni <sub>2</sub> In
<b>15:10</b>	<b>15:25</b>	<b>O6-03, M. Mihalik</b> MAGNETISM IN NdMnO <sub>3+δ</sub> AND NdMn <sub>0.8</sub> Fe <sub>0.2</sub> O <sub>3+δ</sub> STUDIED BY THE NEUTRON DIFFRACTION EXPERIMENTS
<b>15:25</b>	<b>15:40</b>	<b>O6-04, J. Pospíšil</b> COMPLEX MAGNETIC PHASE DIAGRAM OF A GEOMETRICALLY FRUSTRATED SM LATTICE: SmPd <sub>2</sub> Al <sub>3</sub> CASE
<b>15:40</b>	<b>15:55</b>	<b>O6-05, G. Zwirnagl</b> HEAVY QUASIPARTICLES IN Yb COMPOUNDS: THE RENORMALIZED BAND APPROACH
<b>15:55</b>	<b>16:10</b>	<b>O6-07, J. Prchal</b> MAGNETISM IN RCo <sub>2</sub> UNDER AMBIENT AND HYDROSTATIC PRESSURE
<b>16:10</b>	<b>16:30</b>	<b>Coffee break</b>
<b>16:30</b>	<b>18:00</b>	<b>Poster sessions P1, P4, P5</b>

08:20	09:00	<b>I7-01, H. Suderow (invited)</b> THE VORTEX LATTICE VIEWED BY VERY LOW TEMPERATURE SCANNING TUNNELING MICROSCOPY AND SPECTROSCOPY
09:00	09:15	<b>O7-01, R. Hlubina</b> ANOMALOUS SPECTRAL FUNCTIONS IN SUPERCONDUCTORS
09:15	09:30	<b>O7-02, J. Spalek</b> INTRINSIC <i>versus</i> EXTRINSIC STRONGLY CORRELATED MAGNETIC SUPERCONDUCTORS
09:30	09:45	<b>O7-03, J. Kačmarčík</b> SPECIFIC HEAT STUDY OF SUPERCONDUCTIVITY IN $\text{Cu}_x\text{TiSe}_2$
09:45	10:00	<b>O7-04, M. Kratochvílová</b> AMBIENT PRESSURE SUPERCONDUCTIVITY IN THE ANTIFERROMAGNETIC COMPOUND $\text{Ce}_2\text{PtIn}_8$
10:00	10:15	<b>O7-05, M. Jirsa</b> ELECTROMAGNETIC PROPERTIES OF MELT-TEXTURED $\text{YBaCuO}$ SUPERCONDUCTORS DOPED BY Gd AND Sm
10:15	10:30	<b>O7-06, M. Woch</b> STUDY OF RESISTIVE SUPERCONDUCTING TRANSITION OF BULK $(\text{Bi}_{0.6}\text{Pb}_{0.4})_2\text{Sr}_2\text{Ca}_2\text{Cu}_3\text{O}_x$
10:30	10:50	<b>Coffee break</b>
10:50	11:30	<b>I1-02, G. Durin (invited)</b> MAGNETIZATION DYNAMICS IN SOFT MAGNETS: UNIVERSAL FEATURES FROM RIBBONS TO NANOSTRIPS
11:30	11:45	<b>O1-06, P. Frydrych</b> MAGNETIC FLUXGATE SENSOR CHARACTERISTICS MODELING USING EXTENDED PREISACH MODEL
11:45	12:00	<b>O1-07, V.O. Cheranovskii</b> THE ENERGY SPECTRUM AND THERMODYNAMICS OF THE SPIN MODEL FOR QUASI-ONE-DIMENSIONAL MAGNET $[\text{Mn}(\text{phen})_3](\text{TCNQ})_2\cdot\text{H}_2\text{O}$
12:00	12:15	<b>O1-08, T. Lučivjanský</b> THE FRUSTRATED ISING ANTIFERROMAGNET ON THE HONEYCOMB LATTICE

12:15	12:30	<b>O1-09, A. Grechnev</b> EXACT GROUND STATE OF THE SHASTRY-SUTHERLAND LATTICE WITH CLASSICAL HEISENBERG SPINS
12:30	14:00	<b>Lunch</b>
14:00	14:40	<b>I7-02, A. M. Strydom (invited)</b> SUPERCONDUCTIVITY, MAGNETISM, AND ATOMIC RATTLING PHENOMENA IN $R_3\text{Rh}_4\text{Ge}_{13}$ ( $R=\text{Yb, Lu}$ )
14:40	14:55	<b>O7-07, M. M. Abd-Elmeguid</b> CHARGE FLUCTUATION ACROSS THE QUANTUM CRITICAL POINT OF $\text{EuCu}_2(\text{Ge}_{1-x}\text{Six})_2$
14:55	15:10	<b>O7-08, A. Ślebarski</b> ELECTRONIC, MAGNETIC, AND ELECTRIC TRANSPORT PROPERTIES OF $\text{Ce}_3\text{Co}_4\text{Sn}_{13}$ AND $\text{Ce}_3\text{Rh}_4\text{Sn}_{13}$ : A COMPARATIVE STUDY
15:10	15:25	<b>O7-09, M. Vališka</b> MAGNETISM IN $\text{UCo}_{0.88}\text{Ru}_{0.12}\text{Ge}$ STUDIED BY POLARIZED NEUTRONS
15:25	15:40	<b>O7-10, N. E. Sluchanko</b> MAGNETORESISTANCE ANISOTROPY AND $H$ - $T$ - $x$ MAGNETIC PHASE DIAGRAM OF $\text{Tm}_{1-x}\text{Yb}_x\text{B}_{12}$
15:40	15:55	<b>O7-11, J. Pietosa</b> STABILIZATION OF ANTIFERROMAGNETIC PHASE UNDER HYDROSTATIC PRESSURE IN $\text{Nd}_{1-x}\text{Ca}_x\text{BaCo}_2\text{O}_{5.5}$ ( $x = 0-0.06$ )
15:55	16:10	<b>O7-12, E. Fertman</b> TERAHERTZ STUDIES OF CHARGE ORDERING IN $\text{Nd}_{2/3}\text{Ca}_{1/3}\text{MnO}_3$ PEROVSKITE
16:10	16:30	<b>Coffee break</b>
16:30	18:00	<b>Poster sessions P6, P7, P8, P9</b>
18:30		<b>Barbeque</b>

## FRIDAY, JUNE 21

08:20	08:35	<b>O9-01, R. Aogaki</b> MAGNETO-ROTATIONAL SYMMETRY IN CHIRAL MAGNETOELECTRODEPOSITION
08:35	08:50	<b>O9-02, I. Mogi</b> CHIRALITY INDUCED BY MAGNETOELECTROLYSIS
08:50	09:05	<b>O9-03, M. Nowicki</b> MAGNETOVISION SCANNING SYSTEM FOR DETECTION OF DANGEROUS OBJECTS
09:05	09:20	<b>O9-04, J. Hudák</b> NOISE CHARACTERISTICS OF MICROWIRE MAGNETOMETER
09:20	09:35	<b>O9-05, M. Precner</b> HIGH RESOLUTION TIPS FOR SWITCHING MAGNETIZATION MAGNETIC FORCE MICROSCOPY
09:35	09:50	<b>O9-06, O. Štrbák</b> CALCULATION OF THE MAGNETIC FIELD PARAMETERS OF THE BIOGENIC IRON OXIDES ENSEMBLE FOR THE MRI APPLICATIONS
09:50	10:05	<b>O9-07, T. Ščepka</b> VORTEX DYNAMICS IN FERROMAGNETIC NANOELEMENTS OBSERVED BY MICRO-HALL PROBES
10:05	10:20	<b>O9-08, D. Jackiewicz</b> APPLICATION OF EXTENDED JILES-ATHERTON MODEL FOR MODELLING THE INFLUENCE OF STRESS ON MAGNETIC CHARACTERISTICS OF THE CONSTRUCTION STEEL
10:20	10:40	<b>Coffee break</b>
10:40	10:55	<b>O9-09, K. Draganová</b> NOISE ANALYSIS OF MAGNETIC SENSORS USING ALLAN VARIANCE
10:55	11:10	<b>O6-06, J. Ruz</b> FIRST PRINCIPLES CALCULATIONS OF XMCD SPECTRA OF ACTINIDE CUBIC LAVES PHASE COMPOUNDS
11:10	11:25	<b>O7-13, V. H. Tran</b> FERROMAGNETISM IN THE KONDO-LATTICE CePd <sub>2</sub> P <sub>2</sub> COMPOUND

11:25	11:40	<b>O7-14, A. Bogach</b> MAGNETIZATION IN $\text{Tm}_{1-x}\text{Yb}_x\text{B}_{12}$ DODECABORIDES WITH METAL-INSULATOR TRANSITION
11:40	11:55	<b>O7-15, P. Husaníková</b> MAGNETIZATION STUDY OF $\text{Cu}_x\text{TiSe}_2$ SINGLE CRYSTALS
11:55	12:10	<b>O5-07, E. Čížmár</b> OBSERVATION OF ANISOTROPIC EXCHANGE IN SPIN LADDERS BY ELECTRON SPIN RESONANCE
12:10	12:25	<b>Closing</b>
12:25	13:30	<b>Lunch</b>
13:30		<b>Trip to Tokaj</b>



# **INDEX OF ABSTRACTS**

- II-01** A. Zhukov, M. Ipatov, J.M. Blanco, A. Chizhik, A. Talaat and V. Zhukova  
**FAST MAGNETIZATION SWITCHING IN AMORPHOUS MICROWIRES**
- II-02** G. Durin  
**MAGNETIZATION DYNAMICS IN SOFT MAGNETS:  
UNIVERSAL FEATURES FROM RIBBONS TO NANOSTRIPS**
- 01-01** J. Richter, M. Härtel, A. Lohmann, D. Ihle, H.-J. Schmidt, S.-L. Drechsler  
**THERMODYNAMICS OF FRUSTRATED QUANTUM J1-J2 HEISENBERG  
MAGNETS**
- 01-02** R.C. Carvalho, M.S.S. Pereira, M.L. Lyra, O. Rojas and J. Strecka  
**KINETICALLY-DRIVEN FRUSTRATION IN HYBRID LADDERS WITH  
LOCALIZED AND DELOCALIZED SPINS**
- 01-03** K. Carva, D. Legut, P. M. Oppeneer and M. Battiato  
**ULTRAFAST DEMAGNETIZATION AND ELECTRON-PHONON SPIN-FLIP  
PROCESSES FROM FIRST PRINCIPLES**
- 01-04** D. Legut and U. D. Wdowik  
**VIBRATIONAL PROPERTIES AND THE ENERGETIC STABILITY OF THE  
MAGNETIC  $KCuF_3$  PHASES – A QUASI-ONE-DIMENSIONAL MAGNET**
- 01-05** M. Borovský, M. Žukovič and A. Bobák  
**THERMAL PROPERTIES OF A DILUTED TRIANGULAR ISING  
ANTIFERROMAGNET IN A FIELD**
- 01-06** P. Frydrych, R. Szewczyk and J. Salach  
**MAGNETIC FLUXGATE SENSOR CHARACTERISTICS MODELING USING  
EXTENDED PREISACH MODEL**
- 01-07** V.Chernanovskii, M.Botko, G.Vasilets, M.Kaynakova, V. Starodub and A. Feher  
**THE ENERGY SPECTRUM AND THERMODYNAMICS OF THE SPIN MODEL  
FOR QUASI-ONE-DIMENSIONAL MAGNET  $[Mn(phen)_3](TCNQ)_2 \cdot H_2O$**
- 01-08** T. Lučivjanský, A. Bobák, M. Borovský, M. Žukovič and T. Balcerzak  
**THE FRUSTRATED ISING ANTIFERROMAGNET ON THE HONEYCOMB  
LATTICE**
- 01-09** Alexei Grechnev  
**EXACT GROUND STATE OF THE SHASTRY-SUTHERLAND LATTICE WITH  
CLASSICAL HEISENBERG SPINS**
- P1-01** O. Derzhko, J. Richter, O. Krupnitska, and T. Krokhmalkskii  
**LOW-ENERGY THEORY OF SOME FRUSTRATED QUANTUM  
ANTIFERROMAGNETS AT HIGH MAGNETIC FIELDS**
- P1-02** T. Verkholyak and J. Strečka  
**THERMODYNAMICS OF SPIN-1/2 ORTHOGONAL-DIMER CHAIN WITH ISING  
AND ANISOTROPIC HEISENBERG INTERACTIONS**
- P1-03** J. Strečka, F. Michaud and F. Mila  
**EXACT VALENCE-BOND-SOLID GROUND STATES OF FRUSTRATED SPIN-1  
ISING-HEISENBERG AND HEISENBERG LADDERS IN A MAGNETIC FIELD**
- P1-04** O. Krupnitska, O. Derzhko and J. Richter  
**LOW-TEMPERATURE THERMODYNAMICS  
OF THE DIAMOND-CHAIN HEISENBERG ANTIFERROMAGNET  
AT HIGH MAGNETIC FIELDS**
- P1-05** K. Szałowski and T. Balcerzak  
**CRITICAL TEMPERATURE OF SITE-DILUTED SPIN-1/2 SYSTEMS WITH LONG-  
RANGE FERROMAGNETIC INTERACTIONS**
- P1-06** J. Čisárová and J. Strečka  
**MAGNETIZATION PROCESS AND ADIABATIC DEMAGNETIZATION OF THE  
ANTIFERROMAGNETIC SPIN-1/2 HEISENBERG CUBE**

- P1-07** R. Pelka  
**HYSTERESIS EFFECT IN MEAN-FIELD MODEL**
- P1-08** J. Kostyk, R. Varga and M. Vazquez  
**SINGLE DOMAIN WALL PROPAGATION AT LOW FIELDS**
- P1-09** M. Šulek, J. Tóvik and V. Cambel  
**SYMMETRY BROKEN TIME EVOLUTION OF MAGNETIC STRUCTURE IN PL NANODOT**
- P1-10** J. Chovan, M. Marder and N. Papanicolaou  
**WEAK FERROMAGNETISM IN THE DZYALOSHINSKII-MORIYA HELIMAGNET  $\text{Ba}_2\text{CuGe}_2\text{O}_7$**
- P1-11** V. Ilkovič  
**MAGNETIC REORIENTATION IN TWO-SUBLATTICE HEISENBERG FERRIMAGNETIC SYSTEM**
- P1-12** M. Žukovič and M. Jaščur  
**MONTE CARLO SIMULATION OF SPIN-3/2 BLUME-EMERY-GRIFFITHS MODEL**
- P1-13** S. Hrivňák and M. Žukovič  
**DYNAMIC EFFECTS IN RANDOM FIELD ISING MODEL**
- P1-14** L. Mižišin, M. Žukovič and A. Bobák  
**LOW-TEMPERATURE BEHAVIOR OF A STACKED TRIANGULAR LATTICE ISING ANTIFERROMAGNET**
- P1-15** K. Kouřil, H. Štěpánková, V. Chlan, J. Englich, J. Töpfer, D. Seifert  
**HYPERFINE INTERACTIONS IN HEXAGONAL FERRITES OF THE Sr-Fe-O SYSTEMS**
- P1-16** V. Chlan, K. Kouřil, H. Štěpánková, R. Řezníček  
**STUDY OF Y-TYPE HEXAFERRITE BY MEANS OF  $^{57}\text{Fe}$  NMR AND ELECTRONIC STRUCTURE CALCULATIONS**
- P1-17** P. Farkasovsky and H. Cencarikova  
**THERMODYNAMICS OF COUPLED ELECTRON AND SPIN SYSTEMSON THE SHASTRY-SUTHERLAND LATTICE**
- P1-18** H. Cencarikova, P. Farkasovsky and P. Puchala  
**GROUND-STATE PHASE DIAGRAM OF THE EXTENDED ISING MODEL ON THE SHASTRY-SUTHERLAND LATTICE**
- P1-19** M. Jaščur, V. Štubňa, K. Szalowski and T. Balcerzak  
**FRUSTRATION IN A MIXED-SPIN ISING MODEL WITH MULTI-SPIN INTERACTIONS**
- P1-20** R. Sýkora, D. Legut and U. D. Wdowik  
**EXCHANGE INTERACTIONS AND ELASTICITY OF  $\text{Cu}(\text{H}_2\text{O})_2(\text{ethylenediamine})\text{SO}_4$  – QUASI-2D MAGNETIC SYSTEM**

- I2-01** Giselher Herzer  
**STATUS AND TRENDS OF AMORPHOUS AND NANOCRYSTALLINE ALLOYS FOR SOFT MAGNETIC APPLICATIONS**
- I2-02** F. Mazaleyrat  
**TRENDS AND CHALLENGES IN SOFT MAGNETS FOR HIGHER FREQUENCY APPLICATIONS**
- O2-01** R. Szewczyk, Peter Svec Sr., Jacek Salach, Peter Švec, Adam Bieńkowski, Jozef Hoško, Dorota Jackiewicz, Marcin Kamiński and Wojciech Winiarski  
**INFLUENCE OF THERMOMAGNETIC TREATMENT ON MAGNETOELASTIC PROPERTIES OF FeNiMoB AMORPHOUS ALLOY**
- O2-02** M. Pavlovič, M. Miglierini, E. Mustafin, T. Seidl, M. Šoka, I. Strašík and W. Ensinger  
**INFLUENCE OF HIGH-ENERGY HEAVY IONS ON MAGNETIC SUSCEPTIBILITY OF SOFT MAGNETIC METALLIC GLASSES**
- O2-03** S. Michalik, J. Bednarcik, J. Kovac and P. Sovak  
**IDENTIFICATION OF THE CURIE POINT IN FINEMET BASED ALLOYS USING IN-SITU X-RAY DIFFRACTION**
- O2-04** M. Miglierini, T. Hatala and M. Bujdoš  
**DEPTH-SELECTIVE STUDY OF SURFACE CRYSTALLIZATION IN NANOPERM-TYPE ALLOYS**
- O2-05** A. Lancok, N. Mahmed, S-P. Hannula and O. Heczko  
**MÖSSBAUER AND MAGNETIC STUDY OF THE MAGNETITE NANOPARTICLES**
- O2-06** A. Hendrych, O. Životský, and Y. Jirásková  
**THE SURFACE STRUCTURE AND MAGNETIC PROPERTIES OF Fe-Al ALLOYS**
- O2-07** M. Čillíková, J. Dubec, M. Neslušan, H. Mičietová and D. Blažek  
**MAGNETIC EVALUATION OF RESIDUAL STRESSES AND STRUCTURE TRANSFORMATIONS INDUCED IN SOFT STEEL AFTER TURNING**
- O2-08** Z. Śniadecki, B. Idzikowski, J. Marcin, J. Kováč and I. Škorvánek  
**GLASS FORMING ABILITY AND MAGNETISM OF Co-BASED TERNARY METALLIC GLASSES**
- P2-01** P. Klein, R. Varga and M. Vazquez  
**TEMPERATURE DEPENDENCE OF THE SWITCHING FIELD IN NANOCRYSTALLINE FeNiMoB MICROWIRES**
- P2-02** Y. Jirásková, J. Buršík, I. Turek, M. Hapla, J. Čížek  
**STRUCTURAL AND MAGNETIC RELAXATIONS OF MECHANICALLY ALLOYED Fe-Mo**
- P2-03** S. Michalik, J. Bednarcik, P. Pawlik, R. Matija and P. Sovak  
**STRUCTURAL STABILITY OF SOFT MAGNETIC Fe-Co-Zr-W-B METALLIC GLASSES INVESTIGATED BY THE IN-SITU XRD**
- P2-04** E. Ušák, M. Šoka, M. Ušáková and E. Dobročka  
**STRUCTURAL AND MAGNETIC PROPERTIES OF NANO-SIZED NiZn FERRITES**
- P2-05** P. Klein, R. Varga, R. El Kammouni and M. Vazquez  
**MAGNETIC PROPERTIES OF GLASS-COATED FeWB MICROWIRES**
- P2-06** K. Richter, A. Thiaville and R. Varga  
**MAGNETO-OPTICAL OBSERVATION OF SURFACE DOMAIN STRUCTURE IN AMORPHOUS GLASS-COATED MICROWIRES**
- P2-07** E. Komová, Ž. Barlíková and R. Varga  
**MAGNETIC CHARACTERIZATION OF CoFeSiB MICROWIRES USING IMPEDANCE SPECTROSCOPY**

- P2-08** E. Komová, F. Šidík, P.Klein, R.Varga and M.Vazquez  
**GMI EFFECT IN ANNEALED  $\text{Fe}_{40}\text{Ni}_{38}\text{Mo}_4\text{B}_{18}$  MICROWIRES**
- P2-09** B. Dolník, J. Kurimský, K. Marton, M. Kolcun, L. Tomčo, J. Briančin, M. Fabián, M. Halama, M. Vojtko and M. Rajňák  
**THE HALL EFFECT IN POLYCRYSTALLINE ZINC OXIDE BASED COMPOSITE**
- P2-10** A. Lovas, J. Kravčák and L. Novák  
**THERMOPOWER AND MAGNETIC MONITORING OF RELAXATION AND DEVITRIFICATION IN Fe-BASED GLASSY ALLOYS**
- P2-11** J. Onufer, J. Ziman and M. Kladivová  
**STRESS-INDUCED CHANGES IN CLOSURE DOMAIN STRUCTURE DYNAMICS IN BISTABLE FERROMAGNETIC MICROWIRE**
- P2-12** J. Ziman, V. Šuhajová and M. Kladivová  
**SINGLE DOMAIN WALL CONTRIBUTION TO THE IMPEDANCE OF AMORPHOUS FERROMAGNETIC WIRE**
- P2-13** J. Sitek, J. Dekan, M.Pavlovič  
**RADIATION DAMAGE STUDY OF Fe-BASED NANOCRYSTALLINE MATERIALS**
- P2-14** V. Kusigerski, M. Perovic, V. Nikolic, A. Mrakovic, J. Blanusa and V. Spasojevic  
**COMPLEX SUPERSPIN DYNAMICS IN INTERACTING  $\text{Fe}_3\text{O}_4$  NANOPARTICLE SYSTEM**
- P2-15** M. Perovic, V. Kusigerski, J. Blanusa, A. Mrakovic and V. Spasojevic  
**AGING AND MEMORY EFFECTS IN TEMPERATURE CYCLING EXPERIMENTS ON SUPER SPIN GLASS NANOPARTICLE LCMO SYSTEM**
- P2-16** D. Praslička, M. Šmelko J. Blažek, J.Hudák, P. Lipovský and N. Flachbartl  
**ADVANCED METHOD FOR MAGNETIC MICROWIRES NOISE SPECIFICATION**
- P2-17** J. Füzér, S. Dobák and J. Füzérová  
**AC MAGNETIC FIELD EFFECT ON THE COMPLEX PERMEABILITY SPECTRA OF SOFT MAGNETIC  $\text{Fe}_{73}\text{Cu}_1\text{Nb}_3\text{Si}_{16}\text{B}_7$  POWDER CORES**
- P2-18** V. Jančárik, E. Ušák, M. Šoka and M. Ušáková  
**MAGNETIC PROPERTIES OF YTTRIUM-SUBSTITUTED  $\text{NiZn}$  FERRITES**
- P2-19** M. Strečková, M. Bařková, I Bařko, H. Hadraba, R. Bureš  
**IMAGING OF MAGNETIC DOMAINS AND DOMAIN WALLS IN SPHERICAL Fe-Si POWDER USING MAGNETIC FORCE MICROSCOPY**
- P2-20** B. David, O. Schneeweiss, A. Rek, V. Kudrle and O. Jašek  
**NANOSTRUCTURED  $\alpha$ -Fe LAYER SYNTHESIZED BY A PECVD METHOD AND EXAMINED WITH MÖSSBAUER SPECTROMETRY**
- P2-21** J. Miskuf, K. Csach, A. Juríková  
**NANOSCALE FRACTURE MORPHOLOGIES OF SOFT MAGNETIC  $\text{CoFeTaB}$  AMORPHOUS ALLOY**
- P2-22** K. Csach, J. Miskuf, A. Juríková  
**INFLUENCE OF PLASTIC DEFORMATION ON DEVITRIFICATION OF  $\text{Fe}_{73.5}\text{Nb}_3\text{Cu}_1\text{Si}_{13.5}\text{B}_9$  AMORPHOUS ALLOY**
- P2-23** A. Lovas, L. Hubač, L. Novák  
**PULSE HEAT TREATMENT OF FINEMET ALLOYS UNDER TENSION**
- P2-24** T.V. Kalmykova, S.I. Tarapov, V.N. Krivoruchko  
**INFLUENCE OF TEMPERATURE ON MAGNETIC AND STRUCTURAL PROPERTIES OF NANOCRYSTALLINE COMPOSITE BASED ON MAGNETIC PEROVSKITE**

- P2-25** J. Salach, D. Jackiewicz, A. Bienkowski and R. Szewczyk  
**AMORPHOUS SOFT MAGNETIC  $\text{Fe}_{80}\text{B}_{11}\text{Si}_9$  ALLOY IN TENSILE STRESS SENSORS APPLICATION**
- P2-26** M. Janošek, J. Vyhnanek, P. Butvin and B. Butvinová  
**EFFECTS OF CORE DIMENSIONS AND MANUFACTURING PROCEDURE ON FLUXGATE NOISE**
- P2-27** Paweł Pietrusiewicz, Katarzyna Bloch, Joanna Gondro, Marcin Nabiałek, Marcin Dośpiał, Michał Szota  
**MAGNETIC RELAXATIONS IN AMORPHOUS  $\text{Fe}_{61}\text{Co}_{10}\text{Y}_8\text{Zr}_1\text{B}_{20}$  ALLOY**
- P2-28** Katarzyna Bloch, Joanna Gondro, Paweł Pietrusiewicz, Marcin Dośpiał, Marcin Nabiałek, Michał Szota, Konrad Gruszka  
**TIME AND THERMAL STABILITY OF MAGNETIC PROPERTIES IN  $\text{Fe}_{61}\text{Co}_{10}\text{Y}_8\text{Nb}_1\text{B}_{20}$  BULK AMORPHOUS ALLOYS**
- P2-29** Michał Szota, Marcin Dośpiał, Paweł Pietrusiewicz, Marcin Nabiałek, Konrad Gruszka, Tomasz Kaczmarzyk  
**INFLUENCE OF ANNEALING BELOW THE CRYSTALLIZATION TEMPERATURE ON THE STRUCTURAL AND MAGNETIC PROPERTIES OF Fe-based AMORPHOUS ALLOY**
- P2-30** Marcin Nabiałek, Anna Dobrzańska-Danikiewicz, Paweł Pietrusiewicz, Marcin Dośpiał, Michał Szota, Joanna Gondro, Sabina Lesz  
**INFLUENCE OF THE MANUFACTURING METHOD ON MAGNETIZATION PROCESS OF  $\text{Fe}_{61}\text{Co}_{10}\text{Y}_8\text{Mo}_1\text{B}_{20}$  BULK AMORPHOUS ALLOYS**
- P2-31** K. Bán, J. Kovác and A. Lovas  
**CROSSOVER EFFECTS IN MAGNETIC PROPERTY CHANGES OF  $\text{Fe}(\text{SiB})_{25}$  AND  $\text{Fe}_x\text{Ni}_{80-x}(\text{SiB})_{20}$  GLASSES DURING STRUCTURAL RELAXATION AND HYDROGEN ABSORPTION**
- P2-32** Z. Birčáková, P. Kollár, V. Vojtek, R. Bureš and M. Fáberová  
**INFLUENCE OF VITROPERM CONTENT ON THE ENERGY LOSSES IN COMPOSITE MATERIALS BASED ON THE MIXTURE OF TWO FERROMAGNETS**
- P2-33** V. Nemcová, V. Girman, V. Hrabčáková, Š. Michalík, J. Bednarčík, and P. Sovák  
**EFFECT OF ANNEALING TIME ON STRUCTURE OF  $\text{Fe}_{72.5}\text{Cu}_1\text{Nb}_2\text{Mo}_2\text{Si}_{15.5}\text{B}_7$  ALLOY**
- P2-34** M. Hasiak, M. Miglierini, M. Łukiewska, J. Kaleta, J. Zbroszczyk  
**LOW FIELD MAGNETIC PROPERTIES OF FeCo-BASED ALLOYS**
- P2-35** M. Capik, J. Marcin, J. Kováč, P. Švec Jr., D. Janičkovič, P. Švec, I. Škorvánek  
**EFFECT OF TEMPERATURE ON MAGNETIZATION PROCESSES IN RAPIDLY SOLIDIFIED FeSiB/CoSiB BILAYER RIBBONS**
- P2-36** M. Varga, J. Marcin, M. Capik, D. Janičkovič, P. Švec, I. Škorvánek  
**MAGNETOIMPEDANCE EFFECT IN FIELD ANNEALED  $(\text{FeNi})_{78}\text{Nb}_7\text{B}_{15}$  AMORPHOUS AND NANOCRYSTALLINE RIBBONS**
- P2-37** M. Miglierini and M. Pavúk  
**MÖSSBAUER AND MFM INVESTIGATIONS OF SURFACE MAGNETISM IN NANOPERM NANOCRYSTALLINE ALLOYS**
- P2-38** T.-A. Óvári and H. Chiriac  
**TAILORING OF MAGNETOELASTIC ANISOTROPY IN RAPIDLY SOLIDIFIED ULTRATHIN AMORPHOUS WIRES**

- P2-39** J. Kováč, L. Novák  
**STUDY OF THE MAGNETIZATION PROCESSES IN AMORPHOUS AND NANOCRYSTALLINE FINEMET BY THE DECOMPOSITION OF THE HYSTERESIS LOOPS**
- P2-40** L. Novák and J. Kováč  
**RAYLEIGH REGION IN AMORPHOUS AND NANOCRYSTALLINE FINEMET ALLOY**
- P2-41** D. Olekšáková, J. Füzer, P. Kollár, J. Bednarčík, C. Lathe  
**ISOBARIC THERMAL EXPANSION AND ISOTHERMAL COMPRESSION OF POWDERED NiFe BASED ALLOYS STUDIED BY IN-SITU EDX**
- P2-42** V. Hrabčáková, V. Girman, K.B. Borisenko, Š. Michalik, V. Nemcová and P. Sovák  
**STUDY OF LOCAL STRUCTURE OF AMORPHOUS ALLOY Fe<sub>84</sub>B<sub>16</sub> BY ELECTRON AND X-RAY DIFFRACTION**
- P2-43** F. Borza, S. Corodeanu, T.-A. Ovari, and H.Chiriac  
**TENSILE STRESS AND TORQUE INFLUENCE ON THE MI EFFECT IN MULTILAYER MICROWIRES**
- P2-44** J. Kravčák  
**HYSTERESIS IN ASYMMETRICAL GMI EFFECT IN AMORPHOUS MICROWIRES**
- P2-45** M. Kabátová, J. Füzer, J. Füzerová, E. Dudrová, P. Kollár  
**Fe/SiO<sub>2</sub>/RESIN SOFT MAGNETIC COMPOSITE POWDER MATERIALS PREPARED BY MIXING AND VACUUM/PRESSURE IMPREGNATION**
- P2-46** R. Brzozowski, E. Frąteczk, M. Antoszevska and M. Moneta  
**INFLUENCE OF SLOW HEAVY ION IMPACT ON SURFACE TRANSFORMATION OF VP800 AMORPHOUS ALLOY**
- P2-47** P. Křišťan, V. Chlan, H. Štěpánková, R. Řezníček, P. Görnert, P. Payer  
**STRUCTURE OF IRON OXIDE NANOPARTICLES STUDIED BY 57Fe NMR**
- P2-48** Vít Procházka, Helena Štěpánková, Vojtěch Chlan, Petr Křišťan, Martin Hermanek, Jiří Tuček, Radek Zbořil, Kateřina Poláková, Jan Filip, Josef Štěpánek  
**HYPERFINE INTERACTIONS AND STRUCTURE OF NANOCRYSTALLINE MAGHEMITE**
- P2-49** R. Bureš, M. Fáberová, M. Strečková, P. Kollár, J. Füzer  
**STRUCTURE AND PROPERTIES OF HYBRID COMPOSITES BASED ON TWO DIFFERENT FERROMAGNETS**
- P2-50** T. Žák, B. David, A. Čosović, V. Čosović, D. Živković, N. Talijan  
**STRUCTURE AND MAGNETIC PROPERTIES OF NANOCRYSTALLINE NiFe<sub>2</sub>O<sub>4</sub> PREPARED VIA PRECIPITATION ROUTE**
- P2-51** M. Lauda, J. Füzer, J. Füzerová, P. Kollár, M. Strečková and M. Fáberová  
**MAGNETIC PROPERTIES OF SOFT MAGNETIC FeSi COMPOSITE POWDER CORES**
- P2-52** G. Ababei, L. Budeanu, G. Stoian, N. Lupu and H. Chiriac  
**CHARACTERIZATION OF GLASS COATED MAGNETIC NANOWIRES BY UHR-TEM**
- P2-53** H. Chiriac, S. Corodeanu, M. Grigorás, G. Ababei, N. Lupu and T.-A. Óvári  
**DOMAIN WALL PROPAGATION IN FINEMET NANOWIRES**
- P2-54** A. Talaat, V. Zhukova, M. Ipatov, J. M. Blanco, M. Churyukanova, S. Kaloshkin, E. Zamiatkina, E. Shuvaeva, L. Gonzalez-Legarreta, B. Hernando and A. Zhukov  
**MAGNETIC PROPERTIES AND GIANT MAGNETOIMPEDANCE IN AMORPHOUS AND NANOCRYSTALLINE MICROWIRES**

- P2-55** K. Brzózka, P. Sovak, T. Szumiata, P. Kollár, J. Füzer, M. Fáberová, R. Bureš, B.Górka, M. Gawroński and M. Gzik-Szumiata  
**MÖSSBAUER AND MAGNETIC STUDY OF Fe+VITROPERM+PLASTIC SYSTEM**
- P2-56** M. Butta, M. Janosek, I. Pilarcikova, L. Kraus  
**FINE SMOOTHING OF CONDUCTIVE SUBSTRATE FOR PERMALLOY LAYER ELECTROPLATING**
- P2-57** K. Pekała, M. Trzaska, M. Gostomska, M. Pekała  
**ELECTRICAL RESISTIVITY AND THERMOELECTRIC POWER OF NANOCOMPOSITE FILMS OF NICKEL / CARBON NANOTUBES**
- P2-58** P. Butvin, B. Butvinová, M. Kuzminski, A. Slawska-Waniewska, J. Sitek, I. Mat'ko and M. Kadlečiková  
**EFFECT OF SURFACES IN FeNbCuBSiP RIBBONS**
- P2-59** R. Bidulský, J. Bidulská, T. Kvačkaj, M. Actis Grande  
**ANALYSIS OF THE FRACTURE SURFACES OF A NEW DEVELOPMENT INSULATED IRON POWDER COMPOUNDS**



- I3-01** Michael McHenry  
**NANOCOMPOSITE MAGNETS FOR POWER ELECTRONIC APPLICATIONS**
- I3-02** V. Franco and A. Conde  
**THE MAGNETOCALORIC EFFECT OF MULTIPHASE MATERIALS AND NANOSTRUCTURES**
- O3-01** Bianca Frincu, Rajasekhar Madugundo, Olivier Geoffroy, Thierry Waeckerle and Sophie Rivoirard  
**MAGNETIC FIELD ENHANCED SOFT MAGNETIC PROPERTIES OF Fe-Co ALLOYS**
- O3-02** Lajos K. Varga, Jozef Kovac  
**MINOR LOOP SCALING RULES FOR SOFT MAGNETIC CORES**
- P3-01** J. Repková, M. Mahuliaková, M. Lesňák, J. Luňáček, D. Ciprian  
**COMPUTER MODELS OF THE MAGNETIZATION VECTOR DISTRIBUTION IN THE PERMANENT MAGNETS HALBACH ARRAYS**
- P3-02** T. Toliński, K. Synoradzki  
**GRAIN-SIZE EFFECT ON THE MAGNETOCALORIC PROPERTIES OF THE  $\text{DyCo}_3\text{B}_2$  COMPOUND**
- P3-03** M. Falkowski, W. Kowalski, K. Synoradzki, T. Toliński and A. Kowalczyk  
**MAGNETIC PROPERTIES AND MAGNETOCALORIC EFFECT OF THE  $\text{DyNi}_4\text{Si}$  COMPOUND**
- P3-04** J. Kamarád, J. Kaštil, Z. Arnold  
**DIRECT MEASUREMENT OF MAGNETO-CALORIC EFFECT IN AMORPHOUS AND CRYSTALLINE 3d-ELEMENTS ALLOYS**
- P3-05** K. Filipecka, K. Pawlik, P. Pawlik, J.J. Wysocki, P. Gębara, A. Przybył, M. Szwaja, I. Wnuk  
**PHASE COMPOSITION AND MAGNETIC PROPERTIES OF THE NANOCRYSTALLINE  $\text{Fe}_{64,32}\text{Pr}_{9,6}\text{B}_{22,08}\text{W}_4$  ALLOY**
- P3-06** P. Gębara, P. Pawlik, I. Skorvanek, J. Marcin, K. Pawlik, A. Przybył, J.J. Wysocki, M. Szwaja, K. Filipecka  
**TERMOMAGNETIC PROPERTIES OF THE  $\text{La}(\text{Fe,Si})_{13}$ -TYPE ALLOYS**
- P3-07** J. Marcin, J. Kováč, D. Janičkovič, P. Švec, I. Škorvánek  
**TUNING OF MAGNETOCALORIC EFFECT IN  $\text{FeCrNbB}$ -BASED AMORPHOUS COMPOSITES**
- P3-08** K. Zmorayova, V. Antal, S. Piovarci, M. Radusovska, J. Kovac and P. Diko  
**MICROSTRUCTURE AND PROPERTIES OF  $\text{La-Ca-Sr-Mn-O}$  MAGNETOCALORIC CERAMICS**
- P3-09** Marcin Dośpiał, Marcin Nabiałek, Michał Szota, Paweł Pietrusiewicz, Konrad Gruszka, Katarzyna Błoch  
**MODELING THE HYSTERESIS LOOP IN HARD MAGNETIC MATERIALS USING  $T(x)$  MODEL**
- P3-10** Marcin Dośpiał, Marcin Nabiałek, Krzysztof Chwastek, Michał Szota, Paweł Pietrusiewicz, Jakub Gawroński  
**INTERPRETATION OF LINEAR PART OF EQUATION, IN HYPERBOLIC  $T(x)$  MODEL, APPLIED FOR HYSTERESIS ANALYSIS IN HARD MAGNETIC MATERIALS**
- P3-11** J. Sláma, A. Grusková, A. Gonzáles Angeles, M. Šoka, R. Dosoudil  
**MAGNETIC COMPARISON OF SEVERAL DIVALENT AND TETRAVALENT IONS MIXTURES SUBSTITUTED  $\text{Ba}$  FERRITE**
- P3-12** G. Ziolkowski, A. Chrobak, N. Randrianantoandro  
**PHASE STRUCTURE AND MAGNETIC PROPERTIES OF  $\text{Fe-Nb-B-Pt}$  TYPE OF BULK NANOCRYSTALLINE ALLOYS**

- P3-13** A. Chrobak, G. Ziółkowski, N. Randrianantoandro  
**PHASE STABILITY OF  $(\text{Fe}_{80}\text{Nb}_6\text{B}_{14})_{0.9}\text{Tb}_{0.1}$  BULK NANOCRYSTALLINE HARD MAGNET**
- P3-14** A. Chrobak, G. Ziółkowski, G. Haneczok  
**INFLUENCE OF COOLING RATE ON MAGNETIC PROPERTIES OF  $(\text{Fe}_{80}\text{Nb}_6\text{B}_{14})_{1-x}\text{Tb}_x$  TYPE OF BULK NANOCRYSTALLINE ALLOYS**
- P3-15** Krzysztof Ociepka, Anna Bajorek, Artur Chrobak, Grażyna Chełkowska  
**MAGNETIC PROPERTIES OF  $\text{Tb}(\text{Ni}_{1-x}\text{Fe}_x)_3$  : ( $x = 0.2, 0.6$ ) CRYSTALLINE COMPOUNDS AND POWDERS**
- P3-16** I. Petryshynets, F. Kováč, J. Marcin and I. Škorvánek  
**IMPROVED PROCESSING TECHNIQUE FOR PREPARATION OF NON-ORIENTED ELECTRICAL STEELS WITH LOW COERCIVITY**
- P3-17** M. Actis Grande, R. Bidulský, M. Maccarini, J. Bidulská, I. Forno  
**EFFECT OF COMPACTION ON THE BEHAVIOUR OF THE SOFT MAGNETIC MATERIAL**
- P3-18** Kvačkaj T., Bella P., Bidulský R., Kočiško R., Bidulská J., Lupták M., Kováčová A.  
**INFLUENCE OF ANNEALING CONDITIONS ON STRUCTURAL DEVELOPMENT OF CRYO ROLLED C-Si STEEL**
- P3-19** K. Pawlik, P. Pawlik, W. Kaszuwara, J.J. Wysocki  
**MAGNETIZATION REVERSAL PROCESSES IN Pr-Fe-B-TYPE NANOCRYSTALLINE MAGNETS**
- P3-20** M. Neslušan, D. Blažek, D. Hrabovský and M. Bukovina  
**MAGNETIC ANISOTROPY IN HARD TURNED SURFACES**

- I4-01** S. Lipiński and D. Krychowski  
**CORRELATION EFFECTS AND SPIN DEPENDENT TRANSPORT IN CARBON NANOSTRUCTURES**
- O4-01** M. Gmitra, D. Kochan and J. Fabian  
**SPIN-ORBIT COUPLING ENHANCEMENT AND EXCHANGE INTERACTIONS IN HYDROGENATED GRAPHENE**
- O4-02** S. Krompiewski  
**ELECTRONIC TRANSPORT IN MULTI-TERMINAL GRAPHENE DEVICES WITH VARIOUS ARRANGEMENTS OF ELECTRODES**
- O4-03** J. Hamrle, J. Hamrlová, D. Legut, J. Pištora  
**QUADRATIC MAGNETO-OPTICAL KERR EFFECT SPECTRA IN 3d METALS Fe, Co AND Ni**
- O4-04** D. Kubániová, P. Brázda, J. Kohout, A. Lančok, E. Šantavá, M. Klementová and K. Závěta  
**PHASE COMPOSITION OF FERRIC OXIDE IN  $\text{Fe}_2\text{O}_3/\text{SiO}_2$  SYSTEM**
- O4-05** I. Turek, K. Carva, J. Kudrnovský and V. Drchal  
**MAGNETIC ANISOTROPIES IN TETRAGONAL Fe-Co ALLOYS**
- O4-06** Karel Výborný, Nad'a Tesařová, John Černe, and Tomáš Ostatnický  
**MAGNETIC LINEAR DICHROISM AND BIREFRINGENCE IN DILUTE MAGNETIC SEMICONDUCTOR (Ga,Mn)As**
- P4-01** Š. Zajac and L. Wojtczak  
**THE TOPICALITY OF THE VALENTA MODEL OF THE MAGNETIZATION IN THIN FILMS AND SURFACES**
- P4-02** T. Ryba, Z. Vargova, R. Varga, J. Kovac, V. Zhukova and A. Zhukov  
**MAGNETIC CHARACTERIZATION OF  $\text{Co}_2\text{MnSi}$  HEUSLER MICROWIRES**
- P4-03** T. Balcerzak and K. Szalowski  
**FERRIMAGNETISM IN THE HEISENBERG-ISING BILAYER WITH MAGNETICALLY NON-EQUIVALENT PLANES**
- P4-04** M. Molčan, A. Hashim, J. Kováč, M. Rajňák, P. Kopčanský, M. Makowski, H. Gojzewski, M. Timko  
**CHARACTERIZATION OF MAGNETOSOMES AFTER EXPOSURE TO THE EFFECT OF THE SONICATION AND ULTRACENTRIFUGATION**
- P4-05** T. Szumiata, M. Gzik-Szumiata  
**SURFACE MAGNETOSTRICTION MODEL FOR MagNEMS**
- P4-06** J. Kopiński, D. Krychowski and S. Lipiński  
**FANO-KONDO EFFECT OF MAGNETIC IMPURITY WITH SIDE-COUPLED GRAPHENE FLAKE**
- P4-07** A. Szabo, R. Varga, F. Ujhelyi, V. Komanicky, A. Zorkovska and A. Lovas  
**THERMOPOWER AND SURFACE MAGNETIC CHARACTERIZATION OF NI THIN LAYERS**
- P4-08** T. Ryba, Z. Vargová, R. Varga, S. Ilkovic, M. Reiffers, V. Haskova, P. Szabo, J. Kravčák, R. Gyepes  
**STRUCTURAL AND MAGNETIC CHARACTERIZATION OF NiMnSb HALF-HEUSLER ALLOY PREPARED BY RAPID QUENCHING**
- P4-09** P. Vlaic and E. Burzo  
**ELECTRONIC AND SPIN DEPENDENT TRANSPORT PROPERTIES OF Fe/CaSe/Fe (001) HETEROJUNCTIONS**
- P4-10** A. Urbaniak-Kucharczyk  
**LOW TEMPERATURE MAGNETIC PROPERTIES OF FERROMAGNETIC LAYERED COMPOSITES**
- P4-11** V. Štrbík, M. Reiffers, Š. Chromik and M. Španková  
**APPROXIMATION OF ELECTRICAL AND MAGNETO TRANSPORT PROPERTIES OF LSMO THIN FILMS USING POLYNOMIAL FIT EXPRESSION**

- P4-12** M. Španková, Š. Chromík, I. Vávra, A. Rosová, E. Dobročka and V. Štrbík  
**GROWTH AND CHARACTERIZATION OF LSMO FILMS WITH INCREASED TEMPERATURE OF MI TRANSITION**
- P4-13** A. Józefczak, A. Hashim, M. Molčan, T. Hornowski, A. Skumiel, P. Kopčanský, M. Timko  
**ACOUSTIC AND MAGNETIC PROPERTIES OF BACTERIAL MAGNETITE NANOPARTICLES SUSPENSION**
- P4-14** V. Haskova, P. Szabo, P. Samuely, J. Kovac, T. Ryba, Z. Vargova, R. Varga  
**ANDREEV REFLEXION SPECTROSCOPY STUDY OF SPIN POLARIZATION IN  $\text{Co}_2\text{Cr(Fe)Al}$  HEUSLER ALLOYS**
- P4-15** Ewelina Zofia Frątczak, José Emilio Prieto, Marek Edward Moneta  
**MAGNETIC STUDY OF ALPHA, EPSILON AND GAMMA -PHASES OF IRON NITRIDE THIN FILMS**
- P4-16** P. Hrubovčák A. Zeleňáková, V. Zeleňák, N. Murafa, and J. Kováč  
**SUPERPARAMAGNETISM IN COBALT NANOPARTICLES COATED BY PROTECTIVE GOLD LAYER**
- P4-17** J. Kohout, T. Kmjec, K. Závěta, P. Brázda, M. Klementová, A. Lančok, D. Nižňanský  
**DEPENDENCE OF MORIN TEMPERATURE ON THE SIZE OF  $\alpha\text{-Fe}_2\text{O}_3$  NANOPARTICLES**
- P4-18** O. Kapusta, A. Zeleňáková, V. Zeleňák  
**ORDERED NANOPOROUS SILICA MODIFIED WITH MAGNETIC LANTHANIDES NANOPARTICLES**
- P4-19** M. Grigoras, N. Lupu, H. Chiriac, F. Borza and M. Urse  
**INFLUENCE OF Ta AND Mo INTERLAYERS ON THE MAGNETIC PROPERTIES AND OUT-OF-PLANE TEXTURE OF Nd-Fe-B MULTILAYER FILMS**
- P4-20** H. Głowiński, A. Żywcza, T. Stobiecki and J. Dubowik  
**BROAD-BAND VNA-FMR EXPERIMENTS IN OLD AND NEW PROBLEMS OF MAGNETIZATION DYNAMICS**
- P4-21** J. Dubowik, I. Gościńska  
**EXCHANGE-BIAS IN THIN FILM STRUCTURES : A MICROMAGNETIC APPROACH**
- P4-22** A. Zeleňáková, V. Zeleňák, and J. Kováč  
**AC MAGNETIC SUSCEPTIBILITY STUDY OF Fe AND Co BASED NANOPARTICLES**
- P4-23** G. Michałek and B. R. Bułka  
**INFLUENCE OF THE SIDE-ELECTRODE ON TRANSPORT THROUGH HYBRID NANODEVICES**
- P4-24** M. Sopko, O. Milkovič, Š. Nižník, I. Škorvánek  
**STRUCTURE AND MAGNETIC PROPERTIES OF IRON/IRON-OXIDE NANOPARTICLES PREPARED BY PRECIPITATION FROM SOLID STATE SOLUTION**
- P4-25** E. Valušová, M. Antalík, P. Pristaš, P. Javorský, J. Kováč, M. Timko and P. Kopčanský  
**MAGNETIC CHARCOAL SUPPORTING SILVER AS A WATER DISINFECTANT**
- P4-26** P. Trocha and W. Rudziński  
**SPIN-POLARIZED TUNELLING THROUGH A DOUBLE QUANTUM DOT INTERACTING WITH A POLARON**
- P4-27** K.P. Wójcik and I. Weymann  
**TWO-STAGE KONDO EFFECT IN THE T-SHAPED QUANTUM DOTS WITH FERROMAGNETIC LEADS**

- 15-01** F. Mila  
**NEW DEVELOPMENTS IN QUANTUM MAGNETISM WITH  $S > 1/2$**
- 05-01** J.-H. Park, O. N. Risset, M. Shiddiq, M. K. Peprah, E. S. Knowles, M. J. Andrus, C. C. Beedle, G. Ehlers, A. Podlesnyak, E. Čižmár, S. E. Nagler, S. Hill, D. R. Talham, and M. W. Meisel  
**MAGNETIC RESPONSE OF Mn(III)F(salen) AT LOW TEMPERATURES**
- 05-02** I. Radelytsky, H.A.Dabkowska, R.Szymczak, A.Dabkowski, J.Fink-Finowicki H.Szymczak  
**SPIN-GLASS TRANSITION IN THE  $RCoGaO_4$  ( $R=Lu, Yb, Tm$ ) LAYERED COBALTITES**
- 05-03** R. Pelka, M. Czapla, P.M. Zieliński, M. Fitta, M. Bałanda, D Pinkowicz, F.L. Pratt, M. Mihalik, J. Przewoźnik, A. Amato, B. Sieklucka, T. Wasiutyński  
**CRITICAL BEHAVIOR OF  $Mn_2[Nb(CN)_8]$  MOLECULAR MAGNET THROUGH COMPLEMENTARY EXPERIMENTAL METHODS**
- 05-04** R. Tarasenko, A. Orendáčová, E.Čižmár, S. Maťaš, M. Orendáč, I. Potočný, V. Pavlík, K. Siemensmeyer, S. Zvyagin, J. Wosnitza and A. Feher  
**NEUTRON AND EPR STUDY OF  $Cu(tn)Cl_2$  – A TWO-DIMENSIONAL SPATIALLY ANISOTROPIC TRIANGULAR LATTICE ANTIFERROMAGNET**
- 05-05** G. Kamieniarz, M. Antkowiak, P. Kozłowski, L. Kucharski, A. Barasiński, B. Brzostowski, A. Drzewiński, M. Wojciechowski, G. A. Timco, F. Tuna and R. E. P. Winpenny  
**ASSESSMENT OF SPIN HAMILTONIAN PARAMETERS FOR MOLECULAR NANOMAGNETS BY THE SINGLE-CRYSTAL MAGNETIZATION PROFILES AND DFT CALCULATIONS**
- 05-06** K. Szałowski  
**INDIRECT COUPLING BETWEEN LOCALIZED MAGNETIC MOMENTS IN GRAPHENE NANOSTRUCTURES**
- 05-07** E. Čižmár, M. Ozerov, S. Wang, K.W. Krämer, Ch. Rüegg and S.A. Zvyagin  
**OBSERVATION OF ANISOTROPIC EXCHANGE IN SPIN LADDERS BY ELECTRON SPIN RESONANCE**
- P5-01** M. Miglierini, R. Boča, M. Kopáni and A. Lančok  
**MÖSSBAUER AND SQUID CHARACTERIZATION OF IRON IN HUMAN TISSUE: CASE OF *GLOBUS PALLIDUS***
- P5-02** P. Rubin, A.Sherman and M. Schreiber  
**THE SPIN-1  $J_1 - J_3$  HEISENBERG ANTIFERROMAGNET ON A TRIANGULAR LATTICE**
- P5-03** V. Tkáč, K. Tibenská, A. Orendáčová, M. Orendáč, A. G. Anders and A. Feher  
**THE RARE-EARTH BASED SINGLE-ION MAGNET  $CsNd(MoO_4)_2$**
- P5-04** E. S. Knowles, C. H. Li, M. J. Andrus, M. K. Peprah, J. van Tol, S. Hill, D. R. Talham and M.W. Meisel  
**PHOTOCONTROLLED MAGNETISM IN CORE@SHELL PBAs**
- P5-05** R. Pelka, P. Konieczny, P.M. Zieliński, Y. Miyazaki, A. Inaba, D. Pinkowicz, B. Sieklucka and T. Wasiutyński  
**MAGNETOCALORIC EFFECT In  $\{[M(\text{pyrazole})_4]_2[Nb(CN)_8] \cdot 4H_2O\}_n$  ( $M=Fe, Co, Fe_{0.5}Co_{0.5}$ ) ISOSTRUCTURAL MOLECULAR MAGNETS**
- P5-06** J. Kurimský, B. Dolník, K. Marton, M. Kolcun, L. Tomčo, M. Rajňák, M. Timko and P. Kopčanský  
**THE INVESTIGATION OF THE *E-J* CHARACTERISTICS AND THE ROLE OF NANOPARTICLE CONCENTRATION IN WEAKLY POLAR MAGNETIC FLUIDS**
- P5-07** M. Rajňák, L. Tomčo, K. Marton, J. Kurimský, B. Dolník, M. Molčan, P. Kopčanský, M. Timko  
**INFLUENCE OF MAGNETIC FIELD ON DIELECTRIC BREAKDOWN IN TRANSFORMER OIL BASED FERROFLUIDS**

- P5-08** P. Konieczny, M. Grzesiak-Nowak, A. Szymańska, W. Łasocha and T. Wasiutyński  
**MAGNETIC PROPERTIES OF TRANSITION METAL MOLYBDATES**
- P5-09** P. Konieczny, R. Pelka, P. M. Zieliński, F.L. Pratt, Y. Miyazaki, A. Inaba, D. Pinkowicz, B. Sieklucka and T. Wasiutyński  
**STUDY THE IMPACT OF COMPOUND COMPOSITION IN A 3D MOLECULAR MAGNET  $\{[M^{II}(\text{pirazol})_4]_2[\text{Nb}^{IV}(\text{CN})_8]\cdot 4\text{H}_2\text{O}\}_n$**
- P5-10** M. Botko, E. Čižmár, M. Kajňáková and A. Feher  
**EPR SPECTRA OF GENUINE-ORGANIC AND METAL-ORGANIC TCNQ-BASED ANION RADICAL SALTS**
- P5-11** M. Kajňáková, M. Botko, V. A. Starodub, E. Čižmár and A. Feher  
**SPIN-PEIERLS TRANSITION IN NEW MATERIAL (N-Me-Tetra-Me-Pz)(TCNQ)<sub>2</sub>**
- P5-12** L. Baranová, R. Tarasenko, A. Orendáčová, M. Orendáč, V. Pavlík and A. Feher  
**EXPERIMENTAL STUDY OF THE MAGNETOCALORIC EFFECT IN THE TWO-DIMENSIONAL QUANTUM SYSTEM  $\text{Cu}(\text{tn})\text{Cl}_2$**
- P5-13** M. Šviková, M. Liščinský, P. Rabatin and M. Géci  
**STUDY OF TWO-DIMENSIONAL MELTING IN SYSTEM OF SMALL MAGNET**
- P5-14** J. Majorošová, N. Tomašovičová, M. Timko, M. Koneracká, Z. Mitróová, I.P. Studenyak, O.V. Kovalchuk, J. Jadzyn and P. Kopčanský  
**SENSITIVITY OF 6CHBT LIQUID CRYSTAL DOPED WITH FERROELECTRIC OR MAGNETIC PARTICLES ON ELECTRIC AND MAGNETIC FIELDS**
- P5-15** J. Majorošová, N. Tomašovičová, M. Timko, Z. Mitróová, A. Juriková, K. Fodor-Csorba, A. Vajda, N. Éber, T. Tóth-Katona, X. Chaud and P. Kopčanský  
**MAGNETIC FIELD INDUCED ISOTROPIC-NEMATIC PHASE TRANSITION IN FERRONEMATICS BASED ON MIXTURE OF BENT-CORE AND ROD-SHAPED LIQUID CRYSTALS**
- P5-16** N. Tomašovičová, I. Haysak, J. Kováč, M. Kubovčíková, V. Závišová, M. Timko, A. Okunev and P. Kopčanský  
**RADIATION STABILITY OF THE BOVINE SERUM ALBUMIN STABILIZED BIOCOMPATIBLE MAGNETIC FLUID**
- P5-17** N. A. Ali Alghamdi, A. Orendáčová, V. Pavlík, and M. Orendáč  
**THERMODYNAMIC PROPERTIES OF GEOMETRICALLY FRUSTRATED  $S = 1/2$  XY PYROCHLORE ANTIFERROMAGNET  $\text{Er}_2\text{Sn}_2\text{O}_7$**
- P5-18** P. Vrábek, E. Čižmár, A. Orendáčová, S. Gao, and M. Orendáč  
**SPIN GLASS STATE IN  $S = 3/2$  KAGOMÉ ANTIFERROMAGNET  $\text{Co}(\text{N}_3)_2(\text{bpg})[(\text{CH}_3)_2(\text{NCOH})]_{4/3}$**
- P5-19** M. Kubovčíková, I. Antal, J. Kováč, V. Závišová, M. Koneracká and P. Kopčanský  
**PREPARATION, CHARACTERIZATION AND COMPARISON OF SCANNING ELECTRON MICROSCOPY, DYNAMIC LIGHT SCATTERING AND ANALYTICAL ULTRACENTRIFUGATION FOR MAGNETIC NANOPARTICLES SIZING**
- P5-20** Bartosz Brzostowski, Michał Wojciechowski, Romuald Lemański and Grzegorz Kamieniarz  
**CHROMIUM-BASED MOLECULAR RINGS WITHIN THE DFT AND FALICOV-KIMBALL MODEL APPROACH**
- P5-21** V. Bunda, S. Bunda, V. Komanický and A. Feher  
**RAMAN SPECTRA OF BISMUTH OXYHALIDE SINGLECRYSTALS**
- P5-22** V. Bunda, S. Bunda, V. Komanický and A. Feher  
**ANIZOTROPY OF PHOTOCONDUCTIVITY IN  $\text{BiOX}$  ( $X=\text{Cl}, \text{Br}, \text{I}$ ) SINGLE CRYSTALS**
- P5-23** J. Parnica, P. Keša, J. Kováč, M. Timko and M. Antalík  
**IONIC LIQUID BASED FERROFLUIDS**
- P5-24** J. Tothová, J. Kováč, P. Kopčanský, M. Rajňák, M. Timko  
**UNUSUAL VISCOSITY DEPENDENCE OF A MAGNETIC FLUID ON NANOPARTICLES CONCENTRATION**

- I6-01** C. Lacroix  
**THE KONDO LATTICE: SOME NEW ASPECTS**
- O6-01** P. Javorský, J. Prchal, M. Klicpera, J. Kaštil, M. Míšek  
**PRESSURE INFLUENCE ON STRUCTURAL AND MAGNETIC PROPERTIES OF TbNiAl**
- O6-02** S. Mašková, S. Daniš, A. Llobet, H. Nakotte and L. Havela  
**LARGE MAGNETOCALORIC EFFECT IN Nd<sub>2</sub>Ni<sub>2</sub>In**
- O6-03** M. Mihalik jr., M. Mihalik, S. Mařař, A. Hoser and M. Vavra  
**MAGNETISM IN NdMnO<sub>3+δ</sub> AND NdMn<sub>0.8</sub>Fe<sub>0.2</sub>O<sub>3+δ</sub> STUDIED BY THE NEUTRON DIFFRACTION EXPERIMENTS**
- O6-04** J. Pospíšil, G. Nénert, S. Miyashita, H. Kitazawa, Y. Skourski, M. Diviš, J. Prokleřka and V. Sechovský  
**COMPLEX MAGNETIC PHASE DIAGRAM OF A GEOMETRICALLY FRUSTRATED SM LATTICE: SmPd<sub>2</sub>Al<sub>3</sub> CASE**
- O6-05** Gertrud Zwicknagl  
**HEAVY QUASIPARTICLES IN YB COMPOUNDS: THE RENORMALIZED BAND APPROACH**
- O6-06** J. Ruzs, P. M. Oppeneer, F. Wilhelm, E. Colineau, R. Caciuffo, G. Lander  
**FIRST PRINCIPLES CALCULATIONS OF XMCD SPECTRA OF ACTINIDE CUBIC LAVES PHASE COMPOUNDS**
- O6-07** J. Prchal, J. Valenta, J. řebesta, M. Míšek, D. Turčinková, L. Lapčák, J. Prokleřka, M. Kratochvílová, and V. Sechovský  
**MAGNETISM IN RCo<sub>2</sub> UNDER AMBIENT AND HYDROSTATIC PRESSURE**
- P6-01** M. Klicpera, P. Javorský, P. řermák, A. Rudajevořá, S. Daniš, T. Brunátová and I. Čiřařová  
**INVESTIGATION OF CRYSTAL STRUCTURE, MAGNETIC AND TRANSPORT PROPERTIES IN CeCuAl<sub>3</sub> SINGLE CRYSTAL**
- P6-02** I. Tkach, N.T.H. Kim-Ngan, S. Mařková, A.V. Andreev, Z. Mařěj, L. Havela  
**AMORPHOUS 5f FERROMAGNETIC HYDRIDES UH<sub>3</sub>Mo<sub>x</sub>**
- P6-03** V. Glushkov, M. Anisimov, R. Baybakov, S. Demishev, V. Filipov, K. Flachbart, A. Kuznetsov, N. Shitsevalova and N. Sluchanko  
**REENTRANT METAL-INSULATOR TRANSITION IN Ca<sub>1-x</sub>Eu<sub>x</sub>B<sub>6</sub>**
- P6-04** M. Antoňák, M. Mihalik, M. Zentková, M. Mihalik jr., M. Vavra, J. Lazurova, M. Fitta, M. Balanda  
**MAGNETIC PROPERTIES OF La<sub>(1-x)</sub>Ag<sub>x</sub>MnO<sub>3</sub> NANOPOWDERS UNDER PRESSURE**
- P6-05** M. Gmitra, H. Cencarikova and P. Farkasovsky  
**FIRST-PRINCIPLES STUDY OF KONDO INSULATOR SmB<sub>6</sub>**
- P6-06** K. Synoradzki and T. Toliński  
**MAGNETIC PROPERTIES OF Ce(Cu<sub>x</sub>Ni<sub>1-x</sub>)<sub>4</sub>Mn COMPOUNDS**
- P6-07** M. Diviš  
**TRANSITION METALS DOPING OF LaFe<sub>2</sub>Si<sub>2</sub>**
- P6-08** **MAGNETIC PROPERTIES OF RE<sub>2</sub>Pd<sub>3</sub>In COMPOUNDS AND THEIR HYDRIDES**  
S. Mařková, A. Kolomiets, A.V. Andreev, P. Svoboda and L. Havela
- P6-09** R. Klement, B. Hruřka, V. Hronský, D. Olčák  
**PREPARATION AND CHARACTERIZATION OF BASIC AND Nd<sup>3+</sup>/Er<sup>3+</sup> DOPED GLASSES IN THE SYSTEM Y<sub>2</sub>O<sub>3</sub>-Al<sub>2</sub>O<sub>3</sub>-ZrO<sub>2</sub>**
- P6-10** M. Vavra, Marián Mihalik, Matuš Mihalik, M. Zentková, J. Lazurová, M. Matik, J. Briančin  
**MAGNETOSTRUCTURAL CORRELATIONS OF NANO-SIZED MANGANITES PREPARED BY DIFFERENT WAYS**
- P6-11** Z. Arnold, L. V. B. Diop, O. Isnard, J. Kamarád  
**MAGNETIC PROPERTIES OF HoCo<sub>12</sub>B<sub>6</sub> COMPOUND UNDER HIGH PRESSURES**

- P6-12** A. Khoroshilov, N. Sluchanko, A. Azarevich, A. Bogach, V. Glushkov, S. Demishev, N. Shitsevalova, V. Filipov, S. Gabani, K. Flachbart  
**SHORT RANGE ORDER EFFECTS IN MAGNETORESISTANCE OF  $\text{Ho}_x\text{Lu}_{1-x}\text{B}_{12}$  ( $x \leq 0.5$ )**
- P6-13** S. Poperezhai, N. Bondar and V. Kut'ko  
**EXCITONIC SPECTRUM OF THE CRYSTAL  $\text{KY}_{0.3}\text{Er}_{0.7}(\text{MoO}_4)_2$  IN VISIBLE RANGE**
- P6-14** P. Svoboda, S. Mašková, A. V. Andreev and L. Havela  
**SPECIFIC HEAT ANALYSIS AND MAGNETIC ENTROPY OF  $\text{U}_2\text{Ni}_2\text{Sn}$**
- P6-15** J. Lazúrová, M. Mihalik, M. Zentková, M. Mihalik jr., J. Briančin, M. Fitta  
**EFFECT OF Mn FOR Fe SUBSTITUTION ON MAGNETIC PROPERTIES OF  $\text{NdFe}_{x-1}\text{Mn}_x\text{O}_3$  SINGLE CRYSTALS**
- P6-16** M. Almási, A. Zelenáková, V. Zelenák, I. Cisařová, J. Bednarčík  
**COMPARATIVE STUDY OF CRYSTAL STRUCTURES AND MAGNETIC PROPERTIES OF TWO LANTHANIDE 3D POLYMERIC COMPLEXES**
- P6-17** J. Fikáček, J. Custers, J. Prchal, and V. Sechovský  
**SYNTHESIS AND MAGNETIC PROPERTIES OF  $\text{Yb}_2\text{Pt}_3\text{Si}_5$**
- P6-18** M. Mihalik, M. Zentková, J. Briančin, M. Fitta, J. Lazúrová, M. Mihalik jr., M. Vavra  
**MAGNETIC PROPERTIES OF  $\text{La}_{0.8}\text{K}_{0.2}\text{MnO}_3$  NANOPARTICLES**
- P6-19** D. Gralak, V. H. Tran  
**THE HYBRIDIZATION OF 5f-CONDUCTION ELECTRONS IN  $\text{URu}_{1-x}\text{Pd}_x\text{Ge}$**
- P6-20** R. J. Radwanski, D. Nalecz and Z. Ropka  
**CRYSTAL-FIELD INTERACTIONS IN  $\text{RAl}_2$  INTERMETALLICS AND  $\text{RAlO}_3$  OXIDES (R = Pr and Nd)**
- P6-21** R. Nagalakshmi, Ruta Kulkarni, S. K. Dhar, A. Thamizhavel, V. Krishnakumar, C. Besnard, Y. Filinchuk, H. Hagemann and M. Reiffers  
**CRYSTAL GROWTH AND STRUCTURAL CHARACTERISATION OF NOVEL TETRAGONAL  $\text{Ce}_2\text{RhGa}_{12}$**
- P6-22** Z. Śniadecki, A. Szczeszak, A. Szajek, and B. Idzikowski  
**MAGNETISM AND DENSITY OF STATES IN  $\text{YCo}_2$  COMPOUND MODIFIED BY Ti or Nb**
- P6-23** A. Musiał, Z. Śniadecki, D. Pagnani, and B. Idzikowski  
**CRYSTALLIZATION PROCESSES AND MAGNETIZATION OF  $\text{R}_{4.5}\text{Fe}_{77}\text{B}_{18.5}$  (R=Pr, Nd) AMORPHOUS GLASSES**



- 17-01** Hermann Suderow  
**THE VORTEX LATTICE VIEWED BY VERY LOW TEMPERATURE SCANNING TUNNELING MICROCOPY AND SPECTROSCOPY**
- 17-02** A. M. Strydom  
**SUPERCONDUCTIVITY, MAGNETISM, AND ATOMIC RATTTLING PHENOMENA IN  $R_3\text{Rh}_4\text{Ge}_{13}$  ( $R=\text{Yb, Lu}$ )**
- 07-01** Tomáš Bzdušek and Richard Hlubina  
**ANOMALOUS SPECTRAL FUNCTIONS IN SUPERCONDUCTORS**
- 07-02** J. Spálek  
**INTRINSIC *versus* EXTRINSIC STRONGLY CORRELATED MAGNETIC SUPERCONDUCTORS**
- 07-03** J. Kačmarčík, Z. Pribulová, V. Soltészová, P. Barančeková-Husaníková, G. Karapetrov, V. Komanický and P. Samuely  
**SPECIFIC HEAT STUDY OF SUPERCONDUCTIVITY IN  $\text{Cu}_x\text{TiSe}_2$**
- 07-04** M. Kratochvilová, J. Prokleška, M. Dušek, J. Custers, V. Sechovský  
**AMBIENT PRESSURE SUPERCONDUCTIVITY IN THE ANTIFERROMAGNETIC COMPOUND  $\text{Ce}_2\text{PtIn}_8$**
- 07-05** M. Jirsa, M. Rameš, D. Volochová, P. Diko, K. Zmorayová and M. Šefčíková  
**ELECTROMAGNETIC PROPERTIES OF MELT-TEXTURED  $\text{YBaCuO}$  SUPERCONDUCTORS DOPED BY  $\text{Gd}$  AND  $\text{Sm}$ .**
- 07-06** W.M. Woch, M. Chrobak, R. Zalecki and A. Kołodziejczyk  
**STUDY OF RESISTIVE SUPERCONDUCTING TRANSITION OF BULK  $(\text{Bi}_{0.6}\text{Pb}_{0.4})_2\text{Sr}_2\text{Ca}_2\text{Cu}_3\text{O}_x$**
- 07-07** M. A. Ahmida, D. Johrendt, Z. Hossain, C. Geibel and M. M. Abd-Elmeguid  
**CHARGE FLUCTUATION ACROSS THE QUANTUM CRITICAL POINT OF  $\text{EuCu}_2(\text{Ge}_{1-x}\text{Six})_2$**
- 07-08** A. Ślebarski, M. Fijałkowski, J. Goraus and M.B. Maple  
**ELECTRONIC, MAGNETIC, AND ELECTRIC TRANSPORT PROPERTIES OF  $\text{Ce}_3\text{Co}_4\text{Sn}_{13}$  AND  $\text{Ce}_3\text{Rh}_4\text{Sn}_{13}$ : A COMPARATIVE STUDY**
- 07-09** M. Vališka, J. Pospíšil, G. Nénert, A. Stunault, K. Prokeš and V. Sechovský  
**MAGNETISM IN  $\text{UCo}_{0.88}\text{Ru}_{0.12}\text{Ge}$  STUDIED BY POLARIZED NEUTRONS**
- 07-10** A.N. Azarevich, N.E. Sluchanko, A.V. Bogach, V.V. Glushkov, S.V. Demishev, S. Yu. Gavrilkin, S. Gabani, K. Flachbart, N.Yu. Shitsevalova, V.B. Filipov, J. Vanacken, V.V. Moshchalkov  
**MAGNETORESISTANCE ANISOTROPY AND  $H$ - $T$ - $x$  MAGNETIC PHASE DIAGRAM OF  $\text{Tm}_{1-x}\text{Yb}_x\text{B}_{12}$**
- 07-11** J. Pietosa, S.Kolesnik and B. Dabrowski  
**STABILIZATION OF ANTIFERROMAGNETIC PHASE UNDER HYDROSTATIC PRESSURE IN  $\text{Nd}_{1-x}\text{Ca}_x\text{BaCo}_2\text{O}_{5.5}$  ( $x = 0-0.06$ )**
- 07-12** E. Fertman, S. Dolya, C. Kadlec, F. Kadlec, and A. Feher  
**TERAHERTZ STUDIES OF CHARGE ORDERING IN  $\text{Nd}_{2/3}\text{Ca}_{1/3}\text{MnO}_3$  PEROVSKITE**
- 07-13** V. H. Tran, Z. Bukowski, L. M. Tran, A. J. Zaleski  
**FERROMAGNETISM IN THE KONDO-LATTICE  $\text{CePd}_2\text{P}_2$  COMPOUND**
- 07-14** A. Bogach, N. Sluchanko, V. Glushkov, S. Demishev, A. Azarevich, N. Shitsevalova, V. Filipov, S. Gabani, K. Flachbart, J. Stankiewicz, J. Vanacken, V. Moshchalkov  
**PULSED AND STEADY MAGNETIC FIELD STUDIES OF MAGNETIZATION IN  $\text{Tm}_{1-x}\text{Yb}_x\text{B}_{12}$  DODECABORIDES WITH METAL-INSULATOR TRANSITION**
- 07-15** P. Husaníková, J.Fedor, J. Dérer, J. Šoltýs, and G. Karapetrov  
**MAGNETIZATION STUDY OF  $\text{Cu}_x\text{TiSe}_2$  SINGLE CRYSTALS**

- P7-01** M. Zegrodnik, J. Spálek and J. Bünnemann  
**HUND'S RULE INDUCED SPIN-TRIPLET PAIRING FOR ORBITALLY DEGENERATE CORRELATED ELECTRONS**
- P7-02** G.E. Grechnev, A.S. Panfilov, A.V. Fedorchenko, V.A. Desnenko, S.L. Gnatchenko, D.A. Chareev, O.S. Volkova and A.N. Vasiliev  
**MAGNETIC PROPERTIES OF FeSe(Te) SUPERCONDUCTORS**
- P7-03** V. Glushkov, E. Zhukova, B. Gorshunov, S. Demishev, N. Sluchanko, S. Kaiser and M. Dressel  
**SPIN POLARONIC EXCITATIONS IN THE GROUND STATE OF FeSi**
- P7-04** P.A. Alekseev, K.S. Nemkovski, V.N. Lazukov, J.-M. Mignot, R. Stewart, A. P. Menushenkov, A. V. Gribanov  
**MAGNETIC EXCITATION SPECTROSCOPY IN  $\text{EuCu}_2(\text{Si}_{1-x}\text{Ge}_x)_2$  : BETWEEN VALENCE INSTABILITY AND MAGNETISM**
- P7-05** S. Gabáni, K. Flachbart, J. Bednarčík, E. Welter, V. Filipov and N. Shitsevalova  
**INVESTIGATION OF MIXED VALENCE STATE OF  $\text{Sm}_{1-x}\text{B}_6$  and  $\text{Sm}_{1-x}\text{La}_x\text{B}_6$  by XANES**
- P7-07** S. Gabáni, G. Pristáš, I. Takáčová, K. Flachbart, P. Samuely, E. Gažo, T. Mori and D. Braithwaite  
**INFLUENCE OF PRESSURE ON SUPERCONDUCTIVITY IN  $\text{YB}_6$**
- P7-08** A.P. Durajski and R. Szcześniak  
**ON THE THERMODYNAMIC CRITICAL FIELD FOR THE FULLERENES  $\text{K}_3\text{C}_{60}$  AND  $\text{Rb}_3\text{C}_{60}$**
- P7-09** D. Szcześniak and R. Szcześniak  
**CRITICAL MAGNETIC FIELD FOR CHLORINE HALIDE SUPERCONDUCTOR AT HIGH PRESSURE**
- P7-10** Gabriel Pristáš, Slavomír Gabáni, Matúš Orendáč, Vladimír Komanický and Emil Gažo  
**STUDY OF NIOBIUM THIN FILMS UNDER PRESSURE**
- P7-11** N. Sluchanko, S. Gavrilkin, K. Mitsen, A. Kuznetsov, I. Sannikov, A. Azarevich, A. Bogach, V. Glushkov, S. Demishev, A. Khoroshilov, A. Lyashenko, N. Shitsevalova, V. Filipov, K. Flachbart, V. Moshchalkov  
**SUPERCONDUCTIVITY IN  $\text{YB}_6$  and  $\text{ZrB}_{12}$  MEDIATED BY QUASILOCAL VIBRATIONS OF TRANSITION METAL IONS**
- P7-12** I.I. Lobanova, V.V. Glushkov, V.Yu. Ivanov, A.V. Semeno, N.E. Sluchanko and S.V. Demishev  
**HIGH FIELD MAGNETIC TRANSITION IN  $\text{MnSi}$**
- P7-13** V. Glushkov, M. Anisimov, I. Lobanova, S. Demishev, N. Sluchanko, N. Kozlovskaya and Ya. Mukovskii  
**HALL EFFECT IN FERROMAGNETIC STATE OF  $\text{La}_{1-x}\text{Ca}_x\text{MnO}_3$  ( $x=0.23, 0.3$ )**
- P7-14** M. Anisimov, V. Glushkov, A. Bogach, S. Demishev, N. Samarin, N. Shitsevalova, A. Levchenko, V. Filipov, A. Kuznetsov, K. Flachbart, N. Sluchanko  
**TRANSPORT PROPERTIES OF  $\text{GdB}_6$**
- P7-15** M. Anisimov, V. Glushkov, A. Bogach, S. Demishev, N. Samarin, S. Gavrilkin, K. Mizen, N. Shitsevalova, A. Levchenko, V. Filipov, S. Gabani, K. Flachbart, N. Sluchanko  
**DEFECT MODE AND HEAVY FERMIONS IN  $\text{Ce}_x\text{La}_{1-x}\text{B}_6$  ( $x \leq 0.03$ )**
- P7-16** V. Pokorný, V. Janiš, M. Žonda and T. Novotný  
**SPECTRAL AND TRANSPORT PROPERTIES OF A SUPERCONDUCTING QUANTUM DOT SYSTEM**
- P7-17** M. Škrátek, A. Cigán, R. Bystrický, J. Maňka, A. Dvurečenskij and M. Majerová  
**EFFECTS OF Ga/ Ba NONSTOICHIOMETRY IN  $\text{Ga}_{1-x}\text{Ba}_{2-x}\text{Cu}_3\text{O}_{7-\delta}$  ON SUPERCONDUCTING AND MAGNETIC PROPERTIES**

- P7-18** S. Gabáni, G. Pristáš, I. Takáčová, K. Flachbart, V. Soltészová, J. Kačmarčík V. Filipov, N. Shitsevalova and K. Siemensmeyer  
**PHASE DIAGRAM OF  $TmB_4$  UNDER PRESSURE**
- P7-19** D. Volochová, K. Jurek, M. Radušovská, S. Piovareči, V. Antal, J. Kováč  
M. Jirsa and P. Diko  
**INFLUENCE OF Sm AND Yb POLLUTION ON SUPERCONDUCTING PROPERTIES OF YBCO BULK SUPERCONDUCTORS**
- P7-20** A. Baran, A. Zorkovská, M. Kajňáková, C. T. Lin and A. Feher  
**THERMODYNAMIC AND MAGNETOTRANSPORT PROPERTIES OF HIGH QUALITY  $Na_{0.77}CoO_2$  SINGLE CRYSTAL**
- P7-21** V. Bunda, S. Bunda, V. Komanický and A. Feher  
**APPLICATION OF SUPERCONDUCTOR/PHOTOSEMICONDUCTOR CONTACT STRUCTURES IN ELECTRONICS**
- P7-22** S. Piovareči, V. Antal, M. Kaňuchová, M. Radušovská, P. Diko  
**CHANGES IN YBCO SINGLE GRAIN BULK SUPERCONDUCTOR EXPOSED TO AIR MOISTURE**
- P7-23** K. Zmorayova, M. Radusovska, S. Piovarci, V. Antal, J. Kovac and P. Diko  
**MICROSTRUCTURE AND PROPERTIES OF Y-123/Y-211 BULK SUPERCONDUSTORS WITH  $BaCeO_3$  AND  $BaO_2$  ADDITION**
- P7-24** M. Sefcikova, S. Piovarci, V. Antal, J. Kovac and P. Diko  
**MICROSTRUCTURE AND PROPERTIES OF Y123/Y211 BULK SUPERCONDUSTORS WITH Y211 ADDITION**
- P7-25** P. Samuely, P. Szabó, P. Neilinger, M. Trgala and M. Grajcar  
**SUPERCONDUCTIVITY NEAR TRANSITION TO INSULATING STATE IN MOLYBDENUM CARBIDE**
- P7-26** Z. Pribulová, J. Kačmarčík, P. Samuely, Z. Medvecká, V. Komanický, T. Klein, P. Barančeková Husaníková, V. Cambel, J. Šoltýs, and Karapetrov  
**LOCAL MAGNETOMETRY USING MINIATURE HALL-PROBE ARRAY ON  $Cu_xTiSe_2$**
- P7-27** Z. BAK  
**FRACTON CONTRIBUTION TO THE ELECTRON AND MAGNON PAIRING**
- P7-28** R. Zalecki, W.M. Woch A. Kołodziejczyk and G. Gritzner  
**PENETRATION DEPTH OF BULK  $Tl_2Ba_2Ca_2Cu_3O_y$  AND  $Tl_{0.58}Pb_{0.4}Sr_{1.6}Ba_{0.4}Ca_2Cu_3O_y$  SUPERCONDUCTORS**
- P7-29** K. Bocian and W.Rudziński  
**ANDREEV REFLECTION EFFECT IN SPIN-POLARIZED TUNNELING THROUGH A QUANTUM DOT INTERACTING WITH A POLARON.**
- P7-30** R. J. Radwanski, D. Nalecz and Z. Ropka  
**CRYSTAL-FIELD INTERACTIONS AND ORBITAL MAGNETISM IN COBALT OXIDES ( $LaCoO_3$ ,  $CoO$ ,  $KCoF_3$ ,  $CoF_3$ )**
- P7-30** R. J. Radwanski, D. Nalecz and Z. Ropka  
**CRYSTAL-FIELD INTERACTIONS AND ORBITAL MAGNETISM IN COBALT OXIDES ( $LaCoO_3$ ,  $CoO$ ,  $KCoF_3$ ,  $CoF_3$ )**

- 18-01** N. Lupu  
**Fe-Ga MAGNETOSTRICTIVE POLYCRYSTALLINE MATERIALS:  
FROM BULK SHAPED SAMPLES TO NANOWIRES**
- 08-01** O. Heczko, L. Fekete, V. Kopecký, J. Kopeček and L. Straka  
**MAGNETIC DOMAINS IN 10M MARTENSITE OF Ni-Mn-Ga EXHIBITING  
MAGNETIC SHAPE MEMORY EFFECT**
- 08-02** Z. Jagličić, D. Pajič, Z. Trontelj, J. Dolinšek and M. Jagodič  
**MAGNETIC MEMORY EFFECT IN  $K_3M_3^{II}M_2^{III}F_{15}$  FAMILY OF MULTIFERROICS**
- 08-03** J. Kaštil, J. Kamarád, S. Fabbri, F. Albertini, Z. Arnold and L. Righi  
**OUTSTANDING MAGNETIC PROPERTIES OF Co-SUBSTITUTED AND Er-  
DOPED  $Ni_2MnGa$  COMPOUND**
- 08-04** Nirina Randrianantoandro, Ivan Škorvánek, Jozef Kováč, Nicoleta Lupu and Horia Chiriac  
**STRUCTURAL AND MAGNETIC PROPERTIES OF GLASS-COVERED  $FePtNbB$ -  
BASED MICROWIRES**
- P8-01** V.A. Bedarev, M.I. Pashchenko, D.N. Merenkov, Yu.O. Savina, V. A. Pashchenko,  
S.L. Gnatchenko, L.N. Bezmaternykh and V.L. Temerov  
**COMPARATIVE STUDY OF THE FARADAY EFFECT IN TERBIUM BORATES  
 $TbFe_3(BO_3)_4$  AND  $TbAl_3(BO_3)_4$**
- P8-02** T. Kmjec, J. Kohout, K. Závěta, D. Kubániová, V. V. Laguta, I. P. Raevski  
**THE STUDY OF MAGNETIC ORDERING IN  $Ba(Fe,Nb)O_3$  BY MÖSSBAUER  
SPECTROSCOPY**
- P8-03** K. Kouřil, V. Chlan, H. Štěpánková, K. Uličná, V. V. Laguta, I. P. Raevski  
**MULTIFERROIC IRON NIOBATE PEROVSKITES STUDIED BY NUCLEAR  
MAGNETIC RESONANCE SPECTROSCOPY**
- P8-04** M. Maryško, V.V.Laguta, I. P. Raevski  
**DETAILS OF MAGNETIC PROPERTIES IN  $Pb(Fe_{1/2}Nb_{1/2})O_3$**

- O9-01** R. Aogaki, R. Morimoto, A. Sugiyama, I. Mogi, M. Asanuma, M. Miura, Y. Oshikiri and Y. Yamauchi  
**MAGNETO-ROTATIONAL SYMMETRY IN CHIRAL MAGNETOELECTRODEPOSITION**
- O9-02** I. Mogi, R. Aogaki, R. Morimoto and K. Watanabe  
**CHIRALITY INDUCED BY MAGNETOELECTROLYSIS**
- O9-03** Michał Nowicki, Roman Szewczyk  
**MAGNETOVISION SCANNING SYSTEM FOR DETECTION OF DANGEROUS OBJECTS**
- O9-04** P. Lipovský, A. Čverha, J. Hudák, J. Blažek, D. Praslička  
**NOISE CHARACTERISTICS OF MICROWIRE MAGNETOMETER**
- O9-05** M. Precner, J. Fedor, J. Tóbiš, J. Šoltýs, and V. Cambel  
**HIGH RESOLUTION TIPS FOR SWITCHING MAGNETIZATION MAGNETIC FORCE MICROSCOPY**
- O9-06** O. Štrbák, A. Krafčík, M. Teplan, D. Gogola, P. Kopčanský and I. Frollo  
**CALCULATION OF THE MAGNETIC FIELD PARAMETERS OF THE BIOGENIC IRON OXIDES ENSEMBLE FOR THE MRI APPLICATIONS**
- O9-07** T. Ščepka, J. Šoltýs, M. Precner, J. Fedor, J. Tóbiš, D. Gregušová, F. Gučmann, R. Kúdela, and V. Cambel  
**VORTEX DYNAMICS IN FERROMAGNETIC NANOELEMENTS OBSERVED BY MICRO-HALL PROBES**
- O9-08** D. Jackiewicz, R. Szewczyk, J. Salach and A. Bieńkowski  
**APPLICATION OF EXTENDED JILES-ATHERTON MODEL FOR MODELLING THE INFLUENCE OF STRESS ON MAGNETIC CHARACTERISTICS OF THE CONSTRUCTION STEEL**
- O9-09** K. Draganová, F. Kmec, J. Blažek, D. Praslička, J. Hudák and M. Laššák  
**NOISE ANALYSIS OF MAGNETIC SENSORS USING ALLAN VARIANCE**
- P9-01** M. Škrátek, I. Šimáček, A. Dvurečenskij and J. Maňka  
**MAGNETOMETRIC MEASUREMENTS OF LOW CONCENTRATION OF COATED  $\text{Fe}_3\text{O}_4$  NANOPARTICLES**
- P9-02** A. Dvurečenskij, P. Billík, A. Cigán, R. Bystrický, J. Maňka, M. Škrátek and M. Majerová  
**MAGNETIC PROPERTIES OF  $\text{V}_2\text{O}_3$  NANO-OXIDE PREPARED MECHANOCHEMICALLY WITH AND WITHOUT SALT MATRIX**
- P9-04** A.S. Panfilov, G.E. Grechnev, V.B. Filipov, A.B. Ljaschenko and G.V. Levchenko  
**MAGNETIC PROPERTIES OF  $\text{MB}_{50}$  COMPOUNDS**
- P9-05** J. Salach and R. Szewczyk  
**HIGH RESOLUTION EDDY CURRENT TOMOGRAPHY SYSTEM FOR NONDESTRUCTIVE TESTING**
- P9-06** R. Dosoudil, M. Ušáková, A. Grusková and J. Sláma  
**EFFECT OF FILLER MIXTURE RATIO ON PERMEABILITY OF MULTICOMPONENT SOFT MAGNETIC COMPOSITES**
- P9-07** Jaroslav Valenta, Jiří Prchal, Marie Kratochvílová, Martin Mišek and Vladimír Sechovský  
**PRESENCE OF PARIMAGNETISM IN  $\text{Ho}(\text{Co}_{1-x}\text{Si}_x)_2$  UNDER HYDROSTATIC PRESSURE**
- P9-08** V. Hronský, P. Vrábel, M. Koval'áková and D. Olčák  
**DEGREE OF CRYSTALLINITY EVALUATION OF PARTIALLY CRYSTALLINE POLYPROPYLENES USING C NMR**
- P9-09** G. Kharchenko and S. Tarapov  
**THE BAND STRUCTURE OF THE MAGNETOPHOTONIC CRYSTAL SPECTRUM IN VICINITY OF ELECTRON SPIN RESONANCE**

- P9-10** Zuzana Bednarikova, Katarina Siposova, Martina Koneracka, Vlasta Zavisova, Martina Kubovcikova, Milan Timko, Erna Demjen, Peter Kopcansky and Zuzana Gazova  
**INFLUENCE OF MAGNETITE NANOSPHERES PROPERTIES ON INSULIN AMYLOID AGGREGATION**
- P9-11** R. Silber, J. Hamrle, D. Hrabovský, J. Pištora  
**MAGNETO-OPTICAL KERR EFFECT SPECTROSCOPY SETUP BASED ON PHOTOELASTIC MODULATOR**
- P9-12** T. Garstka, K. Laber  
**BARKHAUSEN NOISE INVESTIGATIONS OF HOT ROLLED  $\phi 30$  MM STEEL BARS**
- P9-13** N.G. Kostova, A. Zorkovská, J. Kováč, and P. Baláž  
**MAGNETIC PROPERTIES OF MECHANOCHEMICALLY SYNTHESIZED MIXED OXIDES**
- P9-14** L. Glod, J. Tóthová and V. Lisý  
**EFFECT OF MAGNETIC FIELD ON THE FLUCTUATIONS OF CHARGED OSCILLATORS IN VISCOELASTIC FLUIDS**
- P9-15** I. Batko, M. Batkova and F. Lofaj  
**ELECTRICAL RESISTIVITY IN CrN THIN FILMS**
- P9-16** I. Batko and M. Batkova  
**ELECTRICAL CONDUCTIVITY OF Ti/TiO<sub>x</sub>/Ti STRUCTURES AT LOW TEMPERATURES AND HIGH MAGNETIC FIELDS**
- P9-17** Tomasz M. Gwizdała, Ewelina Frątczak, Małgorzata Antoszevska-Moneta, Krzysztof Warda  
**THE EFFICIENCY OF MÖSSBAUER SPECTRA FITTING PERFORMED WITH THE GENETIC ALGORITHM**
- P9-18** R. Hudak, P. Klein, J. Hudak, D. Praslicka, J. Blazek and R. Varga  
**[1] EFFECT OF THE FIXATION PATTERNS ON MAGNETIC CHARACTERISTICS OF AMORPHOUS GLASS-COATED SENSORIC MICROWIRES**
- P9-19** P. Vrabel, O. Fričová, V. Hronský, M. Kovaľaková, D. Olčák and I. Chodák  
**SOLID STATE C NMR STUDIES OF MODIFIED PHB POLYMER**

# **ABSTRACTS**

**FAST MAGNETIZATION SWITCHING IN AMORPHOUS MICROWIRES**A. Zhukov<sup>1,2</sup>, M. Ipatov<sup>1</sup>, J.M. Blanco<sup>3</sup>, A. Chizhik<sup>1</sup>, A. Talaat<sup>1</sup> and V. Zhukova<sup>1</sup><sup>1</sup>*Dpto. Física de Materiales, UPV/EHU, 20018 San Sebastian, Spain*<sup>2</sup>*IKERBASQUE, Basque Foundation for Science, 48011 Bilbao, Spain*<sup>3</sup>*Dpto. de Física Aplicada, EUPDS, UPV/EHU, 20018, San Sebastian, Spain*

Recently studies of current and magnetic field driven domain walls (DW) propagation in thin magnetic wires (planar and cylindrical) attracted considerable attention owing to possibility of application of DW propagation for data storage and logics (magnetic random memory MRAM devices, logic devices). Extremely fast DW propagation at certain conditions has been observed in amorphous microwires. One of the reasons for achievement of such high DW velocity,  $v$ , might be attributed to amorphous structure of such microwires. At the same time the composite origin of such microwire induces considerable internal stresses, which depend on  $\rho$ -ratio between metallic,  $d$  and total,  $D$  diameters. So called magnetic bistability can be observed in Fe-Co based microwires with different magnetostriction constant,  $\lambda_s$ , varying from  $\lambda_s \approx 10^{-7}$  to  $\lambda_s \approx 35 \times 10^{-6}$ . Within each composition of metallic nucleus we also produced microwires with different  $\rho$ -ratio. This allowed us to control residual stresses, since the strength of internal stresses.

Additionally complex technological process introduces defects in such composites microwires. We observed that there is correlation between the distribution of the local nucleation field along the length of as-prepared bistable microwire and the single-domain wall propagation limit. The minimum value of local nucleation field determines the threshold between single and multiple domain wall propagation regimes. Thus we observed spontaneous DW nucleation on local defects limiting single DW dynamics regime in microwires. We observed that both DW velocity and the range of filed limiting single DW dynamics changed after annealing. We attributed these changes to the stress relaxation after annealing.

We also studied the effect of transverse magnetic field on fast magnetization switching of amorphous microwires. We have observed that under certain conditions a controllable domain wall (DW) collision can be realized in different parts of the wire, and that it is possible to manipulate the DW dynamics in a field-driven regime. The DW collisions obtained in this way can be used to release pinned domain walls.



**MAGNETIZATION DYNAMICS IN SOFT MAGNETS:  
UNIVERSAL FEATURES FROM RIBBONS TO NANOSTRIPS**G. Durin<sup>1,2</sup><sup>1</sup>*Istituto Nazionale di Ricerca Metrologica, strada delle Cacce 91,  
10135 Torino, Italy*<sup>2</sup>*ISI Foundation, via Alassio 11/c, 10126 Torino, Italy*

Since the discovery of the Barkhausen effect in 1919, it was clear that the randomness was an essential element of the magnetization dynamics, as a bulk (3D) system responds to a smoothly varied magnetic field with a jerky noise, in terms of pulses or 'avalanches'. Only recently, it was clarified that this behavior is due to the transition across a depinning point, and must to be understood as a critical phenomena. This explain and describe the occurrence of power law distributions and its scaling properties. Remarkably, despite the large variety of magnetic systems, these properties are classified using only two universal classes, which depend on the range of the interactions in the domain wall dynamics. Such universal features were further explored beyond simple power-law scaling, focusing on the average functional form of avalanches, i.e., the average temporal avalanche shape. This shape revealed several unexpected properties, and showed sometime signatures of non-universal effects, as in the presence of eddy currents.

In thin (2D) films, these universal properties are much less understood. On one side, the experimental determination of the spatial and temporal avalanches is not completely fulfilled, as it is complicated, for instance in optical MOKE methods, by the limited field-of-view which tends to split large avalanches in pieces. On the other side, the precise nature of universality classes is far from being completely clear.

Magnetic systems with further reduced dimensions, such as nanostrips and wires, promise to be, for instance, one type of future non-volatile memories. It is thus essential to understand the role of disorder, both under field and/or spin-polarized currents, and the role of any thermal effect. As expected, the domain wall dynamics appears to be highly affected by even a small amount of disorder, namely edge roughness or local point-like defects. Surprisingly, not all the properties deteriorate, as the disorder tends to stabilize the internal domain wall structure, and increases the maximum speed by suppressing the Walker breakdown. This suggests to deliberately engineer disorder, to accurately control the dynamics, and limiting the effects of thermal fluctuations.

# THERMODYNAMICS OF FRUSTRATED QUANTUM J1-J2 HEISENBERG MAGNETS

J. Richter<sup>1</sup>, M. Härtel<sup>1</sup>, A. Lohmann<sup>1</sup>, D. Ihle<sup>2</sup>, H.-J. Schmidt<sup>3</sup>, S.-L. Drechsler<sup>4</sup>

<sup>1</sup>*Universität Magdeburg, P.O. Box 4120, 39016 Magdeburg, Germany*

<sup>2</sup>*Universität Leipzig, Germany*

<sup>3</sup>*Universität Osnabrück, Germany*

<sup>4</sup>*IFW Dresden, Germany*

Motivated by recent experiments on quasi-one-dimensional [1] and quasi-two-dimensional [2] frustrated quantum magnets with competing nearest-neighbor exchange coupling  $J_1$  and next-nearest-neighbor exchange coupling  $J_2$  we calculate the thermodynamic properties of the corresponding  $J_1$ - $J_2$  Heisenberg magnets by means of exact diagonalization, second-order Green's function theory [3] as well as high-temperature series expansion [4].

In particular, we examine the temperature dependence of the susceptibility, the specific heat and the correlation length varying the strength of frustration  $J_2/J_1$ . We compare our theoretical data for the susceptibility and the correlation length with recent experimental results for quasi-two-dimensional oxovanadates [2].

We also put a particular focus on the thermodynamic behavior near quantum phase transition points present in frustrated  $J_1$ - $J_2$  models. For models with ferromagnetic nearest-neighbor coupling  $J_1$  and moderate strength of  $J_2$  such that the ground state is ferromagnetic we discuss the influence of the frustration on the critical properties of the susceptibility and the correlation length when approaching zero temperature.

- [1] S. Nishimoto, S.-L. Drechsler, R.O. Kuzian, J. van den Brink, J. Richter, W.E.A. Lorenz, Y. Skourski, R. Klingeler, and B. Büchner, *Phys. Rev. Lett* **107**, 097201 (2011).
- [2] L. Bossoni, P. Carretta, R. Nath, M. Moscardini, M. Baenitz, and C. Geibel, *Phys. Rev. B* **83**, 014412 (2011).
- [3] M. Härtel, J. Richter, D. Ihle, J. Schnack, and S.-L. Drechsler, *Phys. Rev. B* **84**, 10441 (2011), M. Härtel, J. Richter, O. Götze, D. Ihle, and S.-L. Drechsler, *Phys. Rev. B* **87**, 054412 (2013).
- [4] H.-J. Schmidt, A. Lohmann, and J. Richter, *Phys. Rev. B* **84**, 104443 (2011).

# KINETICALLY-DRIVEN FRUSTRATION IN HYBRID LADDERS WITH LOCALIZED AND DELOCALIZED SPINS

R.C. Carvalho<sup>1</sup>, M.S.S. Pereira<sup>1</sup>, M.L. Lyra<sup>1</sup>, O. Rojas<sup>2</sup> and J. Strečka<sup>3</sup>

<sup>1</sup>*Instituto de Física, Universidade Federal de Alagoas, 57072-970, Maceió-AL, Brazil*

<sup>2</sup>*Departamento de Ciências Exatas, Universidade Federal de Lavras, 37200-000, Lavras-MG, Brazil*

<sup>3</sup>*Department of Theoretical Physics and Astrophysics, Faculty of Science, P.J. Šafárik University, Park Angelinum 9, 040 01 Košice, Slovakia*

The presence of spin frustration has been pointed in the literature as a favorable scenario for achieving an enhanced magnetocaloric effect. Recently, the thermodynamic properties of diamond chains on which competing interactions emerge from the local quantum hopping of interstitial  $S=1/2$  spins intercalated between nodal Ising spins have been investigated. Magnetization plateaus of  $1/3$  and an enhanced magnetocaloric effect were observed and related to field-driven transitions. In this work, we introduce an exactly solvable model of a  $2N$  linear strip with Ising spins occupying the nodal sites and mobile interstitial spins. The electrons of the interstitial sites are allowed to hop between the two interstitial sites, but are forbidden to hop to the nodal sites. The hopping process is restricted by Pauli's exclusion rule to occur only when the two mobile electrons have opposite spins. In such a case, a hopping amplitude  $t$  accounts for the kinetic energy associated with the electron mobility. The nodal electrons interact with the mobile electrons through exchange couplings  $J$  along each bond orientation. The interaction between nodal spins of each strip is represented by an exchange coupling  $J_1$ . It is possible to solve exactly this model employing an exact diagonalization technique and the decoration-iteration transformation to map it into a model with four distinct temperature dependent effective interactions: nearest-neighbor intra-chain interaction  $J_{1,\text{eff}}$ , inter-chain interaction  $J_{2,\text{eff}}$ , next-nearest neighbor inter-chain interaction  $J_{3,\text{eff}}$  and an additional the four-spin interaction around each square plaquette  $J_{4,\text{eff}}$ . These interactions depict a competitive character when the original inter-chain coupling  $J_1$  has a ferromagnetic nature. We exactly determine the ground-state phase diagram in the  $t/J \times J_1/J$  parameter space. At high temperatures, the correlation functions around an elementary plaquette point towards a frustrated spin configuration. We obtain the frustration temperature diagrams for some representative sets of the model parameters. The emergence of a reentrant behavior is discussed considering the distinct temperature dependence of the effective couplings.

**ULTRAFAST DEMAGNETIZATION AND ELECTRON-PHONON SPIN-FLIP PROCESSES FROM FIRST PRINCIPLES**K. Carva<sup>1,2</sup>, D. Legut<sup>3</sup>, P. M. Oppeneer<sup>2</sup> and M. Battiato<sup>2</sup><sup>1</sup>*Department of Condensed Matter Physics, Charles University,  
Ke Karlovu 5, CZ-12116 Prague 2, Czech Republic*<sup>2</sup>*Department of Physics and Materials Science, Uppsala  
University, Box 530, SE-75121 Uppsala, Sweden*<sup>3</sup>*Nanotechnology Centre, VSB-Technical University of Ostrava, 17. listopadu 15,  
CZ-708 33 Ostrava, Czech Republic*

In recent years it has been demonstrated that magnetization can be changed without applying an external magnetic field in extremely short timescales of the order of hundreds of femtoseconds [1]. We have studied the effect for three ferromagnetic metals Fe, Co and Ni, considering the Elliott-Yafet electron-phonon spin-flip scattering which has been suggested to be the dominant microscopic mechanism [2].

We have calculated the spin-flip Eliashberg function [3] based on ab initio electron-phonon coupling matrix elements. The demagnetization is stimulated by a fs laser pulse and takes place in a strongly non-equilibrium situation. Correct handling of this situation is critical for obtaining reliable information about ultrafast demagnetization, since the spin-flip probability depends strongly on electron energy.

We consider two specific cases for electronic system excited by a laser: thermalized very hot electron distributions, as well as highly non-equilibrium electron distributions that are expected to be present immediately after the fs laser excitation. Employing this approach we compute the electron-phonon SF rates and examine the evolution of the total spin momentum. We find that the demagnetization rate is very low for any thermalized electron distribution (including those with electron temperature of the order of thousands Kelvin) as compared to non-equilibrium distributions present within first femtoseconds following the pump laser [3]. This is due to the density of states and the specific energy-dependence of SF probability. A comparison of SF probabilities and demagnetization rates is provided for all three metals.

[1] E. Beaurepaire, J.-C. Merle, A. Daunois J.-Y. Bigot, Phys. Rev. Lett. 76, 4250 (1996).

[2] B. Koopmans et al., Nature Mater. 9, 259 (2010).

[3] K. Carva, M. Battiato, P. M. Oppeneer, Phys. Rev. Lett., 107, 207201 (2011)

**VIBRATIONAL PROPERTIES AND THE ENERGETIC STABILITY OF THE MAGNETIC  $\text{KCuF}_3$  PHASES – A QUASI-ONE-DIMENSIONAL MAGNET**D. Legut<sup>1</sup> and U. D. Wdowik<sup>2</sup><sup>1</sup>*Nanotechnology Centre, VSB Technical University of Ostrava, 17. listopadu 15, CZ-708 33, Ostrava, Czech Republic*<sup>2</sup>*Institute of Technology, Pedagogical University, ulica Podchorążych 2, PL-30-084, Cracow, Poland*

We report theoretical investigations of the lattice dynamics of quasi-1 dimensional magnetic compound  $\text{KCuF}_3$ . The magnetic couplings are highly anisotropic with strong antiferromagnetic exchange interactions between adjacent  $\text{Cu}^{2+}$  ions along the c-axis and weak ferromagnetic exchange coupling between  $\text{Cu}^{2+}$  nearest-neighbor ions within the tetragonal a–b plane [1-3]. Energetic stability of tetragonal and orthorhombic polymorphic structures of  $\text{KCuF}_3$  is analyzed. Our results show that the orthorhombic polymorph is energetically not preferred. Vibrations of the  $\text{KCuF}_3$  lattice are studied within the harmonic approximation. The Raman and infrared-active phonon modes in two distinct tetragonal polymorphs of  $\text{KCuF}_3$  are discussed with respect to the available experimental data. A detailed examination of the phonon densities of states in both tetragonal polymorphic structures of  $\text{KCuF}_3$  is provided together with discussion on similarities and differences between the vibrational dynamics of two distinct tetragonal lattices of the  $\text{KCuF}_3$  system. Our calculations are based the generalized gradient approximation and parametrization of Perdew–Burke–Ernzerhof to the density functional theory corrected for the on-site Coulomb interaction (GGA + U) using state-of-the-art projected augmented plane-wave method implemented in the VASP code.

[1] J. C. Bonner and M. E. Fisher, Phys. Rev. B, **135** 640 (1964).

[2] T. Oguchi, Phys. Rev. **133**, 1098 ( 1964).

[3] S. K. Satija, J. D. Axe, G. Shirane, H. Yoshizawa and K. Hirakawa, Phys. Rev. B **21**, 2001 (1980).

[4] D. Legut and U. D. Wdowik, J. Phys.: Condensed Matter **25**, 115404 (2013).

**THERMAL PROPERTIES OF A DILUTED TRIANGULAR ISING ANTIFERROMAGNET IN A FIELD**

M. Borovský, M. Žukovič and A. Bobák

*Department of Theoretical Physics and Astrophysics, Faculty of Science, P. J. Šafárik University in Košice, Park Angelinum 9, 041 54 Košice, Slovak Republic*

A triangular Ising antiferromagnet (TIA) is known to show no long-range ordering at any finite temperature due to high degree of geometrical frustration. However, the degeneracy can be at least partially lifted by various perturbations, such as an external magnetic field or quenched nonmagnetic impurities, which can lead to long-range ordering even at finite temperatures. In the presence of the external field the system can display a phase transition between the low-temperature ferrimagnetic and high-temperature paramagnetic phases. Another kind of perturbation is injection of nonmagnetic impurities, either in a uniform or selective fashion. In the former case, the geometrical frustration is relieved only locally, supposedly leading to a spin-glass state. On the other hand, in the latter case, different sublattices are magnetically diluted with different probabilities and then the frustration is relieved globally, giving rise to long-range magnetic ordering phenomena even in the absence of the field.

Within the framework of the effective field theory with correlations we study thermal behavior of the TIA in a broad parameter space of the applied field and both the uniform and selective ways of dilution with nonmagnetic impurities. In particular, we study thermal and field dependencies of some basic thermodynamic quantities, such as the magnetization and the internal energy along with the corresponding response functions, i.e., the magnetic susceptibility and the specific heat. In some regions of the parameter space these functions display a peculiar behavior with various anomalies as a result of joint effects of the geometrical frustration, magnetic dilution, thermal fluctuations and the applied magnetic field.

*Acknowledgments: This work was supported by the Scientific Grant Agency of Ministry of Education of Slovak Republic (Grant No. 1/0234/12).*

**MAGNETIC FLUXGATE SENSOR CHARACTERISTICS MODELING USING EXTENDED PREISACH MODEL**

P. Frydrych, R. Szewczyk and J. Salach

*Institute of Metrology and Biomedical Engineering, Warsaw University of Technology, ul. A. Boboli 8 02-525 Warsaw*

This paper presents the implementation of the extended Preisach model to fluxgate sensor characteristics modeling. The developed model enables optimization of fluxgate sensor parameters for given core material. The model consist of two parts.

First part is extended Preisach model of magnetic characteristics, which is able to simulate the nonsymmetrical hysteresis loops for wide range of field amplitude. The model is strongly connected with physical magnetization mechanism and material properties. The model is defined by four parameters specified for particular material and assumes two dimensional normal distribution of domain coercive field. Distribution position against increasing and decreasing axis and its standard deviation is correlated with material properties. The model was optimized for amorphous alloys using evolution  $\mu+\lambda$  strategy.

In second part simulated hysteresis loop for given external field and excitation field is used to calculate induction in core branches. These results are used to calculation of voltage signal in sensing coils due to windings parameters. Excitation coil parameters and excitation current signal parameters are calculated from excitation field assumed during modeling.

The model enables to achieve best functional characteristics of the fluxgate sensor for particular core material. It is also possible to utilize the modeling results for optimization of material composition and treatment of cores of sensors. The model can lower the costs of research and production of sensors. Presented model can be used as valuable alternative to prototype testing for miniature fluxgate sensors.

# THE ENERGY SPECTRUM AND THERMODYNAMICS OF THE SPIN MODEL FOR QUASI-ONE-DIMENSIONAL MAGNET

[Mn(phen)<sub>3</sub>](TCNQ)<sub>2</sub>·H<sub>2</sub>O

V.Chernanovskii<sup>1</sup>, M.Botko<sup>2</sup>, G.Vasilets<sup>1</sup>, M.Kaynakova<sup>2</sup>, V. Starodub<sup>3</sup> and A. Feher<sup>2</sup>

<sup>1</sup>*Department of Chemistry, V.N. Karazin Kharkiv National University, 4 Svobody Sq., 61077, Kharkiv, Ukraine*

<sup>2</sup>*Institute of Physics, Faculty of Science, Pavol Jozef Šafárik University, Park Angelinum 9, SK-04154 Kosice, Slovakia*

<sup>3</sup>*Institute of Chemistry, Jan Kochanowski University of Humanities and Sciences, 15G Świętokrzyska Str., 25-406 Kielce, Poland*

On the base of *X*-ray and *ESR* data, we propose to describe the low-energy states of the magnetic sublattice of [Mn(phen)<sub>3</sub>](TCNQ)<sub>2</sub>·H<sub>2</sub>O by the following Heisenberg spin Hamiltonian with single-ion anisotropy:

$$\mathbf{H} = \sum_{i=1}^N \sum_{j=1}^2 \left[ J_1 \mathbf{S}_{i,j} (\mathbf{s}_{i,2j-1} + \mathbf{s}_{i,2j} + \mathbf{s}_{i+1,2j}) + J_2 \mathbf{s}_{i,2} \mathbf{s}_{i,4} + D (\mathbf{S}_{i,j}^z)^2 \right],$$

where  $\mathbf{S}_{i,j}$  is a  $S = 5/2$  spin operator which corresponds to Mn<sup>+2</sup> cation and  $\mathbf{s}_{i,j}$  is  $s = 1/2$  spin operator of TCNQ anion; the first index  $i$  enumerates lattice unite cells, the second index enumerates spins inside the unit cell.

In the case of  $D=0$  this Hamiltonian has a singlet ground state at any positive values of coupling constant  $J_1, J_2$  and total number of unit cells  $N$ . At  $J_1 \ll J_2$  two neighboring TCNQ radicals inside the unit cell form singlet pair. This leads to weak effective magnetic interactions of the two-spin structural units TCNQ-Mn(phen)<sub>3</sub> with total spin  $S=2$ . In the absence of magnetic field and single ion anisotropy this unit has two-level energy spectrum, which lead to Shottky anomaly (peak) in temperature dependence of specific heat  $C_v$ . This behavior is in agreement with the experimental data and permits us to estimate the value of coupling  $J_1 \sim 25K$ . On the base of exact diagonalization study of small lattice clusters we had shown that the lattice Hamiltonian can be mapped to the frustrated  $S=2$  spin ladder with the weak antiferromagnetic rung and diagonal couplings  $J_a \ll J_1$  and ferromagnetic coupling in legs. This ladder was used for the study of model thermodynamics. The comparison of the results of our numerical study with the experimental data is discussed.



# THE FRUSTRATED ISING ANTIFERROMAGNET ON THE HONEYCOMB LATTICE

T. Lučivjanský<sup>1</sup>, A. Bobák<sup>1</sup>, M. Borovský<sup>1</sup>, M. Žukovič<sup>1</sup> and T. Balcerzak<sup>2</sup>

<sup>1</sup>*Department of Theoretical Physics and Astrophysics, University of P.J. Šafárik, Park Angelinum 9, 041 54 Košice, Slovak Republic*

<sup>2</sup>*Department of Solid State Physics, University of Łódź, Pomorska 149/153, 90-236 Łódź, Poland*

We study the phase diagram and magnetic properties of the frustrated spin-1/2 Ising model on the honeycomb lattice with first- and second-nearest neighbor antiferromagnetic interactions ( $J_1$  and  $J_2$ ) by the use of two-site cluster effective-field theory. This approach is based on exact Ising-spin identities for the two-site cluster, utilizes a differential operator technique and takes the single-site kinematic relations exactly into account through the exact Van der Waerden identities. The frustration in this bipartite lattice is incorporated via competing nearest-neighbor and next-nearest-neighbor pairs of spins. In particular, we have found that the transition temperature is suppressed to  $T = 0$  K at the critical interaction ratio  $J_2/\square J_1\square = -1/4$ , where the ground state is highly frustrated with the order parameter equal to zero. Thus, without thermal fluctuations the transitions in the system are driven solely by frustration due to the inherent competition between the interactions. Furthermore, it is shown that for  $J_2/\square J_1\square > -1/4$  the ground state is the simple Néel antiferromagnet and in the case of  $J_2/\square J_1\square < -1/4$  the system minimizes its energy by ordering in alternate ferromagnetic rows of opposite oriented spins (superantiferromagnet).

Finally, we study the magnetic behavior at the particular point  $J_2/\square J_1\square = -1/4$ . As mentioned above, due to high degeneracy at  $T = 0$  K, there is no long-range order at finite temperatures and the staggered magnetization (order parameter) is equal to zero. Because the results for the specific heat and the staggered (ordering) susceptibility are also very similar to those of the Ising chain, we conclude that the frustrated two-dimensional Ising antiferromagnet on the honeycomb lattice with  $J_2/\square J_1\square = -1/4$  behaves like a one-dimensional Ising system.

*This work was supported by the Scientific Grant of Ministry of Education of Slovak Republic (Grant VEGA No. 1/0234/12 and Grant VEGA No. 1/0222/13).*

**EXACT GROUND STATE OF THE SHASTRY-SUTHERLAND LATTICE WITH CLASSICAL HEISENBERG SPINS**

Alexei Grechnev

*B.Verkin Institute for Low Temperature Physics and Engineering  
of the National Academy of Sciences of Ukraine, 47 Lenin Ave., Kharkov 61103 ,  
UKRAINE*

The exact ground state of the isotropic classical Heisenberg model on the Shastry-Sutherland lattice in external magnetic field  $H$  is found for an arbitrary ratio  $J_2/J_1$  of the diagonal ( $J_2$ ) and edge ( $J_1$ ) exchange constants. The phase diagram of this model in the  $(J_2/J_1, H/J_1)$  plane is presented. It includes spin-flop, spin-flip and umbrella phases, as well as the special degenerate line ( $J_2/J_1=2$ ). The magnetization curves are found to be linear until saturation for all values of  $J_2/J_1$ , with no magnetization steps.

It is shown numerically with discrete micromagnetic simulations that the inclusion of the easy-axis anisotropy into the model leads to the appearance of the  $M/M_s=1/3$  fractional magnetization plateau, corresponding to the collinear up-up-down spin structure. This explains the appearance of the  $1/3$  magnetization plateau in rare earth tetraborides  $RB_4$ . Also, the  $M=0$  plateau, corresponding to either Neel (for  $J_2/J_1<2$ ) or dimer (for  $J_2/J_1>2$ ) collinear structure, can appear for strong enough anisotropy. The magnetization curve of the compound  $HoB_4$ , which includes the  $M=0$  and  $M/M_s=1/3$  magnetization steps is explained.

# LOW-ENERGY THEORY OF SOME FRUSTRATED QUANTUM ANTIFERROMAGNETS AT HIGH MAGNETIC FIELDS

O. Derzhko<sup>1</sup>, J. Richter<sup>2</sup>, O. Krupnitska<sup>3</sup>, and T. Krokhumalskii<sup>1</sup>

<sup>1</sup>*Institute for Condensed Matter Physics NASU, 79011 L'viv, Ukraine*

<sup>2</sup>*Universität Magdeburg, P.O. Box 4120, 39016 Magdeburg, Germany*

<sup>3</sup>*Ivan Franko National University of L'viv, 79005 L'viv, Ukraine*

We consider the spin-1/2 antiferromagnetic Heisenberg model on several frustrated one- and two-dimensional lattices with an almost dispersionless lowest magnon band. The aim of our study is to develop a systematic theory of low-temperature high-field properties of the models at hand. For this purpose we eliminate high-energy degrees of freedom at high magnetic fields arriving at effective low-energy spin-1/2 Hamiltonians. The obtained effective models are much simpler than the initial ones. Firstly, the effective models have smaller number of sites and secondly, and most importantly, they are unfrustrated. As a result, one can apply well elaborated methods of the quantum spin systems theory to discuss the properties of the initial frustrated quantum antiferromagnets at high fields and low temperatures. In our study we compare different versions of perturbation theory which yields the effective Hamiltonians and analyze the region of their applicability. Furthermore, we focus on the case of a generalized diamond chain model [1,2] which is known to be realized in the natural mineral azurite  $\text{Cu}_3(\text{CO}_3)_2(\text{OH})_2$  [3]. We suggest a number of theoretical predictions for the set of parameters which corresponds to azurite [2,3]. These results may be of interest for explaining of the high-field low-temperature measurements for azurite.

[1] A. Honecker and A. Läuchli, Phys. Rev. B **63**, 174407 (2001).

[2] A. Honecker, S. Hu, R. Peters, and J. Richter, J. Phys.: Condens. Matter **23**, 164211 (2011).

[3] H. Jeschke, I. Opahle, H. Kandpal, R. Valenti, H. Das, T. Saha-Dasgupta, O. Janson, H. Rosner, A. Brühl, B. Wolf, M. Lang, J. Richter, S. Hu, X. Wang, R. Peters, T. Pruschke, and A. Honecker, Phys. Rev. Lett. **106**, 217201 (2011).

**THERMODYNAMICS OF SPIN-1/2 ORTHOGONAL-DIMER CHAIN WITH ISING AND ANISOTROPIC HEISENBERG INTERACTIONS**T. Verkholyak<sup>1,2</sup> and J. Strečka<sup>2</sup><sup>1</sup>*Institute for Condensed Matter Physics, National Academy of Sciences of Ukraine, 1 Svientsitskii Street, 79011 Lviv, Ukraine*<sup>2</sup>*Department of Theoretical Physics and Astrophysics, Faculty of Science, P. J. Šafárik University, Park Angelinum 9, 04001 Košice, Slovak Republic*

The orthogonal-dimer chain [1] constitutes a one-dimensional counterpart of the well-known Shastry-Sutherland lattice. The spin models on the latter lattice are intensively studied in connection with a number of fractional magnetization plateaux experimentally observed in  $\text{SrCu}_2(\text{BO}_3)_2$ ,  $\text{RB}_4$  (R denotes the rare-earth element) and other magnetic compounds with competing interactions [2]. In this work, we will rigorously treat the quantum spin-1/2 version of the orthogonal-dimer chain with the anisotropic Heisenberg intra-dimer and Ising inter-dimer couplings. This simplification renders the model into an integrable case, since z-component of the total spin on the Heisenberg dimers becomes a conserved quantity. As a result, the model under investigation can be presented as a classical spin chain and solved exactly using the transfer-matrix method. The investigated quantum spin system exhibits at zero temperature the fractional plateaux at 1/4 and 1/2 of the saturated magnetization and it has a highly degenerate ground state at the critical fields where the magnetization jumps. We analyze the effect of the anisotropy of the Heisenberg interaction and external magnetic field on the thermodynamic properties, whereas our attention is mainly focused on the temperature behaviour of the specific heat in the vicinity of the critical fields.

*T.V. acknowledges the support of the National Scholarship Programme of the Slovak Republic. J.S. acknowledges the financial support provided under the grant VEGA 1/0234/12.*

[1] J. Richter, N. B. Ivanov, and J. Schulenburg, J. Phys.: Condens. Matter 10 (1998) 3635.

[2] M. Takigawa, F. Mila, Introduction to Frustrated Magnetism, edited by C. Lacroix, P. Mendels, and F. Mila (Springer, New York, 2011), p. 241.

# EXACT VALENCE-BOND-SOLID GROUND STATES OF FRUSTRATED SPIN-1 ISING-HEISENBERG AND HEISENBERG LADDERS IN A MAGNETIC FIELD

J. Strečka<sup>1</sup>, F. Michaud<sup>2</sup> and F. Mila<sup>2</sup>

<sup>1</sup>*Department of Theoretical Physics and Astrophysics, Faculty of Science, P. J. Šafárik University, Park Angelinum 9, 040 01, Košice, Slovak Republic*

<sup>2</sup>*Institute of Theoretical Physics, Ecole Polytechnique Fédérale de Lausanne (EPFL), CH-1015 Lausanne, Switzerland*

Ground states of the frustrated spin-1 Ising-Heisenberg two-leg ladder with Heisenberg intra-rung couplings and equal Ising interactions along legs and diagonals are rigorously found by taking advantage of the local conservation of the total spin of each rung. The ground-state phase diagram consists in total of eight different ground states, two of which are classical and six quantum in character. All six quantum ground states can be conveniently represented within the valence-bond-solid picture, and the translational symmetry is spontaneously broken in four of them with a doubling of the unit cell. It is demonstrated that the frustrated spin-1 Ising-Heisenberg ladder generally exhibits three different magnetization scenarios, which involve intermediate plateaus at one-quarter, one-half and three-quarters of the saturation magnetization.

Taking advantage of the conservation of the total spin of each rung, the frustrated spin-1 Heisenberg two-leg ladder can be decomposed into the direct sum of quantum spin chains with spin 0, 1 or 2 at each site. The ground state of such a system can be shown to be either a homogeneous chain, with the same spin at all sites, or a chain with alternating spins on every other site. Comparing the energy of the different chains, obtained either analytically or using DMRG simulations, the exact ground-state phase diagram of the frustrated spin-1 Heisenberg ladder can be constructed. It is shown that the sequence of plateaus exactly coincides with that of the Ising-Heisenberg ladder if the intra-rung coupling is at least twice as large as the inter-rung interaction. The most significant difference between the magnetization process of the frustrated Ising-Heisenberg and Heisenberg ladders can be accordingly found in the parameter region with a strong enough inter-rung coupling, where the Heisenberg ladder exhibits a field-induced transition from the Haldane phase towards the gapless Luttinger liquid phase with a continuously varying magnetization, to be contrasted to the stepwise magnetization curve of the Ising-Heisenberg ladder with three different intermediate magnetization plateaus.

**LOW-TEMPERATURE THERMODYNAMICS  
OF THE DIAMOND-CHAIN HEISENBERG ANTIFERROMAGNET  
AT HIGH MAGNETIC FIELDS**O. Krupnitska<sup>1</sup>, O. Derzhko<sup>2</sup>, and J. Richter<sup>3</sup><sup>1</sup>*Ivan Franko National University of L'viv, 79005 L'viv, Ukraine*<sup>2</sup>*Institute for Condensed Matter Physics NASU, 79011 L'viv, Ukraine*<sup>3</sup>*Universität Magdeburg, P.O. Box 4120, 39016 Magdeburg, Germany*

We consider the spin-1/2 antiferromagnetic Heisenberg model on a diamond chain with almost dispersionless (almost flat) lowest magnon band (distorted diamond spin chain) in the presence of a magnetic field. The high-field low-temperature properties of the distorted diamond spin chain can be examined using a localized-magnon picture [1]. Within such an approach we have obtained (approximate) analytical results for the high-field magnetization curve at low temperatures and have demonstrated that these results are in a reasonable agreement with exact diagonalization data for finite systems [2].

In our present work we apply the approach of Ref. 2 for the investigation of other properties of the antiferromagnetic Heisenberg diamond chain in proximity to the flat-band point. In particular, we focus on the low-temperature high-field behavior of the specific heat, the entropy, and on the magnetocaloric effect. Furthermore, we apply our analysis to the natural mineral azurite  $\text{Cu}_3(\text{CO}_3)_2(\text{OH})_2$ , the magnetic properties of which can be explained within the spin-1/2 antiferromagnetic Heisenberg diamond spin-chain model with slightly dispersive lowest magnon band [3]. We compare our results with the ones obtained earlier numerically using a transfer-matrix variant of the density-matrix renormalization group [3]. Our theoretical predictions may be of interest for interpreting the high-field low-temperature measurements for azurite.

[1] O. Derzhko, J. Richter, A. Honecker, and H.-J. Schmidt, *Fiz. Nizk. Temp. (Kharkiv)* **33**, 982 (2007) [*Low Temp. Phys.* **33**, 745 (2007)].

[2] O. Derzhko, J. Richter, and O. Krupnitska, *Condensed Matter Physics (L'viv)* **15**, 43702 (2012).

[3] A. Honecker, S. Hu, R. Peters, and J. Richter, *J. Phys.: Condens. Matter* **23**, 164211 (2011).

**CRITICAL TEMPERATURE OF SITE-DILUTED SPIN-1/2 SYSTEMS WITH LONG-RANGE FERROMAGNETIC INTERACTIONS**

K. Szałowski and T. Balcerzak

*Department of Solid State Physics, University of Łódź, ulica Pomorska 149/153, PL 90-236 Łódź, Poland*

The diluted magnets with long-range interactions belong to an interesting class of physical systems, the studies of which are stimulated for example by the contemporary achievements of semiconductors physics. Theoretical description of thermodynamics of such systems is a challenging problem for simulational methods due to the range of interactions, especially in the regime of strong dilution. Therefore, an interest arises in approximate analytical methods capable of describing this class of magnets.

In the present paper we formulate the generalization of the Pair Approximation (PA) method to study site-diluted spin-1/2 systems of arbitrary dimensionality with the long-range ferromagnetic interactions, basing on the previously developed method for magnets with nearest-neighbour coupling. The method allows to take into account arbitrary anisotropy of the interactions in the spin space, not being limited to purely Ising couplings. Within this approach, the Gibbs free energy is obtained, which allows to derive all the further interesting thermodynamic properties. In particular, we obtained an equation for the critical temperature of the second-order phase transitions for the model in question.

In the study we focus our attention on the systems with ferromagnetic interactions decaying with the distance according to the power law  $J(r) \sim (r/r_{NN})^{-n}$ , where  $r_{NN}$  is the nearest-neighbour distance. We discuss the dependence of the critical temperature on the concentration of magnetic component and the index  $n$  for selected one-, two- and three-dimensional lattices. In the limiting case of  $n \rightarrow \infty$  we reproduce the results of PA for nearest-neighbour interaction, while the lowest  $n$  value is limited by the system dimensionality. We confirm the absence of the critical concentration for a diluted magnet with infinite interaction range.

In the regime of low concentrations of magnetic component, we find a non-linear increase of the critical temperature with the concentration, dependent on the system dimensionality and the index  $n$ . This is in sharp contrast with the Mean Field Approximation result, which predicts always a linear dependence.

*This work has been supported by Polish Ministry of Science and Higher Education on a special purpose grant to fund the research and development activities and tasks associated with them, serving the development of young scientists and doctoral students.*

**MAGNETIZATION PROCESS AND ADIABATIC DEMAGNETIZATION OF THE ANTIFERROMAGNETIC SPIN-1/2 HEISENBERG CUBE**

J. Čisárová and J. Strečka

*Department of Theoretical Physics and Astrophysics, Faculty of Science,  
P. J. Šafárik University, Park Angelinum 9, 040 01, Košice, Slovak Republic*

A full energy spectrum of the spin-1/2 Heisenberg cubic cluster is obtained from the group-theoretical calculation and the exact numerical diagonalization in order to investigate the low-temperature magnetization process and adiabatic demagnetization of this zero-dimensional  $2 \times 2 \times 2$  quantum spin system. It is evidenced that the antiferromagnetic spin-1/2 Heisenberg cube exhibits at zero temperature an interesting stepwise magnetization curve with four intermediate magnetization plateaus at zero, one quarter, one half, and three quarters of the saturation magnetization, whereas all the level-crossing fields associated with the magnetization jumps are exactly found from a comparison of the lowest-energy level from the sectors with different total spin of the cubic spin cluster. An effect of temperature upon a gradual smoothing of the magnetization curve is investigated in detail.

Our particular attention is also focused on the adiabatic demagnetization of the antiferromagnetic spin-1/2 Heisenberg cube, which may lead upon certain conditions to the enhanced magnetocaloric effect. It is shown that the temperature shows a marked isentropic dependence on the external magnetic field in a close vicinity of the level-crossing fields, where an abrupt drop in the temperature is subsequently followed by a successive increase. An optimal value of the entropy for observing the enhanced magnetocaloric effect is found. Last but not least, the specific heat dependence on the magnetic field is examined in detail at different temperatures. It is demonstrated that the specific heat displays an intriguing double-peak structure close to the level-crossing fields, whereas the width of both peaks becomes broader upon increasing the temperature.

*This work was supported by the grant of the Slovak Research and Development Agency under the contract No. APVV-0132-11 and by the grant VEGA 1/0234/12.*



**P1-07**

**HYSTERESIS EFFECT IN MEAN-FIELD MODEL**

R. Pełka

*The H. Niewodniczański Institute of Nuclear Physics Polish Academy of Sciences,  
Radzikowskiego 152, 31-342 Kraków, Poland*

A simple feedback loop and a mean-field theory are employed to simulate the memory effect in the exchange-coupled magnetic system. The nonlinearity of the feedback turns out to be the crucial factor for the appearance of hysteresis loops. A threshold value above which the hysteresis disappears is the mean-field transition temperature. Temperature dependence of the coercive field is investigated.

**SINGLE DOMAIN WALL PROPAGATION AT LOW FIELDS**

J. Kostyk<sup>1</sup>, R. Varga<sup>1</sup> and M. Vazquez<sup>2</sup>

<sup>1</sup>*Institute of Physics, Faculty of Sciences, P. J. Safarik University, Park Angelinum 9, 041 54 Kosice, Slovakia*

<sup>2</sup>*Instituto de Ciencia de Materiales, CSIC 28049 Madrid, Spain*

Domain wall propagation is used in many magnetic devices such as magnetic random access memory, spintronics and sensor devices [1]. The speed of such devices depends on the velocity of the magnetic domain wall. One of the problems is understanding the domain wall propagation through a real material containing defects will help us in controlling of such devices.

Amorphous glass-coated microwires with positive magnetostriction prepared by Taylor-Ulitovski method are characterized by depinning and subsequent propagation of the single closure domain wall in one large Barkhausen jump. Because of amorphous nature, they contain defects (local density fluctuations), which act as pinning centers. That is why the magnetic microwires are ideal to study the single domain wall dynamics in defective material.

It was shown, that the classical linear dependence of the domain wall velocity on the applied magnetic field in microwires is not valid at low fields, where domain wall dynamics can be successfully described by a power law:  $v = S'(H-H_0)^q$ , where  $S'$  is domain wall mobility parameter,  $H_0$  is a dynamic coercive field and  $q$  is the power exponent. Such behaviour results from the interaction of the propagating domain wall with the defects presented in the material [2].

In the given contribution we present a detail study on the domain wall propagation at low fields regime under different external conditions (temperature, magnetic field frequency,...).

*This work was supported by the project NanoCEXmat No. ITMS 26220120019, Slovak VEGA grant. No. 1/0060/13, APVV-0027-11, APVV-0266-10 and by Spanish MEC under project MAT2010-20798-C05-01.*

- [1] D. A. Allwood, G. Xiong, C. C. Faulkner, D. Atkinson, D. Petit, and R. P. Cowburn, *Science* 309 (2005), 1688.
- [2] R. Varga, Y. Kostyk, A. Zhukov, M. Vazquez, *Journal of Non-Crystalline Solids* 354 (2008) 5101-5103.

**SYMMETRY BROKEN TIME EVOLUTION OF MAGNETIC STRUCTURE IN PL NANODOT**

M. Šulek, J. Tóbkik and V. Cambel

*Department of Physics at Nanoscale, Institute of Electrical Engineering SAS,  
Dúbravská cesta 9, 841 04 Bratislava*

In this work we present results of numerical simulations of magnetic structure in magnetic PL nanodot at finite temperature. Pacman-like (PL) nanodot is a magnetic dot of cylindrical shape with removed sector in order to lower symmetry. Magnetic structure of the ground state without magnetic field is magnetic vortex. Magnetic vortex is characterized by two parameters – polarity – an out of plane magnetization of the vortex core and chirality – direction of the twist of the magnetization on the nanodot perimeter. The ground-state of PL nanodot is fourfold degenerated as both chirality and polarity have two possible states. It was found that the each particular final state can be chosen by direction of applied external field slowly (adiabatically) decreased to zero. In this work we focus on temperature effect. Temperature is included to simulations via stochastic Langevin term in the time evolution equation. Dynamics of magnetization is described by Landau-Lifshitz-Gilbert equation. By looking at simulations results we have identified two modes of behavior. In one case the thermal fluctuations are dominant, and the resulting vortex polarity is random. In other case the polarity of the nucleated vortex is deterministic, regardless of the temperature. We analyze the Landau-Lifshitz-Gilbert equation with stochastic term in order to identify origin of the directional preferences of the vortex nucleation process.

**WEAK FERROMAGNETISM IN THE DZIALOSHINSKII-MORIYA  
HELMAGNET  $\text{Ba}_2\text{CuGe}_2\text{O}_7$** J. Chovan<sup>1</sup>, M. Marder<sup>2</sup> and N. Papanicolaou<sup>3</sup><sup>1</sup>*Department of Physics, Matej Bel University, Banská Bystrica, Slovakia*<sup>2</sup>*Center for Nonlinear Dynamics and Department of Physics, The University of Texas at Austin, Austin, Texas 787 12*<sup>3</sup>*Department of Physics and Institute of Plasma Physics, University of Crete, Heraklion, Greece*

Recent experiments on  $\text{Ba}_2\text{CuGe}_2\text{O}_7$  have observed an unexpected incommensurate-to-commensurate magnetic phase transition induced by an external field applied perpendicular to the  $c$  axis. A subsequent theoretical analysis suggested a nonzero weak-ferromagnetic component in the underlying Dzyaloshinskii-Moriya anisotropy and estimated its strength.

Here we theoretically examine some finer issues related to weak ferromagnetism in the system. In particular, we show that the weak-ferromagnetic anisotropy plays an important role in a sudden  $\pi/2$  rotations of the spin spiral propagation direction in canted magnetic fields nearly parallel to the  $c$  axis. We also briefly discuss the dynamics of a new type of domain walls in weak-ferromagnetic helimagnets.

**MAGNETIC REORIENTATION IN TWO-SUBLATTICE HEISENBERG FERRIMAGNETIC SYSTEM**

V. Ilkovič

*Institute of Physics, Faculty of Science, P.J.Šafarik University, Jesenná 5, 040 01 Košice, Slovak Republic*

The method of the double-time Green function is used to study theoretically the phenomenon reorientation of magnetization in the ferrimagnetic layer system. We consider a model for two-sublattice ferrimagnet by expressing the two-sublattice Green functions in terms of matrix and find the equation of motion it satisfies. The algebraic procedure of solution is then greatly simplified. The model Hamiltonian includes the operator of the inter-sublattice antiferromagnetic exchange interaction energy between the nearest neighbor spins, two operators of the intra-sublattice ferromagnetic exchange interaction energy between the next nearest neighbor spins, the anisotropic energy due to the coupling of the crystal field and spin-orbit interaction (single-ion anisotropy), and the Zeeman term which corresponds to the transverse magnetic field. The magnetization and reorientation temperature of individual sublattices are calculated for different spin values and as well as the spin wave spectrum for different parameters of the system.

**MONTE CARLO SIMULATION OF SPIN-3/2  
BLUME-EMERY-GRIFFITHS MODEL**

M. Žukovič and M. Jaščur

*Department of Theoretical Physics and Astrophysics, Faculty of Science, P. J. Šafárik University in Košice, Park Angelinum 9, 041 54 Košice, Slovak Republic*

The spin-3/2 Blume-Emery-Griffiths (BEG) model is a spin-3/2 Ising model which includes both bilinear and biquadratic interactions, as well as a single-ion uniaxial crystal-field anisotropy. It was introduced to understand behavior of some real physical systems, such as ternary mixtures. The model has been intensively studied by various approaches, nevertheless, its critical behavior is far from being well understood. Even in the most studied case with zero biquadratic interactions, i.e., the Blume-Capel (BC) model, no consensus among various approaches has been established regarding whether the first-order line separating  $(1/2, 1/2)$  and  $(3/2, 3/2)$  ferromagnetic phases at low temperatures extends to the disordered phase boundary line or it terminates at an isolated point. The spin-3/2 BEG model with finite biquadratic interactions was much less investigated. The calculations by an effective field theory with correlations (EFT) for the system on a honeycomb lattice produced some peculiar features that could not be observed in the spin-3/2 BC model. Particularly interesting was the step-wise dependence of the phase boundary on the single-ion anisotropy parameter for larger negative values of the biquadratic interactions strength.

In the present investigations we employ Monte Carlo (MC) simulations with the aim to verify whether the features predicted by the EFT, in particular the step-wise behavior of the phase boundary, are real or just artifacts of the used approximation. We measure some relevant quantities, such as the magnetization and the magnetic susceptibility, based on which we estimate the locations as well as the character of the order-disorder phase boundaries. For positive values of the biquadratic interactions the MC results confirm the discontinuous character of the critical line as a function of the single-ion anisotropy strength. However, for positive values of the biquadratic interactions the step-like variation of the critical frontier is not reproduced. Namely, only one step associated with the phase transition from the ferrimagnetic  $(1/2, 3/2)$  to the ferromagnetic  $(3/2, 3/2)$  state is observed and, therefore, the multiple steps in the EFT results are deemed artifacts of the method.

*Acknowledgments: This work was supported by the Scientific Grant Agency of Ministry of Education of Slovak Republic (Grant No. 1/0234/12).*

**DYNAMIC EFFECTS IN RANDOM FIELD ISING MODEL**

S. Hrivňák and M. Žukovič

*Department of Theoretical Physics and Astrophysics, Faculty of Science, P. J. Šafárik University in Košice, Park Angelinum 9, 041 54 Košice, Slovak Republic*

The random field Ising model (RFIM) is a prototypical model for magnetic systems with quenched disorder, in which competing mechanisms for order and disorder coexist. While the local spin interactions favor ferromagnetic ordering, the random field variations tend to destroy it. This competition drastically affects thermodynamic properties. As a result, for example, the two-dimensional (2D) RFIM has been shown to display no long-range at any temperature. Thus, in the 2D RFIM statistical mechanics of interfaces or domain walls becomes the key question. Unlike in the zero-field Ising model, in the RFIM it is not always possible to shrink the domain walls to reduce the surface energy and the domain walls are said to be pinned by the local fields. Thus, when the domain walls evolution is finished the system remains in a disordered state, albeit the resulting ferromagnetic domains may be very large. This gives rise to multimodality of the free energy surface and the resulting long relaxation times.

In the present study we employ Monte Carlo simulations and focus on the dynamics of the magnetization processes and the evolution of the largest domain size. The latter is typically assessed only indirectly by the magnetization fluctuations but we opted for a direct determination by the Hoshen-Kopelman algorithm. We investigate two kinds of random field (RF) distributions – uniform and Gaussian – with varying strengths. For either case, both the magnetization and the growth of the largest domain are found to follow the power law with generally different exponents but all exponentially decaying with the RF strength. Moreover, for small RFs the relaxation is confirmed to follow different regimes at early and later times.

*Acknowledgments: This work was supported by the Scientific Grant Agency of Ministry of Education of Slovak Republic (Grant No. 1/0234/12).*

## LOW-TEMPERATURE BEHAVIOR OF A STACKED TRIANGULAR LATTICE ISING ANTIFERROMAGNET

L. Mižišin, M. Žukovič and A. Bobák

*Department of Theoretical Physics and Astrophysics, Faculty of Science, P. J. Šafárik University in Košice, Park Angelinum 9, 041 54 Košice, Slovak Republic*

An Ising antiferromagnet on a stacked triangular lattice is a relatively simple geometrically frustrated spin model. Nevertheless, its behavior remains an object of controversy even in zero field. There is a broad consensus that at higher temperatures the model exhibits a phase transition from a paramagnetic phase to a partially disordered phase with two sublattices ordered and one disordered. However, as temperature is lowered, some theories predicted the transition to a ferrimagnetic state with one sublattice fully ordered and two partially disordered, while some others suggested that there is no such transition. Furthermore, some studies indicated the possibility of unsaturated magnetization at zero temperature, a so called kinetic effect. Therefore, the character of the low-temperature phase is still not quite understood.

In our study we try to elucidate the above mentioned issues by extensive Monte Carlo simulations. In particular, we focus on the behavior of the sublattice magnetizations in a wide range of the relative strength of the exchange interaction in the stacking direction  $\alpha$ . We expect this parameter to affect the degree of the kinetic freezing since the latter is believed to arise as a result of a sluggish spin-flip dynamics of strongly correlated spin chains in the stacking direction. We find that the low-temperature phase is not ferrimagnetic but remains partially disordered with the sublattice magnetizations  $(m, -m, 0)$ . As the system is cooled at steady rate to zero temperature the saturation value of  $m$  behaves like a step function of  $\alpha$ . More specifically, we find two regimes: if  $\alpha$  is large enough the system kinetically freezes and  $m$  falls short of saturation, with the value little sensitive to change in  $\alpha$ . On the other hand, if the value of  $\alpha$  is relatively small, the presence or absence of the kinetic freezing depends on the cooling rate. Namely, it almost disappears unless the cooling at low temperatures is very slow.

*Acknowledgments: This work was supported by the Scientific Grant Agency of Ministry of Education of Slovak Republic (Grant No. 1/0234/12).*



**HYPERFINE INTERACTIONS IN HEXAGONAL FERRITES  
OF THE Sr-Fe-O SYSTEMS**

K. Kouřil<sup>1</sup>, H. Štěpánková<sup>1</sup>, V. Chlan<sup>1</sup>, J. Englich<sup>1</sup>, J. Töpfer<sup>2</sup>, D. Seifert<sup>2</sup>

<sup>1</sup>*Charles University in Prague, Faculty of Mathematics and Physics,  
V Holešovičkách 2, 180 00 Prague 8, Czech Republic*

<sup>2</sup>*University of Applied Sciences Jena, Dept. SciTec, C.-Zeiss-Promenade 2, 07745  
Jena, Germany*

The hexagonal M-type ferrite  $\text{SrFe}_{12}\text{O}_{19}$  represents a well-known composition belonging to the family of hard ferrite magnets. However, other hexagonal structural types are also found in the  $\text{SrO-FeO-Fe}_2\text{O}_3$  system. Recently, a reinvestigation of the Fe-rich part of the phase diagram has confirmed existence of X-type hexagonal ferrite  $\text{Sr}_2\text{Fe}_{30}\text{O}_{46}$  [1]. We report here on its preparation and properties, and compare hyperfine interactions in  $\text{Sr}_2\text{Fe}_{30}\text{O}_{46}$  ( $\text{SrFe}_2\text{X}$ ) with M-type  $\text{SrFe}_{12}\text{O}_{19}$  ( $\text{SrM}$ ) and W-type  $\text{SrFe}_{18}\text{O}_{27}$  ( $\text{SrFe}_2\text{W}$ ) hexaferrites.

The X-type hexaferrite was synthesized at 1400°C; thermal analysis revealed a narrow stability range of 1350-1420°C only. Rietveld refinement of XRD data results in a unit cell with  $a_0 = 5.8940(2)\text{\AA}$  and  $c_0 = 83.808(8)\text{\AA}$ . A ferrous concentration of 3.4 wt % (theoretical 4.3 %) was measured by titrations. The saturation magnetization is somewhat smaller compared to the M-type which can be interpreted in the collinear Gorter model with ferrous ions on spin-up sites.

All three hexagonal ferrites were studied by  $^{57}\text{Fe}$  NMR spectroscopy. The NMR spectra measured at 4.2 K are interpreted as being due to the superposition of signals from  $^{57}\text{Fe}$  in different  $\text{Fe}^{3+}$  sites: for M-type five well separated resonance lines are observed while the spectrum of X-type is more complex and corresponds approximately to a superposition of  $\text{SrM}$  and  $\text{SrFe}_2\text{W}$  spectra. Based on comparison with  $\text{SrM}$  spectrum and results of electronic structure calculations we were able to partially interpret the  $^{57}\text{Fe}$  NMR patterns observed in  $\text{SrFe}_2\text{X}$ . Further we propose that ferrous ions in  $\text{SrFe}_2\text{W}$  are formed in the octahedral sites inside pairs of adjacent S structural blocks.

[1] N. Langhof, D. Seifert, M. Goebbels, J. Töpfer, J. Solid State Chem. 182 (2009) 2409-2416

**STUDY OF Y-TYPE HEXAFERRITE BY MEANS OF  $^{57}\text{Fe}$  NMR AND ELECTRONIC STRUCTURE CALCULATIONS**

V. Chlan, K. Kouřil, H. Štěpánková, R. Řezníček

*Charles University in Prague, Faculty of Mathematics and Physics,  
V Holešovičkách 2, 180 00 Prague 8, Czech Republic*

Multiferroic Y-type hexaferrites are complex systems where properties are influenced by substitutions and their distribution among cationic sites, which can be well investigated by local methods such as nuclear magnetic resonance (NMR) spectroscopy. The local structure and site preferences of cations in the crystal structure of  $\text{Ba}_2\text{Zn}_2\text{Fe}_{19}\text{O}_{22}$  were studied from the electronic structure calculations and nuclear magnetic resonance.

In calculations we investigated Zn and Fe site preference and determined hyperfine magnetic fields on  $^{57}\text{Fe}$  nuclei using WIEN2k and corrections for hyperfine contact interaction. The calculated fields were compared to experimental  $^{57}\text{Fe}$  NMR spectra of  $\text{Ba}_2\text{Zn}_2\text{Fe}_{19}\text{O}_{22}$  single crystal.

In this contribution we aimed on interpretation of  $^{57}\text{Fe}$  NMR. The spectra were measured at 4.2 K in external magnetic field 0 – 1.5 T. Field dependence and comparison of calculated fields with the experiment allowed for interpretation of complicated  $^{57}\text{Fe}$  spectra.

**THERMODYNAMICS OF COUPLED ELECTRON AND SPIN SYSTEMSON THE SHASTRY-SUTHERLAND LATTICE**

P. Farkasovsky and H. Cencarikova

*Institute of Experimental Physics, Slovak Academy of Sciences, Watsonova 47, 040 01 Košice, Slovakia*

The thermodynamics of a simple electron-spin model proposed recently for a description of magnetization processes in rare-earth tetraborides is studied numerically by the canonical Monte Carlo method in two-dimensions. The model is based on the coexistence of two subsystems, and namely, the spin subsystem described by the Ising model and the electronic subsystem described by the free-electron model on the Shastry-Sutherland lattice. Moreover, both subsystems are coupled by the anisotropic spin-dependent interaction of the Ising type. At  $T=0$  the system exhibits magnetization plateaus at  $m/m_s=1/2, 1/3, 1/5, 1/7, 1/9$  and  $1/11$  of the saturated spin magnetization  $m_s$ . The ground states corresponding to magnetization plateaus have the same spin structure consisting of parallel antiferromagnetic bands (of the width  $w=1, 2, 4, 6, 8$  and  $10$ ) separated by ferromagnetic stripes. For the largest phases corresponding to  $m/m_s=0, 1/3$  and  $1/2$  we have examined the nature of the phase transitions from the low-temperature ordered phase to the high-temperature disordered phase. It is shown that all phases persist also at finite temperatures (up to the critical temperature  $T_c$ ) and that the phase transition at the critical point is of the second order for the  $m/m_s=0$  phase and of the first order for the  $m/m_s=1/3$  and  $1/2$  phases. The results obtained are used for a description of thermodynamic properties (the specific heat and magnetization curves) of rare-earth tetraborides.

*This work was supported by the ERDF EU (European Union European regional development fond) under the contract No. ITMS 26220120047.*

**GROUND-STATE PHASE DIAGRAM OF THE EXTENDED ISING MODEL ON THE SHASTRY-SUTHERLAND LATTICE**H. Cencarikova<sup>1</sup>, P. Farkasovsky<sup>1</sup> and P. Puchala<sup>2</sup><sup>1</sup>*Institute of Experimental Physics, Slovak Academy of Sciences, Watsonova 47, 040 01 Košice, Slovakia*<sup>2</sup>*Department of Theoretical Physics and Astrophysics, Faculty of Science, P. J. Šafárik University, Park Angelinum 9, 040 01 Košice, Slovakia*

The ground-state phase diagram of the Ising model on the Shastry-Sutherland lattice with the first ( $J_1$ ), second ( $J_2$ ), third ( $J_3$ ) and fourth ( $J_4$ ) nearest-neighbour spin couplings is studied using the exact and well controlled numerical methods. It is shown that the switching on the  $J_3$  and  $J_4$  interactions (in addition to usually considered  $J_1$  and  $J_2$  interactions) leads to a stabilization of the following magnetic phases with  $m/m_s=1/9, 1/6, 1/2$  and  $5/9$ , that reflect in an appearance of new magnetization plateaus on the magnetization curve of the model at given values of  $m/m_s$ . The results obtained are consistent with experimental measurements of magnetization curves in selected rare-earth tetraborides.

*This work was supported by the ERDF EU (European Union European regional development fond) under the contract No. ITMS 26220120047.*

**FRUSTRATION IN A MIXED-SPIN ISING MODEL WITH MULTI-SPIN INTERACTIONS**

M. Jaščur<sup>1</sup>, V. Štubňa<sup>1</sup>, K. Szalowski<sup>2</sup> and T. Balcerzak<sup>2</sup>

<sup>1</sup>*Department of Theoretical Physics and Astrophysics, Institute of Physics, P.J. Šafárik University in Košice, Park Angelinum 9, 040 01 Košice, Slovakia*

<sup>2</sup>*Department of Solid State Physics, University of Lodz, ul. Pomorska 149/153, 90-236 Lodz, Poland*

In this work we investigate a mixed spin-1/2 and spin-1 Ising model on a decorated square lattice. In addition to standard pair interactions between nearest neighbors, we also consider in our calculations three-site four-spin interactions and the effect of single ion anisotropy. Applying the well-known decoration-iteration transformation, we derive a simple relation between the partition function of the model under investigation and the Onsager's partition function for the simple square lattice. With the help of this mapping relation we are able to calculate exact expressions for all relevant physical quantities of the system (for example, the magnetization, internal energy, Gibbs free energy, entropy and specific heat).

From the physical point of view, the model under investigation is very interesting because it represents a very rare case in which the many-body interactions can be studied without mathematical approximations. In this work we particularly concentrate on the investigation of phase transitions and magnetic ordering in the system. For this purpose, we study in detail the ground-state and also finite-temperature phase diagrams in the whole parameter space. Our analysis of the system with pure three-site four-spin interaction reveals that excepting the standard ordered and disordered phases, there also appears an interesting phase which is ordered only partially. Analyzing relevant physical quantities of the system, we show that the partial ordering is closely related to very strong frustration which leads to non-zero entropy at absolute zero temperature. On the other hand, the specific heat goes to zero for  $T \rightarrow 0$  in agreement with the Nernst principle. Finally, we also investigate dependence of physical quantities on the sign of multi-spin and pair interactions.

*This work has been supported by the Scientific Grant of the Ministry of Education of Slovak Republic (Grant VEGA No. 1/0234/12)*

## EXCHANGE INTERACTIONS AND ELASTICITY OF

**Cu(H<sub>2</sub>O)<sub>2</sub>(ethylenediamine)SO<sub>4</sub> – QUASI-2D MAGNETIC SYSTEM**R. Sýkora<sup>1</sup>, D. Legut<sup>1</sup> and U. D. Wdowik<sup>2</sup><sup>1</sup>*Nanotechnology Centre, VSB Technical University of Ostrava, 17. listopadu 15, CZ-708 33, Ostrava, Czech Republic*<sup>2</sup>*Institute of Technology, Pedagogical University, ulica Podchorążych 2, PL-30-084 Cracow, Poland*

We report a theoretical *ab-initio* investigation of magnetic ordering (exchange interaction between Cu atoms) and mechanical behaviour (elastic constants) of Cu(H<sub>2</sub>O)<sub>2</sub>(*en*)SO<sub>4</sub>, *en*=C<sub>2</sub>H<sub>8</sub>N<sub>2</sub> (ethylenediamine), a compound with a quasi-2D antiferromagnetic magnetic order. Its structure is composed of a stacking along c-axis of weakly interacting (over the *en* group) *ab* planes that are formed by a triangular lattice of Cu atoms with two different exchange-coupling constants (to the 1<sup>st</sup> neighbours): one coupling atoms within a linear chain along the *a* axis (over the SO<sub>4</sub> group), the other coupling Cu atoms in the neighbouring chains [1]. The system, as was reported in [2], can be phenomenologically described by an *S*=1/2 Heisenberg-like Hamiltonian with the above-mentioned exchange-coupling constants entering as parameters. We calculated these exchange-coupling constants using the state-of-the-art first-principles codes WIEN2k and VASP, based on the density functional theory and with no empirical parameters. Subsequently, we determined the Néel temperature using a mean-field model. We also calculated the material elastic constants and from them determined the longitudinal and transverse shear velocities (within the *ab* and *ac* planes). The calculated quantities are compared with available experimental data and empirical models. Our calculations use the generalized gradient approximation and parametrization of Perdew–Burke–Ernzerhof to the density functional theory corrected for on-site Coulomb interaction (GGA + U).

[1] V. Manríquez et al., J. Chem. Crystall., **26**, 15 (1996).

[2] M. Kajňáková et al., Phys. Rev. B, **71**, 014435 (2005).

**STATUS AND TRENDS OF AMORPHOUS AND NANOCRYSTALLINE ALLOYS FOR SOFT MAGNETIC APPLICATIONS**

Giselher Herzer

*Vacuumschmelze GmbH & Co. KG, D-63450 Hanau, Germany*

The talk surveys characteristic features of amorphous and nanocrystalline alloys for soft magnetic applications. Both materials have much in common starting from their way of production by rapid solidification as a thin ribbon and including the key factors which determine their properties. Thus, the magneto-crystalline anisotropy is randomly fluctuating on a scale much smaller than the domain wall width and, as a consequence, is averaged out by exchange interaction so that there is no anisotropy net effect on the magnetisation process, the prerequisite for good soft magnetic behaviour. Superior soft magnetic properties additionally require a low magnetostriction which is true for amorphous Co-based alloys and for nanocrystalline Fe-base alloys. Due to their production inherent low thickness and relatively high electrical resistivity both materials additionally reveal favourably low losses up to several 100 kHz making them even competitive with MnZn ferrites.

Soft magnetic applications require a well defined shape of the hysteresis loop with a specific level of permeability. This is accomplished by annealing induced magnetic anisotropies. Their orientation relative to the magnetic path controls the shape of the hysteresis loop and the magnitude,  $K_u$ , determines the permeability. In particular magnetic field annealing is a powerful tool in tailoring the hysteresis loop according to the demands of various applications. Still, tensile stress annealing provides a further opportunity to control the induced anisotropy. Appropriate choice of the alloy composition and the annealing conditions, thus, ultimately allows to vary  $K_u$  by about four orders of magnitude.

Nanocrystalline alloys provide a particularly unique combination of high saturation induction, low magnetostriction, high permeability, low losses and good thermal stability. This allows to reduce the size and the weight of magnetic components. Apart from its technical performance, the material is also based on the inexpensive raw materials iron and silicon. Accordingly, nanocrystalline alloys are found in a steadily increasing number of applications previously served by amorphous Co-based alloys or MnZn ferrites.

**TRENDS AND CHALLENGES IN SOFT MAGNETS FOR HIGHER FREQUENCY APPLICATIONS**

F. Mazaleyrat

*SATIE, CNRS, ENS Cachan, 61 av. President Wilson, 91230, Cachan, France*

Today's applications in power electronics and electrical machines requires constantly increasing power density, a demand that can only be satisfied if working frequencies are pushed over the usual limits of magnetic materials.

In power electronics, chopping frequencies above 100 kHz are usual for switch-mode-power-supplies (SMPS) even for several kW units and can reach 1 MHz for several 100 W units. Mn-Zn ferrites are perfectly adapted to power applications below 1 MHz, but the core losses are rather high because of their low resistivity, so skin effect is no more negligible. In addition, the Mn-Zn ferrites are quite tricky to produce (the O<sub>2</sub> partial pressure as to be controlled during sintering) and not adapted to low temperature co-fired ceramics technology (LTCC) or spark plasma sintering (SPS). By opposition, partially Cu substituted Ni-Zn ferrites are well adapted to these technologies but rather lossy for power applications. Co-doped NiZnCu ferrites appear as a promising material compatible with the new manufacturing technologies of magnetic components and with low power loss around 1 MHz.

High speed multi-poles electrical machines are today feed at frequencies above 1 kHz which causes problems with classical Fe-Si sheets. Reducing the thickness is a good solution for classical machines, but more and more machines have 3D flux paths making mandatory the used of soft magnetic composites (SMC). Although SMC are produced in industry, the modelization of the losses is still difficult. The two scales nature of the eddy currents, offers no straightforward way to apply Bertotti's theory of separation of losses. An attempt to modelize losses in SMC will be discussed and new directions for improving SMCs will be discussed.



**INFLUENCE OF THERMOMAGNETIC TREATMENT ON MAGNETOELASTIC PROPERTIES OF FeNiMoB AMORPHOUS ALLOY**

R. Szewczyk<sup>1</sup>, Peter Svec Sr.<sup>2</sup>, Jacek Salach<sup>1</sup>, Peter Švec<sup>2</sup>, Adam Bieńkowski<sup>1</sup>, Jozef Hoško<sup>2</sup>, Dorota Jackiewicz<sup>1</sup>, Marcin Kamiński<sup>3</sup> and Wojciech Winiarski<sup>3</sup>

<sup>1</sup>*Institute of Metrology and Biomedical Engineering, Warsaw University of Technology, sw. A. Boboli 8, 02-525 Warsaw, Poland*

<sup>2</sup>*Institute of Physics, Slovak Academy of Sciences, Dúbravská cesta 9, 845 11 Bratislava, Slovak Republic*

<sup>3</sup>*Industrial Research Institute for Automation and Measurements PIAP, Al. Jerozolimskie 202, 02-486 Warsaw, Poland*

Rapidly quenched, amorphous alloys are widely used as the cores of inductive components for switching mode power conversion, current transformers as well as cores of mechatronic sensors. For all these applications specific, magnetic properties are required. These properties of amorphous alloys are determined by its thermomagnetic treatment.

On the other hand, magnetoelastic properties of amorphous alloy are very important from practical point of view. Especially for miniaturized components even relatively small forces applied during assembling process may generate significant mechanical stresses, causing decreasing of core permeability up to 80%. These phenomena may cause malfunction of device with such miniaturized inductive component.

In spite of the fact, that both influence of thermomagnetic annealing on magnetic properties of amorphous alloys as well as its magnetoelastic properties were recently intensively investigated, these properties are still not linked together. This paper is filling this gap.

Paper presents the results of magnetoelastic tests of ring-shaped cores made of Fe<sub>40</sub>Ni<sub>38</sub>Mo<sub>4</sub>B<sub>18</sub> amorphous alloy. Cores were subjected to thermomagnetic annealing in diversified temperature and under different values of magnetic field. For magnetoelastic tests special method was used. As a result uniform distribution of mechanical stresses on all length of magnetic circuit was achieved.

Achieved results enabled linking the magnetoelastic sensitivity of Fe<sub>40</sub>Ni<sub>38</sub>Mo<sub>4</sub>B<sub>18</sub> amorphous alloy with conditions of its thermomagnetic treatment. It should be indicated, that achieved results may be generalized for amorphous alloy with other chemical compositions, subjected to similar thermomagnetic treatment.

## INFLUENCE OF HIGH-ENERGY HEAVY IONS ON MAGNETIC SUSCEPTIBILITY OF SOFT MAGNETIC METALLIC GLASSES

M. Pavlovič<sup>1</sup>, M. Miglierini<sup>1,2</sup>, E. Mustafin<sup>3</sup>, T. Seidl<sup>3,4</sup>, M. Šoka<sup>5</sup>, I. Strašík<sup>3</sup> and W. Ensinger<sup>4</sup>

<sup>1</sup>*Institute of Nuclear and Physical Engineering FEI STU, Slovak University of Technology in Bratislava, Ilkovičova 3, 812 19 Bratislava, Slovak Republic*

<sup>2</sup>*RCATM, Palacky University, 17. listopadu 12, 771 46 Olomouc, Czech Republic*

<sup>3</sup>*GSI Helmholtzzentrum für Schwerionenforschung GmbH, Planckstrasse 1, 642 91 Darmstadt, Germany*

<sup>4</sup>*Darmstadt University of Technology, Karolinenplatz 5, 642 89 Darmstadt, Germany*

<sup>5</sup>*Institute of Electrical Engineering FEI STU, Slovak University of Technology in Bratislava, Ilkovičova 3, 812 19 Bratislava, Slovak Republic*

Some soft magnetic metallic glasses are considered to be used for magnetic cores of accelerator RF-cavities. Due to the losses of the circulating ion beam, they may be exposed to irradiation of different ions at different energies including high-energy heavy ions. This contribution presents experimental data concerning the influence of high-energy heavy-ions on magnetic susceptibility of VITROVAC- and VITROPERM-type metallic glasses.

Samples of magnetic ribbons were irradiated by Au, Ta, and U ions at 11.1 MeV/A (energy per nucleon) and 5.9 MeV/A, respectively. The irradiation fluences varied from  $5 \times 10^{10}$  up to  $1.2 \times 10^{13}$  ions/cm<sup>2</sup>. Relative change of the samples' magnetic susceptibility after and before irradiation was evaluated as a function of the irradiation fluence. The irradiation experiments were performed at the UNILAC accelerator at GSI Helmholtzzentrum für Schwerionenforschung GmbH. They were simulated in SRIM2010 in order to get ionization densities (electronic stopping, dE/dx) and dpa (displacements per atom) caused by the ion beams in the sample material. The dpa were related to elastic nuclear scattering.

As a result, we observed that VITROPERM-type samples showed less drop of magnetic susceptibility in comparison with the VITROVAC-type ones and this drop occurred at higher fluences. This indicates higher radiation hardness of VITROPERM compared with VITROVAC. In addition, heavier ions caused larger change of magnetic susceptibility than the lighter ones and the effect could be roughly scaled with the level of electronic stopping. This suggests mechanisms of material damage different from structural changes due to elastic nuclear scattering. The later finding is supported also by the fact that changes of magnetic susceptibility were present also at dpa less than  $1 \times 10^{-5}$ .

# IDENTIFICATION OF THE CURIE POINT IN FINEMET BASED ALLOYS USING IN-SITU X-RAY DIFFRACTION

S. Michalik<sup>1,2</sup>, J. Bednarcik<sup>3</sup>, J. Kovac<sup>4</sup> and P. Sovak<sup>2</sup>

<sup>1</sup>*Institute of Physics of the ASCR, v.v.i., Na Slovance 2, 18221 Praha 8, The Czech Republic*

<sup>2</sup>*Institute of Physics, Park Angelinum 9, 041 54 Kosice, Slovakia*

<sup>3</sup>*Deutsches Elektronen-Synchrotron, Notkestrasse 85, 22607 Hamburg, Germany*

<sup>4</sup>*Institute of Experimental Physics, Slovak Academy of Sciences, Watsonova 47, 040 01 Košice, Slovakia*

The thermal expansion behaviour of  $\text{Fe}_{(73.5-x)}\text{Mn}_x\text{Si}_{13.5}\text{Cu}_1\text{Nb}_3\text{B}_9$  ( $x = 1, 3, 5, 7$  and  $9$ ) amorphous ribbon samples below the crystallization temperature was investigated on the atomic scale using in-situ high-energy X-ray diffraction (HEXRD). The tracing the position of the first diffuse diffraction maximum was used to follow the thermal expansion behavior of the studied samples. It was observed that the thermal volume coefficient is able to reflect the ferromagnetic transition. The temperatures at which the expansion curves changes their slopes are in good accordance with Curie temperatures extracted from thermomagnetic measurements. In order to get more information about structural changes, the atomic pair distribution function were calculated. Our results suggest that in-situ HEXRD provide enough sensitivity to detect the transition from the ferromagnetic to the paramagnetic state in the case of FINEMET based alloys.

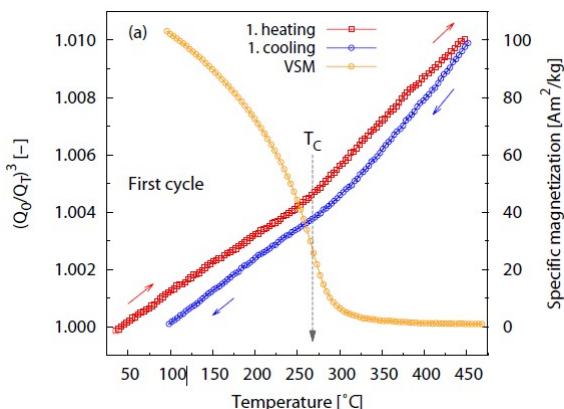


Fig. 1. Comparison of the relative peak changes of the first diffraction maximum scaled to the third power  $(Q_0/Q_T)^3$  with the thermomagnetic curve.

**DEPTH-SELECTIVE STUDY OF SURFACE CRYSTALLIZATION IN NANOPERM-TYPE ALLOYS**M. Miglierini<sup>1,2</sup>, T. Hatala<sup>1</sup> and M. Bujdos<sup>3</sup><sup>1</sup>*Institute of Nuclear and Physical Engineering, Slovak University of Technology, Ilkovičova 3, 812 19 Bratislava, Slovakia*<sup>2</sup>*Regional Centre of Advanced Technologies and Materials, Faculty of Science, Palacky University, 17. listopadu 12, 771 46 Olomouc, Czech Republic*<sup>3</sup>*Institute of Laboratory Research on Geomaterials, Faculty of Natural Sciences, Comenius University, Mlynská dolina, 842 15 Bratislava, Slovakia*

Magnetic properties of nanocrystalline alloys play an important role when employed in practical applications. Bulk properties of these alloys are sufficiently well understood. Surface features, however, deserve still more close inspection. Particular attention is paid to different sides of ribbon-shaped samples, viz. the wheel and the air surface. Due to diverse quenching conditions at both sides of the ribbons, distinctions in the progress of crystallization, and hence magnetic microstructure can be expected.

In this contribution, we report on the surface crystallization of Fe<sub>79</sub>Mo<sub>8</sub>Cu<sub>1</sub>B<sub>12</sub> alloy prepared by rapid quenching. Chemical composition of the alloy was checked by ICP-MS (inductively coupled plasma mass spectrometry). Structure and magnetic order of the as-quenched (amorphous) and partially crystallized (nanocrystalline) samples were studied by surface sensitive techniques of <sup>57</sup>Fe Mössbauer spectrometry such as Conversion Electron Mössbauer Spectrometry (CEMS) and Conversion X-ray Mössbauer Spectrometry (CXMS). They provide depth selective information from the subsurface layers of about 200 nm and 1 000 nm, respectively.

Complementary information on the kinetics of crystallization at both sides of the ribbons is derived from *in situ* diffraction of synchrotron radiation. In addition, vibration properties of the bulk of amorphous and nanocrystalline samples are presented. They were obtained from experiments of nuclear inelastic scattering of synchrotron radiation using partial densities of phonon states. The calculated parameters such as sound velocity and the Debye temperature are compared with those that characterize a fully crystalline material (bcc-Fe foil). The nanocrystals formed during heat treatment of the investigated NANOPERM-type alloy show a tendency to reach the values observed for bulk bcc-Fe.

*This work was supported by the research projects VEGA 1/0286/12, SK-PL-0032-12, CZ.1.05/2.1.00/03.0058, and CZ.1.07/2.3.00/20.0155.*

**MÖSSBAUER AND MAGNETIC STUDY OF THE MAGNETITE NANOPARTICLES**

A. Lancok<sup>1</sup>, N. Mahmed<sup>2,3</sup>, S-P. Hannula<sup>2</sup> and O. Heczko<sup>1</sup>

<sup>1</sup>*Institute of Physics AS CR, v. v. i., Na Slovance 2, 182 21 Prague, Czech Republic*

<sup>2</sup>*Department of Materials Science and Engineering, Aalto University School of Chemical Technology, P.O.Box 16200, FI-00076 Aalto, Finland*

<sup>3</sup>*School of Materials Engineering, Kompleks Pusat Pengajian UniMAP, Taman Muhibbah, Universiti Malaysia Perlis, 02600 Jejawi, Perlis, Malaysia*

The synthesis of magnetite nanoparticles was attempted by using only ion ferrous salt ( $\text{Fe}^{2+}$ ) under ambient atmosphere. The room temperature reverse coprecipitation method was used, with ammonium hydroxide ( $\text{NH}_4\text{OH}$ ) as a precipitating agent. The freshly prepared iron oxide was also immediately coated with Stöber silica ( $\text{SiO}_2$ ) layer, forming the core-shell structure.

The phase, crystallite and the particle size of the synthesized powders were determined by using X-ray diffraction and transmission electron microscope, while the magnetic and oxidation behaviors were studied by using the vibrating sample magnetometer and Mössbauer spectroscopy.

Based on the results, the bare iron oxide nanoparticles is in the stoichiometry in between the magnetite and the maghemite stoichiometries, i.e., oxidation occurs. This oxidation is also due to the large surface area of the synthesized 13 nm size particles. With the silica coating, the magnetite phase retained in the core-shell structure, i.e., oxidation is prevented, as suggested by the Mössbauer measurement. The observed Curie temperature at 850 K for the core-shell powder further confirmed the magnetite phase in the structure.

The Mössbauer study suggested the formation of maghemite rather than magnetite. This oxidation can be prevented by introducing an amorphous silica coating, in the form of core-shell structure. This was inferred from the fitting parameters of difference spectrum obtained from the spectra of bare and silica-coated iron oxide powder.

*Acknowledgments*

*This work was supported by the Czech Scientific Foundation No. P107/11/0391 and No. P204/10/0035.*

**THE SURFACE STRUCTURE AND MAGNETIC PROPERTIES OF Fe-Al ALLOYS**A. Hendrych<sup>1,2</sup>, O. Životský<sup>1,2</sup>, and Y. Jirásková<sup>3</sup><sup>1</sup>*Department of Physics, <sup>2</sup>Nanotechnology Centre, VŠB-Technical University of Ostrava, Ostrava, CZ 70833, Czech Republic*<sup>3</sup>*Institute of Physics of Materials, Academy of Sciences of the Czech Republic, Brno, CZ 61662, Czech Republic*

The Fe-Al alloys attract ongoing interest of the wide scientific community. The reason is their outstanding corrosion and oxidation resistance, mechanical properties, low material costs, and last but not least a relatively large possibility of alloying with other elements or compounds as, e.g., with yttrium oxide in the known oxide dispersion strengthened alloys for high temperature applications. The present paper is devoted to Fe-Al alloys with aluminum content of 28, 33, and 35 at.% prepared by standard technological procedures. The attention concentrates above all on their surface structure and magnetic properties using the surface-sensitive methods, namely, magneto-optical Kerr effect (MOKE), atomic and magnetic force microscopy (AFM, MFM), and conversion electron Mössbauer spectrometry (CEMS). The obtained results are completed by selected methods yielding the bulk properties with the aim to obtain more comprehensive view on these alloys.

From the viewpoint of magnetic behavior, the investigated alloys can be divided into two groups. The alloys Fe<sub>67</sub>Al<sub>33</sub> and Fe<sub>65</sub>Al<sub>35</sub> show a paramagnetic behavior while the alloy with 28 at.%Al is ferromagnetic at room temperature. This is well documented by the CEMS as well as volume magnetic and Mössbauer measurements. However, from the viewpoint of MOKE and MFM observations, all alloys exhibit ferromagnetic behavior. This is surprising especially for alloys with Al content equal or higher than 33 at.%. We ascribe this feature to depletion by Al atoms of the surface in the depth of a few nanometers. The MOKE hysteresis loop measurements are well supported by magnetic domain structure. Moreover, due to the round form of the samples and relatively large grains, the MOKE technique has also allowed us to detect changes in anisotropy inside the grains and at grain boundaries.

**MAGNETIC EVALUATION OF RESIDUAL STRESSES AND STRUCTURE TRANSFORMATIONS INDUCED IN SOFT STEEL AFTER TURNING**

M. Čilliková, J. Dubec, M. Neslušan, H. Mičietová<sup>1</sup> and D. Blažek<sup>2</sup>

<sup>1</sup>*Department of Machining and Production Technologies, University of Žilina, Univerzitná 1, 010 26 Žilina, Slovakia*

<sup>2</sup>*Nanotechnology Centre, VŠB-Technical university of Ostrava, 17. listopadu 15, 70833 Ostrava, Czech Republic*

This contribution deals with the stress and temperature induced microstructure transformations in a soft bearing steel 100Cr6 after turning operation. Investigation is carried out through a technique based on Barkhausen effect.

Many aspects of a magnetic evaluation such as the raw Barkhausen noise signal, its envelopes and corresponding hysteresis loops are presented. Further, evaluation of surface integrity via structure transformations, X - ray diffraction as well as microhardness inspection is carried out. A surface integrity is investigated with the respect to the variable tool wears and consequent mechanical and thermal loads applied on the inspected surfaces. Different surface microstructures caused by the mechanical and associated thermal aspects of the surface formation are discussed and correlated with the parameters obtained from the measured Barkhausen emissions.

It should be noticed that durability and usability of the product strongly depends on the state of surface, which can be expressed in the terms of final microstructure and residual stresses. Therefore well calibrated nondestructive magnetic evaluation of produced parts can be successfully adopted to suppress unacceptable discrepancies.

**GLASS FORMING ABILITY AND MAGNETISM OF Co-BASED  
TERNARY METALLIC GLASSES**Z. Śniadecki<sup>1</sup>, B. Idzikowski<sup>1</sup>, J. Marcin<sup>2</sup>, J. Kováč<sup>2</sup> and I. Škorvánek<sup>2</sup><sup>1</sup>*Institute of Molecular Physics, Polish Academy of Sciences,  
M. Smoluchowskiego 17, 60-179 Poznań, Poland*<sup>2</sup>*Institute of Experimental Physics, Slovak Academy of Sciences, Watsonova 47,  
040 01 Košice, Slovakia*

A new method based on the semi-empirical Miedema's model and geometric approach [1] was used to calculate the glass forming ranges (GFR) and glass forming abilities (GFA) in ternary RE-Co-B (RE –rare earth element) system. The formation enthalpies of amorphous alloys, of their solid solution counterparts and the difference between both energies were calculated. Additionally, the normalized entropy change and the glass forming ability parameter were determined. Calculation results of all mentioned parameters indicate the stoichiometric ranges with the highest GFA. This was the basis for further experimental works concerning synthesis of Co<sub>70</sub>B<sub>30</sub>-based RE<sub>8</sub>Co<sub>62</sub>B<sub>30</sub> (RE = Y, Tb, Ho) metallic glasses and subsequent structural and magnetic investigations. Especially influence of RE substitution on magnetocaloric effect was analyzed. The magnetic entropy changes,  $\Delta S_M$ , were calculated from the magnetization vs. applied magnetic field dependences measured by SQUID magnetometry. The value of the magnetic entropy change found in Y<sub>8</sub>Co<sub>62</sub>B<sub>30</sub> metallic glass in the magnetic field change from 0 to 6 T at 210 K is  $\Delta S_M = 1.11$  J/kgK. The  $\Delta S_M$  value decreases after substitution of Y by Ho and Tb. All observed effects are connected with the coupling between RE and Co sublattices. Ho and Tb containing alloys show the compensation of magnetization at about 50 K and the ferromagnetic ordering of Co-sublattice just above 200 K. Magnetic phase transitions are broadened due to disordered crystalline structures. It is the origin of the increased refrigeration capacity values ( $RC = 105$  J/kg,  $\mu_0 H = 5$  T) in comparison with Co-based intermetallic compounds of similar  $\Delta S_M$ .

The research is now focused on disordered and nanoscale structures because of distribution of magnetic transitions, which leads to broader magnetic entropy curves. There is a need of understanding the role of disorder, surfaces and interfaces, as it will allow tunability of magnetocaloric properties [2].

*This work was supported by Iuventus Plus grant (IP2011 055671) of the Polish Ministry of Science and Higher Education.*

[1] Z. Śniadecki, J.W. Narojczyk, B. Idzikowski, *Intermetallics* **26** (2012) 72

[2] H. Ucar, J.J. Ipus, V. Franco, M.E. McHenry, D.E. Laughlin, *JOM*. **64** (2012) 782



**TEMPERATURE DEPENDENCE OF THE SWITCHING FIELD IN NANOCRYSTALLINE FeNiMoB MICROWIRES**

P. Klein<sup>1</sup>, R. Varga<sup>1</sup> and M. Vazquez<sup>2</sup>

<sup>1</sup>*Institute of Physics, Faculty of Science, P. J. Safarik University, Park Angelinum 9, 041 54 Kosice, Slovakia*

<sup>2</sup>*Institute of Materials Science of Madrid, CSIC, 28049 Madrid, Spain*

Glass-coated microwires with positive magnetostriction are characterized by a magnetic bistability due to their magnetization process that runs through the single large Barkhausen jump when the external field exceeds the so-called switching field. Such bistability can be used in many applications like magnetic coding, sensors of magnetic field, mechanical stress, etc. However, the crucial parameter for their application is the time and temperature stability. From these reasons we have studied the switching field in nanocrystalline microwires prepared by the heat treatment from amorphous precursors which exhibit much higher stability and very good soft magnetic properties typical for nanocrystalline alloys. We have studied the temperature dependencies of the switching field in nanocrystalline Fe<sub>40</sub>Ni<sub>38</sub>Mo<sub>4</sub>B<sub>18</sub> microwires annealed below (650 K and 675 K) and at optimum annealing temperature (700 K). The switching field decreases with increasing temperature mainly due to different thermal expansion coefficients of the glass-coating and the metallic nucleus in nanocrystalline microwires annealed below optimum annealing temperature. Moreover, in nanocrystalline microwire annealed at 650 K the switching field decreases in monotonous way in whole temperature range and therefore it is suitable as temperature sensor.

*This work was supported by the project NanoCEXmat No. ITMS 26220120019, Slovak VEGA grant. No.1/0060/13, APVV-0027-11, APVV-0266-10 and by Spanish MEC under project MAT2010-20798-C05-01.*

**STRUCTURAL AND MAGNETIC RELAXATIONS OF MECHANICALLY ALLOYED Fe-Mo**

Y. Jirásková<sup>1</sup>, J. Buršík<sup>1</sup>, I. Turek<sup>1</sup>, M. Hapla<sup>1</sup>, J. Čížek<sup>2</sup>

<sup>1</sup>*Institute of Physics of Materials, Academy of Sciences of the Czech Republic, Žitkova 22, CZ-616 62 Brno, Czech Republic*

<sup>2</sup>*Charles University in Prague, Faculty of Mathematics and Physics, Department of Low Temperature Physics, V Holešovičkách 2, CZ-18000 Praha 8, Czech Republic*

Two Fe-Mo samples prepared by mechanical alloying in time duration of 250 hrs under air and nitrogen atmospheres are exposed to series of isothermal and isochronal treatments. The aim of present studies is to follow changes in the structure and magnetic properties regarding relaxations of defects and stability of chemical composition.

The initial states of samples are characterized by scanning electron microscopy, X-ray diffraction, positron annihilation, Mössbauer spectrometry, and differential thermal analysis supported by magnetic measurements. The temperatures, at which the magnetic characteristics were consequently measured, were determined from the thermomagnetic curves of samples in the initial states and the time interval of isothermal treatments was chosen between 0 and 300 min.

The content of molybdenum in the bcc-Fe(Mo) solid solution, achieved in the sample milled in air (14 at. %) and in nitrogen (11 at.%) atmospheres, exceeds substantially the equilibrium solubility limit. Moreover, the N processing contributes to asymmetry of the bcc Fe(Mo) (110) peak in X-ray diffraction pattern due to a small additional line at lower  $2\theta$  belonging to a bct-Fe(N) phase. The crystallite size of powder samples is approximately 20 nm.

The coercivity and remnant polarization decrease with temperature reflect annealing out of defects and structural homogenizing. From the changes of magnetic parameters with time at selected temperatures the characteristic relaxation times were obtained and used for calculation of activation energies of relaxation processes. They range between 0.4 and 0.6 eV.

# STRUCTURAL STABILITY OF SOFT MAGNETIC Fe-Co-Zr-W-B METALLIC GLASSES INVESTIGATED BY THE IN-SITU XRD

S.Michalik<sup>1,2</sup>, J. Bednarcik<sup>3</sup>, P. Pawlik<sup>4</sup>, R. Matija<sup>5</sup> and P. Sovak<sup>2</sup>

<sup>1</sup>*Institute of Physics of the ASCR, v.v.i., Na Slovance 2, 18221 Praha 8, The Czech Republic*

<sup>2</sup>*Institute of Physics, Park Angelinum 9, 041 54 Kosice, Slovakia*

<sup>3</sup>*Deutsches Elektronen-Synchrotron, Notkestrasse 85, 22607 Hamburg, Germany*

<sup>4</sup>*Institute of Physics, Czestochowa University of Technology, Al. Armii Krajowej 19, 42-200 Czestochowa, Poland*

<sup>5</sup>*Faculty of manufacturing technologies of Technical University of Kosice with a seat in Presov, Sturova 31, 080 01 Presov, Slovakia*

The atomic structure of as-prepared  $\text{Fe}_{61}\text{Co}_{(14-x)}\text{Zr}_5\text{W}_x\text{B}_{20}$  ( $x = 1, 2$  and  $4$ ) ribbon samples and their thermal stability were investigated by in-situ high-energy X-ray diffraction experiments. It was observed that higher W concentration causes the tiny shift of the main peak of the reduced atomic pair distribution function  $D(r)$  to higher values of interatomic distances as shown in figure 1. Additionally the tracing of the position of the main diffraction peak with temperature was used to determine the thermal behavior of the investigated ribbons during heating (see figure 2). It was revealed that higher W concentration invokes the increase of the coefficient of the volume thermal expansion. Analysis of diffraction profiles obtained during the heating revealed that the crystallization process occurs in two steps. Firstly the  $\text{Fe}_{23}\text{B}_6$  phase is created and later is transformed to other types of borides together with the creation of a Fe-based phase. The formation of the  $\text{Fe}_3\text{Zr}$  phase was suggested by the phase analysis as well. The process of crystallization is qualitatively the same for all studied ribbons.

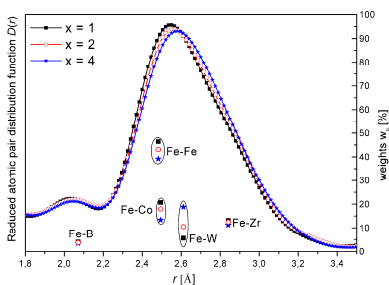


Fig. 1. The first maximum of  $D(r)$  shown  $\text{Fe}_{61}\text{Co}_{(14-x)}\text{Zr}_5\text{B}_{20}\text{W}_x$  ribbons.

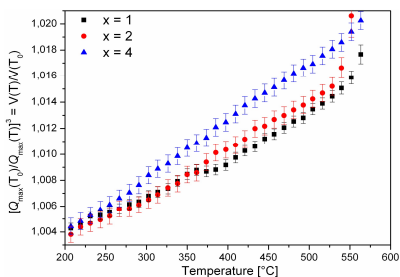


Fig. 2 Relative volume changes of  $\text{Fe}_{61}\text{Co}_{(14-x)}\text{Zr}_5\text{B}_{20}\text{W}_x$  ribbons.

**STRUCTURAL AND MAGNETIC PROPERTIES OF NANO-SIZED NiZn FERRITES**

E. Ušák<sup>1</sup>, M. Šoka<sup>1</sup>, M. Ušáková<sup>1</sup> and E. Dobročka<sup>1, 2</sup>

<sup>1</sup>*Faculty of Electrical Engineering and Information Technology, Slovak University of Technology in Bratislava, Ilkovičova 3, 812 19 Bratislava, Slovak Republic*

<sup>2</sup>*Institute of Electrical Engineering, Slovak Academy of Sciences, Dúbravská cesta 9, 841 04 Radlinského 9, Bratislava, Slovak Republic*

Various structural and magnetic properties of nano-sized NiZn ferrites having the structural formula  $\text{Ni}_{0.33}\text{Zn}_{0.67}\text{Fe}_2\text{O}_4$  prepared by means of auto-combustion method based on glycine precursor, sintered at various temperatures  $t_s$ , ranging from 450 to 850°C for 6 hours have been studied. XRD analysis was used for the investigation of the structure and crystallite size of the powder samples. The Curie temperatures of the prepared samples were found from the temperature dependencies of the magnetic susceptibility measured by means of balanced alternating current (AC) bridge method. The magnetisation curves of ring-shaped samples obtained by pressing the prepared powders into the form of tablet followed by cautious drilling of the central hole by water beam cutter machine were measured using the hysteresisgraph built-up from commercially available stand-alone instruments controlled by tailor-made software.

XRD confirmed a single-phase material in all the samples regardless of the sintering temperatures, meanwhile the size of crystallites  $D$  changed from about 17.5 nm to 157 nm within given temperature range. The dependence  $D$  upon  $t_s$  can be fitted by the second-order polynomial function. Thus, the sintering temperature was proven as an efficient and simple tool for controlling the particle size. Since the size of crystallite particles affects the resulting magnetic properties, the thermal management of ferrite preparation along with varying chemical composition and/or substitution of Ni and Zn ions in the structural formula by other proper elements, such as rare-earths, etc. allow the preparation of diverse magnetic materials needed for any particular application.

*This work was supported by the Slovak Research and Development Agency under the contract No. APVV-0062-11 and by the Scientific Grant Agency of the Ministry of Education, Science, Research and Sport of the Slovak Republic and the Slovak Academy of Sciences (VEGA), projects No. VG-1/1163/12 and VG-1/1325/12.*

**MAGNETIC PROPERTIES OF GLASS-COATED FeWB MICROWIRES**P. Klein<sup>1</sup>, R. Varga<sup>1</sup>, R. El Kammouni<sup>2</sup> and M. Vazquez<sup>2</sup><sup>1</sup>*Inst. Phys., Fac. Sci., UPJS, Park Angelinum 9, 041 54 Kosice, Slovakia*<sup>2</sup>*ICMM, CSIC, 28049 Madrid, Spain*

Glass-coated amorphous microwires are ideal material for miniature sensing applications [1]. Having positive magnetostriction, they show magnetic bistability – magnetization has only two value  $\pm M_s$  (e.g. their hysteresis loop is perfectly rectangular). Switching between the two values appears at the switching field that is strongly dependent on external parameters like temperature, magnetic field, mechanical stress, etc... [2].

The dimensions, electrical and mechanical properties of glass-coated microwires allows easy application for measuring the temperature, mechanical stress or magnetic field contactlessly [3]. For such applications, the strong dependence of the switching field on external parameters is required. One possibility how to enhance the temperature dependence of magnetic properties is to use the material with the Curie temperature close to the temperature of application [4].

In the given contribution we present the temperature dependence of magnetic properties of amorphous  $\text{Fe}_{78}\text{W}_5\text{B}_{17}$  microwires. We show the peculiarities that arise from the glass-coating that induces high mechanical stresses on the metallic nucleus. Such a stresses influence the Curie temperature, too. Moreover, effect of thermal treatment on improving the magnetic properties is shown.

*This work was supported by the project NanoCEXmat Nr. ITMS 26220120019, Slovak VEGA grant. No.1/0060/12, APVV-0027-11, APVV-0266-10 and by Spanish MEC under project MAT2010-20798-C05-01.*

[1] M. Vazquez, H. Chiriac, A. Zhukov, L. Panina, T. Uchiyama, *Phys. Stat. Sol. A* **208** (2011), 493.

[2] R. Sabol, R. Varga, J. Hudak, J. Blazek, D. Praslicka, P. Vojtanik, G. Badini, and M. Vazquez, *J. Appl. Phys.* **111** (2012), 053919.

[3] D. Praslička, J. Blázek, M. Šmelko, J. Hudák, A. Čverha, I. Mikita, R. Varga, A. Zhukov, *IEEE Trans Magn.* **49** (2013), 128

[4] N. Lupu, H. Chiriac, S. Corodeanu, G. Ababei, *IEEE Trans Magn.* **47** (2011), 3791.

**MAGNETO-OPTICAL OBSERVATION OF SURFACE DOMAIN STRUCTURE IN AMORPHOUS GLASS-COATED MICROWIRES**

K. Richter<sup>1</sup>, A. Thiaville<sup>2</sup> and R. Varga<sup>1,2</sup>

<sup>1</sup>*Department of Physics, University of Pavol Jozef Safarik, Park Angelinum 9, 041 54 Kosice, Slovakia*

<sup>2</sup>*Laboratoire de Physique des Solides, Université Paris-Sud 11, 914 00 Orsay, France*

The domain wall dynamics in amorphous glass-coated microwires attracts attention due to the very high domain wall velocities that reach up to 15km/s. In the previous works, the domain wall dynamics in microwires was tuned by the magnetic anisotropies introduced to the wire. However, along with the geometry of anisotropies, the domain wall dynamics can be influenced by surface domain structure. Here, we perform the study of surface domain structure and its interplay on fast domain wall propagation in FeSiB microwires by combination of the three competitive methods.

Imaging by Bitter colloid confirmed the presence of periodic surface domain structure with inclination of about 40° with respect to the axis of the wire. Thermal annealing at 300° increased the domain wall velocity more than tree times; however, the surface domain structure was not changed.

In order to perform magneto-optical observation of surface structure by MOKE microscope a detail theoretical analysis was done. It was shown, that the non-plane cylindrical surface of observed microwires leads to the additional magneto-optical effects that must be taken into account. A theoretical model describing the magneto-optical observation of cylindrical surface was compared to the real images obtained by microscope.

Finally, a detailed analysis of surface domain structure was done by measuring of surface hysteresis loops in longitudinal and transverse configuration. It confirmed that the surface of the wire is characterized by multi-axis stress field, which can be important factor for fast domain wall propagation.

*This work was supported by the project NanoCEXmat Nr. ITMS 26220120019, Slovak VEGA grant. No.1/0060/12, APVV-0027-11 and APVV-0266-10.*

**MAGNETIC CHARACTERIZATION OF CoFeSiB MICROWIRES USING IMPEDANCE SPECTROSCOPY**

E. Komová<sup>1</sup>, Ž. Barliková<sup>1</sup> and R. Varga<sup>2</sup>

<sup>1</sup>*Faculty of Aeronautics of Technical University, Rampova 7, 04121 Kosice, Slovakia*

<sup>2</sup>*Inst. Phys., Fac. Sci., UPJS, Park Angelinum 9, 041 54 Kosice, Slovakia*

Apart from practical applications, impedance spectroscopy is an alternating current technique that can be used to probe some properties of magnetic materials. We apply impedance spectroscopy methodology to analyze the magnetization mechanism in low-magnetostrictive ferromagnetic microwires of CoFeSiB composition. The impedance behavior as a function of the frequency depends on the distribution of the magnetic field inside the specimen. At low frequencies the magnetization mechanism can be emphasized through the evaluation of the complex permeability  $\mu = \mu_{Re} - j \mu_{Im}$ , ( $\mu_{Re}$  corresponds to the wire circumferential permeability and  $\mu_{Im}$  is associated with dissipative processes). At higher frequencies, skin effect must be taken into account in order to explain field dependence of magnetoimpedance effect.

*This work was supported by the project NanoCEXmat Nr. ITMS 26220120019, Slovak VEGA grant. No.1/0060/12, APVV-0027-11 and APVV-0266-10.*

**GMI EFFECT IN ANNEALED  $\text{Fe}_{40}\text{Ni}_{38}\text{Mo}_4\text{B}_{18}$  MICROWIRES**E. Komová<sup>1</sup>, F. Šidík<sup>1</sup>, P. Klein<sup>2</sup>, R. Varga<sup>2</sup> and M. Vazquez<sup>3</sup><sup>1</sup>*Faculty of Aeronautics of Technical University, Rampova 7, 04121 Kosice, Slovakia*<sup>2</sup>*Inst. Phys., Fac. Sci., UPJS, Park Angelinum 9, 041 54 Kosice, Slovakia*<sup>3</sup>*ICMM, CSIC, 28049 Madrid, Spain*

Amorphous glass-coated microwires are ideal material for miniaturized applications for sensing the temperature, stress and magnetic field [1]. One of the key parameters for future applications is their time and thermal stability. It has been shown that stability can be improved by using nanocrystalline materials that combine good soft magnetic properties of amorphous matrix with high structural stability of crystalline grains [2]. Such nanocrystalline materials are usually obtained by controlled annealing of amorphous precursor.

In the given contribution, influence of dc current annealing on the domain structure and GMI effect optimization in the amorphous and nanocrystalline  $\text{Fe}_{40}\text{Ni}_{38}\text{Mo}_4\text{B}_{18}$  magnetic microwires have been studied. The annealing induces additional circular magnetic anisotropy and consequently, provides an improved the magnetic field sensitivity and increased GMI effect. Annealing of amorphous wires below the crystallisation temperature results in an increase of the relative permeability due to the formation of the nanosized  $\gamma$ -FeNi grains.

*This work was supported by the project NanoCEXmat Nr. ITMS 26220120019, Slovak VEGA grant. No.1/0060/12, APVV-0027-11, APVV-0266-10 and by Spanish MEC under project MAT2010-20798-C05-01.*

[1] M. Vazquez, H. Chiriach, A. Zhukov, L. Panina, T. Uchiyama, *Phys. Stat. Sol. A* **208** (2011), 493.

[2] E. Komova, M. Varga, R. Varga, P. Vojtanik, J. Bednarcik, J. Kovac, M. Provencio, M. Vazquez, *Appl. Phys. Lett.* **93**, (2008), 062502.



**THE HALL EFFECT IN POLYCRYSTALLINE ZINC OXIDE BASED COMPOSITE**

B. Dolník<sup>1</sup>, J. Kurimský<sup>1</sup>, K. Marton<sup>1</sup>, M. Kolcun<sup>1</sup>, L. Tomčo<sup>2</sup>, J. Briančin<sup>3</sup>, M. Fabián<sup>3</sup>, M. Halama<sup>4</sup>, M. Vojtko<sup>4</sup> and M. Rajňák<sup>5</sup>

<sup>1</sup>*Department of Electric Power Engineering, Technical University of Košice, Mäsiarska 74, 041 20 Košice, Slovakia*

<sup>2</sup>*Department of Aerodynamics and Simulations, Technical University of Košice, Rampová 7, 041 21 Košice, Slovakia*

<sup>3</sup>*Institute of Geotechnic, Slovak Academy of Science, Watsonova 45, 043 53 Košice, Slovakia*

<sup>4</sup>*Department of Material Science, Technical University of Košice, Park Komenského 11, 040 01 Košice, Slovakia*

<sup>5</sup>*Institute of Experimental Physics, Slovak Academy of Science, Watsonova 47, 040 01 Košice, Slovakia*

Zinc oxide based extrinsic composite was investigated. The sample was selected from series of components of one production batch that were prepared by standard sintering technology. The content of extrinsic elements in ZnO base were determined by scanning electron microscopy (SEM). Van der Pauw method with four point electrode fixture was used for determination of conducting phenomena across square shaped sample. Normally it wished to be assumed symmetric uniformity of the sample's electrical properties, which sheet resistance, bulk resistivity and Hall mobility, sheet carrier density and carrier concentration can be calculated from. Additionally, when the uniformity of measured parameters is breached, anisotropy in the arrangement of the internal structure may be the cause. There remains the question of whether extrinsic ZnO material can be isotropic related to electric conductivity.

Although the Hall effect has been measured, preliminary measurements indicate the presence of anisotropy on the measured samples. ZnO compounds crystallize in either cubic or hexagonal structure with direct band gap of 3.37 eV and exciton binding energy of approx. 60 meV. Before measuring setup following energy conversions should be taking into account: magneto-electric effect, photo electric effect and moreover isothermal condition should be preserved.

Paper discusses on uniformity deviations for defined setup configurations for positive and negative magnetic field directions. Bulk resistivity has been calculated by numerical solution of van der Pauw equation. Large offset voltage during measurement is discussed.

**THERMOPOWER AND MAGNETIC MONITORING OF RELAXATION AND DEVITRIFICATION IN Fe-BASED GLASSY ALLOYS**A. Lovas<sup>1</sup>, J. Kravčák<sup>2</sup> and L. Novák<sup>2</sup><sup>1</sup>*Department of Automobiles and Vehicle, Budapest H-1111, Bertalan Lajos utca 2. Hungary*<sup>2</sup>*Department of Physics, Technical University of Košice, Park Komenského 2, 042 00 Košice, Slovakia*

The glassy alloys are single phase systems, so the thermopower ( $S$ ) continuously changes with the concentration of components. On the other hand,  $S$  is also influenced by the overall stress level, arising from the rapid quenching process.

In this contribution the consequence of stress relaxation and the thermal decomposition of glassy state on the  $S$  evolution will be presented. The altering  $S$  values are compared with simultaneous structural and magnetic property changes (X-ray and  $H_c$  measurements). It is found, that  $H_c$  decrease is universal in the stress lowering period, being always coupled with the negative shift in the thermopower. Though the negative shift is universal, the degree is highly composition dependent. It is interpreted as the thermodynamic stabilization of the glassy structure during the structural relaxation.

Contrast to the generally observed negative shift of  $S$ , characteristic to the stress relaxation, definite reversal can be detected, when the traces of crystalline phases has started during the heat treatments. The reversal in the sign of  $S$  takes place simultaneously with the sudden uprise of the coercive force ( $H_c$ ) during the run of thermomagnetic measurements.

The observed trends, is also supported by the DSC measurements and the X-ray phase analyses.

**STRESS-INDUCED CHANGES IN CLOSURE DOMAIN STRUCTURE DYNAMICS IN BISTABLE FERROMAGNETIC MICROWIRE**

J. Onufer, J. Ziman and M. Kladivová

*Department of Physics, Technical University of Košice, Letná 9, 042 00 Košice, Slovakia*

Recently a new experimental method for the study of closure domain structure dynamics in bistable ferromagnetic microwires was presented. The basic idea of this experiment consists in finding critical parameters of a well-defined rectangular magnetic field pulse (length and magnitude of the pulse) applied to the microwire, for which a domain wall is just released from the wire end. Modelling the wall depinning process from the closure domain structure at the wire end and comparing the results of this model with experimental data can give useful information about the parameters of this process.

In this contribution a slight modification of the experimental method is presented. It simplifies the experimental set-up and the detection of free domain wall presence after the rectangular magnetic field pulse is applied. It also makes it possible to carry out this experiment for different tensile stresses applied to the microwire. Results of this type of measurements are presented for glass-coated  $\text{Fe}_{77.5}\text{B}_{15}\text{Si}_{7.5}$  amorphous ferromagnetic microwire. Closure domain structure at the wire end is modelled by a single domain wall located in a potential well. Confrontation of the model with experimental data gives information about the parameters of the potential well as well as about the dynamic parameters of the wall (mobility, inertial mass). Changes in these parameters caused by tensile stress are discussed.

**SINGLE DOMAIN WALL CONTRIBUTION TO THE IMPEDANCE OF AMORPHOUS FERROMAGNETIC WIRE**

J. Ziman, V. Šuhajová and M. Kladivová

*Department of Physics, Technical University of Košice, Letná 9, 042 00 Košice, Slovakia*

Giant magneto-impedance (GMI) effect in thin ferromagnetic wires has been intensively studied for about two decades. This interest was strongly motivated by promising application potential. For better understanding of GMI effect many aspects have to be taken into account. One of them is the role of domain structure. Our contribution presents an experiment in which we studied the contribution of a single boundary between circular domains to the impedance in  $\text{Co}_{68.2}\text{Fe}_{4.3}\text{Si}_{12.5}\text{B}_{15}$  amorphous ferromagnetic wire.

The wire was annealed under simultaneous application of tensile and torsion stresses. In this way a small helical anisotropy was induced. The deviation of the easy axis from circular direction was very small (about  $4^\circ$ ), however this still enabled the creation of a single domain wall between circular domains (with negligible axial component of magnetization) in the wire. This wall was created by applying an inhomogeneous axial field generated by Helmholtz coils connected in anti-parallel combination. The presence of the wall was verified by circular magnetization flux measurements. The wire impedance measured with and without presence of the domain wall provided the possibility of estimating the single domain wall contribution to the impedance. Results of measurements for different AC current amplitudes in the frequency range 0.1 – 10 MHz are presented.

**RADIATION DAMAGE STUDY OF Fe-BASED NANOCRYSTALLINE MATERIALS**

J. Sitek, J. Dekan, M.Pavlovič

*Institute of Nuclear and Physical Engineering, Faculty of Electrical Engineering and Information Technology, Slovak University of Technology, Ilkovičova 3, Bratislava, Slovakia*

Amorphous and nanocrystalline  $(\text{Fe}_{1-x}\text{Ni}_x)_{81}\text{Nb}_7\text{B}_{12}$  ( $x = 0, 0.25, 0.5, 0.75$ ) and Vitrovac alloys were studied by Mössbauer spectroscopy after neutron irradiation of fluency of  $10^{16} \text{ n/cm}^2$  and  $10^{17} \text{ n/cm}^2$ . From structure analyses we identified in nanocrystalline state ferromagnetic bcc-FeNi and fcc-FeNi phases and paramagnetic  $(\text{Fe-Ni})_{23}\text{B}_6$  phase. Neutron irradiation has an influence on the magnetic microstructure, which reflects at the Mössbauer parameters as a change in direction of net magnetic moment intensity and distribution of internal magnetic field. It was shown that the most sensitive parameters of Mössbauer spectra are the intensities of 2nd and 5th lines. Rather small changes were observed also in the case of internal magnetic field values. Our results showed that amorphous precursor exhibits more sensitivity to neutron irradiation influence than the nanocrystalline one. We observed radiation damage of crystalline components of nanocrystalline alloys and change of magnetic parameters. The results indicated at the changes of the microscopic magnetic parameters induced by neutron irradiation and their dependence at the neutron fluency and different iron and nickel content.

**COMPLEX SUPERSPIN DYNAMICS IN INTERACTING  $\text{Fe}_3\text{O}_4$  NANOPARTICLE SYSTEM**

V. Kusigerski, M. Perovic, V. Nikolic, A. Mrakovic, J. Blanus and V. Spasojevic  
*The "Vinca" Institute of Nuclear Sciences, University of Belgrade, POB 522,  
11001 Belgrade, Serbia*

Nanoparticle magnetite system has been synthesized by thermal decomposition of the iron (III) acetylacetonate complex in organic medium. HRTEM micrographs revealed that system consisted of 5 nm nanoparticles with narrow size distribution of  $\pm 1$  nm, and with a moderate particle agglomeration. SAED pattern was successfully indexed in SG Fd3m corresponding to  $\text{Fe}_3\text{O}_4$  oxide.

Comprehensive investigation of the system magnetic properties has been conducted by applying different DC and AC measurement protocols on the SQUID-based magnetometer (QD MPMS XL-5). Relatively narrow zero field cooled (ZFC) magnetization maximum located at  $T_m = 34$  K possesses properties typical of interacting nanoparticle system, such as nonlinear dependence of the peak position vs. applied field, and small shift of the peak position with AC field frequencies. In addition, field cooled (FC) magnetization branch displays slow increase below  $T_m$  with the saturation tendency at the lowest temperatures, thus pointing to the possible superspin-glass (SSG) state of the system below  $T_m$ .

To gain the deeper insight into the nature of the magnetic state below  $T_m$  we have investigated magnetic dynamics by performing different memory, ageing and cycling experiments. Although the obtained results possess many features that point to interacting superspins in the whole temperature interval below  $T_m$ , we have obtained typical fingerprint of the magnetically frozen state (SSG) only at temperatures below 10 K, since a waiting-time  $t_w$  dependent dip in ZFC magnetization was present at temperatures below 10 K, and absent at higher temperatures. Additional hint on the frozen state below 10 K was given by a drop in ZFC magnetization relaxation in field during the temperature quench in the 10 K  $\rightarrow$  5 K  $\rightarrow$  10 K cycle, while its increase was recorded during cycles performed at temperatures above 10 K. Results gathered in this investigation point to a presence of complex superspin dynamics below  $T_m$ , and the quest for the adequate explanation of this behavior is still in progress.

## AGING AND MEMORY EFFECTS IN TEMPERATURE CYCLING EXPERIMENTS ON SUPER SPIN GLASS NANOPARTICLE LCMO SYSTEM

M. Perovic, V. Kusigerski, J. Blanus, A. Mrakovic and V. Spasojevic  
*Laboratory for Condensed Matter Physics, The 'Vinca' Institute of Nuclear Sciences, University of Belgrade, P.O.BOX 522, 11001 Belgrade, Serbia*

Within the comprehensive investigation of spin-glass like  $\text{La}_{0.7}\text{Ca}_{0.3}\text{MnO}_3$  (LCMO) nanoparticle system [1-4], the nature of low-temperature collective state was studied by employing temperature cycling protocols for measurement of thermoremanent (TRM) magnetization.

The experimental procedure consisted of the following steps: (1) sample cooling in constant low magnetic field from high temperature ( $T > 4T_{\text{SSG}}$ ) to the measuring temperature  $T_1$  ( $T_1 < T_{\text{SSG}}$ ), (2) setting the magnetic field to zero (3) aging during time period  $t_{w1}$ , (4) subsequent quench for  $\Delta T$  to  $T_2$  ( $T_2 < T_1$ ), (5) aging during time period  $t_{w2}$ , (6) reheating to the temperature  $T_1$  and (7) aging during time period  $t_{w3}$ . Relaxation of TRM magnetization was recorded during the each aging period.

Investigation showed that the occurrence of nonequilibrium collective phenomena such as aging and memory effects were significantly affected by different temperature steps  $\Delta T$  used in cycling protocols. The presence of aging and memory phenomena is expected for SSG nanoparticles regarding the fact that system behaviour is strongly dependent on magnetothermal history. Surprisingly, the cycling experiment showed that for certain temperature window, memory effect vanished and independent aging evolutions appeared at different temperatures.

A framework for explanation of these effects was proposed within droplet and hierarchical spin glass models.

- [1] Spasojevic V, Mrakovic A, Perovic M, Kusigerski V and Blanus J 2011 *J. Nanopart. Res.* **13** 763
- [2] Perovic M, Mrakovic A, Kusigerski V, Blanus J and Spasojevic V 2011 *J. Nanopart. Res.* **13** 6805
- [3] Perovic M, Mrakovic A, Kusigerski V, Blanus J and Spasojevic V 2012 *Mat. Chem. Phys.* **136** 196
- [4] Perovic M, Kusigerski V, Spasojevic V, Mrakovic A, Blanus J, Zentkova M and Mihalik M 2013 submitted to *J. Phys. D: Appl. Phys.*

**ADVANCED METHOD FOR MAGNETIC MICROWIRES NOISE SPECIFICATION**

D. Praslička<sup>1</sup>, M. Šmelko<sup>1</sup>, J. Blažek<sup>1</sup>, J. Hudák<sup>1</sup>, P. Lipovský<sup>1</sup> and N. Flachbart<sup>1</sup>

<sup>1</sup>*Department of Aviation Technical Studies, Faculty of Aeronautics, Technical University of Košice, Rampová 7, 041 21 Košice, Slovakia*

Magnetic measurements are nowadays more and more influenced by ambient electromagnetic noise. There are many sources of ambient noise and they vary from power line noise, radio-frequency noise, vibrations, geomagnetic and atmospheric phenomena etc. This noise, deterministic and stochastic, can distort the precise measurement either partially or even completely.

The article points to the effects of the noise and its possible influences on quantification of inherent switching field noise of magnetic microwires. Let's note that the switching field is a carrier of several physical quantities and its inherent noise is a limiting factor in sensor applications. Hence, during the quantification of inherent material noise the decomposition of noise origins and monitoring of the magnetic environment during measurement together with recording of physical conditions as for example temperature or measurement duration is essential. Presented results of short-term and long-term measurements highlight the need to pay attention to the noise ratio in the workplace. Identified interference can reach amplitudes up to the 400 nT so measuring of weak fields is therefore particularly critical.

Based on the observed effects, advanced methodology was developed to quantify the impact of the ambient noise. During measurements a multi-channel system with applied correlation methods was used. The proposed method determines the percentage contribution of the ambient noise variance to the magnetic microwires switching field noise.

*This work was supported by the Slovak Research and Development Agency under Contract No. APVV 0266-10.*



**AC MAGNETIC FIELD EFFECT ON THE COMPLEX PERMEABILITY SPECTRA OF SOFT MAGNETIC  $\text{Fe}_{73}\text{Cu}_1\text{Nb}_3\text{Si}_{16}\text{B}_7$  POWDER CORES**J. Füzér<sup>1</sup>, S. Dobák<sup>1</sup> and J. Füzérová<sup>2</sup><sup>1</sup>*Department of Condensed Matter Physics, Institute of Physics, Faculty of Science, P. J. Šafárik University, Park Angelinum 9, 041 54 Košice, Slovakia*<sup>2</sup>*Faculty of Mechanical Engineering, Technical University, 042 00 Košice, Slovakia*

Soft magnetic powder cores of amorphous and nanocrystalline alloys are well-known ferromagnetic materials with excellent soft magnetic properties, e. g., high permeability, low coercivity and low core loss. Powder cores offer prospective supersession of traditional ferrite materials and electrical steels in high-frequency electromagnetic applications.

In this work, two soft magnetic  $\text{Fe}_{73}\text{Cu}_1\text{Nb}_3\text{Si}_{16}\text{B}_7$  powder core samples were investigated. Samples were prepared by a milling of amorphous  $\text{Fe}_{73}\text{Cu}_1\text{Nb}_3\text{Si}_{16}\text{B}_7$  ribbon at different temperature conditions: sample R by milling at room temperature and sample L by cryomilling at temperature of liquid nitrogen.

Influence of applied exciting ac magnetic field with various amplitudes was studied on the complex permeability spectra. For very small amplitude of applied ac magnetic field, the real part of complex permeability of the sample L shows a low-frequency plateau, which is associated with reversible bulging of domain walls pinned at the original pinning sites in the material. This behaviour is caused by the elastic deformation of domain walls around their equilibrium positions under the “pressure” of the ac magnetic field. On the contrary, the real part of complex permeability of the sample R decreases relatively steeply, but its static value is approximately four times higher than for the sample L. However, as the amplitude of ac magnetic field increases, a decreasing frequency dependence of real parts of complex permeability of both samples is observed in the whole measured frequency band and their static values increases. The relaxation frequency of the sample R shifts toward lower values with increasing of the amplitude of applied ac magnetic field. A similar behaviour is observed for the sample L. The decrease of the relaxation frequency could reflect the decrease in pinning force to hinder the domain wall movement and the relaxation phenomenon occurs earlier with the increasing of the amplitude of the ac magnetic field.

# MAGNETIC PROPERTIES OF YTTRIUM-SUBSTITUTED NiZn FERRITES

V. Jančárik<sup>1</sup>, E. Ušák<sup>1</sup>, M. Šoka<sup>1</sup> and M. Ušáková<sup>1</sup>

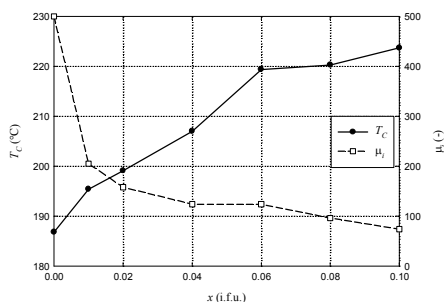
<sup>1</sup>*Institute of Electrical Engineering, Faculty of Electrical Engineering and Information Technology, Slovak University of Technology, Ilkovičova 3, 812 19 Bratislava, Slovakia*

NiZn ferrites still belong to of interesting magnetic materials for high-frequency applications thanks to their relatively high initial permeability and low power losses. The substitution and, consequently, the chemical composition yield changes of ferrite structure. Several substitutions by rare-earth ions are made to improve magnetic and structural properties of these ferrites. They are affected by chemical composition, i.e. type and amount of the substituent, as well as sintering conditions, grain size, impurities and the preparation procedure.

Polycrystalline NiZn ferrite substituted with a small content of  $Y^{3+}$  ions of composition  $Ni_{0.42}Zn_{0.58}Y_xFe_{2-x}O_4$ , where  $x = 0.00, 0.01, 0.02, 0.04, 0.06, 0.08$  and  $0.10$  was analysed. Specimens were prepared by the ceramic technology with reaction temperature of  $1200^\circ\text{C}$ .

Thermo-magnetic analysis and evaluation of hysteresis loops parameters were chosen as main examination methods in this study. Temperature dependence of initial susceptibility  $\chi(T)$  is very sensitive to phase composition and presence of chemical impurities. Moreover, it indicates the thermal stability of prepared ferrite materials. Various parameters, such as e.g. Curie temperature  $T_C$ , coercive field  $H_C$ , remanent magnetic flux density  $B_r$ , hysteresis loop area and amplitude permeability were studied at low frequencies.

Curie temperature increases almost linearly, whereas a strong drop of initial permeability appears at room temperature even for a small amount of  $Y^{3+}$  ions substitution (see figure).



**IMAGING OF MAGNETIC DOMAINS AND DOMAIN WALLS IN SPHERICAL Fe-Si POWDER USING MAGNETIC FORCE MICROSCOPY**M Strečková<sup>1</sup>, M. Bařková<sup>2</sup>, I Bařko<sup>2</sup>, H. Hadraba<sup>3</sup>, R. Bureř<sup>1</sup><sup>1</sup>*Institute of Materials Research, Slovak Academy of Sciences, Watsonova 47, 043 53 Kořice, Slovak Republic*<sup>2</sup>*Institute of Experimental Physics, Slovak Academy of Sciences, Watsonova 47, 043 53 Kořice, Slovak Republic*<sup>3</sup>*Institute of Physics of Materials, Academy of Sciences of Czech Republic, řiřkova 22, 616 62 Brno, Czech Republic*

The commercial Fe-Si powder, produced by Högānas Corporation, represents promising soft magnetic material for technological applications. The powder contains spherical particles having diameter about 150  $\mu\text{m}$ . Internal microstructure of the powder consists of grains of diameter about 30  $\mu\text{m}$ . Each separate grain has a random orientation of the easy magnetization axis and is sufficiently large to split into several magnetic domains. The standard powder metallurgical process of the Fe-Si powder requires a thermal treatment, which consequently leads to an internal recrystallization of the original grains. The present work takes advantage of the magnetic force microscopy (MFM) for imaging the magnetic domains and domain walls of the original Fe-Si powder and the Fe-Si powder annealed at 500°C in protective He atmosphere. A comparative study of the AFM topography and the corresponding MFM images was employed in order to examine the correlation between the grain size, grain orientation and characterization of the magnetic domains, which gives us an important knowledge for further utilization of the spherical Fe-Si particles in electrotechnical industry. The grain size and crystallographic orientation of grains before and after heat treatment were analyzed by the electron backscatter diffraction (EBSD) technique. The annealing process led to recrystallization of grains constituting the particles. Recrystallized grains had slightly smaller size about 20  $\mu\text{m}$ . No preferential crystallographic orientation of the grains was found both in as-received state and after annealing. The MFM images of the original (non-annealed) Fe-Si particles serve in evidence of a presence of various kinds of domain structures and domain walls. Contrary to this, the MFM imaging of the annealed Fe-Si particles imply predominantly stripe and meander domain structures, which arise mainly because of different grain size after the recrystallization of the Fe-Si particles.

**NANOSTRUCTURED  $\alpha$ -Fe LAYER SYNTHESIZED BY A PECVD METHOD AND EXAMINED WITH MÖSSBAUER SPECTROMETRY**B. David<sup>1</sup>, O. Schneeweiss<sup>1</sup>, A. Rek<sup>2</sup>, V. Kudrle<sup>3</sup> and O. Jašek<sup>3,4</sup><sup>1</sup>*CEITEC IPM, Institute of Physics of Materials, ASCR, v.v.i.,**Žitkova 22, CZ-61662 Brno, Czech Republic*<sup>2</sup>*Institute of Scientific Instruments, ASCR, v.v.i., Královopolská 147, CZ-61264 Brno, Czech Republic*<sup>3</sup>*Department of Physical Electronics, Faculty of Science, Masaryk University, Kotlářská 2, CZ-61137 Brno, Czech Republic*<sup>4</sup>*CEITEC MU, Central European Institute of Technology, Masaryk University, Kamenice 753/5, CZ-62500 Brno, Czech Republic*

We have used low-pressure microwave plasma for the synthesis of nanostructured  $\alpha$ -Fe layers, which were deposited on a glass substrate immersed in Ar plasma. Iron pentacarbonyl  $\text{Fe}(\text{CO})_5$  was flown over the substrate and its decomposition resulted in the formation of a few micrometers thick nanostructured layer. The deposition pressure was 2 kPa and the deposition time was 60 seconds. The synthesized samples were studied with XRD, SEM and EDAX. In the XRD pattern only  $\alpha$ -Fe phase was observed with the mean crystallite size of 14 nm which was subsequently confirmed by TEM. The  $\alpha$ -Fe sextet dominated the transmission Mössbauer spectrum (taken at 5 K) and a surprisingly low amount of iron oxide phases was present (about 1% of the whole spectrum area). The layer was very weakly oxidized. The remaining 4 sextets ( $16 \text{ T} < B_{\text{HF}} < 38 \text{ T}$ ) needed to fit the spectrum properly were ascribed to the surfaces/interfaces of the  $\alpha$ -Fe nanograins inside the layer.

**NANOSCALE FRACTURE MORPHOLOGIES OF SOFT MAGNETIC CoFeTaB AMORPHOUS ALLOY**

J. Miskuf, K. Csach, A. Juríková

*Institute of Experimental Physics, Slovak Academy of Science, Watsonova 47, 040 01 Košice, Slovakia*

The metallic glass  $\text{Co}_{43}\text{Fe}_{20}\text{Ta}_{5.5}\text{B}_{31.5}$  is characterized by excellent soft magnetic properties (low coercivity, ultra-high permeability) and high corrosion resistance. The main limitation for their application is the large brittleness under an external loading. Fundamental understanding of the deformation and fracture mechanisms in various bulk metallic glasses has motivated numerous experimental investigations. In this work we analyzed the failure characteristics of ultra-high strength  $\text{Co}_{43}\text{Fe}_{20}\text{Ta}_{5.5}\text{B}_{31.5}$  metallic glass at the room temperature. The bulk samples (cylinders with diameter of 2 and 3 mm) were deformed in compression, whereas the ribbons (30  $\mu\text{m}$  thick) were tested under a uniaxial tension. Co-based glass often breaks into small particles or powder, exhibiting a fragmentation mode. The river-like pattern with fine dimples was observed on the fracture surface. At low deformation rate, the high stored elastic energy is released and the failure process occurs by the fragmentation producing a lot of fine fragments with an accompanying sound effect. On the microscale the fracture surface consists of the smooth mirror cleavage zone and the river pattern zone. The nanosized dimples are arranged in lines respecting the periodic corrugation zones perpendicular to the crack propagation direction. The samples in bulk and ribbon forms have a large difference in the free volume amount due to the difference in the cooling rate. For both, the bulk and the ribbon samples, the oscillation on the fracture surface have the period under 100 nm. The period of oscillation does not depend on the structure (free volume amount) of the material, only small influence on the striation period decreasing was observed as the crack propagation rate increases.

**Acknowledgement**

*This work was supported by the Slovak Academy of Sciences – project VEGA No.0185/11, the Slovak Research and Development Agency – contract No.APVV-0171-10 and by the implementation of the project No.26220120021 provided by the European Regional Development Fund.*

**INFLUENCE OF PLASTIC DEFORMATION ON DEVITRIFICATION OF  $\text{Fe}_{73.5}\text{Nb}_3\text{Cu}_1\text{Si}_{13.5}\text{B}_9$  AMORPHOUS ALLOY**

K. Csach, J. Miskuf, A. Juríková

*Institute of Experimental Physics, Slovak Academy of Science, Watsonova 47, 040 01 Košice, Slovakia*

The amorphous alloy of the nominal composition  $\text{Fe}_{73.5}\text{Nb}_3\text{Cu}_1\text{Si}_{13.5}\text{B}_9$  was found to be a representative precursor for nanocrystalline soft magnetic materials prepared by the crystallization in the solid state. Thermomagnetometry revealed the Curie transition in the amorphous state was below the crystallization temperature. Under the subsequent heating, the crystallization of the Fe-Si nanosized particles causes the increase in the magnetization. Under the cooling, the partially crystallized amorphous alloy saves its magnetic nature. It was shown that the intensive plastic deformation localized into adiabatic shear bands causes the intensive heating and some structural changes in the amorphous alloy. During the ball milling the present extreme plastic deformation tends to the crystallization of the amorphous structure. The influence of the plastic deformation of the amorphous Finemet alloy deformed by the bending and the simulated shot peening on the devitrification of amorphous structure were studied.

***Acknowledgement***

*This work was supported by the Slovak Academy of Sciences – project VEGA No.0185/11, the Slovak Research and Development Agency – contract No.APVV-0171-10 and by the implementation of the project No.26220120021 provided by the European Regional Development Fund.*

**PULSE HEAT TREATMENT OF FINEMET ALLOYS UNDER TENSION**

A. Lovas<sup>1</sup>, L. Hubáč<sup>2</sup>, L. Novák<sup>2</sup>

<sup>1</sup>*Department of Automobiles and Vehicle, Budapest University of Technology and Economics, Stoczek u. 2. 1111., Hungary*

<sup>2</sup>*Department of Physics, Technical University of Košice, Park Komenského 2, 042 00 Košice, Slovakia*

The nanocrystallization from FINEMET-type amorphous precursors opens a wide-range possibility for the property-tailoring in soft magnetic alloys. Not only the exceptional magnetic softness (minimization of coercive force ( $H_c$ ), efficient lowering of power loss ( $P$ ), but the shape of magnetization curve can easily be altered in these alloys by applying appropriate field and stress annealings. In the large scale (industrial) production, the traditional crystallization heat treatments are applied (often in magnetic field).

In this contribution two, less common experimental parameters are simultaneously applied for the magnetic property tailoring: electrical pulse heating and, longitudinal mechanical stress. (along the ribbon length) The stress annealing was carried out under protecting atmosphere in a vertical tube furnace by applying a weight at the free, cold bottom end of the ribbon.

In these circumstances neither final concentration, nor grain-size distribution are developed in the period of thermal decomposition. Nevertheless, significant flattening of the magnetization curve is experienced, due to the stress-induced atomic pair ordering.

# **INFLUENCE OF TEMPERATURE ON MAGNETIC AND STRUCTURAL PROPERTIES OF NANOCRYSTALLINE COMPOSITE BASED ON MAGNETIC PEROVSKITE**

T.V. Kalmykova<sup>1</sup>, S.I. Tarapov<sup>1</sup>, V.N. Krivoruchko<sup>2</sup>

<sup>1</sup>*Institute of Radiophysics and Electronics NAS of Ukraine 12 Ac. Proskura st., Kharkov, 61085, Ukraine*

<sup>2</sup>*Donetsk Physics & Technology Institute NAS of the Ukraine, 72 R.Luxemburg St., 83114 Donetsk, Ukraine.*

The steady interest to study magnetic and electromagnetic properties of manganites perovskites, with the general formula  $\text{La}_{1-x}\text{A}_x\text{MnO}_3$ , where the A-alkaline or alkaline-earth element, is called by colossal magnetoresistance (CMR) effect, which occurs in these structures. A lot of experimental and theoretical researches in this area directed to study the possibilities of desing the data recorders and data readers, high-sensitive sensors of magnetic field, etc..

In this work we describe the interaction of microwave field of the millimeter waveband with samples, composites containing submicron  $\text{Y}_1\text{Ba}_2\text{Cu}_3\text{O}_{7-x}$  powder and  $\text{La}_{0.7}\text{Sr}_{0.3}\text{MnO}_3$  (LSMO) nanoparticles (about 20–30 nm in size) have been produced. Samples differ by the contents of component s as well as by the manufacturing technique of these samples. Samples #1 and #2 are made by of static pressure technique, and #3 is made by the sintering at  $T=650^\circ\text{C}$ . Measurements were carried out at temperature  $T=4.2\text{ K}$  in the frequency range 68 - 80 GHz.

It was shown that with temperature falling down towards helium ones, the peak of electron magnetic resonance (detected experimentally) broadens twice in comparison with peak obtained at room temperature. The sufficient variation of the spectroscopic splitting factor with temperature has been is revealed. The analysis of the possible reasons of such variation and the most likely reasons of temperature variation of the magnetic phase structure is presented in the given report.



**AMORPHOUS SOFT MAGNETIC  $\text{Fe}_{80}\text{B}_{11}\text{Si}_9$  ALLOY IN TENSILE STRESS SENSORS APPLICATION**J. Salach<sup>1</sup>, D. Jackiewicz<sup>1</sup>, A. Bieńkowski<sup>1</sup> and R. Szewczyk<sup>2</sup><sup>1</sup>*Institute of Metrology and Biomedical Engineering, Warsaw University of Technology, sw. A. Boboli 8, 02-525 Warsaw, Poland*<sup>2</sup>*Industrial Research Institute for Automation and Measurements PIAP, Al. Jerozolimskie 202, 02-486 Warsaw, Poland*

Iron-rich amorphous alloys, such as  $\text{Fe}_{80}\text{B}_{11}\text{Si}_9$  alloy, exhibit high permeability and limited value of coercive force. As a result, such alloys are used as the cores of inductive components of switching mode power supplies, as well as the cores of power and current transformers. Moreover, the magnetic characteristics of iron-rich amorphous alloys change significantly under the influence of mechanical stresses. These changes may be so considerable due to the fact, that amorphous alloys do not have a crystalline structure. As a result, in the total balance of free energy of amorphous alloy sample the energy of magnetocrystalline anisotropy is absent. This leads to a high stress sensitivity connected with the fact that significant changes of magnetic properties are caused by even quite small stress induced magnetoelastic anisotropy energy.

Influence of compressive stresses on magnetic properties of  $\text{Fe}_{80}\text{B}_{11}\text{Si}_9$  amorphous alloy was elaborated previously. This paper presents the experimental results focused on the influence of tensile stresses on properties of the  $\text{Fe}_{80}\text{B}_{11}\text{Si}_9$  amorphous alloy, annealed without magnetic field, as well as in the field perpendicular to the direction of magnetization of the core. It is expected, that such thermo-magnetic treatment will reduce the magnetomechanical hysteresis, what is especially important in stress sensor-oriented applications.

In the magnetoelastic investigation the tensile stresses were applied to the ring core perpendicularly to the magnetizing field direction. Due to the fact, that cores with closed magnetic circuits were used, demagnetization energy in the core was negligible.

Results of investigation indicate a significant stress sensitivity of  $\text{Fe}_{80}\text{B}_{11}\text{Si}_9$  amorphous alloy. Moreover, thermo-magnetic annealing reduced the magnetoelastic hysteresis, what is especially important from the point of view of further practical application of  $\text{Fe}_{80}\text{B}_{11}\text{Si}_9$  amorphous alloy in magnetoelastic stress sensor development.

**EFFECTS OF CORE DIMENSIONS AND MANUFACTURING PROCEDURE ON FLUXGATE NOISE**M. Janošek<sup>1</sup>, J. Vyhnánek<sup>1</sup>, P. Butvin<sup>2</sup> and B. Butvinová<sup>2</sup><sup>1</sup>*Czech Technical University in Prague, Technická 2, 16627 Praha CZ*<sup>2</sup>*Institute of Physics, Slovak Academy of Sciences, Dubravská cesta 9, 84511 Bratislava SK*

The coupling of internal noise of the magnetic material to the noise of fluxgate sensors manufactured from that material is ruled according to commonly agreed practice by the so called demagnetizing factor of the probe. This factor can be altered by changing the geometry of the probe. For tape-wound ring-cores, core radius can be modified or the number of tape-turns can be altered. For ring-core and race-track geometries etched from tapes, changing the width of the annulus or stacking of the cores brings similar results. Effect of demagnetizing factor on noise was already proved by the authors for as-cast tape-wound ring cores. However modification of the dimensions brings problems for the tape-wound cores: they exhibit increased noise, if the bending radius of the tape is small, i.e. in small ring cores.

In this work, Co-Cr-Fe-B-Si metallic glass is used, with an average thickness of 20 $\mu$ m with tape widths of 2.6-mm (wound cores) and 20, respectively 40-mm (etched cores). For the tape-wound cores, the magnetoelastic effects can be evidently seen by using the same material for 12-mm and 50-mm diameter. From the B-H loops and measured fluxgate noise, it is evident that even for tapes with magnetostriction of  $\sim 1\text{E-}7$  this effect is present. As for the 2.6-mm tape width, the Co-Cr-Fe based metallic glass used, either as-cast or appropriately annealed, did not show any appreciable macroscopic heterogeneity, which otherwise causes poorly reproducible inhomogeneous magnetic anisotropy brought about by macroscopic stress between surfaces and interior of many Fe-based ribbons (e.g. Finemets). The absence of this heterogeneity in Co-Cr-Fe-B-Si has been verified by comparing hysteresis loops prior to and after surfaces removal when the ribbon thickness was reduced by 10 $\div$ 15 % (2 $\div$ 3  $\mu$ m).

The risk of macroscopic heterogeneity is seen to increase with tape width; this affects mainly the etched flat cores. Measures to avoid or reduce the impact of heterogeneity on flat core properties were taken and are discussed. The etched cores had the same dimensions as the tape-wound cores in order to compare the noise in fluxgate mode; the noise differences are yet to be discussed.

**MAGNETIC RELAXATIONS IN AMORPHOUS  $\text{Fe}_{61}\text{Co}_{10}\text{Y}_8\text{Zr}_1\text{B}_{20}$  ALLOY**

Paweł Pietrusiewicz<sup>1</sup>, Katarzyna Błoch<sup>1</sup>, Joanna Gondro<sup>1</sup>, Marcin Nabiałek<sup>1</sup>, Marcin Dośpiał<sup>1</sup>, Michał Szota<sup>2</sup>

<sup>1</sup> *Czestochowa University of Technology, Faculty of Materials Processing Technology and Applied Physics, Institute of Physics*

<sup>2</sup> *Czestochowa University of Technology, Faculty of Materials Processing Technology and Applied Physics, Materials Engineering Institute*

Effects of annealing treatment on the disaccommodation phenomenon of bulk amorphous alloys obtained by injection-casting method has been studied. The amorphous structure has been confirmed using X-ray diffractometer. The annealing process has been performed at temperature below crystallization temperature. For all samples in as-cast state and after heat treatment the disaccommodation curves has been determined. The susceptibility and its disaccommodation has been used for define thermal and time stability of magnetic properties in studied alloys. These data have also been used for determination of activation energy of elementary processes.

**TIME AND THERMAL STABILITY OF MAGNETIC PROPERTIES IN  $\text{Fe}_{61}\text{Co}_{10}\text{Y}_8\text{Nb}_1\text{B}_{20}$  BULK AMORPHOUS ALLOYS**

Katarzyna Błoch<sup>1\*</sup>, Joanna Gondro<sup>1</sup>, Paweł Pietrusiewicz<sup>1</sup>, Marcin Dośpiał<sup>1</sup>, Marcin Nabiałek<sup>1</sup>, Michał Szota<sup>2</sup>, Konrad Gruszka<sup>1</sup>

<sup>1</sup> *Czestochowa University of Technology, Faculty of Materials Processing Technology and Applied Physics, Institute of Physics*

<sup>2</sup> *Czestochowa University of Technology, Faculty of Materials Processing Technology and Applied Physics, Materials Engineering Institute*

The paper presents studies of time and thermal stability of magnetic properties in  $\text{Fe}_{61}\text{Co}_{10}\text{Y}_8\text{Nb}_1\text{B}_{20}$  bulk amorphous alloys. The investigated sample was prepared by suction-casting method in the form of plate. The structure was studied using X-ray diffractometry. It was found that alloy was amorphous in the as-cast state. The magnetic properties were determined using completely automated set up for measuring susceptibility and its disaccommodation. The disaccommodation curve was decomposed into three elementary processes, each of them was described by Gaussian distribution of relaxation times. From fit of theoretical curve the peak temperature, intensity at peak temperature, average activation energies, distribution parameter and pre-exponential factor of the Arrhenius law were determined. The obtained results indicate that the disaccommodation phenomenon in these samples is related with directional ordering of atom pairs near the free volumes.

**INFLUENCE OF ANNEALING BELOW THE CRYSTALLIZATION TEMPERATURE ON THE STRUCTURAL AND MAGNETIC PROPERTIES OF Fe-based AMORPHOUS ALLOY**

Michał Szota<sup>1,\*</sup>, Marcin Dośpiał<sup>2</sup>, Paweł Pietrusiewicz<sup>2</sup>, Marcin Nabiałek<sup>2</sup>, Konrad Gruszka<sup>2</sup>, Tomasz Kaczmarzyk<sup>2</sup>

<sup>1</sup> *Czestochowa University of Technology, Faculty of Materials Processing Technology and Applied Physics, Materials Engineering Institute*

<sup>2</sup> *Czestochowa University of Technology, Faculty of Materials Processing Technology and Applied Physics, Institute of Physics*

In amorphous materials, as the threshold of structure stability is treated the crystallization onset temperature above which in the amorphous material, occurs to the formation of heterogeneous grains. However, in the amorphous material can be also identified the presence of the so-called frozen nuclei, arisen during manufacturing. These nuclei have a major impact on the properties of amorphous alloys. The growth of the frozen nuclei is possible already below the crystallization onset temperature. The control of process of their growth allows to adjust the operating parameters e.g. magnetic one. Influence of a two-step isothermal annealing, below onset crystallization temperature (at 700 and 770K, respectively for 1 and 3.5 h), on structure and magnetic properties of Fe-based amorphous alloys.

## INFLUENCE OF THE MANUFACTURING METHOD ON MAGNETIZATION PROCESS OF $\text{Fe}_{61}\text{Co}_{10}\text{Y}_8\text{Mo}_1\text{B}_{20}$ BULK AMORPHOUS ALLOYS

Marcin Nabiałek<sup>1</sup>, Anna Dobrzańska-Danikiewicz<sup>2</sup>, Paweł Pietrusiewicz<sup>1</sup>, Marcin Dośpiał<sup>1</sup>, Michał Szota<sup>3</sup>, Joanna Gondro<sup>1</sup>, Sabina Lesz<sup>4</sup>

<sup>1</sup> *Czestochowa University of Technology, Faculty of Materials Processing Technology and Applied Physics, Materials Engineering Institute*

<sup>2</sup> *Silesian University of Technology, Faculty of Mechanical Engineering, Institute of Engineering Processes Automation and Integrated Manufacturing Systems*

<sup>3</sup> *Czestochowa University of Technology, Faculty of Materials Processing Technology and Applied Physics, Institute of Physics*

<sup>4</sup> *Silesian University of Technology, Faculty of Mechanical Engineering, Institute of Engineering Materials and Biomaterials*

The aim of the paper was to show the influence of the type of manufacturing method of bulk amorphous alloys on the magnetization processes. Samples in the form of plates were prepared by the injection or suction of liquid alloy into the copper mold. In order to determine the type and quantity of structural defects present in the bulk amorphous alloys, the indirect method i.e. the approach to the ferromagnetic saturation, was applied. Studies have shown the presence of point defects conglomerates, for both alloys. These defects were pinning sites of domain walls and their number had a direct impact on the coercivity. Alloy produced by suction-casting method, had the highest their number, and thus a higher coercivity value.

**CROSSOVER EFFECTS IN MAGNETIC PROPERTY CHANGES OF  $\text{Fe}(\text{SiB})_{25}$  AND  $\text{Fe}_x\text{Ni}_{80-x}(\text{SiB})_{20}$  GLASSES DURING STRUCTURAL RELAXATION AND HYDROGEN ABSORPTION**K. Bán<sup>1</sup>, J. Kovác<sup>2</sup> and A. Lovas<sup>1</sup><sup>1</sup>*Department of Automobiles and Vehicle Manufacturing, Budapest University of Technology and Economics, Stoczek u .2., 1111 Budapest, Hungary*<sup>2</sup>*Institute of Experimental Physics, Slovak Academy of Sciences, Watsonova 47, 040 01 Košice, Slovakia*

The interaction between relaxation kinetics and the H-absorption is investigated in the amorphous Curie point wandering and the permeability changes in  $\text{Fe}_{75}(\text{SiB})_{25}$  and  $\text{Fe}_x\text{Ni}_{40-x}(\text{SiB})_{20}$  glasses. Two relaxation types are applied: isotherm heat treatments at various temperatures, and low temperature storage at 77K. Saturation of electrochemical hydrogen absorption were performed subsequently the various isothermal heat treatments.

Both the structural relaxation and the H-absorption do contribute individually to the net thermal history of the glassy sample, resulting structural imprints in the glassy structure. The sign of Curie temperature shift due to the H-absorption can be identical, or even opposite compared to that caused by the irreversible structural relaxation. The absorption ability of H, as well as the desorption kinetic strongly depends on the previous relaxation history of the samples.

## INFLUENCE OF VITROPERM CONTENT ON THE ENERGY LOSSES IN COMPOSITE MATERIALS BASED ON THE MIXTURE OF TWO FERROMAGNETS

Z. Birčáková<sup>1</sup>, P. Kollár<sup>1</sup>, V. Vojtek<sup>1</sup>, R. Bureš<sup>2</sup> and M. Fáberová<sup>2</sup>

<sup>1</sup>*Institute of Physics, Faculty of Science, P. J. Šafárik University, 041 54 Košice, Slovakia*

<sup>2</sup>*Institute of Materials Research, Slovak Academy of Sciences, 040 01 Košice, Slovakia*

Soft magnetic composites (SMCs) have been used in various applications thanks to their useful properties like low core losses, isotropic magnetic properties and high electrical resistivity.

In this work we investigated samples consisting of mixture of commercially available materials: Somaloy® 700 iron based material provided by Höganäs AB, Sweden and Vitroperm® 800 amorphous alloy in the form of flakes provided by Vacuumschmelze, GmbH & Co. KG, Germany. The SMC samples were prepared by conventional powder metallurgy in the form of a ring by mixing weight fractions of polycrystalline iron based Somaloy powder with amorphous Vitroperm powder (5-50 %). Reference material was prepared from Somaloy® 700 powder by producer-developed technology.

The morphology of samples was documented using scanning electron microscopy. The dc and ac hysteresis loops (up to 100 Hz) were measured by fluxmeter-based hysteresisgraphs. Total losses were calculated directly from measured hysteresis loops.

Total energy losses were analysed into components: hysteresis losses, eddy current losses and anomalous losses. The hysteresis losses were obtained from dc measurements, the inter-particle eddy current losses were calculated using the measured value of electrical resistivity of each sample, the intra-particle eddy current losses were calculated in iron powder particles as well as in amorphous flakes and the anomalous losses were obtained by subtracting the components from total losses. All the components of losses were compared in relation to the Vitroperm to Somaloy ratio.

*This work was realized within the frame of the project, nanoCEXmat I. – Centre of excellence of progressive materials with nano and submicro structure ITMS 26220120019, which is supported by the Operational Program “Research and Development” financed through European Regional Development Fund.*



# EFFECT OF ANNEALING TIME ON STRUCTURE OF $\text{Fe}_{72.5}\text{Cu}_1\text{Nb}_2\text{Mo}_2\text{Si}_{15.5}\text{B}_7$ ALLOY

V. Nemečová<sup>1</sup>, V. Girman<sup>1</sup>, V. Hrabčáková<sup>1</sup>, Š. Michalík<sup>2</sup>, J. Bednarčík<sup>3</sup>, and P. Sovák<sup>1</sup>

<sup>1</sup>*Institute of Physics, P. J. Šafárik University, Park Angelinum 9, 041 54 Košice, Slovakia*

<sup>2</sup>*Institute of Physics of the ASCR, v. v. i., Na Slovance 2, 18221 Praha 8, The Czech Republic*

<sup>3</sup>*HASYLAB am DESY, Notkestrasse 85, D-22503 Hamburg, Germany*

The Fe-based amorphous and nanocrystalline alloys have been confirmed as excellent soft magnetic materials and therefore large interest has been devoted to them [1]. Amorphous ribbons of the chemical composition  $\text{Fe}_{72.5}\text{Cu}_1\text{Nb}_2\text{Mo}_2\text{Si}_{15.5}\text{B}_7$  were prepared by melt spinning technique. Vitroperm type soft magnetic materials with a small content of Mo were investigated in both as-prepared and nanocrystalline state. The aim of this work was to investigate the process of a primary crystallization. For that reason as-prepared specimens were isothermally annealed in vacuum at 520 °C in times 6, 15 and 150 minutes. Then the annealed samples were characterized by the transmission electron microscopy (TEM), X-ray powder diffraction (XRD) and differential thermal analysis (DTA).

The grain size distribution and an amount of crystalline phase were determined from TEM images. Amount of amorphous phase was reduced but average particle size was unchanged with increasing annealing time. DTA measurements showed that the first exothermic peak corresponding to the first crystalline temperature was diminished and the second crystalline temperature was moved to lower values with the increase of the annealing time. The reduced radial distribution function  $G(r)$  was calculated from TEM (Figure) and XRD diffraction patterns.  $G(r)$  obtained from TEM and XRD showed a good agreement.

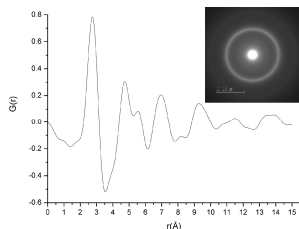


**Figure:** Electron diffraction pattern and radial distribution function of  $\text{Fe}_{72.5}\text{Cu}_1\text{Nb}_2\text{Mo}_2\text{Si}_{15.5}\text{B}_7$ .

*Acknowledgment: This work was realized within the frame of the project „Infrastructure Improving of Centre of Excellence of Advanced Materials with Nano- and Submicron-Structure“, which is supported by the Operational Program “Research and Development” financed through European Regional Development Fund.*

[1] McHenry M.E., Willard M.A., Laughlin D.E.: Amorphous and nanocrystalline materials for applications as soft magnets. Progress in Materials Science 44 1999, p. 291

**LOW FIELD MAGNETIC PROPERTIES OF FeCo-BASED ALLOYS**M. Hasiak<sup>1</sup>, M. Miglierini<sup>2,3</sup>, M. Łukiewska<sup>4</sup>, J. Kaleta<sup>1</sup>, J. Zbroszczyk<sup>4</sup><sup>1</sup>*Institute of Materials Science and Applied Mechanics, Wrocław University of Technology, Wrocław, Poland*<sup>2</sup>*Institute of Nuclear and Physical Engineering, Slovak University of Technology, Bratislava, Slovakia*<sup>3</sup>*Research Centre of Advanced Technologies and Materials, Palacky University, Olomouc, Czech Republic*<sup>4</sup>*Institute of Physics, Częstochowa University of Technology, Częstochowa, Poland*

Amorphous magnetic materials are very interesting because of their excellent soft magnetic properties. The role of small addition of Mo, Nb, Hf, Mn, and Ti on microstructure and magnetic properties has been reported in several papers. Partial replacement of Fe atoms by Co in NANOPERM-type alloys leads to changes both in the structures and in increase of magnetic inductions at elevated temperatures. The aim of this paper is to study low field magnetic properties of amorphous  $(\text{Fe}_x\text{Co}_{1-x})_{76}\text{Mo}_8\text{Cu}_1\text{B}_{15}$  alloys ( $x = 3, 6$  and  $9$ ). The samples were produced by a rapid quenching method on a single roller in a form of thin ribbons. The amorphicity of the alloys was checked at room temperature by X-ray diffractometry and Mössbauer spectroscopy in transmission geometry. Magnetic characterization of amorphous  $(\text{Fe}_x\text{Co}_{1-x})_{76}\text{Mo}_8\text{Cu}_1\text{B}_{15}$  alloys ( $x = 3, 6$  and  $9$ ) was done by investigations of magnetic after-effect, initial magnetic susceptibility, as well as tangent losses. The magnetic after-effect was investigated by decomposition of isochronal disaccommodation curves, which were constructed according to the formula:

$$\Delta(1/\chi) = 1/\chi_2 - 1/\chi_1 = f(T)$$

where:  $\chi_1$  and  $\chi_2$  are susceptibilities at times  $t_1 = 2$  s and  $t_2 = 120$  s after the demagnetization.

Using the lognormal distributions of relaxation times, the values of activation energies and pre-exponential factor in Arrhenius law were calculated. Moreover, the analysis of  $\Delta(1/\chi) = f(H)$  versus magnetic field amplitude was also accomplished. Others DC and AC magnetic characteristics were studied by VersaLab system and AMH-50K-S hysteresisgraph, respectively.

*This work was partially supported by the grants SK-PL-0032-12, VEGA 1/0286/12, CZ.1.05/2.1.00/03.0058, and CZ.1.07/2.3.00/20.0155.*

**EFFECT OF TEMPERATURE ON MAGNETIZATION PROCESSES IN RAPIDLY SOLIDIFIED FeSiB/CoSiB BILAYER RIBBONS**

M. Capik<sup>1</sup>, J. Marcin<sup>1</sup>, J. Kováč<sup>1</sup>, P. Švec Jr.<sup>2</sup>, D. Janičkovič<sup>2</sup>, P. Švec<sup>2</sup>,  
I. Škorvánek<sup>1</sup>

<sup>1</sup>*Institute of Experimental Physics, Slovak Academy of Sciences, Watsonova 47,  
040 01 Košice, Slovakia*

<sup>2</sup>*Institute of Physics, Slovak Academy of Sciences, Dúbravská cesta 9, 845 11  
Bratislava, Slovakia*

Magnetic bilayer systems are attracting a great deal of scientific interest from both fundamental and application points of view. The aim of this work is focused on the high temperature magnetic behavior of amorphous bilayer system composed of two ferromagnetic layers with markedly different magnetostriction values. Rapidly solidified bilayers consisting of Fe-Si-B and Co-Si-B layers have been prepared by planar flow casting from a single crucible with two nozzles close to each other and with a partition between them forming two separate vessels. Such an arrangement has allowed to obtain ribbons with two homogeneous layers, one on top of the other, along the whole ribbon length with high quality surface and with contact interlayer having submicron thickness. Ribbons with typical thickness of 45-50 microns and 6 mm width exhibited amorphous structure of both layers in as-quenched state. Temperature dependencies of magnetization and magnetic reversal process have been investigated in a wide temperature range covering the ferro-paramagnetic transitions and primary crystallization temperatures of both layers. The effects of interphase magnetic interactions arising from a presence of the positive and negative values of saturation magnetostriction constant in two mechanically interconnected soft magnetic layers resulted in a rounded shape of hysteresis loops at ambient temperatures. The loops became squared in a temperature range between the Curie temperature of two constituent layers, which points out the important role of magnetoelastic coupling in investigated bilayer ribbons. The observed features of magnetic behavior are discussed in view of the potential applications as sensor elements.

**MAGNETOIMPEDANCE EFFECT IN FIELD ANNEALED (FeNi)<sub>78</sub>Nb<sub>7</sub>B<sub>15</sub> AMORPHOUS AND NANOCRYSTALLINE RIBBONS**M. Varga<sup>1</sup>, J. Marcin<sup>1</sup>, M. Capik<sup>1</sup>, D. Janičkovič<sup>2</sup>, P. Švec<sup>2</sup>, I. Škorvánek<sup>1</sup><sup>1</sup>*Institute of Experimental Physics, Slovak Academy of Sciences, Watsonova 47, 040 01 Košice, Slovakia*<sup>2</sup>*Institute of Physics, Slovak Academy of Sciences, Dúbravská cesta 9, 845 11 Bratislava, Slovakia*

The giant magnetoimpedance effect (GMI) is attracting a great deal of scientific and technological interest because of its applications in sensing of magnetic field, current or stress. Extensive research activities in this area have been focused on the soft magnetic amorphous and nanocrystalline alloys in the form of ribbons and wires. In order to achieve the requested properties, these alloys often require specific annealing conditions. This work deals with the experimental study of the influence of longitudinal (LF) as well as transversal (TF) magnetic field annealing at various temperatures (from 673K to 773K) on the magnetoimpedance in (FeNi)<sub>78</sub>Nb<sub>7</sub>B<sub>15</sub> ribbons in the form of monolayers and bilayers. The maximum intensity of magnetic field applied during field annealing was 640kA/m. Reference samples were annealed in zero field (ZF). GMI characteristics were measured in the frequency range from 100 kHz up to 10 MHz.

The magnetoimpedance in bilayers after ZF - and LF - annealing show markedly higher values as compared their monolayer counterparts. The highest impedance ratio value,  $(\Delta Z/Z)_{\max}=72\%$ , was obtained in the (FeNi)<sub>78</sub>Nb<sub>7</sub>B<sub>15</sub> bilayer, after LF - annealing at 500°C, with maximum field sensitivity  $\eta_{\max}=12\%/Oe$ . The TF-annealing brings about well-defined two-peak character of the magnetoimpedance, which is connected with transverse domain structure. The observed field annealing sensitivity of the GMI response in investigated mono- and bilayer ribbons can be used for tuning of their characteristics for the potential sensing elements.

**MÖSSBAUER AND MFM INVESTIGATIONS OF SURFACE  
MAGNETISM IN NANOPERM NANOCRYSTALLINE ALLOYS**M. Miglierini<sup>1,2</sup> and M. Pavúk<sup>1</sup><sup>1</sup>*Institute of Nuclear and Physical Engineering, Slovak University of Technology,  
Ilkovičova 3, 812 19 Bratislava, Slovakia*<sup>2</sup>*Regional Centre of Advanced Technologies and Materials, Faculty of Science,  
Palacky University, 17. listopadu 12, 771 46 Olomouc, Czech Republic*

Nanocrystalline alloys are obtained by controlled annealing from amorphous precursors. The latter are usually prepared in the form of ribbons by rapid quenching on a rotating wheel. This preparation procedure leads to noticeable differences between the bulk and the surfaces of the ribbons. In addition, structural deviations are observed at the opposite sides of the ribbons.

This contribution reports on characterization of magnetic behaviour of  $^{57}\text{Fe}_{90}\text{Zr}_7\text{B}_3$  NANOPERM nanocrystalline alloys at their surfaces. We have employed surface sensitive analytical techniques. Conversion electron Mössbauer spectroscopy (CEMS) scans the surface regions down to the depth of about 200 nm whereas detection of conversion X-rays (CXMS) examines deeper regions to about 1 000 nm. To enhance the diagnostic potential we have used samples enriched to isotope  $^{57}\text{Fe}$ . The surface morphology was examined using tapping mode atomic force microscopy (AFM). Magnetic arrangement of the alloys' surfaces was described by magnetic force microscopy (MFM).

Using the above mentioned techniques, we can differentiate among contributions from structurally different regions in nanocrystalline alloys which are also different at both sides of the ribbon-shaped samples. Magnetic dipole interactions develop in the alloys when sufficient number of ferromagnetic nanograins is created after heat treatment. The air side of the ribbons, i.e. which was exposed to the surrounding atmosphere during the preparation, exhibits well developed magnetic domain patterns. This is also the side at which crystallization expands more rapidly than at the opposite, i.e. the wheel side of the ribbon.

*This work was supported by the research projects VEGA 1/0286/12, SK-PL-0032-12, CZ.1.05/2.1.00/03.0058, and CZ.1.07/2.3.00/20.0155.*

**TAILORING OF MAGNETOELASTIC ANISOTROPY IN RAPIDLY SOLIDIFIED ULTRATHIN AMORPHOUS WIRES**

T.-A. Óvári and H. Chiriac

*National Institute of R&D for Technical Physics, 47 Mangeron Boulevard, 700050 Iași, Romania*

Rapidly solidified glass-coated magnetic amorphous submicron wires and nanowires with metallic nucleus diameters from 100 to 950 nm and the glass coating from 1 to 50  $\mu\text{m}$  exhibit a suitable magnetic behavior for domain wall logic applications. The magnetoelastic anisotropy which results from the coupling between the mechanical stresses induced during their preparation and magnetostriction is the key towards understanding their magnetic behavior.

In this work we analyze the effect of wire dimensions (metallic nucleus diameter and glass coating thickness) on the magnetoelastic anisotropy of rapidly solidified glass-coated  $\text{Fe}_{77.5}\text{Si}_{7.5}\text{B}_{15}$  nanowires and submicron wires. Since magnetoelastic anisotropy has a radial distribution, we focused on its maximum value on the axial direction, given that axial internal stresses dominate on 80 to 95% of the nucleus diameter.

For a glass coating between 5 and 20  $\mu\text{m}$ , the influence of the glass thickness on the axial magnetoelastic anisotropy is virtually negligible, with only the metallic nucleus diameter affecting the magnitude of the anisotropy constant. For instance, the axial magnetoelastic anisotropy constant of a nanowire with a 100 nm nucleus diameter and a glass coating of 5  $\mu\text{m}$  is 151.5  $\text{kJ/m}^3$  and it changes to 151.49  $\text{kJ/m}^3$  for a glass coating of 20  $\mu\text{m}$  and the same nucleus diameter. For a glass thickness of 5  $\mu\text{m}$ , the anisotropy constant decreases from 151.5  $\text{kJ/m}^3$  to 65  $\text{kJ/m}^3$  for a metallic nucleus diameter increase from 100 nm to 950 nm. For thinner glass coating, the anisotropy decreases from 65  $\text{kJ/m}^3$  for the wire with a 950 nm metallic nucleus and 5  $\mu\text{m}$  glass coating to 59  $\text{kJ/m}^3$  for the same nucleus diameter and 1  $\mu\text{m}$  glass coating thickness, and further down to 52  $\text{kJ/m}^3$  for the same nucleus diameter and 0.5  $\mu\text{m}$  glass coating. This shows that thinning of the glass coating and even its full removal is an effective tool to decrease the magnetoelastic anisotropy in a controlled way.

The results show that an accurate control over the wire dimensions allow one to tailor their magnetoelastic anisotropy, and subsequently their magnetic behavior for domain wall logic applications.

*Work supported by the Romanian Ministry of National Education through projects PN 09-43 01 01 and PN-II-ID-PCE-2012-4-0424.*

**STUDY OF THE MAGNETIZATION PROCESSES IN AMORPHOUS AND NANOCRYSTALLINE FINEMET BY THE DECOMPOSITION OF THE HYSTERESIS LOOPS**J. Kováč<sup>1</sup>, L. Novák<sup>2</sup><sup>1</sup>*Inst. of Exp. Physics, Slovak Academy of Sciences, Watsonova 47,  
040 01 Košice, Slovakia*<sup>2</sup>*Department of Physics, Faculty of Electrical Engineering and Informatics,  
Technical University of Košice, Letná 9, 042 00 Košice, Slovakia*

The magnetization processes in amorphous and nanocrystalline FINEMET ribbons were studied by the decomposition of the quasi-static hysteresis loop to the contributions of the rotational magnetization (DR) the domain wall movement (DWM) and the domain wall annihilation and nucleation (DWAN) processes following the hyperbolic model of hysteresis. The hysteresis data measured during decreasing of the excitation magnetic field were used for the separation of these processes.

The significant differences in behavior of these two materials were found. The process of the domain wall annihilation is most dominant in the amorphous alloy. The domain wall movement is blocked in this material by internal stresses introduced during the process of preparation. On the contrary, this process - the domain wall movement - is markedly prevailing in nanocrystalline ribbon. In this material, the internal stresses are removed by thermal treatment. In addition, as it is well known, the magnetic anisotropy in nanocrystalline FINEMET reaches very low values. The result is that the DWM is energetically the most advantageous process to change magnetization in this material.

**RAYLEIGH REGION IN AMORPHOUS AND NANOCRYSTALLINE FINEMET ALLOY**

L. Novák<sup>1</sup> and J. Kováč<sup>2</sup>

<sup>1</sup>*Department of Physics, Technical University of Košice, Park Komenského 2, 042 00 Košice, Slovakia*

<sup>2</sup>*Inst. of Exp. Physics, Slovak Academy of Sciences, Watsonova 47, 040 01 Košice, Slovakia*

Magnetization processes in ferromagnetic materials can be described in four ways - reversible and irreversible domain wall motion, rotation of the vector of magnetic polarization and paraprocess in high magnetic fields. The process of reversible domain wall motion is characteristic for the range of small exciting magnetic fields - Rayleigh region. The results of magnetic measurements in this region obtained on the FINEMET samples are presented. The study is focused on the changes in the reversible domain wall motion due to the change of material structure after its transformation from amorphous to nanocrystalline state.

Besides magnetization processes in Rayleigh region full hysteresis loops for both amorphous and nanocrystalline samples were also measured. Processing of these measurements provides other magnetic parameters as coercivity, magnetoelastic anisotropy as well as thickness of domain walls. The comparison of magnetic properties of both types of samples can help to explain the different mobility of domain walls in Rayleigh region in amorphous and nanocrystalline materials.



**ISOBARIC THERMAL EXPANSION AND ISOTHERMAL COMPRESSION OF POWDERED NiFe BASED ALLOYS STUDIED BY IN-SITU EDX**

D. Olekšáková<sup>1</sup>, J. Füzér<sup>2</sup>, P. Kollár<sup>2</sup>, J. Bednarčík<sup>3</sup>, C. Lathe<sup>4</sup>

<sup>1</sup>*Department of Applied Mathematics and Informatics, Faculty of Mechanical Engineering, Technical University in Košice, Letná 9, 042 00 Košice, Slovakia*

<sup>2</sup>*Institute of Physics, Faculty of Science, P. J. Šafárik, Park Angelinum 9, Košice 04154, Slovakia*

<sup>3</sup>*HASYLAB am Deutschen Elektronen Synchrotron, DESY, Notkestrasse 85, D-22607 Hamburg, Germany*

<sup>4</sup>*Geo Forschungszentrum Potsdam at DESY/HASYLAB, Notkestrasse 85, D-22607 Hamburg, Germany*

The Ni-Fe based alloy system shows excellent soft magnetic properties and these alloys have been widely applied in the field of electronic devices and industry. Bcc structure dominates in the iron-rich range whereas fcc structure occurs in the nickel-rich one.

Mechanical milling is a useful technique that can produce a variety of equilibrium and non-equilibrium alloy phases leading to size reduction and particle shape modification. The advantage of this process technology is that the powder can be produced in large quantities and the processing parameters can be easily controlled. Some magnetic properties can be changed when the crystallite size is reduced, while the presence of stresses and defects introduced by mechanical milling and compaction impairs the magnetic property.

The aim of the present work was to study the isothermal compression and isobaric thermal expansion behaviour of ball-milled NiFe (81 wt. % of Ni) and NiFeMo (79 wt. % of Ni, 16 wt. % of Fe) alloy and follow its phase evolution when exposed to high pressure and temperature. In-situ pressure–temperature energy dispersive X-ray diffraction experiments were performed at the MAX80 instrument (beamline F2.1). The compressibility of NiFe alloy at 400 °C was evaluated for pressure values of up to 3.5 GPa. The EDX spectra revealed the presence of cubic FeNi<sub>3</sub> phase as determined from the shift of (111), (200) and (220) reflection lines in corresponding EDX spectra.

*This work was realized within the frame of the project, nanoCEXmat I. – Centre of excellence of progressive materials with nano and submicro structure ITMS 26220120019, which is supported by the Operational Program “Research and Development” financed through European Regional Development Fund.*

# STUDY OF LOCAL STRUCTURE OF AMORPHOUS ALLOY $\text{Fe}_{84}\text{B}_{16}$ BY ELECTRON AND X-RAY DIFFRACTION

V. Hrabčáková<sup>1</sup>, V. Girman<sup>1</sup>, K.B. Borisenko<sup>2</sup>, Š. Michalik<sup>3</sup>, V. Nemcová<sup>1</sup> and P. Sovák<sup>1</sup>

<sup>1</sup>*Department of Condensed Matter Physics, Institute of Physics, P.J. Šafárik University, Park Angelinum 9, 041 54 Košice, Slovakia*

<sup>2</sup>*Department of Materials, University of Oxford, Parks Road, Oxford, OX1 3PH, United Kingdom*

<sup>3</sup>*Institute of Physics of the ASCR, v. v. i., Na Slovance 2, 18221 Praha 8, The Czech Republic*

Metal-metalloid amorphous systems belong to often studied materials in last years because of their unique combination of mechanical, physical and magnetic properties and a number of possible technological applications [1]. Knowledge of their local atomic structure through radial distribution function is important for understanding changes in their properties with composition and preparation method and for improving the production technology.

Short range order in  $\text{Fe}_{84}\text{B}_{16}$  soft magnetic metallic glass was studied by pair distribution function  $G(r)$  calculated from electron and X-ray diffraction patterns. Sample was prepared by melt spinning technique in Ar atmosphere.

Pair distribution functions obtained from electron and X-ray diffraction patterns were compared and showed good agreement (see Fig.1) and atomic structure model have been constructed with using of Reverse Monte Carlo simulation from the obtained electron diffraction data.

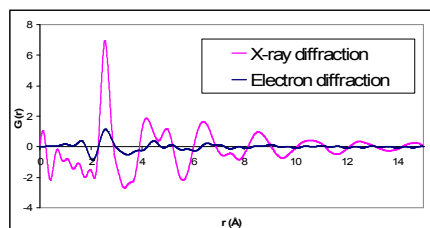


Fig.1: Comparison of pair distribution functions of  $\text{Fe}_{84}\text{B}_{16}$  calculated from X-ray and electron diffraction data.

*This work was realized within the frame of the project „Infrastructure Improving of Centre of Excellence of Advanced Materials with Nano- and Submicron- Structure“, which is supported by the Operational Program “Research and Development” financed through European Regional Development Fund.*

[1] McHenry M.E., Willard M.A., Laughlin D.E.: Amorphous and nanocrystalline materials for applications as soft magnets. Progress in Materials Science 44 1999, p. 291

## TENSILE STRESS AND TORQUE INFLUENCE ON THE MI EFFECT IN MULTILAYER MICROWIRES

F. Borza, S. Corodeanu, T.-A. Ovari, and H.Chiriac

*National Institute of R&D for Technical Physics, 700050 Iasi, Romania*

The deposition of nonmagnetic or magnetic materials on the glass-coated amorphous wires leads to changes in the magnetic behaviour of these materials due to the contribution of the nature of the deposited material and to the supplementary stresses induced by the deposited material.

Considering the importance of the role of internal stresses induced by the glass-coating and by the deposited metallic layer it is expected that the externally induced stresses (tension or torsion) will affect, at their turn, the magnetic behaviour of the composite magnetic multilayer microwires.

Amorphous  $\text{Co}_{68.5}\text{Fe}_{4.5}\text{Si}_{12.5}\text{B}_{15}$  glass-coated microwires with diameters of 23  $\mu\text{m}$  and the thickness of the glass cover of 14.5  $\mu\text{m}$  have been coated with Co layers with various thicknesses (125, 250, and 450 nm) by RF sputtering. Hysteresis loops and magneto-impedance (MI) measurements at 100 and 500 Hz have been performed in an applied field of up to 30 kA/m, under tension (up to 0.7 N) and torsion (up to 540 degrees).

After the deposition of Co layer on the as-cast microwires, the resulted CoFeSiB/Co composite multilayer microwires present a bi-phase behaviour as a result of the coupling between the ultra-soft magnetic phase of the amorphous CoFeSiB microwire and of the magnetic “harder” Co layer.

The tensile stresses applied along the wires' axis lead to the increase of the coercive field due to the magnetostatic coupling between the Co layer, with the crystallographic axis along the wire length, and the inner magnetic core. The MI response first increases slightly and then decreases drastically under tensile applied stresses, the effect being more pronounced for the measurements performed at 500 Hz. This behaviour can be related to the decrease of the penetration depth determined by the smaller transverse permeability in this area.

The application of torsional stresses leads to the deterioration of MI response due to the increase of the magnetoelastic anisotropy which affects the transverse susceptibility. A 45 degrees oriented helicoidal anisotropy is induced at the wire's surface which determines the decrease of permeability and consequently of the penetration depth.

*Work supported by the Ministry of Education and Research, NUCLEU Programme, Projects PN 09-43 01 01 and PN 09-43 02 03.*

**HYSTERESIS IN ASYMMETRICAL GMI EFFECT IN AMORPHOUS MICROWIRES**

J. Kravčák

*Department of Physics, Technical University of Košice, Park Komenského 2,  
042 01 Košice, Slovakia*

The double-peak behaviour of giant magneto-impedance (GMI) dependence on the external magnetic field strength  $H$  is observed in as cast glass-covered amorphous thin wire  $\text{Co}_{70.5}\text{Fe}_{4.5}\text{Si}_{15}\text{B}_{10}$  (microwire). The position of sharp peaks is symmetrical with respect to zero external magnetic field strength ( $H=0$ ) and corresponds to the anisotropy field  $H=\pm H_K$ . The maximum GMI ratio  $(\Delta Z/Z)_{\text{max}}$  dependence on the amplitude  $i_{ac}$  in the frequency range from 0.5 to 50 MHz is analyzed by means of the helical anisotropy ( $0<\alpha<90^\circ$ ) induced during preparation of the microwire. The additional dc bias current  $i_{dc}$  in the interval from 0 to 10 mA with variable  $i_{ac}$  is applied in order to achieve the asymmetrical GMI effect. The asymmetrical GMI dependences exhibit hysteresis which can be explained by an irreversible magnetization rotation at the ferromagnetic surface of the microwire.

**Fe/SiO<sub>2</sub>/RESIN SOFT MAGNETIC COMPOSITE POWDER MATERIALS PREPARED BY MIXING AND VACUUM/PRESSURE IMPREGNATION**M. Kabátová<sup>1</sup>, J. Füzér<sup>2</sup>, J. Füzérová<sup>3</sup>, E. Dudrová<sup>1</sup>, P. Kollár<sup>2</sup><sup>1</sup> *Institute of Materials Research, Slovak Academy of Sciences, Watsonova 47, 040 01 Košice, Slovak Republic*<sup>2</sup> *Institute of Physics, Faculty of Science, Pavol Jozef Šafárik University in Košice, Park Angelinum 9, 040 01 Košice, Slovak Republic*<sup>3</sup> *Institute of Special Technical Sciences, Department of Applied Mathematics, Faculty of Mechanical Engineering, Technical University of Košice, Letná 9, 042 00 Košice, Slovak Republic*

Fe/SiO<sub>2</sub>/resin soft magnetic composite (SMC) materials based on commercial iron powder with irregular and/or spherical shaped particles coated with sol-gel SiO<sub>2</sub> layer and/or with an addition of SiO<sub>2</sub> nano-particles were prepared. Resin (Shellac) was applied in two ways a) by mixing the Fe/SiO<sub>2</sub> powder with 1.0 wt.% of Shellac dissolved in ethylalcohol; after drying (RT, air) the mixture was compacted at 400-600 MPa into cylindrical samples and treated at 100°C in air, b) by vacuum/pressure impregnation (VPI) of low-temperature sintered Fe/SiO<sub>2</sub> cylindrical compacts with Shellac dissolved in ethylalcohol. VPI processing was performed in a steel container ( $\sim 10^{-2}$  kPa/15 min,  $\sim 500$  kPa/N<sub>2</sub>/15 min). The effect of the density, iron particle shape, method of introducing insulating layer (SiO<sub>2</sub>+Shellac) was microscopically evaluated and correlated with electrical resistivity and coercivity H<sub>c</sub>. The results showed that the integrity of electrical-insulating phase is controlled by the complex effect of micro-morphology iron particle surfaces and by the method of insulating layer creating. Using VPI method, the irregular surface of iron particles may result in local discontinuities of the insulating layer and thus in a low electrical resistivity. An addition of evenly distributed SiO<sub>2</sub> nanoparticles has a positive effect on elimination of Fe/Fe contacts. For vacuum/pressure impregnated composites based on spherical iron particles the insulating layer becomes continuous and well consistent with iron particles surface which results in a favorable combination of electrical resistivity and coercivity (780-1120  $\mu\Omega\text{m}$  and 177-290 A/m). For irregular shaped iron particles is preferably a mixing of the Fe+SiO<sub>2</sub> powder with Shellac. Electrical resistance of this material is higher (3700-10700  $\mu\Omega\text{m}$ ) but the value of coercivity (430 A/m) is also higher when compared with VPI processed material.

**INFLUENCE OF SLOW HEAVY ION IMPACT ON SURFACE TRANSFORMATION OF VP800 AMORPHOUS ALLOY**

R. Brzozowski, E. Frątczk, M. Antoszevska and M. Moneta

*Uniuersytet Łódzki, Wydział Fizyki Stosowanej*

*Pomorska 149, PL 90-236 Łódź, Poland*

Modification of surface properties of amorphous alloys under a single ion impact is related to thresholds, either in the potential energy - 10keV deposited by a highly charged ion (HCI) [1] or to the threshold in electronic energy loss - 5keV/nm transferred by a swift heavy ion (SHI) [2].

In this communication thin foils of VP800 ( $\text{Fe}_{73}\text{Si}_{16}\text{B}_7\text{Cu}_1\text{Nb}_3$ ) amorphous alloy [3] were irradiated with slow heavy ions (200 keV Ar) at very low doses varying from  $10^{10}$  to  $10^{13}$  Ar/cm<sup>2</sup>. With the use of *ex-citu* Mossbauer spectroscopy (CEMS) Fe and Fe(Si) clusters accompanied by  $\text{F}_3\text{Si}$  and even  $\text{Fe}_{23}\text{B}_6$  nano-crystals were found in the samples irradiated at lower doses  $10^{10}$  Ar/cm<sup>2</sup>, whereas rather amorphous structures can be found in samples more heavily implanted, at  $10^{13}$  Ar/cm<sup>2</sup>.

[1] A. S. El-Said et al, Phys. Rev. Lett. 100 (2008) 237601

[2] M. Toulemonde, C. Dufour, E. Paumier, Phys. Rev. B 46(1992)14362

[3] R. Brzozowski, M. Moneta, Nucl.Instr.Meth Phys.Res. B297 (2012) 208

**STRUCTURE OF IRON OXIDE NANOPARTICLES STUDIED  
BY  $^{57}\text{Fe}$  NMR**

P. Křišťan<sup>1</sup>, V. Chlan<sup>1</sup>, H. Štěpánková<sup>1</sup>, R. Řezníček, P. Görnert<sup>2</sup>, P. Payer<sup>2</sup>

<sup>1</sup>*Charles University in Prague, Faculty of Mathematics and Physics,  
V Holešovičkách 2, 18000, Prague 8, Czech Republic*

<sup>2</sup>*Innovent e.V. Technologieentwicklung, Prüssingstr. 27 B, D-07745 Jena,  
Germany*

Small particles of magnetic iron oxides are functional materials in various fields of technical and medical applications. Numerous preparation techniques are used to prepare magnetite/maghemite systems. The properties of the products are usually characterized by macroscopic magnetic methods, their composition and structure by X-ray diffraction. However the standard magnetic measurements do not offer detail information on magnetic sublattices and moreover they are hardly applicable for compound mixtures or inhomogeneous systems. X-ray diffraction is not able quite well distinguish magnetite from vacant magnetite or maghemite structure. Under these circumstances, application of hyperfine methods is worthwhile because of their microscopic insight into the studied systems. In this work we apply nuclear magnetic resonance (NMR) spectroscopy of  $^{57}\text{Fe}$  nuclei for investigation of submicron and nanocrystalline iron oxide materials.

The iron oxide particles studied in this work are obtained from ferrous hydroxide gels (prepared from  $\text{FeCl}_2$  and  $\text{KOH}$ ) by aging at elevated temperatures ( $90^\circ\text{C}$ ) with  $\text{KNO}_3$  as oxidant. For further investigation, samples of various particle sizes are used.  $^{57}\text{Fe}$  NMR spectra of the samples are measured in a wide temperature range (4.2–370 K) in zero external magnetic field. Signals of  $^{57}\text{Fe}$  nuclei assigned to tetrahedral and octahedral iron sites are well resolved. The NMR spectra and their temperature dependences are compared with those of magnetite single crystals (stoichiometric sample and sample with cation vacancies), as well as with bulk and nanoparticle samples of maghemite.

**HYPERFINE INTERACTIONS AND STRUCTURE  
OF NANOCRYSTALLINE MAGHEMITE**

Vít Procházka<sup>1</sup>, Helena Štěpánková<sup>2</sup>, Vojtěch Chlan<sup>2</sup>, Petr Křišťan<sup>2</sup>,  
Martin Hermanek<sup>1</sup>, Jiří Tuček<sup>1</sup>, Radek Zbořil<sup>1</sup>, Kateřina Poláková<sup>1</sup>, Jan Filip<sup>1</sup>,  
Josef Štěpánek<sup>2</sup>

<sup>1</sup>*Faculty of Science, Palacky University, Svobody 26, 771 46 Olomouc,  
Czech Republic*

<sup>2</sup>*Faculty of Mathematics and Physics, Charles University, V Holešovičkách 2, 180  
00 Prague 8, Czech Republic*

Maghemite ( $\gamma\text{-Fe}_2\text{O}_3$ ) is one of the four existing structural forms of  $\text{Fe}_2\text{O}_3$ . It exhibits a spinel structure as magnetite  $\text{Fe}_3\text{O}_4$ , but one sixth of the octahedral iron positions are vacant and therefore only ferric ( $\text{Fe}^{3+}$ ) cations are present for the exact  $\text{Fe}_2\text{O}_3$  stoichiometry. Ordering of vacancies on the octahedral sites in maghemite can induce lowering of the crystal symmetry. The local arrangement of vacancies is also supposed to influence the maghemite magnetic properties. There are no available common experimental techniques for direct determination of the vacancy distribution.  $^{57}\text{Fe}$  NMR spectra are, however, sensitive to the local surrounding of resonating nuclei. They can thus reflect the configuration of the vacancies providing a good spectral resolution is reached.

Two sample series of maghemite ( $\gamma\text{-Fe}_2\text{O}_3$ ) fine particles of average size of 3-10 nm were synthesized by thermal decomposition of either iron(II) oxalate dihydrate or iron(II) acetate dihydrate. The  $^{57}\text{Fe}$  NMR spectra were measured in the temperature range of 4.2-355 K in zero magnetic field and at the temperature of 4.2 K also in external magnetic field of 0-2 T. The spectra consisted of partly overlapped signals of iron nuclei in both tetrahedral (A) and octahedral (B) sites. The obtained spectral shapes depended on the preparation protocol including the temperature of decomposition. The dependence of the spectra on the temperature of measurement provided dependence of A and B sublattice magnetizations. Analysis of measurements in external magnetic field enabled unambiguous separation of A and B sublattice spectra. Resulting A and B spectral shapes were interpreted in terms of vacancy distribution in the vicinity of resonating nuclei.



**STRUCTURE AND PROPERTIES OF HYBRID COMPOSITES BASED ON TWO DIFFERENT FERROMAGNETS**

R. Bureš<sup>1</sup>, M. Fáberová<sup>1</sup>, M. Strečková<sup>1</sup>, P. Kollár<sup>2</sup>, J. Füzér<sup>2</sup>

<sup>1</sup>*Institute of Materials Research, Slovak Academy of Sciences, 040 01 Košice, Slovakia*

<sup>2</sup>*Institute of Physics, Faculty of Science, P. J. Šafárik University, 041 54 Košice, Slovakia*

Soft magnetic composites (SMC) are basically iron powder particles separated with an electrically insulated layer. The group of SMC-materials has been expanded by the introduction of new materials. These materials are based on high performance ferromagnetic particles and electric insulation without limitation to processing conditions.

The samples based on mixture of two commercially successful materials were prepared to study the influence of particle morphology on structure and properties of composite. Iron based SMC powder system Somaloy® 700 is produced by Höganäs AB, Sweden and flakes of Vitroperm® 800 is product of Vacuumschmelze, GmbH & Co. KG, Germany. Irregular spherical particles of Somaloy were mixed with 5-50 wt.% of Vitroperm flaky powder. Conventional powder metallurgy technology consists of cold pressing and heat treatment was used to prepare compact samples. Heat treatment in air and in protective atmosphere of argon was used to investigate the development of the structure and properties of the composites.

The microstructure and fractures of samples were investigated using light optical microscopy and scanning electron microscopy. Density was measured using He pycnometry. Mechanical, magnetic and electric properties were measured using standard methods. Properties of the composites were analysed in connection to structure and density. Topology of interphases and interparticle connection were documented by AFM technique. Magnetic properties measured at AC and DC magnetic field (hysteresis loops, coercivity and losses) and mechanical properties (Young modulus, hardness and flexural strength) were compared in relation to technology of compaction with goal to clear the process of densification of SMC materials consist of mixed morphology.

*This work was realized within the frame of the project, nanoCEXmat I, ITMS 26220120019, supported by the Operational Program "Research and Development" financed through European Regional Development Fund and under the project VEGA 2/0155/12.*

# STRUCTURE AND MAGNETIC PROPERTIES OF NANOCRYSTALLINE $\text{NiFe}_2\text{O}_4$ PREPARED VIA PRECIPITATION ROUTE

T. Žák<sup>1</sup>, B. David<sup>1</sup>, A. Čosović<sup>2</sup>, V. Čosović<sup>3</sup>, D. Živković<sup>4</sup>, N. Talijan<sup>3</sup>

<sup>1</sup>CEITEC IPM, Institute of Physics of Materials AS CR, v.v.i., Žitkova 22, CZ-616 62 Brno, Czech Republic

<sup>2</sup>Institute for Technology of Nuclear and Other Mineral Raw Materials, Franse d' Eperea 86, 11000 Belgrade, Serbia

<sup>3</sup>Institute of Chemistry, Technology and Metallurgy, University of Belgrade, Njegoševa 12, 11000 Belgrade, Serbia

<sup>4</sup>Technical Faculty in Bor, University of Belgrade, Vojske Jugoslavije 12, 19210 Bor, Serbia

As one of the most commonly used soft magnetic materials Nickel ferrites represent very important functional materials. Although synthesis of nanosized  $\text{NiFe}_2\text{O}_4$  has been extensively studied over the years, recent developments in nanotechnology have opened new research areas and widened their range of application, thus making investigation of alternative and innovative processing routes still current topic.

Nanocrystalline Ni-ferrite was synthesized by modified precipitation method in which soluble starch is used as dispersing agent and  $\text{Na}_2\text{CO}_3$  as a precipitating agent.  $\text{NiSO}_4 \cdot 6\text{H}_2\text{O}$  and  $\text{Fe}(\text{NO}_3)_3 \cdot 9\text{H}_2\text{O}$  were used as precursors for nickel and ferric oxide, respectively.

Taking into consideration direct relation between magnetic properties, structure and phase composition of nanocrystalline Ni-ferrites, obtained material was analyzed and discussed through structural, compositional and magnetic characterization. Formation of pure  $\text{NiFe}_2\text{O}_4$  phase with average crystallite size of 21 nm has been confirmed by X-ray diffraction analysis (XRD). Determined phase composition was additionally supported by results of  $^{57}\text{Fe}$  Mössbauer phase (MS) analysis and material's nanocrystalline structure by field emission scanning electron microscopy (FESEM). Thermomagnetic behaviour of the obtained nanocrystalline  $\text{NiFe}_2\text{O}_4$  was studied using measurement up to 800°C. The obtained room temperature magnetic hysteresis loop, measured on vibrating sample magnetometer (VSM), exhibits characteristic "S" shape of the soft magnetic material with values of magnetic properties within expected range for this type of material: coercivity of the order of  $10^1$  kA/m and the specific moment up to 40 Am<sup>2</sup>/kg.

**MAGNETIC PROPERTIES OF SOFT MAGNETIC FeSi COMPOSITE POWDER CORES**

M. Lauda<sup>1</sup>, J. Füzér<sup>1</sup>, J. Füzérová<sup>2</sup>, P. Kollár<sup>1</sup>, M. Strečková<sup>3</sup> and M. Fáberová<sup>3</sup>

<sup>1</sup>*Department of Condensed Matter Physics, Institute of Physics, Faculty of Science, P. J. Šafárik University, Park Angelinum 9, 041 54 Košice, Slovakia*

<sup>2</sup>*Faculty of Mechanical Engineering, Technical University, 042 00 Košice, Slovakia*

<sup>3</sup>*Institute of Materials Research, Slovak Academy of Sciences, 040 01 Košice, Slovakia*

Soft magnetic composites (SMC) challenge traditional materials such as soft magnetic ferrites and electrical steels in applications with alternating magnetic fields. Soft magnetic composites, which are used in electromagnetic applications, can be described as ferromagnetic powder particles surrounded by an electrical insulating film. New developments in magnetic materials and new production techniques make SMC material interesting for application in electrical machines.

FeSi powder was used as a base ferromagnetic material for a preparation of soft magnetic composites. The commercial FeSi particles of a precise spherical shape are available in two granulometric fractions (40  $\mu\text{m}$  -125  $\mu\text{m}$  or 60  $\mu\text{m}$  – 355  $\mu\text{m}$ ). The phenol-formaldehyde resin modified by SiO<sub>2</sub> nanoparticles was used as an electroinsulating layer. The FeSi particles covered by the synthesized resin were compacted at 800 MPa to the ring samples for magnetic measurements. The final samples were treated thermally under the curing schedule, which was suggested according to thermal degradation of the modified resin.

Magnetic properties measured at AC and DC magnetic field (hysteresis loops, coercivity and losses) and complex permeability spectra were compared in relation to the initial properties of FeSi powder with goal to clear the process of densification of SMC materials consist of different morphology.

*This work was realized within the frame of the project, nanoCEXmat I, ITMS 26220120019, supported by the Operational Program “Research and Development” financed through European Regional Development.*

**CHARACTERIZATION OF GLASS COATED MAGNETIC NANOWIRES BY UHR-TEM**

G. Ababei, L. Budeanu, G. Stoian, N. Lupu and H. Chiriac

*Department of Materials and Magnetic Devices, National Institute of Research & Development for Technical Physics, 47 Mangeron, 700050 Iasi, Romania*

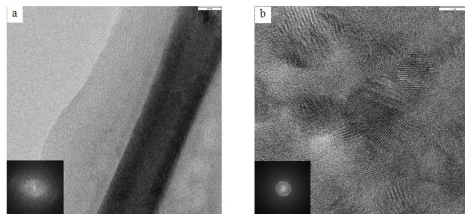
Glass-coated magnetic nanowires (GCNWs) are promising candidates for high frequency applications such as sensors, racetrack memory, magnetic domain wall logic devices, etc. GCNWs were obtained by rapid solidification with diameters of the metallic nucleus ranging from 180 nm to 900 nm and glass coating thickness of 1  $\mu\text{m}$  to 30  $\mu\text{m}$ .

When it's coming to the structural characterization of such tiny materials the conventional methods (e.g. XRD) are almost useless. A powerful method to acquire such information is the ultra-high resolution transmission electron microscopy (UHR-TEM). However, the quality of the TEM samples is critical in this case. The classical methods for the preparation of TEM samples, especially when they contain fiber/wires, imply more working steps such as resin embedding, ultrasonic cutting, dimpling and ion milling.

Because of the particular small size of our GCNWs as well as the presence of the glass coat, we adapted the classical TEM samples preparation techniques to answer to our needs.

First, the GCNW is fixed on both ends with resin on a TEM copper grid and the glass coat layer is then removed using a HF solution (10%) for 20 minutes. In the second step the metallic NW is polished by ion milling. By varying the energy and the angle of the ion beam we were able to obtain thin samples down to electron transparency.

UHR-TEM images were obtained with a LIBRA200MC microscope, with monochromator and image corrector (Cs) operated at 200 kV.



UHR-TEM images FINEMET nanowire with amorphous (a) and nanocrystalline (b) structure.

*Financial support from the NUCLEU Project PN 09-43 01 02 is highly acknowledged.*

**DOMAIN WALL PROPAGATION IN FINEMET NANOWIRES**

H. Chiriac, S. Corodeanu, M. Grigoras, G. Ababei, N. Lupu and T.-A. Óvári  
*National Institute of R&D for Technical Physics, 47 Mangeron Boulevard,  
 700050 Iasi, Romania*

$\text{Fe}_{73.5}\text{Cu}_1\text{Nb}_3\text{Si}_{13.5}\text{B}_9$  glass-coated nanowires and submicron wires with metallic nucleus diameters ( $\Phi_m$ ) between 100 and 500 nm and the glass coating thickness ( $t_g$ ) of 5  $\mu\text{m}$  were prepared using a modified Taylor technique. All samples were annealed in vacuum at 500, 550, 600 and 650 $^\circ\text{C}$ , respectively, for 60 min. The annealing was done in zero field by introducing the samples into the oven at the annealing temperature and taking them out of the oven after 60 min.

The domain wall velocity along the wire length was studied by using a modified Sixtus-Tonks (S-T) method specially designed in our lab for very thin samples. Domain wall shape has been studied using a recently developed simultaneous S-T and magneto-optical Kerr effect method (MOKE). The MOKE signal provides information about changes in the surface magnetization of wires, whilst the S-T one offers information about the wall propagation in their volume.

The domain wall velocity is generally small in the as-cast state and it increases significantly following the annealing performed to induce the nanocrystalline state, reaching values as high as 2,500 m/s. Annealing at larger temperatures leads to a decrease of the domain wall velocity due to the crystallization of the samples. The exact value of the annealing temperature (in the range 500 to 600 $^\circ\text{C}$ ) which corresponds to the maximum value of the domain wall velocity depends on the sample diameter.

The investigation of the domain wall shape with respect to the propagation direction shows that the wall propagates with a different velocity in the middle of the wire as compared to the surface, displaying a curvature which indicates a delay in the surface velocity. The curvature decreases following the annealing for nanocrystallization. This behavior is linked to the different evolutions of the nanocrystalline phase in the middle of the wire as compared to its surface. Ultra-high resolution transmission electron microscopy (UHR-TEM) studies have emphasized the formation of the nanocrystalline phase and its evolution to be in agreement with the observed magnetic behavior of the investigated samples.

*Work supported by the Romanian Ministry of National Education through project number PN 09-43 01 01 (NUCLEU Programme).*

## MAGNETIC PROPERTIES AND GIANT MAGNETOIMPEDANCE IN AMORPHOUS AND NANOCRYSTALLINE MICROWIRES

A. Talaat<sup>1</sup>, V. Zhukova<sup>1</sup>, M. Ipatov<sup>1</sup>, J. M. Blanco<sup>2</sup>, M. Churyukanova<sup>3</sup>, S. Kaloshkin<sup>3</sup>, E. Zamiatkina<sup>3</sup>, E. Shuvaeva<sup>3</sup>, L. Gonzalez-Legarreta<sup>4</sup>, B. Hernando<sup>4</sup> and A. Zhukov<sup>1,5</sup>

<sup>1</sup>*Dpto. Física de Materiales, UPV/EHU, 20018 San Sebastian, Spain*

<sup>2</sup>*Dpto. de Física Aplicada, EUPDS, UPV/EHU, 20018, San Sebastian, Spain*

<sup>3</sup>*National Univer. of Science and Technology «MISIS», Moscow, 119049, Russia*

<sup>4</sup>*Dpto de Física, Universidad de Oviedo, Calvo Sotelo s/n, 33007 Oviedo, Spain*

<sup>5</sup>*IKERBASQUE, Basque Foundation for Science, 48011 Bilbao, Spain*

Ferromagnetic wires (diameters 5-120  $\mu\text{m}$ ) gained considerable interest owing to their good soft magnetic properties and giant magneto-impedance, GMI, effect. Latest development of industrial applications required miniaturization of the magnetic sensors. Therefore reduction of diameters of magnetically soft wires is one of the priority tasks in the field of applied magnetism. Consequently soft magnetic wires with reduced dimensionality and outstanding magnetic characteristics, such as glass-coated microwires with thin diameters (between 1-40  $\mu\text{m}$ ) recently gained much attention. The shape of magnetic field dependence of the GMI effect (usually presented as magnetic field dependence of magnetoimpedance ratio,  $\Delta Z/Z$ ) is determined by the magnetic anisotropy.

At certain annealing conditions and for certain composition amorphous microwires can exhibit nanocrystalline structure after partial crystallization. In some cases, nanocrystallization allows achieving good magnetic softness and enhanced GMI effect in ferromagnetic microwires. Like for conventional nanocrystalline Finemet-type materials, average anisotropy for randomly oriented  $\alpha\text{-Fe}(\text{Si})$  grains is negligibly small when the average grain is about 10-20 nm.

We studied GMI effect and magnetic properties of Finemet-type FeCuNbSiB microwires. We observed that GMI magnetic field and frequency dependences and magnetic softness of composite microwires produced by the Taylor-Ulitovski technique can be tailored either controlling magnetoelastic anisotropy of as-prepared FeCuNbSiB microwires or controlling their structure by heat treatment or changing the fabrication conditions. GMI effect has been observed in as-prepared Fe-rich microwires with nanocrystalline structure. We observed micro-seized defects and interfacial layer between the metallic nucleus and glass coating that considerably affect magnetic properties and GMI effect of studied microwires.

**MÖSSBAUER AND MAGNETIC STUDY OF Fe+VITROPERM+PLASTIC SYSTEM**

K. Brzózka<sup>1</sup>, P. Sovak<sup>2</sup>, T. Szumiata<sup>1</sup>, P. Kollár<sup>2</sup>, J. Füzer<sup>2</sup>, M. Fáberová<sup>3</sup>,  
R. Bureš<sup>3</sup>, B.Górka<sup>1</sup>, M. Gawroński<sup>1</sup> and M. Gzik-Szumiata<sup>1</sup>

<sup>1</sup>*Department of Physics, University of Technology and Humanities in Radom,  
Krasickiego 54, 26-600 Radom, Poland*

<sup>2</sup>*Institute of Physics, P.J. Šafárik University, Park Angelinum 9, 041 54 Košice,  
Slovakia*

<sup>3</sup>*Institute of Materials Research, Slovak Academy of Sciences, 040 01 Košice,  
Slovakia*

Atomic structure and magnetic properties of Somaloy® 700 iron based material provided by Höganäs AB, Sweden and Vitroperm® 800 amorphous alloy in the form of flakes provided by Vacuumschmelze, GmbH & Co. KG, Germany compacted to the form of a cylinder were the subject of investigations. The relative content of Vitroperm in relation to the whole magnetic material had the values: 0.05, 0.1, 0.2, 0.3, 0.5. Conversion electron Mössbauer spectroscopy (CEMS) was employed in order to identify phase composition of the surface layer and bulk regions. Magnetic properties were investigated at room temperature by use of alternating gradient force magnetometer (AGFM), with the magnetic field applying in-plane of the sample. The results were completed with data of mass density and electrical resistivity. The observations showed that the samples were fragile – especially the specimens with large content of Vitroperm.

CEMS spectra, which give information about the surface of sample, proved that a great content (up to 80 %) of the component characteristic of iron oxides occurred, superimposed with those of  $\alpha$ -iron and amorphous or nanocrystalline Vitroperm. The results reveal small resistance of the samples to oxidation and its dependence on external conditions. After manual rub of the surface layer of the width of 0.2 mm and subsequent measurements it was stated that the subspectrum of iron oxides was reduced (up to several percent) or fully eliminated, making possibility for more precise analysis of the other phases.

On the basis of AGFM investigations it was found that the magnetic saturation field had the similar value for all the samples – about 500 mT. Moreover, a trend of rather faster saturation of magnetization was observed for samples of smaller content of the magnetic phase. This result was probably related to the demagnetization effects. The magnetization curves did not reveal hysteresis – it means that *de facto* the coercive field induction was smaller than 0.5 mT, the value which is related to the limit of our AGFM system.

**FINE SMOOTHING OF CONDUCTIVE SUBSTRATE FOR PERMALLOY LAYER ELECTROPLATING**

M. Butta<sup>1</sup>, M. Janosek<sup>1</sup>, I. Pilarcikova<sup>1</sup>, L. Kraus<sup>2</sup>

<sup>1</sup>*Faculty of Electrical Engineering, Czech Technical University in Prague, Technická 2, 16627 Praha, Czech Republic*

<sup>2</sup>*Czech Academy of Science, Na Slovance 2, 18221 Prague, Czech Republic*

Permalloy films electroplated on conductive substrate are currently investigated due to their feasibility as core for fluxgates. It has been shown that by properly choosing the electroplating parameters the magnetic properties of the Permalloy film can be easily tuned to the desired values.

This has been extensively studied for Permalloy films electroplated on copper wires, whose roughness is typically negligible. In our study we consider racetrack cores for parallel fluxgate. The permalloy film is electroplated on PCB copper film. By lithographic method we obtain copper film already shaped to the designed form, such as racetrack shape, and this makes this technique suitable because no further mechanical machining of the core is required.

A critical parameter is the roughness of the copper substrate: any defect on the copper layer will be reflected on the Permalloy layer we electroplate on it, therefore we need a very smooth and defect free surface as base for Permalloy electroplating. Moreover, we want to reduce the thickness of the copper layer as much as possible in order to reduce the eddy currents and make the fluxgate suitable also at high frequency.

We achieved both these goals by electropolishing the copper substrate in orthophosphoric acid. By properly tuning the electropolishing current we reduced the roughness from  $\sim 1 \mu\text{m}$  to  $\sim 0.1 \mu\text{m}$  rms, without adding any defect. The absence of defects caused by gas evolution is obtained by electropolishing the layer on a specific point of the V-A characteristic of the bath.

Moreover, we implemented a system for monitoring the thickness of the substrate during electropolishing by precise measurement of the layer resistance. In this way we managed to reduce the thickness from  $18 \mu\text{m}$  to  $7 \mu\text{m}$ , without altering the uniformity of the substrate. The thickness of the layer has been confirmed by talstep profilometry.

Finally we will show the effect of roughness and surface defects of the conductive layer on the Permalloy layer electroplated on it.



# **ELECTRICAL RESISTIVITY AND THERMOELECTRIC POWER OF NANOCOMPOSITE FILMS OF NICKEL / CARBON NANOTUBES**

K. Pękała<sup>1</sup>, M. Trzaska<sup>2</sup>, M. Gostomska<sup>3</sup>, M. Pękała<sup>4</sup>

<sup>1</sup>*Faculty of Physics, Warsaw University of Technology, Koszykowa 58, 00-662 Warsaw*

<sup>2</sup>*Institute of Precision Mechanics, Duchnicka 3, 01-796 Warsaw*

<sup>3</sup>*Faculty of Material Science and Engineering, Warsaw University of Technology, Wołoska 141, 02-507 Warsaw,*

<sup>4</sup>*Faculty of Chemistry, Warsaw University, Żwirki i Wigury 101, 02-089 Warsaw*

Thin film composites of nickel / carbon nanotubes (Ni/CNTs) have been produced by the electrochemical method in Watts bath on carbon steel substrate (St3S). The used Watts bath has been filled with organic substances and contained disperse phase of carbon nanotubes (CNTs). The bath was enriched with 0.2 g/l of CNTs. The electrodeposition process was performed with constant current density 3 A/dm<sup>2</sup> at temperature 45°C. Prior to the process beginning the bath was intensively stirred ultrasonically in order to obtain a homogenous CNTs suspension. During the entire deposition process the bath was stirred mechanically at a speed of 400 rev/min. The structure and morphology of composites were analyzed by transmission and scanning electron microscopy. Electrical resistivity and thermoelectric power were measured by the four probe and differential methods, respectively, for the microcrystalline, nanocrystalline and composite films. Temperature variation of electrical resistivity exhibits two ranges of distinct behavior, which are separated somewhat above the Curie temperature of pure nickel. At high temperature paramagnetic phase the linear variation of resistivity occurs due to the electron scattering on phonons and disordered spins. In the ferromagnetic phase the second order polynom is related to the magnon and structural components of resistivity. The electron transport parameters are correlated with a microstructure of thin films studied. The room temperature resistivity increases from 8 to 10.5 μΩcm, when the mean grain size varies in range 3÷10 μm in microcrystalline film in range 30÷40 nm in the nanocrystalline one. This is accompanied by a reduction in thermoelectric power from -23.2 to -20.1 μV/K. These changes are caused by the additional electron scattering on grain boundaries as the grain surface to volume ratio  $S/V \sim (1/r)$  becomes enhanced for the nanograins of radius  $r$ . Moreover, it is also observed that phonons and magnons exhibit a weaker influence onto temperature variation of resistivity. The resistivity and structural data show that about 580 K the nanocrystalline films undergo a crystallization to the microcrystalline structure. An embedding of nanocrystalline carbon tubes into the microcrystalline nickel films enhances electrical resistivity by 30 % and reduces thermoelectric power by 10 %. According to Maxwell - Garnett relation a fraction of nanocrystalline carbon tubes is less than 1 vol % . Such a content does not affect temperature variation of electrical resistivity and thermoelectric power.

**EFFECT OF SURFACES IN FeNbCuBSiP RIBBONS**

P. Butvin<sup>1</sup>, B. Butvinová<sup>1</sup>, M. Kuzminski<sup>2</sup>, A. Slawska-Waniewska<sup>2</sup>, J. Sitek<sup>3</sup>, I. Maľko<sup>1</sup> and M. Kadlečíková<sup>4</sup>

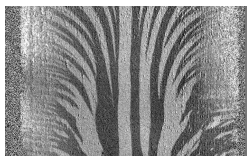
<sup>1</sup>*Institute of Physics Slovak Academy of Sciences, 845 11 Bratislava, Slovakia*

<sup>2</sup>*Institute of Physics Polish Academy of Sciences, 02-668 Warszawa, Poland*

<sup>3</sup>*Institute of Nuclear and Physical Engineering, FEI STU, Bratislava, Slovakia*

<sup>4</sup>*Institute of Electronics and Photonics, FEI STU, 812 19 Bratislava, Slovakia*

Two rapidly quenched ribbons of phosphorus-doped Fe<sub>78</sub>or<sub>74</sub>-Nb<sub>3</sub>-Cu<sub>1</sub>-B<sub>10</sub>-Si<sub>5</sub>or<sub>9</sub>-P<sub>3</sub> annealed 1 hour at 500°C in vacuum or Ar (thus partly nanocrystalline) were investigated by various methods to see mainly the effect of phosphorus on surface-based macroscopic heterogeneity (MH) and its impact on magnetic properties. Domain structure (DS) showing the whole ribbon width shows best the transversal MH. The image shows clearly different anisotropy near



ribbon edges and the central part. There is another MH – across the ribbon thickness, where surfaces can cause stress that induces magnetoelastic anisotropy. Although DS study did not reveal a principal difference of MH formation in Finemet ribbons due to P, the purposeful change of surface properties results in well resolved reduction of MH-induced magnetic anisotropy. This is best seen on hysteresis loops, which show almost 10% lesser reduction of MH-induced anisotropy after equivalent (~15 %) thickness reduction when comparing P-doped and P-free Si<sub>5</sub>-Finemet respectively. Then the weaker MH-induced anisotropy observed on Ar-annealed P-doped samples (as compared to P-free ones) can be understood as due to weaker in-plane compression exerted by genuine surfaces on the ribbon interior of the P-doped ribbon. The P-doped materials (annealed) are slightly more magnetostrictive (~5%) than its P-free counterparts. Thus if sole magnetoelastic contribution to MH-induced anisotropy is anticipated, P reduced the ability of genuine surfaces to exert the compressive stress.

Raman spectroscopy reproducibly identified the presence of Fe-oxides on surfaces of all Si<sub>5</sub> Ar-annealed samples, less so for Si<sub>9</sub> samples. X-rays excited by electrons from annealed ribbon surfaces did not reveal any phosphorus concentration significantly different from nominal one. The P-caused differences seen by Mössbauer spectroscopy reflect mainly the shift of crystallization temperatures. Unlike Si<sub>5</sub>, Si<sub>9</sub> shows DO<sub>3</sub> structure like the P-free counterparts do. The advanced crystalline share after Ar-annealing could also be ascribed to preferred surface crystallization.

**ANALYSIS OF THE FRACTURE SURFACES OF A NEW  
DEVELOPMENT INSULATED IRON POWDER COMPOUNDS**

R. Bidulský<sup>1</sup>, J. Bidulská<sup>1</sup>, T. Kvačkaj<sup>1</sup>, M. Actis Grande<sup>2</sup>

<sup>1</sup> *Technical University of Košice, Faculty of Metallurgy, Letná 9, 042 00 Košice, Slovakia*

<sup>2</sup> *Politecnico di Torino, Department of Applied Science and Technology, V. Teresa Michel 5, 15100 Alessandria, Italy,*

Goal of the present paper is the analysis of the fracture surfaces of an Insulated Iron Powder Compound (IIPC) with different additions of aluminium alloy (0, 5 and 10 wt. %), in order to improve the mechanical properties, evaluated as the transverse rupture strength (TRS) and impact energy values. Investigation of fracture surfaces concluded that improvements in bending strength and impact values require the reduction of surface oxides during the heat treatment, in order to get a proper load bearing area between the adjacent particles.

### **I3-01**

## **NANOCOMPOSITE MAGNETS FOR POWER ELECTRONIC APPLICATIONS**

Michael McHenry

*Materials Science and Engineering Department, Carnegie Mellon University, Pittsburgh, PA 15213*

Recent USDOE workshops highlight the need for advanced soft magnetic materials leveraged in novel designs of power electronic components and systems for power conditioning and grid integration. Similarly soft magnetic materials figure prominently in applications in electric vehicles and high torque motors. Dramatic weight and size reductions are possible in such applications by hold potential for applications in active magneocaloric cooling of such devices. Bulk and thin film soft magnet sensors can contribute to the search for oil and critical materials. Opportunities for state of the art soft magnetic to impact such applications have been furthered by investment by USDOD Programs and other world wide efforts to advance these materials for applications in military electric vehicle technologies.

This talk will focus on the framework for developing high frequency (f) magnetic materials for grid integration of renewable energy sources bridging the gap between materials development, component design, and system analysis. Examples from recent efforts to develop magnetic technology for lightweight, solid-state, medium voltage (>13 kV) energy conversion for MW-scale power applications will be illustrated. The potential for materials in other energy applications (motors, cooling, sensors, RF metal joining, etc.) will also be discussed. The scientific framework for nanocomposite magnetic materials that make high frequency components possible will be presented in terms of the materials paradigm of synthesis → structure → properties → performance. In particular, novel processing and the control of phase transformations and ultimately nanostructures has relied on the ability to probe structures on a nanoscale. Examples of nanostructural control of soft magnetic properties will be illustrated.

**THE MAGNETOCALORIC EFFECT OF MULTIPHASE MATERIALS AND NANOSTRUCTURES**

V. Franco and A. Conde

*Dpto. Física de la Materia Condensada, ICMSE-CSIC, Universidad de Sevilla.  
Apdo. 1065. 41080-Sevilla, Spain*

Although still a large proportion of the magnetocaloric studies is devoted to bulk alloys and compounds and concentrates on the optimization of the properties by designing new phases with enhanced performance [1], it is worth stressing that there is the alternative of using materials engineering techniques for the optimization of already existing materials. The use of known materials as building blocks for developing composites, nanostructures, graded materials, etc. is already giving promising results. One of the reasons for that success is the deep knowledge of the constituent phases that has already been achieved.

In this talk, we will overview our recent results on how, by nanostructuring, well known magnetic phases can lead to magnetocaloric responses which are qualitatively different from the behavior found in the bulk. Nanostructuring can also be used to optimize the magnetic field responsiveness of the materials, a behavior which is intimately related to the magnetocaloric response of multiphase materials and composites. Therefore, we will also focus on the possibility of increasing the refrigerant capacity and obtaining table-like magnetocaloric effect by combining different magnetic phases. These studies, which include both models and experiments, allow us to estimate the influence on the magnetocaloric response of magnetic interactions between phases.

*This work was supported by the Spanish Ministry of Science and Innovation and EU FEDER (Project MAT 2010-20537), the PAI of the Regional Government of Andalucía (Project P10-FQM-6462), and the United States Office of Naval Research (Project N00014-11-1-0311).*

[1] V. Franco, J. S. Blázquez, B. Ingale, and A. Conde, *Annual Review of Materials Research* 42, 305 (2012).

### **O3-01**

#### **MAGNETIC FIELD ENHANCED SOFT MAGNETIC PROPERTIES OF Fe-Co ALLOYS**

Bianca Frincu<sup>1</sup>, Rajasekhar Madugundo<sup>1</sup>, Olivier Geoffroy<sup>2</sup>, Thierry Waeckerle<sup>3</sup> and Sophie Rivoirard<sup>1</sup>

<sup>1</sup> *CNRS/CRETA, Grenoble, France*

<sup>2</sup> *Grenoble Electrical Engineering Laboratory (G2Elab), Saint Martin d'Hères, France*

<sup>3</sup> *Aperam Research Center, Imphy, France*

Reducing the energy consumption is one of the driving forces for the development of improved materials. In this respect, both new metallurgical processes and improved magnetic materials can provide future solutions for a sustainable development. In this work, thermo-magnetic processing is presented as a new technology with the goal of developing improved soft magnetic properties in FeCo alloys unattainable through conventional processing. Developing the permeability of FeCo alloys and decreasing their coercivity are the two main challenges for embarked electrotechnics. In this work, the ferrite phase is found to be stabilised together with a coarse grain microstructure during recrystallisation and growth of two FeCo alloy grades under magnetic field. As a result of recrystallization of cold rolled sheets of the Fe-49%Co-2%V alloy, soft magnetic properties are developed through an extended field induced anisotropy. A decrease of ~40% of the coercivity and of 15% of the total losses as compared to the commercial values is reported. Beside, improved functional properties are obtained by a magnetic field induced Goss texture enhancement in the Fe-27%Co alloy sheet. The coercivity is improved by a factor of almost 3.5 compared to the commercial value as well as the induction level. The total magnetic losses are reduced.

**MINOR LOOP SCALING RULES FOR SOFT MAGNETIC CORES**Lajos K. Varga<sup>1</sup>, Jozef Kovac<sup>2</sup><sup>1</sup>*Wigner Research Center for Physics, Institute for Solid State Physics and Optics, Hungarian Academy of Sciences, 1525 Budapest, P.O.B.49, Hungary*<sup>2</sup>*Laboratory of Nanomaterials and Applied Magnetism, Institute of Physics, Slovak Academy of Sciences, Watsonova 47, SK-04000 Košice, Slovak Republic*

The validity of the Steinmetz law ( $P = K \cdot B^n$ ) has been studied for ultrasoft, Finemet type, nanocrystalline core and has been compared with the result obtained on Mn-Zn ferrite and NO-Fe-Si steels cores. It is shown that, for all the investigated materials, the original Steinmetz law with the exponent  $n = 1.6$  is valid only at intermediate and high induction values, where irreversible magnetization processes dominate. At small magnetization levels the exponent is about 2.2-2.9, much higher than the original proposed value. The interplay of reversible and irreversible processes can be followed on scaling curves as a function of the peak magnetic induction as the change of the slope values. As a function of the remanence however, a unique exponent is found in the whole range of magnetization. The results will be discussed in the frame of tanh model at all levels of excitation, taking into account that the magnetization process can be composed by the following possible components: domain wall displacement, domain rotation and domain wall nucleation and annihilation.

**COMPUTER MODELS OF THE MAGNETIZATION VECTOR DISTRIBUTION IN THE PERMANENT MAGNETS HALBACH ARRAYS**

J. Repková<sup>1</sup>, M. Mahuliaková<sup>1</sup>, M. Lesňák<sup>1</sup>, J. Luňáček<sup>1</sup>, D. Ciprian<sup>1</sup>

<sup>1</sup>*Department of Physics, VŠB – Technical University of Ostrava, 17. listopadu 15, 708 33 Ostrava – Poruba, Czech Republic*

Magnetic separation is one of the promising methods which are used to separate the magnetic and non-magnetic components from an input mixture. The effectiveness of magnetic separation depends strongly on the magnitude and distribution of magnetic field in the separator. One of the possibilities how to economically create suitable magnetic field is to use Halbach arrays of permanent magnets, because the permanent magnets do not require electric power and fundamentally do not change their properties. However, some problems connected with precise magnetization vector orientation can be encountered.

The contribution is oriented on computer models to show the effect of a combination of the different magnetization vectors orientations of individual components Halbach arrays on the size and distribution of the magnetic field in an expected area of the separator. The analysis has been carried out for several types of Halbach arrays containing from four to six permanent magnets. Typical AlNiCo, SmCo and NdFeB magnets of the cubic shape (50x50x50 mm) were used as elementary building blocks for Halbach arrays.



**GRAIN-SIZE EFFECT ON THE MAGNETOCALORIC PROPERTIES OF THE  $\text{DyCo}_3\text{B}_2$  COMPOUND**

T. Toliński, K. Synoradzki

*Institute of Molecular Physics, Polish Academy of Sciences, M Smoluchowskiego 17, 60-179 Poznań, Poland*

$\text{DyCo}_3\text{B}_2$  belongs to the family of the intermetallic compounds represented by the general formula  $R_{1+n}\text{Co}_{5+3n}\text{B}_{2n}$  ( $R$  = rare earth), where  $\text{RCO}_3\text{B}_2$  corresponds to  $n = \infty$ . The crystallographic structure is hexagonal and the general formula originates from the boron substitution for Co in the  $\text{RCO}_5$  compounds.

The  $R$ - $R$  sublattice of  $\text{DyCo}_3\text{B}_2$  orders ferromagnetically at  $T_C = 22$  K and the magnetic moment on Co is absent for  $R = \text{Y}$ ; however, a small antiparallel magnetic moment is induced at the presence of the rare earth ion. Around the ordering temperature of 22 K we have recently observed a significant magnetocaloric effect (MCE). A maximum isothermal magnetic entropy change  $-\Delta S_M = 17.5 \text{ J kg}^{-1} \text{ K}^{-1}$  and the adiabatic temperature change  $\Delta T_{ad} = 14$  K at the magnetic field change of 9 T have been determined. It has been also found that the relative cooling power (RCP), which is a product of the maximum value of MCE and the full width at half maximum of the temperature dependence of MCE, is relatively large if compared with MCE materials of similar ordering temperature.

In the present studies we have investigated the influence of the mechanical milling on the structural, magnetic and thermodynamic properties of  $\text{DyCo}_3\text{B}_2$ , with special emphasis on the evolution of the MCE parameters, i.e.  $\Delta S_M(T)$ ,  $\Delta T_{ad}(K)$  and RCP, with the size of the grains. The latter has been verified by the analysis of the X-ray diffraction patterns collected after various times of the milling. It has been found that the compound studied is very resist to the undertaken mechanical milling process and the characteristic parameters are stable even after long-lasting milling. The reduction of the parameters values proceeds slowly with the milling time.

**MAGNETIC PROPERTIES AND MAGNETOCALORIC EFFECT OF THE DyNi<sub>4</sub>Si COMPOUND**

M. Falkowski, W. Kowalski, K. Synoradzki, T. Toliński and A. Kowalczyk  
*Institute of Molecular Physics, Polish Academy of Sciences, M. Smoluchowskiego 17, 60-179 Poznań, Poland*

DyNi<sub>4</sub>Si crystallizes in the hexagonal CaCu<sub>5</sub>-type structure (space group P6/mmm). At  $T_C = 11$  K a second order phase transition to a ferromagnetic order has been observed.

The heat capacity measurements have shown that DyNi<sub>4</sub>Si is characterized by the enhanced electronic specific heat coefficient  $\gamma = 72$  mJ/mol K<sup>2</sup>. In the low-temperature dependence of  $C_p(T)$  a well defined  $\lambda$ -type anomaly appears near  $T_C$  for zero magnetic field. The externally applied magnetic fields lead to the quenching and shifting of the peak in the vicinity of  $T_C$  to higher temperatures, typical of ferromagnets.

We have investigated the magnetocaloric effect (MCE) on the basis of the specific heat measurements. It exhibits relatively large values of the isothermal entropy change  $-\Delta S_M$  (up to  $6.4 \text{ J kg}^{-1} \text{ K}^{-1}$  at magnetic field of 2 T) and the isoentropic temperature change  $\Delta T_{ad}$  (up to 7.8 K at 2 T) around the magnetic ordering temperature.

We have additionally performed a detailed studies of the effect of the grains size on the maximum value and the temperature dependence of MCE. The modification of the grains size have been obtained by mechanical milling and the size of the grains have been checked after various milling times by analysis of the X-ray diffraction measurements. A decrease and broadening of MCE has been observed.

**DIRECT MEASUREMENT OF MAGNETO-CALORIC EFFECT IN AMORPHOUS AND CRYSTALLINE 3d-ELEMENTS ALLOYS**

J. Kamarád, J. Kaštil, Z. Arnold

*Institute of Physics ASCR, v.v.i., Na Slovance 2, 182 21 Prague 8, Czech Republic*

The magneto-caloric effect (MCE) attracts an attention since the first successful application of Gd and its compounds in magnetic refrigeration technics. An intensive searching for less expensive magnetic materials for this application was based mainly on the indirect methods of the MCE measurements, e.g. using the Maxwell relations and results of simple magnetic measurements. In this case, MCE is characterized by the isothermal change of entropy induced by external magnetic field. However, it seems to be a misleading way for an assessment of magnetic materials with the first order magnetic and/or structural transitions. We have fabricated a device for the direct MCE measurements that provides a solid possibility to measure adiabatic changes of temperature induced by very rapid change of external field up to 4.7 T in temperature range from 80 K up to 500 K. Substantial features of the device will be described. Magnetic moment of 3d-elements is much lower in comparison with Gd, but, pronounced magneto-volume effects that are observed namely in the Fe-based alloys and compounds point to a strong coupling between magnetic moments and crystal structure. We have tested a group of the Fe-based crystalline and amorphous alloys and intermetallic compounds with the aim to receive and to collect the basic MCE data by the direct measurement of the adiabatic changes of temperature,  $\Delta T_{ad}$ . The studied amorphous  $\text{Fe}_{91.5}\text{Zr}_{8.5}$  and  $\text{Fe}_{76}\text{Cr}_9\text{B}_{15}$  alloys exhibit the second order ferro-paramagnetic transitions at  $T_C = 225$  K and 350 K, resp., where we have observed the maximum of  $\Delta T_{ad}$ . The maximum values of  $\Delta T_{ad}$  are only 0.7 K and 0.9 K, resp., in the case of the field span 4.7 T. The first order ferro-paramagnetic transition in the  $\text{Hf}_{0.83}\text{Ta}_{0.17}\text{Fe}_2$  intermetallic compound at  $T_C = 245$  K is accompanied by very pronounced decrease of volume. Temperature of the transition increases significantly with increasing external field. The maximum MCE,  $\Delta T_{ad} = 2.4$  K with field span 4.7 T, was reached at temperature 250 K and this value of  $\Delta T_{ad}$  is constant up to temperature 260 K. The identical value of  $\Delta T_{ad}$  was reached with field span 3 T at temperature 250 K only. Field of 1 T is not able to induce the total ferro-paramagnetic transition and hence, the maximum value of  $\Delta T_{ad} = 1.2$  K with field span 1 T has been observed. A simple description of the peculiar MCE behaviour in the  $\text{Hf}_{0.83}\text{Ta}_{0.17}\text{Fe}_2$  compound will be presented.

### P3-05

#### PHASE COMPOSITION AND MAGNETIC PROPERTIES OF THE NANOCRYSTALLINE $\text{Fe}_{64,32}\text{Pr}_{9,6}\text{B}_{22,08}\text{W}_4$ ALLOY

K. Filipecka<sup>1</sup>, K. Pawlik<sup>1</sup>, P. Pawlik<sup>1</sup>, J.J. Wysocki<sup>1</sup>, P. Gębara<sup>1</sup>, A. Przybył<sup>1</sup>, M. Szwaja<sup>1</sup>, I. Wnuk<sup>1</sup>

<sup>1</sup>*Institute of Physics, Faculty of Materials Processing, Technology and Applied Physics, Czestochowa University of Technology, Armii Krajowej 19, 42-200 Czestochowa, Poland*

The aim of the present work was to study the influence of annealing conditions on magnetic properties and the phase constitution of rapidly solidified  $\text{Fe}_{64,32}\text{Pr}_{9,6}\text{B}_{22,08}\text{W}_4$  alloy ribbons.

The base alloy was prepared by arc-melting of the high purity elements under an Ar atmosphere. Subsequently the ribbon samples were obtained by melt-spinning technique under low pressure of Ar. In order to develop nanocrystalline structure samples were annealed at 1003 K for 5, 10, 20 and 30 min. The room temperature magnetic properties were determined from hysteresis loops measured by VSM magnetometry in the external magnetic field up to 2T. The magnetization reversal processes were carried out by the analysis of recoil curves. For comparison the influence of annealing temperature on magnetic properties were studied for the same alloy composition. The ribbons were annealed at temperature from 929 K to 1023 K for 5 min. X-ray diffractometry and Mössbauer spectroscopy were used to determine the phase composition of annealed ribbons. Heat treatment resulted in an evolution of the phase constitution that caused changes in magnetic properties of the alloy.

*Work supported by the research project N N507 240840 financed by Polish National Science Centre in years 2011–2014.*

**TERMOMAGNETIC PROPERTIES OF THE  $\text{La(Fe,Si)}_{13}$ -TYPE ALLOYS**

P. Gębara<sup>1</sup>, P. Pawlik<sup>1</sup>, I. Skorvanek<sup>2</sup>, J. Marcin<sup>2</sup>, K. Pawlik<sup>1</sup>, A. Przybył<sup>1</sup>, J.J. Wysocki<sup>1</sup>, M. Szwaja<sup>1</sup>, K. Filipecka<sup>1</sup>

<sup>1</sup>*Institute of Physics, Częstochowa University of Technology, Armii Krajowej 19, 42-200 Częstochowa, Poland*

<sup>2</sup>*Institute of Experimental Physics, Slovak Academy of Sciences, Watsonova 47, 040 01 Kosice, Slovakia*

Pseudobinary  $\text{La(Fe,Si)}_{13}$ -type alloys revealing excellent magnetocaloric properties near room temperature seems to be a good candidates for application as an active elements in magnetic refrigerators. In the present work, Curie temperature, refrigeration capacity and relative cooling power of the  $\text{LaFe}_{11.0}\text{Co}_{0.8}(\text{Si}_{1-x}\text{Al}_x)_{1.2}$  (where  $x=0, 0.6$ ) alloys, were investigated. Samples were prepared by arc-melting of high purity constituent elements under the low pressure of Ar atmosphere. The as-cast  $\text{LaFe}_{11.0}\text{Co}_{0.8}\text{Si}_{1.2}$  and  $\text{LaFe}_{11.0}\text{Co}_{0.8}(\text{Si}_{0.4}\text{Al}_{0.6})_{1.2}$  were sealed-off in quartz tubes under low pressure of inert gas and annealed at 1323 K, respectively, for 28 and 49 days. X-ray diffractometer Bruker D8 Advance with semiconductor detector LynxEye was used to study of the phase constitution. The samples in the as-cast state shown presence of dominant bcc  $\alpha$ -Fe and minor LaFeSi phases. After annealing samples were almost single phase with fcc  $\text{NaZn}_{13}$ -type structure and space group  $\text{Fm}\bar{3}\text{c}$ . Magnetic properties of the samples were measured in external magnetic fields up to 6 T at the temperature range 100-400 K. Curie temperature of both samples were investigated using Arrot plots technique and first derivative of the temperature dependences of magnetization  $dM(T)/dT$ . In order to determine the cooling power and refrigeration capacity, temperature dependences of the magnetic entropy change  $\Delta S_M$  were used.

*Work supported by the research project NN 507 233 040 financed by Polish National Science Centre in years 2011 – 2014.*

**TUNING OF MAGNETOCALORIC EFFECT IN FeCrNbB-BASED AMORPHOUS COMPOSITES**J. Marcin<sup>1</sup>, J. Kováč<sup>1</sup>, D. Janičkovič<sup>2</sup>, P. Švec<sup>2</sup>, I. Škorvánek<sup>1</sup><sup>1</sup>*Institute of Experimental Physics, Slovak Academy of Sciences, Watsonova 47, 040 01 Košice, Slovakia*<sup>2</sup>*Institute of Physics, Slovak Academy of Sciences, Dúbravská cesta 9, 845 11 Bratislava, Slovakia*

The magnetocaloric effect (MCE) is a basis of novel environmental friendly cooling technology. In order to ensure the requested energy efficiency of related cooling devices it is of high importance to search for magnetic materials with suitable magnetic entropy characteristics and a sufficiently large refrigerant capacity (RC). One possible way how to expand the temperature range over which the appreciable magnetic entropy changes can be attained is the use of magnetic composites or multiphase materials with suitably distributed values of the Curie temperature. Here, we report on the magneto-caloric effect in FeNbB-based amorphous ribbons where the tuning of MCE was performed by doping of the parent ternary system with a different addition of Cr. We have prepared a series of  $\text{Fe}_{81-x}\text{Cr}_x\text{Nb}_7\text{B}_{12}$  ( $x = 0, 1, 2, 3.5, 4$  and  $5$ ) alloys where the gradual substitution of Cr for Fe results in a decrease of the Curie temperature from 332 K to 260 K. The selected combinations of these alloys with different  $T_c$  served as a model system for tailoring of shape and width of the temperature dependencies of magnetic entropy change. Such modeling allowed us to perform an optimum adjustment of the weight ratio of the individual constituent alloys in the final composite in order to maximize its refrigerant capacity and to reach a flattening of magnetic entropy that leads to table-like MCE response in the vicinity of room temperature

**MICROSTRUCTURE AND PROPERTIES OF La-Ca-Sr-Mn-O  
MAGNETOCALORIC CERAMICS**

K. Zmorayova, V. Antal, S. Piovarci, M. Radusovska, J. Kovac and P. Diko  
*Institute of experimental physics Slovak academy of sciences, Watsonova 47,  
040 01 Košice, Slovakia*

A  $\text{La}_{0.67}\text{Ca}_{0.33-x}\text{Sr}_x\text{MnO}_3$  ( $x = 0.33; 0.03; 0$ ) perovskite magnetocaloric powders were prepared by solid state synthesis in air. Phase transformations were characterized by thermal analyses and the phase composition was checked by x-ray powder diffraction. Pressed pellets were sintered at different temperatures. Microstructure analyses were done by polarized light microscopy and scanning electron microscopy with EDAX and WDX microanalyses. The influence of sintering conditions on porosity, grain size and content of secondary phases is discussed. The magnetocaloric properties have been investigated. Magnetic measurements were performed using a commercial Physical Properties Measurement System (PPMS).

**MODELING THE HYSTERESIS LOOP IN HARD MAGNETIC MATERIALS USING T(x) MODEL**

Marcin Dośpiał<sup>1</sup>, Marcin Nabiałek<sup>1</sup>, Michał Szota<sup>2</sup>, Paweł Pietrusiewicz<sup>1</sup>, Konrad Gruszka<sup>1</sup>, Katarzyna Błoch<sup>1</sup>

<sup>1</sup> *Czestochowa University of Technology, Faculty of Materials Processing Technology and Applied Physics, Institute of Physics*

<sup>2</sup> *Czestochowa University of Technology, Faculty of Materials Processing Technology and Applied Physics, Materials Engineering Institute*

The possibility of decomposing of static hysteresis loop to the contributions of reversible and irreversible processes is demonstrated experimentally and modeled theoretically by the hyperbolic T(x) model. The method of decomposition described in this paper is related with analysis of reversal magnetization curves. Obtained results are applicable in analysis of reversal magnetization processes in hard magnetic materials.



**INTERPRETATION OF LINEAR PART OF EQUATION, IN  
HYPERBOLIC  $T(x)$  MODEL, APPLIED FOR HYSTERESIS ANALYSIS IN  
HARD MAGNETIC MATERIALS**

Marcin Dośpiał<sup>1</sup>, Marcin Nabiałek<sup>1</sup>, Krzysztof Chwastek<sup>2</sup>, Michał Szota<sup>3</sup>, Paweł Pietrusiewicz<sup>1</sup>, Jakub Gawroński<sup>4</sup>

<sup>1</sup> *Czestochowa University of Technology, Faculty of Materials Processing  
Technology and Applied Physics, Institute of Physics*

<sup>2</sup> *Czestochowa University of Technology, Faculty of Electrical Engineering,  
Institute of Electrical Power*

<sup>3</sup> *Czestochowa University of Technology, Faculty of Materials Processing  
Technology and Applied Physics, Materials Engineering Institute*

<sup>4</sup> *Technical University of Lodz, Faculty of Mechanical Engineering*

The presence of linear part of equation in the Takacs  $T(x)$  model raises a lot of questions. Its presence, results in that the material does not reach saturation irrespective of the applied external magnetic field. The inherency of this part of equation in the model was forced by adjustment difficulties arising from the inclination of the magnetic hysteresis loops obtained from the experimental data. In this paper the interpretation of the circumstances, in which was used the above mentioned part of the equation, and what limits its application are described.

# **MAGNETIC COMPARISON OF SEVERAL DIVALENT AND TETRAVALENT IONS MIXTURES SUBSTITUTED Ba FERRITE**

J. Sláma<sup>1</sup>, A. Grusková<sup>1</sup>, A. Gonzáles Angeles<sup>2</sup>, M. Šoka<sup>1</sup>, R. Dosoudil<sup>1</sup>

<sup>1</sup>*Institute of Electrical Engineering, Faculty of Electrical Engineering and Information Technology, Slovak University of Technology, Ilkovičova 3, 812 19 Bratislava, Slovakia*

<sup>2</sup>*Facultad de Ingenieria, Universidad Autónoma de Baja California, Blvd. Benito Juárez s/n, Cp 21280 Mexicali, B. C., México.*

M-type Ba hexaferrite is interesting in high saturated magnetic polarisation  $J_s$ , strong uniaxial crystalline anisotropy and large coercivity  $H_C$  for several research and technical applications. For recording magnetic media and VHF electronic applications the great anisotropy can be diminished substituting  $\text{Fe}^{3+}$  ions by selected metal cation combinations. One aim of substitutions was to decline the magnetisation of one of the sublattices from antiferromagnetic axis. It is an efficient way for controlling the value of  $H_C$ , which is preserving the value of  $J_s$ , this offers very effective media for data recording as example. The magnetic structure and properties of substituted M-type Ba-hexaferrites with composition  $\text{BaFe}_{12-2x}(\text{Me}_1\text{Me}_2)_x\text{O}_{19}$  were prepared, studied, compared and overviewed. Divalent  $\text{Me}_1 = \text{Ni}, \text{Sn}, \text{Zn}$  and tetravalent  $\text{Me}_2 = \text{Ir}, \text{Ru}, \text{Ti}, \text{Zr}$  ion combinations were used in various compounds. We found marked reduction of  $H_C$  and slowly variation of the  $J_s$ , which are related to preferential occupation of divalent and tetravalent cations in the lattice sites. For example  $\text{Ru}^{4+}$  as  $\text{Me}_2$  ions substituted  $\text{Fe}^{3+}$  in  $4f_1$  and  $2b$  sites in  $\text{NiRu}$  and  $\text{SnRu}$  samples.  $\text{Zn}$  and  $\text{Ru}$  occupied first octahedral sites  $4f_2$  and  $2a$  and then bipyramidal  $2b$  sites. The  $\text{Zr}^{4+}$  preferably replaced  $\text{Fe}^{3+}$  ions in  $2b$  and then in tetrahedral sites  $4f_1$  for  $\text{Ni}^{2+}$  as partner ion, which occupies octahedral sites  $4f_2$  and  $12k$  in this mixture. It is well known that  $2b$  lattice is a main contributor to the magnetocrystalline anisotropy and hence  $H_C$ . For other tetravalent  $\text{Me}_2$  ions it was found at certain substitution ratio  $x$  that  $(\text{Me}_1, \text{Me}_2)$  substituted  $\text{Fe}^{3+}$  in BaM-ferrite and then reduced anisotropy by change to planar anisotropy, to shift the FMR frequency bellow 20 GHz. One of goals of that was to develop new compounds with great potential for electronic applications in the region of millimeter waves and with suitable properties for high density recording applications. Coercivity, temperature coefficient of coercivity and temperature behaviour of susceptibility were studied as important magnetic parameters mainly. Behind the presented magnetic parameters, the magnetocrystalline structure, shape and size of grains were investigated too.

# PHASE STRUCTURE AND MAGNETIC PROPERTIES OF Fe-Nb-B-Pt TYPE OF BULK NANOCRYSTALLINE ALLOYS

G. Ziółkowski<sup>1</sup>, A. Chrobak<sup>1</sup>, N. Randrianantoandro<sup>2</sup>

<sup>1</sup> *Institute of Physics, Silesian University, Uniwersytecka 4, 40-007 Katowice, Poland*

<sup>2</sup> *Institut des Molécules et des Matériaux du Mans, UMR CNRS 6283, Université du Maine, 72085 Le Mans cedex 9, France*

A progress in modern technologies requires new materials with specific properties for different kind of applications. In the field of magnetism very promising are FeNb-B type of nanocrystalline alloys. It is well known that such alloys exhibit, in a comparison with their crystalline form, unique and mostly superior magnetic properties [1]. From practical point of view especially interesting are nanocrystalline alloys in the so-called bulk form i.e. rods, ingots etc. with dimensions in order of several mm [2]. Recently, we have reported structural and magnetic properties of  $(\text{Fe}_{80}\text{Nb}_6\text{B}_{14})_{1-x}\text{M}_x$  ( $\text{M} = \text{Au}, \text{Ni}, \text{Gd}, \text{Tb}$ ) bulk nanocrystalline alloys prepared by mould casting technique [3]. These preliminary studies reveal that the alloys with Tb can be considered as high coercive magnetic materials [4], but values of saturation magnetization  $M_s$  are relatively low due to antiferromagnetic coupling of Fe and Tb.

In this work we present phase structure and magnetic properties of the  $(\text{Fe}_{80}\text{Nb}_6\text{B}_{14})_{1-x}\text{Pt}_x$  ( $x=0.15, 0.3, 0.4, 0.6$ ) bulk alloys prepared by making use of the mould casting technique. Magnetic measurements were carried out in the temperature range 2 K – 1100 K and magnetic field up to 7 T. It was observed a formation of mainly two phases (i.e. magnetically soft  $\text{Fe}_2\text{Pt}$  and magnetically hard FePt) with different contributions dependently on the  $x$  parameter. Such coexistence of the phases cause a magnetic hardening of the alloys with  $x \geq 0.4$  with relatively high saturation magnetization. In the presented paper magnetic properties in a context of structural changes are also widely discussed.

- [1] A Chrobak, D. Chrobak, G. Haneczok, P. Kwapuliński, Z. Kwolek and M. Karolus, *Mater. Sci. and Eng. A*, 382,(2004) 401-406.
- [2] A.Chrobak, M.Karolus, G.Haneczok, *Solid State Phenomena*, Vol. 163 (2010) pp 233-238.
- [3] G.Ziółkowski, N.Randrianantoandro, A.Chrobak, J.Klimontko, M.Kądziołka-Gaweł, G.Haneczok, *Acta Physica Polonica A*, No.5-6, 121 (2012) 1266-1269.
- [4] A.Chrobak G. Ziółkowski, N. Randrianantoandro, J. Klimontko, G. Haneczok, *Journal of Alloys and Compounds*, 537 (2012) 154–158.

### P3-13

#### PHASE STABILITY OF $(\text{Fe}_{80}\text{Nb}_6\text{B}_{14})_{0.9}\text{Tb}_{0.1}$ BULK NANOCRYSTALLINE HARD MAGNET

A. Chrobak<sup>1</sup>, G. Ziółkowski<sup>1</sup>, N. Randrianantoandro<sup>2</sup>

<sup>1</sup> *Institute of Physics, Silesian University, Uniwersytecka 4, 40-007 Katowice, Poland*

<sup>2</sup> *Institut des Molécules et des Matériaux du Mans, UMR CNRS 6283, Université du Maine, 72085 Le Mans cedex 9, France*

A progress in modern technologies requires new materials with specific properties for different kind of applications. In the field of magnetism very interesting are Fe-Nb-B type of nanocrystalline alloys. It is well known that such alloys exhibit, in a comparison with their crystalline form, unique and mostly superior magnetic properties. Recently we have reported that the  $(\text{Fe}_{80}\text{Nb}_6\text{B}_{14})_{1-x}\text{Tb}_x$  bulk nanocrystalline series of alloys can be considered as high coercive materials [1]. It was shown (Mössbauer spectra, XRD spectra) that the examined samples contain magnetically hard  $\text{Tb}_2\text{Fe}_{14}\text{B}$  and other  $\text{TbFe}_2$ ,  $\alpha\text{-Fe}$  soft phases - the higher Tb content the higher contribution of  $\text{TbFe}_2$ . Interesting are the samples with  $x = 0.1$  (69 % of  $\text{Tb}_2\text{Fe}_{14}\text{B}$ ) and  $x = 0.12$  (76 % of  $\text{Tb}_2\text{Fe}_{14}\text{B}$ ) for which the magnetic hardening is significant i.e. at  $T=300\text{ K}$   $H_c=1.46\text{ T}$  and  $1.16\text{ T}$ , respectively.

In this work we present structural and magnetic properties of  $(\text{Fe}_{80}\text{Nb}_6\text{B}_{14})_{0.9}\text{Tb}_{0.1}$  bulk nanocrystalline alloy after annealing up to 900 K. The samples were prepared by means of the vacuum suction casting technique in the form of rods with diameters of 2 mm, 1.5 mm, 1 mm and 0.5 mm [2]. Phase changes were studied using scanning differential calorimetry (DSC), Mössbauer spectra and magnetic measurements. It was shown that annealing leads to a formation of crystalline iron which significantly changes a balance between the magnetically hard and soft phases. It has a great influence on magnetic properties which is widely discussed in the paper.

[1] A.Chrobak G. Ziółkowski, N. Randrianantoandro, J. Klimontko, G. Haneczok, *Journal of Alloys and Compounds*, 537 (2012) 154–158.

[2] A.Chrobak, M.Karolus, G.Haneczok, *Solid State Phenomena*, Vol. 163 (2010) pp 233-238

# INFLUENCE OF COOLING RATE ON MAGNETIC PROPERTIES OF $(\text{Fe}_{80}\text{Nb}_6\text{B}_{14})_{1-x}\text{Tb}_x$ TYPE OF BULK NANOCRYSTALLINE ALLOYS

A. Chrobak<sup>1</sup>, G. Ziółkowski<sup>1</sup>, G. Haneczok<sup>2</sup>

<sup>1</sup> *Institute of Physics, Silesian University, Uniwersytecka 4, 40-007 Katowice, Poland*

<sup>2</sup> *Institute of Materials Science, Silesian University, 75 Pułku Piechoty 1, 41-500 Chorzów, Poland*

Among well known permanent magnets, such as Co-Sm, Fe-Pt or Fe-B-Nb types of alloys and compounds, the Fe-Nb-B-Tb alloy family plays an important role. Recently we have reported that the  $(\text{Fe}_{80}\text{Nb}_6\text{B}_{14})_{1-x}\text{Tb}_x$  bulk nanocrystalline series of alloys can be considered as high coercive materials [1]. It was shown (Mossbauer spectra, XRD spectra) that the examined samples contain magnetically hard  $\text{Tb}_2\text{Fe}_{14}\text{B}$  and other  $\text{TbFe}_2$ ,  $\alpha$ -Fe soft. Interesting are the samples with  $x = 0.1$  (69 % of  $\text{Tb}_2\text{Fe}_{14}\text{B}$ ) and  $x = 0.12$  (76 % of  $\text{Tb}_2\text{Fe}_{14}\text{B}$ ) for which the magnetic hardening is significant i.e. at  $T=300$  K  $H_c=1.46$  T and 1.16 T, respectively. The samples were obtained by means of the so-called vacuum suction casting technique in the form of rods with diameter of 1.5 mm [2]. We concluded that the observed magnetic hardening is attributed to additional magnetic anisotropy introduced by the preparation method. The aim of this work is to study an influence of cooling rate on magnetic properties of the  $(\text{Fe}_{80}\text{Nb}_6\text{B}_{14})_{1-x}\text{Tb}_x$  bulk nanocrystalline alloys.

In this work we present magnetic properties of the  $(\text{Fe}_{80}\text{Nb}_6\text{B}_{14})_{1-x}\text{Tb}_x$  ( $x=0.06, 0.08, 0.1$ ) bulk alloys prepared by making use of the mould casting technique with different diameters  $d$  equal to 1.5mm, 1 mm, and 0.5 mm. The difference of sample diameter influences cooling rate. For the alloys with  $x \geq 0.08$  a significant magnetic hardening as a function of  $d$  was observed. For example, for the  $(\text{Fe}_{80}\text{Nb}_6\text{B}_{14})_{0.92}\text{Tb}_{0.08}$  alloy and  $d = 0.5$  mm coercive field  $H_c = 2.4$  T (at 300 K). This means that structural and magnetic disorder cause by the casting technique and high enough cooling rate lead to enhancement of hard magnetic properties. It has also an economic meaning because one can obtain good hard magnets but with lower rare earth content.

[1] A.Chrobak G. Ziółkowski, N. Randrianantoandro, J. Klimontko, G. Haneczok, Journal of Alloys and Compounds, 537 (2012) 154-158.

[2] A.Chrobak, M.Karolus, G.Haneczok, Solid State Phenomena, Vol. 163 (2010) pp 233-238

**MAGNETIC PROPERTIES OF  $\text{Tb}(\text{Ni}_{1-x}\text{Fe}_x)_3$  : ( $x = 0.2, 0.6$ ) CRYSTALLINE COMPOUNDS AND POWDERS**

Krzysztof Ociepka, Anna Bajorek, Artur Chrobak, Grażyna Chełkowska  
*A. Chełkowski Institute of Physics, University of Silesia, ul. Uniwersytecka 4,  
40 – 007 Katowice, Poland*

In the paper we present and discuss magnetic properties of the  $\text{Tb}(\text{Ni}_{1-x}\text{Fe}_x)_3$  ( $x = 0.2, 0.6$ ) crystalline compounds and their ball-milled powders. The crystal structure of all samples was checked at the room temperature by means of X-ray diffraction. The investigated compounds are polycrystalline and crystallize in the rhombohedral  $\text{PuNi}_3$  type of crystal structure (space group  $R\bar{3}m$ ). After 6h milling time SEM results show the presence of nanoflakes with thickness up to 100 nm or even smaller. The Curie temperature ( $T_C$ ) of both studied materials seems to be independent of particle size and indicate almost the same value for the bulk as well as powder compounds. The saturation magnetic moment ( $M_S$ ) decreases while the coercivity ( $H_C$ ) increases with increasing degree of fineness of the material. Moreover, after 6h of milling the significant decrease of magnetocaloric effect (MCE) is also observed.

**IMPROVED PROCESSING TECHNIQUE FOR PREPARATION OF NON-ORIENTED ELECTRICAL STEELS WITH LOW COERCIVITY**I. Petryshynets<sup>1</sup>, F. Kováč<sup>1</sup>, J. Marcin<sup>2</sup> and I. Škorvánek<sup>2</sup><sup>1</sup>*Department of Microstructural Engineering of Steels, Institute of Materials Research, Watsonova 47, 04 001 Košice, Slovakia*<sup>2</sup>*Laboratory of Nanomaterials and Applied Magnetism, Institute of Experimental Physics, Watsonova 47, 04 001 Košice, Slovakia*

Non-oriented electrical steels belong to important group of the soft magnetic materials that are typically used as core parts in a variety of electrical rotating equipments. Their good soft magnetic characteristic strongly rely on the ability of technological processes to precise control the grain size and texture as well as chemistry of the final steel sheets products.

In the present paper, an adjusted temper rolling process for development of particular textures  $\{100\}\langle 0vw \rangle$  in vacuum degassed NO steels was used. The main idea behind the improvement of soft magnetic properties relies on a deformation induced grain growth promoting the preferable formation of grains with desired orientation. Two vacuum degassed NO steels with silicon content 2,4 and 0,6 % wt, taken from industrial line after final industrial annealing, were chosen as an experimental material. In both cases, a coarse grained microstructure with pronounced intensity of cube and Goss texture components in the investigated NO steels were achieved by using deformation induced growth of ferrite grains during the continuous final annealing of the material under laboratory conditions. The obtained microstructure leads to a significant decrease of coercivity measured in DC magnetic field. In the case of steel with silicon content 2,4 % wt. the coercivity decreased from 42 A/m to 17 A/m. Even more remarkable improvement of the soft magnetic properties was observed for the steel with Si 0.6 % wt., where the coercivity value dropped from 68 A/m to 12 A/m.

### **P3-17**

#### **EFFECT OF COMPACTION ON THE BEHAVIOUR OF THE SOFT MAGNETIC MATERIAL**

M. Actis Grande<sup>1</sup>, R. Bidulský<sup>2</sup>, M. Maccarini<sup>1</sup>, J. Bidulská<sup>2</sup>, I. Forno<sup>1</sup>

<sup>1</sup>*Politecnico di Torino, Department of Applied Science and Technology, V. Teresa Michel 5, 15100 Alessandria, Italy, michele.maccarini@polito.it*

<sup>2</sup>*Technical University of Košice, Faculty of Metallurgy, Letná 9, 042 00 Košice, Slovakia*

The main aim of the present work was to study the physical properties (apparent and tap density) and the effect of different compacting pressures on the behaviour of a Powder Metallurgy soft magnetic material - Insulated Iron Powder Compound (IIPC). Different stages during compaction were identified and evaluated in terms of particle rearrangement and plastic deformation.



**INFLUENCE OF ANNEALING CONDITIONS ON STRUCTURAL DEVELOPMENT OF CRYO ROLLED C-Si STEEL**

Kvačkaj T., Bella P., Bidulský R., Kočiško R., Bidulská J., Lupták M., Kováčová A.

*Department of Metal Forming, Faculty of Metallurgy, Technical University of Košice, Vysokoškolská 4, 042 00 Košice, Slovakia*

Non-oriented electrical steel commercially called (NGOES) in ambient and cryogenic temperature conditions was investigated. The plastic deformations in cryogenic temperature are forming stronger structural heterogeneities in sample thickness than at ambient temperature. The structural heterogeneities in deformed structure are as potential places for formation of nuclei for material recrystallization. Samples processing by cryo rolling are shown bigger storage energy. The annealing conditions were applied on deformed samples with the aim abnormal grain growth by static recrystallization process. Moreover, minimal magnetic losses are reached when mean grain size is approximately 150  $\mu\text{m}$ .

**MAGNETIZATION REVERSAL PROCESSES IN Pr-Fe-B-TYPE NANOCRYSTALLINE MAGNETS**K. Pawlik<sup>1</sup>, P. Pawlik<sup>1</sup>, W. Kaszuwara<sup>2</sup>, J.J. Wysocki<sup>1</sup><sup>1</sup>*Institute of Physics, Częstochowa University of Technology, Al. Armii Krajowej 19, 42-200 Częstochowa, Poland*<sup>2</sup>*Faculty of Materials Science and Engineering, Warsaw University of Technology, ul. Wołoska 141, 02-507 Warsaw, Poland*

The magnetization reversal processes in magnets derived from rapidly solidified  $\text{Pr}_9\text{Fe}_{52}\text{Co}_{13}\text{Zr}_1\text{Nb}_4\text{B}_{21}$  alloy samples were studied by analysis of minor hysteresis loops and recoil curves measured by VSM magnetometry.

The studies were carried out on suction-cast 1 mm diameter rod, 1 mm thick plate, 3 mm outer diameter (o.d.) tube and melt-spun ribbon samples subjected to short time annealing.

Preliminary structural studies shown that in as-cast state rod and ribbon samples were amorphous while tube and plate were partially crystalline. Subsequent annealing of all investigated samples at 983K for 5 min resulted in formation of nanocrystalline multiphase microstructure and emerging hard magnetic properties. The X-ray diffraction analysis and Mössbauer spectroscopy shown presence of hard magnetic and paramagnetic phases diluted within the amorphous matrix. Structural and magnetic studies indicated that the initial state of microstructure and phase composition affects the magnetization reversal processes in annealed samples due to a variation of microstructure in samples of various shapes. Combined magnetic studies allowed estimating the mean values of nucleation and pinning fields that control the magnetization reversal processes.

**MAGNETIC ANISOTROPY IN HARD TURNED SURFACES**

M. Neslušan<sup>1</sup>, D. Blažek<sup>2</sup>, D. Hrabovský<sup>3</sup> and M. Bukovina<sup>4</sup>

<sup>1</sup>*Department of Machining and Production Technologies, Faculty of Mechanical Engineering, University of Žilina, Univerzitná 1, 010 26 Žilina, Slovakia*

<sup>2</sup>*Nanotechnology Centre, VŠB-Technical university of Ostrava, 17. listopadu 15, 70833 Ostrava, Czech Republic*

<sup>3</sup>*RMTVC, VŠB-Technical university of Ostrava, 17 listopadu 15, 70833 Ostrava, Czech Republic*

<sup>4</sup>*Department of Materials Engineering, Faculty of Mechanical Engineering, University of Žilina, Univerzitná 1, 010 26 Žilina, Slovakia*

This paper deals with a pronounced magnetic anisotropy found in a hard turned surface as well as a recovery of magnetic isotropy obtained after grinding operation, both made on bearing steel.

The high magnetic anisotropy of the steel surface after hard turning operation occurs due to the significant plastic deformation and due to a temperature exposure exceeding the Currie temperature in the cutting zone followed by rapid cooling. The transformed microstructure of the material in a conjunction with the uniaxial residual stresses near the surface causes the magnetic anisotropy and magnetic domains reconfiguration.

On the contrary, the residual stress state is more balanced after grinding operations and the temperatures in the grinding wheel (workpiece contact) do not exceed Currie temperature. Therefore, smaller mechanic and magnetic anisotropy after grinding operations is obtained.

The magnetic properties of the studied surfaces are analyzed by Barkhausen noise emission as well as magneto-optical methods. Both of these methods are sensitive to the surface volume of the specimen. The results of these two techniques are compared from the point of view of the studied magnetic anisotropy. Due to the very different physical background of these methods a better understanding of the processes can be achieved.

**CORRELATION EFFECTS AND SPIN DEPENDENT TRANSPORT IN CARBON NANOSTRUCTURES**

S. Lipiński and D. Krychowski

*Institute of Molecular Physics, Polish Academy of Sciences,  
M. Smoluchowskiego 17, 60-179 Poznań, Poland*

Currently, there is a widespread interest in developing new types of spintronic devices and carbon nanotubes and graphene nanostructures deserve special attention in this respect due to their long spin lifetimes. With the decrease of the size of the objects increases the role of correlations and due to symmetry of carbon systems highly symmetric Kondo effects result.

In carbon nanotube (CNT) quantum dots Kondo physics is especially exciting, since in addition to spin degeneracy there occurs also orbital degeneracy. The use of single wall carbon nanotubes has pushed the Kondo temperatures to the range of several K, in graphene nanostructures even higher Kondo temperatures are expected. The spin-orbital entanglement observed in CNTs is interesting for quantum computing, since it enables operating with four state bits, what doubles the storage density. The impact of symmetry breaking perturbations including the effect of magnetic field, polarizations of electrodes and spin – orbit interaction on spin dependent transport will be discussed. We will propose carbon based low field spin filter, spin valve and spin battery, all working in the Kondo regime. We will show that in carbon nanotube quantum dots in the Kondo range tunnel magnetoresistance can reach values as large as several hundred. The analysis will be completed by the discussion of spin-dependent shot noise.

Even more attractive materials for spintronic applications are graphene nanostructures (GN), where in tunability of their electronic, magnetic and transport properties the decisive role play the edges. The functionalities of these systems can be enriched by doping the magnetic atoms, what allows the band gap engineering and designing different types of magnetic order. We will present first principles analysis of gate evolution of electronic structure of GNs and discuss energetics of embedded magnetic impurities. The electronic structure of nanosystems is dominated by confinement effects and Van Hove singularities. Since the chemical potential of GNs can be tuned, a formation of local moment, as well as interplay of magnetic ordering tendencies and Kondo correlations can be controlled by gate voltage and one expects particularly strong gate dependence near singularities.

**SPIN-ORBIT COUPLING ENHANCEMENT AND EXCHANGE INTERACTIONS IN HYDROGENATED GRAPHENE**M. Gmitra<sup>1</sup>, D. Kochan<sup>2</sup> and J. Fabian<sup>1,2</sup><sup>1</sup>*Institute for Theoretical Physics, University of Regensburg, Universitaetsstrasse 31, 93040 Regensburg, Germany*

We will present first-principles calculations of the spin-orbit coupling effects in hydrogenated graphene structures, for varying hydrogen coverage densities, using the linearized augmented plane wave method. The covalent bond between the hydrogen and carbon atoms locally deforms graphene sheets, giving rise to an overlap between the Dirac and sigma electrons and a giant enhancement (from roughly 0.01 to 1 meV) of the local spin-orbit interaction. Based on group theoretical principles we derive an effective tight-binding Hamiltonian models and identify dominant contribution to the spin-orbit coupling that comes from breaking of pseudospin inversion symmetry. The calculated spin-orbit coupling induced splittings on the band structure and the emerging spin patterns of the electronic states well agree with first-principles calculations.

Absorption of the hydrogen adatom on graphene induces in addition local magnetic moment. Phenomenological theory, based on first-principles calculations, of the exchange splitting and spin relaxation in graphene with hydrogen adatoms will be presented. The phenomenological modeling includes a symmetry based tight-binding model with the adatom interaction and local exchange couplings that are fitted to the first-principles electronic band structure data in the magnetic ground state of hydrogenated graphene. We will show that resonant scattering and the exchange interaction with the paramagnetic impurities at the adatom site can explain the experimentally observed short spin relaxation times, providing a competitive mechanism to that based on spin-orbit coupling.

*This work is supported by the DFG SPP 1285, SFB 689, and GRK 1570.*

**ELECTRONIC TRANSPORT IN MULTI-TERMINAL GRAPHENE DEVICES WITH VARIOUS ARRANGEMENTS OF ELECTRODES**

S. Krompiewski

*Institute of Molecular Physics, Polish Academy of Sciences, ul. M. Smoluchowskiego 17, 60-179 Poznań, Poland*

This study is devoted to the problem of charge and spin transport in graphene nanodevices in 4-terminal systems with various arrangements of electrodes. The electrodes are attached to square and rectangular graphene nanoflakes with armchair ( $a$ ) and zigzag ( $z$ ) edges. Apart from the case of the  $zzzz$ -configuration (with all the electrodes coupled to the zigzag fragments of the edges, see [1]), also the  $aaaa$ - and  $zaza$ -type cases are considered here. On the one hand the results help to choose an optimum configuration which maximizes the conductance, and on the other hand they shown that in some cases the devices may act as gate-voltage controlled switches. The adopted theoretical approach is based on a tight-binding method combined with the wideband approximation for electrodes, and an effective iterative "knitting"-type ([2]) Green's function algorithm.

*Acknowledgment: This work was supported by the Polish Ministry of Science and Higher Education as a research project No. N N202 199239 for 2010-2013.*

[1] K. Sääskilahti, A. Harju, and P. Pasanen, Appl. Phys. Lett. **95**, 092104 (2009)

[2] K. Kazyrenko and X. Waintal, Phys. Rev. B **77**, 115119 (2008)

**QUADRATIC MAGNETO-OPTICAL KERR EFFECT SPECTRA  
IN 3d METALS Fe, Co AND Ni**J. Hamrle<sup>1</sup>, J. Hamrlová<sup>1</sup>, D. Legut<sup>1</sup>, J. Pištora<sup>1</sup><sup>1</sup>*Institute of Physics and Nanotechnology Centre, VSB-Technical University of Ostrava, 17. listopadu 15, 70833 Ostrava, Czech Republic*

The second-order magneto-transport effects, such as anisotropy magneto-resistance (AMR), quadratic magneto-optical Kerr effect (QMOKE), X-ray magnetic linear dichroism (XMLD), magneto-refractivity etc. are described by the second-order magneto-optical permittivity/conductivity coefficients providing phenomenological description of all those effects. From symmetry point of view all those magneto-optical and magneto-conductivity effects are based on equal footing, however the different naming originates from different investigation techniques used as well as the different energy range of the probing photons (zero photon energy means dc).

Using ab-initio calculations, we determine spectra of the second-order magneto-optical permittivity coefficients ( $G_{44}$ ,  $\Delta G$ ) for ferromagnetic bcc Fe, fcc Ni and fcc Co. The calculations of the conductivity/permittivity tensor elements are done within the framework of Density Functional Theory (DFT) using general magnetic orientation with respect to the crystal axis. Then, dependence of the permittivity elements on general magnetization orientation is compared with expected dependences as provided by symmetry arguments and spectra of  $G_{44}$ ,  $\Delta G$  coefficients are extracted.

**PHASE COMPOSITION OF FERRIC OXIDE IN  $\text{Fe}_2\text{O}_3/\text{SiO}_2$  SYSTEM**

D. Kubániová<sup>1</sup>, P. Brázda<sup>2</sup>, J. Kohout<sup>1</sup>, A. Lančok<sup>2</sup>, E. Šantavá<sup>3</sup>, M. Klementová<sup>2</sup> and K. Závěta<sup>1</sup>

<sup>1</sup> Faculty of Mathematics and Physics, Charles University in Prague, V Holešovičkách 2, 180 00 Prague, Czech Republic

<sup>2</sup> Institute of Inorganic Chemistry, ASCR v.v.i., 250 68 Husinec-Řež, Czech Republic

<sup>3</sup> Institute of Physics, ASCR v.v.i., 182 21 Prague, Czech Republic

Maghemite  $\gamma\text{-Fe}_2\text{O}_3$  and thermodynamically stable hematite  $\alpha\text{-Fe}_2\text{O}_3$  are the two well-known natural polymorphs of ferric oxide.  $\beta$  and  $\varepsilon\text{-Fe}_2\text{O}_3$  were prepared just synthetically.

We present measurements on the samples of different iron concentrations prepared by sol-gel technique with the aim to obtain pure  $\varepsilon$ -phase. Samples were characterized by Mössbauer spectroscopy, XRD, EDS and DC magnetic measurements. The measurements of transmission Mössbauer spectra of the  $^{57}\text{Fe}$  nuclei in  $\text{Fe}_2\text{O}_3$  were performed in zero external magnetic field at room temperature. The spectra were fitted by core-shell model, which assumes random order of magnetic moments on surface of the nanoparticles. Phase composition was deduced from the integral intensities of the Mössbauer spectrum components corresponding to the polymorphs and from the XRD patterns. The total concentration of iron in the material was checked by EDS.

All the four phases of  $\text{Fe}_2\text{O}_3$  ( $\alpha$ ,  $\beta$ ,  $\gamma$  and  $\varepsilon$ ) were observed in the samples. Maghemite was identified as the main source of the “necking” of the hysteresis loops. Thanks to this phenomenon low concentrations of  $\gamma\text{-Fe}_2\text{O}_3$  were discerned in some samples. The results also showed that apart from the crystal size, the iron concentration in the samples is the other important factor influencing the ratios of various  $\text{Fe}_2\text{O}_3$  phases.

*Acknowledgment: The authors thank GACR for the support under the grant P204/10/0035.*



**MAGNETIC ANISOTROPIES IN TETRAGONAL Fe-Co ALLOYS**I. Turek<sup>1,2</sup>, K. Carva<sup>2</sup>, J. Kudrnovský<sup>3</sup> and V. Drchal<sup>3</sup><sup>1</sup>*Institute of Physics of Materials, Academy of Sciences of the Czech Republic, Žitkova 22, 61662 Brno, Czech Republic*<sup>2</sup>*Department of Condensed Matter Physics, Faculty of Mathematics and Physics, Charles University, Ke Karlovu 5, 12116 Praha 2, Czech Republic*<sup>3</sup>*Institute of Physics, Academy of Sciences of the Czech Republic, Na Slovance 2, 18221 Praha 8, Czech Republic*

The binary Fe-Co alloy in its equilibrium cubic (bcc) structure represents a well-known ferromagnetic system interesting, e.g., for the maximum saturation magnetization (Slater-Pauling curve) obtained around 25 at% Co. This alloy system has recently attracted renewed interest as a promising material for ferromagnetic ultrathin films applicable in high-density magnetic recording. It was shown that disordered Fe-Co alloy films with tetragonal (bct) structures can be epitaxially grown on non-magnetic fcc(001) surfaces of Rh, Pd, and Pt, and that these films exhibit a perpendicular magnetic anisotropy in a narrow range of concentrations (around 60 at% Co) and tetragonal distortions (around  $c/a = 1.25$ ).

In the present study, we calculated the electronic structure of these bulk tetragonal alloys with different degrees of atomic long-range order by means of an *ab initio* relativistic TB-LMTO method. Special attention has been paid to the uniaxial magnetic anisotropy energy (MAE), to orbital magnetic moments and to the static transport properties, in particular to the anomalous Hall effect (AHE).

We have found that the MAE values and the orbital magnetic moments are enhanced in the same region of alloy concentrations and  $c/a$  ratios as indicated by recent experiments on thin films. Moreover, we have revealed a strong sensitivity of the MAE to the atomic disorder: its proper inclusion reduces the MAE values by a factor of four as compared to ordered alloys.

We have also found that the AHE in the homogeneous disordered alloys depends strongly on the direction of magnetization. The values of the anomalous Hall conductivities for magnetizations pointing along the  $a$  and  $c$  axes can differ by a factor of three. This pronounced anisotropy is comparable to that reported recently for pure hexagonal Co. However, in contrast to the MAE, the AHE anisotropy in the tetragonal Fe-Co alloys is not reduced by chemical disorder. Calculated trends of further transport properties (longitudinal resistivities) will be presented and briefly discussed as well.

**MAGNETIC LINEAR DICHROISM AND BIREFRINGENCE IN DILUTE MAGNETIC SEMICONDUCTOR (Ga,Mn)As**Karel Výborný<sup>1</sup>, Naďa Tesařová<sup>2</sup>, John Černe<sup>3</sup>, and Tomáš Ostatnický<sup>2</sup><sup>1</sup>*Fyzikální ústav AV ČR, v.v.i., Cukrovarnická 10, Praha 6, CZ-16253*<sup>2</sup>*Matematicko-fyzikální fakulta Univerzity Karlovy,**Ke Karlovu 3, Praha 2, CZ-12116*<sup>3</sup>*University at Buffalo, State University of New York, Buffalo, NY-14260 (USA)*

Magneto-optical effects are often used as a tool to probe magnetization of a sample under study. For out-of-plane magnetization, it can be the polar Kerr effect odd in magnetization while for in-plane magnetization, quadratic magneto-optical Kerr effect (QMOKE) will serve the purpose provided it is strong enough at the frequency of used laser. However, much more interesting information pertaining to the electronic structure of the system is contained in the spectral dependence of these effects. Investigation of magnetic linear dichroism and birefringence of (Ga,Mn)As, that manifests itself in QMOKE, allows to identify transitions between individual electronic bands and their changes with manganese doping concentration  $x$ . Measurements on a series of samples grown according to an optimized protocol will be presented; their doping levels span the range from barely ferromagnetic material up to (nearly) the highest values that afford state-of-the-art critical temperature of 186 K. QMOKE measured in the spectral range  $\sim 0.1$  to 2.5 eV turns out to display much sharper features than for instance infrared absorption. A prominent peak at energies slightly above gap is analysed using mean-field kinetic-exchange k.p model and it is concluded that its blue shift with increasing  $x$  agrees with the Moss-Burstein picture, although corrections to strong disorder are necessary to obtain quantitative agreement between theory and experiment. In a broader view, the calculations lend additional credence to our time-proven model of (Ga,Mn)As; despite its complexity (non-zero QMOKE requires both spin-orbit interaction and ferromagnetic splitting of the bands), level of agreement between the model calculations and experimental data is more than satisfactory in the whole spectral range.

**THE TOPICALITY OF THE VALENTA MODEL OF THE  
MAGNETIZATION IN THIN FILMS AND SURFACES**

Š. Zajac<sup>1</sup> and L. Wojtczak<sup>2</sup>

*<sup>1</sup>Faculty of Nuclear Sciences and Physical Engineering, Czech Technical  
University, Prague, Czech Republic*

*<sup>2</sup>Department of Solid State Physics, University of Lodz, Poland*

Fifty five years ago was presented the theory of spontaneous magnetization in magnetic thin films known now as the Valenta model [1]. The model was later developed to its more general form and has been applied for explanation also of crystalline lattice thermodynamic, order-disorder and electronic phenomena, as well as for the phase transitions including the stability considerations and surface melting behaviour.

The Valenta theory of magnetic thin films has been even preceded by his pioneering work [2] on the angular distribution of magnetization in one-dimensional ferromagnetic toroid. This work has been found as good starting basis for explanation of surface deformation of helimagnetism in rare- earth thin films. Spin wave resonances, Mössbauer phenomenon, as well as neutron scattering certify the general non collinear distribution of magnetization in low- dimensional solid magnetic systems.

[1] L.Valenta, Czech. J. Phys. 7 (1957), 127, 136.

[2] L.Valenta, Czech. J. Phys. 5 (1955), 291.

**MAGNETIC CHARACTERIZATION OF Co<sub>2</sub>MnSi HEUSLER MICROWIRES**

T. Ryba<sup>1</sup>, Z.Vargova<sup>2</sup>, R.Varga<sup>1</sup>, J.Kovac<sup>3</sup>, V.Zhukova<sup>4</sup> and A.Zhukov<sup>4</sup>

<sup>1</sup>*Institute of Physics, Fac.Sci., UPJS, Park Angelinum 9, 041 54 Kosice, Slovakia*

<sup>2</sup>*Institute of Inorganic Chemistry, Fac.Sci.,UPJS, Moyzesova 11, 041 54 Kosice, Slovakia*

<sup>3</sup>*Institute of Physics, Slovak Academy of Sciences, Watsonova 47, 040 01 Kosice, Slovakia*

<sup>4</sup>*Departamento de Fisica de Materiales, Universidad del Pais Vasco, 20009 Sab Sebastian, Spain*

Heusler alloys, as new perspective material, are characterized by many interesting properties such as high Curie temperature, large magnetic moment, small Gilbert damping and high spin polarization. Particularly alloys of the chemical composition Co<sub>2</sub>MnSi are perspective group of materials for spintronics. This alloy have large spin polarization in the range 50%-98% , small Gilbert damping and high T<sub>c</sub> (1004K). The samples of Co<sub>2</sub>MnSi microwires were prepared by the Taylor-Ulitovsky technique. Given technique is a method that allows preparation of large amount of very thin wires. Heusler compositions. We report on the basic magnetic properties of glass-coated Co<sub>2</sub>MnSi Heusler microwires. Microwires consisting of a magnetic nucleus ( with diameter 10,2μm and total diamater 22,4μm) are coated by Pyrex-like glass. Measurements of hysteresis loops in different directions show that easy magnetization axis, is identical to the wire's axis. The frequency dependence of the coercive field has been measured at room temperature in the frequency range from 10Hz to 10 KHz. The coercivity decreases with the frequency up to 100 Hz and then increases linearly up to 1kHz

*This work was supported by the project NanoCEXmat No. ITMS 26220120035, Slovak VEGA grant. No.1/0060/13, APVV-0027-11, APVV-0266-10 and EU ERA-NETprogramme under projects, SoMaMicSens, (MANUNET-2010-Basque-3), by EU under FP7, EMSafety project, by Spanish Ministry of Science and Innovation, MICINN under Project MAT2010-18914 and by the Basque Government under Saiotek 09 MICMAGN project (S-PE09UN38).*

**FERRIMAGNETISM IN THE HEISENBERG-ISING BILAYER  
WITH MAGNETICALLY NON-EQUIVALENT PLANES**

T. Balcerzak and K. Szałowski

*Department of Solid State Physics, University of Łódź,  
ul. Pomorska 149/153, 90-236 Łódź, Poland*

In the paper a model of magnetic bilayer with anisotropic Heisenberg-Ising interactions is considered in the Pair Approximation. The method has been developed within the cluster variational scheme and is based on the Gibbs free-energy analysis.

The magnetic bilayer is composed of two s. q. planes:  $A$  and  $B$ , which are magnetically non-equivalent. Magnetic interactions in plane  $B$  are stronger than in plane  $A$  but the plane  $B$  is magnetically diluted. The inter-planar  $A$ - $B$  couplings are antiferromagnetic and of Ising type, whereas the intra-planar  $A$ - $A$  and  $B$ - $B$  couplings are ferromagnetic and of anisotropic Heisenberg-type.

For such a system, which has not been studied before, the phase diagrams, magnetization and spin-pair correlations as a function of temperature are examined. The existence of compensation point in the case of antiferromagnetic  $A$ - $B$  interactions is demonstrated for the properly selected parameters of Hamiltonian.

In particular, the dependence of the critical concentration  $p^*$ , below which the compensation point does not exist, on the interaction anisotropy is studied. It has been shown that increase of the anisotropy in plane  $A$  increases the value of  $p^*$ , whereas increase of the anisotropy in plane  $B$  acts in the opposite direction and diminishes it. For vanishing concentration of magnetic atoms in  $B$ -plane, the presence or absence of the phase transition depends on whether  $A$ -plane is anisotropic or not, and this fact is correlated with the onset of ferromagnetism in that plane. On the other hand, a vanishing of ferromagnetism, observed in magnetically separated planes in case of isotropic intra-planar interactions, remains in agreement with Mermin-Wagner theorem.

The results are illustrated in figures and discussed for a wide range of Hamiltonian parameters. The parameters are the following: concentration of magnetic atoms in  $B$ -plane, exchange anisotropy and unequal values of exchange integrals in  $A$  and  $B$  planes, as well as the inter-planar coupling strength.

The analysis enables to determine a range of parameters where the compensation point can be expected in such system. It also clarifies the role of exchange anisotropy in the shift of compensation point, as well as significance of antiferromagnetic inter-planar couplings in case of partially diluted bilayer.

**CHARACTERIZATION OF MAGNETOSOMES AFTER EXPOSURE TO THE EFFECT OF THE SONICATION AND ULTRACENTRIFUGATION**

M. Molčan<sup>1</sup>, A. Hashim<sup>1</sup>, J. Kováč<sup>1</sup>, M. Rajňák<sup>1</sup>, P. Kopčanský<sup>1</sup>, M. Makowski<sup>2,3</sup>, H. Gojzewski<sup>2,4</sup>, M. Timko<sup>1</sup>

<sup>1</sup>*Institute of Experimental Physics, SAS, Watsonova 47, 040 01 Kosice, Slovakia*

<sup>2</sup>*Institute of Physics, Poznan University of Technology, Niezawska 13A, 60-965 Poznan, Poland*

<sup>3</sup>*Max Planck Institute for Polymer Research, Ackermannweg 10, 55-128 Mainz, Germany*

<sup>4</sup>*Max Planck Institute of Colloids and Interfaces, Department of Interfaces, Wissenschaftspark Potsdam-Golm, Am Mühlenberg 1 OT Golm, 14476 Potsdam, Germany*

Magnetosomes are intracellular organelles of widespread aquatic microorganisms called Magnetotactic bacteria. At present they are under investigation especially in biomedical applications. This ability depends on the presence of intracellular magnetosomes which are composed of two parts: first, nanometer-sized magnetite ( $\text{Fe}_3\text{O}_4$ ) or greigite ( $\text{Fe}_3\text{S}_4$ ) crystals (magnetosome crystal), depending on the bacterial species; and second, the bilayer membrane surrounding the crystal (magnetosome membrane).

The magnetosomes were prepared by biomineralization process of magnetotactic bacteria *Magnetospirillum Magnetotacticum* sp. AMB-1. The isolated magnetosome chains (sample M) were centrifugated at speed of 100 000 rpm for 4 hours (sample UM) and sonicated at power of 120 W for 3 hours (sample SM), respectively. The prepared suspensions were investigated with respect to morphological, structural and magnetic properties. The results from scanning electron microscopy showed that isolated chains of magnetosomes were partially broken to smaller ones after ultracentrifugation. On the other hand the application of the sonication process caused the formation of individual magnetosomes (unordered in chain). These results were confirmed by coercivity and magnetization saturation measurements.

## SURFACE MAGNETOSTRICTION MODEL FOR MagNEMS

T. Szumiata, M. Gzik-Szumiata

*Department of Physics, Faculty of Mechanical Engineering,  
University of Technology and Humanities in Radom,  
Krasickiego 54, 26-600 Radom, Poland*

During last two decades a significant technological progress in the field of MagMEMS (magnetic microelectromechanical systems) has been observed as well as application potential increase of such systems [1]. Typical dimensions of magnetostrictive cantilever-type magMEMS are: thickness of magnetostrictive layer of about several  $\mu\text{m}$ , thickness of substrate - several tens of  $\mu\text{m}$ , total width - of about hundreds of  $\mu\text{m}$  and total lengths - of the order of mm. Next technological step in the miniaturization is transition to nanoscale - from MEMS to NEMS devices (nanoelectromechanical systems) [2]. It is a direct way towards designing of nanosensors and nanoactuators (like motors, pumps and valves) of unique parameters (high frequency operation, low energy consumption) and for their integration with nanoelectronics. In such systems low-dimensional effects (quantum and surface ones) significantly affect their properties.

In this work a surface roughness influence on magnetostrictive nanoactuator parameters has been analyzed theoretically. A mechanical and magnetoelastic behavior of investigated cantilever bimorphic system has been described in the frame of the simple analytical model [3]. Magnetostriction changes due to the presence of rough surfaces has been considered [4]. Realistic material parameters have been incorporated into the model for high-magnetostrictive galfeinol (Fe-Ga) thin films on silicon substrate [5]. Total deflection of the actuator and generated force have been calculated as a function both of magnetostrictive layer and substrate thickness as well as their elastic constants. It has been shown that for 5 nm thick galfeinol film a flat surface magnetostrictive effects modify the cantilever deflection only by 4%, whereas in the case of rough surface this influence increases to about 15%, when dimensions of roughness steps are comparable to the distance between them.

[1] M.R.J. Gibbs, "Applications of magmems", *J. Magn. Magn. Mater.* 290-291 (2005) 1298-1303.

[2] C.T. Leondes, "MEMS/NEMS", Springer, ISBN: 978-0-387-24520-1.

[3] K. Ishiyama, Ch. Yokota, "Cantilever actuator using magnetostrictive thin film", *J. Magn. Magn. Mater.* 320 (2008) 2481-2484.

[4] T. Szumiata, M. Gzik-Szumiata and K. Brzózka, "Pseudodipolar model of surface magnetostriction for thin layers with roughness", *Materials Science - Poland* 26 (2008) 1039-1044.

[5] A. Javed, N.A. Morley, M.R.J. Gibbs, "Structure, magnetic and magnetostrictive properties of as-deposited Fe-Ga thin films", *J. Magn. Magn. Mater.* 321 (2009) 2877-2882.

**FANO-KONDO EFFECT OF MAGNETIC IMPURITY WITH  
SIDE-COUPLED GRAPHENE FLAKE**

J. Kopiński, D. Krychowski and S. Lipiński

*Institute of Molecular Physics, Polish Academy of Sciences,  
M. Smoluchowskiego 17, 60-179 Poznań, Poland*

We examine transport through a spin-1/2 magnetic impurity patterned between atomic scale electrodes in the presence of side-coupled nanographene flake. Impurity is attached to the edge of the flake, what allows to probe the edge states. Graphene flakes of various shapes are considered. Their magnetic properties are determined within Hartree-Fock approximation assuming a finite value of the flake onsite Coulomb interaction. The emerging magnetic moments are localized at zigzaglike segments of the flakes. The Kotliar Ruckenstein slave boson approach is adopted to describe the strongly correlated impurity. The line shape of zero-bias conductance changes with the shift of chemical potential from Kondo resonance when Fermi level is located between discrete energy levels of the flake to antiresonance when levels cross the Fermi energy and destructive interference between direct path and path through the flake results. In both cases local polarization reflects in the spin splitting of transmission lines. Spin polarization of conductance changes with the shift of the chemical potential and in some cases full spin filtering is observed.



# **THERMOPOWER AND SURFACE MAGNETIC CHARACTERIZATION OF NI THIN LAYERS**

A. Szabo<sup>1</sup>, R. Varga<sup>2</sup>, F. Ujhelyi<sup>3</sup>, V. Komanicky<sup>2</sup>, A. Zorkovska<sup>2</sup> and A. Lovas<sup>1</sup>

<sup>1</sup>*Department of Automobiles and Vehicle Manufacturing, Budapest University of Technology and Economics, Stoczek u. 2. 1111 Budapest, Hungary*

<sup>2</sup>*Department of Condensed Matter Physics, Institute of Physics P.J. Šafárik University, Park Angelinum 9 041 54 Košice, Slovakia*

<sup>3</sup>*Department of Atomic Physics, Budapest University of Technology and Economics, Budafoki u. 8. 1111 Budapest, Hungary*

It has been known for some time that for a system of independent electrons interacting with static scatterers, the Mott formula for the thermoelectric power is exact for arbitrary values of the interaction strength:

$$S(T) = \frac{\pi^2}{3} \frac{k^2 T}{e} \left( \frac{\partial \ln \sigma(\varepsilon)}{\partial \varepsilon} \right)_{\varepsilon=\varepsilon_F}$$

Where  $k$  is the Boltzmann's constant,  $e$  is the electron charge,  $\sigma(\varepsilon)$  is the conductivity and  $\varepsilon$  is the Fermi energy.

The measurement of thermoelectric power is successfully applied as non-destructive testing in several metallic substances, especially in structural steels and amorphous materials.

Recently the method is also applied for the thin film characterization, however the interpretation of the observed phenomenon is far from the complete understanding.

In the present contribution, the separation of "thin-layer" and bulk effects is planned, completing the thermopower measurements with surface magnetic and structural (X-ray) characterization. Typical size dependence (a continuous transition from nanoscopic to bulk properties) is found in both properties, with increasing layer thickness, which is also supported by the structural investigations.

# STRUCTURAL AND MAGNETIC CHARACTERIZATION OF NiMnSb HALF-HEUSLER ALLOY PREPARED BY RAPID QUENCHING

T. Ryba<sup>1</sup>, Z. Vargová<sup>2</sup>, R. Varga<sup>1</sup>, S. Ilkovic<sup>3</sup>, M. Reiffers<sup>3</sup>, V. Haskova<sup>1</sup>, P. Szabo<sup>4</sup>, J. Kravčák<sup>5</sup>, R. Gyepes<sup>6</sup>

<sup>1</sup> Inst. Phys., Fac. Sci., UPJS, Park Angelinum 9, 041 54 Košice, Slovakia

<sup>2</sup> Dept. Inorg. Chem., Fac. Sci., UPJS, Moyzesova 11, 041 54 Košice, Slovakia

<sup>3</sup> Univ. of Prešov, Fac. Hum. and Nat. Sci., SK-08078 Prešov, Slovakia

<sup>4</sup> IEF SAS, Watsonova 47, 04001 Košice

<sup>5</sup> Dept. Phys., FEEL, Technical University of Košice, Košice, Slovakia

<sup>6</sup> Dept. of Chemistry, Faculty of Education, J. Selye University, Komárno, Slovakia

The large class of Heusler compounds offer many potential applications. The magnetic  $X_2YZ$  compounds show various magnetic multifunctional properties, such as magneto-optical, magnetocaloric and magnetostructural [1]. The magneto-electrical half-Heusler XYZ compounds, the half-metallic ferromagnets provide nonmagnetic semiconductors, and even superconductors, thermoelectrics, and solar cells [2].

The typical example of half-Heusler alloys that exhibit high spin polarization is NiMnSb. It is commonly prepared by arc-melting method followed by long-term annealing process. The new rapid quenching method has been recently successfully introduced to prepare the Full-Heusler alloy [3]. It allows a fast production of relatively large amount of alloy.

In the given contribution, we have applied the rapid quenching method to produce NiMnSb half-Heusler alloys. Structural and magnetic properties of NiMnSb half-Heusler alloys will be described. The SEM/EDS and powder X-ray characterizations were used to estimate their composition and structure determination. Magnetic properties have been studied by VSM and Spin polarization has been estimated by Andreev reflection.

*This work was supported by Project NanoCEXmat No.ITMS 26220120035, Slovak VEGA Grant no.1/0060/13 and APVV-0027-11.*

[1] T. Graf, C. Felser, S.S.P. Parkin, *Prog. Solid State Chem.* **39** (2011), 1

[2] A. Hirohata, M. Kikuchi, N. Tezuka, K. Inomata, J.S. Claydon, Y.B. Xu, G. van der Laan, *Curr. Opin. Sol. State Mat. Sci.* **10** (2006), 93

[3] B.Hernando, J.L.Sanchez Liamazares, J.D.Santos, V.M.Prida, D.Baldomir, D.Sarentes, R.Varga, J.Gonzales, *Appl. Phys. Lett.* **92** (2008) 132507.

# **ELECTRONIC AND SPIN DEPENDENT TRANSPORT PROPERTIES OF Fe/CaSe/Fe (001) HETEROJUNCTIONS**

P. Vlaic<sup>1,2</sup> and E. Burzo<sup>2</sup>

<sup>1</sup>*University of Medicine and Pharmacy "Iuliu Hatieganu", Biophysics Department, 400023 Cluj-Napoca, Romania*

<sup>2</sup>*Faculty of Physics, Babes-Bolyai University, 400084 Cluj-Napoca, Romania*

Calcium selenide wide band gap semiconductor crystallize under ambient conditions in rock salt (B1)-type structure with a lattice parameter ( $a_{\text{CaSe}}=5.91 \text{ \AA}$ ) rather epitaxially compatible with that of bcc Fe structure. Thus Fe/CaSe/Fe (001) heterostructures represent feasible systems for theoretical investigations as well as practical applications in the context of magnetoelectronics.

Electronic and magnetic properties of Fe/CaSe/Fe (001) magnetic tunnel junctions (MTJs) have been studied by means of a self consistent Green's function technique for surface and interfaces implemented within tight-binding linear muffin-tin formalism (TB-LMTO) [1]. The spin dependent transport properties in current-perpendicular-to-plane (CPP) geometry have been studied by means of the linear response of Kubo-Landauer approach implemented within TB-LMTO formalism [2].

A small charge rearrangement mostly localized at interface layers and the enhancements of the interfacial iron magnetic moments are evidenced. Small exchange couplings with the sign depending on Fe/CaSe (001) interface structure and the strength decaying exponentially with the barrier thickness are observed. Interface resonant states have an important role in the tunneling processes and the main contribution to the ferromagnetic (FM) state conductances is given by the minority spin electrons. High tunneling magnetoresistance (TMR) ratios, beyond 2000 %, are predicted. Electronic, magnetic and spin dependent transport properties of Fe/CaSe/Fe (001) MTJs are sensitive to Fe/CaSe (001) interface structure and rather similar with those of previously studied Fe/CaS/Fe (001) heterojunctions [3].

[1] I. Turek, V. Drchal, J. Kudrnovský, M. Šob and P. Weinberger in "Electronic Structure of Disordered Alloys, Surfaces and Interfaces" (Kluwer Academic Publishers, 1997).

[2] K. Carva, I. Turek, J. Kudrnovský and O. Bengone, Phys. Rev. B 73 (2006) 144421.

[3] P. Vlaic, E. Burzo and K. Carva, J. Apply. Phys. 113 (2013) 053715.

**LOW TEMPERATURE MAGNETIC PROPERTIES OF  
FERROMAGNETIC LAYERED COMPOSITES**

A. Urbaniak-Kucharczyk

*Faculty of Physics and Applied Informatics, University of Łódź, Pomorska 149/153,  
90 236 Łódź, Poland*

In the last decade properties of periodic composite magnetic materials, generated a great deal of interest because of growing technological importance in view of applications of such materials for information storage, magnetic heads and propagation elements as well as developments in experimental techniques. In presented paper a ferromagnetic layered composite (ABAB....ABA, where A and B are different homogeneous ferromagnetic materials) is studied by means of Green function approach. Our attention is focussed on the elementary excitations and low temperature magnetisation behavior. To describe the system we use Heisenberg Hamiltonian consisting of the exchange, single ion anisotropy, Zeeman and dipolar coupling terms, respectively. Parameters of spin wave spectrum are calculated using the transfer matrix method. The cases of disordered surface and of inhomogeneous boundary conditions are considered, respectively.

In the presented paper we take also into account the effects of damping due spin-spin interaction. As a result not only the positions and relative intensities of resonance peaks are obtained but also the resonance line-width is found. On the basis of above described method the temperature dependence of magnetization of a ferromagnetic layered composite is calculated and the spin wave parameter  $B$  in the Bloch's law  $T^{3/2}$  is found and presented in dependence of parameters characterizing the system under consideration.

**APPROXIMATION OF ELECTRICAL AND MAGNETO TRANSPORT PROPERTIES OF LSMO THIN FILMS USING POLYNOMIAL FIT EXPRESSION**

V. Štrbík<sup>1</sup>, M. Reiffers<sup>2</sup>, Š. Chromík<sup>1</sup> and M. Španková<sup>1</sup>

<sup>1</sup>*Institute of Electrical Engineering, Slovak Academy of Sciences, Dúbravská cesta 9, 841 04 Bratislava, Slovak Republic*

<sup>2</sup>*Faculty of Humanities and Natural Sciences, University of Prešov, Ul. 17 novembra 1, 081 16 Prešov, Slovak Republic*

To characterize the electrical and magneto transport properties of  $\text{La}_{0.7}\text{Sr}_{0.3}\text{MnO}_3$  (LSMO) thin films we used the polynomial fit expression consisting of three terms. The first term is determined by a low temperature ( $T < 20$  K) residual resistivity  $\rho_0$ , the second term describes the electron-electron scattering in LSMO and it shows  $\sim T^2$  dependence up to temperature about 160-180 K. At temperatures around 300 K a steep increase of resistivity appears which is described by the third term proportional to  $\sim T^{4.5}$  dependence. This term corresponds to the electron-magnon scattering from double exchange theory.

We show that the polynomial fit expression can be used for analyzing and characterization of LSMO electrical and magneto transport properties in wide temperature range (0-380 K) and magnetic field at least up to 9 T.

**GROWTH AND CHARACTERIZATION OF LSMO FILMS WITH INCREASED TEMPERATURE OF MI TRANSITION**

M. Španková, Š. Chromík, I. Vávra, A. Rosová, E. Dobročka and V. Štrbík  
*Institute of Electrical Engineering SAS, Dúbravská cesta 9, 841 04 Bratislava, Slovakia*

Epitaxial  $\text{La}_{0.67}\text{Sr}_{0.33}\text{MnO}_3$  (LSMO) thin films with a significant increased temperature of metal-insulator transition ( $\sim 450$  K) are prepared on single crystal MgO (001) substrates using different deposition techniques - a *dc* magnetron sputtering or a pulsed laser deposition.

The crystalline perfection of the films, both the sputtered and the laser deposited, are characterized by X-ray diffraction technique, rocking curve measurements and transmission electron microscopy (TEM).

As a consequence of different methods of the film preparation we show various types of the LSMO film microstructure having influence on the electrical properties of the films. The results obtained from these structural and electrical film characterizations are reported.

#### P4-13

### ACOUSTIC AND MAGNETIC PROPERTIES OF BACTERIAL MAGNETITE NANOPARTICLES SUSPENSION

A. Józefczak<sup>1</sup>, A. Hashim<sup>2</sup>, M. Molčan<sup>2</sup>, T. Hornowski<sup>1</sup>,

A. Skumiel<sup>1</sup>, P. Kopčanský<sup>2</sup>, M. Timko<sup>2</sup>

<sup>1</sup>*Institute of Acoustics, Faculty of Physics, Adam Mickiewicz University,  
Umultowska 85, 61-614 Poznań, Poland*

<sup>2</sup>*Institute of Experimental Physics, Slovak Academy of Sciences, Košice,  
Watsonova 47, 040 01 Kosice, Slovakia*

Magnetosomes are bacterial magnetic nanoparticles containing iron mineral crystals of magnetite ( $\text{Fe}_3\text{O}_4$ ) or greigite ( $\text{Fe}_3\text{S}_4$ ). They are the size of nanometer, they disperse very well because they are covered with a stable biological membrane – phospholipid bilayer mixed with proteins.

This paper presents an ultrasound method based on the measurements of compression wave velocities and determination of the phase velocity of a wave. The obtained data allow the determination of the mechanical characteristics of the suspension. Acoustic studies have shown that the propagation velocity of ultrasonic wave in the bacterial magnetic particle suspension is higher in comparison with the liquid carrier (HEPES solution). Magnetosomes suspension behaves inversely in comparison with magnetic fluids with chemically synthesized  $\text{Fe}_3\text{O}_4$ .

Magnetic properties carried out by SQUID magnetometer showed that suspension of magnetosomes behaves as superparamagnetic material without coercivity at room temperature.

*This work was supported by a Polish National Science Centre grant, no DEC-2011/03/B/ST7/00194 and by Slovak Academy of Sciences projects VEGA No. 2/0043/2012, APVV 0171-10 and Ministry of Education Agency for structural funds of EU in frame of projects Nos. 26220220061 and 26220120033.*

# ANDREEV REFLEXION SPECTROSCOPY STUDY OF SPIN POLARIZATION IN $\text{Co}_2\text{Cr(Fe)Al}$ HEUSLER ALLOYS

V. Haskova<sup>1</sup>, P. Szabo<sup>2</sup>, P. Samuely<sup>2</sup>, J. Kovac<sup>2</sup>, T. Ryba<sup>1</sup>, Z. Vargova<sup>3</sup>, R. Varga<sup>1</sup>

<sup>1</sup>*Inst. Exp. Physics, SAS, Watsonova 47, 04001 Kosice*

<sup>2</sup>*Inst. Phys., Fac. Sci., UPJS, Park Angelinum 9, 041 54 Kosice, Slovakia*

<sup>3</sup>*Dept. Inorg. Chem., Fac. Sci., UPJS, Moyzesova 11, 041 54 Kosice, Slovakia*

The large class of Heusler compounds offer many potential applications [1]. One of the most promising application is in spintronics as some Heusler alloys exhibit high spin polarization [2]. The typical example of a such Heusler half-metal is  $\text{Co}_2\text{CrAl}$  [2].

In the present contribution the influence of Fe on the spin polarization of  $\text{Co}_2\text{CrAl}$  will be studied. A recently successfully introduced new rapid quenching method have been used for the sample preparation [3]. The spin polarization parameter P of each sample has been determined from Point-contact Andreev reflexion spectra [4], measured on different microconstrictions between a superconducting Nb tip and  $\text{Co}_2\text{Cr(Fe)Al}$  sample.

*This work was supported by the ERDF EU (European Union European regional development fond) grant, under the contract No. ITMS26220120047.*

[1] A. Hirohata, M. Kikuchi, N. Tezuka, K. Inomata, J.S. Claydon, Y.B. Xu, G. van der Laan, *Curr. Opin. Sol. State Mat. Sci.* **10** (2006), 93

[2] T. Graf, C. Felser, S.S.P. Parkin, *Prog. Solid State Chem.* **39** (2011),

[3] B.Hernando, J.L.Sanchez Liamazares, J.D.Santos, V.M.Prida, D.Baldomir, D.Sarentes, R.Varga, J.Gonzales, *Appl. Phys. Lett.* **92** (2008) 132507.

[4] R.J. Soulen Jr. et al., *Science* **289** (1998) 85., I.I. Mazin et al., *J. Appl. Phys.*, **89** (2001) 7576.



**MAGNETIC STUDY OF ALPHA, EPSILON AND GAMMA -PHASES OF IRON NITRIDE THIN FILMS**Ewelina Zofia Frątczak <sup>1,2</sup>, José Emilio Prieto <sup>1</sup>, Marek Edward Moneta <sup>2</sup><sup>1</sup> *Centro de Microanálisis de Materiales, Universidad Autónoma de Madrid, Campus de Cantoblanco, Ediff. 22, Faraday 3., E-28049 Madrid, Spain*<sup>2</sup> *University of Łódź, Department of Solid State Physics, Pomorska 149, 90-236 Łódź, Poland*

Most of the Fe–nitride phases have been studied in much detail. Nevertheless, there is still a debate about the most efficient, exact and controlled way of obtaining thin films of the different iron nitride phases. Here we present data on the recent state of our investigation and focus on low and high nitrogen-content iron-nitride phases and their transformations by ion irradiation and annealing.

Thin films of iron nitrides were deposited by molecular beam epitaxy in ultra high vacuum conditions. We grew alpha ( $\alpha''$ -Fe<sub>16</sub>N<sub>2</sub>), epsilon ( $\epsilon$ -Fe<sub>x</sub>N,  $2 \leq x \leq 3$ ) and gamma (FeN<sub>y</sub>,  $y > 0.5$ ) phases by evaporating Fe in the presence of a flow of atomic nitrogen and by post-nitriding under controlled conditions a thin epitaxial  $\gamma'$ -Fe<sub>4</sub>N sample.

By adjusting the growth parameters, we tried to obtain the  $\alpha''$ -phase in its possible purest form. In a similar way, we aimed to produce films of the  $\epsilon$  nonmagnetic phase in its possible purest form and to process them by heavy ion irradiation in order to transform it to a magnetic  $\epsilon$  phase. We worked also on iron mononitride, FeN, which is known to exist in different phases. There is a debate on the exact crystal type and on the coexistence of these phases. On the basis of theoretical calculations, two FeN compounds are predicted with different phases:  $\gamma''$ -FeN and  $\gamma'''$ -FeN. However, up to this moment, there is no unambiguous experimental evidence for the existence of these two different phases.

The stoichiometry of the samples was determined by means of resonant RBS with an accuracy of about 1%. The samples were investigated by room temperature conversion electron Mössbauer spectroscopy (CEMS). On the basis of results obtained from Mössbauer analysis supported by RBS data, we studied the dependence of the growth of the samples with different growth parameters and show the results of our attempts of transformations. We achieved as much as 36% of pure  $\alpha''$ -phase, a transformation of nonmagnetic  $\epsilon$ -phase into magnetic  $\epsilon$ -phase after heavy ion irradiation and provide evidence of the existence of  $\gamma''$ -FeN with vacancies.

**SUPERPARAMAGNETISM IN COBALT NANOPARTICLES COATED BY PROTECTIVE GOLD LAYER**

P. Hrubovčák<sup>1</sup>, A. Zelenáková<sup>1</sup>, V. Zelenák<sup>2</sup>, N. Murafa<sup>3</sup>, and J. Kováč<sup>4</sup>

<sup>1</sup>*Department of Solid State Physics, P.J. Šafárik University, Park Angelinum 9, 04154 Košice, Slovakia*

<sup>2</sup>*Department of Inorganic Chemistry, P.J. Šafárik University, Moyzesova 11, 04001 Košice, Slovakia*

<sup>3</sup>*Department of Inorganic Chemistry, Charles University, Prague, Czech Republic*  
*ESY-Hasylab, Notkestrasse 85, Hamburg, Germany*

<sup>4</sup>*Institute of Experimental Physics, SAS, Watsonova 41, 041 54 Košice, Slovakia*

Magnetic nanoparticles are in great interest of study because of its specific properties with comparison to the identical material in bulk form. Origin of these unique qualities stems mainly from the size, structure and character of surface of the particles. In recent years, magnetic nanoparticles are widely used in medicine (MRI, cancer treating, targeted drug delivery), electronics (increase of the density of data recording) as well as in technics (production of ferrofluids).

In this work we prepared core-shell magnetic nanoparticles Co@Au and studied its properties. Particles were synthesized employing the method of microemulsion. Structural analysis was performed by TEM (Transmission electron microscope) and HE XRD (High energy X-ray diffraction). Measurements confirmed spherical shape and core-shell structure of as prepared nanoparticles with narrow size distribution. Average size of Co@Au nanoparticles was estimated to  $d \sim 8$  nm.

Investigation of magnetic properties of the nanoparticles was carried out utilizing SQUID based magnetometer in temperature range of 2-300 K. Employing Langevin fit to the experimental data of  $M(H)$  at 280 K the magnetic moment of individual particle  $m_p \sim 145 \mu_B$  and average size of  $d \sim 7$  nm were established for as-prepared Co@Au nanoparticles. From  $M(T)$  curves critical temperature, below which the magnetic moments of the particles are blocked, was determined below  $T \sim 50$  K.

AC susceptibility dependence on temperature curve measured at different frequencies (0.1 Hz - 1000 Hz) displayed maximum which shifts towards the higher temperature with increasing frequency. Using theoretical Néel-Arrhenius and Vogel-Fulcher models for magnetically non-interacting and interacting particles we assume that interparticle interactions are significant in presented system of nanoparticles.

# DEPENDENCE OF MORIN TEMPERATURE ON THE SIZE OF $\alpha$ -Fe<sub>2</sub>O<sub>3</sub> NANOPARTICLES

J. Kohout<sup>1</sup>, T. Kmjec<sup>1</sup>, K. Závěta<sup>1</sup>, P. Brázda<sup>2</sup>, M. Klementová<sup>2</sup>, A. Lančok<sup>2</sup>, D. Nižňanský<sup>2</sup>

<sup>1</sup> Charles University in Prague, Faculty of Mathematics and Physics,  
V Holešovičkách 2, 180 00 Praha, Czech Republic

<sup>2</sup> Institute of Inorganic Chemistry of the ASCR, v.v.i., 250 68 Husinec-Řež, Czech Republic

Hematite ( $\alpha$ -Fe<sub>2</sub>O<sub>3</sub>) exhibits a spin reorientation transition from antiferromagnetic spin ordering to weak ferromagnetic state above the temperature  $T_M$ , known as the Morin transition [1], which equals 264 ( $\pm 2$ ) K for the bulk material [2]. The value of  $T_M$  depends on the size of the particles. When the size of particles is decreasing to nanodimensions, temperature  $T_M$  is also decreasing [1, 3]. For particles smaller than  $\sim 20$  nm the Morin transition may be even suppressed [4]. Our nanoparticles of  $\alpha$ -Fe<sub>2</sub>O<sub>3</sub> were prepared by sol-gel [5] and hydrothermal [6] techniques. The samples were characterized by powder XRD, TEM and DC magnetic measurements. The X-ray powder diffraction pattern confirmed  $\alpha$ -Fe<sub>2</sub>O<sub>3</sub> as the main phase. The shape of the particles as well as the mean particle size and its distribution were obtained from TEM. The temperature dependence of magnetization after cooling in zero and non-zero magnetic field was measured in a SQUID magnetometer and  $T_M$  was derived from the rapid increase in the magnetization.

We present temperature dependence of transmission Mössbauer spectra in the range 4.2 through 300 K in our samples with distribution of particle sizes. The Mössbauer spectra were fitted by two sextets respectively ascribed to the antiferromagnetic and a weak ferromagnetic phase with relative intensities proportional to their concentrations. Experimental data were compared with the theoretical dependence of  $T_M$  on the particle size [3, 7].

## Acknowledgement

The authors thank the GACR for the support under the grant P204/10/0035.

- [1] Morin F.J. Phys. Rev. 78, 819 (1950)
- [2] Amin N., Araj S., Phys. Rev. B **35** (1987), 4810-4811
- [3] Lu H. M., Meng X. K., J. Phys. Chem. C **114** (2010), 21291-21295
- [4] R.E.Vandenberghe et al., Hyperfine Interactions **53** (1990), 175-196
- [5] P. Brázda, et al., J. Sol-Gel Sci. Technol. **51** (2009) 78-83
- [6] X. Wang, J. Zhuang, Q. Peng, Y. Li, Nature 2005, 437, 121-124
- [7] X. Batlle and A. Labarta J. Phys. D: Appl. Phys. **35** (2002) R15-R42

**ORDERED NANOPOROUS SILICA MODIFIED WITH MAGNETIC LANTHANIDES NANOPARTICLES**O. Kapusta<sup>1</sup>, A. Zeleňáková<sup>2</sup>, V. Zeleňák<sup>1</sup><sup>1</sup>*Department of Inorganic Chemistry, P.J. Šafárik University, Moyzesova 11, 04001 Košice, Slovakia*<sup>2</sup>*Department of Solid State Physics, P.J. Šafárik University, Park Angelinum 9, 04154 Košice, Slovakia*

Lanthanide metals and their alloys have attracted much attention as suitable magnetic materials for a wide range of technological and biomedical applications. For example, Gd and its compounds are of current interest as magnetic resonance contrast media, therapeutic agents in tumor treatment and drug delivery. The well-defined shape and size of nanoparticles is necessary for mentioned application. One of the promising methods how to pack the magnetic nanoparticles into ordered structures with the possibility of controlling their size and shape is nanocasting approach.

In our work, we prepared magnetic nanoparticles of lanthanide oxides Ln= (Gd, Pr, Nd, Eu and La) inside a periodic porous matrix of silica type SBA-15. Nanoparticles were prepared using wet-impregnation method and by nanocasting, where the mesoporous silica acts as a hard template for the growth of the nanoparticles. The structure of prepared samples was characterized by adsorption/desorption of nitrogen, SAXS (Small angle X-ray scattering), XANES (X-ray Near Edge Spectroscopy) and by powder X-ray diffraction. The realized measurements show on the reduction of the pore volume from 720 g/cm<sup>2</sup> for a blank mesoporous matrix to about 35 g/cm<sup>2</sup> for lanthanide/silica nanocomposite due to the lanthanide nanoparticles confined. Also, the presence of lanthanide oxides type of Ln<sub>2</sub>O<sub>3</sub> with cubic symmetry and the lattice parameters refined in space group *Fm3m* was confirmed. Magnetic properties were investigated using a SQUID based magnetometer in external dc field up to 5 T and in the temperature range of 2 – 300 K. The inverse dc susceptibility analysed by a Curie-Weiss law in the Gd<sub>2</sub>O<sub>3</sub> nanoparticles shows on a weak antiferromagnetic behaviour, represented by the Weiss constant of  $\theta = 2.24$  K, what is in a good agreement with previous studies. The magnetic moment of 6.2 Bohr magnetons is lower than the theoretical value of 7.94 Bohr magnetons, which could be due to nanosized character of the sample.

**INFLUENCE OF Ta AND Mo INTERLAYERS ON THE MAGNETIC PROPERTIES AND OUT-OF-PLANE TEXTURE OF Nd-Fe-B MULTILAYER FILMS**

M. Grigoras, N. Lupu, H. Chiriac, F. Borza and M. Urse

*National Institute of Research & Development for Technical Physics,  
47 Mangeron Blvd., 700050 Iasi, Romania*

The anisotropic magnetic thin films, such as out-of-plane-oriented Nd-Fe-B films, for which it is possible to obtain high  $M_r/M_s$  ratio ( $M_r$  - remanent magnetization,  $M_s$  - saturation magnetization), high coercivity,  $H_c$ , and large maximum energy product  $(BH)_{\max}$ , have attracted an increasing attention due to their potential applications in magnetic microelectromechanical systems (MEMS), microstructured magnetic sensors, and ultra-high-density magnetic data storage.

In this paper, the influence of the Ta and Mo interlayers and its thickness, substrate nature and temperature on the hard magnetic properties and out-of-plane texture are investigated and compared for the NdFeB/(Ta,Mo) multilayer films.

The Nd-Fe-B/(Ta,Mo) multilayer films have been prepared by r.f. sputtering deposition on Si and SiO<sub>2</sub>/Si substrates. Ta or Mo buffer layers with thickness of about 40 nm have been used to promote the out-of-plane texture for Nd-Fe-B films.

The Mo interlayers with the thickness  $\leq 10$  nm were found to be most effective for nucleation of the Nd<sub>2</sub>Fe<sub>14</sub>B grains with  $c$ -axis perpendicular to the film plane, when  $T_s \leq 500^\circ\text{C}$ , in comparison with Ta interlayers. The multilayered configuration stimulates the formation, in one-step, of out-of-plane texture for NdFeB/(Mo,Ta) films deposited on substrates heated at the temperatures of  $500^\circ\text{C}$  and  $550^\circ\text{C}$ , respectively. The additional annealing at higher temperatures leads to deterioration of the hard magnetic properties.

The  $c$ -axis texture is not fully developed for NdFeB/(Mo,Ta) multilayer films prepared on heated substrates at temperatures between  $370^\circ\text{C}$  and  $400^\circ\text{C}$ . The postdeposition treatments for NdFeB/(Mo,Ta) multilayer films at temperatures of  $550^\circ\text{C}$  and  $600^\circ\text{C}$ , respectively, are sufficient to develop a strong out-of-plane texture. In comparison with NdFeB/Ta multilayer film, the NdFeB/Mo multilayer film exhibits a decrease in the nanocrystallization temperature of about  $50^\circ\text{C}$  because the Mo film shows to be the better candidate as interlayer for its good lattice match with the Nd-Fe-B layer.

**BROAD-BAND VNA-FMR EXPERIMENTS IN OLD AND NEW PROBLEMS OF MAGNETIZATION DYNAMICS**H. Głowiński<sup>1</sup>, A. Żywczak<sup>2</sup>, T. Stobiecki<sup>2</sup> and J. Dubowik<sup>1</sup><sup>1</sup>*Institute of Molecular Physics Polish Academy of Sciences, Mariana Smoluchowskiego Str. 17, 60-179 Poznań, Poland*<sup>2</sup>*Department of Electronics, AGH University of Science and Technology, Mickiewicza Av. 30, 30-059 Kraków, Poland*

We show versatility of broad-band ferromagnetic resonance technique based on Vector Network Analyzer (VNA-FMR) for magnetic characterization of various samples: bulk ferromagnets, thin films or ultrathin film structures. Due to a broad dynamical range ( $\sim 120$  dB) of VNA spin-wave excitations can be measured both in the bulk ferromagnets as well as in ultrathin structures using the same coplanar waveguide (CPW). We will show new FMR results concerning old and new problems of the spin wave excitations:

- Ferromagnetic resonance and ferromagnetic antiresonance in amorphous metallic NiFeMo ribbons observed in the in-plane configuration. These are representative of spin-wave excitations in bulk metals.
- Standing spin-wave resonance (SSWR) in thin Permalloy films (20 – 40 nm) in the in-plane configuration gives us a new twist in characterization of spin-wave dynamics at frequencies up to 40 GHz. These experiments exemplify usefulness of VNA-FMR for not frequently measured spin-wave excitations in the in-plane configuration.
- Ultrathin ( $\sim 1$  nm) magnetic films are characterized by using VNA-FMR. The films set up multilayer structures ( magnetic tunnel junctions and all-metallic GMR double spin-valves), which are used for spin-transfer-torque devices. Magnetization dynamics as well as anisotropies are characterized in these structures with a high accuracy.

*This work was done in the framework of Project NANOSPIN PSPB-045/2010 supported by a grant from Switzerland through the Swiss Contribution to the enlarged European Union.*

**EXCHANGE-BIAS IN THIN FILM STRUCTURES : A MICROMAGNETIC APPROACH**J. Dubowik<sup>1</sup>, I. Gościańska<sup>2</sup><sup>1</sup>*Institute of Molecular Physics Polish Academy of Sciences, Mariana Smoluchowskiego Str. 17, 60-179 Poznań, Poland*<sup>2</sup>*Department of Physics, A. Mickiewicz University, Umultowska Str. 85, 61-614 Poznań, Poland*

We present experimental results concerning exchange-bias (EB) in thin film systems, in which three types of Heusler alloys ( $\text{Ni}_2\text{MnSn}$ ,  $\text{Co}_2\text{MnSn}$ ,  $\text{Co}_2\text{FeSi}$ ) are in contact with an antiferromagnet. Magnetic exchange interactions between the constituting atoms (i.e., Ni-Mn, Mn-Mn, Co-Mn, and Co-Fe, or Co-Co) differ substantially in these Heusler alloys (HA). We explain the influence of the exchange stiffness  $A$  within the Heusler alloys and of the exchange coupling between Heusler alloy and an antiferromagnet in a finite interface volume.

We show that the origin of exchange bias in Heusler alloy films in contact with an antiferromagnet is more complex than that for conventional FM/AFM structures. We qualitatively explain the strength of EB in HA/AFM structures as depending on magnitude of exchange integrals between magnetic moments localized in HA in a different way. On mesoscopic scale, the exchange interactions are described by the exchange stiffness constant  $A$ . Our results show that EB in HA/IrMn structures is proportional to  $A$  scaled by a reduction factor  $\varepsilon \approx 0.001\text{--}0.01$ , which is ascribed to a small number of the pinned spins. Our experimental results of EB in bilayers and multilayers as well as Co "dusted" multilayers suggest that interface roughness and crystallite sizes determine the magnitude of the reduction factor  $\varepsilon$ . In Mn containing HA/AFM structures a strong increase in EB is observed at low temperatures. We preferably relate this effect to FM/AFM interactions in nanoscale rather than to HA/IrMn coupling at interfaces.

*Authors acknowledge support from Polish Ministry of Higher Education and Science (Grant 733/N-DAAD/2010/0) for financial support.*

**AC MAGNETIC SUSCEPTIBILITY STUDY OF Fe AND Co BASED NANOPARTICLES**A. Zelenáková<sup>1</sup>, V. Zelenák<sup>2</sup>, and J. Kováč<sup>3</sup><sup>1</sup>*Department of Solid State Physics, P.J. Šafárik University, Park Angelinum 9, 04154 Košice, Slovakia*<sup>2</sup>*Department of Inorganic Chemistry, P.J. Šafárik University, Moyzesova 11, 04001 Košice, Slovakia*<sup>3</sup>*Institute of Experimental Physics, SAS, Watsonova 41, 041 54 Košice, Slovakia*

Mono-domain metal nanoparticles based on iron and cobalt are of great interest due to their intrinsic physical properties, such as macroscopic quantum tunnelling (MQT), quantum size effects, giant magnetic moment and surface spin frustration interplaying between the surface and core atoms. In particular, metal magnetic nanoparticles have attracted the attention of the scientific community because the application in information storage and for biomedical uses: magnetic nanoparticles have been proposed as contrast agents for magnetic resonance imaging, carriers for drug or gene delivery systems, and hyperthermal treatment of tumours. If magnetic interactions between the particles are not negligible, they can have a significant influence on the superparamagnetic relaxation. Furthermore, the spin structure of nanoparticles can be affected by inter-particle interactions. An assembly of nanoparticles coupled by sufficiently weak inter-particle interactions show a superparamagnetic behaviour, while stronger interactions between densely packed nanoparticles can stabilize superspin glass or superferromagnetic state. One of the powerful ways how to get a better insight into the nature of inter-particle interactions and estimate their strength is the analysis of ac magnetic susceptibility.

In this context, in our work we have prepared and studied the inter-particle interactions of iron and cobalt based nanoparticles of Fe, Fe<sub>2</sub>O<sub>3</sub>, Co and CoO coated by different non-magnetic surfaces shells. Magnetic measurements were performed on a commercial superconducting quantum interference device (SQUID) magnetometer (Quantum Design MPMS XL5) over a range of temperatures (2-300 K) and applied dc fields (up to 5 T). The complex ac magnetic susceptibility  $\chi'(f) + i\chi''(f)$ , where  $\chi'$  represents in-phase ac susceptibility (real part) and  $\chi''$  out-of-phase (imaginary part) susceptibility, was registered by the same instruments in the temperature interval 2-300 K and in the frequency interval 0.1-1000 Hz. We have analysed the experimental data of real and imaginary component of ac susceptibility for various nanoparticle systems through theoretical laws for non-interacting and interacting particles and we have estimated the strength of magnetic interaction and their influence of total magnetic processes in nanoparticles.



**INFLUENCE OF THE SIDE-ELECTRODE ON TRANSPORT THROUGH HYBRID NANODEVICES**

G. Michałek and B. R. Bułka

*Institute of Molecular Physics, Polish Academy of Sciences,  
ul. M. Smoluchowskiego 17, 60-179 Poznań, Poland*

Recently, devices which consists of the quantum dot (QD) coupled with superconducting and normal leads are extensively studied because of their potential application in nanoelectronic, spintronic and quantum computation processing, see [1].

In the paper a quantum dot coupled to two semi-infinite one-dimensional wires (source and side) and one superconducting (drain) electrode is studied. The wires are treated within the tight-binding approximation for the semi-infinite chain of atoms. The superconducting (SC) electrode is described in the BCS approximation. Currents, which originate from various type of tunneling processes are calculated using the equation of motion technique for the non-equilibrium Green function.

Our attention is focused on the influence of the side-wire on the transport between remaining source and drain (SC) terminals. The side-wire acts as an inelastic scatterer because opening of a new conductance channel in the side-electrode activates additional tunneling processes: direct electron transfer (ET) and crossed Andreev reflection (CAR). These processes influence source-drain current caused by the direct Andreev reflection (DAR) processes. The most noticeable changes one can see when the gate potential shifts the edge of the conduction channel in the side-wire. In the case, one observes in the conductance threshold effects (so called Wigner singularities [2]) caused by the back action from the side-wire. A shape of the singularities depends on interference conditions when the additional conducting channel becomes activated. A detailed analysis of various contributions to transmission and conductance allows one to identify microscopic processes, which are responsible for the particular shape of the Wigner effects. An additional gate voltage applied to the QD breaks electron-hole symmetry, so a shape of the Wigner singularities is different near positive and negative gate voltages. The calculations are performed for both linear and non-linear regimes.

[1] A. Martín-Rodero and A. Levy Yeyati, *Advances in Physics* **60**, 899 (2011); S. De Franceschi, L. Kouwenhoven, C. Schönenberger and W. Wernsdorfer, *Nature Nanotechnology* **5**, 703 (2010).

[2] B. R. Bułka and A. Tagliacozzo, *Physical Review B* **79**, 075436 (2009); E. P. Wigner, *Physical Review* **73**, 1002 (1948).

**STRUCTURE AND MAGNETIC PROPERTIES OF IRON/IRON-OXIDE NANOPARTICLES PREPARED BY PRECIPITATION FROM SOLID STATE SOLUTION**M. Sopko<sup>1</sup>, O. Milkovič<sup>2</sup>, Š. Nižník<sup>2</sup>, I. Škorvánek<sup>3</sup><sup>1</sup>*The Institute of Materials Research of SAS, Watsonova 47, 040 01 Košice, Slovakia*<sup>2</sup>*Department of Material Science, Technical University of Košice, Park Komenského 11, 042 00 Košice, Slovakia*<sup>3</sup>*Institute of Experimental Physics, Slovak Academy of Sciences, Watsonova 47, 040 01 Košice, Slovakia*

The iron/iron-oxide nanoparticles were prepared by a precipitation from the solid state. The binary Cu-Fe alloy with 1.23 wt.% Fe was used as starting material for a growth of the nano-sized precipitates. The precipitates were subsequently extracted from the parent alloy by using a solution method. The structural and magnetic properties of the produced nanoparticles were studied by Transmission Electron Microscopy (TEM) and SQUID magnetometry. For the samples annealed at 600 and 700 °C, TEM investigations revealed the existence of Fe core and Fe<sub>3</sub>O<sub>4</sub> shell. The samples annealed at 500 °C showed the presence of iron oxides only. The average diameter of the nanoparticles increased with annealing temperature from 8.5 nm for the sample annealed at 500 ° to 32.5 nm for the sample annealed at 700 °C. All nanoparticles exhibited spherical shape.

The temperature dependencies of coercivity and magnetization were measured from 5 K to 200 K. The reduction of saturated magnetic polarization with a decrease of particle size confirms an important role of oxide phases at the particle surface. The coercive field at 5 K attained a maximum value of 1000 Oe for the sample annealed at 500 °C, which indicates a presence of relatively large magnetic anisotropies at low temperatures.

**MAGNETIC CHARCOAL SUPPORTING SILVER AS A WATER DISINFECTANT**

E. Valušová<sup>1</sup>, M. Antalík<sup>1,2</sup>, P. Pristaš<sup>3</sup>, P. Javorský<sup>3</sup>, J. Kováč<sup>1</sup>, M. Timko<sup>1</sup>  
and P. Kopčanský<sup>1</sup>

<sup>1</sup>*Institute of Experimental Physics, Slovak Academy of Sciences, Watsonova 47, 040 01 Košice, Slovakia*

<sup>2</sup>*Department of Biochemistry, Faculty of Science, P. J. Šafárik University, Moyzesova 11, 040 01 Košice, Slovakia*

<sup>3</sup>*Institute of Animal Physiology, Slovak Academy of Sciences, Šoltésovej 4-6, 040 01 Košice, Slovakia*

In this study, we employed a technique for the preparation of charcoal composite with magnetite (MC) in order to give the material magnetic properties. Using a coprecipitation method, the MC exhibited high efficiency in adsorption with Ag<sup>+</sup> ions. The adsorption capacities of MC were 32 µg AgNO<sub>3</sub> per 1 mg of MC. Moreover, one hour was defined as adequate time for adsorption of silver ions. This MCAG composite seems to have stability against Ag<sup>+</sup> leaching and could be adopted for further treatment studies.

The elimination of bacteria from surface water samples was examined and the results clearly demonstrate the inhibitory effect of MCAG on total river water bacteria and on *Pseudomonas koreensis* and *Bacillus mycoides* cultures isolated from river water. The bacterial counts in river water samples were reduced by five orders of magnitude following 30 min of treatment using 1 g l<sup>-1</sup> of MCAG at room temperature. The MCAG thus act as a magnetic filter uptaking bacteria. This idea confirmed the PCR analysis in which the bacterial DNA was detectable in the sediment after treatment processing.

The magnetic behavior of MCAG composites has been validated by the hysteresis loop measured using SQUID magnetometer at 293 K. The magnetic properties of MCAG composites allow use a permanent magnet to remove them easily from water after each processing. Thus, MCAG would be an excellent candidate for the simple ambulatory disinfection of surface water.

**Acknowledgements.** *The authors wish to thank the Slovak Grant Agency for support through VEGA grants No. 2/0025/12, 2/0016/12, APVV grant No. APVV-0171-10 and the European Union Structural Funds under ITMS project code 26220120033 and project code 26220220061.*

**SPIN-POLARIZED TUNELLING THROUGH A DOUBLE QUANTUM DOT INTERACTING WITH A POLARON**

P. Trocha and W. Rudzinski

*Faculty of Physics, Adam Mickiewicz University, ul. Umultowska 85, 61-614 Poznan, Poland*

Phonon-assisted electronic transport in mesoscopic systems is studied theoretically in case of tunneling through a double quantum dot coupled to ferromagnetic electrodes. The occupation numbers on the dot and current-voltage characteristics for the system are derived by means of the nonequilibrium Green function technique based on equation of motion in the Hubbard I approximation. Phonon spectra are analyzed for quantum dots and coupled to the leads in series, parallelly as well as in the T-shape geometry. Moreover, in calculations arbitrary Coulomb correlations are taken into account. It is found that at sufficiently low temperatures additional phonon-induced resonance peaks appear in the linear spectral function on both sides of the main resonances corresponding to the quantum dot energy levels. It is shown that the bonding and antibonding resonances are reproduced in the phonon side bands in the differential conductance. Such effects as the Franck-Condon blockade of the electric current, TMR oscillations and TMR inversion due to the electron-phonon interactions, as well as interference effects in the presence of the phonon field are also discussed.

**TWO-STAGE KONDO EFFECT IN THE T-SHAPED QUANTUM DOTS WITH FERROMAGNETIC LEADS**

K.P. Wójcik and I. Weymann

*Department of Physics, Adam Mickiewicz University,  
Umultowska 85, 61-614 Poznań, Poland*

I will present our results of calculation of the linear conductance of the system consisted of two single-level quantum dots with finite Coulomb interaction coupled to two ferromagnetic leads. One of the dots is tunnel-coupled to the leads, and the dots are coupled with each other. The second dot is not directly coupled to the leads, forming a T-shape configuration. The calculations are performed with the aid of numerical renormalization group method, and the temperature averages are obtained using the full density matrix of the system. We calculate the temperature dependence of the conductance in parallel and antiparallel magnetic configurations of the device. In the case of particle-hole symmetric dots, we find that the Kondo effect develops and is then suppressed with decreasing temperature. We also study how this situation is affected by changing the energies of the dots' levels. In the parallel configuration we observe a strong suppression of the Kondo effect due to the exchange field that splits the levels of the dots. On the contrary, in the antiparallel configuration the exchange field is absent and the Kondo effect is not suppressed.

**I5-01****NEW DEVELOPMENTS IN QUANTUM MAGNETISM WITH  $S > 1/2$** 

F. Mila

*Institute of Theoretical Physics, Ecole Polytechnique Federale de Lausanne, CH-1015 Lausanne, Switzerland*

30 years after Haldane's prediction that integer spin chains are gapped while half-integer spin chains are gapless, the field of quantum magnetism with spins larger than  $1/2$  has been relatively little explored as compared to the spin- $1/2$  case. The situation is rapidly changing however, and in this talk, I will try to give an overview of some of the recent developments in this field, with emphasis on the following topics: 1) The possibility to stabilize quadrupolar order in two-dimensional spin-1 models with biquadratic interactions; 2) The generalization of Majumdar-Ghosh point of the frustrated spin- $1/2$  chain to larger spins, and the evidence that, at least for spins 1,  $3/2$  and 2, the dimerization transition is in the  $SU(2)$  level 2S Wess-Zumino-Witten universality class; 3) The intriguing topological transitions that take place in antiferromagnetic spin- $S$  ladders as a function of the rung coupling.

## 05-01

### MAGNETIC RESPONSE OF Mn(III)F(salen) AT LOW TEMPERATURES

J.-H. Park,<sup>1</sup> O. N. Risset,<sup>2</sup> M. Shiddiq,<sup>3</sup> M. K. Peprah,<sup>4</sup> E. S. Knowles,<sup>4</sup>  
M. J. Andurs,<sup>2</sup> C. C. Beedle,<sup>1</sup> G. Ehlers,<sup>5</sup> A. Podlesnyak,<sup>5</sup> E. Čížmár,<sup>6</sup>  
S. E. Nagler,<sup>3</sup> S. Hill,<sup>3</sup> D. R. Talham,<sup>2</sup> and M. W. Meisel<sup>4,6</sup>

<sup>1</sup> National High Magnetic Field Laboratory (NHMFL), Florida State University,  
Tallahassee, FL 32310-3706, USA

<sup>2</sup> Department of Chemistry, University of Florida, Gainesville, FL 32611-7200,  
USA

<sup>3</sup> Department of Physics and NHMFL, Florida State University, Tallahassee, FL  
32310-3706, USA

<sup>4</sup> Department of Physics and NHMFL, University of Florida, Gainesville, FL  
32611-8440, USA

<sup>5</sup> Quantum Condensed Matter Division, Spallation Neutron Source (SNS), Oak  
Ridge National Laboratory (ORNL), Oak Ridge, TN 37831-6477, USA

<sup>6</sup> Institute of Physics, Faculty of Science, P. J. Šafárik University, 04154 Košice,  
Slovakia

Due to a report suggesting Mn(III)F(salen), salen = H<sub>14</sub>C<sub>16</sub>N<sub>2</sub>O<sub>2</sub>, may be an  $S = 2$  Haldane system with  $J/k_B \approx 50$  K and no long-range order down to 2 K [1], we have studied its magnetic response. Using a single crystal with the field applied perpendicular to the chain direction, torque magnetometry, down to 20 mK and up to 18 T, revealed a feature at 3.8 T when  $T \leq 400$  mK. ESR ( $\approx 200$  GHz) studies, using single crystals at 4 K and in 5 T, have not detected any signal. In 10 mT, the temperature dependence of the susceptibility of powder-like samples can be reasonably fit when  $J/k_B = 50$  K and  $g = 2$  [2]. In addition, these data are unchanged for  $P \leq 1.0$  GPa. Using a randomly-oriented, powder-like, deuterated (12 of 14 H replaced by D) sample of 2.2 g, neutron scattering data, acquired with the CNCS (Cold Neutron Chopper Spectrometer) at SNS (Spallation Neutron Source) show strong, dispersionless excitations that may be associated with the zero-field, high energy levels of antiferromagnetic  $S = 2$  spins with  $g = 2$ ,  $J/k_B = 50$  K,  $D/k_B = 1.4$  K, and  $E/k_B = 0.25$  K. These data and analyses will be presented.

*Supported by NSF via DMR-1005581 (DRT), DMR-0804408 (SH), DMR-1202033 (MWM), and DMR-1157490 (NHMFL); by the DOE BES Scientific User Facilities Division for work at ORNL; and by the Fulbright Commission in Slovakia (MWM).*

[1] T. Birk *et al.*, Inorg. Chem. **50** (2011) 5312.

[2] J. M. Law, H. Benner, and R. K. Kremer, J. Phys. Condens. Matter **25** (2013) 065601.

**SPIN-GLASS TRANSITION IN THE RCoGaO<sub>4</sub> (R=Lu, Yb, Tm) LAYERED COBALTITES**

I. Radelytsky<sup>1</sup>, H.A.Dabkowska<sup>2</sup>, R.Szymczak<sup>1</sup>, A.Dabkowski<sup>2</sup>, J.Fink-Finowicki<sup>1</sup>  
H.Szymczak<sup>1</sup>

<sup>1</sup>*Institute of Physics, Polish Academy of Sciences, 02668 Warsaw, Poland*

<sup>2</sup>*Department of Physics and Astronomy, McMaster University, Hamilton, Ontario, Canada*

We present magnetic measurements (ac and dc susceptibilities and magnetization) performed on single crystals of RCoGaO<sub>4</sub> (R=Lu, Yb, Tm) layered cobaltites as a function of frequency, temperature and hydrostatic pressure. Typical Ising-like spin glass features are observed in the frequency and temperature dependence of the ac susceptibility but only in longitudinal configuration. In transverse configuration the system is pure paramagnetic. The spin glass behavior of these cobaltites is due to frustration arising from random distribution of magnetic ions and specific geometry of the lattice. The dynamical scaling analysis confirms above conclusions.

*Acknowledgments*

*This paper was partially supported by the Ministry of Science and Higher Education (Poland) through grant No. N202 125135*



# CRITICAL BEHAVIOR OF $\text{Mn}_2[\text{Nb}(\text{CN})_8]$ MOLECULAR MAGNET THROUGH COMPLEMENTARY EXPERIMENTAL METHODS

R. Pełka<sup>1</sup>, M. Czapla<sup>1</sup>, P.M. Zieliński<sup>1</sup>, M. Fitta<sup>1</sup>, M. Bałanda<sup>1</sup>, D Pinkowicz<sup>2</sup>, F.L. Pratt<sup>3</sup>, M. Mihalik<sup>4</sup>, J. Przewoźnik<sup>5</sup>, A. Amato<sup>6</sup>, B. Sieklucka<sup>2</sup>, T. Wasiutyński<sup>1</sup>

<sup>1</sup>*The H. Niewodniczański Institute of Nuclear Physics Polish Academy of Sciences, Radzikowskiego 152, 31-342 Kraków, Poland*

<sup>2</sup>*Faculty of Chemistry, Jagiellonian University, Ingardena 3, 30-060 Kraków, Poland*

<sup>3</sup>*ISIS Facility, Rutherford Appleton Laboratory, Chilton, Oxfordshire OX11 0QX, UK*

<sup>4</sup>*Institute of Experimental Physics, Slovak Academy of Sciences, Watsonova 47, 040 01 Kosice, Slovakia*

<sup>5</sup>*AGH University of Science and Technology, 30 Mickiewicza Av., 30-059 Kraków, Poland*

<sup>6</sup>*Laboratory of Muon-Spin Spectroscopy, Paul Scherrer Institute, 5232 Villigen-PSI, Switzerland*

Important feature of most molecular magnets is the fact that the constituent magnetic moments are well localized providing a natural testing ground for the predictions of the existing spin models. The present contribution reports a comprehensive analysis of the critical behavior of a unique ferrimagnetic molecular magnet

$\{[\text{Mn}^{\text{II}}(\text{pydz})(\text{H}_2\text{O})_2][\text{Mn}^{\text{II}}(\text{H}_2\text{O})_2][\text{Nb}^{\text{IV}}(\text{CN})_8] \cdot 2\text{H}_2\text{O}\}_n$  with  $T_c \approx 42$  K. As a probe of critical behavior complementary experimental methods have been employed such as  $\mu\text{SR}$  spectroscopy, ac magnetometry, and relaxation calorimetry. A full set of critical exponents is determined. Static exponents  $\alpha$ ,  $\beta$ ,  $\gamma$ , and the dynamic exponent  $w$  are extracted directly from the measurements. Further critical exponents  $\nu$ ,  $\eta$ , and  $z$  are derived on the basis of scaling or hyperscaling relations. The knowledge of the thermal dependence of the order parameter combined with the results of the calorimetric measurements allowed for the determination of two further static critical exponents  $\kappa$  and  $\kappa'$ . The system shows a close affinity to the three-dimensional Heisenberg model. Ferrimagnetism of the compound leads to a coexistence of typically ferro- and antiferromagnetic characteristics.

# NEUTRON AND EPR STUDY OF $\text{Cu}(\text{tn})\text{Cl}_2$ – A TWO-DIMENSIONAL SPATIALLY ANISOTROPIC TRIANGULAR LATTICE ANTIFERROMAGNET

R. Tarasenko<sup>1</sup>, A. Orendáčová<sup>1</sup>, E. Čižmár<sup>1</sup>, S. Mařaš<sup>2</sup>, M. Orendáč<sup>1</sup>, I. Potočník<sup>3</sup>, V. Pavlík<sup>4</sup>, K. Siemensmeyer<sup>2</sup>, S. Zvyagin<sup>5</sup>, J. Wosnitza<sup>5</sup> and A. Feher<sup>1</sup>

<sup>1</sup>*Institute of Physics, Faculty of Science, P.J. Šafárik University, Park Angelinum 9, 041 54 Košice, Slovak Republic*

<sup>2</sup>*Helmholtz-Zentrum Berlin, Hahn-Meitner Platz 1, D-14109 Berlin, Germany*

<sup>3</sup>*Institute of Chemistry, Department of Inorganic Chemistry, Faculty of Science, P.J.Šafárik University, Moyzesova 11, 041 54 Košice, Slovak Republic*

<sup>4</sup>*Institute of Experimental Physics, Slovak Academy of Sciences, Watsonova 47, 040 01 Košice, Slovak Republic*

<sup>5</sup>*Dresden High Magnetic Field Laboratory (HLD), Helmholtz-Zentrum Dresden-Rossendorf and TU Dresden, 01314 Dresden, Germany*

$\text{Cu}(\text{tn})\text{Cl}_2$  ( $\text{tn} = 1,3$ -diaminopropane) has been previously identified as a potential realization of a quasi-two-dimensional, spatially-anisotropic triangular Heisenberg antiferromagnet with spin  $1/2$ , intralayer exchange coupling  $J/k_B \approx -3$  K, and interlayer exchange coupling  $J' \approx 0.001 J$ . Previous specific-heat studies in zero magnetic field did not show a phase transition to long-range magnetic order down to 60 mK. These studies indicated a field-induced anomaly forming below 1 K in magnetic fields up to 7 T and this anomaly was assigned to a Berezinskii-Kosterlitz-Thouless phase transition. The structure of  $\text{Cu}(\text{tn})\text{Cl}_2$  consists of covalently bonded ladders running along the  $c$ -axis, while adjacent ladders are linked through hydrogen bonds. Powder neutron diffraction studies were performed in the temperature range from 0.4 K to 100 K. A rather large contraction of the  $a$  and  $b$  lattice parameters observed at low temperatures has been attributed to the presence of the hydrogen bonds, while no pronounced change of the  $c$  parameter was observed. X-band powder EPR measurements have been performed in the temperature range from 2 K to 300 K and the analysis of resonance fields revealed the presence of an exchange anisotropy in the studied system. The phonon modulation of the spin anisotropies can be responsible for the increase of the EPR linewidth observed above 100 K. On the other hand, the upturn of the linewidth appearing below 20 K can be ascribed to the development of intralayer magnetic correlations.

*This work was supported by the projects APVV LPP-0202-09, the DFG and EuroMagNET (EU contract No. 228043).*

# ASSESSMENT OF SPIN HAMILTONIAN PARAMETERS FOR MOLECULAR NANOMAGNETS BY THE SINGLE-CRYSTAL MAGNETIZATION PROFILES AND DFT CALCULATIONS

G. Kamieniarz<sup>1</sup>, M. Antkowiak<sup>1</sup>, P. Kozłowski<sup>1</sup>, L. Kucharski<sup>1</sup>, A. Barasiński<sup>2</sup>, B. Brzostowski<sup>2</sup>, A. Drzewiński<sup>2</sup>, M. Wojciechowski<sup>2</sup>, G. A. Timco<sup>3</sup>, F. Tuna<sup>3</sup> and R. E. P. Winpenny<sup>3</sup>

<sup>1</sup>*Faculty of Physics, A. Mickiewicz University, Poznań, Poland*

<sup>2</sup>*Institute of Physics, University of Zielona Gora, Zielona Gora, Poland*

<sup>3</sup>*Department of Chemistry, University of Manchester, Manchester M13 9PL, UK*

We demonstrate numerically that for the strongly anisotropic homometallic  $S=2$  canted single chain magnet described by the quantum antiferromagnetic Heisenberg model the correlation energy and exchange coupling constant can be directly estimated from the in-field-magnetization profile found along the properly selected crystallographic direction. In the parameter space defined by the spherical angles ( $\varphi$ ,  $\vartheta$ ) determining the axes orientation, four regions are identified with different sequences of the characteristic field-dependent magnetization profiles representing the antiferromagnetic, metamagnetic and weak ferromagnetic type behavior.

The static thermodynamic properties observed for the tetranuclear oxalato-bridged  $\text{Re}_3(\text{IV})\text{Ni}(\text{II})$  complex demonstrating the Single Molecule Magnet behavior are described by a single quantum anisotropic spin Heisenberg model. Our comprehensive phenomenological analysis is based on an exact diagonalization technique combined with the genetic algorithm ideas and leads to the quantitative agreement of the low-lying energy levels with the EPR resonances measured in a powder sample and interpreted as transitions appearing between Kramers doublets.

The nine-numbered frustrated homometallic chromium based molecular ring with a single bond defect is synthesized, experimentally characterized by low temperature magnetic measurements and analyzed within the microscopic quantum model. From fitting the susceptibility and magnetization curves, the strength of the coupling corresponding to the defect is estimated at 52% of the bulk value inside the ring, preserving the typical values of remaining parameters. on of the quantum states and couplings and may supplement the standard INS and EPR techniques. Moreover all non-equivalent spin configurations with  $S=\pm 3/2$  are considered and the corresponding differences between the total energies are calculated using DFT approach and the exchange interaction parameter  $J$  extracted from the spin model, using different scenarios.

**INDIRECT COUPLING BETWEEN LOCALIZED MAGNETIC MOMENTS IN GRAPHENE NANOSTRUCTURES**

K. Szałowski

*Department of Solid State Physics, University of Łódź, ulica Pomorska 149/153, PL 90-236 Łódź, Poland*

Emerging interest in spintronic applications of graphene motivates theoretical and experimental studies of its magnetic properties. In particular, the geometrically confined graphene-based systems attract considerable efforts. This encourages the studies of charge-carrier mediated interactions of localized magnetic moments in graphene and its derivatives.

In the paper we present the results of non-perturbational calculations of the Ruderman-Kittel-Kasuya-Yosida (RKKY) coupling in graphene systems, focusing our attention mainly on nanoflakes and nanoribbons.

The electronic structure is described by means of the tight-binding Hamiltonian, supplemented with an Anderson-Kondo term to account for the presence of magnetic impurities. Additional terms are included in order to incorporate such factors as the Rashba spin-orbit coupling or Zeeman splitting of energy states in selected systems. Coulombic interactions are incorporated by on-site Hubbard term in the mean field approximation. The total energy calculations allow to determine an indirect coupling energy in a non-perturbational way.

In the paper, the influence of the mentioned factors on the RKKY interaction in geometrically confined graphene structures is extensively discussed. For instance, the presence of the energy states occupied by single electrons in nanostructures enables an additional indirect coupling mechanism resembling the double exchange. This mechanism is frequently a dominant one and may mediate both ferro- or antiferromagnetic interactions. Moreover, an indirect coupling in graphene nanoflakes is often highly sensitive to doping even with a single charge carrier. In all these nanostructures, the pronounced quantum size effects are present in the RKKY coupling, accompanied by a substantial modification of its distance dependence in nanoribbons. On the other hand, such factors as the spin-orbit coupling and Zeeman splitting result in appearance of highly anisotropic RKKY interaction, also influencing the coupling sign.

*This work has been supported by Polish Ministry of Science and Higher Education on a special purpose grant to fund the research and development activities and tasks associated with them, serving the development of young scientists and doctoral students.*

# OBSERVATION OF ANISOTROPIC EXCHANGE IN SPIN LADDERS BY ELECTRON SPIN RESONANCE

E. Čížmár<sup>1</sup>, M. Ozerov<sup>2</sup>, S. Wang<sup>3</sup>, K.W. Krämer<sup>4</sup>, Ch. Rüegg<sup>5</sup> and S.A. Zvyagin<sup>2</sup>

<sup>1</sup>*Institute of Physics, Faculty of Science, P.J. Šafárik University, SK-041 54 Košice, Slovakia*

<sup>2</sup>*Dresden High Magnetic Field Laboratory (HLD), Helmholtz-Zentrum Dresden-Rossendorf, D-01314 Dresden, Germany*

<sup>3</sup>*Laboratory for Developments and Methods, Paul Scherrer Institut, CH-5232 Villigen PSI, Switzerland*

<sup>4</sup>*Department of Chemistry and Biochemistry, University of Bern, CH-3012 Bern, Switzerland*

<sup>5</sup>*Laboratory for Neutron Scattering, Paul Scherrer Institut, CH-5232 Villigen PSI, Switzerland*

The study of magnetic excitations in the spin-ladder materials  $(\text{C}_5\text{H}_{12}\text{N})_2\text{CuBr}_4$  and  $\text{BiCu}_2\text{PO}_6$  was performed by high resolution X-band and multi-frequency electron spin resonance (ESR) spectroscopy. While  $(\text{C}_5\text{H}_{12}\text{N})_2\text{CuBr}_4$  was proposed as the best realization of a spin-ladder in the strong-coupling limit ( $J_{\text{rung}} \sim 4J_{\text{leg}}$ ), comparable  $J_{\text{rung}}$  and  $J_{\text{leg}}$  including substantial frustration along the ladder legs are present in  $\text{BiCu}_2\text{PO}_6$ . Our experiments provide a direct evidence for the presence of anisotropy in  $(\text{C}_5\text{H}_{12}\text{N})_2\text{CuBr}_4$  in contrast to a fully isotropic spin-ladder model employed for this system previously. The angular dependence and frequency-field diagram of ESR transitions are analyzed within a simple model of triplet excitations split by a biaxial anisotropy of 0.55 K. It is argued that the anisotropy is caused by spin-orbit coupling, specifically by the symmetric anisotropic interaction, as confirmed by the theoretical work of Furuya *et al.* [Phys. Rev. Lett. 108 (2012) 037204]. In  $\text{BiCu}_2\text{PO}_6$ , we report on observation of ESR modes with the energy lower than the singlet-triplet gap of 460 GHz estimated from neutron-scattering experiments in the quantum disordered phase [Plumb *et al.*, arXiv:1301.5324v1]. The most pronounced mode was observed with an energy gap 312 GHz (corresponding to 15 K) at zero magnetic field with non-linear field dependence. We discuss the origin of observed modes taking into account frustration and the presence of antisymmetric Dzyaloshinskii-Moriya interaction.

*Supported by EuroMagNET (EU contract No. 228043) and ERDF EU via contract No. ITMS26220120005.*

**MÖSSBAUER AND SQUID CHARACTERIZATION OF IRON IN HUMAN TISSUE: CASE OF *GLOBUS PALLIDUS***

M. Miglierini<sup>1,2</sup>, R. Boča<sup>3</sup>, M. Kopáni<sup>4</sup> and A. Lančok<sup>5</sup>

<sup>1</sup>*Institute of Nuclear and Physical Engineering, Slovak University of Technology, Ilkovičova 3, 812 19 Bratislava, Slovakia*

<sup>2</sup>*Regional Centre of Advanced Technologies and Materials, Faculty of Science, Palacky University, 17. listopadu 12, 771 46 Olomouc, Czech Republic*

<sup>3</sup>*Department of Chemistry, FPV, University of SS. Cyril and Methodius, 917 01 Trnava, Slovakia*

<sup>4</sup>*Department of Pathology, Faculty of Medicine, Comenius University, Sasinkova 4, 811 08 Bratislava, Slovakia*

<sup>5</sup>*Institute of Inorganic Chemistry AS CR, v. v. i., 250 68 Husinec-Řež 1001, Czech Republic*

Iron is the most important metal with high concentration in some regions of the brain. *Basal ganglia* have the highest iron concentration in the brain, in particular in the regions identified as *globus pallidus* and *substantia nigra*. Iron catalyzes reactions forming reactive oxygen species and it is one of the major factors associated with neurodegenerative diseases. But its activity depends greatly on its ligand-based environment.

This contribution aims in characterization of magnetic behaviour of iron in *globus pallidus*. <sup>57</sup>Fe Mössbauer spectroscopy (MS) was employed as a principal method of investigation that provides information both on structural arrangement and magnetic states of the resonant <sup>57</sup>Fe nuclei. Histochemical findings indicated a presence of iron accumulation in its physiological form, i.e. ferritin. A considerable amount of biomineralized iron-oxides was found also in the extracellular matter. Subsequent SQUID magnetometry experiments have revealed different magnetic states of the investigated samples.

MS was performed in transmission geometry at room temperature. The resulting doublet-like spectra suggested superparamagnetic behaviour that is governed mainly by the size of ferritin nanoparticles. Consequently, low temperature MS experiments have been employed which provide the information on magnetic states as well as the blocking temperature. Results obtained from human brain tissues are compared with those of horse ferritin that serves as generally accepted reference material.

*This work was supported by the research projects VEGA 1/0220/12, P204/10/0035, CZ.1.05/2.1.00/03.0058, and CZ.1.07/2.3.00/20.0155.*

**THE SPIN-1  $J_1$  -  $J_3$  HEISENBERG ANTIFERROMAGNET  
ON A TRIANGULAR LATTICE**P. Rubin<sup>1</sup>, A.Sherman<sup>1</sup> and M. Schreiber<sup>2</sup><sup>1</sup>*Institute of Physics, University of Tartu, Riia 142, 51014 Tartu, Estonia*<sup>2</sup>*Institut für Physik, Technische Universität, D-09107 Chemnitz, Germany*

Motivated by the recent experiment in  $\text{NiGa}_2\text{S}_4$ , the spin-1 Heisenberg model on a triangular lattice with the ferromagnetic nearest- and antiferromagnetic third-nearest-neighbor exchange interactions,  $J_1 = -(1-p)J$  and  $J_3 = pJ$ ,  $J > 0$ , is studied in the range of the parameter  $0 \leq p \leq 1$ . Mori's projection operator technique is used as a method which retains the rotation symmetry of spin components and does not anticipate any magnetic ordering. For zero temperature several phase transitions are observed.

At  $p \approx 0.2$  the ground state is transformed from the ferromagnetic spin structure into a disordered state, which in its turn is changed to an antiferromagnetic long-range ordered state with the incommensurate ordering vector  $Q \approx (1.16, 0)$  at  $p \approx 0.31$ . With growing  $p$  the ordering vector moves along the line  $Q - Q_1$  to the commensurate point  $Q_1 = (2\pi/3, 0)$  which is reached at  $p = 1$ . The final state with an antiferromagnetic long-range order can be conceived as four interpenetrating sublattices with the  $120^\circ$  spin structure on each of them. The model is able to describe the state with the incommensurate short-range order observed in  $\text{NiGa}_2\text{S}_4$ .

## P5-03

### THE RARE-EARTH BASED SINGLE-ION MAGNET $\text{CsNd}(\text{MoO}_4)_2$

V. Tkáč<sup>1</sup>, K. Tibenská<sup>2</sup>, A. Orendáčová<sup>1</sup>, M. Orendáč<sup>1</sup>, A. G. Anders<sup>3</sup> and A. Feher<sup>1</sup>

<sup>1</sup>*Institute of Physics, P. J. Šafárik University in Košice, Park Angelinum 9, 040 00 Košice, Slovakia*

<sup>2</sup>*Faculty of Aeronautics, Technical University, Rampová 7, 041 21 Košice, Slovak Republic*

<sup>3</sup>*Institute of Low Temperature Physics and Engineering, Lenin Av. 47, 3 101 64 Kharkov, Ukraine*

Single molecule magnets (SMMs) represent an attractive area for the investigation of quantum phenomena such as quantum tunneling, quantum spin coherence and others. The present work is devoted to the study of  $\text{CsNd}(\text{MoO}_4)_2$ , the candidate for novel mononuclear lanthanide-based SMMs (single-ion magnets). This material crystallizes in the orthorhombic system with the cell parameters  $a = 9.55 \text{ \AA}$ ,  $b = 8.23 \text{ \AA}$  and  $c = 5.13 \text{ \AA}$ .  $\text{Nd}^{3+}$  with the ground state  $^4\text{I}_{9/2}$  is responsible for the magnetic properties. Low-symmetry crystal field splits this state to 5 doublets. Specific heat has been experimentally studied in the temperature range from 120 mK to 20 K in magnetic field up to 4 T. No phase transition to long-range magnetic order has been observed down to lowest temperatures in zero magnetic field, which indicates weak magnetic correlations in the studied system. The behavior of the specific heat in non-zero magnetic field can be described with a two-level model with the  $g$ -factor 3.08. A good agreement with the data suggests that higher energy doublets do not contribute to the specific heat at low temperatures and the approximation of the effective spin  $S^* = 1/2$  can be applied in further analysis. The magnetization measurement has been performed at the temperature 5 K in the magnetic field up to 5 T. The data are well described using Brillouin function with  $g = 3.08$ . DC susceptibility studied in the temperature range from 2 to 300 K in the magnetic field 10 mT was fitted to Curie Weiss law. The analysis provided Curie paramagnetic temperature  $\theta = -1.05 \text{ K}$  and  $g = 3.3$  when assuming  $S^* = 1/2$ . This is in good agreement with the value obtained from the analysis of the magnetic specific heat and magnetization. Analysis of specific heat, magnetization and DC susceptibility indicate surprisingly very weak magnetic correlations in  $\text{CsNd}(\text{MoO}_4)_2$  and rather large energy separation between the ground and first excited doublet. These features suggest  $\text{CsNd}(\text{MoO}_4)_2$  might be a representative of a single-ion magnet.

*This work was supported by the projects APVV 0132-11 and VEGA 1/0143/13.*



**PHOTOCONTROLLED MAGNETISM IN CORE@SHELL PBAs**

E. S. Knowles<sup>1</sup>, C. H. Li<sup>2</sup>, M. J. Andrus<sup>2</sup>, M. K. Peprah<sup>1</sup>, J. van Tol<sup>3</sup>, S. Hill<sup>3</sup>, D. R. Talham<sup>2</sup>, and M.W. Meisel<sup>1,†</sup>

<sup>1</sup>*Department of Physics and NHMFL, University of Florida, 2001 Museum Road, Gainesville, FL 32611-8440 USA*

<sup>2</sup>*Department of Chemistry, University of Florida, P.O. Box 117200, Gainesville, FL 32611-7200 USA*

<sup>3</sup>*Department of Physics and NHMFL, Florida State University, 1800 E. Paul Dirac Drive, Tallahassee, FL 32310-3706 USA*

<sup>†</sup>*Present address: Department of Condensed Matter Physics, Institute of Physics, P.J. Šafárik University, Park Angelinum 9, 041 54 Košice, Slovakia*

Novel photoeffects in heterostructured Prussian blue analogues (PBAs), consisting of  $A_i\text{Co}[\text{Fe}(\text{CN})_6]_j \cdot n\text{H}_2\text{O}$  (CoFe-PBA) and  $A_i\text{Ni}[\text{Cr}(\text{CN})_6]_j \cdot n\text{H}_2\text{O}$  (NiCr-PBA), which extend the magnetic photocontrol temperature to 70 K and reverse the sign of the photoeffect<sup>1,2</sup> from that of the pure CoFe-PBA<sup>3</sup>, sparked investigations into the microscopic mechanism of the photoinduced decrease in magnetism. Due to the similarity with pressure-induced effects in a single-phase NiCr-PBA<sup>4,5</sup>, we propose that these photoeffects in the heterostructures arise from a photoinduced strain on the NiCr-PBA caused by the expansion of the CoFe-PBA lattice upon irradiation. The static magnetization and EPR signals from a series of core@shell particles of CoFe@NiCr-PBAs, with a common cubic core of size nominally 350 nm and varying shell thicknesses of 80 nm to 160 nm, are studied to determine if this strain induces spin canting, linkage isomerism, or some other mechanism. A quantitative model is used to describe the magnitude of the photoeffect as a function of shell thickness, thereby providing a test of the plausible mechanisms. An understanding of the extent and implications of the photoinduced strain will inform efforts to prepare materials with yet higher photocontrol temperatures.

*Supported, in part, by the NSF via DMR-1202033 (MWM), DMR-1005581 (DRT), and DMR-1157490 (NHMFL), and by the Fulbright Program (MWM).*

<sup>1</sup> D. M. Pajeroski *et al.*, J. Am. Chem. Soc. **132** (2010) 4058.

<sup>2</sup> M. F. Dumont *et al.*, Inorg. Chem. **50** (2011) 4295.

<sup>3</sup> O. Sato *et al.*, Science **272** (1996) 704.

<sup>4</sup> M. Zentková *et al.*, J. Phys.: Condens. Matter **19** (2007) 266217.

<sup>5</sup> M. K. Peprah *et al.*, unpublished.

**MAGNETOCALORIC EFFECT In  $\{[M(\text{pyrazole})_4]_2[\text{Nb}(\text{CN})_8] \cdot 4\text{H}_2\text{O}\}_n$  ( $M=\text{Fe}$ ,  $\text{Co}$ ,  $\text{Fe}_{0.5}\text{Co}_{0.5}$ ) ISOSTRUCTURAL MOLECULAR MAGNETS**

 R. Pelka<sup>1</sup>, P. Konieczny<sup>1</sup>, P.M. Zieliński<sup>1</sup>, Y. Miyazaki<sup>2</sup>, A. Inaba<sup>2</sup>,

 D. Pinkowicz<sup>3</sup>, B. Sieklucka<sup>3</sup> and T. Wasiutyński<sup>1</sup>
<sup>1</sup>*The H. Niewodniczański Institute of Nuclear Physics Polish Academy of Sciences, Radzikowskiego 152, 31-342 Kraków, Poland*
<sup>2</sup>*Research Center for Structural Thermodynamics, Graduate School of Science, Osaka University, Toyonaka, Osaka 560-0043, Japan*
<sup>3</sup>*Faculty of Chemistry, Jagiellonian University, Ingardena 3, 30-060 Kraków, Poland*

Magnetocaloric effect in isostructural  $\{[M(\text{pyrazole})_4]_2[\text{Nb}(\text{CN})_8] \cdot 4\text{H}_2\text{O}\}_n$  ( $M=\text{Fe}$  **1**,  $\text{Co}$  **2**,  $\text{Fe}_{0.5}\text{Co}_{0.5}$  **3**, pyrazole= $\text{C}_3\text{H}_4\text{N}_2$ ) molecular magnets is reported. They crystallize in tetragonal  $I4_1/a$  space group [1]. The compounds exhibit a phase transition to a long range magnetically ordered state at  $T_c \approx 8.5$  K (**1**), 4.8 K (**2**), 7.0 K (**3**). The magnetic entropy change  $\Delta S_m$  as well as the adiabatic temperature change  $\Delta T_{ad}$  due to applied field change  $\mu_0\Delta H=0.1, 0.2, 0.5, 1, 2, 5, 9$  T, as a function of temperature were determined by the relaxation calorimetry measurements. The maximum value of  $\Delta S_m$  for  $\mu_0\Delta H=5$  T is  $4.9 \text{ J mol}^{-1} \text{ K}^{-1}$  ( $4.8 \text{ J kg}^{-1} \text{ K}^{-1}$ ) at 10.33 K for **1**,  $7.0 \text{ J mol}^{-1} \text{ K}^{-1}$  ( $6.8 \text{ J kg}^{-1} \text{ K}^{-1}$ ) at 6.91 K for **2**, and  $5.3 \text{ J mol}^{-1} \text{ K}^{-1}$  ( $5.1 \text{ J kg}^{-1} \text{ K}^{-1}$ ). The maximum value of  $\Delta T_{ad}$  for  $\mu_0\Delta H=5$  T is 2.0 K at 9.81 K for **1**, 4.2 K at 5.32 K for **2**, and 2.5 K at 7.46 K for **3**. The temperature dependences of the  $n$  exponent characterizing the dependence of  $\Delta S_m$  on  $\Delta H$  have been estimated. They all exhibit a minimum slightly above the transition temperature with values 0.64, 0.44, and 0.65 for **1**, **2**, and **3**, respectively. For **1** and **3** the values of  $n$  are consistent with the 3D Heisenberg model. The low value of  $n$  for **2** suggests a different universality class.

[1] D. Pinkowicz, R. Pelka, O. Drath, W. Nitek, M. Balanda, A.M. Majcher, G. Poneti, B. Sieklucka, *Inorg. Chem.* **49** (2010) 7565.

**THE INVESTIGATION OF THE *E-J* CHARACTERISTICS AND THE ROLE OF NANOPARTICLE CONCENTRATION IN WEAKLY POLAR MAGNETIC FLUIDS**

J. Kurimský<sup>1</sup>, B. Dolník<sup>1</sup>, K. Marton<sup>1</sup>, M. Kolcun<sup>1</sup>, L. Tomčo<sup>2</sup>, M. Rajňák<sup>3</sup>, M. Timko<sup>3</sup> and P. Kopčanský<sup>3</sup>

<sup>1</sup>*Department Electrical Power Engineering, Technical University of Košice, Mäsiarska 74, 040 01 Košice, Slovakia*

<sup>2</sup>*Faculty of Aeronautic, Technical University of Košice, Rampová 7, 041 2P51 Košice, Slovakia*

<sup>3</sup>*Institute of Experimental Physics SAS, Watsonova 47, 040 01 Košice, Slovakia*

Magnetic fluids are perspective and promising material of the future technologies. Full application potential is unleashed step-by-step sequentially through research on many different physical phenomena related to their nature.

The paper presents investigation on the magnetic fluids that are stable colloidal suspensions of single-domain magnetic particles in a liquid carrier of dielectrics nature. Studies were made on the electric field-current density (*E-J*) characterization commonly observed in insulating liquids under uniform electrical field. High performance oil was used as the dielectrics carrier. The experiments were carried out at different mass concentrations of magnetite nanoparticles up to 4 %. These materials belong to group of weak polar liquid in dependence on concentration of magnetic particles. During experiments, samples were placed in anechoic chamber in the dark, so measurements were free of both the optical and the electro-magnetic interference. The current density between parallel plates has been observed in magnetic fluids for over series of electrical intensity levels up to  $5 \cdot 10^5$  V/m of both the direct and reversal directions, too, at ambient temperature and pressure. At each level, the physical quantities have been recorded.

The current density is driven by free charge carriers of nano-sized metal oxide particles and by the accumulation of space charge near the electrodes in the volume of the liquid. *E-J* characteristics were determined over a given range of magnetic fluid concentrations, influenced by static external magnetic field. The dependence of current density on volume concentration of magnetic nanoparticles in magnetic fluids has been observed. In applied fields, it is suggested possible generation of colloidal aggregates in the form of strings which can bridge inter-electrode space. The obtained local *E-J* curves showed significant contribution of magnetite particles to the linearization of characteristics and increase of overall fluid electrical conductivity.

**INFLUENCE OF MAGNETIC FIELD ON DIELECTRIC BREAKDOWN IN TRANSFORMER OIL BASED FERROFLUIDS**

M. Rajňák<sup>1</sup>, L. Tomčo<sup>2</sup>, K. Marton<sup>3</sup>, J. Kurimský<sup>3</sup>, B. Dolník<sup>3</sup>, M. Molčan<sup>1</sup>, P. Kopčanský<sup>1</sup>, M. Timko<sup>1</sup>

<sup>1</sup>*Institute of Experimental Physics SAS, Watsonova 47, 04353 Košice, Slovakia*

<sup>2</sup>*Department of Aerodynamics and Simulations, Faculty of Aviation, Technical University, Rampová 7, 04121 Košice, Slovakia*

<sup>3</sup>*Department of Electric Power Engineering, Faculty of Electrotechnics and Informatics, Technical University, Letná 9/A, 04121 Košice, Slovakia*

An analysis of experimental study of dielectric breakdown and possible partial discharges (PD) occurrence in transformer oil based ferrofluids under the influence of magnetic field is presented. The basic ferrofluid was synthesized by coprecipitation method. The three main constituents of the studied ferrofluid are transformer oil Mogul, magnetite nanoparticles and oleic acid which are acting as carrier liquid, magnetic solid substance and surfactant, respectively. In order to reveal a degree of magnetite contribution to the dielectric behavior and finely to the PD and breakdown occurrence, we prepared four ferrofluid samples with different magnetic volume fraction determined by means of saturation magnetization measurements and Langevin theory of superparamagnetism.

In our experimental study the enhanced dielectric properties of the ferrofluid were confirmed in comparison with the pure transformer oil. A model of electron scavenging by magnetite nanoparticles is considered as a possible reason of slower streamer development leading to increased voltage breakdown level in the ferrofluid. Except of that enhancement we could observe an influence of external magnetic field on the investigated dielectric behavior. Magnetic field induced formation of needle shape magnetite clusters is analyzed. The increased inhomogeneity due to the presence of magnetic nanoparticles in oil and on the surface of electrodes is also responsible for possible partial discharges initiation.

**MAGNETIC PROPERTIES OF TRANSITION METAL MOLYBDATES**

P. Konieczny<sup>1</sup>, M. Grzesiak-Nowak<sup>2</sup>, A. Szymańska<sup>2</sup>, W. Łasocha<sup>2,3</sup> and T. Wasiutyński<sup>1</sup>

<sup>1</sup>*Department of Structural Research, Institute of Nuclear Physics PAN, Radzikowskiego 152, 31-342 Kraków, Poland*

<sup>2</sup>*XRD and Thermoanalysis Laboratory, Jerzy Haber Institute of Catalysis and Surface Chemistry PAN, Niezapominajek 8, 30-239 Kraków, Poland*

<sup>3</sup>*Faculty of Chemistry, Jagiellonian University, Ingardena 3, 30-060 Kraków, Poland*

Two examples of transition metal molybdates were studied with the use of X-ray diffraction and magnetometry techniques. Structures of copper dimolybdate trihydrate  $\text{CuMo}_2\text{O}_7 \cdot 3\text{H}_2\text{O}$  and fibrillar cobalt trimolybdate pentahydrate  $\text{CoMo}_3\text{O}_{10} \cdot 8\text{H}_2\text{O}$  were obtained. First compound contains two dimensional layers of dimolybdate chains connected by  $[\text{Cu}_2\text{O}_4(\text{H}_2\text{O})_6]^{4+}$  dimers. Second one consists of zigzag anionic chains of  $\text{Mo}_3\text{O}_{10}^{2-}$  which are separated by  $[\text{Co}(\text{H}_2\text{O})_6]^{2+}$  and water molecules.

Magnetic properties of those low dimensional compounds were studied with the use of an AC/DC magnetometer in the range 0-7 T.

# STUDY THE IMPACT OF COMPOUND COMPOSITION IN A 3D MOLECULAR MAGNET $\{[M^{II}(\text{pirazol})_4]_2[\text{Nb}^{IV}(\text{CN})_8]\cdot 4\text{H}_2\text{O}\}_n$

P. Konieczny<sup>1</sup>, R. Pełka<sup>1</sup>, P. M. Zieliński<sup>1</sup>, F.L. Pratt<sup>2</sup>, Y. Miyazaki<sup>3</sup>, A. Inaba<sup>3</sup>, D. Pinkowicz<sup>4</sup>, B. Sieklucka<sup>4</sup> and T. Wasiutyński<sup>1</sup>

<sup>1</sup>*Department of Structural Research, Institute of Nuclear Physics PAN, Radzikowskiego 152, 31-342 Kraków, Poland*

<sup>2</sup>*ISIS Facility, Rutherford Appleton Laboratory, Chilton, Oxfordshire OX11 0QX, United Kingdom*

<sup>3</sup>*Research Center for Structural Thermodynamics, Graduate School of Science, Osaka University, Toyonaka, Osaka 560-0043, Japan*

<sup>4</sup>*Department of Chemistry, Jagiellonian University, Ingardena 3, 30-060 Kraków, Poland*

The magnetic properties and critical behavior of three dimensional (3D) ferromagnetic molecular magnets  $\{[M^{II}(\text{pirazol})_4]_2[\text{Nb}^{IV}(\text{CN})_8]\cdot 4\text{H}_2\text{O}\}_n$ , where  $M^{II}=\text{Fe}$ ,  $\text{Co}$  or  $\text{FeCo}$ , have been studied with the use of ac/dc magnetometry, zero-field  $\mu\text{SR}$  spectroscopy and relaxation calorimetry. All the compounds crystallize in the  $I4_1/a$  space group where cyanido-bridged structure is decorated with pyrazole molecules coordinated to  $M^{II}$  centers. The study concentrates on phase transitions and on the influence of  $M^{II}$  composition on magnetic properties. Moreover, a set of critical exponents were determined which points to 3D Heisenberg model.

**EPR SPECTRA OF GENUINE-ORGANIC AND METAL-ORGANIC TCNQ-BASED ANION RADICAL SALTS**M. Botko<sup>1</sup>, E. Čižmár<sup>1</sup>, M. Kajňáková<sup>1</sup> and A. Feher<sup>1</sup><sup>1</sup>*Institute of Physics, Faculty of Science, P.J. Šafárik University in Košice, Park Angelinum 9, 04154 Košice, Slovak republic*

Ever since their discovery, the organic anion-radical charge-transfer complexes have attracted significant interest thanks to the variety of their physical properties, for example, a wide range of conductive behavior, from insulator to superconductor and the ability to tune the magnetic ordering predetermines their suitability for practical applications. The most interesting materials are those with 7,7,8,8-tetracyanoquinodimethane (TCNQ) in role of acceptor molecule.

As the structural and magnetic properties of these anion-radical salts (ARS) are strongly dependent on the cation present in the compound, the understanding of magneto-structural correlations is crucial for any further practical applications. In our previous work, the thermodynamic and magnetic properties of several genuine-organic and metal-organic ARS systems are studied.

In this work, we present the results of a comparison study of electron paramagnetic spectra of genuine-organic and metal-organic TNCQ-based ARS. The genuine-organic ARS examined are: [N-Me-OH-Me-Py](TCNQ)<sub>2</sub>, [N-Et-OH-Me-Py](TCNQ)<sub>2</sub>, [Me-2,6-di-Me-Py](TCNQ)<sub>2</sub>, [Me-3,5-di-Me-Py](TCNQ)<sub>2</sub>, [Me-Qn-Ox](TCNQ)<sub>2</sub>, [Et-2,6-di-Me-Pz](TCNQ)<sub>2</sub> and [Et-Qn-Ox](TCNQ)<sub>2</sub> as well as the metal-organic ARS of: [Mn-phen<sub>3</sub>](TCNQ)<sub>2</sub>·2H<sub>2</sub>O. The spectroscopic properties were examined using Bruker ELEXSYS E500 X-band spectrometer in the temperature range from 2 K to 300 K. All the samples were in the form of powders. The spectra were fitted in order to obtain the *g*-factor values and linewidths for each sample.

The comparison of shape of the spectra, *g*-factors and linewidths suggests that, in genuine-organic ARS, a signal arising from the magnetic moment of the TCNQ radicals is observed. However, in metal-organic ARS, only contributions of transition metal ions are detectable.

Our analyses of temperature behavior of the EPR spectra are consistent with the results of the temperature dependences of magnetic susceptibility.

*This work was supported by the Slovak Research and Development Agency under the contract No. APVV-0132-11 and VEGA 1/0145/13*

## SPIN-PEIERLS TRANSITION IN NEW MATERIAL

(N-Me-Tetra-Me-Pz)(TCNQ)<sub>2</sub>M. Kajňáková<sup>1</sup>, M. Botko<sup>1</sup>, V. A. Starodub<sup>2</sup>, E. Čižmár<sup>1</sup> and A. Feher<sup>1</sup><sup>1</sup> *Institute of Physics, Faculty of Science, P. J. Šafárik University in Košice, 04154, Košice, Slovakia*<sup>2</sup> *Institute of Chemistry, Jan Kochanowski University of Humanities and Sciences, 5G Świętokrzyska Str., 25-406 Kielce, Poland*

Organic magnets based on TCNQ anion-radical salts (ARS) are considered as useful systems for the study of low-dimensional magnetic models since a subtle modification of their crystal structure has a substantial impact on their physical properties. The compound (N-Me-tetra-Me-Pz(TCNQ)<sub>2</sub> (Pz = pyrazine) represents a structurally quasi-two-dimensional system mediated by hydrogen bonds, in contrast to the one-dimensional character of the majority of recent TCNQ ARS.

The magnetic susceptibility of the studied system shows a plateau at temperatures above 250 K, whereas a sudden exponential decrease appears below 42 K. Strikingly similar behavior is observed in the temperature dependence of the EPR signal intensity. This exponential decrease of the magnetic moment indicates a transition from the magnetic state to the state with  $S=0$ , which indicates existence of the spin-Peierls (sP) transition in the studied system.

According to the formula proposed by Orignac *et al.*,  $\Delta(T=0)/T_{\text{SP}} \approx 2.47$  is given for the sP transition, where  $\Delta$  is the energy gap due to the sP transition and  $T_{\text{SP}}$  is the transition temperature. The fits of the susceptibility and EPR data provide  $\Delta \sim 108$  K and  $T_{\text{SP}} \sim 42$  K, thus the ratio is equal to 2.57, which suggests the presence of the sP transition.

As was shown in work by Nakazawa *et al.*, the sP transition can be detected and confirmed in the derivative of the temperature dependence of the heat capacity in the vicinity of the  $T_{\text{SP}}$ . The calculation of the magnetic entropy, removed below the heat-capacity peak (*i.e.* peak area above the polynomial function fit of the experimental data), gives value of 2.08 J/K·mol, which yields 36% of the total entropy of the system with the spin  $S = 1/2$ . This value of removed magnetic entropy supports the spin-Peierls nature of the transition.

*This work was supported by the projects: CFNT MVEP - the Centre of Excellence of the Slovak Academy of Sciences, the Slovak Research and Development Agency under the contract No. APVV-0132-11 and the Slovak Grant Agency VEGA 1/0145/13.*



# EXPERIMENTAL STUDY OF THE MAGNETOCALORIC EFFECT IN THE TWO-DIMENSIONAL QUANTUM SYSTEM $\text{Cu}(tn)\text{Cl}_2$

L. Baranová<sup>1</sup>, R. Tarasenko<sup>2</sup>, A. Orendáčová<sup>2</sup>, M. Orendáč<sup>2</sup>, V. Pavlík<sup>3</sup> and A. Feher<sup>2</sup>

<sup>1</sup>*Department of Applied Mathematics, Technical University of Košice, Vysokoškolská 4, 042 00 Košice, Slovak Republic*

<sup>2</sup>*Institute of Physics, Faculty of Science, P.J. Šafárik University, Park Angelinum 9, 041 54 Košice, Slovak Republic*

<sup>3</sup>*Institute of Experimental Physics of SAS, Watsonova 47, 040 01 Košice, Slovak Republic*

$\text{Cu}(tn)\text{Cl}_2$  ( $tn = 1,3$ -diaminopropane= $\text{C}_3\text{H}_{10}\text{N}_2$ ) has been previously identified as a potential realization of the quasi-two-dimensional spatially anisotropic triangular Heisenberg antiferromagnet with spin  $1/2$  and with nearest-neighbour ( $J/k_B = 3$  K), frustrating next-nearest-neighbor ( $0 < J'/J < 0.6$ ), and interlayer ( $|J''/J| \approx 10^{-3}$ ) interactions with the collinear Néel ground state. Previous thermodynamic studies identified the response of the system in nonzero magnetic field as a field-induced Berezinskii-Kosterlitz-Thouless (BKT) phase transition below 1 K [1].

Magnetocaloric studies have been performed in the temperature range from 0.2 K to 4 K in magnetic fields up to 2 T by adiabatic magnetization and demagnetization measurements. The aim of the magnetocaloric measurements was tracking of the phase transition to the magnetically ordered state which was not indicated in the previous specific heat studies. Furthermore, the interplay of the magnetic-field induced easy-plane anisotropy and the intrinsic spin anisotropy present in the studied system should manifest in low magnetic fields.

The obtained results of the magnetocaloric experiments of  $\text{Cu}(tn)\text{Cl}_2$  indicate a double crossover from the normal to inverse magnetocaloric effect (MCE). The first crossover from the normal to inverse MCE occurring at about 0.3 K can be attributed to the competition of the aforementioned anisotropies. The second crossover from the inverse to normal MCE observed at about 2 K might be ascribed to the formation of spin vortices stabilized by the easy-plane anisotropy introduced by magnetic field.

*The work was supported by the projects VEGA 1/0143/13 and APVV LPP -0202-09.*

[1] A. Orendáčová, et al., Phys. Rev. B 80 (2009) 144418.

**STUDY OF TWO-DIMENSIONAL MELTING IN SYSTEM OF SMALL MAGNETS**

M. Šviková<sup>1</sup>, M. Liščinský<sup>1</sup>, P. Rabatin<sup>2</sup> and M. Géci<sup>1</sup>

<sup>1</sup> *High School of st. Thomas Akvinas, Zbrojnicna 3, Kosice 040 01, Slovakia*

<sup>2</sup> *Department of Cybernetics and Artificial Intelligence, Faculty of Electrical Engineering and Informatics, Technical University of Košice, Letná 9, 042 00 Košice, Slovakia*

Two-dimensional melting has been an area of intense research and continuous debate over the past three decades. Several theoretical models, computer simulations, and experimental studies have been dedicated to the subject of melting in two dimensions, with predictions and results that are often contradictory.

In our work a new experimental system in which formation of two-dimensional crystal can be studied is suggested. It is macroscopic system of small cylindrical magnets moving on air layer produced by air table. Magnetic moments of magnets are oriented perpendicularly to the layer. Kinetic energies of particles are influenced by intensity of flowing air. From video records of particles motions temperature and pressure for different degrees of intensity of air flowing and different particle concentrations are determined. A next analysis contains determination of particles velocity distribution, pair correlation function, diffusion coefficient and plotting of particles trajectories. At high temperature irregular trajectory of every particle almost fill up the area of the system as is expected for random walking. At lower temperature particle moves around all system area however trajectory of one particle creates regions with larger probability of finding particle arranged in square lattice. At much lower temperature particles oscillate around their equilibrium positions and 2D crystal with triangular lattice is formed.

In 2D melting thermally generated topological defects are important. From Voronoi polyhedron analysis and the Delaunay triangulation analysis average number of n-fold coordinated particles in dependence on temperature is evaluated. The sudden drop of number of 6-fold coordinated particles and the increase of number of 5-fold and 7-fold coordinated particles with increasing temperature are observed indicating transition from ordered crystalline phase to less-ordered one.

# **SENSITIVITY OF 6CHBT LIQUID CRYSTAL DOPED WITH FERROELECTRIC OR MAGNETIC PARTICLES ON ELECTRIC AND MAGNETIC FIELDS**

J. Majorošová<sup>1</sup>, N. Tomašovičová<sup>1</sup>, M. Timko<sup>1</sup>, M. Koneracká<sup>1</sup>, Z. Mitróová<sup>1</sup>, I.P. Studeniyak<sup>2</sup>, O.V. Kovalchuk<sup>3</sup>, J. Jadzyn<sup>4</sup> and P. Kopčanský<sup>1</sup>

<sup>1</sup>*Institute of Experimental Physics, Slovak Academy of Sciences, Watsonova 47, 040 01 Košice, Slovakia*

<sup>2</sup>*Uzhorod National University 46 Pidhirna St., Uzhorod 88000, Ukraine*

<sup>3</sup>*Institute of Physics, National Academy of Science of Ukraine, 46, prospect Nauky, 03028 Kyiv, Ukraine*

<sup>4</sup>*Institute of Molecular Physics, Polish Academy of Sciences, Smoluchowskiego 17, 60179 Poznan, Poland*

System of colloidal particles dispersed in liquid crystals present a rich variety of phenomena. Introduction of ferroelectric or magnetic nanoparticles into nematic liquid crystal is promising method for improvemet electro-optic or magneto-optic properties of different nematic liquid crystals by non-chemical way. The giant nanoparticle-nematic coupling might then be fruitfully used in devices controlled by electric or magnetic field.

This work is devoted to the study of composite systems of liquid crystal with spherical ferroelectric or magnetic nanoparticles with aim to study their sensitivity to electric and magnetic fields. The thermotropic nematic 4-(trans-4'-n-hexylcyclohexyl)-isothiocyantobenzene (6CHBT) liquid crystal was doped with SbSI ferroelectric particles or with spherical Fe<sub>3</sub>O<sub>4</sub> magnetic particles. The structural transitions in ferronematic samples were indicated by capacitance measurements in a capacitor made of ITO-coated glass electrodes in combined electric and magnetic fields. The obtained results showed the increase of the shift in critical voltage with increasing magnetic field in both kind of samples. However, the shift is higher in the case of doping with magnetic particles.

*This work was supported by the Slovak Academy of Sciences grants VEGA 2/0045/13, Slovak Research and Development Agency under the contract No. APVV-0171-10, Ministry of Education of Slovakia - Agency for Structural Funds of EU in frame of project No. 26110230061, 6220120021 and 6220120033, and the Grenoble High Magnetic Field Laboratory (CRETA).*

# MAGNETIC FIELD INDUCED ISOTROPIC-NEMATIC PHASE TRANSITION IN FERRONEMATICS BASED ON MIXTURE OF BENT-CORE AND ROD-SHAPED LIQUID CRYSTALS

J. Majorošová<sup>1</sup>, N. Tomašovičová<sup>1</sup>, M. Timko<sup>1</sup>, Z. Mitróová<sup>1</sup>, A. Juríková<sup>1</sup>, K. Fodor-Csorba<sup>2</sup>, A. Vajda<sup>2</sup>, N. Éber<sup>2</sup>, T. Tóth-Katona<sup>2</sup>, X. Chaud<sup>3</sup> and P. Kopčanský<sup>1</sup>

<sup>1</sup>*Institute of Experimental Physics, Slovak Academy of Sciences, Watsonova 47, 040 01 Košice, Slovakia*

<sup>2</sup>*Institute for Solid State Physics and Optics, Wigner Research Centre for Physics, Hungarian Academy of Sciences, H-1525 Budapest, P.O.Box 49, Hungary*

<sup>3</sup>*Grenoble High Magnetic Field Laboratory, CNRS, 25 Avenue des Martyrs, Grenoble, France*

The possibility to alter the nematic-isotropic transition temperature  $T_{NI}$  in liquid crystals (LCs) with an external field has been known for a long time [1]. However, the effect has not been produced via magnetic field until recently [2], when a magnetic-field induced alteration of  $T_{NI}$  has been achieved in a bent-core nematic LC using a powerful electromagnet ( $B$  up to 30T). In our previous work [3] we have shown that the ferronematic consisting of the calamitic nematic LC 4-(trans-4-n-hexylcyclohexyl)-isothiocyanato-benzene (6CHBT) doped with rod-like magnetic particles can be just as effective in demonstrating the magnetic field induced isotropic-nematic phase transition shift in the magnetic field range of 10T as pure bent-core nematics.

In this work we investigate the influence of an external magnetic field on the  $T_{NI}$  of the binary mixture of the bent-core 4,6-dichloro-1,3-phenylene-bis [4'-(9-decen-1-yloxy)-1,1'-biphenyl] 4-carboxylate (10DC1PBBC) and the rod-shaped 4-n-octyloxyphenyl 4-n-hexyloxybenzoate (6OO8) LCs doped with spherical magnetic particles (in volume concentration of  $8 \times 10^{-4}$ ) in order to increase the magnetic sensitivity. Structural transitions in the prepared samples were detected by capacitance measurements in a capacitor made of ITO-coated glass electrodes. The magnetic field was applied either parallel with, or perpendicular to the electrodes. Due to the presence of magnetic particles, depending on the magnetic field direction a positive or negative shift of  $T_{NI}$  was observed with a linear  $T_{NI}(B^2)$  relation.

[1] W. Helfrich, Phys. Rev. Lett. **24**, 201 (1970).

[2] T. Ostapenko, et al., Phys. Rev. Lett. **101**, 247801 (2008).

[3] P. Kopčanský, et al., IEEE T. Magn. **47**, 4409 (2011).

**RADIATION STABILITY OF THE BOVINE SERUM ALBUMIN  
STABILIZED BIOCOMPATIBLE MAGNETIC FLUID**

N. Tomašovičová<sup>1</sup>, I. Haysak<sup>2</sup>, J. Kováč<sup>1</sup>, M. Kubovčíková<sup>1</sup>, V. Závišová<sup>1</sup>, M. Timko<sup>1</sup>, A. Okunev<sup>2</sup> and P. Kopčanský<sup>1</sup>

<sup>1</sup>*Institute of Experimental Physics, Slovak Academy of Sciences, Watsonova 47, 040 01 Košice, Slovakia*

<sup>2</sup>*Uzghorod National University, Kapitulna 9A, 880 00 Uzghorod, Ukraine*

The aim of the presented work was to investigate the stability of biocompatible magnetic fluid, i.e. water-based magnetic fluid containing magnetite nanoparticles stabilized by surfactant sodium oleate and modified by bovine serum albumin (BSA) after electron irradiation. Samples with the same initial concentration of Fe<sub>3</sub>O<sub>4</sub> but different mass ratio BSA/Fe<sub>3</sub>O<sub>4</sub> (w/w = 0.25, 1.0 and 2.5) were studied. The irradiation of samples was conducted by electrons with energy 0.6 MeV. The electron irradiation caused about 10% reduction of the saturation magnetization in the samples with w/w BSA/Fe<sub>3</sub>O<sub>4</sub> ratio 0.25 and less than 5% in the samples with w/w BSA/Fe<sub>3</sub>O<sub>4</sub> ratio 1 and 2.5. Size distribution measurements and infrared spectra showed the structural changes in BSA and aggregation of BSA after irradiation. Our results showed that the stability of BSA modified magnetic fluids after irradiation depends on the w/w BSA/Fe<sub>3</sub>O<sub>4</sub> ratio.

*This work was supported by the Slovak Academy of Sciences grants VEGA 2/0045/13, Slovak Research and Development Agency under the contract No. APVV-0171-10, Ministry of Education of Slovakia - Agency for Structural Funds of EU in frame of project No. 26110230061 and 6220120021, and by Ministry of Education and Science of Ukraine in the framework of project No. 0109U000873.*

# THERMODYNAMIC PROPERTIES OF GEOMETRICALLY FRUSTRATED $S = 1/2$ XY PYROCHLORE ANTIFERROMAGNET

**Er<sub>2</sub>Sn<sub>2</sub>O<sub>7</sub>**

N. A. Ali Alghamdi<sup>1</sup>, A. Orendáčová<sup>1</sup>, V. Pavlík<sup>2</sup>, and M. Orendáč<sup>1</sup>

<sup>1</sup>*Institute of Physics, P. J. Šafárik University, Park Angelinum 9, Košice, 040 01, Slovakia*

<sup>2</sup>*Institute of Experimental Physics, SAS, Watsonova 47, Košice 040 01, Slovakia*

The magnetic and thermodynamic properties of the  $S = 1/2$  XY antiferromagnet Er<sub>2</sub>Sn<sub>2</sub>O<sub>7</sub> are reported. The studied material belongs to geometrically frustrated magnets in which simultaneous minimizing of all pair – wise interactions is not possible. Unlike its counterpart Er<sub>2</sub>Ti<sub>2</sub>O<sub>7</sub>, which orders magnetically at  $T_N = 1.2$  K, no indication of long - range ordering has been reported in Er<sub>2</sub>Sn<sub>2</sub>O<sub>7</sub> down to 130 mK. The comparative values of Curie - Weiss temperatures of both compounds suggests that the frustration index

$f = \Theta_{cw}/T_N \approx 14/0.1 = 140$  for Er<sub>2</sub>Sn<sub>2</sub>O<sub>7</sub> is significantly higher than that found in Er<sub>2</sub>Ti<sub>2</sub>O<sub>7</sub>. The obtained value of  $f$  placed the studied material into a highly frustrated regime. However, the presented results of the analysis of the temperature dependence of dc susceptibility studied on powder sample suggest a non - negligible role of single - ion anisotropy. As a result, considering only the contribution of effective exchange coupling to the magnitude of  $\Theta_{cw}$ , the studied material may be characterized by a lower value of the frustration index.

This suggestion was verified indirectly by investigating magnetocaloric effect. The magnetothermal characteristics, namely isothermal change of magnetic entropy  $\Delta S_M(T)$ , were calculated from temperature dependences of specific heat studied systematically in magnetic fields up to 9 T. The used magnetic field range involves  $B_c \approx 1.6$  T which for Er<sub>2</sub>Ti<sub>2</sub>O<sub>7</sub> induces a quantum phase transition. The absence of the enhanced magnetocaloric effect in Er<sub>2</sub>Sn<sub>2</sub>O<sub>7</sub> in the vicinity of  $B_c$  is consistent with weaker exchange interaction in this material. Consequently, the weakening of the effective exchange interaction by replacing Sn for Ti in the pyrochlore lattice may play a significant role in suppressing long - range ordering found in Er<sub>2</sub>Sn<sub>2</sub>O<sub>7</sub>.

*This work has been supported by the project ITMS 26220120005.*

## P5-18

### SPIN GLASS STATE IN $S = 3/2$ KAGOMÉ ANTIFERROMAGNET

$\text{Co}(\text{N}_3)_2(\text{bpg})[(\text{CH}_3)_2(\text{NCOH})]_{4/3}$

P. Vrábek<sup>1</sup>, E. Čižmár<sup>1</sup>, A. Orendáčová<sup>1</sup>, S. Gao<sup>2</sup>, and M. Orendáč<sup>1</sup>

<sup>1</sup>*Institute of Physics, P. J. Šafárik University, Park Angelinum 9, Košice, 040 01, Slovakia*

<sup>2</sup>*State Key Laboratory of Rare Earth Materials Chemistry and Applications, Peking University, Beijing 100871, China*

The magnetic and thermodynamic properties of the  $S = 3/2$  compound  $\text{Co}(\text{N}_3)_2(\text{bpg})[(\text{CH}_3)_2(\text{NCOH})]_{4/3}$  are reported. The structure of the studied material consists of Kagomé layers in which Co(II) magnetic ion is coordinated with six N atoms, two from *trans*-bpg ligands and four from azido ligands. The azido ligands link the Co(II) ions creating a Kagomé layer featuring vertex-sharing triangles along the *bc* plane. The wavy Kagomé layers are bridged by *bpg* ligands and generate a three – dimensional framework whose hexagonal channels are filled by  $(\text{CH}_3)_2(\text{NCOH})$  molecules.

Specific heat study performed from 2 K to 40 K in magnetic fields up to 2 T revealed the existence of a small spike at 16 K indicating long - range ordering. The magnetic transition has been confirmed also by the temperature dependence of the ac susceptibility and magnetization studied in FC and ZFC regime. In addition to the anomaly associated with the magnetic ordering, distinct broad maxima were observed in the ac susceptibility at 9 K, well below magnetic ordering. The analysis of the frequency dependence of ac susceptibility using Cole - Cole diagrams revealed wide distribution of relaxation times characteristic for a spin glass state. Calculation of isothermal susceptibility suggests gradual freezing of spins below 4 K at a time scale much longer than the experimental window for the ac susceptibility measurements. The long relaxation time was confirmed by a subsequent study of the time dependence of the magnetization performed from 4.2 K to 9 K using various thermal protocols. The observed spin relaxation occurring in various time scales is in accord with the model of a topological spin glass, in which the coexistence of geometrical frustration and chirality leads to the formation of spin glass even in a system without structural defects.

*This work has been supported by the project ITMS 26220120005.*

**PREPARATION, CHARACTERIZATION AND COMPARISON OF SCANNING ELECTRON MICROSCOPY, DYNAMIC LIGHT SCATTERING AND ANALYTICAL ULTRACENTRIFUGATION FOR MAGNETIC NANOPARTICLES SIZING**

M. Kubovčíková, I. Antal, J. Kováč, V. Závišová, M. Koneracká and P. Kopčanský  
*Institute of Experimental Physics, SAS, Watsonova 47, 04001 Košice, Slovakia*

Magnetic fluids (MFs) are stable colloidal suspensions of magnetic nanoparticles (around 10 nm in diameter) in a liquid carrier. To meet biomedical requirements they have to be superparamagnetic (SPM), meaning that they are attracted by a magnetic field but retain no residual magnetism after the field is off. Due to their small size and SPM behaviour, MFs offer a variety of uses in the field of biomedicine.

This paper deals with magnetite nanoparticles (MNPs) that were synthesized by the co-precipitation method from ferric and ferrous salts using ammonium hydroxide, then sodium oleate (SO) was applied as a surfactant in order to prevent their agglomeration. The complex physicochemical characterization of the prepared MFs has been accomplished by the routine methods such as infrared spectroscopy (FTIR), magnetic measurements, scanning electron microscopy (SEM) and dynamic light scattering (DLS). The FTIR spectra showed that SO molecules were linked to MNPs through chemical bond. Magnetic measurements proved that the MNPs are superparamagnetic in nature. Knowing the particle size is considered to be one of the basic preconditions if it is to be used effectively in biomedicine, which made us focus on study of particle-size distribution of MNPs. Four different methods were used to determine the size and size distribution of the MNPs: SEM, DLS, analytical ultracentrifugation (ANUC) and magnetic measurements. SEM analysis showed a relatively narrow size distribution of roughly spherical MNPs with a mean diameter of 67 nm. DLS analysis confirmed monodispersed MFs production with hydrodynamic diameter of 75 nm. The size distribution determined by ANUC using sedimentation velocity analysis was found to be 69 nm.

Finally, the calculated magnetic core diameter obtained from magnetization curve was 6.85 nm. The comparison of the size and size distributions determined by each technique for MFs, their advantages, disadvantages and limitations is included as well.

*Acknowledgement: This work was supported within the projects SF of EU 26110230061, VEGA 0041, APVV 0171-10 and APVV 0742-10.*



**CHROMIUM-BASED MOLECULAR RINGS WITHIN THE DFT AND FALICOV-KIMBALL MODEL APPROACH**

Bartosz Brzostowski<sup>1</sup>, Michał Wojciechowski<sup>1</sup>, Romuald Lemański<sup>2</sup> and Grzegorz Kamieniarz<sup>3</sup>

<sup>1</sup>*Institute of Physics, University of Zielona Góra, Zielona Góra (Poland)*

<sup>2</sup>*Institute of Low Temp. & Struct. Research, Polish Academy of Sciences, Wrocław (Poland)*

<sup>3</sup>*Faculty of Physics, A. Mickiewicz University, Poznań (Poland)*

Based on first principles density functional theory (DFT) calculations, we present a comprehensive study of electronic and magnetic properties of non-metallic homo-nuclear chromium-based molecular rings  $\text{Cr}_9\text{F}_9\text{Cl}_2(\text{O}-\text{C}-\text{CH}_3)_{17}$ . The total, local and orbital projected density of states are presented, magnetic moments are calculated using different approaches as well as the electron density and spin density maps are discussed. All non-equivalent broken-symmetry spin configurations with  $S=\pm 3/2$  are considered, the corresponding differences between the total energies calculated and the exchange interaction parameter  $J$  extracted from the spin model, using different scenarios.

Moreover, the complementary studies are carried out using the Falicov-Kimball model, which incorporates the Hund coupling. In this model magnetic interactions between ions are generated by local (on-site) couplings between the ions and itinerant electrons. This approach allows us to determine the magnetic coupling constant  $J$  between ions in terms of Hund coupling  $J_h$  and the hopping amplitude  $t$  of electrons for the molecular rings in question. It appears that the approach reproduces very well the energy levels determined by different magnetic broken symmetry configurations obtained by DFT.

**RAMAN SPECTRA OF BISMUTH OXYHALIDE SINGLECRYSTALS**V. Bunda<sup>1</sup>, S. Bunda<sup>1</sup>, V. Komanicky<sup>2</sup> and A. Feher<sup>2</sup><sup>1</sup> *Faculty of Information technologies, Transcarpathian State University, Zankovetska 87-B, 880 15 Uzhgorod, Ukraine*<sup>2</sup> *Centre of Low Temperature Physics, Faculty of Science P. J. Šafárik University & Institute of Experimental Physics, Slovak Academy of Sciences, Park Angelinum 9, Kosice 04154, Slovakia*

Oxyhalogenides of bismuth BiOHal (Hal = Cl, Br and I) are very interesting materials which find various applications as X-ray luminescent screens, as anti-Stokes (frequency upshift) converters, usual luminophors, and photoconducting analyzer of linear polarized radiation.

The Raman spectral data of solid state (as a singlecrystals) bismuth oxyhalides have not as yet been extensively studied. In the present study, the Raman active vibrational fundamentals of the singlecrystalline bismuth oxyhalides, BiOCl, BiOBr and BiOI, are discussed using the results of the factor group analysis. The optically active normal vibrations are discussed by comparison with the results of the calculations of phonon spectra in terms of rigid ion model.

The BiOHal singlecrystals were grown either by the chemical gas transport reactions method (typically of the order  $10 \times 10 \times 0.5 \text{ mm}^3$ ). The BiOHal singlecrystals crystallize with the tetragonal Matlokit (PbFCl) type structure (space group  $P4/nmm - D_{4h}^7$ ;  $Z = 2$ ). The bismuth ions have a monocapped square antiprismatic surrounding of four oxygen and five halogen atoms. Since each primitive cell consist of six monoatomic sites, the structure of the reduced representation of the 15 normal modes of vibration is found to be

$$\Gamma = 2A_{1g}(Ra.) + B_{1g}(Ra.) + 3E_g(Ra.) + 2A_{2u}(i.r.) + 2E_u(i.r.),$$

in which the vibrations of  $A_{1g}$ ,  $B_{1g}$  and  $E_g$  species are active in the Raman spectrum and those of  $A_{2u}$  and  $E_u$  species are active in the infrared (i.r.) spectrum. There are no optically inactive fundamentals. In the present Raman investigation, however, only five fundamental bands were found for the BiOCl, BiOBr and BiOI. The Raman active modes are observed in frequency range 55 - 225; 50 - 185; 45 - 175 for the BiOCl, BiOBr and BiOI singlecrystals, respectively.

The halogen substitution effect on the Raman spectra of the BiOHal (Bismocklit family) crystals and the correlation's between experimental and calculated results are observed.

# ANIZOTROPY OF PHOTOCONDUCTIVITY IN BiOX (X=Cl, Br, I) SINGLE CRYSTALS

V. Bunda<sup>1</sup>, S. Bunda<sup>1</sup>, V. Komanicky<sup>2</sup> and A. Feher<sup>2</sup>

<sup>1</sup> *Faculty of Information technologies, Transcarpathian State University, Zankovetska 87-B, 880 15 Uzhgorod, Ukraine*

<sup>2</sup> *Centre of Low Temperature Physics, Faculty of Science P. J. Šafárik University & Institute of Experimental Physics, Slovak Academy of Sciences, Park Angelinum 9, Kosice 04154, Slovakia*

Oxyhalides of bismuth BiOX (X = Cl, Br, I) are very interesting materials which find various applications as X-ray luminescent screens, as anti-Stokes converters, photocatalist, usual luminophors and as photoconductive analyzer of linear polarized radiation in the 0.24 - 1.2 $\mu$ m spectral region. Bismuth oxyhalides provides a very convenient matrix for activation by various rare-earth and 3d-elements: by doping this matrix with different, is possible to obtain a wide variety of optical, luminescent and photoconductive properties. Moreover, these crystals are of essential interest in connection with the research and development work on laser materials. The great interest for these materials is strongly related to the influence of dimensionality on the behaviour of physical properties (they are 2D structured materials). Bismuth oxyhalides are one of the V-VI-VII group compound semiconductors belonging to the tetragonal system. The structure of BiOX is known to have a layered structure, which is constructed by the combination of the halide ion layer and the bismuth oxygen layer.

We present results of the study of photoconducting spectra anisotropy of the BiOX single crystals, obtained with the polarization of electrical vector  $\vec{E}$  of the electromagnetic wave parallel and perpendicular to each of the two axes ([100] or [010]) of the unit cell. The BiOHal compounds are broad-band (1.80 - 3.50 eV) photo-semiconductors. The maxima of their photoconductivity are in the interval of 0.24-1.2  $\mu$ m and theirs photosensitivity's are  $S = 10^4 - 10^8$  arbitrary units at the temperature 80K. The anisotropy of photoconducting spectra is believed to be the results of the layer matlockite-type (PbFCl) crystal structure of all bismuth oxyhalide compounds.

The position of electrical vector  $\vec{E}$  can be varied either by rotating of the crystal. Anisotropy in 3 - 5 times was observed for the photosensitive value S. The change in light polarization at the 90 degrees (from [100] to [010] crystallographic direct) leads to the change in the photoconductivity of 50-100 units. The temperature region of BiOX based photoresistors is in the range 80-400K. They are stable in air.

**IONIC LIQUID BASED FERROFLUIDS**

J. Parnica<sup>1</sup>, P. Keša<sup>1</sup>, J. Kováč<sup>2</sup>, M. Timko<sup>2</sup> and M. Antalík<sup>1,2</sup>

<sup>1</sup>*Department of Biochemistry, Faculty of Science, P.J. Šafárik University, Košice, Slovak Republic*

<sup>2</sup>*Institute of Experimental Physics, Slovak Academy of Sciences, Košice, Slovak Republic*

Ionic liquids (ILs) are organic salts composed of organic cations and anions. The possible choices of a cation and an anion can result in the formation of practically unlimited ILs. The unique properties of these fluids include extremely low volatility, high thermal stability, wide temperature range of liquid phase, non-flammability, high chemical stability and high ionic conductivity. Magnetic ionic liquids (MILs) have paramagnetic properties by itself without the need of adding magnetic particles. Room temperature (RT) magnetic chiral ILs derived (methyl ester hydrochlorides) from amino acids (AA) were synthesized and their magnetic properties were investigated.

Magnetoactive metal complex anions, such as  $\text{Fe}^{\text{III}}\text{Cl}_4^-$  anions, have been known to form paramagnetic RT-IL, by pairing with conventional liquid-forming counter cations. Ionic liquids can be obtained simply by mixing the halide salts and neutral metal complexes; for example, dark brown ionic liquids  $[\text{L-AA-OMe}][\text{FeCl}_4]$  are formed by mixing exactly equimolar crystalline  $[\text{L-AA-OMe}]\text{Cl}$  and  $\text{FeCl}_3$  in ethanol at RT. The dark brown liquid may be regarded as a new type of magnetic fluid (group of smart materials whose properties can be controlled by means of external magnetic fields).

The ILs were characterized by Fourier transform infrared–attenuated total reflectance (FTIR-ATR) spectroscopy and by magnetic measurements. The magnetic susceptibility and magnetization of the ILs were measured using a Quantum Design Superconducting Quantum Interference Device (SQUID) magnetometer. Circular dichroism (CD) and magnetic CD (MCD) spectra were also monitored for characterization ILs and UV/Vis spectroscopy shows the coordination around the  $\text{Fe(III)}$  ion. MILs have both general properties of ILs and magnetic response, has a simplicity and demonstrated their advantages and unique properties what suggest opportunities for new applications.

*This research was supported within the projects Nos. 26220120021 a 26220220061 in frame of SF EU, VEGA 2/0025/12 and project APVV-0171-10, APVV-0526-11.*

**UNUSUAL VISCOSITY DEPENDENCE OF A MAGNETIC FLUID ON NANOPARTICLES CONCENTRATION**J. Tothová<sup>1</sup>, J. Kováč<sup>2</sup>, P. Kopčanský<sup>2</sup>, M. Rajňák<sup>2</sup>, M. Timko<sup>2</sup><sup>1</sup>*Department of Physics, Technical University of Košice, Park Komenského 2, 042 00 Košice, Slovakia*<sup>2</sup>*Institute for Experimental Physics, Slovak Academy of Sciences, Watsonova 47, 040 01 Košice, Slovakia*

Ferrofluids or magnetic fluids (MFs) are colloidal suspensions of nanosized ferromagnetic particles coated with surfactants and dispersed in a carrier liquid. Since their physical properties can be easily influenced by external forces such as, for example, a magnetic field, they can be found in various applications ranging from inks to pharmaceuticals. One of many unique properties of ferrofluids is their tunable viscosity by the external magnetic field. This is called the magnetoviscous effect. For a good understanding of this phenomenon, the knowledge of the viscous properties of MFs in the absence of magnetic fields is very important. Particularly its dependence on the amount of suspended magnetic particles (MPs) and temperature is very interesting.

In this work we have studied the effect of temperature on the viscosity of MFs based on the transformed oil ITO 100. The volume concentration of suspended MPs changed from 0.025 to 1 %. Rheological characterization of MFs was performed using a vibroviscometer at working frequency 30 Hz. The temperature dependence of the viscosity was measured in the range from 20 to 80°C. Five different concentrations of MPs in MFs were determined by experiments with the vibrating sample magnetometer. In contrast to the expected behavior of MFs, a decrease of their viscosities in comparison to the carrier liquid has been recorded. From the lowest concentration of MPs in MFs - 0.025% towards 0.25%, the viscosities of these MFs gradually decrease. Further increasing of MPs amount in MFs leads to a slight increase of the MFs viscosities but their values remain smaller than the viscosity of carrier liquid.

**THE KONDO LATTICE: SOME NEW ASPECTS**

C. Lacroix

*Institut Néel, CNRS-UJF, BP 166, 38042 Grenoble Cedex 9, France*

The Kondo lattice model has been proposed by Doniach in 1977. It has been widely used for describing competition between Kondo effect and exchange interactions in Ce compounds. In the last 10 years several improvements have been proposed. Some of these new aspects will be reviewed in this talk:

- In U compounds,  $S=1$  model is sometimes more appropriate. I will present a phase diagram for the  $S=1$  Kondo lattice model. Partial Kondo effect may occur in this model, resulting in a rich phase diagram.

- Geometrical frustration is present in some series of compounds like  $\text{YbPd}_2\text{Sn}$  in which the crystal structure is kagome-like. The phase diagram of the Kondo lattice in presence of frustration exhibits, besides the Kondo and ordered phases, a non-magnetic spin-liquid phase stabilized by frustration.

- Lifshitz-transitions, i.e. change of topology of the Fermi surface, often occur in the Kondo lattice model under magnetic field or pressure. I will show that such transition also occurs under doping in a dilute Kondo alloy.

**PRESSURE INFLUENCE ON STRUCTURAL AND MAGNETIC PROPERTIES OF TbNiAl**

P. Javorský, J. Prchal, M. Klicpera, J. Kaštil, M. Míšek

*Charles University in Prague, Faculty of Mathematics and Physics, Department of Condensed Matter Physics, Ke Karlovu 5, 121 16 Prague 2, Czech Republic*

The application of external pressure is a very powerful tool how to modify the interatomic distances and hence also the electronic properties of a given material. The pressure has a very large effect on e.g. magnetic properties in materials where the electrons responsible for the magnetic behavior have itinerant character. Among the rare earth compounds, the pressure is mainly used to study the Ce or Yb-based compounds in which the 4f electrons lie on a verge between localized and itinerant character. The magnetic properties of compounds containing only localized magnetic moments are usually much less influenced by the external pressure. The TbNiAl intermetallic compound is an example of a system with localized Tb moments, where the the pressure have considerable effects on its properties. The influence of pressure, both hydrostatic and uniaxial, on structural and magnetic properties of TbNiAl is a subject of this work.

TbNiAl crystallizes in the hexagonal ZrNiAl-type structure and shows an abrupt transition in the temperature development of the lattice parameters at around 100 K. This structural transition resides in a sudden change of the lattice parameters when the  $c/a$  ratio approaches the critical region between 0.565 and 0.575 in the temperature dependence. The crystal structure with the  $c/a$  ratio from this forbidden region is energetically less favorable and these  $c/a$  values are not realized. During the transition, the  $a$  and/or  $c$  parameters change by several percent to jump over the forbidden  $c/a$  region, while keeping volume unchanged. We show that this structural transition is rapidly shifted to lower temperatures with applied hydrostatic pressure.

The magnetic properties of TbNiAl are only very weakly influenced by the above described structural transition. TbNiAl orders antiferromagnetically below  $T_N = 45$  K. The magnetic order is characterized by a propagation vector ( $\frac{1}{2}$  0  $\frac{1}{2}$ ) with Tb magnetic moments oriented along the  $c$ -axis. The antiferromagnetic order can be easily disrupted by a small ( $\sim 0.3$  T at 2 K) magnetic field applied along the  $c$ -axis or by substitutions like in the Tb(Ni,Cu)Al or TbNi(Al,In) series, leading to a collinear ferromagnetic structure. We show that the application of hydrostatic pressure stabilizes the antiferromagnetic order in TbNiAl, whereas the uniaxial pressure along the  $c$ -axis leads to its suppression and transition to the ferromagnetic order.

**LARGE MAGNETOCALORIC EFFECT IN Nd<sub>2</sub>Ni<sub>2</sub>In**S. Mašková<sup>1</sup>, S. Daniš<sup>1</sup>, A. Llobet<sup>2</sup>, H. Nakotte<sup>3</sup> and L. Havela<sup>1</sup><sup>1</sup>*Department of Condensed Matter Physics, Ke Karlovu 5, 12116 Prague 2, The Czech Republic*<sup>2</sup>*LANSCE, Los Alamos National Laboratory, Los Alamos, NM 87545, USA*<sup>3</sup>*New Mexico State University, 88003-8001 Las Cruces, USA-NM*

Nd<sub>2</sub>Ni<sub>2</sub>In belongs to a large family of RE<sub>2</sub>T<sub>2</sub>X (RE = rare-earth or actinide, T = transition metal, X = *p*-metal) compounds crystallizing in the Mo<sub>2</sub>FeB<sub>2</sub> structure type (space group *P4/mbm*). The RE atoms form a triangular motif which, depending on the type of exchange interactions, can bring a geometrical frustration into the system, as it is equivalent to the 2-dimensional Shastry-Sutherland lattice arrangement [1]. Nd<sub>2</sub>Ni<sub>2</sub>In orders antiferromagnetically below  $T_N \approx 8$  K. Magnetic susceptibility even in very low magnetic fields do not exhibit any cusp, which would be characteristic of common antiferromagnetic ordering. Instead a plateau appears below the critical temperature. The plateau extends down to  $T = 3.5$  K and the magnetization in low fields decreases weakly at the low- $T$  end (even if measured in the field-cooled mode). Under weak magnetic field (0.3 T) the magnetic behavior changes to ferromagnetic. The magnetic structure was determined using neutron diffraction experiment. It revealed the non-collinear arrangement of magnetic moments in the basal plane. The size of magnetic moment is only slightly decreasing with increasing temperature (2.49  $\mu_B$ /Nd at  $T = 4$  K and 2.01  $\mu_B$ /Nd at  $T = 8$  K). The relatively weak decrease of the size of Nd moments and the sudden disappearance above 8 K can point to 1<sup>st</sup> order magnetic transition. The peak in specific heat related to magnetic ordering does not form any  $\lambda$ -type anomaly, expected for the 2<sup>nd</sup> order magnetic phase transition, but there is a concentration of entropy in the temperature range 7.5-8.5 K. Relatively weak fields shift a lot of entropy by several Kelvin up, testifying a certain magnetocaloric potential, with  $\Delta S > 5$  J/mol f.u. K in quite low fields (below 1 T). The fact that weak fields change the entropy considerably can be related to the magnetic frustration, making the magnetic order very sensitive. The large change of magnetic entropy indicates that such frustrated systems could be suitable magnetocaloric media, especially if similar effect is found for heavy rare-earths, which can develop higher magnetic entropy due to the higher multiplicity of magnetic moments in the paramagnetic state.

[1] B. Shastry and B. Sutherland, Physica B+C 108 (1981) 1069.



# MAGNETISM IN $\text{NdMnO}_{3+\delta}$ AND $\text{NdMn}_{0.8}\text{Fe}_{0.2}\text{O}_{3+\delta}$ STUDIED BY THE NEUTRON DIFFRACTION EXPERIMENTS

M. Mihalik jr.<sup>1</sup>, M. Mihalik<sup>1</sup>, S. Maťaš<sup>2</sup>, A. Hoser<sup>2</sup> and M. Vavra<sup>1,3</sup>

<sup>1</sup>*Institute of Experimental Physics SAS, Watsonova 47, 040 01 Košice, Slovak Republic*

<sup>2</sup>*Helmholtz-Zentrum Berlin, Hahn Meitner Platz 1, D-14109 Berlin, Germany*

<sup>3</sup>*Faculty of Science, P.J. Šafárik University, Moyzesova 11, 041 54 Košice, Slovak Republic*

The  $\text{NdMnO}_3$  compound attracted the attention because of three possible magnetic interactions in this compound (Mn - Mn; Nd - Nd and Mn - Nd magnetic interaction) could be observed. Previous neutron powder diffraction (NPD) experiments revealed that the Mn - Mn interaction leads to the antiferromagnetic ordering of Mn sublattice ( $T_N = 82$  K, magnetic moments parallel to  $b$ -axis) [1]. However, description of Nd - Mn magnetic interaction remained controversial: One group of authors state that Nd sublattice orders ferromagnetically (moments parallel to  $c$ -axis) at  $T_1 < 20$  K [1] as a consequence of the polarization of Nd ions by Mn ions. The second group of authors claim that Nd sublattice possess ordered magnetic moment already below  $T_N$  [2]. To solve this controversy we have performed the single crystal neutron diffraction experiment. In the contribution we will suggest more realistic ordering of magnetic moments in the  $\text{NdMnO}_{3+\delta}$  compound and we compare our results with results from previous NPD experiments.

Substitution of  $\text{Fe}^{3+}$  ions for  $\text{Mn}^{3+}$  ions weakens the interaction in the Mn/Fe sublattice resulting to decrease of  $T_N$  to 55.4 K for  $\text{NdMn}_{0.8}\text{Fe}_{0.2}\text{O}_{3+\delta}$ . Thence the strength of Mn/Fe - Nd interaction becomes more comparable to the strength of the Mn - Mn interaction. As a consequence the temperature dependence of magnetization ( $M(T)$ ) exhibits the compensation temperature at  $T_{\text{comp}} = 26.6(2)$  K and magnetization reaches negative values at lower temperatures. Such an effect can be described by the interplay of two different magnetic sublattices in the compound. We have studied this interplay using NPD, we will present the results from this neutron experiment and we will compare our results with other results obtained on similar compounds.

[1] T. Chatterji, B. Ouladdiaf, D. Bhattacharya, J. Phys.: Condens. Matter **21** (2009), 306001

[2] F. Bartolomé, J. Herrero-Albillos, L. M. García, J. Bartolomé, N. Jaouen, A. Rogalev, J. Appl. Phys. **97** (2005), 10A503

# COMPLEX MAGNETIC PHASE DIAGRAM OF A GEOMETRICALLY FRUSTRATED SM LATTICE: $\text{SmPd}_2\text{Al}_3$ CASE

J. Pospíšil<sup>1</sup>, G. Nénert<sup>2</sup>, S. Miyashita<sup>3</sup>, H. Kitazawa<sup>4</sup>, Y. Skourski<sup>5</sup>, M. Diviš<sup>1</sup>,  
J. Prokleška<sup>1</sup> and V. Sechovský<sup>1</sup>

<sup>1</sup>*Faculty of Mathematics and Physics, Department of Condensed Matter Physics, Charles University, Ke Karlovu 5, 121 16 Prague 2, The Czech Republic*

<sup>2</sup>*Institut Laue Langevin, BP 156, 6 rue Jules Horowitz, 38042, Grenoble Cedex 9, France*

<sup>3</sup>*Department of Physics, School of Science, The University of Tokyo 7-3-1 Hongo, Bunkyo-ku, Tokyo, 113-0033 Japan*

<sup>4</sup>*National Institute for Materials Science, Tsukuba, Ibaraki 305-0047, Japan*

<sup>5</sup>*Dresden High Magnetic Field Laboratory, Helmholtz-Zentrum Dresden Rossendorf, D-01314 Dresden. Germany*

$\text{SmPd}_2\text{Al}_3$  represents an example of Sm magnetism with a complex magnetic phase diagram where four consecutive magnetic phase transitions (MPT) at 3.4, 3.8, 4.3 and 12.5 K have been observed. The complexity of magnetism in this compound is caused by specific features of the  $\text{Sm}^{3+}$  ion, namely by nearness of the ground-state multiplet  $J = 5/2$  and the first excited multiplet  $J = 7/2$  in conjunction with strong crystal field influence. We have established a magnetic phase diagram of this compound. Since the magnetic characteristics had been obtained from bulk measurements detailed information regarding the magnetic structure of each magnetic phase was lacking and neutron diffraction was highly desirable. To reduce the problem of the strong neutron absorption by the natural Sm isotope we performed the experiment at the ILL Grenoble D9 diffractometer with the hot source providing neutrons of a short wavelength ( $\lambda = 0.5 \text{ \AA}$ ). We will report on the temperature evolution of the magnetic reflections in comparison with bulk data. The  $(5/3 \ 5/3 \ 0)$  and  $(4/3 \ 1/3 \ 0)$  reflections emerged at 12.5 K which is in good agreement with bulk magnetic and specific-heat data. The maximum of the intensity was found at 4.3 K, where the second MPT occurs. Further lowering temperature leads to gradual suppression of these reflections and emerging new magnetic reflections, which reflect formation of another magnetic structure. This observation classifies the  $\text{SmPd}_2\text{Al}_3$  compound as a magnetically frustrated system. The complex magnetic behavior of this material is further illustrated by kinetic effects of the magnetization inducing rather complicated magnetic structure with various metastable states.

**O6-05**

**HEAVY QUASIPARTICLES IN Yb COMPOUNDS: THE  
RENORMALIZED BAND APPROACH**

Gertrud Zwicknagl

*Institut für Mathematische Physik, TU Braunschweig, Mendelssohnstr. 3, 38106  
Braunschweig, Germany*

Results for the dispersion of "heavy" 4f-derived quasiparticles in Yb-based compounds are presented. The bands are determined by means of the Renormalized Band method. The topology of the Fermi surface differs from the one predicted by standard band structure calculations based on Density Functional Theory. This is in marked contrast to the situation encountered in Ce-based Heavy Fermion Systems where standard band structure calculation usually provide reliable models for the Fermi surface. Calculations of the magnetic-field-induced changes of the heavy quasiparticles in  $\text{YbRh}_2\text{Si}_2$  are presented. The progressive de-renormalization of the quasiparticles in the magnetic field is accounted for using field-dependent quasiparticle parameters deduced from Numerical Renormalization Group studies. The results are related to recent measurements of thermodynamic and transport properties.

**FIRST PRINCIPLES CALCULATIONS OF XMCD SPECTRA OF ACTINIDE CUBIC LAVES PHASE COMPOUNDS**J. Ruzs<sup>1</sup>, P. M. Oppeneer<sup>1</sup>, F. Wilhelm<sup>2</sup>, E. Colineau<sup>3</sup>, R. Caciuffo<sup>3</sup>, G. Lander<sup>3</sup><sup>1</sup>*Department of Physics and Astronomy, Uppsala University, Sweden*<sup>2</sup>*European Synchrotron Radiation Facility, Grenoble, France*<sup>3</sup>*Joint Research Centre, ITU, Karlsruhe, Germany*

The actinide cubic Laves compounds  $\text{NpAl}_2$ ,  $\text{NpOs}_2$ ,  $\text{NpFe}_2$ , and  $\text{PuFe}_2$  have been examined by X-ray magnetic circular dichroism (XMCD) at the actinide  $M_{4,5}$  absorption edges [1]. We have performed electronic structure calculations of these compounds using the WIEN2k package. To deal with the strongly correlated nature of unfilled  $5f$ -electron shells, we have performed both local spin density approximation (LSDA) calculations as well as LSDA+ $U$  calculations using both the most common variants, namely the around mean-field (AMF) and fully localized limit (FLL) formulations. The x-ray absorption spectra (XAS) have been simulated by the initial state approximation in which the absorption strength at the  $M_{4,5}$  edges is a function of the projected density of states of unoccupied  $5f$  states of the actinide element. For every treated system we have performed several independent simulations - varying the strength of the onsite Coulomb repulsion characterized by the  $U$  parameter in the LSDA+ $U$  method. Typically we have calculated the spectra for  $U$  within the range from 0 to 4 eV. The value of  $J$  was set to 0.6 eV for both Np and Pu  $5f$  electrons. Comparing the theoretical and experimental XAS spectra, the first-principles calculations reproduce the experimental findings with a good qualitative accuracy with regard to the peak shapes, distance and branching ratio. Best agreement between theory and experiment is obtained for small values of  $U$ . The XMCD spectra reveal more details. Generally, the XMCD signal of  $\text{NpFe}_2$  on the  $M_5$  edge is very weak, compared to the XAS intensity. In the experimental spectra there is a sine-like oscillation, starting with negative values, switching the sign to a positive peak and monotonously decreasing to zero. The theoretical XMCD spectra at the  $M_5$  edge show an interesting, rather strong sensitivity on the chosen model of the description of the  $5f$  states. The sine-like signal is best reproduced by low  $U$  values. For  $\text{PuFe}_2$ , it is the FLL variant of LSDA+ $U$  that provides the most satisfactory agreement with experimental spectra. The AMF LSDA+ $U$  calculations lead to a far too weak XMCD signal at the  $M_5$  edge.

[1] F. Wilhelm, R. Eloiardi, J. Ruzs, R. Springell, E. Colineau, P. M. Oppeneer, R. Caciuffo, A. Rogalev, and G. H. Lander, submitted.

**MAGNETISM IN  $\text{RCO}_2$  UNDER AMBIENT AND HYDROSTATIC PRESSURE**

J. Prchal<sup>1</sup>, J. Valenta<sup>1</sup>, J. Šebesta<sup>1</sup>, M. Míšek<sup>1</sup>, D. Turčínková<sup>1</sup>, L. Lapčák<sup>1</sup>, J. Prokleška<sup>1</sup>, M. Kratochvílová<sup>1</sup>, and V. Sechovský<sup>1</sup>

<sup>1</sup>*Charles University in Prague, Department of Condensed Matter Physics, Ke Karlovu 5, 121 16 Prague, Czech Republic*

The  $\text{RCO}_2$  (R = Dy, Ho, Er, Tm) compounds crystallize in the cubic Laves phase structure. The rare-earth localized 4f-electron magnetic moments coexist together with the itinerant Co 3d moments, which appear on the verge of magnetism. Below  $T_C$ , the large exchange field due to the ferromagnetically ordered R moments polarizes the Co 3d-electron states and the emerged moments in the Co sublattice orient antiparallel to the R sublattice. Recent reports propose that weak Co moments survive rather far above  $T_C$  in Co magnetic clusters remaining coupled antiparallel to paramagnetic R moments forming a parimagnetic configuration in the paramagnetic phase [1,2]. The onset of this phenomenon causes an anomaly in the magnetic susceptibility at the “parimagnetic transition temperature”  $T_f$ .

The ordering temperature appears to be very sensitive to applied hydrostatic pressure. The same pressure coefficient has been found for  $T_f$  that indicates a common underlying mechanism of ferrimagnetism and parimagnetism.

We will present variations of the transition temperatures  $T_C$  and  $T_f$  in compounds with R = Dy, Ho, Er and Tm with applying hydrostatic pressures up to 3 GPa. The results will be discussed in term of suppressing the Co magnetic moments and varying the exchange and crystal-field interactions with applying the hydrostatic pressure.

[1] J. Herrero-Albillos et al., Phys.Rev.B **76** (2007) 094409.

[2] C.M. Bonila et al., J.Appl.Phys. **111** (2012) 07E315.

**INVESTIGATION OF CRYSTAL STRUCTURE, MAGNETIC AND TRANSPORT PROPERTIES IN CeCuAl<sub>3</sub> SINGLE CRYSTAL**

M. Klicpera<sup>1</sup>, P. Javorský<sup>1</sup>, P. Čermák<sup>1</sup>, A. Rudajevová<sup>1</sup>, S. Daniš<sup>1</sup>, T. Brunátová<sup>1</sup> and I. Cisařová<sup>2</sup>

<sup>1</sup>*Charles University in Prague, Faculty of Mathematics and Physics, Department of Condensed Matter Physics, Ke Karlovu 5, 121 16 Prague 2, Czech Republic.*

<sup>2</sup>*Department of Inorganic Chemistry, Faculty of Science, Charles University in Prague, Hlavova 8, 128 43 Prague 2, Czech Republic*

Cerium intermetallic compounds stay in the foreground of interest already many years and the research of them escalates in the last time. The various properties as heavy-fermion behavior, unconventional superconductivity, valence fluctuations and complex magnetic order at low temperatures are the main reasons why to study these compounds. Ce atom has only one 4f-electron which is very weakly shielded by 5d- and 6s-levels. The small energy differences between electronic levels make the 4f-electron unstable what results in various unique physical properties. The competition between RKKY interaction and Kondo interaction, screening of localized 4f-moments by conduction electrons and effect of crystal field are crucial for magnetic behavior of these compounds.

Very suitable group of compounds for study of above phenomena is the CeTX<sub>3</sub> family crystallizing in tetragonal BaNiSn<sub>3</sub>-type structure, where *T* means transition d-metal and *X* p-metal. In our presentation we focus on structural, magnetic and transport properties of CeCuAl<sub>3</sub> single crystal. This compound is of particular interest as it was recently found to be one of few compounds in which the strong electron-phonon coupling is present and results in the formation of a new quantum state, called vibron quasi-bound state. CeCuAl<sub>3</sub> orders antiferromagnetically below 2.5 K. Its magnetic behavior is generally discussed as a result of interplay between the magnetic RKKY, Kondo interactions and influence of crystal field. It is also often labeled as a heavy-fermion system. Despite the fact that numerous studies of magnetic and transport properties of CeCuAl<sub>3</sub> were performed, there are still many contradictory statements about magnetization easy-axis, details of the magnetic order at low temperatures and even the crystal structure type in which this compound crystallizes. We present the thorough study of crystal structure as well as the consistent information about the low temperature magnetic properties of CeCuAl<sub>3</sub> single crystal.

**AMORPHOUS 5f FERROMAGNETIC HYDRIDES  $\text{UH}_3\text{Mo}_x$** 

I. Tkach<sup>1</sup>, N.T.H. Kim-Ngan<sup>2</sup>, S. Mašková<sup>1</sup>, A.V. Andreev<sup>3</sup>, Z. Matěj<sup>1</sup>,  
L. Havela<sup>1</sup>

<sup>1</sup>*Faculty of Mathematics and Physics, Charles University, Ke Karlovu 5, 12116, Prague, Czech Republic*

<sup>2</sup>*Institute of Physics, Pedagogical University, Podchorazych 2, 30-084 Krakow, Poland*

<sup>3</sup>*Institute of Physics, ASCR, Na Slovance 2, 18221, Prague, Czech Republic*

Samples of uranium metal with cubic structure ( $\gamma$ -phase) were stabilized to room temperature by splat cooling technique and with addition of Mo. Such  $\gamma$ -U materials have to be hydrogenated at elevated  $\text{H}_2$  pressures. The product is hydrides with hydrogen concentration 3 H/U atom. Unlike standard  $\beta$ - $\text{UH}_3$ , our samples turn amorphous. A large surprise is the lack of fragmentation: the material remains compact.

The amorphous hydride  $\text{UH}_3\text{Mo}_{0.18}$  exhibits ferromagnetic order with Curie temperature around 195 K and magnetisation  $1.2 \mu_B/\text{U}$  in magnetic field 14 T (compare with 175 K and  $0.93 \mu_B/\text{U}$ , respectively, for crystalline  $\beta$ - $\text{UH}_3$ ). A broad hysteresis appears on magnetization curves at low temperature, the coercive force reaching enormous 3.5 T at  $T = 1.7$  K. The magnetisation reversal is characterised by a sharp jump at temperatures below 5 K, which can be associated with HARD (high anisotropy random distribution) phenomenon.

The shift of  $T_C$  to  $\approx 200$  K is for  $\text{UH}_3\text{Mo}_{0.18}$  revealed also by specific heat. A linear fit of  $C_p/T$  vs.  $T^2$  at low temperatures yields the Sommerfeld coefficient  $\gamma_e = 27.6 \text{ mJ/mol K}^2$ , which is approximately 3 times higher than for  $\alpha$ -U and 2 times higher than for  $\gamma$ -U (initial splat sample  $\text{U}_{0.85}\text{Mo}_{0.15}$ ). The increase of  $\gamma_e$  indicates increasing  $N(E_F)$  and narrowing of the 5f band.

The temperature dependence of electrical resistivity of  $\text{UH}_3\text{Mo}_{0.18}$  exhibits a negative slope ( $d\rho/dT < 0$ ) similar to  $\gamma$ -phase U-Mo alloys. A small cusp observed at 200 K is related to  $T_C$ . The absolute values of resistivity for  $\text{UH}_3\text{Mo}_{0.18}$  are unusually high, exceeding  $1000 \mu\Omega\text{cm}$ .

We can conclude that we described a novel type of material: 5f amorphous ferromagnet with high  $T_C$ . The dependence on Mo concentration is currently investigated and will be presented.

## P6-03

### REENTRANT METAL-INSULATOR TRANSITION IN $\text{Ca}_{1-x}\text{Eu}_x\text{B}_6$

V. Glushkov<sup>1,2</sup>, M. Anisimov<sup>1</sup>, R. Baybakov<sup>3</sup>, S. Demishev<sup>1,2</sup>, V. Filipov<sup>4</sup>, K. Flachbart<sup>5</sup>, A. Kuznetsov<sup>3</sup>, N. Shitsevalova<sup>4</sup> and N. Sluchanko<sup>1</sup>

<sup>1</sup>*Prokhorov General Physics Institute of RAS, 38, Vavilov str., Moscow 119991 Russia*

<sup>2</sup>*Moscow Institute of Physics and Technology, 9, Institutskii per., Dolgoprudny, Moscow Region 141700 Russia*

<sup>3</sup>*National Research Nuclear University "MEPhI", 31, Kashirskoe Shosse, Moscow 115409 Russia*

<sup>4</sup>*Frantsevich Institute for Problems of Materials Science NAS, 3, Krzhizhanovskiy str., Kiev 03680 Ukraine*

<sup>5</sup>*Institute of Experimental Physics, Slovak Academy of Sciences, Watsonova 47, 040 01 Košice, Slovak Republic*

The nature of concentration driven metal-insulator transition (MIT) in the ferromagnetic phase of  $\text{Ca}_{1-x}\text{Eu}_x\text{B}_6$  [1] is still under debates. Magneto-optical studies reveal zeroing of field induced spectral weight below  $x \sim 0.5$  [2], while optical experiments favor the suppression of free carrier contribution for  $x < 0.65$  [3]. Recent study of charge transport proves the onset of dielectric ground state in  $\text{Ca}_{1-x}\text{Eu}_x\text{B}_6$  below  $x_{\text{MIT}} \approx 0.8$  [4]. However, the crossover from electron ( $x > x_{\text{MIT}}$ ) to hole ( $x < x_{\text{MIT}}$ ) conductivity accompanied by the increase of magnetoresistance to  $\rho(0)/\rho(7 \text{ T}) \sim 7 \cdot 10^5$  ( $x = 0.756$ ) [4] assumes a qualitative transformation of band structure, which is not treated in the original model [1].

Here we report a study of resistivity, Hall and Seebeck effects measured on  $\text{Ca}_{1-x}\text{Eu}_x\text{B}_6$  ( $0 \leq x \leq 1$ ) single crystals in magnetic fields up to 8 T. The maximum of  $\rho(0)/\rho(7 \text{ T}) = 1.3 \cdot 10^6$  is shown to be observed for  $x = 0.63$  compound below 10 K, while hole conductivity could be identified only in the narrow range of  $0.7 \leq x \leq 0.8$ . Rising of Ca content for  $x < 0.6$  restores the metallic ground state characterized by moderate values of  $\rho(0) \sim 1 \div 5 \text{ m}\Omega\cdot\text{cm}$  and  $\rho(0)/\rho(7 \text{ T}) < 7$ . A correlation between the enhancement of magnetoresistance, positive sign of diffusion thermopower and large anomalous Hall effect established for  $0.6 \leq x \leq 0.85$  allows to define the smooth change of band structure as a main factor governing this reentrant MIT in  $\text{Ca}_{1-x}\text{Eu}_x\text{B}_6$ .

[1] V.M. Pereira et al., Phys. Rev. Lett., 93, 147202 (2004).

[2] G. Caimi et al., Phys. Rev. Lett. 96, 016403 (2006).

[3] J. Kim et al., J. Phys.: Condens. Matter, 19, 106203 (2007).

[4] V.V. Glushkov et al., Phys. Stat. Sol. B, 247, 650 (2010).



# MAGNETIC PROPERTIES OF $\text{La}_{(1-x)}\text{Ag}_x\text{MnO}_3$ NANOPOWDERS UNDER PRESSURE

M.Antoňák<sup>1</sup>, M.Mihalik<sup>1</sup>, M.Zentková<sup>1</sup>, M.Mihalik<sup>1,j,r</sup>, M.Vavra<sup>1,2</sup>, J.Lazurova<sup>1</sup>, M. Fitta<sup>3</sup>, M. Balanda<sup>3</sup>

<sup>1</sup>*Institute of Experimental Physics, SAS, Watsonova 47, 040 01 Košice, Slovakia*

<sup>2</sup>*P. J. Šafárik University, Moyzesova 11, 041 54 Košice, Slovakia*

<sup>3</sup>*Institute of Nuclear Physic, PAS, Radzikowskiego 152, 31-342 Kraków, Poland*

Most of the studies of hole-doped  $\text{R}_{1-x}\text{A}_x\text{MnO}_3$  manganites have been performed on systems where rare earth ion R was partially substituted by a divalent alkaline-earth-metal A. In contrast, monovalent metal doped systems exhibit similar and very interesting properties but are less-studied. Therefore, the study of monovalent metal doping would offer a complementary understanding on the structural and magnetic properties of these systems.

In our paper we present study of pressure effect on magnetic properties of  $\text{La}_{(1-x)}\text{Ag}_x\text{MnO}_3$  nanopowders ( $x = 0.10, 0.15, 0.20$ ), which were prepared by glycine – nitrate method. Hydrostatic pressure was generated in the CuBe pressure cell up to 0.9 GPa. Magnetization measurements were performed by SQUID magnetometer (MPMS) in the temperature range 1.8 K – 350 K. The particle size was modified by heat treatment and increases with heat treatment. As prepared and annealed samples at  $T = 300^\circ\text{C}$  crystallize in orthorhombic crystal structure (space group  $Pnma$ ). The average size of nanoparticles for both series of samples is about 25 nm. Samples annealed at  $T = 600^\circ\text{C}$  adopt rhombohedral structure (space group  $R\bar{3}c$ ) and average size of nanoparticles is about 55 nm.

The exchange bias phenomenon was observed on samples with particle size smaller than 30 nm. We have studied pressure effect on the Curie temperature  $T_C$ , saturated magnetization  $\mu_s$  and exchange bias field  $H_E$  on a set of powders with different chemical composition and particle size. We have found that  $T_C$ ,  $\mu_s$  and  $H_c$  increase with pressure markedly and  $H_E$  is affected by pressure only slightly. Effects of pressure and effect of cooling in magnetic field  $H_{cf}$  on exchange bias phenomenon will be discussed.

**FIRST-PRINCIPLES STUDY OF KONDO INSULATOR  $\text{SmB}_6$** M. Gmitra<sup>1,2</sup>, H. Cencarikova<sup>2</sup> and P. Farkasovsky<sup>2</sup><sup>1</sup>*Institute for Theoretical Physics, University of Regensburg, Universitaetsstrasse 31, 93040 Regensburg, Germany*<sup>2</sup>*Institute of Experimental Physics, Slovak Academy of Sciences, Watsonova 47, 040 01 Kosice, Slovakia*

Kondo insulators are highly correlated electron systems with a narrow hybridization gap that manifests in steeply increase in electrical resistivity at low temperatures. Transport, thermal and optical properties of the hybridization gap in exemplary Kondo insulator,  $\text{SmB}_6$  has been studied for several decades. Periodic arrangement of the spins in  $\text{SmB}_6$  creates Kondo lattice, where hybridization between localized  $f$  electrons and conduction bands leads to the characteristic energy gap opening in density of states. However, this signature in the electronic structure has not yet been unambiguously observed in  $\text{SmB}_6$ .

In this contribution we present first-principles calculations of  $\text{SmB}_6$  electronic properties using on-site hybrid functional PBE0 as implemented in Wien2k code [1]. We found that PBE0 separates the localized  $\text{Sm } f$  states of about 7 eV in agreement with standard optical experiments [2]. The unoccupied  $f_{7/2}$  states hybridize with the  $d$  states in the range of 2 eV. The occupied  $f$  states form two narrow peaks in density of states just below the Fermi level. They are split due to spin-orbit coupling of about 1 eV as observed in recent ARPES measurement [3]. The peak in vicinity of the Fermi level is dominated by the  $f_{5/2}$  states, while the other peak is formed with both the  $f_{5/2}$  and  $f_{7/2}$  relativistic states. We also found that GGA+U can not reproduce the spin-orbit splitting and narrow localization of the occupied  $f$  states.

*This work was supported by the ERDF EU (European Union European regional development fond) under the contract No. ITMS 26110230061.*

[1] K. Schwarz and P. Blaha, *Comput. Mater. Sci.* **28**, 259 (2003).

[2] J. M. Tarascon et al., *J. Physique* **41**, 1141 (1980).

[3] H. Miyazaki et al., *Phys. Rev. B* **86**, 075105 (2012).

**MAGNETIC PROPERTIES OF  $\text{Ce}(\text{Cu}_x\text{Ni}_{1-x})_4\text{Mn}$  COMPOUNDS**

K. Synoradzki and T. Toliński

*Institute of Molecular Physics, Polish Academy of Sciences, Smoluchowskiego 17, 60-179 Poznań, Poland*

The effect of the Cu substitution on magnetic properties of  $\text{CeNi}_4\text{Mn}$  has been investigated. The intermetallic compounds  $\text{Ce}(\text{Cu}_x\text{Ni}_{1-x})_4\text{Mn}$  were prepared from the pure elements in argon atmosphere in a water-cooled sample chamber of an induction furnace. X-ray diffraction of polycrystalline samples confirmed that all the prepared compounds crystallize in the hexagonal  $\text{CaCu}_5$ -type structure (space group  $P6/mmm$ ). The lattice parameters of  $\text{Ce}(\text{Cu}_x\text{Ni}_{1-x})_4\text{Mn}$  obey the Vegard's law.

We have previously shown for a single Cu substitution ( $x = 0.25$ ) that a spin-glass behaviour develops, whereas the parent compound  $\text{CeNi}_4\text{Mn}$  is a ferromagnet with  $T_C = 130$  K. In the present studies a wide range of  $x$  values is studied. The magnetic properties are determined from the temperature dependence of the dc and ac magnetization. A large irreversibility is observed between the zero-field cooled (ZFC) and field-cooled (FC) curves with a cusp in the ZFC one. An increase in the magnetic field strength tends to smoothen the dc magnetic susceptibility anomaly and reduces the magnitude of the susceptibility. The ac magnetic susceptibility also shows a cusp, which shifts to higher temperatures with increasing frequencies, which is typically observed in spin-glass systems. The observation of the spin-glass behaviour is further supported by a very slow decay of the isothermal remanent magnetization. The easiness of the spin-glass state formation by small substitutions in  $\text{CeNi}_4\text{Mn}$  is helpful in better understanding of the peculiar, resembling half-metallic behaviour, ferromagnetism of  $\text{CeNi}_4\text{Mn}$ .

**TRANSITION METALS DOPING OF  $\text{LaFe}_2\text{Si}_2$** 

M. Diviš

*Department of Condensed Matter Physics, Charles University of Prague, Faculty of Mathematics and Physics, Ke Karlovu 5, 121 16 Prague 2, Czech Republic*

The intermetallic  $\text{LaFe}_2\text{Si}_2$  compound is a Pauli paramagnet as was confirmed by Mössbauer measurements and first principles density functional theory (DFT) fixed spin moment calculations [1]. In this work we have studied the influence of transition metals ( $T = \text{Cr, Mo, Tc, W, Re}$ ) doping into the iron position on the magnetism of ground state electronic structure of  $\text{La}(\text{Fe}_{1-x}\text{T}_x)_2\text{Si}_2$ . The coherent potential approximation (CPA) in the framework of DFT was used to treat the positional disorder in the iron lattice site. The dopings were from one to five percent of transition metal atom  $T$ . The ferromagnetic ground state was found upon Cr substitution and the Cr and Fe atoms have nonzero local magnetic moment. On the other hand the paramagnetic ground state with (Mo, Tc, W and Re) zero local moments were found.

[1] I. Turek, M. Diviš, D. Nižňanský, J. Vejpravová, JMMM 316 (2007) e403.

**MAGNETIC PROPERTIES OF RE<sub>2</sub>Pd<sub>2</sub>In COMPOUNDS AND THEIR HYDRIDES**

S. Mašková<sup>1</sup>, A. Kolomiets<sup>1,2</sup>, A.V. Andreev<sup>3</sup>, P. Svoboda<sup>1</sup> and L. Havela<sup>1</sup>

<sup>1</sup>*Department of Condensed Matter Physics, Charles University, Ke Karlovu 5, 12116 Prague 2, the Czech Republic*

<sup>2</sup>*Department of Physics, Lviv Polytechnic National University, Lviv, Ukraine*

<sup>3</sup>*Institute of Physics, AVCR, Na Slovance 2, 18221 Prague 8, the Czech Republic*

We compare the impact of hydrogen absorption on RE<sub>2</sub>Pd<sub>2</sub>In compounds. The amorphization of the structure due to the high H absorption (> 4 H/f.u.) is found for RE<sub>2</sub>Pd<sub>2</sub>In with light RE (La, Nd). RE<sub>2</sub>Pd<sub>2</sub>In with heavy RE behave similar way as was found for isostructural U<sub>2</sub>T<sub>2</sub>X compounds (2 H/f.u., crystal structure type not changed). For the RE<sub>2</sub>Pd<sub>2</sub>In compounds, the lattice parameters *a* and *c* decrease linearly with increasing atomic number of RE. Upon hydrogenation the crystal structure is expanded. The lattice parameter *a* for the hydrides is also linearly decreasing with increasing atomic number but the slope is much higher. For first part of RE (La-Gd) the hydrogen absorption leads to expansion along the *a*-axis while for the others the *a* parameter is contracted. On the other hand the lattice is expanding along the *c*-axis in all studied RE<sub>2</sub>Pd<sub>2</sub>In compounds in such way, that it compensates the lattice contraction along *a*-axis leading to volume expansion in all cases. Magnetic properties of RE<sub>2</sub>Pd<sub>2</sub>In series are interestingly complicated. RE atoms form a triangular motif within the tetragonal crystal structure bringing magnetic frustration into the system. The crystal structure resembles 2D Shastry-Sutherland lattice [1]. We have found from measurements on single crystals of selected compounds that magnetic properties of these compounds are highly anisotropic, showing several metamagnetic transitions in different crystallographic directions. The magnetic ordering temperatures of all RE-compounds studied are dramatically reduced by hydrogenation. Such general dramatic weakening of the RKKY exchange interaction should have a strong reason – most likely the impact of hydrogen bonding on the system of conduction electrons. Few percent volume expansion cannot have such a dramatic consequence. As H typically behaves as acceptor in a compound with strongly electropositive elements, it induces a drain of electrons from RE into the H-1s states, affecting the situation around the Fermi level.

[1] B. Shastry and B. Sutherland, *Physica B+C* 108 (1981) 1069.

**PREPARATION AND CHARACTERIZATION OF BASIC AND Nd<sup>3+</sup>/Er<sup>3+</sup> DOPED GLASSES IN THE SYSTEM Y<sub>2</sub>O<sub>3</sub>–Al<sub>2</sub>O<sub>3</sub>–ZrO<sub>2</sub>**R. Klement<sup>1</sup>, B. Hruška<sup>1</sup>, V. Hronský<sup>2</sup>, D. Olčák<sup>2</sup><sup>1</sup> *Vitrum Laugaricio – Joint Glass Centre of the IIC SAS, TnU AD, FChPT STU and RONA, a.s., Študentská 2, SK-911 50 Trenčín, Slovak Republic*<sup>2</sup> *Department of Physics, Faculty of Electrical Engineering and Informatics, The Technical University of Košice, Park Komenského 2, SK-042 00 Košice, Slovak Republic*

Rare earth (RE) aluminate glasses have been of great interest due to their high elastic modulus and hardness, high refraction index, excellent optical properties, and good corrosion resistance. Moreover, RE aluminate glasses are known for their ability to accommodate high concentration of rare earth photoluminescence active ions (e.g. Nd<sup>3+</sup>, Er<sup>3+</sup>, etc.), and low phonon energy due to the aluminate network. These properties predetermine such glasses as potential candidates for various applications e.g. in solid state lasers, optical waveguides and optical amplifier hosts.

In the present work we report on the preparation and characterization of the yttrium aluminozirconate (YAZ) glasses and their Nd- and Er- doped analogues. The undoped, and Nd-, Er-doped low zirconia high alumina yttrium aluminozirconate (YAZ) glasses were prepared from sol-gel derived precursors (Pechini method) by flame synthesis in the form of transparent glass microbeads. The ZrO<sub>2</sub> content was maintained in the range of 5-20 mol. %. The prepared glass microbeads were characterized by optical microscopy, SEM, XRD, DSC, FT-IR/Raman spectroscopy, <sup>27</sup>Al MAS NMR, UV-VIS-NIR and fluorescence spectroscopy. The thermal stability of non-doped YAZ glasses is surprisingly not significantly affected by ZrO<sub>2</sub> content. On the other hand, second crystallization peak exhibits compositional dependence. To solve this finding from DSC measurements, high temperature XRD experiment was used to study the phase evolution during crystallization process. The <sup>27</sup>Al MAS NMR spectra of glass samples studied reveal that Al atoms are predominantly 4-coordinated; relative abundance of Al-species was calculated from the spectra. The doping of YAZ5 and YAZ10 glasses with Nd<sup>3+</sup>/Er<sup>3+</sup> at the level of 1-5 mol. % leads to decrease of thermal stability of glasses. The UV-VIS-NIR/fluorescence spectra show characteristic absorptions/emissions, due to the optically active Nd<sup>3+</sup> and Er<sup>3+</sup> ions in the host glass. The absorption/emission properties of guest ions are not significantly affected by the glass host. At higher concentrations of Nd<sup>3+</sup>/Er<sup>3+</sup> ions in glasses, the concentration quenching was observed.

**MAGNETOSTRUCTURAL CORRELATIONS OF NANO-SIZED MANGANITES PREPARED BY DIFFERENT WAYS**

M. Vavra<sup>1,2</sup>, Marián Mihalík<sup>1</sup>, Matúš Mihalík<sup>1</sup>, M. Zentková<sup>1</sup>, J. Lazurová<sup>1</sup>, M. Matík<sup>3</sup>, J. Briančin<sup>3</sup>

<sup>1</sup>*Institute of Experimental Physics SAS, Watsonova 47, 040 01 Košice, Slovak Republic*

<sup>2</sup>*Faculty of Science, P.J. Šafárik University, Moyzesova 11, 041 54 Košice, Slovak Republic*

<sup>3</sup>*Institute of Geotechnics SAS, Watsonova 45, 040 01 Košice, Slovak Republic*

Complicated binary oxides based on the manganese, called manganites, are frequently studied for their interesting magnetic properties in nano-sized dimensions. Reducing the size of material particles down to nanosize range can cause not only remarkable changes in physical properties but also the emergence of the qualitatively new one. From the magnetic point of view, this refers to superparamagnetism, change in transition temperatures and formation of new magnetic phases, size dependence of saturation magnetization and coercivity.

The simplest ways of its preparation are sol-gel method and the precipitation of metal hydroxides from a solution. These hydroxides become after exsiccation and heating oxides. Another procedure of binary oxides preparation in a wet way is nitrate-glycine synthesis, where individual metal nitrates are in solution mixed with organic fuel (glycine) and after dehydration on a hot plate a solution becomes a viscous gel which underwent an autoignition after some time followed by a short combustion. Slightly different procedure is self-combustion high temperature synthesis, where instead of organic fuel, a redox mixture containing glucose and potassium nitrate is dissolved in solution together with metal nitrates. Final solution is evaporated until a formation of a brown caramel mass, which is formed in a cylindrical shape and ignited.

Obtained as-prepared and annealed samples prepared by different ways have been characterized using X-ray powder diffraction, SEM and TEM. Magnetization and AC susceptibility measurements have been performed by commercial SQUID magnetometer (MPMS) and VSM magnetometer (PPMS). In our paper we present study of magneto-structural correlation in nano-sized manganites prepared by several techniques. We have focus on the study of sample preparation, size of particles and crystal structure on magnetic properties of prepared materials.

# MAGNETIC PROPERTIES OF HoCo<sub>12</sub>B<sub>6</sub> COMPOUND UNDER HIGH PRESSURES

Z. Arnold<sup>1</sup>, L. V. B. Diop<sup>2</sup>, O. Isnard<sup>2</sup>, J. Kamarád<sup>1</sup>

<sup>1</sup>*Institute of Physics AS CR v.v.i., Na Slovance 2, 18221, Prague 8, Czech Rep.*

<sup>2</sup>*Institut Néel, CNRS/Univ. J. Fourier, BP166, 38042 Grenoble cedex, France*

The RCo<sub>12</sub>B<sub>6</sub> borides (R- rare earth) crystallize in the rhombohedral structure of the SrNi<sub>12</sub>B<sub>6</sub> type (space group R-3m). Their low Curie temperatures and low Co magnetic moment ( $T_C = 150$  K and  $m_{Co} = 0.45 \mu_B/\text{Co atom}$  for YCo<sub>12</sub>B<sub>6</sub>) are attributed to hybridization of B(p) and Co(d) electrons bands as a consequence of small interatomic distances between Co and B atoms (2.05 Å). HoCo<sub>12</sub>B<sub>6</sub> compound with antiparallel coupling of the magnetic moments of Ho and Co sublattices is characterized by the magnetic ordering temperature ( $T_C = 146$  K), spin reorientation temperature ( $T_{SR} = 79$  K) and compensation temperature ( $T_{COMP} = 50$  K). To get information about the nature of Co magnetism and the role of the Ho sublattice on the character of magnetism and exchange interactions we have studied effects of hydrostatic pressure up to 10 kbar on magnetic properties of polycrystalline HoCo<sub>12</sub>B<sub>6</sub> compound in temperature range 5 – 200 K using a SQUID magnetometer with magnetic field up to 7T and miniature Cu-Be pressure cell.

Both the  $T_C$  and  $T_{SR}$  decreases linearly with pressure with moderate slopes ( $dT_C/dp = -0.34 \pm 0.04$  K.kbar<sup>-1</sup>,  $dT_{SR}/dp = -0.42 \pm 0.04$  K.kbar<sup>-1</sup>). The spontaneous magnetization  $M_S$  at 5 K and  $T_{COMP}$  are pressure insensitive within the experimental error. The situation is more complex at higher temperatures where the pressure slope of  $M$  is becoming negative, reaching the value of  $d \ln M_S/dp = -0.0041$  kbar<sup>-1</sup> at 130 K. The pressure effect on  $T_C$  and  $M_S$  can be attributed mostly to the volume dependence of both the Co magnetic moment and the exchange interactions. The results obtained on HoCo<sub>12</sub>B<sub>6</sub> compound confirmed the remarkably higher volume stability of its magnetic properties than the RCo<sub>4</sub>B compounds (R - Y, Gd), where more than two times higher values of  $dT_C/dp$  and  $d \ln M_S/dp$  were observed. The relative volume stability of magnetic properties, namely the spontaneous magnetization of compound with the itinerant character of magnetism can be attributed to the remarkable role of the hybridization of B(p) and Co(d) electronic states and to the crucial role of exchange interaction. Similarly the volume stability of the highly reduced Co magnetic moment was recently observed for tetravalent Th state in ThCo<sub>4</sub>B compound.



# SHORT RANGE ORDER EFFECTS IN MAGNETORESISTANCE OF $\text{Ho}_x\text{Lu}_{1-x}\text{B}_{12}$ ( $x \leq 0.5$ )

A. Khoroshilov<sup>1,2</sup>, N. Sluchanko<sup>1</sup>, A. Azarevich<sup>1,2</sup>, A. Bogach<sup>1</sup>, V. Glushkov<sup>1,2</sup>, S. Demishev<sup>1,2</sup>, N. Shitsevalova<sup>3</sup>, V. Filipov<sup>3</sup>, S. Gabani<sup>4</sup>, K. Flachbart<sup>4</sup>

<sup>1</sup>*A.M. Prokhorov General Physics Institute of RAS, 119991 Moscow, Russia*

<sup>2</sup>*Moscow Institute of Physics and Technology, Moscow Region 141700 Russia*

<sup>3</sup>*Institute for Problems of Materials Science, NASU, 03680 Kiev, Ukraine*

<sup>4</sup>*Institute of Experimental Physics of SAS, 040 01 Košice, Slovak Republic*

It was discovered recently [1] that the loosely bounded state of the rare earth ion in combination with 1-3% of boron vacancies in lutetium dodecaboride ( $\text{LuB}_{12}$ ) causes an unusual cage-glass state in the crystal at temperatures below  $T^* \sim 50\text{-}70\text{ K}$ . It was proposed that at  $T < T^*$  the centrosymmetric position of  $\text{Lu}^{3+}$  ions embedded in  $\text{B}_{24}$  truncated cubooctahedrons is mostly destroyed and leads to an emergence of strong structural disorder of  $\text{Lu}^{3+}$  ions in the  $\text{LuB}_{12}$  matrix.

In this study we report results of transverse magnetoresistance  $\Delta\rho/\rho(T, H)$  measurements that were carried out on high quality single crystals of  $\text{Ho}_x\text{Lu}_{1-x}\text{B}_{12}$  where  $\text{Ho}^{3+}$  magnetic impurity ions are randomly arranged in the cage glass state. Data obtained at temperatures 1.9-120 K and in magnetic field up to 80 kOe both for the dilute magnetic impurity limit ( $x=0.01$  and 0.1) and for concentrated  $\text{Ho}_x\text{Lu}_{1-x}\text{B}_{12}$  solid solutions ( $x=0.3$  and 0.5) allowed to separate and to classify various contributions to magnetoresistance, and provide a description of charge transport regimes in this model system with randomly distributed magnetic impurities. Revealed was a crossover from a rather complicated large positive magnetoresistance ( $\Delta\rho/\rho_+$ ) observed for all Ho contents at intermediate temperatures to a negative quadratic ( $-\Delta\rho/\rho_- \propto H^2$ ) dependence which dominates in the paramagnetic state at liquid helium temperatures and in small magnetic field  $H < 30\text{ kOe}$ . A tendency to saturation of the negative magnetoresistance ( $\Delta\rho/\rho_-$ ) was observed for  $H \geq 50\text{ kOe}$ , and the negative term can be described quantitatively by relation  $(\Delta\rho/\rho_-) \sim L^2(H/T)$  ( $L(H/T)$  - Langevin function). The applied fitting allowed us to deduce values of effective magnetic moments  $2.9\text{-}8.7\mu_B$  which are small in comparison with  $\mu_{\text{eff}}(\text{Ho}^{3+})=10.7\mu_B$ . The received results are interpreted in terms of short range order effects - formation of  $\text{R}^{3+}$  dimers and trimers with antiferromagnetic exchange in the  $\text{Ho}_x\text{Lu}_{1-x}\text{B}_{12}$  matrix. In the antiferromagnetic state achieved for  $x=0.5$  ( $T_N \approx 3.4\text{ K}$ ) a large positive magnetoresistance was observed and analyzed in detail. It enabled to construct the  $H$ - $T$  magnetic phase diagram of  $\text{Ho}_{0.5}\text{Lu}_{0.5}\text{B}_{12}$ .

[1] N. E. Sluchanko, A. N. Azarevich, A. V. Bogach, et al., JETP **113**, 468 (2011)

# EXCITONIC SPECTRUM OF THE CRYSTAL $\text{KY}_{0.3}\text{Er}_{0.7}(\text{MoO}_4)_2$ IN VISIBLE RANGE

S. Poperezhai, N. Bondar and V. Kuřko

*B.I. Verkin Institute for Low Temperature Physics and Engineering of the NAS of Ukraine 61103, Lenin ave. 47, Kharkov, Ukraine*

Crystal  $\text{KY}_{0.3}\text{Er}_{0.7}(\text{MoO}_4)_2$  belongs to a series of rare-earth compounds in which phase transitions occur at low-temperatures due to the cooperative Jahn-Teller effect. These compounds are interested as low dimensional magnetic structure magnetic materials.

Crystal  $\text{KY}_{0.3}\text{Er}_{0.7}(\text{MoO}_4)_2$  is a rhombic system with four formula units in a unit cell. It has a layered structure which is formed by the layers  $\text{K}_{\infty}^{+}$  and layer packets  $[\text{Y}_{0.3}\text{Er}_{0.7}(\text{MoO}_4)_2]_{\infty}^{-}$  alternate in the compound along the direction b. We believe that the low-frequency acoustic spectrum of the crystal is formed by the shear vibrations of the layer packets  $[\text{Y}_{0.3}\text{Er}_{0.7}(\text{MoO}_4)_2]_{\infty}^{-}$  as whole along different crystallographic directions. Assumption has allowed us to use a one-dimensional model for calculating the dispersion of the acoustic vibration branches in the Brillouin zone. Excitonic absorption bands can have sidebands caused by simultaneous excitations of low-energy excitons and phonons and high frequency excitations in the visible range. The goal of this study was to investigate the structure of low energy electronic and vibrational excitations of the crystal  $\text{KY}_{0.3}\text{Er}_{0.7}(\text{MoO}_4)_2$  using excitonic transmission spectra in the visible range. For this purpose the transmission spectra of the crystal  $\text{KEr}_{0.7}\text{Y}_{0.3}(\text{MoO}_4)_2$  have been measured at the temperatures 6K and 150K. At the temperature 150K the spectrum contains absorption bands having the energies  $12550 \text{ cm}^{-1}$ ,  $12568 \text{ cm}^{-1}$ ,  $12578 \text{ cm}^{-1}$  and  $12587 \text{ cm}^{-1}$ . As the temperature decreases to 6K the additional band with the frequency  $12562 \text{ cm}^{-1}$  appears in the absorption spectrum. This is a sideband for the band with frequency  $12550 \text{ cm}^{-1}$ . A comparison of the distance between the main and the side bands and the frequency of the acoustic phonon at the Brillouin zone boundary shows their good agreement. This implies that some excitations are observed in the optic spectrum, which is caused by the excitation of the exciton-acoustic phonon pair at the Brillouin zone boundary. This band is unobservable at high temperature because the band broadens significantly due to the appreciable temperature-induced occupation excitations of the low frequency vibrational branch. Thus we can conclude that it is possible to find the limiting frequencies of low-energy vibrational spectra at the Brillouin zone boundary of double alkali rare-earth molybdates using the visible-range spectra of these materials.

**SPECIFIC HEAT ANALYSIS AND MAGNETIC ENTROPY OF  $\text{U}_2\text{Ni}_2\text{Sn}$** P. Svoboda<sup>1</sup>, S. Mašková<sup>1</sup>, A.V. Andreev<sup>2</sup> and L.Havela<sup>1</sup><sup>1</sup>*Department of Condensed Matter Physics, Charles University, Faculty of Mathematics and Physics, Ke Karlovu 5, 121 16 Prague 2, The Czech Republic*<sup>2</sup>*Institute of Physics, ASCR, Na Slovance 2, 182 21 Prague 8, The Czech Republic*

$\text{U}_2\text{Ni}_2\text{Sn}$  crystallizes in the tetragonal structure and orders antiferromagnetically below  $T_N = 26$  K [1]. Here we present the analysis of the low-temperature specific heat data obtained on  $\text{U}_2\text{Ni}_2\text{Sn}$  single crystal in zero magnetic field. The data have been analyzed in terms of an additive contribution of electronic, phonon and magnetic heat capacities to the total heat capacity and to the total entropy of this system.

Phonon specific heat analysis is based on separate Debye-model analysis of acoustic phonon branches, optical branches are analyzed within the Einstein model, each model grouping several branches. Electronic specific heat is based on Sommerfeld model, strong enhancement of the Sommerfeld coefficient has been observed in the very low temperatures region.

The magnetic part of specific heat was obtained by subtraction of electronic and phonon model curves from the total specific heat. Calculated magnetic entropy well corresponds to  $R\ln 2$ , i.e. to the entropy of the doublet just above the Néel temperature.

[1] e.g. V. Sechovsky, L. Havela, in E.P. Wohlfarth, K.H.J. Buschow (Eds.), *Ferromagnetic Materials*, Vol. 4, North-Holland, Amsterdam (1988), p. 309

**EFFECT OF Mn FOR Fe SUBSTITUTION ON MAGNETIC PROPERTIES OF NdFe<sub>x-1</sub>Mn<sub>x</sub>O<sub>3</sub> SINGLE CRYSTALS**

J. Lazúrová<sup>1</sup>, M. Mihalik<sup>1</sup>, M. Zentková<sup>1</sup>, M. Mihalik jr.<sup>1</sup>, J. Briančin<sup>2</sup>, M. Fitta<sup>3</sup>

<sup>1</sup>*Institute of Experimental Physics SAS, Watsonova 47, Košice, Slovak Republic*

<sup>2</sup>*Institute of Geotechnics SAS, Watsonova 45, Košice, Slovak Republic*

<sup>3</sup>*Institute of Nuclear Physics, PAN, Radzikowskiego 152, Kraków, Poland*

Magnetic properties of NdFeO<sub>3</sub> are mostly determined by three magnetic interactions (Fe-Fe, Fe-Nd and Nd-Nd), which are present in this material. Magnetic ordering of Fe<sup>3+</sup> ions creates a canted antiferromagnet below the Néel temperature at about 690 K [1]. Upon cooling the magnetic moments of Fe<sup>3+</sup> exhibit reorientation from the *a*-axis to the *c*-axis in the spin reorientation region (103-165 K) [2]. Low temperature heat capacity measurements revealed a Shottky anomaly at about 2 K which is connected with the Nd-Fe interaction and small sharp peak associated with Nd ordering below 1 K [3]. In our paper we study effect of Mn for Fe substitution on magnetic properties of NdMn<sub>x-1</sub>Fe<sub>x</sub>O<sub>3</sub> compounds which have been grown by the optical floating zone technique in a mirror furnace equipped with four mirrors. Prepared crystals were characterized by powder diffraction, SEM and EDX analysis. Magnetic properties were measured by SQUID magnetometer on MPMS and VSM magnetometer on PPMS in temperature range from 2 to 400 K and magnetic flux up to 9 T. Substitution of Mn for Fe affects the reorientation temperature only slightly and Fe-Nd interactions are practically intact. Measurements of heat capacity were performed in temperature range from 2 K to 200 K and in magnetic fields up to 9 T. Low temperature heat capacity measurement for sample with *x* = 0.1 revealed that doping will strengthen Nd-Fe magnetic interaction because a Schotky maximum in low temperatures heat capacity shifts to higher temperatures. Another anomaly is generated by doping at about 11 K. The anomaly is smeared out by magnetic field confirming magnetic origin of the anomaly.

[1]. K.P. Belov, et al. Phys. Solid State 13 (1971) 518, D. Treves, J. Appl. Phys. 3a, 1033 (1965).

[2] I. SOSNOWSKA, et al., Physica 136B (1986) 394-396

[3] F. Bartolomé, et al., Solid State Communications, Vol. 91, No. 3, pp. 177-182, 1994

**COMPARATIVE STUDY OF CRYSTAL STRUCTURES AND MAGNETIC PROPERTIES OF TWO LANTHANIDE 3D POLYMERIC COMPLEXES**M. Almáši<sup>1</sup>, A. Zeleňáková<sup>2</sup>, V. Zeleňák<sup>1</sup>, I. Císařová<sup>3</sup>, J. Bednarčík<sup>4</sup><sup>1</sup>*Department of Inorganic Chemistry, P.J. Šafárik University, Moyzesova 11, SK-04154 Košice, Slovak Republic*<sup>2</sup>*Department of Solid State Physics, P.J. Šafárik University, Park Angelinum 9, SK-04154 Košice, Slovak Republic*<sup>3</sup>*Department of Inorganic Chemistry, Charles University, Hlavova 2030, CZ-12843 Prague, Czech Republic*<sup>4</sup>*DESY/HASYLAB, P.J. Šafárik University, Notkestraße 85, D-22607 Hamburg, Germany*

During the last decade, polymeric complexes have attracted considerable attention because of their structural diversity as well as their potential applications in practical areas, such as catalysis, gas storage and magnetism. Rare earth metal ions are less frequently chosen for the node of coordination polymers because of their notorious variability with respect to both coordination number and geometry. However, the lanthanide ions exhibit unique topological structure leading to interesting magnetic properties.

In our present work we have focused on the preparation of coordination polymers using Eu(III) and Gd(III) cations as nodes and formate ( $\text{HCOO}^-$ ) anion as the smallest and the simplest carboxylate anion. Two three-dimensional (3D) complexes with general formula  $\{[\text{Ln}(\text{FOR})_3]\}_n$  were prepared and characterized by different physicochemical measurements. Single-crystal X-ray diffraction (SC-XRD) and high-energy powder X-ray diffraction (HE-XRD) reveal that complexes are isostructural and formed 3D polymeric network with Gd-Gd, Eu-Eu distances 3.998 Å and 4.003 Å, respectively. Magnetic properties were investigated using a SQUID based magnetometer in external dc field up to 5 T in the temperature range of 2 - 300 K. The inverse dc susceptibility analysed by a Curie-Weiss law shows on the typical paramagnetic behaviour for Gd(III) complex with the Weiss constant equal to zero. The value of effective magnetic moment  $\mu_{\text{eff}} = 7,57 \mu_{\text{B}}$  from the experimental data is close to the theoretical value for  $S = 7/2$ . Detailed correlation between crystal structure of complexes and magnetic properties will be presented.

**SYNTHESIS AND MAGNETIC PROPERTIES OF  $\text{Yb}_2\text{Pt}_3\text{Si}_5$** J. Fikáček<sup>1</sup>, J. Custers<sup>1</sup>, J. Prchal<sup>1</sup>, and V. Sechovský<sup>1</sup><sup>1</sup>*Department of Condensed Matter Physics, Faculty of Mathematics and Physics, Charles University in Prague, Ke Karlovu 5, 121 16 Praha 2*

We report on the synthesis, crystal structure and basic physical properties of a new ternary compound  $\text{Yb}_2\text{Pt}_3\text{Si}_5$ . Single crystalline samples have been prepared by solvent growth method using tin flux and non-stoichiometric amounts of pure elements.

Crystal structure has been examined on selected single-crystals by X-ray Laue diffraction and powder X-ray diffraction (on pulverized crystals). It has been found that  $\text{Yb}_2\text{Pt}_3\text{Si}_5$  adopts the orthorhombic  $\text{U}_2\text{Co}_3\text{Si}_5$ -type structure (space group *Ibam*). The correct stoichiometry has been confirmed by EDX analysis.

Before and after annealing (300 °C, 2 days), the electrical resistivity, magnetization and specific heat were measured between 1.8 and 300 K. Annealing has no effect on measured data. Electrical resistivity data confirmed a very good quality of our single-crystals having residual resistivity ratio  $\sim 100$ . The magnetic susceptibility decreases with decreasing temperature down to 80 K where it shows a shallow minimum then it gradually increases with further cooling. These features indicate influence of spin fluctuations. Specific heat and electrical resistivity show no anomaly in the investigated temperature range. The gamma coefficient of specific heat reaches a moderately enhanced value  $(34.5 \pm 0.5) \text{ mJ.mol.K}^{-2}$ . These findings suggest lack of magnetic ordering at least down to 1.8 K in contrary to the case of  $\text{Ce}_2\text{Pt}_3\text{Si}_5$ , which is a Kondo lattice antiferromagnet.

**MAGNETIC PROPERTIES OF  $\text{La}_{0.8}\text{K}_{0.2}\text{MnO}_3$  NANOPARTICLES**

M. Mihalik<sup>1</sup>, M. Zentková<sup>1</sup>, J. Briančin<sup>3</sup>, M. Fitta<sup>4</sup>, J. Lazúrová<sup>1</sup>, M. Mihalik jr.<sup>1</sup>, M. Vavra<sup>1,2</sup>

<sup>1</sup>*Institute of Experimental Physics, SAS, Watsonova 47, Košice, Slovak Republic*

<sup>2</sup>*Faculty of Science, UPJŠ, Moyzesova 11, 041 54 Košice, Slovak Republic*

<sup>3</sup>*Institute of Geotechnics SAS, Watsonova 45, 040 01 Košice, Slovak Republic*

<sup>4</sup>*Institute of Nuclear Physics, PAS, Radzikowskiego 152, Kraków, Poland*

In our paper we study magnetic properties of  $\text{La}_{0.8}\text{K}_{0.2}\text{MnO}_3$  nano-sized powders with particular emphasis on the exchange bias (EB) phenomena in this system. The EB effect was discovered more than 55 years ago by Meiklejohn and Bean [1], and its characteristic signature is the shift of the centre of magnetic hysteresis loop from its normal position at  $H = 0$  to  $H_E \neq 0$ . EB usually occurs in systems, which are composed by an antiferromagnet (AFM) that is in atomic contact with a ferromagnet (FM) after the system is cooled, below the respective Néel temperature  $T_N$  and Curie temperature  $T_C$ , in an external cooling field  $H_{cf}$ . The EB effect in manganites has attracted attention for their potential application and was studied e.g. on  $\text{La}_{1-x}\text{Ca}_x\text{MnO}_3$  [2]. Although the complex AFM background accompanied with FM component in these materials has already been found, the EB effect remains unclear and needs further investigation.

The preparation of nano-sized powders followed the glycine-nitrate method [3]. As-prepared  $\text{La}_{0.8}\text{K}_{0.2}\text{MnO}_3$  were characterised by X-ray powder diffraction and by electron microscopy including SEM and TEM. The mean particle size of as prepared nanoparticles was about 30 nm. Magnetization measurements were performed in magnetic fields up to 9 T and in the temperature range between 1.8 K and 400 K by a SQUID magnetometer on MPMS and VSM magnetometer in PPMS. The effect of external cooling field  $H_{cf}$  and training effect on EB phenomena was studied. Study of correlations between magnetic properties and particle size, which was modified by heat treatment, will be presented and discussed in our paper.

[1] W. P. Meiklejohn and C. P. Bean, Phys. Rev. 102, 1413 (1956).

[2] Xiao H. Huang et al. J. Am. Ceram. Soc., 94, 1324 (2011)

[3] S.B. Boskovic et al., Ceram Int 33:89 (2007) doi: 10.1016/j.ceramint.2005.07.022

**THE HYBRIDIZATION OF 5f-CONDUCTION ELECTRONS  
IN  $\text{URu}_{1-x}\text{Pd}_x\text{Ge}$** 

D. Gralak, V.H. Tran

*W. Trzebiatowski Institute of Low Temperature and Structure Research,  
Polish Academy of Science, 50-422 Wrocław, Poland*

We present a systematic study of the  $\text{URu}_{1-x}\text{Pd}_x\text{Ge}$  solid solutions by means of X - ray diffraction, dc-magnetization, specific heat and electrical resistivity. The studied alloys ( $0.1 \leq x \leq 0.9$ ) crystallize in the orthorhombic  $\text{TiNiSi}$  - type structure with space group  $\text{Pnma}$ . Analysis of the X-ray diffraction data using Rietveld refinement method reveals the Vegard's law behaviour of the unit cell volume through the  $b$  - and  $c$  axis parameters exhibit an anomaly around  $x = 0.7$ . It is found that the magnetic behavior of  $\text{URu}_{1-x}\text{Pd}_x\text{Ge}$  strongly depends upon the Pd substitution. The compositions with  $x < 0.3$  are nonmagnetic down to 2 K. In the concentration range  $0.3 < x < 0.8$  the magnetic ground state is antiferromagnetic with a maximum value of  $T_N = 32$  K at  $x = 0.7$ . The  $x = 0.9$  composition alike  $\text{UPdGe}$  undergoes two successive magnetic phase transitions: antiferromagnetic at  $T_N = 35$  K and ferromagnetic at  $T_C = 31$  K. In the nonmagnetic-magnetic crossover region ( $x \sim 0.3$ ) the magnetic and electron transport properties display non Fermi liquid behavior. The observed development of magnetism corresponds well to changes in the degree of 5f electron localization as well as in the Kondo interactions, resulting mainly from increased 5f conduction electron hybridization.

*Acknowledgements : The authors acknowledge for the financial support from the project 2011/01/B/ST3/04553 of the National Science Centre of Poland.*



**CRYSTAL-FIELD INTERACTIONS IN  $\text{RAl}_2$  INTERMETALLICS AND  $\text{RAlO}_3$  OXIDES (R = Pr and Nd)**R. J. Radwanski<sup>1,2</sup>, D. Nalecz<sup>1,2</sup> and Z. Ropka<sup>2</sup><sup>1</sup>*Institute of Physics, Pedagogical University, Podchorążych 2, 30-084 Krakow, Poland*<sup>2</sup>*Center of Solid State Physics, Snt Filip 5, 31-150 Krakow, Poland*

We have analyzed crystal-field (CEF) interactions in  $\text{PrAl}_2$  and  $\text{NdAl}_2$  intermetallics in order to compare them with interactions in  $\text{PrAlO}_3$  and  $\text{NdAlO}_3$ . Our studies have been motivated by a recent claim of Novak, Knizek and Kunes (arXiv: 1303.1281) of the ability to calculate *ab-initio* CEF parameters for rare-earth aluminates  $\text{RAlO}_3$ . Novak *et al.* have used a Hamiltonian expressed in basis of Wannier functions and the density functional theory. In these oxides rare-earth ion has twelve nearest-neighbour oxygen ions typical for the perovskite structure. Similarly to Novak *et al.* we are interested in explanation of properties of cobalt perovskites  $\text{RCoO}_3$ . For  $\text{R}=\text{La}$ , i.e. in  $\text{LaCoO}_3$  the cobalt state is extensively studied theoretically by more than 50 years due to its surprising nonmagnetic ground state. By changing R we can modify the Co state by the chemical-pressure mechanism simultaneously introducing the magnetism of rare-earth ions. We have proved that very thin and well-defined crystal-field states of the  $\text{Co}^{3+}$  ion exist in  $\text{LaCoO}_3$  (Phys. Rev. **67** (2003) 172401).

The derived set of CEF parameters explains, for instance, the magnetic ground state for  $\text{PrAl}_2$  and for  $\text{NdAl}_2$  below 33 K and 63 K, respectively, with the easy magnetic  $\langle 100 \rangle$  axis. Within the Quantum Atomistic Solid State theory (QUASST) we consistently have explained the ground-state properties and thermodynamics, both in the paramagnetic and magnetic state, together with the reproduction of the  $\lambda$ -type peak at the phase transition. Within QUASST we anticipate properties of ideal cubic perovskites  $\text{PrAlO}_3$  and  $\text{NdAlO}_3$  as well as properties of  $\text{PrCoO}_3$  and  $\text{NdCoO}_3$ . The influence of orthorhombic distortions will be also discussed.

# CRYSTAL GROWTH AND STRUCTURAL CHARACTERISATION OF NOVEL TETRAGONAL $Ce_2RhGa_{12}$

R. Nagalakshmi<sup>1</sup>, Ruta Kulkarni<sup>2</sup>, S.K. Dhar<sup>2</sup>, A. Thamizhavel<sup>2</sup>, V. Krishnakumar<sup>3</sup>, C. Besnard<sup>4</sup>, Y. Filinchuk<sup>5</sup>, H. Hagemann<sup>6</sup> and M. Reiffers<sup>7</sup>

<sup>1</sup>*Department of Physics, National Institute of Technology, Tiruchirappalli – 620 0015, India*

<sup>2</sup>*DCMPMS, Tata Institute of Fundamental Research, Mumbai – 400 005, India*

<sup>3</sup>*Department of Physics, Periyar University, Salem – 636 011, India*

<sup>4</sup>*Lab. of Crystallography, Univ. of Geneva, 24, q. E. Ansermet, 1211 Geneva 4 Switzerland*

<sup>5</sup>*Swiss-Norwegian Beamlines at ESRF, BP-220, 38043 Grenoble, France.*

<sup>6</sup>*Department of Physical Chemistry, University of Geneva, Geneva, Switzerland.*

<sup>7</sup>*Faculty of Humanities and Natural Sciences, Presov University, Presov, Slovakia.*

Single crystals of  $Ce_2RhGa_{12}$  have been synthesized using Ga flux and their structure was determined by single-crystal X-ray diffraction. The  $Ce_2RhGa_{12}$  crystallizes in the tetragonal  $P4/nbm$  space group (No. 125), which is isostructural to  $Ce_2PdGa_{12}$ , with  $Z = 2$  and lattice parameters  $a \approx 6.0405 \text{ \AA}$  and  $c = 15.706 \text{ \AA}$ . Data were collected at the Swiss Norwegian Beam Line at the European Synchrotron Facility, Grenoble France. Also the Laue diffraction was carried to confirm the single crystal quality and it shows the well defined spots possessing tetragonal symmetry.

The heat capacity, electrical resistivity and magnetic properties are presented. We observed transition into the magnetically oriented state.

**MAGNETISM AND DENSITY OF STATES IN YCo<sub>2</sub> COMPOUND  
MODIFIED BY Ti or Nb**

Z. Śniadecki, A. Szczeszak, A. Szajek, and B. Idzikowski

*Institute of Molecular Physics, Polish Academy of Sciences*

*M. Smoluchowskiego 17, PL 60-179 Poznań, Poland*

The YCo<sub>2</sub> intermetallic compound is a Pauli exchange-enhanced paramagnet. In fine crystalline form it becomes ferromagnetic in the whole grains volume. Also in amorphous state the magnetic ordering appears. In our current studies the magnetic properties of rapidly quenched YCo<sub>2</sub>-type compositions are described, where nanocrystalline state is obtained in rapid quenching process by appropriate cooling rate. To modify electronic structure of such prepared intermetallics, 30 at.% of Y atoms were substituted by Nb or Ti.

The studied intermetallic compounds Y<sub>0.7</sub>Nb<sub>0.3</sub>Co<sub>2</sub> and Y<sub>0.7</sub>Ti<sub>0.3</sub>Co<sub>2</sub> were examined with X-ray diffraction (XRD) and vibrating sample magnetometry (VSM). The samples with 10 at.% substitution consist of single phase (not discussed here), but for 30 at.% substitution of Y by Nb a small amount of additional phase appears. This is NbCo<sub>2</sub> phase, also with the same *Fd-3m* space group, but with lattice constant  $a = 6.782$  Å. For Y<sub>0.7</sub>Ti<sub>0.3</sub>Co<sub>2</sub>, three phases are observed, with the same structures but different lattice constants:  $a = 7.198$ ,  $7.088$  and  $6.772$  Å. In both compositions all nanocrystalline phases grow simultaneously after replacing Y atoms of initial YCo<sub>2</sub> by Nb or Ti.

The Y<sub>0.7</sub>Nb<sub>0.3</sub>Co<sub>2</sub> and Y<sub>0.7</sub>Ti<sub>0.3</sub>Co<sub>2</sub> compounds exhibit the maximum on M(T) curves and linear, paramagnetic M(H) dependence in higher magnetic fields. An increase of magnetization at low temperatures is observed and hysteresis loops are visible on M(H) curves. These characteristics evidence the presence of ferromagnetic ordering with small coercive fields, in opposite to paramagnetic YCo<sub>2</sub>.

The electronic band structures of YCo<sub>2</sub> systems were calculated using *ab-initio* Full Potential - Linearized Augmented Plane Wave method where Nb or Ti substitutions were considered as point defects. Theoretically predicted magnetically ordered ground states for YCo<sub>2</sub> system with Y atoms substituted by Ti or Nb find experimental confirmation.

*This work was supported by the National Science Centre within the research project no. N202 381740.*

# CRYSTALLIZATION PROCESSES AND MAGNETIZATION OF $R_{4.5}Fe_{77}B_{18.5}$ (R=Pr, Nd) AMORPHOUS GLASSES

A. Musiał<sup>1,2</sup>, Z. Śniadecki<sup>1</sup>, D. Pagnani<sup>1</sup>, and B. Idzikowski<sup>1</sup>

<sup>1</sup>*Institute of Molecular Physics, Polish Academy of Sciences*

*M. Smoluchowskiego 17, PL 60-179 Poznań, Poland*

<sup>2</sup>*The NanoBioMedical Centre, Adam Mickiewicz University, Umultowska 85*

*PL 61-614 Poznań, Poland*

The amorphous  $R_{4.5}Fe_{77}B_{18.5}$  (R=Pr, Nd) alloys were prepared by melt-spinning technique under argon atmosphere on a cooper wheel rotating with  $25 \text{ ms}^{-1}$ . The ribbons have been investigated by means of differential scanning calorimetry (DSC), X-ray diffraction (XRD) and thermomagnetic measurements. DSC measurements have been realized with different heating rates from 10 to 50 K/min. DSC curves clearly show the glass transition and crystallization temperatures. Temperatures of crystallization for  $Pr_{4.5}Fe_{77}B_{18.5}$  (at heating rates 10 K/min) are (i) for the first exothermic effect  $T_{x1} = 589,7^\circ\text{C}$  and (ii) for the second  $T_{x2} = 600,1^\circ\text{C}$ , whereas at the heating rate of 50 K/min these values are  $T_{x1} = 603,5^\circ\text{C}$  and  $T_{x2} = 615,8^\circ\text{C}$ , respectively. The magnetic properties has been analyzed by using of an alternate current magnetometer and have been compared with DSC results.

The identification of the structural phases were made by analysis of X-ray diffraction patterns. In the investigated amorphous ribbons initially crystallizes  $Fe_3B$  alloy and the crystallization of  $Pr_2Fe_{23}B_3$  particles occurs immediately after the  $Fe_3B$  formation. Then, fine hard magnetic  $Pr_2Fe_{14}B$  particles nucleate directly at  $Fe_3B$  interfaces [1]. In further crystallization processes  $Pr_2Fe_{14}B$  and  $Pr_2Fe_{23}B_3$  particles grow by the coalescence of fine structure [2].

*This work was supported by the National Centre for Research and Development within the project no. POKL.04.03.00-00-015/12 and partially (Z.Ś.) by the Polish Ministry of Science and Higher Education (Iuventus Plus grant IP2011 055671).*

[1] Y-C. Jung, Y. Ohmori, K. Nakai, S. Hirose, H. Kanekiyo, Mater. Trans. 43 (2002) 660

[2] Y-C. Jung, Y. Ohmori, K. Nakai, S. Hirose, H. Kanekiyo, Mater. Trans. 42 (2001) 2102

**I7-01**

**THE VORTEX LATTICE VIEWED BY VERY LOW TEMPERATURE  
SCANNING TUNNELING MICROSCOPY AND SPECTROSCOPY**

Hermann Suderow

*Universidad Autónoma de Madrid, Spain*

During past years we have been developing dilution refrigerator scanning tunnelling microscopy to achieve atomic size real space mapping with high energy resolution. I will review the basics of this technique, and present new developments such as local Josephson spectroscopy, Andreev spectroscopy and current drive microscopy, which provide powerful methods to map out the phase and spin of superconducting condensates. I will further present methods to obtain the local magnetic field, based on the use of superconducting tips. I will discuss recent measurements in disordered superconducting thin films under magnetic fields.

**SUPERCONDUCTIVITY, MAGNETISM, AND ATOMIC RATTLING PHENOMENA IN  $R_3\text{Rh}_4\text{Ge}_{13}$  ( $R=\text{Yb}, \text{Lu}$ )**

A. M. Strydom

*Department of Physics, University of Johannesburg, PO Box 524, Auckland Park 2006, South Africa*

$\text{Yb}_3\text{Rh}_4\text{Ge}_{13}$  and  $\text{Lu}_3\text{Rh}_4\text{Ge}_{13}$  are members of a large ternary intermetallic series of compounds. They form in a cubic crystal structure and whereas unique atomic sites are provided respectively for the rare-earth and Rh atoms, Ge occupies two different positions in this structure. The 3:4:13 series of compounds are well-known for a fascinating variety of physical properties such as strongly correlated and heavy-fermion behaviour, superconductivity, and magnetic ordering. In previous work of ours on the compound  $\text{Yb}_3\text{Ir}_4\text{Ge}_{13}$  we found that this structure type is interestingly also amenable to the unusual occurrence of charge ordering among the magnetic Yb ions.

The unit cell of these compounds may furthermore be described in terms of two filled atomic cages with conditions favorable for the phenomenon of *rattling* or anharmonic and off-centre motion of the atoms located inside oversized atomic cages. This leads to interesting anomalies in the phononic spectra of such materials. The 3:4:13 crystal structure is related to that of the skutterudite class of compounds and these two structure types share many common physical properties.

In this work we turn to an exploratory study of  $\text{Yb}_3\text{Rh}_4\text{Ge}_{13}$  and its Lu-based counterpart.  $\text{Lu}_3\text{Rh}_4\text{Ge}_{13}$  superconducts below 2.5K, its magnetic susceptibility being overall diamagnetic below room temperature. Our analysis of the specific heat reveals the presence of optical lattice modes that are reconcilable with details of the crystal structure.

$\text{Yb}_3\text{Rh}_4\text{Ge}_{13}$  displays a temperature-dependent magnetic susceptibility characteristically associated with paramagnetic Yb spins at high temperature. The electrical resistivity is in evidence of intermediate valence behaviour through strongly curved behaviour as function of temperature below ~80K, but interestingly at 2.5K  $\text{Yb}_3\text{Rh}_4\text{Ge}_{13}$  becomes magnetically ordered with the specific heat and magnetic susceptibility reminiscent of nominally antiferromagnetic type ordering.

We present here a study of physical properties that seeks to investigate the interplay between different cooperative phenomena in the ground states of  $\text{Lu}_3\text{Rh}_4\text{Ge}_{13}$  and  $\text{Yb}_3\text{Rh}_4\text{Ge}_{13}$ .

**ANOMALOUS SPECTRAL FUNCTIONS IN SUPERCONDUCTORS**

Tomáš Bzdušek and Richard Hlubina

*Department of Experimental Physics, Comenius University, Mlynská dolina F2, 842 48 Bratislava, Slovakia*

Within the Nambu-Gorkov formulation of the BCS theory, a superconductor is characterized by a  $2 \times 2$  matrix of Green's functions. The spectral functions of the diagonal components are well studied in the literature, not only theoretically but also experimentally – since they are measurable, at least in principle, by the angle-resolved photoemission and inverse photoemission spectroscopies. However, much less is known about the spectral properties of the off-diagonal (or anomalous) components of the matrix Green's function. The present contribution aims at filling in this gap in the literature by establishing what can be said exactly about the anomalous spectral functions and suggesting procedures for their experimental determination.

That this is a relevant problem is apparent already from the Eliashberg approach to phonon-mediated superconductivity. Within that formalism, the superconducting state is described by *two* functions  $Z(\omega)$  and  $\Delta(\omega)$ , but the photoemission and tunneling experiments provide access to only *one* function of frequency. Of course, in conventional superconductors this is not perceived as a real problem, but in less understood cases such as the cuprates it might be valuable to possess a new tool in studying their physical mechanism.

We will start by presenting exact sum rules for a few moments of the anomalous spectral functions, as obtained within the Eliashberg theory and for the repulsive Hubbard model, which is believed to exhibit d-wave superconductivity. The sum rules imply important differences of the spectral functions with respect to the predictions of the BCS theory, which will be explicitly checked by a direct calculation within the Eliashberg theory.

Next we propose a procedure for separating the contributions of the normal and anomalous Green's functions to the spin-spin and density-density response functions. We show that convolutions of the anomalous spectral function are in principle observable and we present the expected results within the Eliashberg theory. Finally we conclude with some notes on the solution of the inverse problem.

**INTRINSIC *versus* EXTRINSIC STRONGLY CORRELATED MAGNETIC SUPERCONDUCTORS**J. Spałek<sup>1,2</sup><sup>1</sup>*Marian Smoluchowski Institute of Physics, Jagiellonian University, Reymonta 4, 30-059 Kraków, Poland*<sup>2</sup>*Faculty of Physics and Applied Computer Science, AGH University of Science and Technology, Reymonta 19, 30-059 Kraków, Poland*

I overview our recent results for the t-J model of high-temperature superconductivity, both within the statistically consistent renormalized mean field theory (SC-RMFT) and those comprising diagrammatic expansion to higher orders. A quantitative comparison with experiment is made for selected quantities.

In the second part, I discuss our most recent results concerning an application of SC-RMFT to the Anderson-Kondo lattice model, with inclusion of the Kondo-type pairing, as well as elaborate on phase diagram involving pure magnetic and superconducting phases, and coexistent antiferromagnetic-superconducting states. I discuss also in qualitative terms the relevance of the last results to the selected heavy-fermion systems.

*The author acknowledges the cooperation with his coworkers/students: J. Kaczmarczyk, D. Goc-Jagło, J. Jędrak, and O. Howczak. He was also supported by the Foundation for Polish Science (FNP) through the Grant TEAM, as well as by the National Science Center (NCN) through the special Grant MAESTRO.*



**SPECIFIC HEAT STUDY OF SUPERCONDUCTIVITY IN  $\text{Cu}_x\text{TiSe}_2$** 

J. Kačmarčík<sup>1</sup>, Z. Pribulová<sup>1</sup>, V. Soltészová<sup>2</sup>, P. Barančeková-Husaníková<sup>3</sup>, G. Karapetrov<sup>4</sup>, V. Komanický<sup>2</sup> and P. Samuely<sup>1</sup>

<sup>1</sup>*Centre of Very Low Temperature Physics at Institute of Experimental Physics, Slovak Academy of Sciences, Watsonova 47, 040 01 Košice, Slovakia*

<sup>2</sup>*Faculty of Natural Sciences, University of P.J. Šafárik, Park Angelinum 9, 040 01 Košice, Slovakia*

<sup>3</sup>*Institute of Electrical Engineering, Slovak Academy of Sciences, Dúbravská cesta 9, 841 04 Bratislava, Slovakia*

<sup>4</sup>*Department of Physics, Drexel University, 3141 Chestnut Street, Philadelphia, PA 19104, USA*

In  $\text{TiSe}_2$  the charge density wave (CDW) order exists below  $T_{\text{CDW}}=200$  K. When the system is intercalated by copper, in  $\text{Cu}_x\text{TiSe}_2$  for  $x=0.04$  superconductivity appears. This is accompanied by a rapid suppression of  $T_{\text{CDW}}$  order but CDW still overlaps with the superconductivity in the underdoped superconducting region for  $x$  between 0.04 and 0.06. The way how superconducting and CDW orders compete is still unresolved but interesting physical problem. The maximum superconducting transition temperature  $T_c$  around 4 K is observed for  $x=0.08$ .

Here we report a calorimetric study performed on the superconducting single crystals of  $\text{Cu}_x\text{TiSe}_2$  measured by a sensitive ac technique in the temperature range down to 0.6 K and magnetic fields up to several Teslas. We have measured two underdoped samples with  $x = 0.0605$  and  $0.068$  of  $T_c = 2.75$  K and  $3.2$  K, resp. and one slightly overdoped sample with  $x=0.086$  and  $T_c = 3.85$  K. All the measurements show sharp and well defined specific heat anomaly at the superconducting transition. We will analyze the results in terms of the superconducting coupling strength, the upper critical fields and their angular dependence.

# **AMBIENT PRESSURE SUPERCONDUCTIVITY IN THE ANTIFERROMAGNETIC COMPOUND $\text{Ce}_2\text{PtIn}_8$**

M. Kratochvilová<sup>1</sup>, J. Prokleška<sup>1</sup>, M. Dušek<sup>2</sup>, J. Custers<sup>1</sup>, V. Sechovský<sup>1</sup>

<sup>1</sup>*Department of Condensed Matter Physics, Faculty of Mathematics and Physics, Charles University, Prague, Ke Karlovu 5, 121 16, Czech Republic*

<sup>2</sup>*Department of Structure Analysis, Institute of Physics, Prague, Cukrovarnická 10, 162 00, Czech Republic*

The family of  $\text{Ce}_n\text{T}_m\text{In}_{3n+2m}$  ( $n = 1, 2$ ;  $m = 1$ ;  $T$  = transition metal) heavy fermion compounds are known to be on the verge of a magnetic to non-magnetic quantum critical point (QCP) [1]. In the vicinity of the materials' QCP an unconventional superconducting state has been reported which attracted much of the attention in the past decades. However, this family of compounds is interesting for some other reason. The compounds crystallize in the tetragonal  $\text{Ho}_n\text{Co}_m\text{Ga}_{3n+2m}$  structures. The structures consist of  $m$   $\text{TIn}_2$ -layers alternating with  $n$ -layers of  $\text{CeIn}_3$  along the  $c$ -axis. By adding an additional  $\text{CeIn}_3$  stacking block the structural dimensionality changes from more 2D to 3D ( $127 \rightarrow 115 \rightarrow 218$ ). This makes them ideal candidates to investigate the influence of the parameter „dimensionality“ with respect to quantum criticality [2].

Here, we report on  $\text{Ce}_2\text{PtIn}_8$  which is the compound within the family showing superconductivity below an antiferromagnetic transition at ambient pressure. In the specific heat, resistivity and ac susceptibility two magnetic transitions are observed; the compound orders antiferromagnetically below  $T_N = 2.1$  K and further cooling reveals another, order-to-order transition just below at  $T_m = 2$  K. Contrary to  $\text{Ce}_2\text{RhIn}_8$ , the two transitions merge at magnetic field around 4 T and split again in higher magnetic fields pointing on a different character of magnetic ordering. Finally, superconductivity emerges at  $T_C = 0.39$  K. Application of hydrostatic pressure leads to formation of a superconducting dome with the highest  $T_C = 0.7$  K at 1 GPa. The magnetic field-pressure-temperature phase diagram will be discussed in the context of superconductivity and magnetism evolution in related compounds.

[1] J. D. Thompson *et al.*, J. Magn. Magn. Mater. **226-230**, 5 (2001).

[2] J. Custers *et al.*, Nature Mat. **11**, 189 (2012).

**ELECTROMAGNETIC PROPERTIES OF MELT-TEXTURED YBaCuO SUPERCONDUCTORS DOPED BY Gd AND Sm**

M. Jirsa<sup>1</sup>, M. Rameš<sup>1</sup>, D. Volochová<sup>2</sup>, P. Diko<sup>2</sup>, K. Zmorayová<sup>2</sup> and M. Šefčíková<sup>2</sup>

<sup>1</sup>*Institute of Physics ASCR, Na Slovance 2, CZ-18221 Praha 8, Czech Republic*

<sup>2</sup>*Institute of Experimental Physics SAS, SK-04353 Watsonova 47, Slovakia*

Magnetic rare earth (RE) ions represent a great potential for melt-textured YBaCuO bulks to form effective point-like vortex pinning defects. Only a small amount of RE is needed for optimum pinning. We report on electromagnetic properties of YBa<sub>2</sub>Cu<sub>3</sub>O<sub>y</sub> samples melt-grown in air, pure and doped by 0.1 mol % Gd and Sm. Magnetic behavior was studied in both tetragonal (nonsuperconducting) and orthorhombic (superconducting) forms of the composites. In connection with the point-like disorder due to the RE doping and other sources a second peak on the magnetization curve is formed. Beside the magnetization loop and the critical current density associated with it, also the average magnetic moment  $M_{av}$  (the mean value of the upper and lower branches of the hysteresis loop) was studied in the orthorhombic forms of the materials.  $M_{av}$ , commonly regarded as an equilibrium moment, joins at the irreversibility field,  $B_{irr}$ , with the reversible curve observed above  $B_{irr}$ . The joined curve should be close to the thermodynamic reversible magnetization and follow the theoretical logarithmic field dependence. However, a rather strong temperature-dependent disturbance is observed on  $M_{av}(B)$  just below  $B_{irr}$ , which is evidently connected with the mechanism of the second peak formation. This feature, starting already slightly above  $B_{irr}$ , scales with temperature, but in a different way than both the second peak and the logarithmic relaxation rate.

**STUDY OF RESISTIVE SUPERCONDUCTING TRANSITION OF BULK  $(\text{Bi}_{0.6}\text{Pb}_{0.4})_2\text{Sr}_2\text{Ca}_2\text{Cu}_3\text{O}_x$** 

W.M. Woch, M. Chrobak, R. Zalecki and A. Kołodziejczyk

*AGH University of Science and Technology, Faculty of Physics and Applied Computer Science, Solid State Physics Dept., Al. Mickiewicza 30, PL 30-059, Kraków, Poland*

The width of the resistive transition as well as the thermal fluctuations of bulk  $(\text{Bi}_{0.6}\text{Pb}_{0.4})_2\text{Sr}_2\text{Ca}_2\text{Cu}_3\text{O}_x$  superconductor were analyzed within the theoretical models. The applied magnetic field widens the resistive transition according to the following formula:  $\Delta T = CH^m + \Delta T_0$ . The exponent  $m$  varies around  $2/3$  and it depends on the vortex structure and the strength of the pinning force. The thermal fluctuations were analyzed from the magnetoresistance measurements. The critical exponents have been calculated within the temperature interval from the zero resistance critical temperature to well above the onset temperature. The critical as well as the Gaussian fluctuations have been discussed.

# CHARGE FLUCTUATION ACROSS THE QUANTUM CRITICAL POINT OF $\text{EuCu}_2(\text{Ge}_{1-x}\text{Si}_x)_2$

M. A. Ahmida<sup>1</sup>, D. Johrendt<sup>2</sup>, Z. Hossain<sup>3</sup>, C. Geibel<sup>4</sup> and M. M. Abd-Elmeguid<sup>1</sup>

<sup>1</sup>*II Physikalisches Institut, Universität zu Köln, Zùlpicher Str. 77, 50937 Köln, Germany*

<sup>2</sup>*Department Chemie and Biochemie der Ludwig-Maximilians-Universität München, Butenandtstrasse 5-13 (Haus D), 81377 München, Germany*

<sup>3</sup>*Department of Physics, Indian Institute of Technology, Kanpur-208016, India*

<sup>4</sup>*Max Planck Institut für Chemische Physik fester Stoffe, Nöthnitzer Strasse 40, 01187 Dresden, Germany*

The intermetallic series  $\text{EuCu}_2(\text{Ge}_{1-x}\text{Si}_x)_2$  crystallizing in the tetragonal  $\text{ThCr}_2\text{Si}_2$ -type structure combines the antiferromagnetic (AF) compound  $\text{EuCu}_2\text{Ge}_2$  ( $T_N=14$  K) with the homogenous intermediate valent (IV) compound  $\text{EuCu}_2\text{Si}_2$ . Thus, the system offers the opportunity to investigate the crossover from a magnetically ordered state to a nonmagnetic IV state through a quantum critical point (QCP) at  $x = 0.65$ . To gain a microscopic insight into the change of the magnetic and valence states and their competition at the QCP, we have performed systematic  $^{151}\text{Eu}$  Mössbauer effect and x-ray diffraction measurements on  $\text{EuCu}_2(\text{Ge}_{1-x}\text{Si}_x)_2$  as a function of concentration ( $0 < x < 1$ ) as well as external pressure at different temperatures (300 to 4 K).

The analysis of the results shows that the collapse of AF ordering for  $x > 0.50$  is connected with a simultaneous sharp change of the valence state of Eu towards a homogeneous IV state, leading to a first order quantum phase transition from the AF state to a nonmagnetic IV state at a QCP ( $X= 0.7$ ). Both values of the Eu mean valence at/ near the QPT induced by doping or external pressure are found to be enhanced, indicating enhanced charge fluctuations. The nature of valence fluctuations at/ near the QPT and their coupling to the lattice are discussed.

# **ELECTRONIC, MAGNETIC, AND ELECTRIC TRANSPORT PROPERTIES OF $\text{Ce}_3\text{Co}_4\text{Sn}_{13}$ AND $\text{Ce}_3\text{Rh}_4\text{Sn}_{13}$ : A COMPARATIVE STUDY**

A. Ślebarski<sup>1</sup>, M. Fijałkowski<sup>1</sup>, J. Goraus<sup>1</sup> and M.B. Maple<sup>2</sup>

<sup>1</sup>*Institute of Physics, University of Silesia, 40-007 Katowice, Poland*

<sup>2</sup>*Department of Physics, University of California, San Diego, La Jolla, CA 92093, USA*

$\text{Ce}_3\text{Co}_4\text{Sn}_{13}$  and  $\text{Ce}_3\text{Rh}_4\text{Sn}_{13}$  crystallize in the cubic  $\text{Yb}_3\text{Rh}_4\text{Sn}_{13}$  structure, which is closely related to the one of skutterudites, well known thermoelectric materials. Both compounds exhibit novel physical properties, a large increase in electronic specific heat  $C(T)/T$  was recently observed at low temperatures with a maximum value of about  $4 \text{ J/K}^2\text{mol}_{\text{Ce}}$ . The first reason of our investigations is to compare the physical properties of the both compounds and to explain the abnormal electrical resistivity behaviour in  $\text{Ce}_3\text{Co}_4\text{Sn}_{13}$  above  $\sim 160 \text{ K}$ , which has not been observed in  $\text{Ce}_3\text{Rh}_4\text{Sn}_{13}$ . Second, we investigate the quantum criticality of  $\text{Ce}_3\text{Co}_4\text{Sn}_{13}$ . The specific heat data suggested that  $\text{Ce}_3\text{Co}_4\text{Sn}_{13}$  is likely near a magnetic quantum critical point (QCP). To investigate this idea further, we measured a low-temperature specific heat and magnetic and electronic transport properties of  $\text{Ce}_{3-x}\text{La}_x\text{Co}_4\text{Sn}_{13}$  in order to study the proximity of  $\text{Ce}_3\text{Co}_4\text{Sn}_{13}$  to the possible magnetic QCP. We found the critical concentration  $x_c \approx 0.6$  which separates the magnetically correlated state with a maximum in  $C(T)/T$  at  $\sim 0.7 \text{ K}$  for  $x < x_c$ , and a single Kondo impurity state for  $x > x_c$  in heavy fermion  $\text{Ce}_{3-x}\text{La}_x\text{Co}_4\text{Sn}_{13}$  system. The QCP has been, however, excluded. For the critical doping  $x_c$  of La, the low-temperature T-dependencies of the susceptibility, specific heat,  $C(T)/T$  and resistivity are not characteristic of the QCP.

**MAGNETISM IN  $\text{UCo}_{0.88}\text{Ru}_{0.12}\text{Ge}$  STUDIED BY POLARIZED NEUTRONS**M. Vališka<sup>1</sup>, J. Pospíšil<sup>1</sup>, G. Nénert<sup>2</sup>, A. Stunault<sup>2</sup>, K. Prokeš<sup>3</sup> and V. Sechovský<sup>1</sup><sup>1</sup> *Faculty of Mathematics and Physics, Charles University, DCMF, Ke Karlovu 5, CZ-12116 Praha 2, Czech Republic*<sup>2</sup> *Institut Laue Langevin, 6 rue Jules Horowitz, 38042 Grenoble, France*<sup>3</sup> *HZB Berlin, Hahn-Meitner Platz 1 14109 Berlin, Germany*

UCoGe is an archetype of coexisting the 5f-electron ferromagnetism ( $T_C \sim 3$  K) and superconductivity ( $T_{SC} \sim 0.6$  K) at ambient pressure. The low spontaneous magnetic moment of UCoGe ( $0.03\mu_B/\text{f.u.}$ ) indicates nearness of ferromagnetic instability. We have prepared a series of  $\text{UCo}_{1-x}\text{Ru}_x\text{Ge}$  polycrystals in order to study development of magnetism and superconductivity. The Ru doping leads to an initial sharp increase of the Curie temperature up to the maximum of  $T_C = 8.5$  K for  $x = 0.12$  and suppression of superconductivity. Further increase of Ru content yields gradual decrease of  $T_C$  towards the ferromagnetic quantum critical point at  $x \approx 0.3$ . We have grown the  $\text{UCo}_{0.88}\text{Ru}_{0.12}\text{Ge}$  single crystal and observed that it exhibits strong magnetocrystalline anisotropy analogous to UCoGe and a spontaneous magnetization considerably higher than found in the parent compound. To see the microscopic background of these findings we have performed a polarized neutron diffraction experiment at D3 in ILL. In contrast to the antiparallel orientation of the Co and U moments in UCoGe (in 12 T  $\mu_{Co} = -0.27\mu_B$ ,  $\mu_U = \mu_{U,L} + \mu_{U,S} = 0.49 - 0.17 = 0.32\mu_B$ ) we have found that the Co and U moments are parallel in  $\text{UCo}_{0.88}\text{Ru}_{0.12}\text{Ge}$  (in 9 T  $\mu_{Co} = 0.069\mu_B$ ,  $\mu_U = \mu_{U,L} + \mu_{U,S} = 0.457 - 0.20 = 0.257\mu_B$ ). This stands behind the magnetization increase with Ru doping which evokes a question whether the magnetic state of Co can be a critical parameter for presence of superconductivity in U(Co,Ru)Ge compounds.

# MAGNETORESISTANCE ANISOTROPY AND $H$ - $T$ - $x$ MAGNETIC PHASE DIAGRAM OF $\text{Tm}_{1-x}\text{Yb}_x\text{B}_{12}$

A.N. Azarevich<sup>1,2</sup>, N.E. Sluchanko<sup>2</sup>, A.V. Bogach<sup>2</sup>, V.V. Glushkov<sup>1,2</sup>, S.V. Demishev<sup>1,2</sup>, S. Yu. Gavrilkin<sup>3</sup>, S. Gabani<sup>4</sup>, K. Flachbart<sup>4</sup>, N.Yu. Shitsevalova<sup>5</sup>, V.B. Filipov<sup>5</sup>, J. Vanacken<sup>6</sup>, V.V. Moshchalkov<sup>6</sup>

<sup>1</sup>*Moscow Institute of Physics and Technology, 141700 Moscow Region, Russia*

<sup>2</sup>*General Physics Institute of RAS, 119991 Moscow, Russia*

<sup>3</sup>*Physical Institute of RAS, 53 Leninsky pr., 119991 Moscow, Russia*

<sup>4</sup>*Institute of Experimental Physics of SAS, 040 01 Košice, Slovak Republic*

<sup>5</sup>*Institute for Problems of Materials Science NASU, 03680 Kiev, Ukraine*

<sup>6</sup>*Inst. for Nanoscale Physics and Chemistry, KU Leuven, Leuven 3001, Belgium*

It was shown recently that  $\text{Tm}_{1-x}\text{Yb}_x\text{B}_{12}$  solid solutions may be considered as model compounds which enable to choose between various scenarios of antiferromagnetic (AF) instability, quantum critical behavior and mechanisms responsible for metal-insulator transition in strongly correlated electron systems [1]. In this study magnetic phase transitions inside the AF state as well as between the AF and paramagnetic (P) phase in  $\text{Tm}_{1-x}\text{Yb}_x\text{B}_{12}$  with Yb concentration  $x \leq 0.3$  are investigated. Measurements of heat capacity, magnetoresistance and magnetization have been carried out on high quality single crystals of  $\text{Tm}_{1-x}\text{Yb}_x\text{B}_{12}$  family at low temperatures 1.8 - 30 K and in magnetic field up to 12 T. The received data allow construct the  $H$ - $T$ - $x$  magnetic phase diagram of the AF state in  $\text{Tm}_{1-x}\text{Yb}_x\text{B}_{12}$ . We conclude that additionally to indirect exchange (RKKY-mechanism) the spin polarization of  $5d$ - type electronic states should be considered as another important factor which determinates the formation of the complex magnetic structure in these *fcc* crystals. As a result of the spin-polaron effect the  $H$ - $T$  magnetic phase diagram becomes significantly anisotropic and the difference between AF-P critical magnetic fields for  $\mathbf{H} // [100]$  and  $[111]$  orientations reaches values  $\Delta H_C / H_C = 0.23$  at  $T = 2.1$  K even for very small Yb concentration  $x = 0.004$ .

Based on the analysis of magnetic, angular and temperature dependences of magnetoresistance it was shown that the depression of spin polarons in magnetic field should be considered as the main factor responsible both for the emergence of the field hysteresis effect and the transformation of magnetic structure which was observed in magnetic field within the AF phase. We discuss also the transformation of the  $5d$ - spin density wave component of the magnetic structure in the AF ground state of  $\text{Tm}_{1-x}\text{Yb}_x\text{B}_{12}$ .

[1] N. E. Sluchanko, A. N. Azarevich, A. V. Bogach, et al., JETP. **115**, 509 (2012).



# STABILIZATION OF ANTIFERROMAGNETIC PHASE UNDER HYDROSTATIC PRESSURE IN $\text{Nd}_{1-x}\text{Ca}_x\text{BaCo}_2\text{O}_{5.5}$ ( $x = 0-0.06$ )

J. Pietosa<sup>1</sup>, S.Kolesnik<sup>2</sup> and B. Dabrowski<sup>2</sup>

<sup>1</sup>*Institute of Physics, Polish Academy of Sciences, Aleja Lotnikow 32/46, 02-668 Warsaw, Poland*

<sup>2</sup>*Department of Physics, Northern Illinois University, De Kalb, Illinois 60115, USA*

The layered perovskites of  $\text{RBaCo}_2\text{O}_{5+\delta}$  ( $R$  = lanthanide ion or Y) have been attracted much interest due to their fascinating physical properties, which can be tuned by a substitution at the  $R$ -, Ba- and Co-sites or by a change of oxygen index  $\delta$ . Compounds with  $\delta = 0.5$  are the most interesting for study as the Co ions are located in two distinct pyramid and octahedral coordinations to oxygen. The following sequence of magnetic and electronic phase transitions have been observed with increasing temperature for pure materials for which cobalt valence is +3 for both coordinations: antiferromagnet–ferro(ferri-)magnet (200 – 250 K), ferro(ferri-)magnet–paramagnet (260 – 290 K) and insulator–metal transition (320 – 350 K). The values of temperatures of these transitions depend on the ionic size of the  $R$ -site ion and on a degree of the oxygen nonstoichiometry  $\delta$ .

The magnetic properties of the hole doped  $\text{Nd}_{1-x}\text{Ca}_x\text{BaCo}_2\text{O}_{5.5}$  ( $x = 0 - 0.2$ ) system, for which both Co coordinations are preserved, have been recently reported. Upon  $\text{Ca}^{2+}$  substitution the temperature of antiferro–ferrimagnetic phase transition is drastically suppressed. At 10% substitution this magnetic transition vanishes and the antiferromagnetic order is absent down to 4 K. We have examined the effect of the hydrostatic pressure on magnetic properties of  $\text{Nd}_{1-x}\text{Ca}_x\text{BaCo}_2\text{O}_{5.5}$  system with  $\text{Ca}^{2+}$  substitution up to 6%, i.e. in the composition range where antiferro-ferrimagnetic phase transition is still present. Our measurements have revealed stabilization of antiferromagnetic phase as was evidenced by an increase of the Néel temperature ( $T_N$ ). The pressure coefficient of  $dT_N/dP$  was found to increase with increasing Ca substitution,  $dT_N/dP = 1.03, 1.43$  and  $3.1$  K/kbar for  $x = 0, 0.02$  and  $0.06$ , respectively. The value of  $dT_C/dP$  ( $0.62$  K/kbar) was smaller than  $dT_N/dP$  ( $1.03$  K/kbar) for  $\text{NdBaCo}_2\text{O}_{5.5}$ . In the case of  $\text{Nd}_{0.94}\text{Ca}_{0.06}\text{BaCo}_2\text{O}_{5.5}$ ,  $dT_C/dP$  changed the sign to negative ( $-0.29$  K/kbar). We also observed a decrease of saturation magnetization under hydrostatic pressure, at the temperature where ferrimagnetic phase is present (235, 225 and 155 K for  $x = 0, 0.02$  and  $0.06$ , respectively). This also points to stabilization of antiferromagnetic interactions under hydrostatic pressure.

*This work was partly supported by National Science Centre of Poland, no. 1662/B/H03/2011/40.*

# **TERAHERTZ STUDIES OF CHARGE ORDERING IN $\text{Nd}_{2/3}\text{Ca}_{1/3}\text{MnO}_3$ PEROVSKITE**

E. Fertman<sup>1</sup>, S. Dolya<sup>1</sup>, C. Kadlec<sup>2</sup>, F. Kadlec<sup>2</sup>, and A. Feher<sup>3</sup>

<sup>1</sup>*B. Verkin Institute for Low Temp. Physics and Eng., 47 Lenin Ave., 61103 Kharkov, Ukraine*

<sup>2</sup>*Institute of Physics, Na Slovance 2, 182 21 Prague 8, Czech Republic*

<sup>3</sup>*Institute of Physics, P. J. Šafárik University in Košice, 04154, Košice, Slovakia*

$\text{Nd}_{2/3}\text{Ca}_{1/3}\text{MnO}_3$  polycrystalline perovskite has been studied in temperatures 2 - 300 K by means of terahertz time-domain spectroscopy at frequencies 0.2 – 2 THz in magnetic fields up to 3 T. The THz measurements were performed in the Voigt geometry. Real and imaginary parts of a refractive index  $N = n + i \cdot \kappa$  were measured. Using the ratio  $N^2 = \varepsilon \cdot \mu$ , where  $\varepsilon$  is a dielectric permittivity and  $\mu$  is a magnetic permeability, temperature dependent  $\text{Re}(\varepsilon \cdot \mu)$  and  $\text{Im}(\varepsilon \cdot \mu)$  have been obtained (Fig. 1). The compound  $\text{Nd}_{2/3}\text{Ca}_{1/3}\text{MnO}_3$  is paramagnetic down to about 130 K and insulating at all temperatures and magnetic fields studied. Charge ordering at  $T_{CO} \sim 212$  K leads to the phase separated state of the compound.

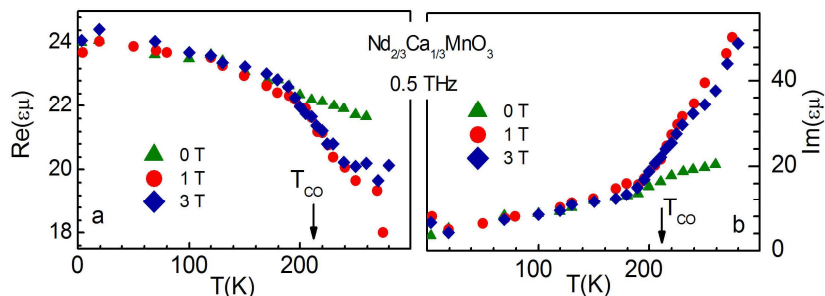


Fig. 1. Temperature dependences of (a)  $\text{Re}(\varepsilon \cdot \mu)$  and (b)  $\text{Im}(\varepsilon \cdot \mu)$ .

Temperature dependences of the  $\text{Re}(\varepsilon \cdot \mu)$  and  $\text{Im}(\varepsilon \cdot \mu)$  are found to change their slopes in the vicinity of  $T_{CO}$ . The refractive index has been found to be strongly magnetic field  $H$  dependent above charge ordering transformation, while it is practically independent on the  $H$  in the charge ordered state (below  $T_{CO}$ ). Above  $T_{CO}$  magnetic field applied leads to the drop of  $\text{Re}(\varepsilon \cdot \mu)$  (Fig. 1 a) and to the huge growth of  $\text{Im}(\varepsilon \cdot \mu)$  (Fig. 1 b). Also  $N$  is depend on the magnetic field history of the sample. Presumably the magnetic field affects the conduction mechanism in the compound above  $T_{CO}$ .

**FERROMAGNETISM IN THE KONDO-LATTICE  $\text{CePd}_2\text{P}_2$  COMPOUND**

V. H. Tran, Z. Bukowski, L. M. Tran, A. J. Zaleski

*Institute of Low Temperature and Structure Research,**Polish Academy of Sciences, P.O. Box 1410, 50-422 Wrocław, Poland*

We have synthesized a polycrystalline sample of intermetallic  $\text{CePd}_2\text{P}_2$  compound and have characterized its basic properties by measurements of x-ray diffraction, ac-magnetic susceptibility, magnetization, specific heat, electrical resistivity, magnetoresistance and Hall effect. The compound crystallizes in the tetragonal  $\text{CaBe}_2\text{Ge}_2$ -type structure (space group  $P4/nmm$ ) with the lattice parameters  $a = 0.41762$  and  $c = 0.95093$  nm at room temperature. The physical properties measurements establish a ferromagnetic ordering with the Curie temperature  $T_C = 28.4 \pm 0.2$  K. The ordered state is characterized by the magnetic moment  $M = 0.98 \mu_B$  and magnon energy gap of the order of magnitude  $\Delta/k_B = 25 - 50$  K. The specific heat and resistivity data, both consistently exhibit characteristic Kondo-lattice features with the Kondo temperature  $T_K \approx 20$  K.  $\text{CePd}_2\text{P}_2$  appears to be a new ferromagnetically ordered Kondo system. We discuss the observed behaviour in  $\text{CePd}_2\text{P}_2$  in the context of magnetic properties of other 122-type families of compounds, including the 122-FeAs-based superconductors.

*Acknowledgements*

*The authors acknowledge for the financial support from the project 2011/01/B/ST3/04553 of the National Science Centre of Poland.*

# **PULSED AND STEADY MAGNETIC FIELD STUDIES OF MAGNETIZATION IN $\text{Tm}_{1-x}\text{Yb}_x\text{B}_{12}$ DODECABORIDES WITH METAL-INSULATOR TRANSITION**

A. Bogach<sup>1</sup>, N. Sluchanko<sup>1</sup>, V. Glushkov<sup>1,2</sup>, S. Demishev<sup>1,2</sup>, A. Azarevich<sup>1,2</sup>,  
N. Shitsevalova<sup>3</sup>, V. Filipov<sup>3</sup>, S. Gabani<sup>4</sup>, K. Flachbart<sup>4</sup>, J. Stankiewicz<sup>5</sup>,  
J. Vanacken<sup>6</sup>, V. Moshchalkov<sup>6</sup>

<sup>1</sup>*A.M. Prokhorov General Physics Institute of RAS, 38 Vavilov str., 119991 Moscow, Russia*

<sup>2</sup>*Moscow Institute of Physics and Technology (State University), Institutskii per. 9, 141700, Dolgoprudnyi, Russia*

<sup>3</sup>*Institute for Problems of Materials Science NASU, 3 Krzhyzhanovsky str., 03680 Kiev, Ukraine*

<sup>4</sup>*Institute of Experimental Physics of SAS, 47 Watsonova, 040 01 Košice, Slovak Republic*

<sup>5</sup>*Instituto de Ciencia de Materiales de Aragón, CSIC-Universidad de Zaragoza, C/ Pedro Cerbuna 12, 50009 Zaragoza, Spain*

<sup>6</sup>*Institute for Nanoscale Physics and Chemistry (INPAC), Celestijnenlaan 200D, KU Leuven, Leuven 3001, Belgium*

Magnetization studies of strongly correlated electron systems - substitutional solid solutions  $\text{Tm}_{1-x}\text{Yb}_x\text{B}_{12}$  ( $x \leq 0.81$ ) with simultaneous antiferromagnetic-paramagnetic and metal-insulator transitions [1-2] have been carried out at low temperatures 1.8-40 K in steady (using SQUID and VSM magnetometers up to 5T and 11T, respectively) and in pulsed (up to 50T, using the INPAC installation of KU Leuven, pulse duration ~20-100 ms) magnetic fields. The detailed analysis of magnetization data yields two main contributions in the paramagnetic response. It is shown that these two paramagnetic components could be attributed to (i) localized magnetic moments ( $\sim 0.8\text{-}3.7 \mu_B$  per unit cell) whose magnetization is saturated at helium temperatures in the range of  $H/T$  values slightly above  $\sim 4$  T/K and to (ii) the Pauli type response from heavy fermions (many body resonance at  $E_F$  in the gap) whose density of states may be estimated to be approximately  $(3\div 4) \cdot 10^{21} \text{ cm}^{-3} \text{ meV}^{-1}$ . In addition, comparison between steady and pulsed field magnetization behaviors provides arguments in favor of the formation of nanosize antiferromagnetic clusters of  $\text{Tm}^{3+}$  and  $\text{Yb}^{3+}$  rare earth ions and the emergence of short range ordering effects in the  $\text{Tm}_{1-x}\text{Yb}_x\text{B}_{12}$  matrix.

[1] N. E. Sluchanko, A. N. Azarevich, A. V. Bogach, et al., JETP. **115**, 509 (2012)

[2] N.E. Sluchanko, A.V. Bogach, V.V. Glushkov et al., JETP Lett. **89**, 256 (2009)

**MAGNETIZATION STUDY OF  $\text{Cu}_x\text{TiSe}_2$  SINGLE CRYSTALS**P. Husaniková<sup>1,2</sup>, J. Fedor<sup>1</sup>, J. Déer<sup>1</sup>, J. Šoltýs<sup>1</sup>, and G. Karapetrov<sup>1,2</sup><sup>1</sup>*Institute of Electrical Engineering, SAS, Bratislava, 84104*<sup>2</sup>*Departement of Physics, Drexel University, Philadelphia, PA 19104*

We study superconducting properties of  $\text{Cu}_x\text{TiSe}_2$  single crystals by means of bulk magnetization measurements. We examine in detail several crystals with different level of copper doping and extract relevant superconducting properties. Our results indicate that anisotropy of upper critical fields is independent of copper doping, whereas penetration depth and Ginzburg-Landau parameter show strong doping dependence. Superconducting penetration depth is extracted from reversible magnetization curves at intermediate fields. We find that temperature dependence of the superconducting penetration depth is consistent with the single-gap BCS theory. Furthermore, superconducting critical current derived from magnetization hysteresis loops is low, decaying exponentially with applied magnetic field. This results in a wide reversible region in the vortex phase diagram of this material.

**HUND'S RULE INDUCED SPIN-TRIPLET PAIRING FOR ORBITALLY DEGENERATE CORRELATED ELECTRONS**M. Zegrodnik<sup>1</sup>, J. Spalek<sup>1</sup> and J. Büneemann<sup>2</sup><sup>1</sup>*AGH University of Science and Technology, Faculty of Physics and Applied Computer Science, Al. Mickiewicza 30, PL-30-059, Kraków, Poland*<sup>2</sup>*Max-Planck Institute for Solid State Research, Heisenbergstr. 1, D-70569 Stuttgart, Germany*

Spin-triplet superconductivity is believed to appear in  $\text{Sr}_2\text{RuO}_4$ ,  $\text{UGe}_2$ ,  $\text{URhGe}$ ,  $\text{UIr}$ , and  $\text{UCoGe}$ . In the last four compounds the paired phase coexists with ferromagnetism, while in others:  $\text{UNi}_2\text{Al}_3$  and  $\text{UPt}_3$ , the coexistence with antiferromagnetism has been observed. The question of microscopic mechanism that induces the spin-triplet paired phase still remains open.

In our considerations we analyze the Hund's-rule induced spin-triplet pairing for the case of two-band Hubbard model. This pairing mechanism can lead to pure superconducting states, as well as coexistent with magnetic ordering. To examine the influence of electron correlations on stability of the considered phases the so-called *statistically consistent Gutzwiller approximation* is applied. The obtained results are compared with those calculated with the use of the Hartree-Fock approximation.

**MAGNETIC PROPERTIES OF FeSe(Te) SUPERCONDUCTORS**

G.E. Grechnev<sup>1</sup>, A.S. Panfilov<sup>1</sup>, A.V. Fedorchenko<sup>1</sup>, V.A. Desnenko<sup>1</sup>,  
S.L. Gnatchenko<sup>1</sup>, D.A. Chareev<sup>2</sup>, O.S. Volkova<sup>3</sup> and A.N. Vasiliev<sup>3</sup>

<sup>1</sup>*B.Verkin Institute for Low Temperature Physics and Engineering, National Academy of Sciences of Ukraine, Kharkov 61013, Ukraine*

<sup>2</sup>*Institute of Experimental Mineralogy, Russian Academy of Sciences, Chernogolovka, Moscow District 142432, Russia*

<sup>3</sup>*Moscow State University, Physics Department, Moscow 119991, Russia*

Detailed magnetization studies for FeSe<sub>1-x</sub>Te<sub>x</sub> superconducting systems are carried out to investigate the behavior of the intrinsic magnetic susceptibility  $\chi$  in the normal state with temperature and under hydrostatic pressure. The intrinsic magnetic susceptibility  $\chi$  was estimated to increase gradually with Te content. A substantial growth of susceptibility with temperature is revealed for FeSe together with large anisotropy  $\Delta\chi$  for magnetic field applied along and perpendicular to tetragonal axis. A drastic drop in  $\chi(T)$  with decreasing temperature was observed in FeTe at  $T_N = 70$  K, which is closely related to the antiferromagnetic ordering.

The measurements of magnetic susceptibility for FeSe and FeTe under hydrostatic pressure revealed a strong positive effect at low temperatures. At room temperature, this effect is found to be also strong, but it is negative for FeSe and positive for FeTe. The estimated spontaneous change in volume of FeTe at the antiferromagnetic ordering is shown to be large enough and presumably hidden from direct detection because of the close interplay of the antiferromagnetic and structural phase transitions.

Ab initio calculations of the pressure dependent electronic structure and magnetic susceptibility in the normal state indicate that FeSe and FeTe are very close to magnetic instability with dominating enhanced spin paramagnetism. The calculated paramagnetic susceptibility exhibits a strong dependence on the unit cell volume and the height  $Z$  of chalcogen species from the Fe plane. The observed large positive pressure effects on  $\chi$  in FeTe and FeSe at low temperatures are related to considerable sensitivity of the paramagnetism to the internal parameter  $Z$ . It is shown that available experimental data on the strong and nonmonotonic pressure dependence of the superconducting transition temperature in FeSe correlate qualitatively with the calculated behavior of the density of electronic states at the Fermi level with pressure.

**SPIN POLARONIC EXCITATIONS IN THE GROUND STATE OF FeSi**

V. Glushkov<sup>1,2</sup>, E. Zhukova<sup>1,2,3</sup>, B. Gorshunov<sup>1,2,3</sup>, S. Demishev<sup>1,2</sup>, N. Sluchanko<sup>1</sup>, S. Kaiser<sup>3</sup> and M. Dressel<sup>3</sup>

<sup>1</sup>*Prokhorov General Physics Institute of RAS, 38, Vavilov str., Moscow 119991 Russia*

<sup>2</sup>*Moscow Institute of Physics and Technology, 9, Institutskii per., Dolgoprudny, Moscow Region 141700 Russia*

<sup>3</sup>*1. Physikalisches Institut, Universität Stuttgart, Pfaffenwaldring 57, Stuttgart 70550 Germany*

Renewed interest to strongly correlated semiconductor FeSi is inspired by recent theoretical and experimental studies [1-3], which treat this compound beyond the Kondo insulator model commonly applied. Our direct measurements of the complex optical conductivity  $\sigma(\nu)$  of FeSi discover a broad absorption in THz range (eigenfrequency  $\nu_0(4.2\text{ K}) \approx 32\text{ cm}^{-1}$ ) appearing in the optical spectra below 20 K [4]. The feature is unambiguously associated with spin-polaronic states formed in the middle of the gap ( $E_g=60\text{ meV}$ ), which contribute to the spin excitations between electron levels split by the exchange field of  $H_e=34 \pm 6\text{ T}$ . The spin-polaronic approach provides a clear interpretation of the double inversion of Hall coefficient established from the study of charge transport (resistivity and Hall effect) in FeSi. Actually, the sign of Hall effect is shown to be changed at  $T_{H1} \approx 75\text{ K}$  due to different temperature behavior of electron and hole mobilities in the regime of intrinsic conductivity, while onset of positive Hall effect below  $T_{H2} \approx 48.5\text{ K}$  is determined by the transition to charge transport via spin polarons. The estimations of concentration and Hall mobility result in the concentration and mobility values of  $n=10^{17}-10^{18}\text{ cm}^{-3}$  and  $\mu_H \leq 5\text{ cm}^2\text{V}^{-1}\text{s}^{-1}$ , respectively, which could be treated as effective characteristics of the states in the spin-polaronic band below 30 K. The results obtained support the Mott-Hubbard scenario of temperature induced metal-insulator transition in FeSi [5] and allow identifying spin fluctuations as the main factor, which determines the formation of spin-polaronic states and the rich magnetic phase diagram of FeSi.

[1] V.V. Mazurenko et al., Phys. Rev. B, **81**, 125131 (2010).

[2] D. Menzel et al., Phys. Rev. B, **79**, 165111 (2009).

[3] M. Arita et al., Phys. Rev. B, **77**, 205117 (2008).

[4] V.V. Glushkov et al., Phys. Rev. B, **84**, 073108 (2011).

[5] N. Sluchanko et al., Europhys.Lett. **51**, 557 (2000).



# **MAGNETIC EXCITATION SPECTROSCOPY IN $\text{EuCu}_2(\text{Si}_x\text{Ge}_{1-x})_2$ : BETWEEN VALENCE INSTABILITY AND MAGNETISM**

P.A. Alekseev<sup>1,5</sup>, K.S. Nemkovski<sup>2</sup>, V.N. Lazukov<sup>1</sup>, J.-M. Mignot<sup>3</sup>, R. Stewart<sup>4</sup>, A. P. Menushenkov<sup>5</sup>, A. V. Gribanov<sup>6</sup>

<sup>1</sup> NRC "Kurchatov Institute", Moscow, Russia

<sup>2</sup> Jülich Centre for Neutron Science, Forschungszentrum Jülich, Germany

<sup>3</sup> LLB, CEA/Saclay, Gif sur Yvette, France

<sup>4</sup> ISIS, Rutherford Appleton Laboratory, Didcot, UK

<sup>5</sup> National Research Nuclear University "MEPhI", Kashirskoe shosse 31, 115409, Moscow, Russia

<sup>6</sup> Department of Chemistry, Moscow State University, Moscow, Russia

$\text{EuCu}_2\text{Si}_x\text{Ge}_{2-x}$  series represents to date the only known case [1], among the variety of Eu- and Sm-based valence-unstable systems, where the state in the phase diagram is tuned from the valence-fluctuating one to heavy-fermion and then to, magnetic-ordered state, with possibility for existing of a quantum critical point near  $x \approx 0.3$ . Here we present the inelastic neutron scattering study of spin dynamics in  $\text{EuCu}_2\text{Si}_x\text{Ge}_{2-x}$  ( $x=1, 0.8, 0.5, 1.2$ ), performed in a wide temperature range (5-200K) related to the balt valence state of Eu defined by  $L_3$ -edge spectroscopy. Neutron scattering provide the detailed information about the spectral structure of dynamical magnetic response.

At  $x=1$  the magnetic excitation spectrum was found to be represented by the double-peak structure just below the energy range of the  $\text{Eu}^{3+}$  spin-orbit (SO) excitation  ${}^7F_0 \rightarrow {}^7F_1$ , so that at least the high-energy spectral component can be assigned to the renormalized SO transition. Change of the Eu valence towards 2+ with increase of the temperature and increase of Ge concentration results in further renormalization (lowering the energy) and gradual suppression of both inelastic peaks in the spectrum, along with developing sizeable quasielastic signal. The origin of the spectral structure and its evolution is discussed in terms of excitonic model for the mixed-valence state. Possible phase diagram of  $\text{EuCu}_2\text{Si}_x\text{Ge}_{2-x}$  is considered in connection with structure and its temperature evolution of magnetic response spectrum.

*This work have been supported by RFBR grant No. 11-02-00121 and 12-02 12077.*

[1] Z. Hossain, C. Geibel, N. Senthilkumaran, M. Deppe, M. Baenitz, F. Schiller, S. L. Molodtsov, Phys. Rev. B **69**, 014422 (2004).

**INVESTIGATION OF MIXED VALENCE STATE OF  $\text{Sm}_{1-x}\text{B}_6$  and  $\text{Sm}_{1-x}\text{La}_x\text{B}_6$  by XANES**

S. Gabáni<sup>1</sup>, K. Flachbart<sup>1</sup>, J. Bednarčík<sup>2</sup>, E. Welter<sup>2</sup>, V. Filipov<sup>3</sup> and N. Shitsevalova<sup>3</sup>

<sup>1</sup>*Centre of Low Temperature Physics, Institute of Experimental Physics, Slovak Academy of Sciences, Watsonova 47, SK-04001 Košice, Slovak Republic*

<sup>2</sup>*Deutsches Elektronen Synchrotron DESY, Notkestrasse 85, D-22603 Hamburg, Germany*

<sup>3</sup>*Institute for Problems of Materials Science, National Academy of Sciences of Ukraine, Krzhyzhanovsky 3, UA 03680 Kiev, Ukraine*

We investigated the valence states of samarium ions in Sm deficient  $\text{Sm}_{1-x}\text{B}_6$  ( $x = 0.03, 0.05, 0.08, 0.1$  and  $0.2$ ) sintered samples, in single crystalline solid solutions  $\text{Sm}_{1-x}\text{La}_x\text{B}_6$  ( $x = 0.16, 0.28, 0.4, 0.6$  and  $0.8$ ) as well as in a  $\text{SmB}_6$  single crystal by X-ray absorption near edge structure (XANES) between 4.2 and 300 K. It was shown that the mixed valence state  $\nu_{\text{Sm}}$  of Sm-ions ( $\nu_{\text{Sm}} \approx 2.53$  for  $\text{SmB}_6$  at 4.2 K) in deficient samples is changed but maintained up to a concentration of 20 % of vacancies and up to a concentration of 80 % in samples doped with trivalent La-ions, and that in both cases it increases with temperature. On the other hand, the value of  $\nu_{\text{Sm}}$  increases with increasing vacancy level whereas it decreases with increasing of  $\text{La}^{3+}$  substitution. The received dependences of Sm-valence in  $\text{SmB}_6$  on vacancy as well as on  $\text{La}^{3+}$  ion concentration are in good agreement with susceptibility measurements and exact numerical calculation of the spinless Falicov-Kimball model in two dimensions.

*This work was supported by the Slovak Scientific Agency VEGA (2/0106/13), the Slovak Research and Development Agency APVV 0132-11, and by the Center of Excellence of the Slovak Academy of Sciences.*

## P7-07

### INFLUENCE OF PRESSURE ON SUPERCONDUCTIVITY IN YB<sub>6</sub>

S. Gabáni<sup>1</sup>, G. Pristáš<sup>1</sup>, I. Takáčová<sup>1</sup>, K. Flachbart<sup>1</sup>, P. Samuely<sup>1</sup>, E. Gažo<sup>1</sup>, T. Mori<sup>2</sup> and D. Braithwaite<sup>3</sup>

<sup>1</sup>*Centre of Low Temperature Physics, Institute of Experimental Physics, Slovak Academy of Sciences, Watsonova 47, SK-04001 Košice, Slovak Republic*

<sup>2</sup>*National Institute for Materials Science, Namiki 1-1, JP-305-0044 Tsukuba, Japan*

<sup>3</sup>*SPSMS, UMR-E CEA / UJF-Grenoble 1, INAC, F-38054 Grenoble, France*

We present electrical resistivity measurements on superconducting system YB<sub>6</sub> ( $T_c \approx 7.5$  K) down to 60 mK at hydrostatic pressures up to 47 kbar. Obtained phase diagrams of the upper critical field,  $H_{c3}$  vs  $T$ , show a typical BCS behavior for all pressures, and a linear decrease of the zero-field transition temperature  $T_c$  as well as the zero-temperature value of  $H_{c3}$  with increasing pressure. The observed pronounced negative pressure effect on the upper critical field,  $d\ln H_{c3}/dp = -1.1\%/kbar$ , is significantly higher than this on critical temperature,  $d\ln T_c/dp = -0.59\%/kbar$ , which provides a critical pressure,  $p_c \approx 180$  kbar, at that  $T_c$  vanishes. Reasons leading to these observations are discussed.

*This work was supported by the Slovak Scientific Agency VEGA (2/0135/13), the Slovak Research and Development Agency APVV 0036-11, and by the Center of Excellence of the Slovak Academy of Sciences.*

**P7-08**

**ON THE THERMODYNAMIC CRITICAL FIELD FOR THE  
FULLERENES  $K_3C_{60}$  AND  $Rb_3C_{60}$**

A.P. Durajski and R. Szczęśniak

*Institute of Physics, Częstochowa University of Technology,  
Ave. Armii Krajowej 19, 42-200 Częstochowa, Poland*

In the paper, the temperature dependence of the thermodynamic critical field for the alkali-metal-doped fullerenes  $K_3C_{60}$  and  $Rb_3C_{60}$  has been considered. The numerical calculations have been conducted in the framework of the Migdal-Eliashberg formalism. It has been shown that the obtained results agree with the experimental data.

**CRITICAL MAGNETIC FIELD FOR CHLORINE HALIDE SUPERCONDUCTOR AT HIGH PRESSURE**D. Szczęśniak<sup>1</sup> and R. Szczęśniak<sup>2</sup><sup>1</sup> *Institute of Physics, Jan Długosz University in Częstochowa, Al. Armii Krajowej 13/15, 42200 Częstochowa, Poland*<sup>2</sup> *Institute of Physics, Częstochowa University of Technology, Al. Armii Krajowej 19, 42200 Częstochowa, Poland*

At present, hydrides are considered as a one of the most perspective high-temperature superconductors with the classical electron-phonon pairing mechanism. In the present work, we provide an analysis of the critical magnetic field ( $H_C$ ) dependence on the temperature for chlorine halide superconductor (HCl) within its new  $P2_1/m$  metallic phase. This is done in the framework of the Eliashberg formalism for selected high values of the pressure (320 and 360 GPa). Our results reveal that the  $H_C(T)$  values increase with the increase of the pressure. Furthermore, we show that the dimensionless ratio  $T_C C^N(T_C)/H_C^2(0)$  differs from the value predicted by the Bardeen-Cooper-Schrieffer theory;  $T_C$  and  $C^N$  denote the critical temperature and the specific heat of the normal state, respectively.

**STUDY OF NIOBIUM THIN FILMS UNDER PRESSURE**

Gabriel Pristáš<sup>1</sup>, Slavomír Gabáni<sup>1</sup>, Matúš Orendáč<sup>2</sup>, Vladimír Komanický<sup>2</sup> and Emil Gažo<sup>1</sup>

<sup>1</sup>*Centre of Low Temperature Physics, Institute of Experimental Physics, Slovak Academy of Sciences, Watsonova 47, 040 01 Košice, Slovakia*

<sup>2</sup>*Faculty of Science, P.J. Šafárik University, Park Angelinum 9, 041 54 Košice, Slovakia*

Niobium is widely used in many important superconducting applications. At ambient pressure, bulk Nb has the highest critical temperature,  $T_C \approx 9.25$  K among the superconducting elements. Thin films of Nb show several differences in behavior in comparison with bulk Nb, e.g. substantial increase in the upper critical field ( $H_{C2}$ ). Critical temperature of superconducting transition is usually lower for thin films than in bulk sample and depend on thickness of film, size of grains etc. In this study, we performed measurements of critical temperature and upper critical field by electrical resistivity measurements of Nb thin film under hydrostatic pressures up to 30 kbar. We prepared 100 nm thick niobium thin films in the high vacuum DC magnetron sputtering system, with  $T_C = 8.95$  K at ambient pressure. We observed increase of  $T_C$  with increasing value of pressure ( $dT_C/dp = 7.3$  mK/kbar) in spite of no change in  $H_{C2}$ . On the other side in the case of bulk sample of Nb we observed decrease of  $T_C$  value ( $dT_C/dp = -2.5$  mK/kbar) with increasing applied pressure. Difference in superconducting properties between niobium bulk and thin film under pressure is discussed.

# **SUPERCONDUCTIVITY IN $\text{YB}_6$ and $\text{ZrB}_{12}$ MEDIATED BY QUASILOCAL VIBRATIONS OF TRANSITION METAL IONS.**

N. Sluchanko<sup>1</sup>, S. Gavrilkin<sup>2</sup>, K. Mitsen<sup>2</sup>, A. Kuznetsov<sup>3</sup>, I. Sannikov<sup>3</sup>, A. Azarevich<sup>1,4</sup>, A. Bogach<sup>1</sup>, V. Glushkov<sup>1,4</sup>, S. Demishev<sup>1,4</sup>, A. Khoroshilov<sup>1,4</sup>, A. Lyashenko<sup>5</sup>, N. Shitsevalova<sup>5</sup>, V. Filipov<sup>5</sup>, K. Flachbart<sup>6</sup>, V. Moshchalkov<sup>7</sup>

<sup>1</sup>*A.M.Prokhorov General Physics Institute of RAS, 119991 Moscow, Russia*

<sup>2</sup>*P.N.Lebedev Physical Institute of RAS, 119991 Moscow, Russia*

<sup>3</sup>*National Research Nuclear University MEPhI, 115409 Moscow, Russia*

<sup>4</sup>*Moscow Institute of Physics and Technology, Moscow Region 141700 Russia*

<sup>5</sup>*Institute for Problems of Materials Science, NASU, 03680 Kiev, Ukraine*

<sup>6</sup>*Institute of Experimental Physics of SAS, 040 01 Košice, Slovak Republic*

<sup>7</sup>*Institute for Nanoscale Physics and Chemistry of KU Leuven, B-3001 Belgium*

On superconductors  $\text{ZrB}_{12}$  and  $\text{YB}_6$ , which exhibit a transition to cage-glass state at  $T^* \sim 100$  K, charge transport (resistivity, Hall and Seebeck coefficients), heat capacity  $C(T)$  and magnetization measurements have been carried out at high quality single crystals with various boron isotopes. From received results critical temperature  $T_C \approx 6$  K, thermodynamic field  $H_C \sim 420$  Oe, density of states (DOS) renormalization effect, electron-phonon interaction  $\lambda \sim 0.4-0.6$  and superconducting gap  $2\Delta(0) \sim 20.5$  K have been estimated and compared among  $\text{Zr}^{10}\text{B}_{12}$ ,  $\text{Zr}^{11}\text{B}_{12}$  and  $\text{Zr}^{\text{nat}}\text{B}_{12}$ . Our experiments reveal only slight changes both of the aforementioned characteristics in  $\text{ZrB}_{12}$  samples with various boron isotopes as well as of the deduced quasi-local mode frequencies  $\theta_{E1}(\text{ZrB}_{12}) \sim 200$  K and  $\theta_{E2,3}(\text{ZrB}_{12}) \sim 420-450$  K, which are responsible for the BCS-type superconductivity in this compound. The possibility of two-gap superconductivity in  $\text{ZrB}_{12}$  is analyzed too. Moreover, the superconducting state parameters observed for  $\text{ZrB}_{12}$  are compared with characteristics obtained in this study for the transition metal superconductor  $\text{YB}_6$  ( $T_C = 6-8.4$  K, depending on the stoichiometry of studied single crystals) in which the electron DOS  $N(E_F)$  is only slightly reduced in comparison with  $N(E_F)$  values of  $\text{ZrB}_{12}$ . It is proposed that the dramatic decrease of Einstein mode frequency in  $\text{YB}_6$  ( $\theta_E(\text{YB}_6) \sim 100$  K) is compensated by a strong enhancement of the electron-phonon interaction up to  $\lambda \sim 1$  in vicinity of the *bcc* lattice instability developed in yttrium hexaboride. We discuss also the formation of two level systems (TLS) in these compounds with loosely bounded states of  $\text{Y}^{3+}$  and  $\text{Zr}^{4+}$  ions embedded in the rigid boron cage, and the role of these TLS in the suppression/enhancement of superconductivity in  $\text{RB}_6$  and  $\text{RB}_{12}$  borides.

**HIGH FIELD MAGNETIC TRANSITION IN MnSi**

I.I. Lobanova<sup>1</sup>, V.V. Glushkov<sup>1,2</sup>, V.Yu. Ivanov<sup>2</sup>, A.V.Semenov<sup>2</sup>, N.E. Sluchanko<sup>2</sup>  
and S.V. Demishev<sup>1,2</sup>

<sup>1</sup>*Moscow Institute of Physics and Technology (State University), 9,  
Institutskiy per., 141700 Dolgoprudny, Russia*

<sup>2</sup>*Prokhorov General Physics Institute, 38, Vavilov street, 119991 Moscow, Russia*

Strongly correlated electron system MnSi is known for decades as an archetypal example of itinerant magnet with helicoidal ordering at  $T=29$  K [1]. The quantum criticality under high pressure [2], the formation of skyrmion state [3] and topological Hall effect observed below 0.6 T near  $T_C$  [4] are hot topics of modern studies of this material. However, recent experiments explain the features of electron spin resonance by the excitations of Heisenberg magnetic moments at  $B>2$  T [5] thus contradicting to the itinerant magnetism of MnSi.

To shed more light on the nature of magnetic states in MnSi, we have probed the paramagnetic (PM) and spin-polarized (SP) phases by resistivity, magnetoresistance (MR) and magnetization (M) measurements in wide temperature range (2-300 K) in magnetic fields up to 8 T. A universal relation between MR and M  $\Delta\rho/\rho = -a_0 M^2$  ( $a_0 = \text{const}(T)$ ) has been discovered in the PM phase of MnSi. This relation is shown to be valid in a wide range of temperatures corresponding to the change of MR by more than 2 orders in magnitude. The breakdown of this relation defines position of the boundary between the PM and SP phases. It was found that in contrast to previous investigations this phase boundary is almost vertical and corresponds to  $T_C \sim 30$  K [6]. The analysis of Hall resistivity shows that Hall coefficient falls down abruptly from  $R_H = 1,64 \cdot 10^{-4} \text{ cm}^3/\text{C}$  (PM,  $T > T_C$ ) to  $R_H = 1,15 \cdot 10^{-4} \text{ cm}^3/\text{C}$  (SP,  $T < T_C$ ) at the transition point to the low-temperature SP phase. The sharp increase in the concentration of the charge carriers in MnSi at  $T \sim T_C$  correlates with the obtained magnetic phase diagram of MnSi [6] and supports the model of localized magnetic moments proposed for this unusual material [5-6].

[1] T. Moriya *Spin fluctuations in itinerant electron magnetism*, Springer-Verlag, 1985

[2] D. Belitz et al., Phys. Rev. Lett., **94**, 247205 (2005)

[3] A. Tonomura et al., Nano Lett., **12**, 1673 (2012)

[4] A. Neubauer et al., Phys. Rev. Lett., **102**, 186602 (2009)

[5] S.V. Demishev et al., JETP Letters, **93**, 231 (2011)

[6] S.V. Demishev et al., Phys. Rev. B, **85**, 045131 (2012)



## P7-13

### HALL EFFECT IN FERROMAGNETIC STATE OF $\text{La}_{1-x}\text{Ca}_x\text{MnO}_3$ ( $x=0.23, 0.3$ )

V. Glushkov<sup>1,2</sup>, M. Anisimov<sup>1</sup>, I. Lobanova<sup>2</sup>, S. Demishev<sup>1,2</sup>, N. Sluchanko<sup>1</sup>, N. Kozlovskaya<sup>3</sup> and Ya. Mukovskii<sup>3</sup>

<sup>1</sup>*Prokhorov General Physics Institute of RAS, 38, Vavilov str., Moscow 119991 Russia*

<sup>2</sup>*Moscow Institute of Physics and Technology, 9, Institutskii per., Dolgoprudny, Moscow Region 141700 Russia*

<sup>3</sup>*National University of Science and Technology "MISiS", 4 Leninskii av., Moscow 119049 Russia*

We report the study of Hall effect carried out on  $\text{La}_{1-x}\text{Ca}_x\text{MnO}_3$  single crystals ( $x=0.23, 0.3$ ) at temperatures 4.2-300K using experimental technique with the step-by-step rotation of sample in steady magnetic field (up to 8 T) [1]. Odd component of transverse resistivity  $\rho_{xy}=\rho_H\cos\varphi$  ( $\varphi$  – the angle between the normal to the plane of sample and applied magnetic field) allows separating between normal and anomalous contributions to Hall resistivity:  $\rho_H=R_H H+\rho_H^{\text{an}}$  ( $R_H$  – Hall coefficient). Reduced carrier concentration  $n/n_{\text{Mn}}=(R_H n_{\text{Mn}} e)^{-1}=1\div 2$  ( $n_{\text{Mn}}$  – concentration of Mn ions) for  $\text{La}_{0.7}\text{Ca}_{0.3}\text{MnO}_3$  seems to result from two groups of charge carriers (holes and electrons) with mobility  $|\mu|=3\div 5 \text{ cm}^2\text{V}^{-1}\text{s}^{-1}$ . The anomalous Hall resistivity  $\rho_H^{\text{an}}$  is found to follow to scaling behavior  $\rho_H^{\text{an}}\sim\rho^{1.5}$ , which differs drastically from  $\rho_H^{\text{an}}\sim\rho^\alpha$  with exponent  $\alpha=0.2\div 0.4$  expected for "bad-metal" regime ( $\rho>10^{-4} \Omega\cdot\text{cm}$ ) [2].

Additionally, even contribution to Hall resistivity  $\rho_{xy}^{\text{S}}=\rho_{\text{H2}}\cos(2\varphi+\Delta\varphi)$  ( $\Delta\varphi\approx\pi/4$ ) is detected below Curie point for  $x=0.3$  compound. The observation that  $\rho_{xy}^{\text{S}}$  is not magnetoresistance artifact is proved by 100-fold difference between  $\rho_{\text{H2}}$  and anisotropy of transverse magnetoresistance. Allowing for the trend  $\rho_{\text{H2}}\rightarrow 0$  with both temperature lowering and field increasing, we argue that the even component  $\rho_{xy}^{\text{S}}$  forbidden by the symmetry of crystal [3] appears as anomalous contribution due to short range antiferromagnetic correlations. Estimation of antiferromagnetic Hall coefficient  $R_H^{\text{L}}$  gives the values of  $R_H^{\text{L}}\geq 0,06\div 0,14 \text{ cm}^3\text{C}^{-1}$ , which exceed the anomalous Hall coefficient  $R_H^{\text{A}}(T\leq 150 \text{ K})=0,002\div 0,03 \text{ cm}^3\text{C}^{-1}$  supporting the suggested interpretation of Hall effect in the ferromagnetic state of optimally doped manganites.

[1] N. Sluchanko et al., JETP, 98, 793 (2004).

[2] N. Nagaosa et al., Rev. Mod. Phys, 82, 1539 (2010).

[3] C.M. Hurd, Adv. Phys., 23, 315 (1974).

**TRANSPORT PROPERTIES OF GdB<sub>6</sub>**

M. Anisimov<sup>1</sup>, V. Glushkov<sup>1,2</sup>, A. Bogach<sup>1</sup>, S. Demishev<sup>1,2</sup>, N. Samarin<sup>1</sup>,  
 N. Shitsevalova<sup>3</sup>, A. Levchenko<sup>3</sup>, V. Filipov<sup>3</sup>, A. Kuznetsov<sup>4</sup>, K. Flachbart<sup>5</sup>,  
 N. Sluchanko<sup>1</sup>

<sup>1</sup>*A.M. Prokhorov General Physics Institute of RAS, Vavilov str. 38, 119991 Moscow, Russia*

<sup>2</sup>*Moscow Institute of Physics and Technology (State University), Institutskii per. 9, 141700, Dolgoprudnyi, Russia*

<sup>3</sup>*I. N. Frantsevich Institute for Problems of Materials Science NASU, Krzhizhanovskiy str. 3, 03680 Kiev, Ukraine*

<sup>4</sup>*Moscow Engineering Physics Institute, Kashirskoe sh. 31, 115409 Moscow, Russia*

<sup>5</sup>*Institute of Experimental Physics of SAS, Watsonova str. 47, 040 01 Košice, Slovak Republic*

In present work transport properties of gadolinium hexaboride (GdB<sub>6</sub>) have been investigated. Although Gd<sup>3+</sup> ion does not have orbital degrees of freedom ( $L=0$ ,  $S=7/2$ ) the compound GdB<sub>6</sub> undergoes two successive phase transitions with simultaneous structural distortion and antiferromagnetic (AF) ordering. Below  $T_N \approx 15.5$  K the magnetic structure is characterized by a wave vector  $\mathbf{k}_m = [1/4, 1/4, 1/2]$  and a structural modulation by  $\mathbf{q}_1 = [0, 0, 1/2]$ . This modulated structure is slightly transformed at  $T^* \approx 4.7-9$  K, and other modulated structures with  $\mathbf{q}_2 = [0, 1/2, 1/2]$  and  $\mathbf{k}_m$  are superimposed. However, the nature of the magnetic ground state in GdB<sub>6</sub> is still a subject of discussion.

To shed more light on the mechanisms responsible for the unusual magnetic ordering, a comprehensive study of transverse magnetoresistance (MR) and Hall effect has been carried out on high quality single crystals of GdB<sub>6</sub> in the temperature range 2-120 K and magnetic fields up to 8 T. The data obtained allow to detect the anomalies on transport characteristics at  $T_N$  including (i) the crossover of MR regimes and (ii) the drastic enhancement of negative Hall coefficient ( $\Delta R_H/R_H \sim 121\%$ ). The transition to AF(II) state below  $T^*$  is accompanied by a complex behavior of MR with field hysteresis on  $\Delta\rho(H)/\rho$  curves. We also detect the appearance of anomalous Hall effect at  $T < T^*$ . The analysis of  $\Delta\rho(H)/\rho$  allows to separate contributions to MR of GdB<sub>6</sub> in accordance with the procedure developed previously for other AF hexaborides (CeB<sub>6</sub>, PrB<sub>6</sub> and NdB<sub>6</sub>). The results of the complex analysis of charge carriers transport allow to support both the hypothesis of Gd<sup>3+</sup> ions displacement and the effects of 5d-states spin density polarization in AF and PM phases of GdB<sub>6</sub>.

## P7-15

### DEFECT MODE AND HEAVY FERMIONS IN $\text{Ce}_x\text{La}_{1-x}\text{B}_6$ ( $x \leq 0.03$ )

M. Anisimov<sup>1</sup>, V. Glushkov<sup>1,2</sup>, A. Bogach<sup>1</sup>, S. Demishev<sup>1,2</sup>, N. Samarin<sup>1</sup>, S. Gavrilkin<sup>3</sup>, K. Mizen<sup>3</sup>, N. Shitsevalova<sup>4</sup>, A. Levchenko<sup>4</sup>, V. Filipov<sup>4</sup>, S. Gabani<sup>5</sup>, K. Flachbart<sup>5</sup>, N. Sluchanko<sup>1</sup>

<sup>1</sup>*A.M. Prokhorov General Physics Institute of RAS, Vavilov str. 38, 119991 Moscow, Russia*

<sup>2</sup>*Moscow Institute of Physics and Technology (State University), Institutskii per. 9, 141700, Dolgoprudnyi, Russia*

<sup>3</sup>*P.N. Lebedev Physical Institute of RAS, Leninskii Prospect 53, 119991 Moscow, Russia*

<sup>4</sup>*I.N. Frantsevich Institute for Problems of Materials Science NASU, Krzhyzhanovskiy str. 3, 03680 Kiev, Ukraine*

<sup>5</sup>*Institute of Experimental Physics of Slovak Academy of Science, Watsonova str. 47, 040 01 Košice, Slovak Republic*

Rare earth (RE) hexaborides  $\text{RB}_6$  represent a class of compounds with a variety of interesting physical properties including antiferromagnetic (R-Ce, Pr, Nd, Gd, Dy, Tb, Ho), ferromagnetic ( $\text{EuB}_6$ ), intermediate valence ( $\text{SmB}_6$ ) and heavy fermion behavior ( $\text{CeB}_6$ ). At the same time the nonmagnetic reference compound  $\text{LaB}_6$  plays an important role for estimating the magnetic contribution in the thermodynamic properties of  $\text{RB}_6$  and dilute systems  $\text{R}_x\text{La}_{1-x}\text{B}_6$ .

In present work we investigate the heat capacity of high quality single crystals of hexaborides  $\text{Ce}_x\text{La}_{1-x}\text{B}_6$  ( $x=0, 0.01, 0.03$ ) in a wide range of temperatures 0.4-300 K. In order to detect the defect-mode contribution  $\text{La}^{\text{N}}\text{B}_6$  single crystals with various boron isotope content ( $N = 10, 11$ , natural) were additionally studied. The data obtained allow to estimate correctly (i) the electronic  $\gamma T$  term of heat capacity ( $\gamma \approx 2.4 \text{ mJ/mol}\cdot\text{K}^2$ ), (ii) the contribution from quasilocal vibrating mode of  $\text{R}^{3+}$  ions ( $\Theta_E \approx 150\text{-}152 \text{ K}$ ), (iii) the Debye-type term from rigid boron cages ( $\Theta_D \approx 1160 \text{ K}$ ). Our data also suggest an additional defect-mode component (iv) which is provided by the contribution of 1.5-2.3% boron vacancies in  $\text{RB}_6$  [1]. The obtained results may be interpreted in terms of two level systems formation, which appear when  $\text{R}^{3+}$  ions are displaced from their centrosymmetric positions in the cavities of rigid boron cages towards randomly distributed boron vacancies in the  $\text{RB}_6$  matrix. Moreover, an alternative scenario of the genesis of heavy fermions is proposed for dilute systems with magnetic impurities  $\text{Ce}_x\text{La}_{1-x}\text{B}_6$  ( $x = 0.01, 0.03$ ).

[1] M.M.Korsukova, V.N.Gurin et al., J. Less-Common. Met. **117**, 73 (1986).

**SPECTRAL AND TRANSPORT PROPERTIES OF A  
SUPERCONDUCTING QUANTUM DOT SYSTEM**V. Pokorný<sup>1</sup>, V. Janiš<sup>1</sup>, M. Žonda<sup>2</sup> and T. Novotný<sup>2</sup><sup>1</sup>*Institute of Physics, Academy of Sciences of the Czech Republic,  
Na Slovance 2, 18221 Prague, Czech Republic*<sup>2</sup>*Faculty of Mathematics and Physics, Charles University in Prague,  
Ke Karlovu 5, 12116 Prague, Czech Republic*

We study the Josephson current through a quantum dot embedded between two superconductors showing a phase difference. The system is described by a single-impurity Anderson model coupled to BCS superconducting leads. We utilize diagrammatic perturbation techniques in the Coulomb interaction to capture the relevant physical phenomena. We study the effect of Coulomb interaction on the Andreev bound states present in the electronic spectrum and transport properties, particularly the current-phase relation and the emergence of the pi-junction behavior. Results of the Hartree-Fock approximation, second-order perturbation theory and the random phase approximation at zero temperature are presented.

# **EFFECTS OF Ga/ Ba NONSTOICHIOMETRY IN $\text{Ga}_{1+x}\text{Ba}_{2-x}\text{Cu}_3\text{O}_{7-\delta}$ ON SUPERCONDUCTING AND MAGNETIC PROPERTIES**

M. Škrátek, A. Cigán, R. Bystrický, J. Maňka, A. Dvurečenskij and M. Majerová

*Department of Magnetometry, Institute of Measurement Science*

*Slovak Academy of Sciences, Dúbravská cesta, 9, 841 04 Bratislava, Slovakia*

Effects of slight nonstoichiometry in  $\text{Ga}_{1+x}\text{Ba}_{2-x}\text{Cu}_3\text{O}_{7-\delta}$  compounds on superconducting and magnetic properties were studied. The compounds belong, e.g., to LRE-123 superconductors, in which LRE - light rare earth cations (where LRE = Nd, Sm, Eu and Gd) can form solid solutions with Ba ions. Among the elements, gadolinium has the highest Gennes factor, which indicates an exchange interaction of Ge ions. Moreover, between them, only its total orbital magnetic moment is zero.

Two series of single-phase samples of  $\text{Gd}_{1+x}\text{Ba}_{2-x}\text{Cu}_3\text{O}_{7-\delta}$  with composition deviation  $x$  from the stoichiometric value of 0 to 0.1 (A samples) and from  $-0.1$  to 0 (B samples) were synthesized by the solid-state reaction method from  $\text{Gd}_2\text{O}_3$ ,  $\text{BaCO}_3$  and  $\text{CuO}$  precursors and sintered at the temperature of  $\sim 1012^\circ\text{C}$  in flowing oxygen. All the samples with  $(-0.02 \leq x \leq 0.01)$  show critical temperature  $T_c$  above 93 K. The 10-90 %  $\Delta T_c$  about 1 K up to almost  $x \leq \pm 0.04$  confirms, together with XRD, good quality samples.

The magnetization  $M(H)$  curves were measured at the temperatures of 20, 77, and 100 K and effects of nonstoichiometry with the point of critical current density have been studied. Temperature dependence of the zero-field cooled (ZFC) and field cooled (FC) DC magnetic moment and magnetization  $M(H)$  curves were measured by the QD SQUID magnetometer MPMS XL-7 at the small and high applied magnetic field  $H$ . The corresponding ZFC dependences of molar susceptibility at field  $H$  ( $1.59 \text{ kAm}^{-1}$ ) were determined and fitted by the Curie–Weiss law. The dependences of values of the Curie constant and the effective magnetic moment on the composition deflection  $x$  have been investigated. In addition, the same was done for the applied magnetic field of  $5.57 \text{ MA m}^{-1}$ . The ZFC molar susceptibilities at the high field show a transition from paramagnetic to antiferromagnetic ordering. The values of the Neel temperature  $T_N$  about 4 K were estimated from the maximum molar susceptibility at low temperatures, as well as the values of Weiss temperature  $\theta$  being of the order of some (negative) units. The obtained results at a low and high magnetic field will be compared and confronted with the public data and discussed with respect to the 3-D ordering of  $\text{Ge}^{3+}$  ions and the mechanism responsible for their ordering without influencing the superconducting state.

**PHASE DIAGRAM OF TmB<sub>4</sub> UNDER PRESSURE**

S. Gabáni<sup>1</sup>, G. Pristáš<sup>1</sup>, I. Takáčová<sup>1</sup>, K. Flachbart<sup>1</sup>, V. Soltészová<sup>1</sup>, J. Kačmarčík<sup>1</sup>, V. Filipov<sup>2</sup>, N. Shitsevalova<sup>2</sup> and K. Siemensmeyer<sup>3</sup>

<sup>1</sup>*Centre of Low Temperature Physics, Institute of Experimental Physics, Slovak Academy of Sciences, Watsonova 47, SK-04001 Košice, Slovak Republic*

<sup>2</sup>*Institute for Problems of Materials Science, NASU, 3 Krzhynanovskiy St., UA-03680 Kiev, Ukraine*

<sup>3</sup>*Helmholtz Zentrum Berlin, Glienicker Str. 100, D-14109 Berlin, Germany*

TmB<sub>4</sub> is a Shastry-Sutherland frustrated system which exhibits very complex magnetic properties. In this contribution the phase diagram magnetic field vs temperature of TmB<sub>4</sub> under hydrostatic pressure up to 31 kbar is investigated using sensitive ac-resistance measurements. Temperature and magnetic field dependences of resistance at various pressures were carried out in a piston cylinder pressure cell between 1.7 and 14 K and in magnetic fields up to 6 T. The received results exhibit shifts of ordering temperature  $T_N$  as well as shifts of boundaries between different magnetic phases. The observed pressure dependence of  $T_N$  can be described by the relation  $d\ln T_N/dp = +0.11\%/kbar$ . The effect of pressure on various interactions in this compound is discussed.

*This work was supported by the Slovak Scientific Agency VEGA (2/0106/13), the Slovak Research and Development Agency APVV 0132-11, and by the Center of Excellence of the Slovak Academy of Sciences.*

## INFLUENCE OF Sm AND Yb POLLUTION ON SUPERCONDUCTING PROPERTIES OF YBCO BULK SUPERCONDUCTORS

D. Volochová<sup>1</sup>, K. Jurek<sup>2</sup>, M. Radušovská<sup>1</sup>, S. Piovarči<sup>1</sup>, V. Antal<sup>1</sup>, J. Kováč<sup>1</sup>  
M. Jirsa<sup>2</sup> and P. Diko<sup>1</sup>

<sup>1</sup> Institute of Experimental Physics SAS, Watsonova 47, 040 01 Košice, Slovak Republic

<sup>2</sup> Institute of Physics ASCR, Na Slovance 2, CZ-182 21 Prague 8, Czech Republic

YBa<sub>2</sub>Cu<sub>3</sub>O<sub>7-δ</sub> (YBCO, Y-123) bulk superconductors with a nominal composition Y<sub>1.5</sub>Ba<sub>2</sub>Cu<sub>3</sub>O<sub>x</sub> and 1 wt% CeO<sub>2</sub> addition were prepared by the Top Seeded Melt Growth (TSMG) process. Small single-crystalline pieces cut from the SmBa<sub>2</sub>Cu<sub>3</sub>O<sub>y</sub> (Sm-123) bulk were used for seeding of epitaxial growth. Wavelength-dispersive spectrometry (WDS) confirmed the presence of 0.1 wt% Sm and 0.25 wt% Yb practically in the whole sample volume. The influence of this Sm and Yb contamination on superconducting properties of grown bulks is shown. Different experiments were realized in order to decrease the pollution of prepared samples. Using a NdBa<sub>2</sub>Cu<sub>3</sub>O<sub>z</sub> (Nd-123) seed and a combination of Y<sub>2</sub>O<sub>3</sub> and Yb<sub>2</sub>O<sub>3</sub> substrate led to a high critical temperature,  $T_c$  of prepared samples. In this case, the pronounced peak effect in  $J_c(B)$  dependence was suppressed (77 K, H // c).

### Acknowledgment

*This work was realized within the framework of the projects: Centre of Excellence of Advanced Materials with Nano- and Submicron Structure (ITMS 26220120019), Infrastructure Improving of Centre of Excellence of Advanced Materials with Nano- and Submicron- Structure (ITMS 26220120035), New Materials and Technologies for Energetics (ITMS 26220220061), Research and Development of Second Generation YBCO Bulk Superconductors (ITMS 26220220041), which are supported by the Operational Programme 'Research and Development' financed through the European Regional Development Fund, VEGA project No. 2/0090/13 and SAS Centre of Excellence: CFNT MVEP.*

# **THERMODYNAMIC AND MAGNETOTRANSPORT PROPERTIES OF HIGH QUALITY $\text{Na}_{0.77}\text{CoO}_2$ SINGLE CRYSTAL**

A. Baran<sup>1</sup>, A. Zorkovská<sup>2</sup>, M. Kajňáková<sup>3</sup>, C. T. Lin<sup>4</sup> and A. Feher<sup>3</sup>

<sup>1</sup>*Faculty of Manufacturing Technologies with seat in Prešov, Technical University of Košice, Bayerova 1, 080 01 Prešov, Slovak Republic*

<sup>2</sup>*Institute of Geotechnics, Slovak Academy of Science, Watsonova 45, 040 01 Košice, Slovak Republic*

<sup>3</sup>*Institute of Physics, Faculty of Science, P.J. Šafárik University, Park Angelinum 9, 041 54 Košice, Slovak Republic*

<sup>4</sup>*Max-Planck-Institute for Solid State Research, Heisenbergstrasse 1, D-70569 Stuttgart, Germany*

Low temperature thermodynamic and transport properties of high- quality  $\text{Na}_{0.77}\text{CoO}_2$  single crystal were systematically studied as a function of temperature and magnetic field. The specific heat and the electrical resistivity in four point arrangement have been measured using the conventional Quantum Design PPMS-9 equipment.

Anomalies at 20 K have been observed both in the specific heat and the electrical resistivity.

The broad bump in the temperature dependence of specific heat indicates a smeared magnetic phase transition. Applied magnetic field up to 9 T reduces the temperature of this anomaly in accordance with the assumption of A-type antiferromagnetic ordering. The electronic specific heat coefficient  $\gamma = 11.1 \text{ mJ/molK}^2$  indicates strong electron correlations.

The observed low temperature upturn in electrical resistivity below 20 K is sensitive to the applied magnetic field: the temperature of resistivity minimum follows the same field dependence as the magnetic transition temperature estimated from the specific heat. On the other hand, magnetic field only slightly suppresses the upturn. The observed anomaly is probably the consequence of the interplay of several various mechanisms. The best fit of the low-temperature resistivity upturn at all magnetic fields can be obtained by considering electron-electron interactions in terms of  $T^{1/2}$  dependence, Kondo-like spin dependent scattering in terms of  $\ln T$  dependence, and electron-phonon scattering in terms of  $T^5$  dependence.



**APPLICATION OF SUPERCONDUCTOR/PHOTOSEMICONDUCTOR CONTACT STRUCTURES IN ELECTRONICS**V. Bunda<sup>1</sup>, S. Bunda<sup>1</sup>, V. Komanicky<sup>2</sup> and A. Feher<sup>2</sup><sup>1</sup> *Faculty of Information technologies, Transcarpathian State University, Zankovetska 87-B, 880 15 Uzhgorod, Ukraine*<sup>2</sup> *Centre of Low Temperature Physics, Faculty of Science P. J. Šafárik University & Institute of Experimental Physics, Slovak Academy of Sciences, Park Angelinum 9, Kosice 04154, Slovakia*

The integration of high temperature superconductors (HTSC's) with conventional semiconductor (SeC) - based technology would have important consequences for micro- and cryophotoelectronics, with the promise of high performance hybrid circuits incorporating the best of what superconductors and semiconductors have to offer as well as the possibility for novel devices.

HTSC's are considered to be low carrier density materials. Therefore, the light can penetrate the superconductor and can effectively excite the quasiparticles in it. The study of light detection by a "HTSC – photosemiconductor" hybrid contact structures (HCS's) is very perspective for fabrication of multifunctional photonic circuits - high speed detectors with reasonable sensitivity covering a broad electromagnetic spectrum.

The special magnetic and transport properties of Cooper pairs provide new applications in the field of tunnel contacts, electronic devices and the generation of very high magnetic fields. Compared to classical ultrasonic sources, superconducting tunnel contacts emit phonons with higher frequency. Therefore, the properties of different HTSC/photosemiconductor heterojunctions are of great interest for the development of new electronic devices such as diodes with very high rectifying parameters and transistors based on the Josephson field effect.

In recent years, two-dimensional (2D) nanostructured materials, such as nanoplates and nanosheets, have attracted much attention because of not only their unique electronic, magnetic, optical, and catalytic properties, which mainly arise from their large surface areas, nearly perfect crystallinity, structural anisotropy, and quantum confinement effects in the thickness. The potential of 2D nanostructured materials uses for building blocks for advanced materials and devices with designed functions in areas as diverse as lasers, transistors, catalysis, solar cells, light emission diodes, chemical and biological sensors. We report physical properties of YBCO/BiOX and Nb/BiOX contact structures (X- halogen).

## CHANGES IN YBCO SINGLE GRAIN BULK SUPERCONDUCTOR EXPOSED TO AIR MOISTURE

S. Piovarči, V. Antal, M. Kaňuchová, M. Radušovská, P. Diko

<sup>1</sup>*Institute of experimental physics Slovak academy of sciences, Watsonova 47, 040 01 Košice, Slovakia*

Influence of exposition of YBCO superconductor on air was studied on bulk single grain samples. Increasing of the sample weight caused by reaction with air moisture was observed by weighing the samples over two months. Thermal analyses and mass spectrometry has shown evolution of water and carbon dioxide during sample heating. Observation with scanning electron microscope confirmed formation of some nanosize phases at the (001) surfaces and on surfaces of pores in the bulk. XPS spectra done on freshly cleaved and air exposed (001) surfaces confirmed changes in Ba and Cu bonds at the surfaces.

### *Acknowledgements*

*This work was realized within the framework of the projects: Centre of Excellence of Advanced Materials with Nano- and Sub- micron Structure (ITMS26220120019), Infrastructure Improving of Centre of Excellence of Advanced Materials with Nano-and Sub- micron- Structure (ITMS26220120035), New Materials and Technologies for Energetics (ITMS26220220061), Research and Development of Second Generation YBCO Bulk Superconductors (ITMS26220220041), which are supported by the Operational Programme 'Research and Development' financed through the European Regional Development Fund, VEGA Project no.2/0090/13, and SAS Centre of Excellence: CFNTMVEP.*

**MICROSTRUCTURE AND PROPERTIES OF****Y-123/Y-211 BULK SUPERCONDUCTORS WITH BaCeO<sub>3</sub> AND BaO<sub>2</sub> ADDITION**

K. Zmorayova, M. Radusovska, S. Piovarci, V. Antal, J. Kovac and P. Diko

*Institute of experimental physics Slovak academy of sciences, Watsonova 47, 040 01 Košice, Slovakia*

YBCO bulk single-grain superconductors were prepared by Top-Seeded Melt-Growth process. CeO<sub>2</sub>, BaCeO<sub>3</sub> and BaO<sub>2</sub> powders were added to nominal composition Y<sub>1.5</sub>Ba<sub>2</sub>Cu<sub>3</sub>O<sub>7</sub> with the aim to refine Y-211 secondary particles, which provide pinning. Added powders were refined by friction milling and characterized by X-ray powder diffractometry. The system behavior was characterized by thermal analyses. Microstructure of prepared samples was studied by polarized light microscopy, scanning electron microscopy with EDAX and WDX microanalyses. Transition temperatures and the field dependences of the magnetic moment for further determination of the critical current densities were obtained using a vibrating – sample magnetometer. Trapped field at 77 K was measured.

**MICROSTRUCTURE AND PROPERTIES OF  
Y123/Y211 BULK SUPERCONDUCTORS WITH Y211 ADDITION**

M. Sefcikova, S. Piovarci, V. Antal, J. Kovac and P. Diko

*Institute of experimental physics Slovak academy of sciences, Watsonova 47, 040  
01 Košice, Slovakia*

The YBCO bulk single-grain superconductors were prepared by Top-Seeded Melt-Growth process. The  $\text{Y}_2\text{BaCuO}_5$  (Y211) phase refined to different particle sizes was added to  $\text{YBa}_2\text{Cu}_3\text{O}_7$  (Y123) powder. The Y211 powder was refined by attrition milling and characterized by laser granulometry and by X-ray powder diffractometry. The system behaviour at heating was characterized by thermal analyses. Microstructure of prepared samples was studied by polarized light microscopy, scanning electron microscopy with EDAX and WDX microanalyses. The transition temperatures and field dependences of magnetic moment for further determination of critical current densities were obtained using a vibrating – sample magnetometer. Trapped field at 77 K was measured. The influence of Y211 powder refinement on the sample microstructure and properties is shown.

*Acknowledgment*

*This work was realized within the framework of the projects: Centre of Excellence of Advanced Materials with Nano- and Submicron Structure (ITMS 26220120019), Infrastructure Improving of Centre of Excellence of Advanced Materials with Nano- and Submicron- Structure (ITMS 26220120035), New Materials and Technologies for Energetics (ITMS 26220220061), Research and Development of Second Generation YBCO Bulk Superconductors (ITMS 26220220041), which are supported by the Operational Programme 'Research and Development' financed through the European Regional Development Fund, VEGA project No. 2/0090/13 and SAS Centre of Excellence: CFNT MVEP.*

**SUPERCONDUCTIVITY NEAR TRANSITION TO INSULATING STATE  
IN MOLYBDENUM CARBIDE**

P. Samuely<sup>1</sup>, P. Szabó<sup>1</sup>, P. Neilinger<sup>2</sup>, M. Trgala<sup>2</sup> and M. Grajcar<sup>2</sup>

<sup>1</sup>*Centre of Low Temperature Physics at the Institute of Experimental Physics,  
Slovak Academy of Sciences, Watsonova 47, 040 01 Košice, Slovakia*

<sup>2</sup>*Comenius University, Dept. Solid State Physics, SK-84248 Bratislava, Slovakia*

Recently, disordered superconductors attract a lot of attention aiming at better understanding the Superconducting Insulator Transition. In the paper we study the thin MoC films with different level of disorder as characterized by the Ioffe–Regel product  $k_F l$  determined from transport and Hall resistance measurements, where  $k_F$  is the Fermi momentum and  $l$  is the electron mean free path. Using scanning tunneling spectroscopy and microscopy below 1 K we address the superconducting density of state on differently disordered films with the superconducting transition temperature  $T_c < 6$  K. In particular the spatial (in)homogeneity of the superconducting energy gap is studied by means of the Continuous Imaging Tunneling Spectroscopy. The broadening of the superconducting density of states is analyzed within different models.

*This work was supported by the ERDF EU (European Union European regional development fund) grant, under the contract No. ITMS26220120047.*

# **LOCAL MAGNETOMETRY USING MINIATURE HALL-PROBE ARRAY ON $\text{Cu}_x\text{TiSe}_2$**

Z. Pribulová<sup>1</sup>, J. Kačmarčík<sup>1</sup>, P. Samuely<sup>1</sup>, Z. Medvecká<sup>2</sup>, V. Komanický<sup>2</sup>, T. Klein<sup>3</sup>, P. Barančková Husaniková<sup>4</sup>, V. Cambel<sup>4</sup>, J. Šoltýs<sup>4</sup>, and Karapetrov<sup>5</sup>

<sup>1</sup> *Institute of Experimental Physics, Slovak Academy of Sciences, Watsonova 47, 040 01 Kosice, Slovakia*

<sup>2</sup> *Faculty of Natural Sciences, University of P.J. Safarik, Park Angelinum 9, 04001 Kosice, Slovakia*

<sup>3</sup> *Institut Néel, CNRS and Université Joseph Fourier, Boite Postale 166, F-38042 Grenoble Cedex 9, France*

<sup>4</sup> *Institute of Electrical Engineering, Slovak Academy of Sciences, Dubravská cesta 9, 84104 Bratislava, Slovakia*

<sup>5</sup> *Department of Physics, Drexel University, 3141 Chestnut St., Philadelphia, PA 19104, USA*

$\text{TiSe}_2$  is a compound with the charge density wave (CDW) transition at 200 K. The CDW state is gradually suppressed when intercalated by copper and for certain amount of Cu superconductivity occurs showing a superconducting dome in the phase diagram  $T_c$  vs. Copper content. We report the studies of the lower critical field  $H_{c1}$  of three different superconducting samples – one sample that is close to optimal doping, and two underdoped samples.  $H_{c1}$  has been extracted from local magnetization measurements using miniature Hall-probes. The temperature dependence of  $H_{c1}$  and its anisotropy will be presented. We show that  $H_{c1}$  increases significantly with increasing Cu doping. Moreover, local magnetometry using array of 7 Hall-probes in a line shows that vortices after penetration into the sample move towards the centre resulting into a dome-shape induction profile suggesting relatively low pinning and importance of geometrical barriers for vortex penetration.

*This work was supported by the ERDF EU (European Union European regional development fund) grant, under the contract No. ITMS26220120047.*

**FRACTON CONTRIBUTION TO THE ELECTRON AND MAGNON PAIRING**

Z. BAK

Institute of Physics, Jan Dlugosz University of Czestochowa,  
al. Armii Krajowej 13/15, 42-200 Czestochowa, Poland

Experimental data show that for some values of oxygen content the copper oxides show fractal distribution of interstitial oxygen atoms. This nonuniform distribution eventually evolves into superstripe structure. In our contribution we present theoretical study of the superconductivity in the copper oxide systems with fractal inhomogeneities on mesoscopic scales. We consider a situation when within the spacer layers of the copper oxides there arises phase separation. The oxygen rich fractal nanoregions are separated by regions with lower interstitial (and consequently charge carrier) concentration. Intrinsic fractal heterogeneity of the composition causes that there appear the fracton excitations.

The collective excitations on fractal systems (fractons) are of localized nature and can contribute to formation of the local Cooper pairs. Fracton pairing along with the conventional mechanisms generates spatially nonuniform, multigap superconductivity. We develop a model in which the fractons-collective excitations on fractals, contribute to the formation of superconducting state. Contrary to earlier studies we assume coupling of charge carriers to the multifracton (bi-fracton) complexes and show its potential importance in the formation of superconducting state.

In our contribution fractons of both elastic and magnetic nature are taken into account. In the latter case we show that onset of superconductivity implies not only coherence of electron condensate but also coherence within fracton/magnon system. The accounting for fractal nanoregions is important since, as it has been proved earlier such symmetry can enhance critical temperature up to the limit set by the pair binding energy. Finally, with the help of Gross-Pitaevski formulas we present the mean field description of the system under consideration and predict magnetic inhomogeneities of the electron-magnon condensate.

**PENETRATION DEPTH OF BULK  $\text{Ti}_2\text{Ba}_2\text{Ca}_2\text{Cu}_3\text{O}_y$  AND  $\text{Ti}_{0.58}\text{Pb}_{0.4}\text{Sr}_{1.6}\text{Ba}_{0.4}\text{Ca}_2\text{Cu}_3\text{O}_y$  SUPERCONDUCTORS**R. Zalecki<sup>1</sup>, W.M. Woch<sup>1</sup>, A. Kołodziejczyk<sup>1</sup> and G. Gritzner<sup>2</sup><sup>1</sup>*AGH University of Science and Technology, Faculty of Physics and Applied Computer Science, Solid State Physics Dept., Al. Mickiewicza 30, PL 30-059, Kraków, Poland*<sup>2</sup>*Institute for Chemical Technology of Inorganic Materials, Johannes Kepler University, 4040 Linz, Austria*

The penetration depths of bulk  $\text{Ti}_2\text{Ba}_2\text{Ca}_2\text{Cu}_3\text{O}_y$  and  $\text{Ti}_{0.58}\text{Pb}_{0.4}\text{Sr}_{1.6}\text{Ba}_{0.4}\text{Ca}_2\text{Cu}_3\text{O}_y$  superconductors with the critical temperatures 112K and 114K respectively were determined from the *a.c.* susceptibility measurements taken for the samples of the thickness of the 0.1 mm and smaller. When the samples are in the Meissner state, the dispersive components of ac susceptibility as well as their temperature dependences, reflect the penetration depths of the measured superconductors. In these bulk ceramic superconductors the penetration depths are of order of few micrometers and that is comparable to the grain size in the ceramics.



**ANDREEV REFLECTION EFFECT IN SPIN-POLARIZED TUNNELING THROUGH A QUANTUM DOT INTERACTING WITH A POLARON.**

K. Bocian and W. Rudziński

*Faculty of Physics, Adam Mickiewicz University, ul. Umultowska 85, 61-614 Poznań, Poland*

Using the nonequilibrium Green's function technique we study theoretically spin-polarized transport due to Andreev reflection (AR) in a hybrid ferromagnet-quantum dot-superconductor junction based on a single-level quantum dot interacting with a local phonon mode. Phonon spectra have been calculated for arbitrary Coulomb correlations on the dot. The phonon-assisted AR phenomenon is analyzed within the Green function approach based on the dot correlators including both hole and electron contributions. Thus, it is shown that the phonon emission satellites in density of states spectrum calculated for the Andreev transmission may appear on both sides of the main resonance peaks corresponding to the quantum dot energy levels. The effect of the intradot Coulomb correlations on behavior of the conductance is shown for phonon-assisted AR transmission in the linear regime of bias voltage as well as in the nonequilibrium situation. In particular it is shown that the Franck-Condon blockade gives rise to a suppression of the transmission through the Andreev bound states and may lead to a significant enhancement of the phonon resonances. An influence of the vibrational modes on the matching condition for the perfect AR phenomenon is analyzed as well.

The numerical results obtained by means of different approximations of the Green's function correlators for the dot interacting with a local phonon mode are compared and discussed in detail.

**CRYSTAL-FIELD INTERACTIONS AND ORBITAL MAGNETISM  
IN COBALT OXIDES (LaCoO<sub>3</sub>, CoO, KCoF<sub>3</sub>, CoF<sub>3</sub>)**R. J. Radwanski<sup>1,2</sup>, D. Nalecz<sup>1,2</sup> and Z. Ropka<sup>2</sup><sup>1</sup>*Institute of Physics, Pedagogical University, Podchorazych 2, 30-084 Krakow, Poland*<sup>2</sup>*Center of Solid State Physics, Snt Filip 5, 31-150 Krakow, Poland*

We have calculated crystal-field (CEF) interactions in a number of cobalt ionic compounds, in oxides LaCoO<sub>3</sub> and CoO, and in fluorides KCoF<sub>3</sub> and CoF<sub>3</sub> from really first-principles calculations.

LaCoO<sub>3</sub> has been extensively studied theoretically by more than 50 years due to its surprising nonmagnetic ground state. The existence of very thin and well-defined crystal-field states in LaCoO<sub>3</sub> have been revealed by electron-paramagnetic resonance. It is important result owing to very general conviction of the continuous energy states in 3d oxides. The physical origin of these states will be discussed. We attribute these states as originating from the Co<sup>3+</sup> ion in the high-spin state. The present possibility of detecting the electron-paramagnetic resonance in the 300-1000 GHz frequency and in applied magnetic field up to 30 T becomes extremely important tool for study of 3d oxides. The discovery of the crystal-field states in LaCoO<sub>3</sub> is important for us because one of the present authors (RJR) has claimed from the very beginning the existence of the localized *d* electrons in oxides in contrary to strong opposition of the "hybridization" community. These *d* electrons in LaCoO<sub>3</sub> form strongly correlated 3d<sup>6</sup> electron system.

In contrary to LaCoO<sub>3</sub> the Co<sup>3+</sup> ions in CoF<sub>3</sub> are in the magnetic ground state. Such the state is responsible for high magnetic-ordering temperature of 460 K. Within the Quantum Atomistic Solid State theory (QUASST) we consistently have explained the ground-state properties of CoF<sub>3</sub> and thermodynamical properties, both in the paramagnetic and magnetic state, together with the reproduction of the λ-type peak at the phase transition at 460 K.

In CoO and KCoF<sub>3</sub> the cobalt ions are in the divalent state with localized seven *d* electrons forming strongly correlated electron system 3d<sup>7</sup>. We claim that for description of magnetic properties and of the electronic structure of 3d compounds the spin-orbit coupling has to be taken into account.

In all these cobalt systems there exists substantial orbital magnetic moment. In fact, the nonmagnetic state of LaCoO<sub>3</sub> can be considered as resulting from large orbital magnetic moment.

**Fe-Ga MAGNETOSTRICTIVE POLYCRYSTALLINE MATERIALS:  
FROM BULK SHAPED SAMPLES TO NANOWIRES**

N. Lupu

*National Institute of Research and Development for Technical Physics, Iasi,  
Romania*

The magnetoelastic properties of Fe-Ga alloys are very sensitive to the microstructure, the solubility of Ga in bcc  $\alpha$ -Fe and the fabrication process. The replacement of Fe by Ga results in a large increase in magnetostriction, approaching 400 ppm for quenched single crystals at room temperature, with low saturation fields of several hundreds of oersted. The highly textured polycrystalline Galfenol show large  $\lambda_{100}$  values with 2 maxima of 265 ppm near 19 at.% Ga and 235 ppm near 27 at.% Ga after annealing at 1000°C. The recent studies shown that the subsequent magnetic field annealing can induce anisotropies along the external field direction, influencing the magnetostriction and magnetoelastic coupling values of bcc Fe-Ga alloys.

Four (4) types of Fe-Ga samples and their structural, magnetic and magnetoelastic features will be presented: (i) bulk-shaped polycrystalline magnetostrictive materials, (ii) melt-spun ribbons (MSRs), (iii) microwires (MW) produced by in-rotating water spinning (INROWASP) method, and (iv) single and multilayered nanowires (NWs).

The magnetostriction of 3-D shaped polycrystalline Fe-Ga bulk samples is dependent on the magnitude of the applied stresses during measurements, because of the stored magnetoelastic energy which strongly depends on samples magnetic structure and the induced anisotropies.

The magnetostriction and magnetoelastic coupling coefficient of Fe-Ga polycrystalline MSRs are dependent on the magnitude of the applied stresses and fields during measurements. The magnetic field annealing leads to the enhancement of the magnetostriction, depending on the external field direction.

INROWASP method employs the directional solidification that enables the fabrication of highly textured Fe-Ga continuous MWs. The  $\langle 100 \rangle$  crystallographic texture is likely due to the directional solidification imposed by the induced radial compressive stresses during the INROWASP process, being an important approach with implications for design and development of miniaturized systems involving magnetostrictive materials.

The deposition potential, concentration of the surfactants and pH of the electrodeposition bath all concur in the composition and magnetic properties of the nanowires.

**MAGNETIC DOMAINS IN 10M MARTENSITE OF Ni-Mn-Ga EXHIBITING MAGNETIC SHAPE MEMORY EFFECT**O. Heczko<sup>1</sup>, L. Fekete<sup>1</sup>, V. Kopecký<sup>1</sup>, J. Kopeček<sup>1</sup> and L. Straka<sup>2</sup><sup>1</sup>*Department of Functional Materials, Institute of Physics, ASCR, Na Slovance 2, CZ-182 02 Prague, Czech Republic*<sup>2</sup>*Laboratory of Engineering Materials, Aalto University School of Engineering, PL 14200, FIN-00076 AALTO, Finland*

Magnetic shape memory (MSM) effect resulting in giant magnetic field induced deformation (up to 12%) is a new paradigm of the deformation in magnetic field and one of multiferroic effect combining ferroelasticity and magnetism. In contrast to magnetostriction the effect is based on martensite structure reorientation. The effect hinges on the highly mobile twin boundaries or interfaces between two differently oriented martensite variants as the reorientation is mediated by their movement. Recently we showed that in Ni-Mn-Ga 10M modulated martensite, which is a prototype of MSM alloy, there are two structurally different twin boundaries (Type I and Type II) which strongly differ by their mobility, about ten times [1]. These macrostructural interfaces have complex layered microstructure consisting of different twinning systems [2]. The structure relief due to martensite twin variant interfaces (ferroelastic domains) and corresponding magnetic domains structure was studied by AFM/MFM and optical microscopy. Magnetic domain structures far from interfaces are typical for uniaxial ferromagnet, however, in the vicinity of the mobile interface they become more complex. For comparison we also studied another ferromagnetic shape memory alloy Co-Ni-Al, which, however, does not exhibit MSM effect. We will discuss the interaction of ferroelastic domains with ferromagnetic domains, which can be important for understanding of the twin boundary mobility and ultimately for the understanding of this multiferroic effect.

- [1] L. Straka, O. Heczko, H. Seiner, N. Lanská, J. Drahokoupil, A. Soroka, S. Fahler, H. Hanninen, A. Sozinov, Highly mobile twinned interface in 10 M modulated Ni-Mn-Ga martensite: Analysis beyond the tetragonal approximation of lattice, *Acta Mater.* 59 (2011) 7450.
- [2] O Heczko, L. Straka, H. Seiner, Different microstructures of mobile twin boundaries in 10 M modulated Ni-Mn-Ga martensite, *Acta Mater.* 61 (2013) 622.

# MAGNETIC MEMORY EFFECT IN $K_3M_3^{II}M_2^{III}F_{15}$ FAMILY OF MULTIFERROICS

Z. Jagličić<sup>1</sup>, D. Pajič<sup>2</sup>, Z. Trontelj<sup>3</sup>, J. Dolinšek<sup>4</sup> and M. Jagodič<sup>3</sup>

<sup>1</sup>*Institute of Mathematics, Physics and Mechanics & University of Ljubljana, Faculty of Civil Engineering and Geodesy, Jamova 2, 1000 Ljubljana, Slovenia*

<sup>2</sup>*Department of Physics, Faculty of Science, University of Zagreb, Bijenička c. 32, 10000 Zagreb, Croatia*

<sup>3</sup>*Institute of Mathematics, Physics and Mechanics, Jadranska 19, 1000 Ljubljana, Slovenia*

<sup>4</sup>*Jožef Stefan Institute, Jamova 39, SI-1000 Ljubljana, Slovenia*

Multiferroic materials combine in one system both ferromagnetic and ferroelectric properties thus achieving rich functionality. Majority of all known inorganic ferroelectrics and multiferroics are oxides, like  $BiFeO_3$  as the most known member. Although much effort has been put into research of oxide multiferroic materials, the coupling between magnetic and electric properties is still relatively weak. In search of new multiferroic materials we turned to a family of fluorides that can be represented by a formula  $K_3M_3^{II}M_2^{III}F_{15}$  where M denotes transition metals (Fe, Mn, Co, Cr) with the orthorhombically deformed tetragonal tungsten bronze structure.

While the ferroelectric transition in these fluorides is well above room temperature the magnetic phase transitions occur below room temperature, for example at 122 K and 35 K for  $K_3Fe_5F_{15}$  and  $K_3Cr_2Fe_3F_{15}$ , respectively. Below magnetic transition temperatures a large difference between zero-field-cooled and field-cooled magnetic susceptibilities has been observed, and a slow magnetic dynamic in both systems have been detected showing a non-ergodic magnetic behaviour of the systems at low temperatures.

In the present work we will describe a magnetic memory effect observed in  $K_3Fe_5F_{15}$  and  $K_3Cr_2Fe_3F_{15}$ . Using the memory effect we succeeded to write, read and erase a digital information written in these materials. In this way we showed the materials exhibit, in addition to already known magneto-electric multiferroic properties, a new level of possible application - as a thermal memory cell material. On the other hand, the observation of the magnetic memory effect confirms a hypothesis of magnetic clusters formation in this family of multiferroics.

## OUTSTANDING MAGNETIC PROPERTIES OF Co-SUBSTITUTED AND Er-DOPED $\text{Ni}_2\text{MnGa}$ COMPOUND

J. Kaštil<sup>1,2</sup>, J. Kamarád<sup>1</sup>, S. Fabbri<sup>3</sup>, F. Albertini<sup>3</sup>, Z. Arnold<sup>1</sup> and L. Righi<sup>4</sup>

<sup>1</sup> Institute of Physics ASCR, v.v.i., Na Slovance 2, 182 21 Prague 8, Czech Republic

<sup>2</sup> Charles University, Faculty of Mathematics and Physics, Department of Condensed Matter Physics, Ke Karlovu 5, 121 16 Prague 2, The Czech Republic

<sup>3</sup> IMEM CNR, Parco Area delle Scienze 37/A, I-43124 Parma, Italy

<sup>4</sup> Dipartimento di Chimica GIAF, Università di Parma, Viale G. Usberti 17/A, I-43100 Parma, Italy

The  $\text{Ni}_2\text{MnGa}$  Heusler compound belongs to family of ferromagnetic shape memory materials. These compounds are very promising smart materials with many applications as medical guide-wires, smart actuators, motor and oscillators. They show magnetic and magneto-structural transitions accompanied with a large set of the giant magneto-elastic, -plastic, -structural and -caloric effects. They undergo the first order structural transition from high temperature cubic austenite to the low temperature martensite phase. The structural and magnetic properties of the Heusler off-stoichiometric  $\text{Ni}_2\text{MnGa}$  alloys are very sensitive to a doping.

We have prepared polycrystalline samples of Co-doped off-stoichiometric  $\text{Ni}_2\text{MnGa}$  alloys with outstanding magnetic properties of their martensitic phases, where a paramagnetic gap has been observed and tuned by composition. Surprisingly, the temperature dependence of their austenitic saturated magnetisation tends to follow one universal curve  $M_s(T/T_C^A)$ . Saturated magnetisation of martensitic phases of these alloys strongly decreases with increasing Co and Mn content, transition into paramagnetic state occurs in the alloys with a rich Co-doping. A presence of the paramagnetic gap at a temperature range between ferromagnetic states of martensite and austenite has been verified by linear dependence of susceptibility  $\chi^{-1}(T)$ . A possible presence of the uncompensated disordered-local moment state in the Mn-rich compounds will be addressed. However, a steep decrease of the martensitic magnetisation with increasing Co-doping is not clear up to now. Based on the presented unforeseen suppression of the martensitic transition by a small amount of rare-earth, we have prepared the Er-doped  $\text{Ni}_{1.72}\text{Co}_{0.28}\text{Mn}_{1.24}\text{Ga}_{0.76}$  alloy, to study magnetic properties of austenite phase of our studied alloys in large temperature range down to 5 K. We will discuss trends in the temperature dependence of austenite and martensite magnetisation with respect to the composition.

**STRUCTURAL AND MAGNETIC PROPERTIES OF GLASS-COVERED FePtNbB-BASED MICROWIRES**

Nirina Randrianantoandro<sup>1</sup>, Ivan Škorvánek<sup>2</sup>, Jozef Kováč<sup>2</sup>, Nicoleta Lupu<sup>3</sup> and Horia Chiriac<sup>3</sup>

<sup>1</sup>*Institut des Molécules et des Matériaux du Mans, UMR CNRS 6283, Université du Maine, 72085 Le Mans cedex 9, France*

<sup>2</sup>*Institute of Experimental Physics, Slovakia Academia of Science, Kosice Slovakia*

<sup>3</sup>*National Institute of Research and Development for Technical Physics, Iasi, Romania*

The interest in Fe-Pt based alloys comes from the good permanent magnet characteristics of these alloys resulting from L1<sub>0</sub> fct FePt phase with very high magnetocrystalline anisotropy of the order of 7 MJ/m<sup>3</sup>. Various techniques have been employed to produce permanent magnets as nanocomposite thin films or nanocrystalline melt spinning ribbons containing L1<sub>0</sub> FePt nanograins. In such cases, the formation of L1<sub>0</sub> phase requires subsequent heat treatments of the as-produced samples consisting only of a mixture of disordered fcc FePt phase dispersed in a residual amorphous phase. The phase transformation from the disordered to the ordered FePt phase occurs in the temperature range 550-600°C, depending on Fe and Pt atomic contents.

Our goal is to produce permanent magnet wires based on the formation of FePt hard magnetic phase. Our study focuses on the structural and magnetic properties of glass covered FePtNbB-based microwires prepared by glass-covered melt spinning method. The studied wires consist of a cylindrical metallic core with the diameter of 10 to 20 µm, covered by Pyrex glass, the average total diameter of the microwires ranging from 20 to 40 µm. The structural and magnetic properties of two sets of samples with nominal compositions Fe<sub>50</sub>Pt<sub>28</sub>Nb<sub>2</sub>B<sub>20</sub> and Fe<sub>46</sub>Pt<sub>27</sub>Nb<sub>2</sub>B<sub>25</sub> were investigated.

In this work, we present our recent results on the effect of isothermal annealing treatment on the structural and magnetic properties of FePtNbB glass-covered wires. X-ray diffraction and <sup>57</sup>Fe Mössbauer spectrometry measurements were carried out and indicated that the as-melted microwires consist of a mixture of nanoscale crystalline grains of fcc FePt phase embedded in an amorphous phase based on Fe-B (Pt, Nb) alloy while in the annealed samples we have identified the presence of the L1<sub>0</sub> fct FePt and Fe<sub>2</sub>B phases. As revealed by SQUID magnetometry, the thermally untreated samples exhibit hysteresis loops characterized by a low coercivity and squared shape, which are typical for microwires with positive magnetostriction. Our results show that an adequate heat treatment favors the magnetic hardening of FePtNbB-based microwires with coercive fields up to 440 kA/m.

*This work is supported by French-Slovakia Bilateral Program "Hubert Curien Stephanik", project code 26359PJ and APVV SK-FR 0035-11.*

**COMPARATIVE STUDY OF THE FARADAY EFFECT IN TERBIUM BORATES  $\text{TbFe}_3(\text{BO}_3)_4$  AND  $\text{TbAl}_3(\text{BO}_3)_4$** V.A. Bedarev<sup>1</sup>, M.I. Pashchenko<sup>1</sup>, D.N. Merenkov<sup>1</sup>, Yu.O. Savina<sup>1</sup>,V. A. Pashchenko<sup>1</sup>, S.L. Gnatchenko<sup>1</sup>, L.N. Bezmaternykh<sup>2</sup> and V.L. Temerov<sup>2</sup><sup>1</sup> *Department of Magnetism, B.I. Verkin Institute of Low Temperature Physics and Engineering, National Academy of Sciences of Ukraine, 47 Lenin Ave, 61103 Kharkov, Ukraine*<sup>2</sup> *L.V. Kirensky Institute of Physics, Siberian Branch of the Russian Academy of Sciences, 660036 Krasnoyarsk, Russia*

Rare-earth borate crystals with general formula  $\text{RM}_3(\text{BO}_3)_4$  (R - rare-earth elements, M – transition metals) have attracted considerable attention as magneto-optic materials. In single crystals  $\text{TbFe}_3(\text{BO}_3)_4$  and  $\text{TbAl}_3(\text{BO}_3)_4$  the terbium subsystem contributes to the Faraday rotation of that borates. The comparison of the values of this rotation in crystals  $\text{TbAl}_3(\text{BO}_3)_4$  and  $\text{TbFe}_3(\text{BO}_3)_4$  at various temperatures can help to determine the contributions of the subsystems of the terbium ions and iron ions in the Faraday rotation in the crystal  $\text{TbFe}_3(\text{BO}_3)_4$ .

The goal of the present work was to determine the contributions of the terbium ions subsystem and the iron ions subsystem to the Faraday rotation in a single crystal  $\text{TbFe}_3(\text{BO}_3)_4$  by a comparative study of the field dependencies of the Faraday rotation of light in single crystals  $\text{TbAl}_3(\text{BO}_3)_4$  and  $\text{TbFe}_3(\text{BO}_3)_4$ .

In this work the field dependences of the Faraday rotation of light and magnetization in single crystals  $\text{TbAl}_3(\text{BO}_3)_4$  and  $\text{TbFe}_3(\text{BO}_3)_4$  were studied. As a result it was obtained that the terbium subsystem brings the dominant magnetic contribution to the Faraday rotation at low temperatures in iron borate  $\text{TbFe}_3(\text{BO}_3)_4$ . Furthermore in the crystal  $\text{TbFe}_3(\text{BO}_3)_4$  magneto-optical constant corresponding to the terbium and iron subsystems were determined. Magneto-optical constant in the crystal  $\text{TbAl}_3(\text{BO}_3)_4$  is close to magnitude of magneto-optical constant corresponding terbium subsystem in  $\text{TbFe}_3(\text{BO}_3)_4$ .



# THE STUDY OF MAGNETIC ORDERING IN Ba(Fe,Nb)O<sub>3</sub> BY MÖSSBAUER SPECTROSCOPY

T. Kmjec<sup>1</sup>, J. Kohout<sup>1</sup>, K. Závěta<sup>1</sup>, D. Kubániová<sup>1</sup>, V. V. Laguta<sup>2</sup>, I. P. Raevski<sup>3</sup>

<sup>1</sup> *Faculty of Mathematics and Physics, Charles University in Prague, V Holešovičkách 2, Prague 8, CZ 180 00*

<sup>2</sup> *Institute of Physics, Academy of Sciences of the Czech Republic, v. v. i., Cukrovarnická 10, Prague 6, CZ 162 53*

<sup>3</sup> *Department of Physics and Research Institute of Physics, Southern Federal University, 344090 Rostov on Don, Russia*

The multiferroic material Ba(Fe,Nb)O<sub>3</sub> (BFN) was prepared by solid state reaction at 1350 °C for 2 hours as a sintered ceramics. The crystal structure is monoclinic with the space group *P2/m* with  $a=4.056$ ,  $b=2.857$ , and  $c=4.039$  Å;  $\alpha=\gamma=90^\circ$ ,  $\beta=90.14^\circ$  [1]. The sample was characterized by XRD to check the phase composition, crystal structure and lattice constant and by ED XRF spectrometry to confirm the chemical composition and its homogeneity.

The Mössbauer spectra of <sup>57</sup>Fe isotope were acquired in a transmission-mode spectrometer with <sup>57</sup>Co source in rhodium matrix moving with constant acceleration with the aim to receive information about the temperature dependence of the magnetic ordering, in particular the transition temperature. The measurements were performed in the temperature range 4.2 through 300 K with in-field spectra taken in external fields up to 6 T below the magnetic ordering temperature of ~32 K.

*The support of the Grant Agency of the Czech Republic under project No. 13-11473S is gratefully acknowledged.*

[1] S. Bhagat and K. Prasad, Phys. Status Solidi A 207, No. 5, 1232–1239 (2010) / DOI 10.1002/pssa.200925476

**MULTIFERROIC IRON NIOBATE PEROVSKITES STUDIED BY NUCLEAR MAGNETIC RESONANCE SPECTROSCOPY**K. Kouřil<sup>1</sup>, V. Chlan<sup>1</sup>, H. Štěpánková<sup>1</sup>, K. Uličná<sup>1</sup>, V. V. Laguta<sup>2</sup>, I. P. Raevski<sup>3</sup><sup>1</sup>*Charles University in Prague, Faculty of Mathematics and Physics,  
V Holešovičkách 2, 180 00 Prague 8, Czech Republic*<sup>2</sup>*Institute of Physics AS CR, Cukrovarnická 10, Prague, Czech Republic*<sup>3</sup>*Institute of Physics, Southern Federal University, Rostov on Don 344090, Russia*

Lead iron niobate  $\text{PbFe}_{0.5}\text{Nb}_{0.5}\text{O}_3$  (PFN) belongs to the family of multiferroic perovskites exhibiting simultaneous ferroelectric and magnetic ordering. This material undergoes several phase transitions between various magnetic and electric phases, also including spin and dipole glass phases induced by ionic site and charge disorder. On contrary, barium iron niobate  $\text{BaFe}_{0.5}\text{Nb}_{0.5}\text{O}_3$  (BFN) exhibits only antiferromagnetic or spin-glass magnetic transition at 23-24 K. The solid solutions PFN-BFN show interesting ferroelectric and magnetic relaxor properties. Our aim is to study the phase transitions in these composites and the role of Fe/Nb local ordering. Nuclear magnetic resonance (NMR) method provides information about distribution of ions and phase composition, structural phase transitions and various dynamical processes and is therefore suitable for investigating these perovskite systems.

The PFN-BFN ceramics was prepared by the solid state reaction route [1]. The phase purity of all the compositions obtained was checked by the X-ray diffraction, which showed a single phase of the perovskite type. We measured frequency swept NMR spectra as well as relaxation times in PFN-BFN systems in magnetic field of 9.4 T at room temperature and at various temperatures in the range 4-400 K. Large quadrupolar broadening of  $^{93}\text{Nb}$  (spin  $I=9/2$ ) resonance was observed.  $^{207}\text{Pb}$  NMR in PFN and  $^{135,137}\text{Ba}$  NMR in BFN was detected. In addition also a weak  $^{17}\text{O}$  resonance was observed. Broad  $^{57}\text{Fe}$  spectrum in PFN was acquired in zero-field at 4.2 K. The measured data are analyzed in order to calculate hyperfine fields at different ions, to determine Fe/Nb local ordering and dynamic properties of relaxor phases.

[1] I. P. Raevski, S. P. Kubrin, S. I. Raevskaya, V. V. Titov, D. A. Sarychev, M. A. Malitskaya, I. N. Zakharchenko, and S. A. Prosandeev, *Phys. Rev. B* **80**, 024108 (2009)

**DETAILS OF MAGNETIC PROPERTIES IN  $\text{Pb}(\text{Fe}_{1/2}\text{Nb}_{1/2})\text{O}_3$** M. Maryško<sup>1</sup>, V.V.Laguta<sup>1</sup>, I. P. Raevski<sup>2</sup><sup>1</sup>*Institute of Physics, ASCR, 16253 Prague 6, Cukrovarnická 10, Czech Republic.*<sup>2</sup>*Department of Physics and Research Institute of Physics, Southern Federal University, 344090 Rostov on Don, Russia.*

The magnetic properties of the multiferroic double perovskite  $\text{Pb}(\text{Fe}_{1/2}\text{Nb}_{1/2})\text{O}_3$  (PFN) has been intensively studied but, in our opinion, up to now the consistent explanation of the magnetic state of this compound is absent (see e.g. [1]). In the framework of our recent study on Ba and Ti doped PFN [2] detailed SQUID measurements on pure PFN were performed and some hitherto unpublished results represent the background for the present contribution. A special emphasis was put on the measurement of the magnetization up to field  $H = 70$  kOe.

At  $T_N \approx 143$  K PFN undergoes a transition from the paramagnetic (PM) to a more complicated state formed by the long - range antiferromagnetism (AFM) and certain AFM or superantiferromagnetic (SAFM) clusters. Above  $T_N$  the virgin magnetization curve  $m(H)$  is strictly linear as expected in the PM state. Below  $T_N$  the  $m(H)$  curves exhibit an inflection point at a critical field  $H_s$  (T) in the field region  $10 - 30$  kOe. This critical field determined from a maximum in  $dm/dH$  is the same when measuring during increasing or decreasing field. The differential susceptibility evaluated between the fields 60 and 70 kOe does not show any maximum at  $T_N$  and an extrapolation of the  $m(H)$  dependence to zero field suggests the presence of a weak ferromagnetic or ferromagnetic arrangement. These results demonstrating the large influence of the magnetic field are discussed in connection with a possible spin - reorientation in the AFM and SAFM clusters. At temperature below 50 K a cluster glass state develops with a freezing temperature  $T_g \approx 10$  K. This region is characterized by a frequency dependent ac susceptibility and the irreversibility of the ZFC and FC susceptibilities.

[1] W.Kleemann et al., Phys.Rev.Letters, **105**,257202-1 (2010).[2] V.V.Laguta et al., Phys.Rev. B **87**, 064403 (2013).

**MAGNETO-ROTATIONAL SYMMETRY IN CHIRAL  
MAGNETOELECTRODEPOSITION**

R. Aogaki<sup>1,8</sup>, R. Morimoto<sup>2</sup>, A. Sugiyama<sup>3</sup>, I. Mogi<sup>4</sup>, M. Asanuma<sup>5</sup>, M. Miura<sup>6</sup>,  
Y. Oshikiri<sup>7</sup> and Y. Yamauchi<sup>8</sup>

<sup>1</sup>*Polytechnic University, 2-20-12-1304 Ryogoku, Sumida, Tokyo, 130-0026, Japan*

<sup>2</sup>*Saitama Prefectural Okubo Water Filtration Plant, Saitama, 338-0814, Japan*

<sup>3</sup>*Waseda University, Shinjuku, Tokyo, 169-0855, Japan*

<sup>4</sup>*IMR, Tohoku University, Katahira, Sendai, 980-8577, Japan*

<sup>5</sup>*Yokohama Harbour Polytechnic College, Yokohama, 231-0811, Japan*

<sup>6</sup>*Polytechnic College Akita, Odate, Akita, 017-0805, Japan*

<sup>7</sup>*Yamagata College of Industry and Technology, Yamagata, 990-2473, Japan*

<sup>8</sup>*National Institute for Materials Science, Tsukuba, Ibaraki, 305-0044, Japan*

Using electrodes fabricated by magnetoelectrodeposition, Mogi has found the appearance of chiral activity in enantiomorphic electrode reactions, which was thought to come from spiral dislocations transcribed by vortex flows. In a vertical magnetic field (MG), a tornado-like stream called vertical MHD flow (VMF) emerges over the electrode surface. Inside the stream, micro-vortexes called micro-MHD flows (MMF) are induced. For the transcription of the vortex motion to a deposit surface, something like atomic-scale lubricant is required. Recently, it has been found that ionic vacancy is created by electrode reaction, acting as a lubricant. In consequence, two types of surface are self-organized; one is ordinal rigid surface with friction, and the other is free surface without friction covered with ionic vacancies. At the same time, two types of MMF with different flow and rotational directions are activated on the rigid and free surfaces, respectively. The rotational directions of these vortexes are determined by the direction of the MG, whereas the rotation of the VMF donates the precessions to them. If the rotational directions activated by the MG are consistent with those of the precession by the VMF, the MMF will develop with time, being transcribed to electrode surface with deposition. If their directions are not consistent with each other, they cannot grow for the transcription. This means that there is a suitable combination of MG direction and VMF rotation. From the theoretical analysis, such combination agrees with that of right-handed system; downward magnetic field with clockwise rotation or upward magnetic field with anti-clockwise rotation. These rotational directions are fortunately the same as those of the VMF induced by a given MG. Therefore, clockwise and anti-clockwise screw dislocations yielded by downward and upward MG's can provide the chiral activities for L- and D-reagents, respectively.

**CHIRALITY INDUCED BY MAGNETOELECTROLYSIS**I. Mogi<sup>1</sup>, R. Aogaki<sup>2</sup>, R. Morimoto<sup>3</sup> and K. Watanabe<sup>1</sup><sup>1</sup>*Institute for Materials Research, Tohoku University, Katahira, Aoba-ku, Sendai 980-8577, Japan*<sup>2</sup>*Polytechnic University, Sagami-hara, Kanagawa 252-5196, Japan*<sup>3</sup>*Saitama Prefectural Okubo Water Filtration Plant, Saitama 338-0814, Japan*

An application of a magnetic field to electrolysis (magnetoelectrolysis) involves various research aspects from viewpoints of electrochemistry, materials processing, magnetohydrodynamics and astrophysical hydrodynamics. Particular concern has been devoted into the chirality induction on the surfaces of electrodeposits, in connection with the origin of the homochirality in molecular evolution of life on the early earth.

When a magnetic field is imposed to an electrochemical cell, the Lorentz force acting on the faradaic currents causes convections around the electrodes in the electrolytic solutions. This is well known as the MHD (magnetohydrodynamic) effect. There are two kinds of the MHD flow in the magnetic field perpendicular to the electrode surface; micro-MHD vortices on a fluctuated surface of the electrodeposits and a macroscopic flow around the electrode edge (the vertical MHD flow). When the micro-MHD vortices have scales of nanometers or sub-micrometers, they could produce chiral defects such as screw dislocations on the electrodeposit surfaces. In the micro-MHD effect, both clockwise and anticlockwise vortices must coexist, resulting in achiral surfaces. The influence of the vertical MHD flow on the micro-MHD vortices could break the symmetry of the micro-MHD vortices, inducing surface chirality.

We have tried to explore chiral surfaces of magnetoelectrodeposited (MED) metal films. The Ag and Cu films were electrodeposited in the magnetic fields of up to 5 T generated by a cryocooled superconducting magnet. The MED films were used as an electrode, and the electrochemical reactions of chiral molecules such as glucose and amino acids were examined by voltammetry. The MED film electrodes exhibited the chiral behavior as the reaction yield (faradaic current) difference between the enantiomers, and the chiral sign in the voltammograms depended on the polarity of the magnetic fields during the electrodeposition. The latter indicates that the surface chirality is determined by the sense of the vertical MHD flow. These results demonstrate that the MED film surfaces possess the chirality and they can recognize the molecular chirality.

**MAGNETOVISION SCANNING SYSTEM FOR DETECTION OF DANGEROUS OBJECTS**Michał Nowicki<sup>1</sup>, Roman Szewczyk<sup>2</sup><sup>1</sup> *Institute of Metrology and Biomedical Engineering, Warsaw University of Technology, ul. Św. Andrzeja Boboli 8, 02-525 Warszawa, Poland*<sup>2</sup> *Industrial Institute for Automation and Measurements, Al. Jerozolimskie 202, 02-486 Warszawa, Poland*

Magnetovision is the measurement of the disturbances of magnetic field induction in a particular plane or in space and presenting it with a 2D image (for the plane) or 3D (for space).

This paper presents an application of magnetovision based measurements to develop a method for passive detection of dangerous ferromagnetic objects. Obtaining magnetovision images of unknown objects from a greater distance and on a larger surface area, required the development of new methods for measurement and signal processing. The use of passive magnetovision system is important because the active metal detectors can provoke a reaction of the specially constructed detonators. This applies particularly to the newer generation of landmines, reacting to the presence of active detectors, which represents a direct threat during demining.

Measuring system was designed and built to study the magnetic field vector distributions. The measurements of the Earth's field disturbances caused by ferromagnetic objects were carried out. The ability for passive detection of selected dangerous objects and was demonstrated. Further data processing allowed for obtaining of (x,y) coordinates of the object relative to the plane of measurement, and even the possibility of determining the distance from the object. A new methodology of measurement for decreasing the impact of magnetic background on the visualization of the results was also developed. The developed methods allow to get a visualization of the distribution of the magnetic induction vector absolute values. Furthermore, it is possible to visualize its gradient, or the value and direction of the magnetic induction vector in different measurement points.

The results obtained indicate that it is possible to detect and determine the location of dangerous ferromagnetic objects. This opens the new way to use magnetovision in public security systems, in particular for the detection of dangerous objects by police and sapper robots. A system of this type can also be used in non-destructive testing, detection of structural defects inside the objects.

**NOISE CHARACTERISTICS OF MICROWIRE MAGNETOMETER**

P. Lipovský<sup>1</sup>, A. Čverha<sup>1</sup>, J. Hudák<sup>1</sup>, J. Blažek<sup>1</sup>, D. Praslička<sup>1</sup>

<sup>1</sup>*Department of Aviation Technical Studies, Technical University of Kosice,  
Rampova 7, 041 21 Kosice, Slovakia*

Magnetometers with ferroprobes provide the possibility to measure magnetic field within the range of 12 orders. Widely spread is their utilization in measurement of weak, stationary and low frequency magnetic fields. Sensitivity of the probe is determined by internal magnetic noise caused by necessary periodical magnetization of its core. This internal magnetic noise depends on the core material and its geometry and is in its principle unremovable. Other sources of noise influencing output signals of magnetometers are introduced by fluctuations of voltages and currents in the electronics of the measurement chain. Their level generally depends on the quality of construction and used components. Fluctuations of the measured magnetic field caused by near and also far sources and processes are considered as an interference and significantly influence overall noise of output signals of magnetometers.

Current trends in modernization and miniaturization of ferroprobe sensors lead to replacement of amorphous ribbon cores with magnetic microwires. The miniaturization often causes degradation in the parameters of sensors, so, considering measurement of weak magnetic fields, it is necessary to explore noise parameters, temperature drift and stability of the magnetometer output value. The noise properties of sensors are sufficiently characterized by power spectral density of the noise and its amplitude distribution.

The article deals with analysis of noise characteristics of one channel of microwire magnetometer based on the experimental data processing. Using 1 second periodograms 24-hour development of power spectral density was processed and average amplitudes and peak values of stimulation signal and noise parameters were calculated. Obtained data are compared with corresponding parameters of relax-type ferroprobe magnetometer.

*This work was supported by the Slovak Research and Development Agency under Contract No. APVV 0266-10.*

**HIGH RESOLUTION TIPS FOR SWITCHING MAGNETIZATION  
MAGNETIC FORCE MICROSCOPY**

M. Precner, J. Fedor, J. Tóvik, J. Šoltýs, and V. Cambel

*Institute of Electrical Engineering, SAS, Bratislava, 841 04 Slovak Republic*

Switching magnetization magnetic force microscopy (SM-MFM) is based on two-pass magnetic force microscopy with reversed tip magnetization between the scans [1]. Within the technique the sum of the scanned data with reversed tip magnetization depicts local van der Waals forces, while their difference maps the local magnetic forces. Here we implement this idea by the fabrication of low-momentum magnetic probes that exhibit magnetic single domain state, which can be easily reversed in low external magnetic field during the scanning. The separation of the forces mapped enables scanning in close proximity of the sample ( $\sim 5$  nm). Therefore, extremely high spatial resolution is achievable by the SM-MFM technique.

Image phase resolution of the MFM method depends on various geometric parameters of the tip, such as tip length, its apex radius and taper angle. The parameters are determined by the evaporation process, within which the standard atomic force microscopy tips are coated with magnetic layer. We show that the thickness of the coated layer is important for the tip spatial resolution. In this work we optimize material and geometric parameters for the SM-MFM high resolution tips.

[1] V. Cambel, M. Precner, J. Fedor, J. Šoltýs, J. Tóvik, T. Ščepka, G. Karapetrov, *High Resolution Switching Magnetization Magnetic Force Microscopy*, Applied Phys. Lett. 102 (2013) 062405. DOI: 10.1063/1.4791591.



**CALCULATION OF THE MAGNETIC FIELD PARAMETERS OF THE BIOGENIC IRON OXIDES ENSEMBLE FOR THE MRI APPLICATIONS**O. Štrbák<sup>1</sup>, A. Krafčík<sup>1</sup>, M. Teplan<sup>1</sup>, D. Gogola<sup>1</sup>, P. Kopčanský<sup>2</sup> and I. Frollo<sup>1</sup><sup>1</sup>*Institute of Measurement Science, Slovak Academy of Sciences, Dúbravská cesta 9, 841 04 Bratislava, Slovakia*<sup>2</sup>*Institute of Experimental Physics, Slovak Academy of Sciences, Watsonova 47, 040 01 Košice, Slovakia*

The iron oxide nanoparticles are due to their unique superparamagnetic properties in a wide range of interest of the biomedical applications, such as targeted drug delivery, hyperthermia, magnetic separation of biomolecules etc. However, the iron oxide nanoparticles produced by living systems have also a big potential in biomedicine, especially in the physiological and pathological processes imaging. In humans, it is mainly the iron storage proteins such as ferritin and hemosiderin, but also the magnetite nanoparticles, which have been found in the human brain tissue. Elevated levels of these particles are usually linked to the pathological processes in the body. Ferritin and hemosiderin are involved in the formation of the so called "iron-overloaded" disorders, such as cirrhosis, diabetes and heart disease, but according to the latest findings also in the breast cancer. Magnetite nanoparticles were found at increased levels in patients with the neurodegenerative disorders.

Since these particles, due to their magnetic properties, can be "visible" by the magnetic resonance imaging (MRI), they can become a biomarker for the noninvasive diagnostics of the above-mentioned disorders. However, the unresolved questions are still remaining. The most important is, to what extent and in what concentration and spatial distribution are these biogenic nanoparticles able to alter the MRI signal sufficiently for the detection by clinical tomographs.

In this paper we present a simple analytical computational method, based on so called "Cube model", which allows the calculation of the magnetic field parameters of the biogenic iron oxides ensembles. This allows the theoretical determination of the minimal concentration and spatial distribution of the particles still visible for the magnetic resonance imaging. Surprisingly, the magnetic field of the just one magnetite nanoparticle reaches values up to 1.2 T in the central ring system, at the proximity of particle's corners. However, its range is only in order of a few nanometers. Conclusions of this paper can push forward the practical applications of the biogenic iron imaging.

**VORTEX DYNAMICS IN FERROMAGNETIC NANOELEMENTS  
OBSERVED BY MICRO-HALL PROBES**

T. Ščepka<sup>1</sup>, J. Šoltýs<sup>1</sup>, M. Precner<sup>1</sup>, J. Fedor<sup>1</sup>, J. Tóbiš<sup>1</sup>, D. Gregušová<sup>1</sup>,  
F. Gucmann<sup>1</sup>, R. Kúdela<sup>1</sup>, and V. Cambel<sup>1</sup>

<sup>1</sup>*Institute of Electrical Engineering, Slovak Academy of Sciences, Dúbravská cesta  
9, 841 04 Bratislava, Slovak Republic*

Developments in controlled manipulation of magnetic domains in ferromagnet nanostructures have opened opportunities for novel fast, high-density, and low-power memories, including their new architectures – race track memories, magnetic random access memories, and bit pattern media. Magnetic properties of the nanomagnets are governed by magnetostatic and exchange energies, and are fundamentally influenced by its dimensions and shape. The micromagnetic objects with lowered symmetry help to explore vortex dynamics, therefore a new prospective shape of a nanomagnet with broken symmetry was proposed (“Pacman-like”, PL) [1].

In this work we measure the nucleation and annihilation of magnetic vortices in PL nanodots prepared from Permalloy ( $\text{Ni}_{81}\text{Fe}_{19}$ , Py) at 77 K. Lateral dimensions of explored objects are below 1  $\mu\text{m}$  with thickness of about 40 nm. The nanodots are located directly on the high-sensitive micro-Hall probe based on GaAs/AlGaAs/InGaP heterostructure by lift-off process. We use both, Hall and bend-resistance measurements for the vortex dynamics characterization. Experiments show good agreement of the magnetization reversal with the micromagnetic simulation. Other shapes of micromagnets are also considered to obtain more precise picture of the vortex dynamics.

[1] Cambel, V. and Karapetrov, G.: Control of vortex chirality and polarity in magnetic nanodots with broken rotational symmetry, Phys. Rev. B **84** (2011) 014424.

**APPLICATION OF EXTENDED JILES-ATHERTON MODEL FOR MODELLING THE INFLUENCE OF STRESS ON MAGNETIC CHARACTERISTICS OF THE CONSTRUCTION STEEL**D. Jackiewicz<sup>1</sup>, R. Szweczyk<sup>2</sup>, J. Salach<sup>1</sup> and A. Bieńkowski<sup>1</sup><sup>1</sup>*Institute of Metrology and Biomedical Engineering, sw. A. Boboli 8, 02-525 Warsaw, Poland*<sup>2</sup>*Industrial Research Institute for Automation and Measurements*

Paper concerns the possibility of using the Jiles-Atherton extended model to describe the magnetic characteristics of construction steel 45 under the influence of tensile stresses.

Experimental data was acquired with use of the frame-shaped sample made of the 45 steel. Sample was subjected to tensile stresses with use the material testing machine. During the measurements, the applied stress was changed from 5 MPa up to the rupture of the sample. The results confirmed that hysteresis loop changes significantly under tensile stresses.

Then influence of stresses on hysteresis loops was modeled with the Jiles-Atherton extended model. Extension of the model was connected with taking into account changes of average pinning energy required to break pinning site for different states of magnetisation of the sample. As a result, extended Jiles-Atherton model enabled modeling of the magnetic hysteresis loop for wide range of the amplitude of magnetising field.

The obtained results of the modeling are consistent with results of the experimental measurements. This consistency was confirmed by the high value of the  $R^2$  determination coefficient.

As a result of modeling changes of model's parameters under the influence of tensile stresses was determined. These changes creates new possibilities of explanation of the physical phenomena connected with magnetisation of the magnetic materials under stresses. Moreover, determination of the influence of stresses on Jiles-Atherton model parameters opens the new possibilities of assessment of the state of construction steel during its exploitation in industrial conditions.

**NOISE ANALYSIS OF MAGNETIC SENSORS USING ALLAN VARIANCE**K. Draganová<sup>1</sup>, F. Kmec<sup>1</sup>, J. Blažek<sup>1</sup>, D. Praslička<sup>1</sup>, J. Hudák<sup>1</sup> and M. Laššák<sup>1</sup><sup>1</sup>*Department of Aviation Technical Studies, Faculty of Aeronautics, Technical University of Kosice, Rampova 7, 041 21 Kosice, Slovakia*

The article deals with the noise analysis of magnetic sensors using Allan variance. In compare with the standard variance based on the variations around the average value, Allan variance provides a measure of the behavior of the variability of a quantity as it is averaged over different measurement time periods, which results into the better convergence and the possibility to distinguish types of noise directly. A significant advantage of this method is that it is based on the analysis of the time sequences of the measured data without the need of any transformations.

According to the IEEE “Recommended practice for inertial sensor test equipment, instrumentation, data acquisition, and analysis”, Allan variance approach and also the power spectral density approach are the preferred methods for the stochastic error identification of inertial sensors – accelerometers and gyroscopes. Allan variance analysis is therefore used to identify the stochastic error sources existing in inertial sensors, including white and quantization noise, random walk and flicker noise. A key aspect of the noise type determination is the dependence of the Allan variance on the averaging time. In such plots applying logarithmic scales for horizontal and also vertical axis, slopes of the dependence show noise properties. Allan variance analysis can identify time regions and provide differentiation between time intervals in which particular noise types are dominant.

Considering that magnetic sensors become even more often a part of inertial measurements units, the goal of this article is to prove that the method using Allan variance analysis can be very successfully applied also for magnetic sensor noise analysis. Therefore the Allan variance methodology was consequently applied to the noise analysis of measurements performed with considerably different types of magnetic sensors, including magnetic sensors based on amorphous magnetic microwires. Results of obtained data analysis graphically presented and statistically evaluated underline the correctness of the initial hypothesis and confirm suitability of the Allan variance approach for the stochastic error identification of magnetic sensors.

*This work was supported by the Slovak Research and Development Agency under Contract No. APVV 0266-10.*

**MAGNETOMETRIC MEASUREMENTS OF LOW CONCENTRATION OF COATED  $\text{Fe}_3\text{O}_4$  NANOPARTICLES**

M. Škrátek, I. Šimáček, A. Dvurečenskij and J. Maňka

*Institute of Measurement Science, Slovak Academy of Sciences, Dúbravská cesta 9, 841 04 Bratislava, Slovakia*

A modified *ac* susceptometric method for the detection of coated  $\text{Fe}_3\text{O}_4$  magnetic nanoparticles (CMNP) at low concentration (of the order of tens of  $\mu\text{g}/\text{cm}^3$ ) in the samples modeling the internal organs of the laboratory animals (Wistar rats) is presented. For this purpose, the *rf* SQUID system with a spectral sensitivity of  $2 \times 10^{-14} \text{ T Hz}^{-1/2}$  (SQS) consisting of gradiometric sensor, magnetization system and the electronics, has been used. The paper presents basic information how to use this method and how to quantify and monitor the distribution of CMNP in the tested biological object. The results from model measurements helped to define achieved sensitivity of the method and to analyze the factors which significantly affect the accuracy of obtained results. It has been shown that in addition to the physical-magnetic properties of CMNP and the intensity of their magnetization, mainly the volume and the shape of measured biological tissue with dispersed CMNP and its position to the sensor influence the results. Also other factors are discussed, such as the effects of surrounding environment and some practical experience gained from measurements with experimental animals. The results of measurements of CMNP low concentrations in aqueous solution realized by SQS were confronted with the measurements of magnetic moments on equivalent microsample solutions using SQUID magnetometer Quantum Design MPMS XL 7 AC.

**MAGNETIC PROPERTIES OF  $V_2O_3$  NANOOXIDE PREPARED MECHANOCHEMICALLY WITH AND WITHOUT SALT MATRIX**

A. Dvurečenskij<sup>1</sup>, P. Billik<sup>1,2</sup>, A. Cigán<sup>1</sup>, R. Bystrický<sup>1</sup>, J. Maňka<sup>1</sup>, M. Škrátek<sup>1</sup> and M. Majerová<sup>1</sup>

<sup>1</sup>*Department of Magnetometry, Institute of Measurement Science*

*Slovak Academy of Sciences, Dúbravská cesta 9, 841 04 Bratislava, Slovakia*

<sup>2</sup>*Department of Inorganic Chemistry, Faculty of Natural Sciences, Comenius University, Mlynská dolina, 842 15 Bratislava, Slovakia*

$V_2O_3$  has been extensively studied as the canonical Mott-Hubbard system.  $V_2O_3$  bulk shows the first-order metal-insulator transition at about 150 - 170 K, with an accompanying seven-order magnitude increase in conductivity and a shift from an antiferromagnetic to paramagnetic behaviour.

Bulk  $V_2O_3$  has been traditionally prepared, by reduction of  $V_2O_5$  with  $H_2$  at a high temperature, however, calcination temperature of  $>800$  °C is often needed to obtain the required  $V_2O_3$  phase. On the other hand, high temperatures result in particle coarsening and agglomeration. An alternative to calcination at an elevated temperature is a mechanochemical synthesis in a high-energy milling process. This processing involves the preparation of nanopowders emended in a salt matrix, which is formed as the second reaction product.

We present a new preparation of  $V_2O_3$  nanocrystals based on mechanochemical reduction of  $V_2O_5$  with  $Na_2SO_3$  as a reductant, followed by vacuum annealing. The magnetic properties of the  $V_2O_3$  nanocrystals were studied. Temperature dependence of the zero-field cooled (ZFC) and field cooled (FC) DC magnetic moment and magnetization  $M(H)$  curves were measured by the QD SQUID magnetometer MPMS XL-7. Molar susceptibilities of the samples were corrected to the effect of the sample holder and next to diamagnetic and paramagnetic temperature independent contributions. ZFC curves were fitted by the Curie-Weiss law,  $\chi = C/(T-\Theta)$  and values of Curie constant  $C$ , Weiss temperature  $\Theta$  and effective magnetic moment were determined. The  $V_2O_3$  sample in the salt matrix shows an expressive ZFC-FC hysteresis effect in the range from 10 to 145 K and magnetic transition from the antiferromagnetic to paramagnetic ordering at the temperature of about 144 K. Moreover, the magnetization curves  $M(H)$  are non-hysteretic at the temperatures from 10 to 300 K. In contrast with the present salt matrix, the  $V_2O_3$  nanocrystals of the samples after wash up the salt matrix do not show ZFC-FC hysteresis and noticeable magnetic transition.

**MAGNETIC PROPERTIES OF MB<sub>50</sub> COMPOUNDS**

A.S. Panfilov<sup>1</sup>, G.E. Grechnev<sup>1</sup>, V.B. Filipov<sup>2</sup>, A.B. Lyaschenko<sup>2</sup>  
and G.V. Levchenko<sup>2</sup>

<sup>1</sup>*B. Verkin Institute for Low Temperature Physics and Engineering, National Academy of Sciences of Ukraine, Kharkov 61013, Ukraine*

<sup>2</sup>*I. Frantsevich Institute for Problems of Materials Sciences, National Academy of Sciences of Ukraine, 03680 Kiev, Ukraine*

Interstitial doping with 3d-elements can substantially affect the electronic structure and magnetic properties of boron. These properties are dependent upon the type of the diluted 3d atoms which generate a magnetic subsystem of localized interacting electronic states within the band gap of boron.

Temperature dependence of the magnetic susceptibility  $\chi(T)$  of MB<sub>50</sub> (M=V, Cr, Mn, Fe, Co and Ni) was measured by a Faraday method in the temperature range 77–300 K in the magnetic field of about 5 kOe. The experimental data obey a modified Curie-Weiss law,  $\chi(T) \cong \chi_0 + C/(T - \theta)$ , wherein the temperature independent term  $\chi_0$  and Curie constant  $C$  are strongly defined by the type of 3d atoms, having their maximum values for M=Mn. Also, the observed negative values of paramagnetic Curie temperature  $\theta$  imply the antiferromagnetic type of interaction between localized 3d states.

The electronic structures and magnetic properties of the tetragonal boron B<sub>50</sub> with intercalated 3d atoms were investigated by means of ab initio calculations with a full potential linear MT orbitals method. The MB<sub>50</sub> elementary cell contains 4 icosahedra of B<sub>12</sub>, whereas two boron atoms and 3d atom  $M$  occupy vacant positions. The ab initio calculations provide a possibility to investigate changes in the electronic structure of B<sub>50</sub> by introducing 3d atoms of various valency. According to the calculations the intercalated 3d atoms form a peak in the density of electronic states (DOS) at the energy gap region. The position of the peak and structure of DOS depend significantly on a type of introduced 3d atom. The hybridization and exchange splitting of the electronic states result in noticeable difference of DOS for the spin-up and spin-down subbands, and also to a possibility of emergence of the half-metal state in MB<sub>50</sub>. The calculations provided the values of magnetic moments which exhibit nonmonotonic behavior within the series of intercalated 3d atoms, with a magnetic moment maximum for MnB<sub>50</sub> in accordance with experimental data.

**HIGH RESOLUTION EDDY CURRENT TOMOGRAPHY SYSTEM FOR NONDESTRUCTIVE TESTING**

J. Salach<sup>1</sup> and R. Szewczyk<sup>2</sup>

<sup>1</sup>*Institute of Metrology and Biomedical Engineering, Warsaw University of Technology, sw. A. Boboli 8, 02-525 Warsaw, Poland*

<sup>2</sup>*Industrial Research Institute for Automation and Measurements PIAP, Al. Jerozolimskie 202, 02-486 Warsaw, Poland*

Tomography creates new possibilities for non-destructive testing technology. However, x-ray based tomography creates safety problems. For this reason application of x-ray for tomography is expensive, problematic and sometimes danger for operators.

Paper presents newly developed experimental setup for high resolution eddy current tomography. Presented solution enable analyze of internal structure of tested sample made of conductive material, both magnetic as well as non-magnetic. Presented eddy current tomography system is safe for operators and can be easily adapted for industrial quality control systems.

Measuring signal from eddy current tomography system consist both amplitude and phase shift on detection coil. As a result internal structure of material, from the point of view of magnetic permeability and conductivity, may be calculated on the base of Maxwell equations. Results of such measurements for both magnetic and non-magnetic testing elements are presented in the paper.

Results presented in the paper open new possibilities of development of data processing algorithms for eddy current tomography. This processing covers non-linear filtration of measuring signal, inverse transformation based on Maxwell equations. Development of each step of this signal processing is very important from both theoretical and practical point of view.



**EFFECT OF FILLER MIXTURE RATIO ON PERMEABILITY OF MULTICOMPONENT SOFT MAGNETIC COMPOSITES**R. Dosoudil<sup>1</sup>, M. Ušáková<sup>1</sup>, A. Grusková<sup>2</sup> and J. Sláma<sup>1</sup><sup>1</sup>*Institute of Electrical Engineering, Slovak University of Technology, Ilkovičova 3, 812 19 Bratislava, Slovakia*<sup>2</sup>*Institute of Power and Applied Electrical Engineering, Slovak University of Technology, Ilkovičova 3, 812 19 Bratislava, Slovakia*

The influence of the mixture ratio of hybrid LiZnTi/FeSiAl filler in LiZnTi/FeSiAl/PVC composite materials on their frequency dispersion of complex permeability  $\mu = \mu' - j\mu''$  has been measured and analyzed. The LiZnTi ferrite of composition  $\text{Li}_{0.525}\text{Zn}_{0.30}\text{Ti}_{0.35}\text{Fe}_{1.825}\text{O}_4$  (synthesized by a ceramic route at 1050°C/3.5h in air) and commercially available FeSiAl alloy (Kovohuty Co., Dolný Kubín, Slovakia) of composition  $\text{Fe}_{82.5}\text{Si}_{15.0}\text{Al}_{0.3}$  (the rest to balance present Mn, C and Cr with amount less than 1%) in bulk and also powder form were used as magnetic fillers. The particle size of fillers was controlled under 250  $\mu\text{m}$  for LiZnTi ferrite and under 160  $\mu\text{m}$  for FeSiAl alloy, respectively. The morphology of fillers was confirmed by scanning electron microscopy (SEM). The powder fillers were uniformly mixed with polyvinylchloride (PVC) at a constant total filler's volume content of 60 vol%. The mixture ratio of hybrid LiZnTi:FeSiAl filler was set to 1:0, 0.75:0.25, 0.5:0.5, 0.25:0.75, and 0:1. Ring shaped composite samples (outer diameter 7.9 mm, inner diameter 3.2 mm and thickness of 1.8 – 2.5 mm) were obtained by thermal pressing the ferrite/alloy/polymer mixture into a brass die under a pressure of 5 MPa and a temperature of 145°C. Complex permeability in the frequency range of 100 Hz – 6.5 GHz was measured on final samples by a combined impedance/network analysis method. The dc electrical conductivity was determined using standard four-probe procedure. Whereas the bulk samples (LiZnTi spinel ferrite and FeSiAl metal alloy) showed the resonance type of permeability dispersion, the composites exhibited both the resonance and relaxation one: the real part ( $\mu'$ ) of permeability at low frequencies decreased owing to demagnetizing effects of filler particles embedded in polymer matrix and the dispersion varied from resonance type to relaxation one with the configuration change from LiZnTi/PVC composite to FeSiAl/PVC one. The dispersion of permeability was due to the domain wall as well as natural ferromagnetic (or spin precession) resonance phenomena. The skin depth effect due to the eddy currents affected the permeability too, especially in samples with higher content of conductive magnetic filler.

**PRESENCE OF PARIMAGNETISM IN  $\text{Ho}(\text{Co}_{1-x}\text{Si}_x)_2$  UNDER HYDROSTATIC PRESSURE**

Jaroslav Valenta<sup>1</sup>, Jiří Prchal<sup>1</sup>, Marie Kratochvílová<sup>1</sup>, Martin Mišek<sup>1</sup> and Vladimír Sechovský<sup>1</sup>

<sup>1</sup> DCMP, Faculty of Mathematics and Physics, Charles University in Prague, Ke Karlovu 5, 121 16 Prague 2, Czech Republic

$\text{HoCo}_2$  belongs to a group of  $\text{RECo}_2$  compounds (RE = rare earth metal) which were mostly studied by the second half of the last century due to presence of two types of magnetism. The localized 4f electrons create localized R magnetic moment while the Co magnetism originates in the splitting of the Co 3d subbands. The corresponding RE and Co magnetic sublattices are both ferromagnetic and antiparallel to each other for  $R \in (\text{Gd}..\text{Tm})$  below  $T_C$ . In 2007 Herrero-Albillos et al. [1] published experimental evidences of the Co moments surviving in paramagnetic state above  $T_C$  in  $\text{ErCo}_2$ . The surviving Co magnetic moments form small (ferromagnetic) clusters couple antiparallel to the nearest RE magnetic moments in the paramagnetic state. These antiparallel short-range Co-Er moment correlations at  $T > T_C$  are denoted as parimagnetism [1]. Above a characteristic temperature  $T_f$  (observed in the AC magnetic susceptibility data as a tiny anomaly) the Co magnetic moment turns to the same direction as Er magnetic moment. The phenomenon of parimagnetism has been recently confirmed for  $\text{HoCo}_2$  [2]. In this contribution we present new results evidencing considerable composition and hydrostatic pressure influence on parimagnetism in  $\text{Ho}(\text{Co}_{1-x}\text{Si}_x)_2$  compounds for  $x \leq 7.5\%$ . The results will be discussed in terms of corresponding variations of the hierarchy inter- and intra-sublattice exchange interactions.

[1] J. Herrero-Albillos et al., Phys.Rev.B **76** (2007) 094409.

[2] C.M. Bonila et al., J.Appl.Phys. **111** (2012) 07E315.

**DEGREE OF CRYSTALLINITY EVALUATION OF PARTIALLY CRYSTALLINE POLYPROPYLENES USING  $^{13}\text{C}$  NMR**V. Hronský<sup>1</sup>, P. Vrábel<sup>1</sup>, M. Kovařáková<sup>1</sup> and D. Olčák<sup>1</sup><sup>1</sup>*Department of Physics, Faculty of Electrical Engineering and Informatics, Technical University of Košice, Park Komenského 2, 042 00 Košice, Slovakia*

The degree of crystallinity is an important morphological characteristic which determines many properties of polymeric materials. It is usually defined in terms of the weight fraction of crystalline domains within a polymer. The evaluation of the degree of crystallinity using  $^{13}\text{C}$  NMR is based on the fact that magnetic moments of the nuclei of the same functional group within crystalline and amorphous domains experience different internal magnetic fields and produce different lines in the  $^{13}\text{C}$  NMR spectra. The relative number of  $^{13}\text{C}$  nuclei within crystalline domains, which is the degree of crystallinity, can be estimated by the deconvolution of  $^{13}\text{C}$  NMR spectra. This approach was used in our previous paper for estimation of the degrees of crystallinity for two pelletized, partially-crystalline polypropylene (PP) materials produced by different technologies. We have found, however, that thin PP foils show three lines in the  $^{13}\text{C}$  NMR spectrum instead of just two, related to crystalline and amorphous domains. For this reason a modification of the experimental technique enabling estimation of the degree of crystallinity of PP is presented in this paper.

The  $^{13}\text{C}$  NMR spectrum obtained using direct polarization has a very low signal to noise ratio and for this reason an accumulation of at least one thousand scans is necessary to obtain highly-resolved spectra. The delay time between two consecutive scans has to be at least  $5T_1$  ( $T_1$  – spin-lattice relaxation time) to allow the spin system to have sufficient time for relaxation. The  $T_1$  for spins associated with crystalline domains is much longer than that associated with amorphous domains. For this reason a very long delay time determined by the  $T_1$  of crystalline domains has to be chosen to detect signals originating from both domains in the  $^{13}\text{C}$  NMR spectra. In direct polarization experiments with a short delay time only signals from amorphous domains can be detected, since the spin system in crystalline domains does not have sufficient time for relaxation. Due to the short delay time the heteronuclear Overhauser enhancement of the  $^{13}\text{C}$  NMR signals was observed in this experiment. The spectra measured with both techniques were used for the estimation of the degree of crystallinity, whereby the heteronuclear Overhauser enhancement of the  $^{13}\text{C}$  NMR signals was taken into account in the calculations.

**THE BAND STRUCTURE OF THE MAGNETOPHOTONIC CRYSTAL SPECTRUM IN VICINITY OF ELECTRON SPIN RESONANCE**G. Kharchenko<sup>1</sup> and S. Tarapov<sup>1</sup><sup>1</sup>*Radiospectroscopy Department, O.Ya. Usikov Institute for Radiophysics and Electronics of the NAS of Ukraine, Ac. Proskury Str. 12, 61085 Kharkiv, Ukraine*

Magnetophotonic crystals (MPC) take a special place among the other electrodynamic materials/structures due to the strong dispersion of the crystal components permeability. One of the promising technological implementation and application of such structures can be their usage as basis for generation of cheap and compact magnetically controlled passive electronic components (couplers, switches, routers). An important issue here is the providing the control of their spectra. In this connection, the most interesting range of frequencies and magnetic fields is the range of maximum dispersion of the permeability, i.e. the range of Electron Spin Resonance (ESR). Since in vicinity of ESR the value of real part of the permeability increases sharply (by known equations of Landau-Lifshitz), this fact can cause very significant, but non-obvious change in the structure of the spectrum.

It is well known that the spectrum of the periodic structure has a band nature and consists of a set of passbands (PB) and stopbands (SB). However, in this case the strong frequency dispersion observed in vicinity of ESR frequency, results in a significant change in the spectrum, namely, in the appearance of the family of narrow transmission peaks – "secondary bands".

During the research the appearance of the set of secondary bands in the MPC spectrum associated with the sharply increasing of the frequency dispersion of the real part of permeability of the ferromagnetic layer (ferrite) has been found theoretically. The analysis of the nature of secondary bands was carried out. It was shown that the origin of secondary bands is connected with the conditions of the known Wolf-Bragg resonance in the primary cell of MPC in vicinity of ESR. The characteristic frequency of each secondary band has been calculated. It was shown that this frequency is determined by the requirement that the integer number of a half-waves should be packed in the primary cell of the magnetophotonic crystal.

## INFLUENCE OF MAGNETITE NANOSPHERES PROPERTIES ON INSULIN AMYLOID AGGREGATION

Zuzana Bednarikova<sup>1,3</sup>, Katarina Siposova<sup>1,3</sup>, Martina Koneracka<sup>2</sup>, Vlasta Zavisova<sup>2</sup>, Martina Kubovcikova<sup>2</sup>, Milan Timko<sup>2</sup>, Erna Demjen<sup>1</sup>, Peter Kopcansky<sup>2</sup> and Zuzana Gazova<sup>1</sup>

<sup>1</sup>*Department of Biophysics, <sup>2</sup>Department of Magnetism, Institute of Experimental Physics, Slovak Academy of Sciences, Watsonova 47, 040 01 Kosice, Slovakia*

<sup>3</sup>*Department of Biochemistry, P J Safarik University, Moyzesova 11, 040 01 Kosice, Slovakia*

Pathogenesis of so-called amyloid diseases is associated with the formation of amyloid aggregates in different parts of the body. Insulin amyloid aggregation have been observed in patients long-term treated with injected insulin and also causes problems in the production and storage of this drug and in application of insulin pumps.

We have investigated interaction of bovine serum albumin modified magnetite nanoparticles (MFBSA) as well as MFBSA wrapped in biocompatible and biodegradable polymer poly(D,L-lactide) (MFNPs) with insulin amyloid aggregation by Thioflavin T (ThT) fluorescence assay and atomic force microscopy. Both types of magnetic nanospheres were characterized by the routine methods such as scanning electron microscopy (SEM), dynamic light scattering (DLS) and magnetic measurements. SEM analysis showed almost spherical shape of the studied nanospheres with hydrodynamic diameters  $D_{\text{hydr}}$  (MFBSA) = 80 nm and  $D_{\text{hydr}}$  (MFNPs) = 200 nm determined by DLS method, respectively. Magnetic measurements confirmed superparamagnetic behaviour of magnetic nanospheres with core magnetic diameter  $D_{\text{Mag}}$  = 9 nm.

Presence of both types of magnetite nanospheres caused depolymerization of insulin amyloid fibrils. The extent of anti-amyloidogenic activity was affected by structure and physico-chemical features of studied magnetite nanospheres. We have found that size of the nanospheres is the main factor affecting the depolymerizing efficiency. The effect of the magnetic field on magnetite induced depolymerization of insulin aggregates was also studied.

*Acknowledgement: This work was supported within the projects SF of EU 26110230061, VEGA 0181, 0041, APVV 0171-10 and VVGS 38/12-13.*

**MAGNETO-OPTICAL KERR EFFECT SPECTROSCOPY SETUP  
BASED ON PHOTOELASTIC MODULATOR**

R. Silber<sup>1</sup>, J. Hamrle<sup>1</sup>, D. Hrabovský<sup>1</sup>, J. Pištora<sup>1</sup>

*<sup>1</sup>Institute of Physics and Nanotechnology Centre, VSB-Technical University of  
Ostrava, 17. listopadu 15, 70833 Ostrava, Czech Republic*

We present magneto-optical setup allowing to measure spectra of the magneto-optical Kerr effect (MOKE). The setup is based on the photoelastic modulator, providing advantages of better signal to noise ratio and simple measurement of Kerr ellipticity, without use of phase plates. On the other hand, the disadvantage is need of detailed calibration of the photoelastic modulation.

Within this work we present detailed principle of the operation of the setup, as well as description of its calibration. We further demonstrate ability to measure both linear and quadratic spectra of MOKE.

**BARKHAUSEN NOISE INVESTIGATIONS OF HOT ROLLED  $\phi 30$  MM STEEL BARS**

T. Garstka, K. Laber

*Faculty of Materials Processing Technology and Applied Physics, Czestochowa University of Technology, Al. Armii Krajowej 19, 42-200 Czestochowa, Poland*

This article presents results of non-destructive examination of hot rolled steel bars by the magnetic Barkhausen method.

During investigations of industrial process of  $\phi 30$  mm bars production, after various, four type kind of controlled cooling variants, the differentiation of mechanical properties was achieved. After microstructure assessment and Vickers hardness test, the Barkhausen Noise (BN) method was applied to find the non destructive way for estimation and properties control of produced bars.

The Barkhausen noise examinations were carried out using the measuring apparatus developed at Faculty of Materials Processing Technology and Applied Physics of Technical University of Czestochowa. On the surface of bars' samples, the measurements of BN were done. The typical parameters of BN like amplitude, root mean square value of BN as well as shape and the time dependences of the BN envelope peak shift were analyzed.

As an effect of these investigations, found and described a link between Barkhausen Noise parameters and the microstructure of subsurface layer of the rods.

**MAGNETIC PROPERTIES OF MECHANOCHEMICALLY SYNTHESIZED MIXED OXIDES**N.G. Kostova<sup>1</sup>, A. Zorkovská<sup>2</sup>, J. Kováč<sup>3</sup>, and P. Baláž<sup>2</sup><sup>1</sup>*Institute of Catalysis, Bulgarian Academy of Sciences, acad. G. Bonchev, Bl.11, 1113 Sofia, Bulgaria*<sup>2</sup>*Institute of Geotechnics, Slovak Academy of Sciences, Watsonova 45, 040 01 Košice, Slovakia*<sup>3</sup>*Institute of Experimental Physics, Slovak Academy of Sciences, Watsonova 47, 040 01 Košice, Slovakia*

Superparamagnetic iron oxide nanoparticles are emerging as promising candidates for biosensors, drug delivery, cancer hyperthermia and magnetic resonance imaging. However, the intrinsic magnetic properties of iron oxide are far from optimal for diverse biomedical applications. Fe<sub>2</sub>O<sub>3</sub>-ZnO mixed oxides and zinc ferrite were synthesized by mechanochemical method. The properties of the powders were characterized by X-ray diffraction, infrared spectroscopy, diffuse reflectance spectroscopy, and magnetic measurements. The influence of thermal treatment conditions on particle size and phase composition of the powders was studied.

The diffraction peaks of the ZnFe<sub>2</sub>O<sub>4</sub> nanoparticles are slightly shifted to small diffraction angles when the calcination temperature increases. This can be attributed to the increase in lattice parameter caused by the successful substitution of Fe<sup>3+</sup> with larger Zn<sup>2+</sup> cations in the spinel structure, which further verifies the formation of zinc ferrite. From the peak widths, the average crystallite size was estimated using Scherrer's formula to be 60 nm.

The magnetic behavior of as-prepared ZnFe<sub>2</sub>O<sub>4</sub> and Fe<sub>2</sub>O<sub>3</sub>-ZnO nanoparticles, for comparison purposes, was investigated using a vibrating sample magnetometer in magnetic field up to 6 T. The magnetization of mechanically activated stoichiometric mixed oxide increases after calcination at 973 K, and the room temperature magnetization of ZnFe<sub>2</sub>O<sub>4</sub> nanoparticles in magnetic field of 6 T reaches 46 emu g<sup>-1</sup>. At 300 K no significant hysteresis was observed and the nanoparticles exhibit superparamagnetic – like behavior.

**Acknowledgement:** *This investigation was financially supported by the National Science Fund of Bulgaria (project DNTS/Slovakia 01/3), by the Slovak Research and Development Agency (project APVV-0189-10), by the projects of Ministry of Education of the Slovak Republic VEGA (project 1/0861/12), and through a bilateral project between Bulgarian Academy of Sciences and Slovak Academy of Sciences.*



**EFFECT OF MAGNETIC FIELD ON THE FLUCTUATIONS OF CHARGED OSCILLATORS IN VISCOELASTIC FLUIDS**L. Glod<sup>1</sup>, J. Tóthová<sup>2</sup> and V. Lisý<sup>2</sup><sup>1</sup>*Department of Mathematics and Physics, The University of Security Management, Kukučínova 17, 040 01 Košice, Slovakia*<sup>2</sup>*Department of Physics, Technical University of Košice, Park Komenského 2, 042 00 Košice, Slovakia*

Stochastic motion of charged particles in magnetic fields was first studied half a century ago in connection with the diffusion of electrons and ions in plasma. In the classical works by Taylor and Kurşunoğlu the long-time limits of the mean square displacement (MSD) of the particles have been found. Later Furuse on the basis of the standard Langevin theory with the white-noise force driving the particles generalized their results for arbitrary times. The currently observed revival of these problems is mainly related to memory effects in the particle diffusion. Such effects appear when more realistic colored random forces act on the particles from their surroundings. In the present work an exact analytical solution of the generalized Langevin equation has been found for the motion of the particle in an external magnetic field when the random force is exponentially correlated in the time. Due to the fluctuation-dissipation theorem this model is consistent with the assumption that the solvent has weakly viscoelastic properties, which corresponds to the theory, originally proposed by Maxwell and later substantiated coming from first principles. The obtained MSD of the particle motion across the field contains a term proportional to the time, a constant term, and contributions exponentially decaying in the time. Also the problem of the fluctuations of charged Brownian particles trapped in the harmonic potential and exposed to the magnetic field is fully solved. These findings are more general than the previous results from the literature and are obtained in a way applicable to many other problems of the Brownian motion with memory.

**ELECTRICAL RESISTIVITY IN CrN THIN FILMS**I. Batko<sup>1</sup>, M. Batkova<sup>1</sup> and F. Lofaj<sup>2</sup><sup>1</sup>*Institute of Experimental Physics, Slovak Academy of Sciences, Watsonova 47, 040 01 Košice, Slovak Republic*<sup>2</sup>*Institute of Materials Research, Slovak Academy of Sciences, Watsonova 47, 040 01 Košice, Slovak Republic*

Chromium nitride (CrN) has received considerable attention due to its high mechanical hardness, high-temperature stability and corrosion resistance for applications in hard, wear, and corrosion resistant coatings. In addition, CrN attracts increasing interest as a potential electronic or spintronic material due to its magnetic ordering and possible band gap, which makes it a promising material for diluted magnetic semiconductors. Another interesting application lies in the field of thermometry, such as CrN thin films fabricated by RF-magnetron sputtering were reported as prospective temperature sensors for cryogenic region with (very) small magnetoresistance.

We present results of electrical resistivity measurements for CrN thin films deposited on glass substrates by DC-magnetron sputtering in Ar + N<sub>2</sub> atmosphere. The studied films have revealed semiconducting behavior of electrical resistivity in the range of tested preparation parameters (such as pressure and composition of Ar-N<sub>2</sub> mixture), whereas the electrical transport regime has been strongly influenced by parameters of preparation. Numerical analysis of experimental data indicates that in selected temperature intervals electrical transport can be adequately described in terms of variable-range hopping conduction. Moreover, S-shape anomaly in  $\rho(T)$  dependence in temperature interval of 230 K - 260 K has been observed for some samples. Possible origin of this anomaly and regimes of electrical transport will be discussed in the paper in more details.

*This work was supported by the ERDF EU (European Union European regional development fond) grant under Contract No. ITMS 26220120005.*

**ELECTRICAL CONDUCTIVITY OF Ti/TiO<sub>x</sub>/Ti STRUCTURES AT LOW TEMPERATURES AND HIGH MAGNETIC FIELDS**

I. Batko and M. Batkova

*Institute of Experimental Physics, Slovak Academy of Sciences, Watsonova 47, 040 01 Košice, Slovak Republic*

Thin films and thin-films structures composed of metal oxides can display a rich variety of electronic and magnetic properties, including colossal magnetoresistance, superconductivity, and multiferroic behaviour. Because of the diversity of properties, many metal-oxide based materials and structures find utilization in various technological applications, such as sensors of temperature, magnetic field, or gas. Electric conduction of metal oxides is as a rule sensitive to concentration of oxygen vacancies. Therefore, electric properties of these materials are strongly influenced by preparation method and parameters of the preparation process, what offers unique opportunity to modify electric properties by modification/variation of synthesis conditions.

In this work we present results of electrical conductivity studies of Ti/TiO<sub>x</sub>/Ti test structures prepared by tip-induced oxidation of titanium thin films by use of atomic force microscope (AFM). For purposes of the presented work, titanium thin films in geometry of micro-bridges were deposited on glass substrates by DC-magnetron sputtering. Consequently, oxide barriers across the bridges were fabricated by AFM at ambient conditions (with humidity kept in the interval between 55 - 60%). The prepared Ti/TiO<sub>x</sub>/Ti structures have revealed almost linear *I-V* curves at temperatures from 300 K down to 30 K; and clearly non-linear *I-V* curves at 10 K. Very interesting property of the studied Ti/TiO<sub>x</sub>/Ti structures is that they reveal very small magnetoresistance in magnetic fields up to 9 T over the whole temperature region of 10 - 300 K. Such property in combination with the high sensitivity of the electric conduction to temperature changes indicates their promising application as temperature sensors for cryogenic region and high magnetic fields. Electric properties and application potential of the studied structures will be discussed in more details in the paper.

*This work was supported by the ERDF EU (European Union European regional development fond) grant under Contract No. ITMS 26220120047.*

**THE EFFICIENCY OF MÖSSBAUER SPECTRA FITTING PERFORMED WITH THE GENETIC ALGORITHM**

Tomasz M. Gwizdała, Ewelina Frątczak, Małgorzata Antoszevska-Moneta, Krzysztof Warda

*Department of Solid State Physics, University of Łódź, Pomorska 149/153, 90-236 Łódź*

The analysis of Mössbauer spectra is one of the fundamental problems of experimental magnetism. Since the determination of experimental distribution can be considered as a curve fitting problem, the numerical methods appropriate for such issues are also in use for the study of Mössbauer effect. Among the potentially efficient methods we can enlist global optimization techniques especially Genetic Algorithm.

In our previous paper [1] we studied the dynamics of the optimization process and emphasized the influence of different factors on the efficiency of optimization. When considering different factors we took into account as well those of experimental character, like the measurement inaccuracy, as the numerical parameters which control the optimization run. The basic assumption was that the optimization process is indeed the hybrid one and much attention had to be paid to the correct choice of switching point which separated the global and local optimization process.

In the paper mentioned above we study the theoretical spectra which contained only sextets built of pure Lorentzians. The number of sextets was limited to four. In the presented paper we are going to show some more advanced results for as well more number of sextets as singlets and doublets included. We study the effect of these changes on the characteristics obtained for pure systems and the some trends observable by increasing the complexity of spectrum. We show also the role of initial parameter tuning.

[1] T.M.Gwizdała, M.E.Moneta, Nucl.Instr.Meth.Phys.Res.B, 279 (2012) 205-207

# **EFFECT OF THE FIXATION PATTERNS ON MAGNETIC CHARACTERISTICS OF AMORPHOUS GLASS-COATED SENSORIC MICROWIRES**

R. Hudak<sup>1</sup>, P. Klein<sup>2</sup>, J. Hudak<sup>3</sup>, D. Praslicka<sup>3</sup>, J. Blazek<sup>3</sup> and R. Varga<sup>2</sup>

<sup>1</sup>*Department of Biomedical Engineering and Measurement, Technical University of Kosice, Letna 9, 042 00 Kosice, Slovakia*

<sup>2</sup>*Department of Physics of Condensed Matters, Pavol Jozef Safarik University in Kosice, Park Angelinum 9, 041 54 Kosice, Slovakia*

<sup>3</sup>*Department of Aviation Technical Studies, Technical University of Kosice, Rampova 7, 041 21 Košice*

One of the frequent reasons of titanium implants' failures in human body are incorrect biomechanical interactions within the tissue – implant interface and inflammatory processes arising around the implant's application area. Within both processes, it is crucial location and in time intervention.

One of the monitoring possibility of the mentioned processes is an application of amorphous glass-coated sensoric microwires (AGCSM).

Magnetic characteristics of these microwires are influenced by both mechanical tension (magnetoelastic interaction of the magnetic moment with mechanical stress) and by temperature (different coefficient of thermal expansion of the metal core and glass coating).

The key task, in order to change the magnetic characteristics of AGCSM from both clinical and scanning point of view, appears to be fixation pattern of AGCSM in the implant's body.

The presented study shows the impact of three types of AGCM fixation (at the endings, in the middle and by sealing the whole wire) on the thermal response process tested in laboratory conditions. The obtained results will enable to establish the AGCM fixation methodology in the implant's body in order to achieve optimal output temperature parameters from the implant and the tissue – implant interface by magnetic contactless measurements.

*Presented research was supported by project Research of New Diagnostic Methods in Invasive Implantology, MŠSR-3625/2010-11, Stimulus for Research and Development of Ministry of Education, Science, Research and Sport of the Slovak Republic, Project NanoCEXmat No.ITMS 26220120019, VEGA Grant no.1/0060/13 and APVV-0266-10.*

**SOLID STATE  $^{13}\text{C}$  NMR STUDIES OF MODIFIED PHB POLYMER**P. Vrábel<sup>1</sup>, O. Fričová<sup>1</sup>, V. Hronský<sup>1</sup>, M. Kovaľáková<sup>1</sup>, D. Olčák<sup>1</sup> and I. Chodák<sup>2</sup><sup>1</sup>*Department of Physics, Faculty of Electrical Engineering and Informatics, Technical University of Košice, Park Komenského 2, 042 00 Košice, Slovakia*<sup>2</sup>*Polymer Institute, Slovak Academy of Sciences, Dúbravská cesta 9, 842 36 Bratislava, Slovakia*

The substitution of conventional polymeric materials by biodegradable materials is one of the most attractive recent trends in material science. PHB (polyhydroxybutyrate) belongs to biologically synthesized polymers. It is non-toxic, biocompatible, biodegradable, and thermoplastic. PHB is semicrystalline and its mechanical properties are similar to those of isotactic polypropylene, except for elongation at break leading to low toughness. Moreover, under ambient conditions its properties change significantly due to physical aging. On the other hand, an application of several modifications results in material with unique mechanical properties.

Properties of polymeric materials are determined by their structure and interactions at molecular as well as supramolecular grade, and molecular motion is closely related to the structure. The present paper is aimed at understanding the influence of thermal treatment, plastification and compatibilization on the structure and molecular dynamics of PHB by means of nuclear magnetic resonance spectroscopy, which is known as a unique tool for the study of the structure and molecular dynamics of polymeric materials. For this purpose the  $^{13}\text{C}$  NMR spectra were measured applying direct polarization technique under magic angle spinning (MAS) at the spinning rate of 10 kHz. The measurements were carried out at ambient temperature and at 98 °C.

PHB contains nuclei of carbons in four different groups, CO, CH, CH<sub>2</sub> and CH<sub>3</sub>, and therefore the magnetic moments of the  $^{13}\text{C}$  nuclei embedded into external magnetic field interact with the four different internal magnetic fields produced by the electrons surrounding them. Owing to these interactions four lines appeared at 170.0, 68.5, 41.3 and 21.4 ppm associated with the CO, CH, CH<sub>2</sub> and CH<sub>3</sub> groups respectively, in the  $^{13}\text{C}$  MAS NMR spectrum. The changes of the structure and molecular motion in PHB as a consequence of its thermal treatment and plastification will be concluded from the shapes and widths of the particular lines of the  $^{13}\text{C}$  MAS NMR spectra.

# **INDEX OF AUTHORS**

Ababei G.	Iași	P2-53	P2-52		
Abd-Elmeguid M.M.	Köln	O7-07			
Actis Grande M.	Alessandria	P2-59	P3-17		
Ahmida M.A.	Köln	O7-07			
Albertini F.	Parma	08-03			
Alekseev P.A.	Moscow	P7-04			
Ali Alghamdi N.A.	Košice	P5-17			
Almáši M.	Košice	P6-16			
Amato A.	Villigen	O5-03			
Anders A.G.	Kharkov	P5-03			
Andreev A.V.	Prague	P6-02	P6-08	P6-14	
Andrus M.J.	Gainesville	O5-01	P5-04		
Anisimov M.	Moscow	P6-03	P7-13	P7-14	P7-15
Antal I.	Košice	P5-19			
Antal V.	Košice	P3-08	P7-19	P7-22	P7-23
		P7-24			
Antalik M.	Košice	P4-25	P5-23		
Antkowiak M.	Poznań	O5-05			
Antoňák M.	Košice	P6-04			
Antoszevska-Moneta M.	Łódź	P2-46	P9-17		
Aogaki R.	Tokyo	O9-01	O9-02		
Arnold Z.	Prague	O8-03	P3-04	P6-11	
Asanuma M.	Yokohama	O9-01			
Azarevich A.N.	Moscow	O7-10	O7-14	P6-12	P7-11
Bajorek A.	Katowice	P3-15			
Bak Z.	Częstochowa	P7-27			
Balanda M.	Kraków	P6-04			
Baláz P.	Košice	P9-13			
Balcerzak T.	Łódź	O1-08	P1-05	P1-19	P4-03
Bałanda M.	Kraków	O5-03			
Bán K.	Budapest	P2-31			
Baran A.	Prešov	P7-20			
Barančeková-Husaníková P.	Bratislava		O7-03	P7-26	
Baranová L.	Košice	P5-12			
Barasiński A.	Zielona Gora	O5-05			
Barlíková Ž.	Košice	P2-07			
Bat'ko I.	Košice	P2-19	P9-15	P9-16	
Bat'ková M.	Košice	P2-19	P9-15	P9-16	
Battiato M.	Uppsala	O1-03			
Baybakov R.	Moscow	P6-03			
Bedarev V.A.	Kharkov	P8-01			
Bednarčík J.	Hamburg, Košice	O2-03	P2-03	P2-33	P2-41
		P6-16	P7-05		
Bednarikova Z.	Košice	P9-10			
Beedlel C.C.	Tallahassee	O5-01			



Bella P.	Košice	P3-18			
Besnard C.	Geneva	P6-21			
Bezmaternykh L.N.	Krasnoyarsk	P8-01			
Bidulská J.	Košice	P2-59	P3-17	P3-18	
Bidulský R.	Košice	P2-59	P3-17	P3-18	
Bieńkowski A.	Warszawa	O2-01	O9-08	P2-25	
Billik P.	Bratislava	P9-02			
Birčáková Z.	Košice	P2-32			
Blanco J.M.	San Sebastian	I1-01	P2-54		
Blanusa J.	Belgrade	P2-14	P2-15		
Blažek D.	Ostrava	O2-07	P3-20		
Blažek J.	Košice	O9-04	O9-09	P9-18	
Błoch K.	Częstochowa	P2-27	P2-28	P3-09	
Bobák A.	Košice	O1-05	O1-08	P1-14	
Boča R.	Trnava	P5-01			
Bocian K.	Poznań	P7-29			
Bogach A.V.	Moscow	O7-10	O7-14	P6-12	P7-11
		P7-14	P7-15		
Bondar N.	Kharkov	P6-13			
Borisenko K.B.	Oxford	P2-42			
Borovský M.	Košice	O1-05	O1-08		
Borza F.	Iași	P2-43	P4-19		
Botko M.	Košice	O1-07	P5-10	P5-11	
Braithwaite D.	Grenoble	P7-07			
Brázda P.	Husinec-Řež	O4-04	P4-17		
Briančin J.	Košice	P2-09	P6-10	P6-15	P6-18
Brunátová T.	Prague	P6-01			
Brzostowski B.	Zielona Góra	O5-05	P5-20		
Brzózka K.	Radom	P2-55			
Brzozowski R.	Łódź	P2-46			
Budeanu L.	Iași	P2-52			
Bujdoš M.	Bratislava	O2-04			
Bukovina M.	Žilina	P3-20			
Bukowski Z.	Wrocław	O7-13			
Bułka B.R.	Poznań	P4-23			
Bunda S.	Uzhgorod	P5-21	P5-22	P7-21	
Bunda V.	Uzhgorod	P5-21	P5-22	P7-21	
Bünemann J.	Stuttgart	P7-01			
Bureš R.	Košice	P2-19	P2-32	P2-49	P2-55
Buršík J.	Brno	P2-02			
Burzo E.	Cluj-Napoca	P4-09			
Butta M.	Prague	P2-56			
Butvin P.	Bratislava	P2-26	P2-58		
Butvinová B.	Bratislava	P2-26	P2-58		
Bystrický R.	Bratislava	P7-17	P9-02		

Bzdušek T.	Bratislava	O7-01			
Caciuffo R.	Karlsruhe	O6-06			
Cambel V.	Bratislava	O9-05	O9-07	P1-09	P7-26
Capik M.	Košice	P2-35	P2-36		
Carva K.	Prague, Uppsala	O1-03	O4-05		
Carvalho R.C.	Maceió	O1-02			
Čenčariková H.	Košice	P1-17	P1-18	P6-05	
Čermák P.	Prague	P6-01			
Černe J.	Buffalo	O4-06			
Chareev D.A.	Moscow	P7-02			
Chaud X.	Grenoble	P5-15			
Chelkowska G.	Katowice	P3-15			
Cheranovskii V.	Kharkov	O1-07			
Chiriac H.	Iași	O8-04	P2-38	P2-43	P2-52
		P2-53	P4-19		
Chizhik A.	San Sebastian	I1-01			
Chlan V.	Prague	P1-15	P1-16	P2-47	P2-48
		P8-03			
Chodák I.	Bratislava	P9-19			
Chovan J.	Banská Bystrica	P1-10			
Chrobak A.	Katowice	P3-12	P3-13	P3-14	P3-15
Chrobak M.	Kraków	O7-06			
Chromik Š.	Bratislava	P4-11	P4-12		
Churyukanova M.	Moscow	P2-54			
Chwastek K.	Częstochowa	P3-10			
Čigán A.	Bratislava	P7-17	P9-02		
Čilliková M.	Žilina	O2-07			
Ciprian D.	Ostrava	P3-01			
Čisárová I.	Prague	P6-01	P6-16		
Čisárová J.	Košice	P1-06			
Čížek J.	Prague	P2-02			
Čižmár E.	Košice	O5-01	O5-04	O5-07	P5-10
		P5-11	P5-18		
Colineau E.	Karlsruhe	O6-06			
Conde A.	Sevilla	I3-02			
Corodeanu S.	Iași	P2-43	P2-53		
Ćosović A.	Belgrade	P2-50			
Ćosović V.	Belgrade	P2-50			
Csach K.	Košice	P2-21	P2-22		
Custers J.	Prague	O7-04	6P-17		
Čverha A.	Košice	O9-04			
Czapla M.	Kraków	O5-03			
Dabkowska H.A.	Hamilton	O5-02			
Dabkowski A.	Hamilton	O5-02			
Dabrowski B.	De Kalb	O7-11			

Daniš S.	Prague	O6-02	P6-01		
David B.	Brno	P2-20	P2-50		
Dekan J.	Bratislava	P2-13			
Demishev S.V.	Moscow	O7-10	O7-14	P6-03	P6-12
		P7-03	P7-11	P7-12	P7-13
		P7-14	P7-15		
Demjen E.	Košice	P9-10			
Derer J.	Bratislava	O7-15			
Derzhko O.	L'viv	P1-01	P1-04		
Desnenko V.A.	Kharkov	P7-02			
Dhar S.K.	Mumbai	P6-21			
Diko P.	Košice	O7-05	P3-08	P7-19	P7-22
		P7-23	P7-24		
Diop L.V.B.	Grenoble	P6-11			
Diviš M.	Prague	O6-04	P6-07		
Dobák S.	Košice	P2-17			
Dobročka E.	Bratislava	P2-04	P4-12		
Dobrzańska-Danikiewicz A.	Gliwice	P2-30			
Dolinšek J.	Ljubljana	O8-02			
Dolník B.	Košice	P2-09	P5-06	P5-07	
Dolya S.	Kharkov	O7-12			
Dosoudil R.	Bratislava	P3-11	P9-06		
Dośpiał M.	Częstochowa	P2-27	P2-28	P2-29	P2-30
		P3-09	P3-10		
Draganová K.	Košice	O9-09			
Drchal V.	Prague	O4-05			
Drechsler S.-L.	Dresden	O1-01			
Dressel M.	Stuttgart	P7-03			
Drzewiński A.	Zielona Gora	O5-05			
Dubec J.	Žilina	O2-07			
Dubowik J.	Poznań	P4-20	P4-21		
Dudrová E.	Košice	P2-45			
Durajski A.P.	Częstochowa	P7-08			
Durin G.	Torino	I1-02			
Dušek M.	Prague	O7-04			
Dvurečenskij A.	Bratislava	P7-17	P9-01	P9-02	
Éber N.	Budapest	P5-15			
Edward M.	Madrid	P4-15			
Ehlers G.	Oak Ridge	O5-01			
El Kammouni R.	Madrid	P2-05			
Emilio J.	Łódź	P4-15			
Englich J.	Prague	P1-15			
Ensinger W.	Darmstadt	O2-02			
Fabbrici S.	Parma	O8-03			
Fáberová M.	Košice	P2-32	P2-49	P2-51	P2-55

Fabian J.	Regensburg	O4-01			
Fabián M.	Košice	P2-09			
Falkowski M.	Poznań	P3-03			
Farkašovský P.	Košice	P1-17	P1-18	P6-05	
Fedor J.	Bratislava	O7-15	O9-05	O9-07	
Fedorchenko A.V.	Kharkov	P7-02			
Fehér A.	Košice	O1-07	O5-04	O7-12	P5-03
		P5-10	P5-11	P5-12	P5-21
		P5-22	P7-20	P7-21	
Fekete L.	Prague	O8-01			
Fertman E.	Kharkov	O7-12			
Fijałkowski M.	Katowice	O7-08			
Fikáček J.	Prague	6P-17			
Filinchuk Y.	Grenoble	P6-21			
Filip J.	Olomouc	P2-48			
Filipecka K.	Częstochowa	P3-05	P3-06		
Filipov V.B.	Kiev	O7-10	O7-14	P6-03	P6-12
		P7-05	P7-11	P7-14	P7-15
		P9-04			
Fink-Finowicki J.	Warszawa	O5-02			
Fitta M.	Kraków	O5-03	P6-04	P6-15	P6-18
Flachbart K.	Košice	O7-14	O7-10	P6-03	P6-12
		P7-05	P7-07	P7-11	P7-14
		P7-15	P7-18		
Flachbart N.	Košice	P2-16			
Fodor-Csorba K.	Budapest	P5-15			
Forno I.	Alessandria	P3-17			
Franco V.	Sevilla	I3-02			
Frątczak E.	Łódź	P2-46	P9-17		
Fričová O.	Košice	P9-19			
Frincu B.	Grenoble	O3-01			
Frollo I.	Bratislava	O9-06			
Frydrych P.	Warszawa	O1-06			
Füzer J.	Košice	P2-17	P2-41	P2-45	P2-49
		P2-51	P2-55		
Füzerová J.	Košice	P2-17	P2-45	P2-51	
Gabáni S.	Košice	O7-10	O7-14	P6-12	P7-05
		P7-07	P7-10	P7-14	P7-15
		P7-18			
Gao S.	Beijing	P5-18			
Garstka T.	Częstochowa	P9-12			
Gavrilkin S.Yu.	Moscow	O7-10	P7-11	P7-15	
Gawroński J.	Łódź	P3-10			
Gawroński M.	Radom	P2-55			
Gažo E.	Košice	P7-07	P7-10		

Gažová Z.	Košice	P9-10			
Gębara P.	Częstochowa	P3-06	P3-05		
Géci M.	Košice	P5-13			
Geibel C.	Dresden	O7-07			
Geoffroy O.	Grenoble	O3-01			
Girman V.	Košice	P2-33	P2-42		
Glod L.	Košice	P9-14			
Glushkov V.V.	Moscow	O7-10	O7-14	P6-03	P6-12
		P7-03	P7-11	P7-12	P7-13
		P7-14	P7-15		
Głowiński H.	Poznań	P4-20			
Gmitra M.	Regensburg	O4-01	P6-05		
Gnatchenko S.L.	Kharkov	P7-02	P8-01		
Gogola D.	Bratislava	O9-06			
Gojzewski H.	Poznań, Potsdam	P4-04			
Gondro J.	Częstochowa	P2-27	P2-28	P2-30	
Gonzáles Angeles A.	Mexicali	P3-11			
Gonzalez-Legarreta L.	Oviedo	P2-54			
Goraus J.	Katowice	O7-08			
Górka B.	Radom	P2-55			
Görnert P.	Jena	P2-47			
Gorshunov B.	Moscow, Stuttgart		P7-03		
Gościańska I.	Poznań	P4-21			
Gostomska M.	Warszawa	P2-57			
Grajcar M.	Bratislava	P7-25			
Gralak D.	Wrocław	P6-19			
Grechnev A.	Kharkov	O1-09			
Grechnev G.E.	Kharkov	P7-02	P9-04		
Gregušová D.	Bratislava	O9-07			
Gribanov A.V.	Moscow	P7-04			
Grigora □ M.	Ia□i	P2-53	P4-19		
Gritzner G.	Linz	P7-28			
Grusková A.	Bratislava	P3-11	P9-06		
Gruszka K.	Częstochowa	P2-28	P2-29	P3-09	
Grzesiak-Nowak M.	Kraków	P5-08			
Gucmann F.	Bratislava	O9-07			
Gwizdała T.M.	Łódź	P9-17			
Gyepes R.	Komárno	P4-08			
Gzik-Szumiata M.	Radom	P2-55	P4-05		
Hadraba H.	Brno	P2-19			
Hagemann H.	Geneva	P6-21			
Halama M.	Košice	P2-09			
Hamrle J.	Ostrava	O4-03	P9-11		
Hamrlová J.	Ostrava	O4-03			
Haneczok G.	Chorzów	P3-14			

Hannula S.-P.	Aalto	O2-05			
Hapla M.	Brno	P2-02			
Härtel M.	Magdeburg	O1-01			
Hashim A.	Košice	P4-04	P4-13		
Hasiak M.	Wrocław	P2-34			
Haskova V.	Košice	P4-08	P4-14		
Hatala T.	Bratislava	O2-04			
Havela L.	Prague	O6-02	P6-02	P6-08	P6-14
Haysak I.	Uzghorod	P5-16			
Heczko O.	Prague	O2-05	O8-01		
Hendrych A.	Ostrava	O2-06			
Hermanek M.	Olomouc	P2-48			
Hernando B.	Oviedo	P2-54			
Herzer G.	Hanau	I2-01			
Hill S.	Tallahassee	O5-01	P5-04		
Hlubina R.	Bratislava	O7-01			
Hornowski T.	Poznań	P4-13			
Hoser A.	Berlin	O6-03			
Hoško J.	Bratislava	O2-01			
Hossain Z.	Kanpur	O7-07			
Hrabčáková V.	Košice	P2-33	P2-42		
Hrabovský D.	Ostrava	P3-20	P9-11		
Hrivňak S.	Košice	P1-13			
Hronský V.	Košice	P6-09	P9-08	P9-19	
Hrubovčák P.	Košice	P4-16			
Hruška B.	Trenčín	P6-09			
Hubač L.	Košice	P2-23			
Hudák J.	Košice	O9-04	O9-09	P2-16	P9-18
Hudak R.	Košice	P9-18			
Husanikova P.	Bratislava	O7-15			
Idzikowski B.	Poznań	O2-08	P6-22	P6-23	
Ihle D.	Leipzig	O1-01			
Ilkovič S.	Prešov	P4-08			
Ilkovič V.	Košice	P1-11			
Inaba A.	Toyonaka, Osaka		P5-05	P5-09	
Ipatov M.	San Sebastian	I1-01	P2-54		
Isnard O.	Grenoble	P6-11			
Ivanov V.Yu.	Moscow	P7-12			
Jackiewicz D.	Warszawa	O9-08	P2-25		
Jadzyn J.	Poznań	P5-14			
Jagličić Z.	Ljubljana	O8-02			
Jagodič M.	Ljubljana	O8-02			
Jančárik V.	Bratislava	P2-18			
Janičkovič D.	Bratislava	P2-35	P2-36	P3-07	
Janiš V.	Prague	P7-16			

Janošek M.	Prague	P2-26	P2-56		
Jaščur M.	Košice	P1-19	P1-12		
Jašek O.	Brno	P2-20			
Javorský P.	Košice	P4-25			
Javorský P.	Prague	O6-01	P6-01		
Jirásková Y.	Brno	O2-06	P2-02		
Jirsa M.	Prague	O7-05			
Johrendt D.	München	O7-07			
Józefczak A.	Poznań	P4-13			
Jurek K.	Prague	P7-19			
Juríková A.	Košice	P2-21	P2-22	P5-15	
Kabátová M.	Košice	P2-45			
Kačmarčík J.	Košice	O7-03	P7-18	P7-26	
Kaczmarzyk T.	Częstochowa	P2-29			
Kadlec C.	Prague	O7-12			
Kadlec F.	Prague	O7-12			
Kadlečíková M.	Bratislava	P2-58			
Kaiser S.	Stuttgart	P7-03			
Kajňáková M.	Košice	O1-07	P5-10	P5-11	P7-20
Kaleta J.	Wrocław	P2-34			
Kalmykova T.V.	Kharkov	P2-24			
Kaloshkin S.	Moscow	P2-54			
Kamarád J.	Prague	O8-03	P3-04	P6-11	
Kamieniarz G.	Poznań	O5-05	P5-20		
Kamiński M.	Warszawa	O2-01			
Kaňuchová M.	Košice	P7-22			
Kapusta O.	Košice	P4-18			
Karapetrov G.	Philadelphia	O7-03	O7-15	P7-26	
Kaštil J.	Prague	O6-01	O8-03	P3-04	
Kaszuwara W.	Warszawa	P3-19			
Keša P.	Košice	P5-23			
Kharchenko G.O.	Kharkov	P9-09			
Khoroshilov A.	Moscow	P6-12	P7-11		
Kim-Ngan N.T.H.	Kraków	P6-02			
Kitazawa H.	Tsukuba, Ibaraki	O6-04			
Kladivová M.	Košice	P2-11	P2-12		
Klein P.	Košice	P2-01	P2-05	P2-08	P9-18
Klein T.	Grenoble	P7-26			
Klement R.	Trenčín	P6-09			
Klementová M.	Husinec-Řež	O4-04	P4-17		
Klicpera M.	Prague	O6-01	P6-01		
Kmec F.	Košice	O9-09			
Kmjec T.	Prague	P4-17	P8-02		
Knowles E.S.	Gainesville	O5-01	P5-04		
Kochan D.	Regensburg	O4-01			

Kočiško R.	Košice	P3-18			
Kohout J.	Prague	O4-04	P4-17	P8-02	
Kolcun M.	Košice	P2-09	P5-06		
Kolesnik S.	De Kalb	O7-11			
Kollár P.	Košice	P2-32	P2-41	P2-45	P2-49
		P2-51	P2-55		
Kolomiets A.	Prague, Lviv	P6-08			
Kołodziejczyk A.	Kraków	O7-06			
Komanický V.	Košice	O7-03	P4-07	P5-21	P5-22
		P7-10	P7-21	P7-26	
Komová E.	Košice	P2-07	P2-08		
Koneracká M.	Košice	P5-14	P5-19	P9-10	
Konieczny P.	Kraków	P5-05	P5-08	P5-09	
Kopáni M.	Bratislava	P5-01			
Kopčanský P.	Košice	O9-06	P4-04	P4-13	P4-25
		P5-06	P5-07	P5-14	P5-15
		P5-16	P5-19	P5-24	P9-10
Kopeček J.	Prague	O8-01			
Kopecký V.	Prague	O8-01			
Kopiński J.	Poznań	P4-06			
Kostova N.G.	Sofia	P9-13			
Kostyk J.	Košice	P1-08			
Kouřil K.	Prague	P1-15	P1-16	P8-03	
Kováč F.	Košice	P3-16			
Kováč J.	Košice	O2-03	O2-08	O3-02	O8-04
		P2-31	P2-35	P2-39	P2-40
		P3-07	P3-08	P4-04	P4-14
		P4-16	P4-22	P4-25	P5-16
		P5-19	P5-23	P5-24	P7-19
		P7-23	P7-24	P9-13	
Kováčová A.	Košice	P3-18			
Kovaľaková M.	Košice	P9-08	P9-19		
Kovalchuk O.V.	Kiev	P5-14			
Kowalczyk A.	Poznań	P3-03			
Kowalski W.	Poznań	P3-03			
Kozlovskaya N.	Moscow	P7-13			
Kozłowski P.	Poznań	O5-05			
Krafčík A.	Bratislava	O9-06			
Krämer K.W.	Bern	O5-07			
Kratochvílová M.	Prague	O6-07	O7-04	P9-07	
Kraus L.	Prague	P2-56			
Kravčák J.	Košice	P2-10	P2-44	P4-08	
Krishnakumar V.	Salem	P6-21			
Křišťan P.	Prague	P2-47	P2-48		
Krivoruchko V.N.	Kharkov	P2-24			



Krokhmalskii T.	L'viv	P1-01			
Krompiewski S.	Poznań	O4-02			
Krupnitska O.	L'viv	P1-01	P1-04		
Krychowski D.	Poznań	I4-01	P4-06		
Kubániová D.	Prague	O4-04	P8-02		
Kubovčíková M.	Košice	P5-16	P5-19	P9-10	
Kucharski Ł.	Poznań	O5-05			
Kúdela R.	Bratislava	O9-07			
Kudrle V.	Brno	P2-20			
Kudrnovský J.	Prague	O4-05			
Kulkarni R.	Mumbai	P6-21			
Kurimský J.	Košice	P2-09	P5-06	P5-07	
Kusigerski V.	Belgrade	P2-14	P2-15		
Kuťko V.	Kharkov	P6-13			
Kuzminski M.	Warszawa	P2-58			
Kuznetsov A.	Moscow	P6-03	P7-11	P7-14	
Kvačkaj T.	Košice	P2-59	P3-18		
Laber K.	Częstochowa	P9-12			
Lacroix C.	Grenoble	I6-01			
Laguta V.V.	Prague	P8-02	P8-03	P8-04	
Lančok A.	Prague, Řež	O2-05	O4-04	P4-17	P5-01
Lander G.	Karlsruhe	O6-06			
Lapčák L.	Prague	O6-07			
Laššák M.	Košice	O9-09			
Lathe C.	Hamburg	P2-41			
Lauda M.	Košice	P2-51			
Lazukov V.N.	Moscow	P7-04			
Lazúrová J.	Košice	P6-04	P6-10	P6-15	P6-18
Legut D.	Ostrava	O1-03	O1-04	O4-03	P1-20
Lemański R.	Wrocław	P5-20			
Lesňák M.	Ostrava	P3-01			
Lesz S.	Gliwice	P2-30			
Levchenko A.	Kiev	P7-14	P7-15		
Levchenko G.V.	Kiev	P9-04			
Li C.H.	Gainesville	P5-04			
Lin C.T.	Stuttgart	P7-20			
Lipinski S.	Poznań	I4-01	P4-06		
Lipovský P.	Košice	O9-04	P2-16		
Liščinský M.	Košice	P5-13			
Lisý V.	Košice	P9-14			
Llobet A.	Los Alamos	O6-02			
Lobanova I.I.	Moscow	P7-12	P7-13		
Lofaj F.	Košice	P9-15			
Lohmann A.	Magdeburg	O1-01			
Lovas A.	Budapest	P2-10	P2-23	P2-31	P4-07

Lučivjanský T.	Košice	O1-08			
Luňáček J.	Ostrava	P3-01			
Lupták M.	Košice	P3-18			
Lupu N.	Ia□i	I8-01	O8-04	P2-52	P2-53
		P4-19			
Lyaschenko A.B.	Kiev	P9-04			
Lyashenko A.	Kiev	P7-11			
Lyra M.L.	Maceió	O1-02			
Łasocha W.	Kraków	P5-08			
Łukiewska M.	Częstochowa	P2-34			
Maccarini M.	Alessandria	P3-17			
Madugundo R.	Grenoble	O3-01			
Mahmed N.	Aalto, Perlis	O2-05			
Mahuliaková M.	Ostrava	P3-01			
Majerová M.	Bratislava	P7-17	P9-02		
Majorošová J.	Košice P5-15	P5-14			
Makowski M.	Poznań, Mainz	P4-04			
Maňka J.	Bratislava	P7-17	P9-01	P9-02	
Maple M.B.	San Diego	O7-08			
Marcin J.	Košice	O2-08	P2-35	P2-36	P3-06
		P3-07	P3-16		
Marder M.	Austin	P1-10			
Marton K.	Košice	P2-09	P5-06	P5-07	
Maryško M.	Prague	P8-04			
Mašková S.	Prague	O6-02	P6-02	P6-08	P6-14
Maťaš S.	Berlin	O5-04	O6-03		
Matěj Z.	Prague	P6-02			
Matija R.	Prešov	P2-03			
Matik M.	Košice	P6-10			
Maťko I.	Bratislava	P2-58			
Mazaleyrat F.	Cachan	I2-02			
McHenry M.	Pittsburgh	I3-01			
Medvecká Z.	Košice	P7-26			
Meisel M.W.	Gainesville, Košice		O5-01	P5-04	
Menushenkov A.P.	Moscow	P7-04			
Merenkov D.N.	Kharkov	P8-01			
Michalik Š.	Prague, Košice	O2-03	P2-03	P2-33	P2-42
Michalek G.	Poznań	P4-23			
Michaud F.	Lausanne	P1-03			
Mičietová H.	Žilina	O2-07			
Miglierini M.	Bratislava, Olomouc		O2-02	O2-04	P2-34
			P2-37	P5-01	
Mignot J.-M.	Gif sur Yvette	P7-04			
Mihalik M.	Košice	O5-03	O6-03	P6-04	P6-10
		P6-15	P6-18		

Mihalik Jr. M.	Košice	O6-03 P6-18	P6-04	P6-10	P6-15
Mila F	Lausanne	I5-01	P1-03		
Milkovič O.	Košice	P4-24			
Míšek M.	Prague	O6-01	O6-07	P9-07	
Miškuf J.	Košice	P2-21	P2-22		
Mitróová Z.	Košice	P5-14	P5-15		
Mitsen K.	Moscow	P7-11			
Miura M.	Odate, Akita	O9-01			
Miyashita S.	Bunkyo-ku, Tokyo		O6-04		
Miyazaki Y.	Toyonaka, Osaka		P5-05	P5-09	
Mizen K.	Moscow	P7-15			
Mižišin L.	Košice	P1-14			
Mogi I.	Katahira, Aoba-ku, Sendai			O9-01	O9-02
Molčan M.	Košice	P4-04	P4-13	P5-07	
Moneta M.	Łódź	P2-46			
Mori T.	Tsukuba	P7-07			
Morimoto R.	Saitama	O9-01	O9-02		
Moshchalkov V.V.	Leuven	O7-10	O7-14	P7-11	
Mrakovic A.	Belgrade	P2-14	P2-15		
Mukovskii Ya.	Moscow	P7-13			
Murafa N.	Košice	P4-16			
Musiś A.	Poznań	P6-23			
Mustafin E.	Darmstadt	O2-02			
Nabiałek M.	Częstochowa	P2-27 P3-09	P2-28 P3-10	P2-29	P2-30
Nagalakshmi R.	Tiruchirappalli	P6-21			
Nagler S.E.	Oak Ridge	O5-01			
Nakotte H.	Las Cruces	O6-02			
Nalecz D.	Kraków	P6-20	P7-30		
Neilinger P.	Bratislava	P7-25			
Nemcová V.	Košice	P2-33	P2-42		
Nemkovski K.S.	Jülich	P7-04			
Nénert G.	Grenoble	O6-04	O7-09		
Neslušán M.	Žilina	O2-07	P3-20		
Nikolic V.	Belgrade	P2-14			
Nižňanský D.	Husinec-Řež	P4-17			
Nižník Š.	Košice	P4-24			
Novák L.	Košice	P2-10	P2-23	P2-39	P2-40
Novotný T.	Prague	P7-16			
Nowicki M.	Warszawa	O9-03			
Ociepka K.	Katowice	P3-15			
Okunev A.	Uzghorod	P5-16			
Olčák D.	Košice	P6-09	P9-08	P9-19	
Olekšáková D.	Košice	P2-41			

Onufer J.	Košice	P2-11			
Oppeneer P.M.	Uppsala	O1-03	O6-06		
Orendáč M.	Košice	O5-04	P5-03	P5-12	P5-17
		P5-18	P7-10		
Orendáčová A.	Košice	O5-04	P5-03	P5-12	P5-17
		P5-18			
Oshikiri Y.	Yamagata	O9-01			
Ostatnický T.	Prague	O4-06			
Óvári T.-A.	Ia□i	P2-38	P2-43	P2-53	
Ozerov M.	Dresden	O5-07			
Pagnani D.	Poznań	P6-23			
Pajič D.	Zagreb	O8-02			
Panfilov A.S.	Kharkov	P7-02	P9-04		
Papanicolaou N.	Heraklion	P1-10			
Park J.-H.	Tallahassee	O5-01			
Parnica J.	Košice	P5-23			
Pashchenko M.I.	Kharkov	P8-01			
Pashchenko V.A.	Kharkov	P8-01			
Pavlík V.	Košice	O5-04	P5-12	P5-17	
Pavlovič M.	Bratislava	O2-02	P2-13		
Pavúk M.	Bratislava	P2-37			
Pawlik K.	Częstochowa	P3-05	P3-06	P3-19	
Pawlik P.	Częstochowa	P2-03	P3-05	P3-06	P3-19
Payer P.	Jena	P2-47			
Pękała K.	Warszawa	P2-57			
Pękała M.	Warszawa	P2-57			
Pelka R.	Kraków	O5-03	P1-07	P5-05	P5-09
Peprah M.K.	Gainesville	O5-01	P5-04		
Pereira M.S.S.	Maceió	O1-02			
Perovic M.	Belgrade	P2-14	P2-15		
Petryshynets I.	Košice	P3-16			
Pietosa J.	Warszawa	O7-11			
Pietrusiewicz P.	Częstochowa	P2-27	P2-28	P2-29	P2-30
		P3-09	P3-10		
Pilarcikova I.	Prague	P2-56			
Pinkowicz D	Kraków	O5-03	P5-05	P5-09	
Piovarci S.	Košice	P3-08	P7-19	P7-22	P7-23
		P7-24			
Pištora J.	Ostrava	O4-03	P9-11		
Podlesnyak A.	Oak Ridge	O5-01			
Pokorný V.	Prague	P7-16			
Poláková K.	Olomouc	P2-48			
Poperezhai S.	Kharkov	P6-13			
Pospíšil J.	Prague	06-04	O7-09		
Potočňák I.	Košice	O5-04			

Praslička D.	Košice	O9-04	O9-09	P2-16	P9-18
Pratt F.L.	Chilton	O5-03	P5-09		
Prechal J.	Prague	O6-01	O6-07	P6-17	P9-07
Precner M.	Bratislava	O9-05	O9-07		
Pribulová Z.	Košice	O7-03	P7-26		
Pristáš G.	Košice	P7-07	P7-10	P7-18	
Pristaš P.	Košice	P4-25			
Procházka V.	Olomouc	P2-48			
Prokeš K.	Berlin	O7-09			
Prokleška J.	Prague	O6-04	O6-07	O7-04	
Przewoźnik J.	Kraków	O5-03			
Przybył A.	Częstochowa	P3-05	P3-06		
Puchala P.	Košice	P1-18			
Rabatin P.	Košice	P5-13			
Radelytsky I.	Warszawa	O5-02			
Radusovska M.	Košice	P3-08	P7-19	P7-22	P7-23
Radwanski R.J.	Kraków	P6-20	P7-30		
Raevski I.P.	Rostov on Don	P8-02	P8-03	P8-04	
Rajňák M.	Košice	P2-09	P4-04	P5-06	P5-07
		P5-24			
Rameš M.	Prague	O7-05			
Randrianantoandro N.	Le Mans	O8-04	P3-12	P3-13	
Reiffers M.	Prešov	P4-08	P4-11	P6-21	
Rek A.	Brno	P2-20			
Repková J.	Ostrava	P3-01			
Řezníček R.	Prague	P1-16	P2-47		
Richter J.	Magdeburg	O1-01	P1-01	P1-04	
Richter K.	Košice	P2-06			
Righi L.	Parma	O8-03			
Risset O.N.	Gainesville	O5-01			
Rivoirard S.	Grenoble	O3-01			
Rojas O.	Lavras	O1-02			
Ropka Z.	Kraków	P6-20	P7-30		
Rosová A.	Bratislava	P4-12			
Rubin P.	Tartu	P5-02			
Rudajevová A.	Prague	P6-01			
Rudzinski W.	Poznań	P4-26	P7-29		
Rüegg Ch.	Villigen	O5-07			
Rusz J.	Uppsala	O6-06			
Ryba T.	Košice	P4-02	P4-08	P4-14	
Salach J.	Warszawa	O1-06	O2-01	O9-08	P2-25
		P9-05			
Samarin N.	Moscow	P7-14	P7-15		
Samuely P.	Košice	O7-03	P4-14	P7-07	P7-25
		P7-26			

Sannikov I.	Moscow	P7-11			
Šantavá E.	Prague	O4-04			
Savina Yu.O.	Kharkov	P8-01			
Ščepka T.	Bratislava	O9-07			
Schmidt H.-J.	Osnabrück	O1-01			
Schneeweiss O.	Brno	P2-20			
Schreiber M.	Chemnitz	P5-02			
Šebesta J.	Prague	O6-07			
Sechovský V.	Prague	O6-04	O6-07	O7-04	O7-09
		6P-17	P9-07		
Šefčíková M.	Košice	O7-05	P7-24		
Seidl T.	Darmstadt	O2-02			
Seifert D.	Jena	P1-15			
Semenov A.V.	Moscow	P7-12			
Sherman A.	Tartu	P5-02			
Shiddiq M.	Tallahassee	O5-01			
Shitsevalova N.Yu.	Kiev	O7-10	O7-14	P6-03	P6-12
		P7-05	P7-11	P7-14	P7-15
		P7-18			
Shuvaeva E.	Moscow	P2-54			
Šidík F.	Košice	P2-08			
Siekłucka B.	Kraków	O5-03	P5-05	P5-09	
Siemensmeyer K.	Berlin	O5-04	P7-18		
Silber R.	Ostrava	P9-11			
Šimáček I.	Bratislava	P9-01			
Siposova K.	Košice	P9-10			
Šitek J.	Bratislava	P2-13	P2-58		
Škorvánek I.	Košice	O2-08	O8-04	P2-35	P2-36
		P3-06	P3-07	P3-16	P4-24
		O6-04			
Skourski Y.	Dresden	P7-17	P9-01	P9-02	
Škrátek M.	Bratislava	P4-13			
Skumiel A.	Poznań	P3-11	P9-06		
Sláma J.	Bratislava	P2-58			
Slawska-Waniewska A.	Warszawa	O7-08			
Ślebarski A.	Katowice	O7-10	O7-14	P6-03	P6-12
Sluchanko N.E.	Moscow	P7-03	P7-11	P7-12	P7-13
		P7-14	P7-15		
		P2-16			
Šmelko M.	Košice	O2-08	P6-22	P6-23	
Śniadecki Z.	Poznań	O2-02	P2-04	P2-18	P3-11
Šoka M.	Bratislava	O7-03	P7-18		
Soltészová V.	Košice	O7-15	O9-05	O9-07	P7-26
Šoltýs J.	Bratislava	P4-24			
Sopko M.	Košice				

Sovák P.	Košice	O2-03 P2-55	P2-03	P2-33	P2-42
Spalek J.	Kraków	O7-02	P7-01		
Španková M.	Bratislava	P4-11	P4-12		
Spasojevic V.	Belgrade	P2-14	P2-15		
Stankiewicz J.	Zaragoza	O7-14			
Starodub V.A.	Kielce	O1-07	P5-11		
Štěpánek J.	Prague	P2-48			
Štěpánková H.	Prague	P1-15 P8-03	P1-16	P2-47	P2-48
Stewart R.	Didcot	P7-04			
Stobiecki T.	Kraków	P4-20			
Stoian G.	Iași	P2-52			
Straka L.	Aalto	O8-01			
Strašík I.	Darmstadt	O2-02			
Štrbák O.	Bratislava	O9-06			
Štrbík V.	Bratislava	P4-11	P4-12		
Strečka J.	Košice	O1-02	P1-02	P1-03	P1-06
Strečková M.	Košice	P2-19	P2-49	P2-51	
Strydom A.M.	Johannesburg	I7-02			
Štubňa V.	Košice	P1-19			
Studeniyak I.P.	Uzhorod	P5-14			
Stunault A.	Grenoble	O7-09			
Suderow H.	Madrid	I7-01			
Sugiyama A.	Shinjuku, Tokyo	O9-01			
Šuhajová V.	Košice	P2-12			
Šulek M.	Bratislava	P1-09			
Švec Jr. P.	Bratislava	O2-01	P2-35		
Švec Sr. P.	Bratislava	O2-01	P2-35	P2-36	P3-07
Šviková M.	Košice	P5-13			
Svoboda P.	Prague	P6-08	P6-14		
Sýkora R.	Ostrava	P1-20			
Synoradzki K.	Poznań	P3-02	P3-03	P6-06	
Szabo A.	Budapest	P4-07			
Szabo P.	Košice	P4-08	P4-14	P7-25	
Szajek A.	Poznań	P6-22			
Szałowski K.	Łódź	O5-06	P1-05	P1-19	P4-03
Szczęśniak D.	Częstochowa	P7-09			
Szczęśniak R.	Częstochowa	P7-08	P7-09		
Szczeszak A.	Poznań	P6-22			
Szewczyk R.	Warszawa	O1-06 P2-25	O2-01 P9-05	O9-03	O9-08
Szota M.	Częstochowa	P2-27 P3-09	P2-28 P3-10	P2-29	P2-30
Szumiaty T.	Radom	P2-55	P4-05		

Szwaja M.	Częstochowa	P3-05	P3-06		
Szymańska A.	Kraków	P5-08			
Szymczak H.	Warszawa	O5-02			
Szymczak R.	Warszawa	O5-02			
Takáčová I.	Košice	P7-07	P7-18		
Talaat A.	San Sebastian	I1-01	P2-54		
Talham D.R.	Gainesville	O5-01	P5-04		
Talijan N.	Belgrade	P2-50			
Tarapov S.I.	Kharkov	P2-24			
Tarasenko R.	Košice	P5-12	O5-04		
Temerov V.L.	Krasnoyarsk	P8-01			
Teplan M.	Bratislava	O9-06			
Tesařová N.	Prague	O4-06			
Thamizhavel A.	Mumbai	P6-21			
Thiaville A.	Orsay	P2-06			
Tibenská K.	Košice	P5-03			
Timco G.A.	Manchester	O5-05			
Timko M.	Košice	P4-04	P4-13	P4-25	P5-06
		P5-07	P5-14	P5-15	P5-16
		P5-23	P5-24	P9-10	
Tkáč V.	Košice	P5-03			
Tkach I.	Prague	P6-02			
Tóbiş J.	Bratislava	O9-05	O9-07	P1-09	
Toliński T.	Poznań	P3-02	P3-03	P6-06	
Tomašovičová N.	Košice	P5-14	P5-15	P5-16	
Tomčo L.	Košice	P2-09	P5-06	P5-07	
Töpfer J.	Jena	P1-15			
Tóth-Katona T.	Budapest	P5-15			
Tothová J.	Košice	P5-24	P9-14		
Tran L.M.	Wrocław	O7-13			
Tran V.H.	Wrocław	O7-13	P6-19		
Trgala M.	Bratislava	P7-25			
Trocha P.	Poznań	P4-26			
Trontelj Z.	Ljubljana	O8-02			
Trzaska M.	Warszawa	P2-57			
Tuček J.	Olomouc	P2-48			
Tuna F.	Manchester	O5-05			
Turčinková D.	Prague	O6-07			
Turek I.	Brno, Prague	O4-05	P2-02		
Ujhelyi F.	Budapest	P4-07			
Uličná K.	Prague	P8-03			
Urbaniak-Kucharczyk A.	Łódź	P4-10			
Urse M.	Iaşi	P4-19			
Ušák E.	Bratislava	P2-04	P2-18		
Ušáková M.	Bratislava	P2-04	P2-18	P9-06	



Vajda A.	Budapest	P5-15				
Valenta J.	Prague	O6-07	P9-07			
Vališka M.	Prague	O7-09				
Valušová E.	Košice	P4-25				
van Tol J.	Tallahassee	P5-04				
Vanacken J.	Leuven	O7-10	O7-14			
Varga L.K.	Budapest	O3-02				
Varga M.	Košice	P2-36				
Varga R.	Košice, Orsay	P1-08	P2-01	P2-05	P2-06	
		P2-07	P2-08	P4-07	P4-08	
		P4-14	P9-18			
Vargova Z.	Košice	P4-08	P4-14			
Vasilets G.	Kharkov	O1-07				
Vasiliev A.N.	Moscow	P7-02				
Vávra I.	Bratislava	P4-12				
Vavra M.	Košice	O6-03	P6-04	P6-10	P6-18	
Vazquez M.	Madrid	P1-08	P2-01	P2-05	P2-08	
Verkholyak T.	Lviv	P1-02				
Vlaic P.	Cluj-Napoca	P4-09				
Vojtek V.	Košice	P2-32				
Vojtko M.	Košice	P2-09				
Volkova O.S.	Moscow	P7-02				
Volochová D.	Košice	P7-19	O7-05			
Vrábel P.	Košice	P5-18	P9-08	P9-19		
Výborný K.	Prague	O4-06				
Vyhnánek J.	Prague	P2-26				
Waeckerle T.	Imphy	O3-01				
Wang S.	Villigen	O5-07				
Warda K.	Łódź	P9-17				
Wasiutyński T.	Kraków	O5-03	P5-05	P5-08	P5-09	
Watanabe K.	Katahira, Aoba-ku, Sendai			O9-02		
Wdowik U.D.	Krakow	O1-04	P1-20			
Welter E.	Hamburg	P7-05				
Weymann I.	Poznań	P4-27				
Wilhelm F.	Grenoble	O6-06				
Winiarski W.	Warszawa	O2-01				
Winpenny R.E.P.	Manchester	O5-05				
Wnuk I.	Częstochowa	P3-05				
Woch W.M.	Kraków	O7-06	P7-28			
Wojciechowski M.	Zielona Góra	O5-05	P5-20			
Wójcik K.P.	Poznań	P4-27				
Wojtczak L.	Łódź	P4-01				
Wosnitza J.	Dresden	O5-04				
Wysłocki J.J.	Częstochowa	P3-05	P3-06	P3-19		
Yamauchi Y.	Tsukuba, Ibaraki	O9-01				

Zajac Š.	Prague	P4-01			
Žák T.	Brno	P2-50			
Zalecki R.	Kraków	O7-06	P7-28		
Zaleski A.J.	Wrocław	O7-13			
Zamiatkina E.	Moscow	P2-54			
Závěta K.	Prague	O4-04	P4-17	P8-02	
Závišová V.	Košice	P5-16	P5-19	P9-10	
Zbořil R.	Olomouc	P2-48			
Zbroszczyk J.	Częstochowa	P2-34			
Zegrodnik M.	Kraków	P7-01			
Zelenák V.	Košice	P4-16	P4-18	P4-22	P6-16
Zelenáková A.	Košice	P4-16	P4-18	P4-22	P6-16
Zentková M.	Košice	P6-04	P6-10	P6-15	P6-18
Zhukov A.	San Sebastian, Bilbao	I1-01	P2-54		
Zhukova E.	Moscow, Stuttgart		P7-03		
Zhukova V.	San Sebastian	I1-01	P2-54		
Zieliński P.M.	Kraków	O5-03	P5-05	P5-09	
Ziman J.	Košice	P2-11	P2-12		
Ziółkowski G.	Katowice	P3-12	P3-13	P3-14	
Živković D.	Bor	P2-50			
Životský O.	Ostrava	O2-06			
Zmorayova K.	Košice	O7-05	P3-08	P7-23	
Zofia E.	Łódź, Madrid	P4-15			
Žonda M.	Prague	P7-16			
Zorkovska A.	Košice	P4-07	P7-20	P9-13	
Žukovič M.	Košice	O1-05	O1-08		
		P1-12	P1-13	P1-14	
Zvyagin S.A.	Dresden	O5-04	O5-07		
Zwicznagl G.	Braunschweig	O6-05			
Żywczak A.	Kraków	P4-20			

## NOTES

## NOTES

## NOTES

## NOTES

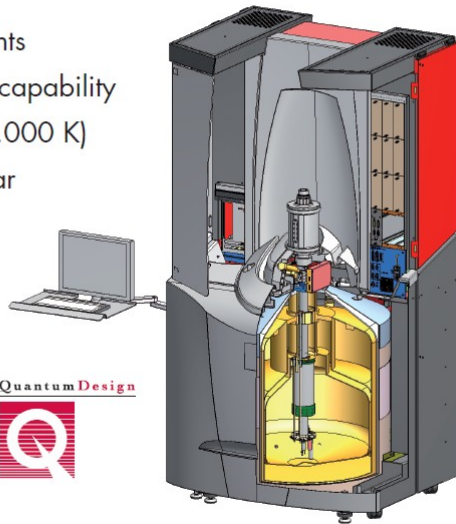
## NOTES

## MPMS SQUID VSM –

*SQUID sensitivity combined with the speed of a vibrating sample magnetometer*

The MPMS SQUID VSM DC magnetometer offers you:

- $10^{-8}$  emu sensitivity
- Up to 7 Tesla magnetic field
- Sample temperature from 1,8 K to 400 K
- Options:
  - AC susceptibility measurements
  - Ultra-low field measurement capability
  - Sample space oven (up to 1.000 K)
  - Cryogen-free EverCool dewar



[www.lot-oriel.com/de](http://www.lot-oriel.com/de)



**LOT-Oriel Group Europe.** Im Tiefen See 58. 64293 Darmstadt.  
phone: +49 6151-8806-0. eMail: [info@lot-oriel.de](mailto:info@lot-oriel.de)





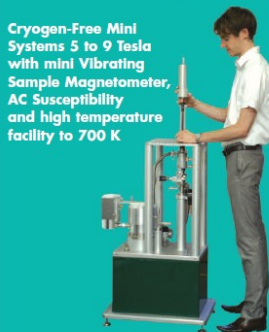
## CRYOGEN FREE MEASUREMENT SYSTEMS 5 TO 25 TESLA

### Measurement Options

- Vibrating Sample Magnetometer (VSM) for measurements of DC magnetic moment with sensitivity of  $10^{-6}$
- AC Calorimeter to measure Specific Heat and Thermal Conductivity
- Resistivity and Hall effect probe with sample rotation in field
- AC Susceptibility probe
- MFM/AFM and Pressure Cell options

### Temperature Ranges

- High Temperature Insert with temperatures to 1000 K
- He-3 Insert with temperatures down to 300 mK and 30 hours hold time
- Ultra low temperatures down to 10 mK with 17 Tesla shielded coil in a Cryogen-Free Dilution Refrigerator



**Cryogenic Limited,**  
Unit 30, Acton Park Industrial Estate,  
The Vale, Acton, London, W3 7QE. United Kingdom.  
Tel: +44 (0) 20 8743 6049  
Fax: +44 (0) 20 8749 5315  
E-mail: [sales@cryogenic.co.uk](mailto:sales@cryogenic.co.uk)

[www.cryogenic.co.uk](http://www.cryogenic.co.uk)

# **C R Y O S O F T spol. s r. o.**

## **LABORATORY EQUIPMENTS A N D S U P P L I E S**

### **OFFERS:**

- **Import/Export services**
- **Laboratory equipments**

### **NIKON MICROSCOPES**

- for metallurgy, electronics, IC inspection, medicine

**ANALYZERS – chromatography**

**VACUUM AND CRYOGENIC TECHNIQUE**

- cryostats, dewars

### ***TEMPERATURE SENSORS***

- Ge sensors with very low magnetoresistance, Pt sensors, thermocouples
- **Magnetic systems, medical equipments**
- **Supplies of liquid helium and nitrogen**
- **Engineering and cryogenic consultations**
- **Computers**

**CONTACT:** Cryosoft spol. s r. o.  
P. O. Box G-14  
040 01 Košice  
Slovakia

Tel./Fax: ++421557295948  
E- mail: stefan.molokac@stonline.sk

Head: Ing. Štefan Molokáč, Csc.



**CHROMSPEC**  
SLOVAKIA  
s.p.o.

Jánošíkova 1827/65, 927 01 ŠAČA

Zápis v Obchodnom registri Okresného súdu Nitra,  
oddiel Šač, vložka číslo: 3339/N

## Laboratórne prístroje a zariadenia

[www.chromspec.sk](http://www.chromspec.sk)

pre aplikácie v oblastiach :

Spektrálna a elementárna analýza  
Analýza životného prostredia  
Materiálová analýza, testovanie materiálov  
Vákuová technika, nízko-teplotné aplikácie  
Príprava vzoriek a čistej vody  
Všeobecné laboratórne zariadenia  
Testovanie a kontrola farmaceutických výrobkov  
Spotrebný materiál





Faculty of Science  
Pavol Jozef Šafárik University, Košice  
[www.science.upjs.sk](http://www.science.upjs.sk)



Institute of Experimental Physics  
Slovak Academy of Sciences, Košice  
[uef.saske.sk](http://uef.saske.sk)



Technical University, Košice  
[www.tuke.sk](http://www.tuke.sk)



Slovak Physical Society  
[www.sfs.sk](http://www.sfs.sk)



Czech Physical Society  
[www-ucjf.troja.mff.cuni.cz/cfs/](http://www-ucjf.troja.mff.cuni.cz/cfs/)



Slovenská magnetická spoločnosť  
(SMAGS)



[www.smags.sk](http://www.smags.sk)



## **Book of Abstracts and Programme**

### **15<sup>th</sup> Czech and Slovak Conference on Magnetism**

Publisher: Pavol Jozef Šafárik University in Košice

Technical editing: the UPJŠ University library in Košice

<http://www.upjs.sk/pracoviska/univerzitna-kniznica>

Year of publication: 2013

Impression: 350 copies

Number of pages: 372

Number of author's sheets: 18, 98

First edition

Printed by: Equilibria s.r.o.

ISBN 978-80-8152-015-0



ISBN 978-80-8152-015-0



9

788081

520150